Technical Report Documentation Page

1. Report No.	2. Government Accession No.	3. Recipient's Catalog No.
FHWA/TX-06/0-5091-3		

4. Title and Subtitle	5. Report Date
ASSESSING THE ABILITY OF FOG SEALS TO SEAL PAVEMENTS, TO REJUVENATE IN SITU BINDER, AND TO RETARD BINDER OXIDATION	February 2007 Published: December 2007
	6. Performing Organization Code

7. Author(s)	8. Performing Organization Report No.
Nikornpon Prapaitrakul, Thomas J. Freeman, and Charles J. Glover	Report 0-5091-3

9. Performing Organization Name and Address	10. Work Unit No. (TRAIS)
Texas Transportation Institute The Texas A&M University System College Station, Texas 77843-3135	11. Contract or Grant No. Project 0-5091

12. Sponsoring Agency Name and Address	13. Type of Report and Period Covered
Texas Department of Transportation Research and Technology Implementation Office P. O. Box 5080 Austin, Texas 78763-5080	Technical Report: September 2004-August 2006
	14. Sponsoring Agency Code

15. Supplementary Notes

Project performed in cooperation with the Texas Department of Transportation and the Federal Highway Administration.

Project Title: Analyze Existing Fog Seal Asphalts and Additives

URL: http://tti.tamu.edu/documents/0-5091-3.pdf

16. Abstract

This work was conducted for the purpose of assessing the effectiveness of fog seal treatments as an aid to highway maintenance managers in making sound decisions for fog seal treatments. Replicate cores of both treated and untreated highway and general aviation pavement sections were analyzed. Whole cores were assessed by water permeability and by susceptibility to permanent deformation. Replicate cores were sawed into one-quarter inch slices which were individually analyzed for total air voids, accessible air voids, binder content, oxidative aging and rheology, and for the presence of fog seal material. The fog seal materials used in this project were emulsions of asphalt materials and coal tar type materials.

Results showed that if the fog seal is penetrating into the pavement, it is not doing so to a detectable level, the permeability of the pavement is not significantly reduced, and APA tests did not show any softening of the pavements by the treatments. Additionally, 1) differences between untreated and treated pavement slices generally seem more likely due to original binder variability with depth than to the fog seal treatments, although coal-tar treatments appear to harden the top layer; 2) effects of the fog seal treatments on oxidative aging were not observed; and 3) previous work, that the aging rates of asphalt binders are decreased by very low accessible air voids is supported.

In summary, the effects of fog seals on pavement durability appear to be minimal, with respect to binder rejuvenation or sealing. Cosmetic effects or protecting against shelling or raveling remain as possible benefits, although they were not assessed by this project. In response to this work, engineers should reassess the cost-benefit balance of fog seal treatments

17. Key Words	18. Distribution Statement
Asphalt, Fog Seal, Binder Rejuvenation, Rejuvenator, Asphalt Durability, Binder Oxidation, Pavement Preservation, Pavement Air Voids, Asphalt Emulsion	No restrictions. This document is available to the public through NTIS: National Technical Information Service Springfield, Virginia 22161 http://www.ntis.gov

19. Security Classif.(of this report)	20. Security Classif.(of this page)	21. No. of Pages	22. Price
Unclassified	Unclassified	362	

Form DOT F 1700.7 (8-72) **Reproduction of completed page author**

ASSESSING THE ABILITY OF FOG SEALS TO SEAL PAVEMENTS, TO REJUVENATE IN SITU BINDER, AND TO RETARD BINDER OXIDATION

by

Nikornpon Prapaitrakul
Graduate Research Assistant
Artie McFerrin Department of Chemical Engineering/Texas Transportation Institute

Thomas J. Freeman
Engineering Research Associate
Texas Transportation Institute

and

Charles J. Glover
Professor/Research Engineer
Artie McFerrin Department of Chemical Engineering/Texas Transportation Institute

Report 0-5091-3
Project 0-5091
Project Title: Analyze Existing Fog Seal Asphalts and Additives

Performed in cooperation with the
Texas Department of Transportation
and the
Federal Highway Administration

February 2007
Published: December 2007

TEXAS TRANSPORTATION INSTITUTE
The Texas A&M University System
College Station, Texas 77843-3135

DISCLAIMER

The contents of this report reflect the views of the authors, who are responsible for the facts and the accuracy of the data presented herein. The contents do not necessarily reflect the official view or policies of the Federal Highway Administration (FHWA) and the Texas Department of Transportation (TxDOT). This report does not constitute a standard, specification, or regulation, nor is it intended for construction, bidding, or permit purposes. The Unites States Government and the State of Texas do not endorse products or manufacturers. Trade or manufacturers' names appear herein solely because they are considered essential to the object of this report. The engineers in charge were Charles J. Glover, P.E. (Texas No. 48732) and Thomas J. Freeman, P.E. (Illinois No. 062-044540).

ACKNOWLEDGMENTS

This project was conducted for TxDOT, and the authors thank TxDOT and FHWA for their support in funding this research project. In particular, the guidance and technical assistance provided by the project director (PD) Gerald Peterson of TxDOT, the project coordinator (PC) Miles Garrison, also of TxDOT, and German Claros of the TxDOT Research and Technology Implementation (RTI) office are greatly appreciated. Special thanks also go to Rick Canatella and Sidney Greer, from the Texas Transportation Institute (TTI) for their assistance with a number of laboratory measurements. The assistance of the various TxDOT district offices that assisted with obtaining the many pavement cores and fog seal materials also is greatly appreciated.

TABLE OF CONTENTS

TABLE OF CONTENTS (continued)

TABLE OF CONTENTS (continued)

TABLE OF CONTENTS (continued)

TABLE OF CONTENTS (continued)

LIST OF FIGURES

Figure **Page**

LIST OF FIGURES (continued)

Figure **Page**

LIST OF FIGURES (continued)

Figure **Page**

LIST OF FIGURES (continued)

Figure **Page**

LIST OF FIGURES (continued)

Figure **Page**

LIST OF TABLES

Table **Page**

LIST OF TABLES (continued)

Table **Page**

LIST OF TABLES (continued)

Table **Page**

LIST OF ABBREVIATIONS AND SYMBOLS

ω	Angular Frequency
$\eta'(\omega)$	Dynamic Shear Viscosity
$\eta^*(\omega)$	Complex Dynamic Shear Viscosity
$G'(\omega)$	Elastic (storage) Dynamic Shear Modulus
$G''(\omega)$	Viscous (loss) Dynamic Shear Modulus
$G'/(\eta'/G')$	DSR Function
SSD	Saturated Surface-Dry Method
CSS-1	Cationic Slow-Setting Asphalt Emulsion
SS-1	Slow-Setting Asphalt Emulsion
MS-2	Medium-Setting Asphalt Emulsion
PASS	Polymer-Modified Asphalt Surface Sealer
COS-50	Cape over Seal
EB44	Engineering Brief No. 44 (Coal-Tar Treatment)
SEC	Size Exclusion Chromatography
CM	Coarse Matrix Mixture
DG	Dense Grade Mixture
SP	SuperPave Mixture
PQI	Pavement Quality Indicator
k_w	Water Permeability (cm/s)
x_i, y_i	Data of Untreated and Treated Samples for Sample i
n	Number of Samples
D_i	Difference for Each Linked Pair
$\overline{D}$	Mean Difference for Each Linked Pair
σ	Standard Deviation
t	t-Statistic
p	Probability That Mean Difference Occurs by Chance

CHAPTER 1

INTRODUCTION AND BACKGROUND

PROBLEM STATEMENT

Fog and rejuvenating seals are presumed to have the potential to reduce and reverse the aging of asphalt pavements, reduce cracking and raveling, and provide a better, longer-lasting pavement. To assess fog seal and rejuvenator seal performance, a 2-year research program was conducted. Pavements sealed within the last several years prior to and during this project were tested each year of the 2-year study to assess the *actual* impact of these treatments on water permeability, strength, binder viscosity, and depth of binder penetration.

Specifically, the objectives of this research were:

1. Determine the fog seal practices and materials that are currently used on highway and airport pavements.
2. Determine and compare properties of asphalt binders from pavements with and without fog seal treatments.
3. Determine fog seal performance on the following categories:
    - Evaluate the effectiveness as a rejuvenator.
    - Evaluate the effectiveness as a sealant.
4. Develop fog seal specification for highway and airport pavements.
5. Make recommendations as to the best pavement maintenance scenario, from a binder rejuvenation perspective.

This report provides comprehensive documentation of background information on sealannt types and usage, and on the methods, results, and conclusions of this research. Guidelines on the application and use of sealants, including advantages and disadvantages of the various types, are summarized in a separate document (Glover and Freeman, 2007).

FOG SEAL AND REJUVENATOR

Fog seals have been used for pavement maintenance purposes for many years. According to the Asphalt Emulsion Manufacturers Association (AEMA), fog seal is defined as “a light spray application of dilute asphalt emulsion used primarily to seal an existing asphalt surface to reduce raveling and enrich dry and weathered surfaces” (The Asphalt Institute, 1999b). Fog seals are referred to as enrichment treatments since fresh asphalt is added to an aged surface to lengthen the pavement surface life (Booth et al., 1988). Fog seals, referred to as flush coats, are also useful in chip seal applications to hold chips in place in fresh seal coats. This method can help prevent vehicle damage due to flying chips. The Asphalt Institute also concludes that small cracks can be sealed by a fog seal (The Asphalt Institute, 1999a; Outcalt, 2001).

Rejuvenators are agents used to restore properties of asphalt. Most rejuvenators are proprietary materials and are difficult to specify except by brand name. Very little information is

available that describes the expected performance when using rejuvenators to maintain pavements (Estakhri and Agarwal, 1991).

Function of a Fog Seal

The purpose of a fog seal is to coat, protect, and/or rejuvenate the existing asphalt pavement. Also, a fog seal can be used to decrease the permeability to water and air. To the extent such permeability reductions occur, a pavement's waterproofing will be improved and aging susceptibility due to binder oxidation will be reduced. Fog seal emulsions must penetrate into the voids in the pavement in order to seal off the surface. A slow setting emulsion diluted in water turns out to be a suitable fog seal material in this case. An emulsion that is too thick may not properly penetrate into the surface voids and will leave behind an excess amount of asphalt on the surface after the emulsion breaks, causing a slippery surface.

A fog seal emulsion wets the surface of pavement then breaks, forming a new asphalt film on the pavement surface. The rate at which the emulsion breaks primarily depends on weather conditions such as wind, rain, and temperature.

Function of a Rejuvenator

Rejuvenating emulsions contain oils that reduce the viscosity of existing asphalt, thereby reducing the cohesive failure of the asphalt as the flexibility of binder is improved. In addition, rejuvenating oils can penetrate to fill voids in the pavement and minimize further binder oxidation since the rate of asphalt oxidation is highly dependent on the voids in the total mixture (VTM) (Brown, 1988). An effective rejuvenator must penetrate into the pavement surface in order to be absorbed by the aged hardened asphalt, but also to avoid causing a binder-slick surface, especially in wet weather (Brown, 1988).

FOG SEAL EMULSION

Fog seal emulsions are presumed to provide multiple improvements to the pavement. Some emulsions are single purpose (seal the pavement, penetrate into voids, or rejuvenate the binder), but most often, more than one function is desired by users of current commercial fog seal emulsions.

In some cases, fog seal emulsion can be positively charged (cationic), which can replace water from the surface of an aggregate or aged asphalt film (California Department of Transportation, 2003). This type of emulsion breaks by loss of water and by chemical action. The cationic emulsified asphalt standard specification can be found in ASTM D-2397. On the other hand, a negatively charged (anionic) emulsion has no interaction with the aggregate surface and breaks due to water loss by evaporation and absorption through voids in the pavement (California Department of Transportation, 2003). Also, emulsion can be categorized by setting time (Transport Research Board, 2006). For example, RS refers to rapid-setting, MS for medium-setting and SS for slow-setting. In addition, local authorities may use other naming

systems according to their properties of interest such as P and LM, which refer to polymer-modified and latex-modified emulsion, respectively.

FOG SEAL CONSTRUCTION

The State of California Department of Transportation general guidelines for fog seal construction are discussed in this section (California Department of Transportation, 2003).

Site Conditions

Warm and dry weather will make the low viscosity emulsion break quickly, which will lead to asphalt film formation on the pavement surface. Atmospheric temperature should be above 10 °C (50 °F), and pavement temperature should be above 15 °C (59 °F).

Surface Conditions

Prior to fog seal application, the pavement surface must be clean and dry. The pavement surface can be cleaned with a road sweeper, power broom, or flushed with a water pump-unit to remove dust, dirt, and debris. If flushing is required, it should be completed 24 hours prior to the application of the fog seal to allow adequate drying.

FOG SEAL PREPARATION

Asphalt emulsions (original emulsions) contain up to 43 percent water, but must be diluted, generally, to 50 percent before further use. This additional dilution reduces viscosity and allows the application of small amounts of residual binder to be adequately controlled as shown in Figure 1-1. Dilution water must be potable and free from detectable solids or incompatible soluble salts (hard water).

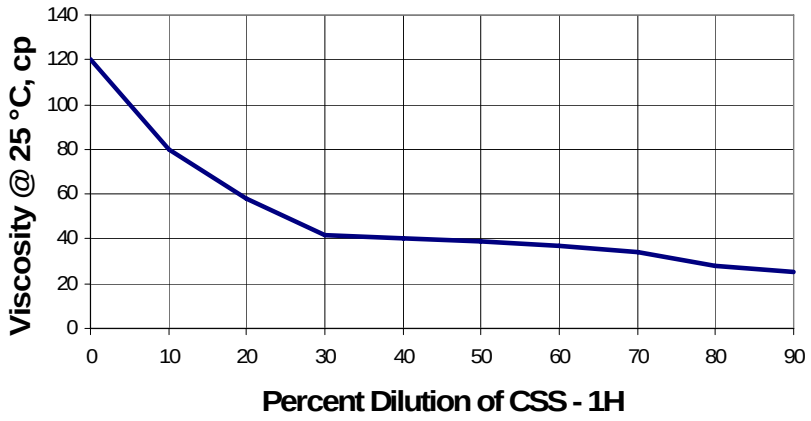

Figure 1-1. Viscosity Change with Dilution (Hicks and Holleran, 2002).

The compatibility of water with the emulsion may be checked by mixing a small amount of the emulsion in a can (approximately 1 liter). After mixing the materials for 2 to 3 minutes

with a stirrer, the resulting mixture is poured through a pre-wetted 150 µm sieve. If more than 1 percent by weight of material is retained on the sieve, the water is not compatible, and clogging in the spray jets may result.

About 0.5 to 1.0 percent of a compatible emulsifier solution can be used to treat incompatible water (the emulsion manufacturer can provide advice regarding compatible solutions). The emulsifier solution should be added to the water tanker and circulated for 10 to 15 minutes via the pump before adding it to the emulsion. The compatibility test should be repeated if a water treatment is used.

The emulsion should be diluted no more than 24 hours before its intended use (Asphalt Emulsion Manufacturer's Association, 1990). This is to avoid settlement of the diluted emulsion. Water is always added to the emulsion and not the other way around. The emulsion may be circulated using a centrifugal or other suitable pump to ensure uniformity (Asphalt Emulsion Manufacturer's Association, 1990).

Application Rates

Properly calibrated distributor trucks are used to apply the emulsion. In some cases, if emulsions are modified, a special distributor may be required (Heydorn, 1998). Spray nozzles with 4 to 5 mm (1/8 to 3/16 inch) openings are recommended (Asphalt Emulsion Manufacturer's Association, 1990). The emulsion may be heated to 50 °C (122 °F) maximum, although, generally the emulsion is sprayed at ambient temperature (Asphalt Emulsion Manufacturer's Association, 1990). The emulsion is sprayed at a rate that is dependent on the surface conditions (see Table 1-1). Typical application rates for diluted emulsion (1:1) range from 0.15 to 1.0 liter per square meter (0.03 to 0.22 gallon per square yard) depending on the surface conditions (Hicks and Holleran, 2002; Minnesota Department of Transportation, 2001). A 1:1 diluted emulsion is an original emulsion that has been subsequently diluted with equal part water.

Table 1-1. AEMA Recommendations for Application Rates (Hicks and Holleran, 2002).

% Original Emulsion	Dilution Rate	Tight Surface *		Open Surface **	
		(l/m^2)	(gal/yd^2)	(l/m^2)	(gal/yd^2)
50	1:1	0.15 – 0.5	0.03 – 0.11	0.4 – 1.0	0.09 – 0.22

** A tight surface is of low absorbance and relatively smooth (Asphalt Emulsion Manufacturer's Association, 1990).*
*** An open surface is relatively porous and absorbent with open voids (Asphalt Emulsion Manufacturer's Association, 1990).*

Ideally, one-half of the application should be sprayed in each direction to prevent buildup on one side of the stones only (this is particularly important in the case of chip seals and rough surfaces). Buildup on one side can result in a slippery surface and inadequate binder to fully enrich the surface or hold the stone (California Department of Transportation, 2003).

The application temperature normally depends upon the type of emulsion. In most cases, emulsions should be applied under relatively warm and dry conditions (Western Emulsion, 2002; Federal Aviation Administration, 1989).

Estimating Application Rates

To estimate the application rate, a 1 liter can of diluted emulsion (usually 1:1 dilution rate) is poured evenly over an area of 1 square meter. This represents a diluted application rate of 1 liter per square meter. The application rate is reduced if the emulsion is not absorbed into the surface after 2 to 3 minutes and repeated until the approximate application rate is found. If, after the first test, the surface looks like it can absorb more emulsion, the application rate of the emulsion is increased and tested over a new 1 square meter area. The process is repeated until the approximate application rate is found. This same procedure can be followed using gallons and square yards to determine application rate.

FOG SEAL EVALUATION METHODS

Pavement Evaluation

After a fog seal application, the treated surface condition and pavement performance may be evaluated as to the effectiveness of the applied fog seal/rejuvenator. This section discusses several methods for pavement evaluation.

Skid Resistance

Skid resistance is the force developed when a tire that is prevented from rotating slides along the pavement surface (Highway Research Board, 1972). Skid resistance is an important pavement evaluation parameter because:

- Inadequate skid resistance will lead to incidences of skid-related accidents.
- Most agencies need to provide a reasonably safe roadway to users.
- Skid resistance measurements can be used to evaluate various types of materials and construction practices.

Skid resistance changes over time. Typically it increases in the first two years of service as the asphalt binder is worn away by traffic, then decreases over the remaining pavement life as aggregates become more polished. Skid resistance typically is higher in the fall and winter and lower in the spring and summer, a seasonal variation that is quite significant and can severely skew skid resistance data if not properly compensated (Jayawickrama and Thomas, 1998).

Cracking

Pavement cracking is a type of distress that is generally caused by inadequate base support or brittle asphalt surface (Texas Department of Transportation, 2005). Since cracks allow surface water to enter the subgrade and further destroy the stability of the subgrade, sealing should be accomplished as soon as practical. When cracking has progressed to the extent that failure of the roadway surface is imminent, repairs should be made as soon as possible. Cracking observations should be done periodically to ensure that corrective or preventive maintenance is implemented at the appropriate time.

Pavement Surface Condition

An excessive amount of asphalt on the pavement would cause a slippery surface, which could lead to vehicle control difficulty especially in wet weather (California Department of Transportation, 2003). Also, fog seal material that is not properly cured will result in developing a soft asphalt binder film on the pavement surface, which can cause pavement deformation such as rutting. After the application of surface treatment, pavement examination is required periodically.

Aggregate Retention

Aggregate loss is one of the criteria used to evaluate the performance of a fog seal on chip seal applications. A convenient method to detect aggregate retention is to use visual examination, which can be subjective. Alternatively, for a more accurate representative method, photorecords were introduced. Rectangles, 12-inch by 9-inch, were painted on the pavement surface both in controlled and treated sections. Then close-up photographs were taken periodically to examine the individual stone lost with time (Estakhri and Agarwal, 1991). Also, surface texture may be determined using the sand-patch method (Texas State Department of Highways and Public Transportation, 1983).

Laboratory Evaluation

In addition to field evaluation, laboratory controlled tests need to be performed to examine the potential effectiveness of the treatment. Furthermore, any change in the property of core sample or asphalt binder due to fog seal/rejuvenating effect should be identified. Chapter 2 discusses the laboratory evaluation methods used in this project. The following tests are generally used methods for assessing mixture/binder properties.

Resilient Modulus

The indirect tension test for resilient modulus of asphalt mixture can be used for both laboratory-fabricated and field-recovered cores of asphalt mixtures. Mixture stiffness is measured in accordance with ASTM D 4123-82 to determine any improvement due to the rejuvenating process. For laboratory-aged samples, aging ratios can be calculated by dividing resilient moduli after aging by the corresponding values before aging.

Vialet Test

The Vialet test has been shown to be an indicator of chip seal aggregate retention (Stroup-Gardiner et al., 1990). Basically, loose hot mix is spread on a 7 by 7 inch steel plate with a 0.25-inch rim to prevent binder runoff. Then the sample is rolled with a hand-held rubber roller and left undisturbed at room temperature for 24 hours. After that, fog seal emulsion is applied and allowed to cure for 24 hours at 140 ^{o}F. The sample is then placed in a testing temperature for 2 hours prior to the testing. A steel ball with a diameter of 2 inches is dropped from a height of 18 inches above the sample. Percentage of material retained after impact is calculated.

Extraction/Recovery

In order to test the properties of asphalt binder from mixture cores, binder needs to be extracted and recovered from the whole mixture. Typical extraction method follows the standard procedure of ASTM D 2172. Asphalt binder is then recovered by using the Abson method, ASTM D 1856. For this specific study, successive extraction/recovery was used to determine the extent to which asphalt binder would be softened by penetrated rejuvenator (Noureldin and Wood, 1987). The penetration phenomenon was proposed and referred to as "Black Rock Model" (Carpenter and Wolosick, 1980).

Asphalt Binder Viscosity

The convenient and appropriate method to determine the softening effect of rejuvenator on asphalt binder is to measure the viscosity of the sample at 140 ^{o}F (Asphalt Institute, 1981). The two main types of viscometer are the tube and rotational instruments (Whorlow, 2005). Typically, the rotational type is more widely used because it is suitable for most applications and for non-Newtonian materials. The vast majority of rotational viscometers fall into two categories: those where two concentric cylinders rotate relative to one another around a common axis; and those consisting of a cone having a large vertex angle (approaching 180 degrees) and plate whose plane is through the apex of the cone. Many variations on this theme are possible, but in all types the test fluid is sheared between the rotating parts. Then the force exerted on the fluid can be used to calculate fluid viscosity.

Fourier Transform Infrared Spectroscopy (FT-IR)

FT-IR can be applied for the study of bitumen characterization. The analysis is able to identify functional groups present in bitumen due to its ability to measure infrared light absorbed by covalent bonds in molecules. Each functional group will result in a unique intensity and frequency of light absorbed. FT-IR has been applied to analyze functional groups in asphalt binder (Jemison et al., 1992) and diffusion of oxygen into bitumen (Jemison et al., 1992; Davison et al., 1994).

BINDER OXIDATION AND EMBRITTLEMENT IN SERVICE

Asphaltic binders experience oxidation and a consequent embrittlement over time that reduces the performance of flexible pavements. The process is relentless and thus, over enough time, can destroy the pavement. The constancy of the hardening rate over time and the depth to which oxidations occurs, based on recent pavement data, are surprising and at the same time critical to understanding and evaluating fog seal performance. These are elaborated on in the text that follows.

In previous research studies, spanning the last 15 years, we have gained considerable improvement in our understanding of the oxidation kinetics of asphalt materials and the resulting binder hardening. As binders oxidize, carbonyl (– C=O) compounds are formed, which increases the polarity of their host compounds and makes them much more likely to associate with other

polar compounds. As they form these associations, they create less soluble asphaltene materials, which behave like solid particles. This composition change, taken far enough, results in orders-of-magnitude increases in both the asphalt's viscous and elastic properties. The end result is a material that increases its stress greatly with deformation (high elastic stiffness) and simultaneously cannot relieve the stress by flow (high viscosity) leading to a pavement binder that is very brittle.

This embrittlement of binders has been captured with the discovery of a correlation between binder ductility (measured at 15 °C, 1 cm/min) and binder DSR properties (dynamic elastic shear modulus, G' and dynamic viscosity, η', equal to G"/ω), shown in Figure 1-2. A very good correlation exists between binder ductility and G'/(η'/G') (or, equivalently G'/(G"/ωG')), demonstrating the interplay between elastic stiffness and ability to flow in determining binder brittleness.

This correlation is depicted on a "map" of G' versus η'/G' (Figure 1-3) which tracks a pavement binder as it ages in service. This particular binder is from SH-21 between Bryan and Caldwell, but represents the trends that we have seen for all conventional binders. On this type of plot, a binder moves, over time, from the lower right toward the upper left, with increased aging as the result of increases in both the elastic stiffness and viscosity (but note that G' increases more than viscosity, i.e., G"/ω, because movement is toward the left, i.e., smaller values of η'/G'). Note also the dashed lines that represent lines of constant ductility, calculated from the correlation of Figure 1-2.

Recent evidence suggests that pavement binders age at surprisingly constant rates and to surprising depths. This conclusion is illustrated in Figure 1-3. This highway was constructed from July 1986 to July1988 in three, 2-inch lifts. The solid symbols (with the exception of the solid diamond) are binder measurements from cores taken from the third lift down from the surface of the pavement, as originally constructed. With each lift being 2 inches thick, this bottom lift had 4 inches of pavement on top of it. (Note: In 2000, this pavement had a chip seal and overlay paced on top of it, burying the original lifts even more.) Yet, even buried this deeply, we see its binder moving across the DSR "map" in a relentless fashion and at about the same pace as the top lift (open symbols). Binder from the 1989 bottom core has an estimated ductility of 20 cm at 15 °C. By 1996, it is reduced by aging to 5.6 cm, and by 2002, it is less than 5 cm. Meanwhile, the top lift binder's ductility was estimated to be 16 cm in 1989, 4.5 cm in 1996, and about 4 cm in 2002. The march across the DSR map was not that different for the top lift, compared to the bottom lift. Binder from the middle lift, taken in 1989 and 1992, is also shown and tracks well with the other lifts. Note that the RTFOT plus PAV laboratory-aged binder matches the 1992 pavement-aged binder, suggesting that for this pavement, RTFOT plus PAV is approximately equivalent to hot-mix and construction aging, plus four years of pavement aging.

These results are rather remarkable and strongly suggest, as noted above, that oxidative aging rates are remarkably constant over time and, beyond the very top portion of the pavement, proceed at remarkably uniform rates, at least to several inches below the surface of the pavement. Figures 1-4 and 1-5 make the rate comparison more directly in terms of viscosity and

the DSR function G'/(η'/G'). While there may be some slowing of the rate after a few years, it is clear that aging does not stop.

It should be noted that the literature reports that ductility values in the range of 2 to 3 cm for 15 °C at 1 cm/min appears to correspond to a critical level for age-related cracking. Thus, the top-left corner of the pavement aging figure is a suspect region for pavement performance. While this region has not yet been verified conclusively to be a critical zone, with recent pavement data, the results (from 0-1872, including several LTPP pavements) are consistent with this early conclusion.

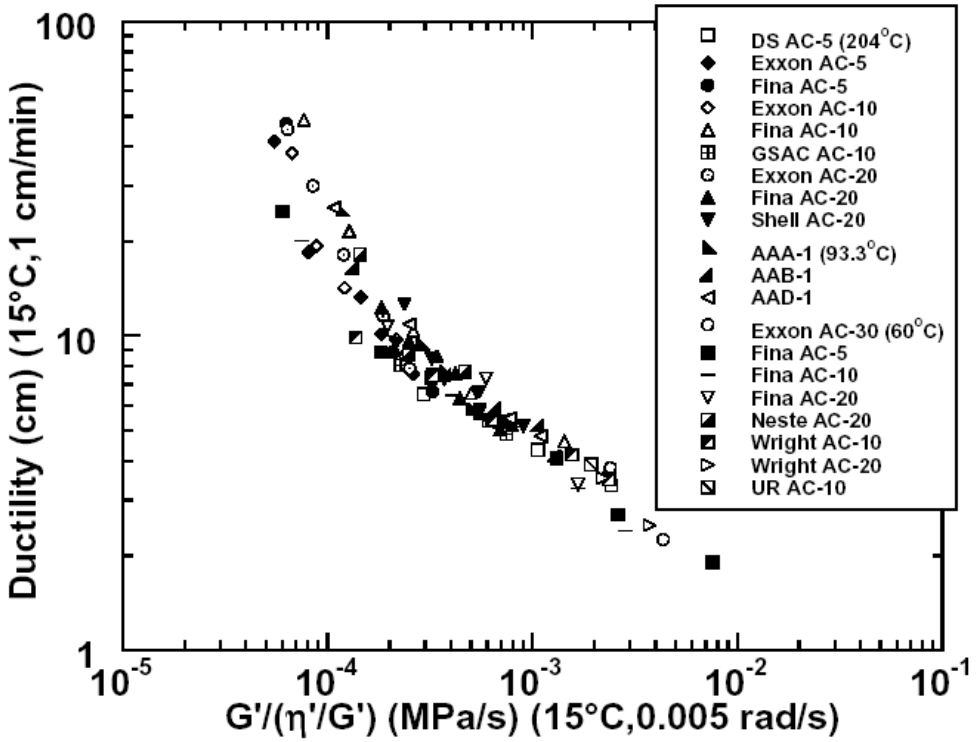

Figure 1-2. Correlation of Aged-Binder Ductility with the DSR Function G'/(η'/G').

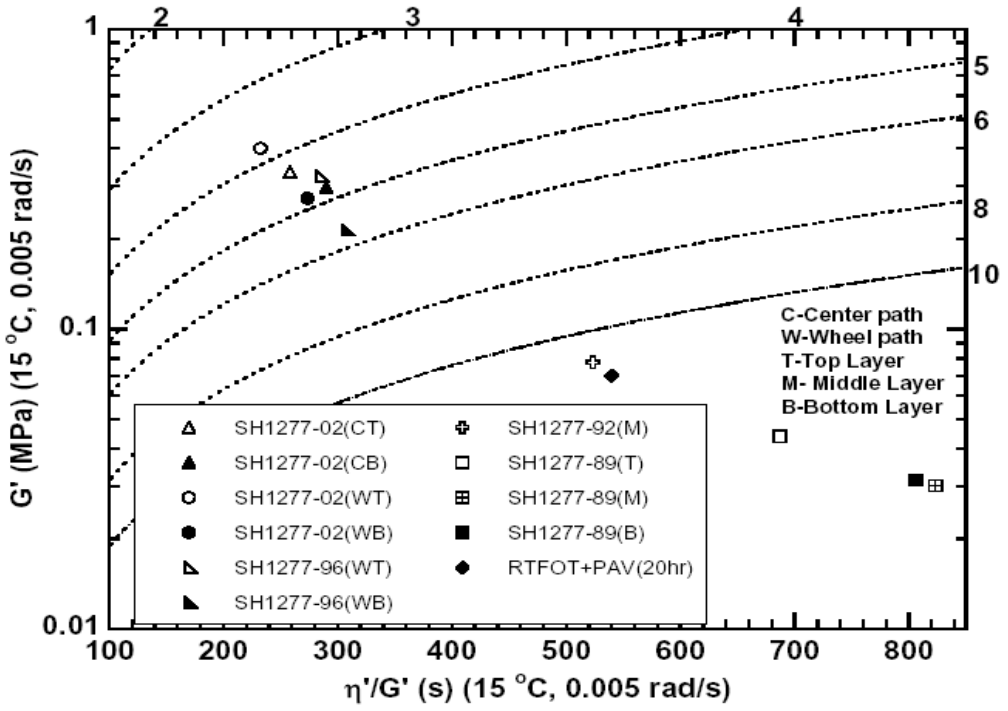

Figure 1-3. Binder Aging Path on a G' Versus η'/G' Map (Pavement-aged Binders).

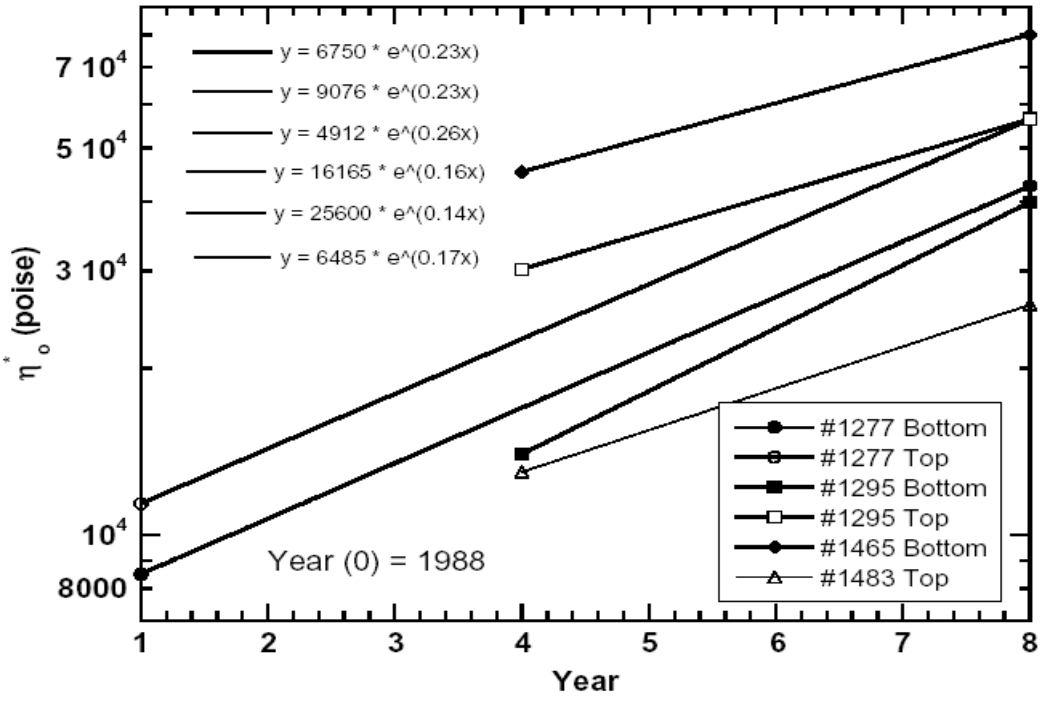

Figure 1-4. Binder Hardening with Oxidation.
The Bottom Lift Is under 4 Inches of Pavement.

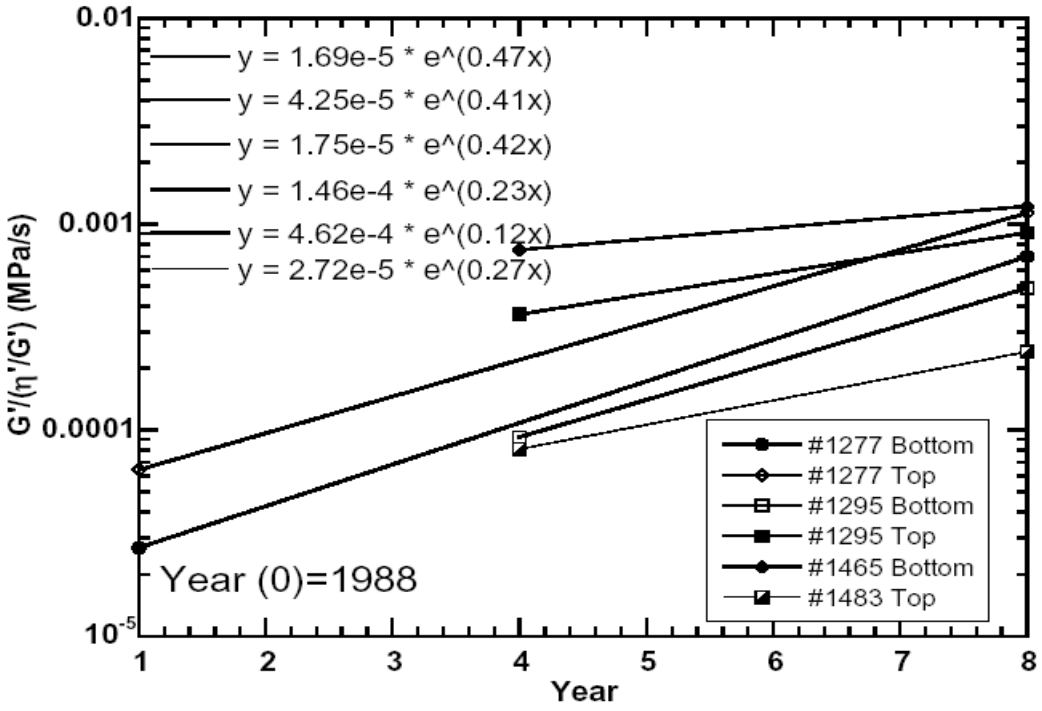

Figure 1-5. Binder Hardening in Terms of the DSR Function G'/(η'/G').

EVIDENCE OF PAVEMENT REJUVENATION AFTER TREATMENT

As pavements are exposed to the environment, they begin to age. The aging, caused by oxidation of the asphalt binder and breakdown of the constitutive materials by ultraviolet rays, takes the form of raveling (Figure 1-6) and cracking as the binder becomes stiffer (especially block cracking, Figure 1-7). The application of a rejuvenating seal (Figure 1-8) is considered to provide significant cosmetic, and perhaps performance, benefits.

Fog seals and seals with a rejuvenating agent have been used for many years to reverse the effects of oxidation and aging of asphalt pavements, reduce the rate of oxidative aging by sealing small cracks and microcracks in the surface, and to hold aggregate on the surface of a seal coat that is shelling or raveling. Additional benefits include a better edge delineation and reduction of weed growth and raveling when placed along the edge of pavement and an increase in contrast and visibility for the fog stripe.

While the typical G' versus η'/G' path for an aging binder is toward the upper left corner, relentlessly moving to a lower ductility, a preponderance of recent field data suggests that hot-applied seal coats can help reverse this movement. Figure 1-9 shows the binder from one station of SH-21. From 1992 to 1996, the binder moved in the direction expected. However, from 1996 to 2002, after a chipseal and overlay were placed in 2000, the binder moved significantly in the opposite direction. Note that the lift tested was the bottom lift that had 4 inches of pavement over it. Figure 1-10 shows G'/(η'/G') versus aging time for other stations, and the significantly

different aging rate after 1996 is evident. Figure 1-11 shows results for all seven LTPP sites for which cores were available in two years (1989 or 1990 and 2002). (Note that different binders were used at the different locations so that the binders don't form a single track across the plot.) In each case where there was no sealant applied between core samples, the binder moved as expected, toward the upper left corner (48-2108 and 48-6086), or did not progress at all (48-3769). However, when a sealant was applied in the interim, the path was retrograde (48-1046, 48-1056, 48-2133, and 48-9005). Note also that 48-3769, which seemed to be protected against aging, was treated with a seal containing rubber. Finally, Figure 1-12 shows calculated ductility values (based on the correlation shown in Figure 1-2 and measured DSR properties) versus years of service. The solid symbols are binders that have had no sealant treatments; open symbols are binders that have been previously treated with sealants.

From the above data, it is unknown whether hot sealants or fog sealants penetrate the pores of an asphalt pavement better. On one hand, the hot sealant asphalt has a much lower viscosity, perhaps allowing it to penetrate easier. On the other hand, the binder in the fog seal (emulsion) materials exists as very fine droplets (less than 10 microns in diameter and may be drawn down into the pavement by the water carrier. In most instances, field data haven't specified whether fog seals or hot sealants were applied.

Figure 1-6. Unsealed, Aged Pavement.

Figure 1-7. Block Cracked Pavement.

Figure 1-8. Sealed Aged Pavement.

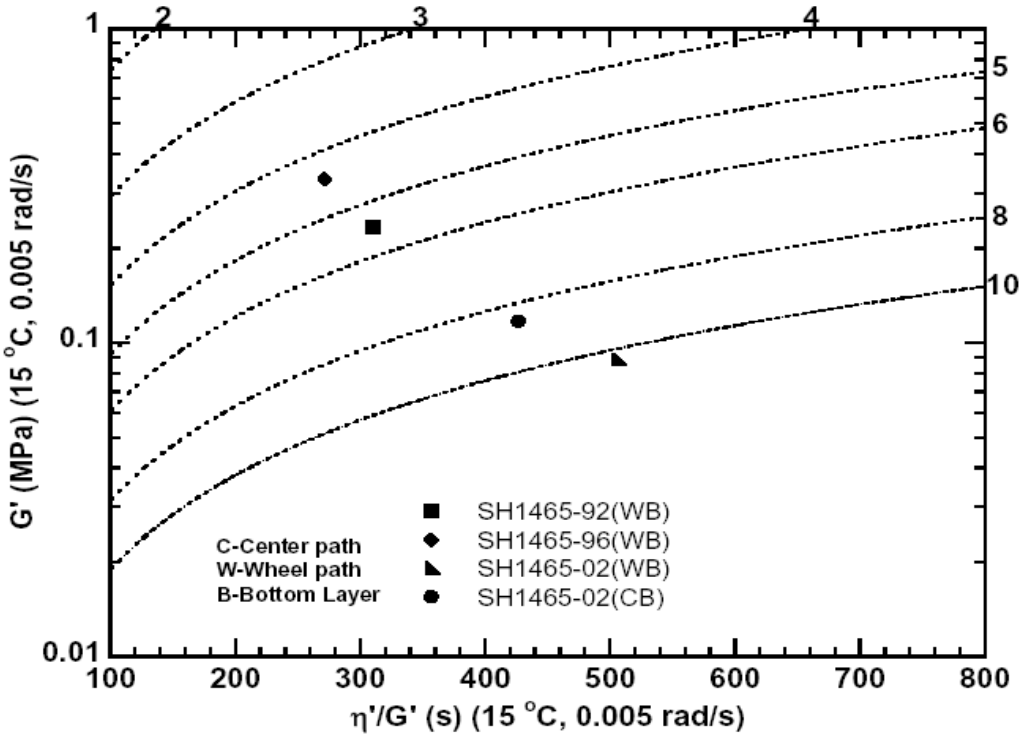

Figure 1-9. Reversal of Binder Properties after Sealant.

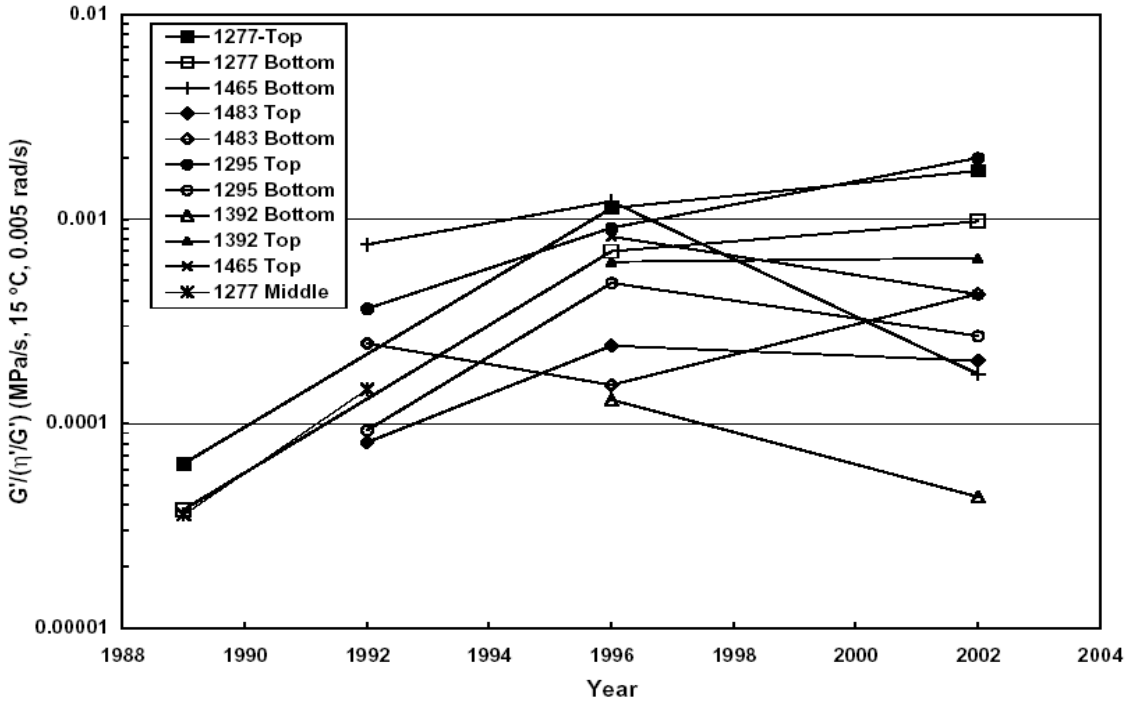

Figure 1-10. DSR Function Properties after the 2000 Sealant.

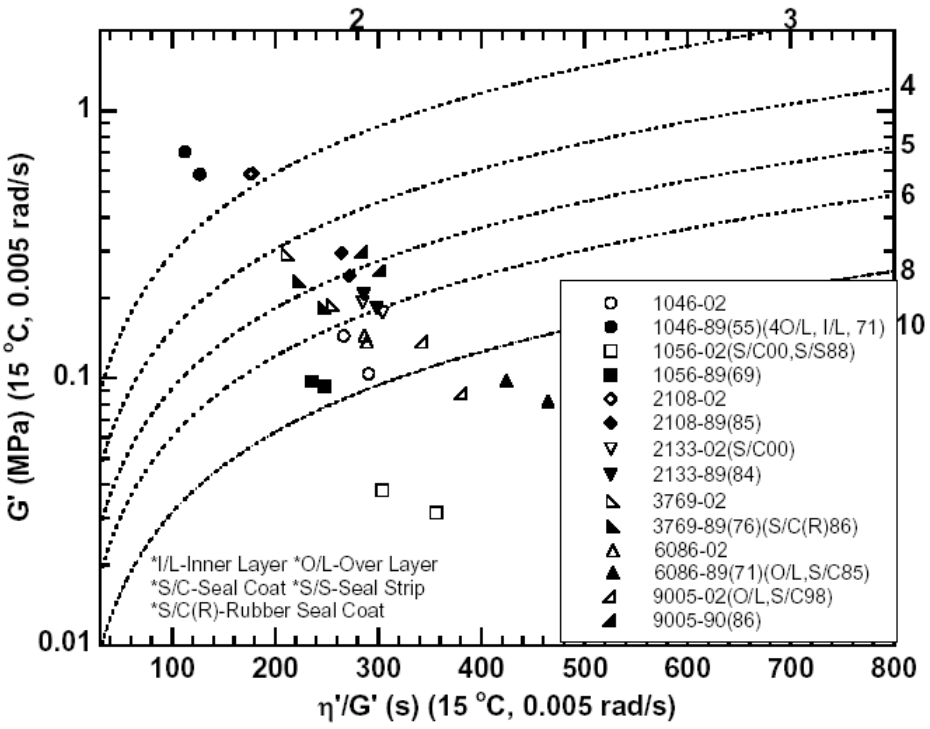

Figure 1-11. LTPP Pavement Binder Property Comparisons from Cores 12 Years Apart.

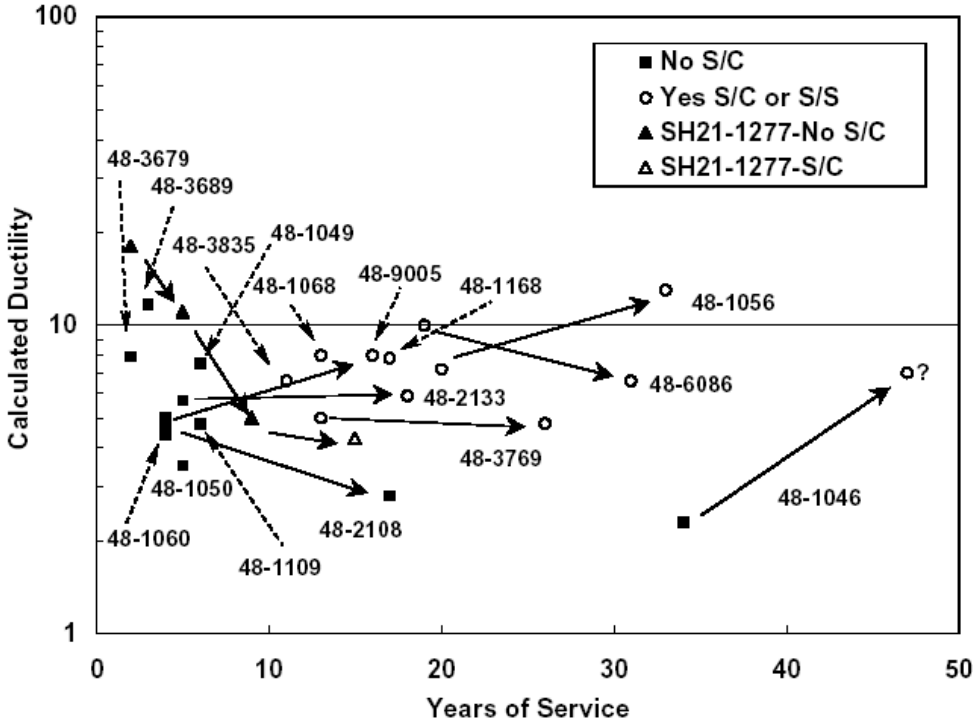

Figure 1-12. Estimated Ductility Changes to Pavement Binders over Years of Service.

In spite of these data, it should be noted that evidence to date is not sufficient to prove that sealants actually rejuvenate in-place binders. Even if the rejuvenating binder penetrates into the pavement, it will not rejuvenate unless it is absorbed into, and thereby softens, the aged binder. Work is needed to address this critical issue.

FOG SEAL USED IN TEXAS

Early versions of fog and rejuvenator seals often caused problems with skid resistance, and their use on roadways was reduced or abandoned due to these problems. Different formulations and innovations in the application of low flow rate distributors have solved many of these problems. On airfield pavements, where skid resistance was less of a problem and aging was more of a problem, they continued to be used. Airfield pavements, especially low-volume general aviation airports, were able to function with lower skid resistance pavements because traffic volumes and speeds are lower, there is little high-speed turning, very little panic braking, and there is much less usage during rainy or wet weather. Likewise, lower volume pavements in the drier areas of Texas are always good candidates, and fog seals continue to be used.

Fog seals, even without a rejuvenating additive, are thought to cause some softening of the binder and to seal the surface. Part of this research was conducted to assess these presumed benefits and to determine whether a fog seal alone can provide the needed benefits at a lower cost.

Some districts have used these seals along the edges of 2-lane roads with no shoulders. On these roads, the outside 1 foot or so (free edge) does not become as compacted as the rest of the pavement and may have higher air voids and permeability. These open areas in the pavement generally exhibit more raveling and allow weed seeds and grasses to take root, which further damages the edge. Eventually, these areas break down and the pavement becomes narrower. A fog seal, typically without any additives, seals these areas and eliminates the problem for a few years. Personal and anecdotal evidence from district personnel verify that these seals are effective in reducing edge problems.

Likewise, fog seals have been used to correct and stop the shelling of seal coat aggregate. The pavement in Figure 1-13 is an aged pavement that is shelling, but the effect on a new pavement is much the same. Loose aggregate is whipped off by passing traffic and becomes a hazard. In these cases, a fog seal is believed capable of holding the rock to the pavement.

Figure 1-13. Aged Pavement with Raveling.

FOG SEAL QUESTIONNAIRE

As part of this project, researchers contacted various districts, divisions, and people outside of TxDOT to determine the general use, suggestions, and cautions that people had about using fog seals and rejuvenators. The results of the questionnaire are included here. Although multiple calls were made (sometimes as many as 5 to 7), not everyone responded, but 30 responses were received. The hurricane experience of the last few years made it difficult to receive responses from some gulf coast districts and states. Appendix A contains the results of the questionnaire.

The questions and a summary of the responses are as follows.

Do you use fog seals or rejuvenators? Table A-1.

Fog seals are used widely throughout TxDOT. In general, the districts that did not use fog seals or rejuvenators were in southeast Texas, where rainfall totals are high. Eighteen districts said they used fog seals, while six said they did not use fog seals or rejuvenators. Six districts use both fog seals and rejuvenators. The Aviation Division primarily uses rejuvenators.

How much do you use? Table A-2.

The six districts that used both treatments tend to use a lot of fog, but much less rejuvenator. Only one district used rejuvenator extensively. Eleven districts had tried rejuvenators, at least as an experiment. The Aviation Division primarily uses rejuvenators extensively.

Do you use more or less than you used to? Table A-3.

The general trend was weak, but there was a slight tendency to use more fog seals and less rejuvenator, except for the Aviation Division.

Why not? (Why are you not using them extensively?) Table A-4.

The primary reason for not using the treatments from the districts that used them was the worry about skid resistance. The districts that did not use them either had never used them or did not think that the treatments provide any benefit.

What type fog seal do you use and at what rate? Table A-5.

For use on either Hot-Mix Asphalt Concrete (HMAC) or seal coat pavements, the responses were nearly evenly split between SS-1h, CRS or CSS, and MS, with a residual asphalt content of approximately 0.06gal/sy.

What type rejuvenator do you use and at what rate? Table A-6.

Most districts responded that when they use a rejuvenator, they used the PASS emulsion for both HMAC and seal coat pavements.

How do you determine application rate? Table A-7.

Most of the districts use the experience of the maintenance supervisor or crew to determine the appropriate application rate. A few used trial applications or manufacturer recommendations, especially for rejuvenators. Most of the districts report the cost of a treatment to be less than $0.10/sy.

What are you trying to correct? Table A-8.

Most responses indicated that the treatment was placed to correct a shelling seal coat, seal the pavement, and stop the loss of fines. Fewer districts thought that the treatments would rejuvenate the pavement or provide some preventive effect. Fog seals are used on patches before applying a seal coat.

When do you NOT use them? Table A-9.

In general, the most common response was that the treatments were not used in high traffic, urban areas. Rutted pavements and open graded friction courses were also mentioned.

What surface preparation do you do beforehand? Table A-9.

Almost all respondents swept the pavement as their only preparation.

How log do you wait before opening to traffic? Table A-10.

Most districts open the pavement to traffic within an hour, with 30 minutes being the most common number. The rest of the districts say that either the time varied, depending on weather conditions, or that the time was close to three hours. Climatic region does not appear to be a factor in opening time as there were districts in dry areas that waited longer and districts in wet areas that had a short delay. Most districts determine when to open the pavement to traffic by a visual inspection, but many others add touching and driving the project to the decision process.

Do you have any suggestions for application? Table A-11.

Almost all responses were that the application should err on the low side and that it is much easier to add some additional material than it is to deal with an overshot. The most common problem encountered was that the material would end up tracking onto cars with reduced skid resistance.

SUMMARY

Fog seal and rejuvenating sealants potentially have the ability to reduce and reverse the effects of oxidative aging of asphalts in pavements. Additionally, they may reduce shelling and raveling and cosmetically improve the appearance of the pavement surface. Whether and to what degree these potential benefits are actually achieved is uncertain. This project was designed to evaluate these questions of fog seal effectiveness.

Performance characteristics for evaluating fog seal treatments include skid resistance; cracking; pavement surface condition and aggregate retention; water permeability; air voids; and recovered binder rheology and oxidation.

In this project, several test methods were used to determine the effectiveness of fog seal treatments on asphalt pavements. Penetration of fog seal material was evaluated by the use of Size Exclusion Chromatography (SEC), while binder rejuvenation and aging improvement was evaluated by rheological and chemical property measurements.

Chapter 2 presents basic information on the sites and fog seal materials that were used in the various pavements. Additionally, the experimental methodologies that were used in this project are presented.

Chapter 3 addresses the extent to which fog seal materials penetrate into and through the pavement, as indicated by Size Exclusion Chromatography (SEC) analysis of recovered binders. In addition, the effectiveness of fog seals as sealants, as indicated by water permeability, is discussed.

Chapter 4 addresses the possiblity that fog seal treatments affect the oxidative aging of asphalt binders in pavements. The degree of oxidative aging, layer-by-layer, of untreated and treated cores is compared using the FT-IR carbonyl area and the rheological DSR function as indicators.

Chapter 5 is a brief chapter that compares layer-by-layer binder properties to total air voids and accessible or interconnected air voids in particular and also to binder content.

Chapter 6 summarizes the objectives, work, and conclusions of this project.

CHAPTER 2

SITE SELECTION AND TEST METHOD

SITE SELECTION

Experiment Design

The original experiment design plan called for 16 sites in a matrix based on climate, surface type (AC or seal coat), and type, or classification, of seal. Researchers solicited test sites during the questionnaire phase of the project when calls were made to the districts. While special care was given to selecting test sections that would fit in the experiment design, only treatments actually being built could be included. Field or other last minute changes caused two sections to be dropped after initial coring and several other sections were moved from one cell to another. The final list of test sections includes these variables and the age of the pavement. Table 2-1 lists the final layout of 20 sites.

Table 2-1. Final Layout of Test Sections.

Age of Pavement	Highway			Airport
	Climate	Fog Seal	Rejuvenator	
0 – 2	Wet			Jacksonville
	Dry		FtW FM4 03 COS-50	
2 – 5	Wet	Atl IH20 CMHB Atl IH20 Dense Graded Atl IH20 Superpave	Atl US 67 PASS Tyl US 79 PASS	
	Dry		FtW FM4 00 COS-50	
> 5 yrs	Wet		Luf BUS 59	Carrizo Springs Georgetown-89 Georgetown-95 Georgetown-95* Pleasanton
	Dry	AB SH 36 R1 MS2 AB SH 36 L2 MS2 Ode SH 191 Ode SH 349	AB SH 36 R1 PASS AB SH 36 L2 PASS	

Where

XX YY ZZ XY = District Highway Lane Treatment

SH – State Highway IH – Interstate Highway

BUS – Business Route US – United States Highway.

R1 – Southbound Outside Lane L1 – Southbound Inside Lane

R2 – Northbound Outside Lane L2 – Northbound Inside Lane

The sites in Abilene (AB SH 36 R1 MS2, L2 MS2, R1 Pass, and L2 PASS), Atlanta (Atl IH20 CMHB, Dense Graded, and Superpave), and Fort Worth (FtW FM4 03 COS-50 and 00

COS-50) were all experimental sites placed by the districts for the purpose of evaluating fog seals and rejuvenators. Rejuvenators, specifically coal tar rejuvenators, are used quite often on airfield pavements. There was no problem in selecting airfield pavements for that part of the experiment. Many more sites could have been chosen, but these sites represented an interesting mix of recently sealed pavements (Jacksonville, Carrizo Springs, and Pleasanton) and pavements where the seal had been placed five years earlier (Georgetown).

CORING PLAN

The research team took cores from each site to provide material to support the testing plan. They determined three cores per site to be sufficient to provide the replicate samples for physical testing and to provide the raw material needed for extraction and asphalt testing. During the first year, coring locations for roadway sections were established that would provide one core from the inside edge of the wheelpath, one from the wheelpath, and one from the outside edge of the wheelpath. Figure 2-1 illustrates this layout and the coring rig used during that first round of coring. The thought process was that selecting the cores from the traveled area (wheelpath) and from the less traveled areas (inside and outside of the wheelpath), would provide a range of in-place densities and air voids, which would result in different permeabilities and absorption of the fog seal or rejuvenator treatment. Figure 2-2 illustrates that this approach was somewhat effective, however there was concern that to be as accurate as possible a better method was needed to ensure that the treated and untreated locations were as similar as possible in air voids permeability, and aging.

NEED FOR PQI TESTING

The testing procedure established for the first round of testing resulted in three cores being taken on the untreated section and three cores being taken on the treated section. Two of the untreated cores and two of the treated cores per site were tested using the Asphalt Pavement Analyzer (APA), which runs a load at elevated temperature over the core. Because this testing damages the core, these cores could not be used to determine air voids. The results of the first round of testing identified an unexpected anomaly in the testing where a majority of the sites had lower air voids for the untreated cores than for the treated cores. Air voids and permeability were expected to have an enormous impact on the penetration of the treatment and thus may have presented a problem. The values may represent the unfortunate differences and variability in an HMAC pavement or they may be real, actual differences in the effect of fog seals and rejuvenators on the air voids in each core.

For the second round of testing, special measures are being taken to ensure that the density of the treated and untreated cores is as close as possible.

Reducing Density Variability in HMAC Pavement

Some measure was needed to try to match up the density of the untreated and treated cores. The test method chosen was the Pavement Quality Indicator (PQI). The PQI was developed as part of the Strategic Highway Research Program (SHRP) Innovations Deserving Exploratory Analysis (IDEA) project to develop a “rapid, non-intrusive, nondestructive, and non-radioactive technique” for measuring asphalt pavement density. Figures 2-3 and 2-4 list pictures and schematics of the device.

Figure 2-1. Layout of Coring Plan and Coring Rig.

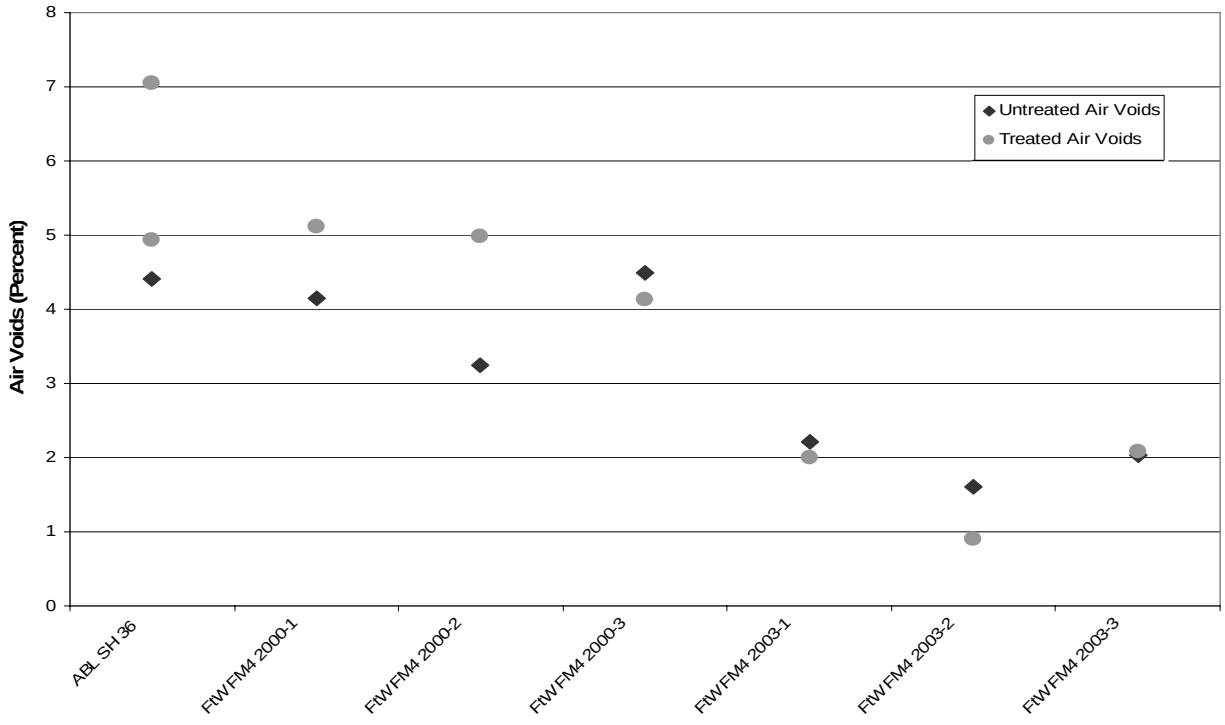

Figure 2-2. Air Voids from Year One Roadway Pavements.

Figure 2-3. Photograph of PQI Instrument.

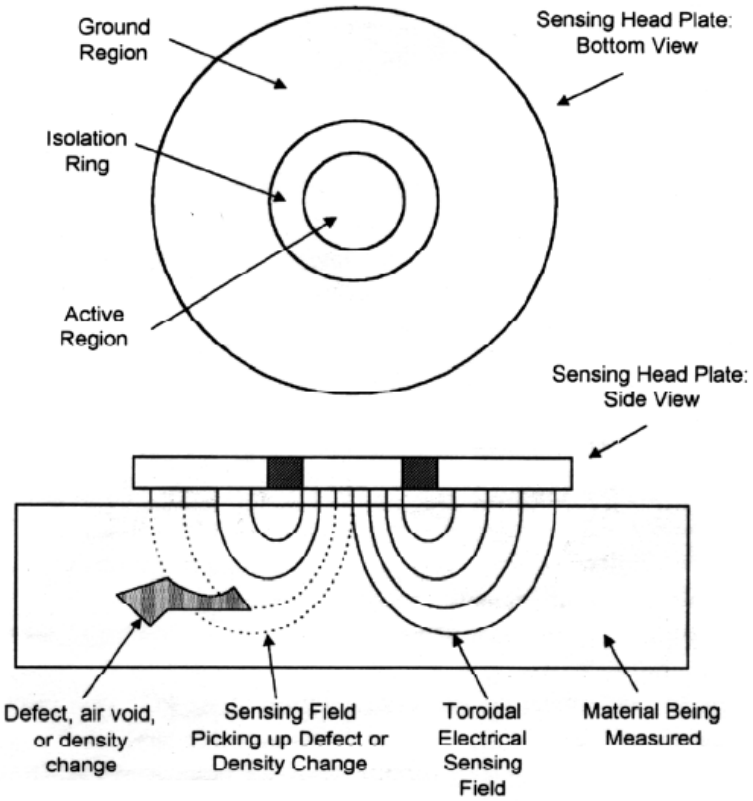

Figure 2-4. Schematic of PQI Instrument.

REVISED CORING PLAN

The implementation of the revised coring plan resulted in at least five areas being identified for the treated and untreated areas, PQI testing performed, results compared, and treated and untreated cores with high, middle, and low readings being selected. Occasionally, a second set of five areas were tested to obtain areas that were sufficiently close. Figure 2-5 illustrates the layout of the five areas. This layout was made possible by the new coring rig purchased by TTI that allows for easy movement of the coring head.

Appendix C contains the results of the PQI testing. Appendix D, which contains the results of the air void testing, illustrates that with the PQI researchers were able to obtain cores in treated and untreated areas that were very similar.

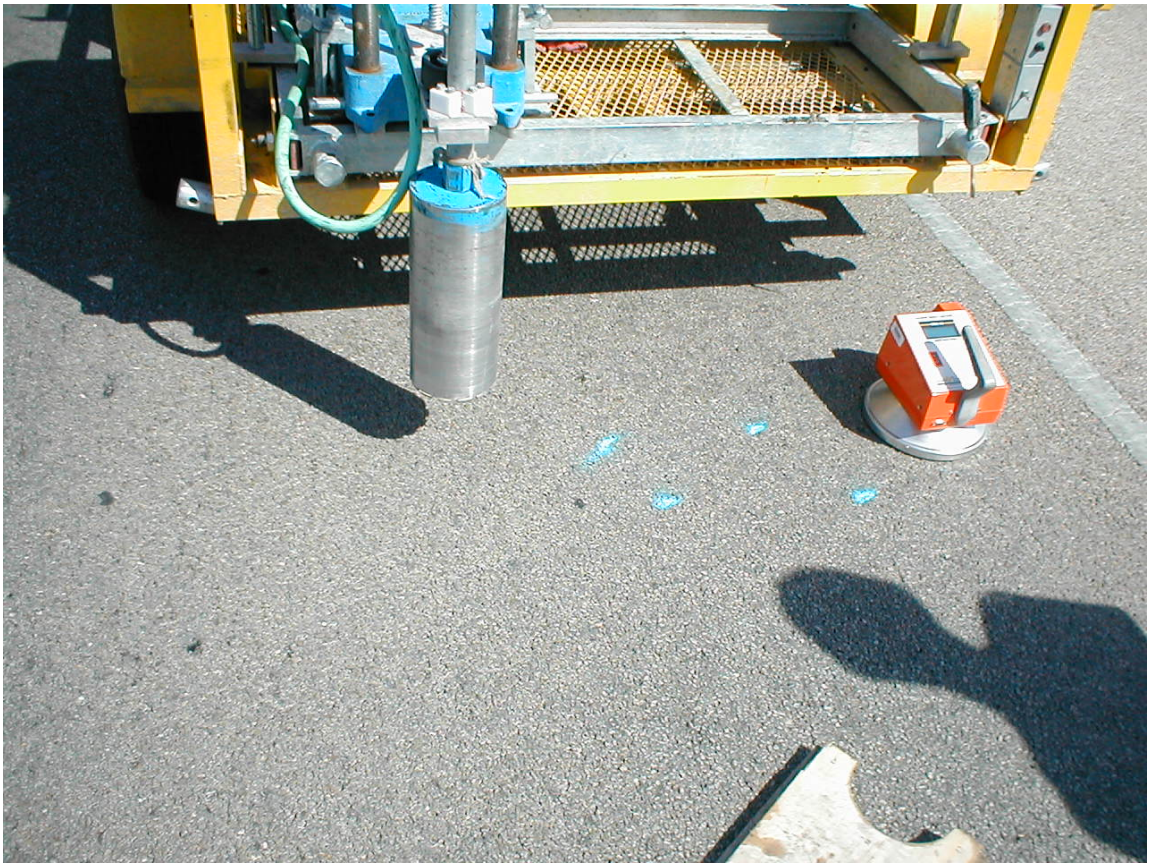

Figure 2-5. Revised Layout of Coring Plan and New Coring Rig.

ORIGINAL TEST METHOD

The original sample preparation and test procedures are as shown in Figure 2-6. Three core samples (replicates) were received from each site. At first, core samples were trimmed and the top approximately 3 inches of samples was tested for water permeability. After that, the cores were tested with APA (Asphalt Pavement Analyzer). However, the first and second replicates, which were exposed to the APA test, could not be used to determine the air voids content due to the compression of the wheel from the APA test. Therefore, the third replicate was arranged to

pass through the process without experiencing the APA environment for more accurate air voids measurement. In the original plan, air voids measurements were conducted on only the third replicate. This third replicate was sliced into ¼-inch disks for further testing. Due to the cutting blade thickness, the real thicknesses of slice samples need to be estimated. Appendix D shows the estimated slice thicknesses and estimated core depths. Then, the binder from each slice was extracted and recovered for further testing. The extracted binders' properties were measured using the DSR, SEC, and FT-IR methods, which are discussed later in this chapter.

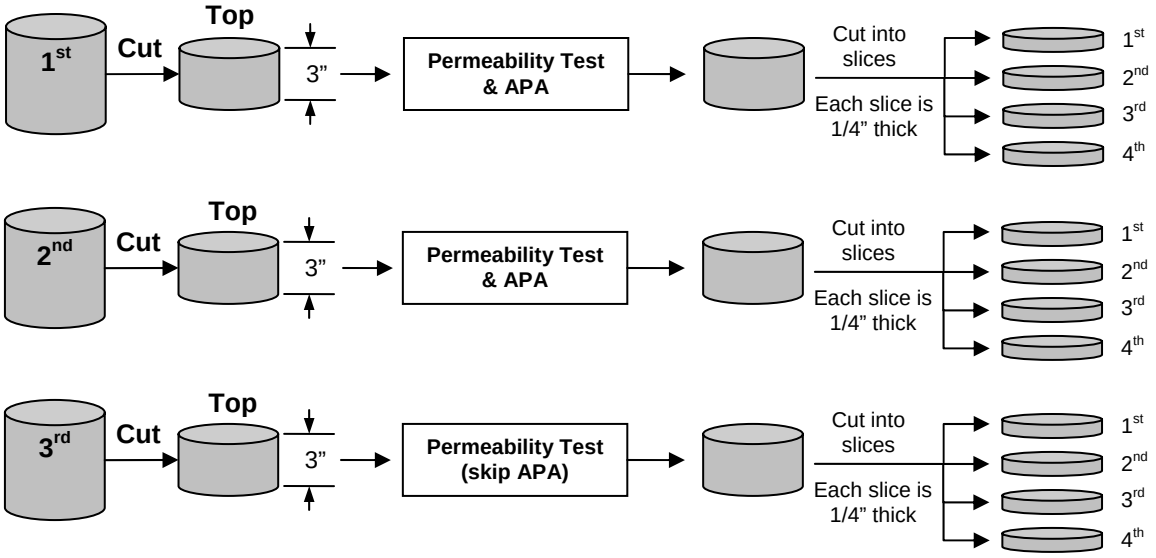

a. Cores Preparation

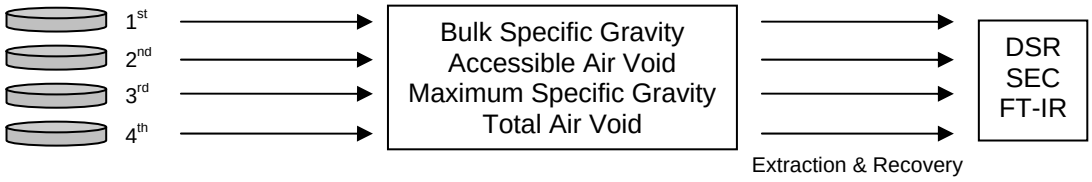

Remarks

DSR: Dynamic Shear Rheometer
SEC: Size Exclusion Chromatography
FT-IR: Fourier Transform Infrared Spectroscopy

b. Physical/Chemical Properties Measurements

Figure 2-6. Test Plan Diagram

REVISED TEST METHOD

In the second year, the APA testing was discontinued, and all cores were then available for permeability testing, slicing, air voids determination, and extraction. Figure 2-7 shows a core being prepared for slicing, and Figure 2-8 shows a set of slices being dried prior to further testing.

Test Method for Core Samples

Constant Head Permeability Test

Once the core samples were received, they were cut to 3 inch lengths, and the permeability of each core was tested in the constant head permeability apparatus (Figure 2-9). In the constant head permeability test, the trimmed core is placed under a pressurized column of water to measure the time it takes for the column of water to drop a specified distance. The water permeability for each sample is then calculated. After the permeability test, the samples were dried prior to conducting additional tests. If the seal treatment seals the surface and reduces the permeability, this test will demonstrate that fact and determine the quantity of reduction. Appendix C contains the data for the permeability testing. Statistical analysis is performed in Chapter 3. A visual review of the data in Appendix C shows that there is no obvious trend, but it does appear that for sites that were permeable, the treatments reduced permeability more often than an increase in permeability, indicating that the treatments were somewhat effective. Sites that were not permeable showed no impact, except that all the Atlanta sites showed increases in permeability. No reason is known for this increase.

Asphalt Pavement Analyzer

The APA test uses a pressurized hose in a heated chamber (Figure 2-10) to simulate somewhat severe wheel loadings. The number of repetitions required to produce a specified rut depth are recorded. The purpose of this test was to verify that the pavements were still strong. If the rejuvenator softened the asphalt binder too much, the pavement would become weaker and prone to rutting. This deficiency would be identified by early rutting in the treated samples. If the rejuvenator penetrated the asphalt binder, but merely filled voids in the binder without interacting, the rut characteristics would not change. Since the APA test was omitted for the second year cores, there were only the APA results of the first year cores (Appendix E). In most cases, the treated pavement had slightly higher rutting at the end of the cycle, but the difference was less than 0.03 inches (0.75 mm). In several cases, the untreated cores had slightly more rutting.

Because there was no clear trend in the APA results, and because the cores originally scheduled to be tested in the APA equipment could be used for additional air void and extraction testing, the APA testing was discontinued and those cores were sliced and tested as described below.

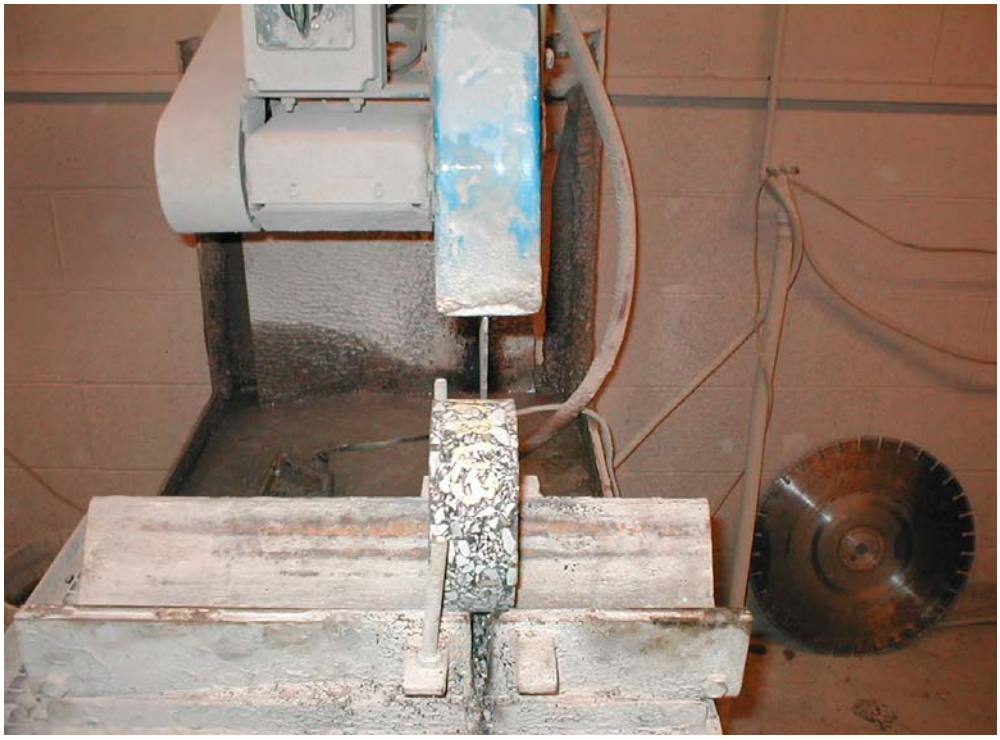

Figure 2-7. Slicing Cores for Further Testing.

Figure 2-8. Core Slices Being Dried.

Figure 2-9. Constant Head Permeability Apparatus.

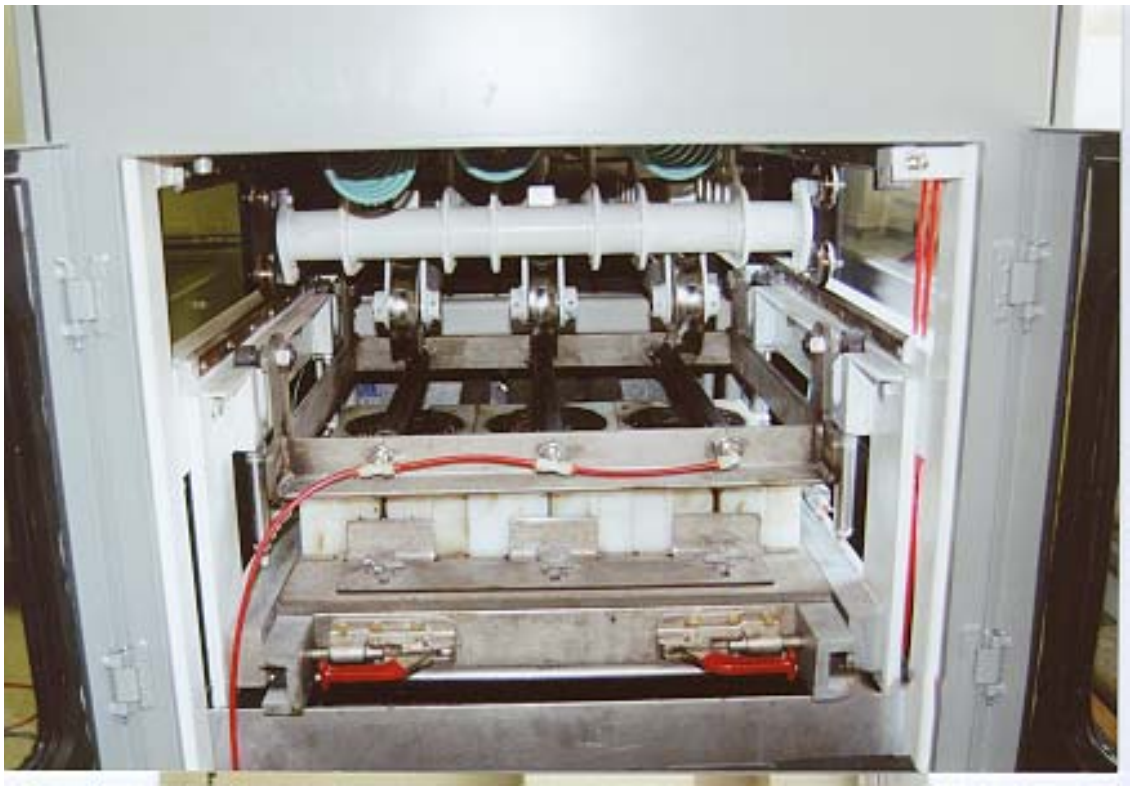

Figure 2-10. APA Test Setup.

Air Voids Measurement

A number of properties of intact pavement cores are of interest. These include the bulk and maximum specific gravities and the total and accessible air voids content. These properties are determined by a number of weight measurements including the weight of the dry core in air, the weight of the saturated core underwater, and the weight of the dry core underwater. Two methods were used to determine these weights, a saturated surface-dry method (SSD, ASTM D 2041-91) and the Corelok method (ASTM D 6752-03, ASTM 6857-03). The SSD method uses measurements of the unsealed core while the core lock method uses underwater measurements of the evacuated core sealed in a plastic bag.

The measurements and the calculations for the two methods are given by the following equations and notation:

$$\text{Bulk Specific Gravity} = \frac{DA}{SaA - SaW} \quad \text{(SSD method)} \tag{2-1}$$

$$\text{Accessible Air Void} = \frac{SaA - DA}{SaA - SaW} \quad \text{(SSD method)} \tag{2-2}$$

$$\text{Bulk Specific Gravity} = \frac{DA}{SeA - SeW} \quad \text{(Corelok method)} \tag{2-3}$$

$$\text{Accessible Air Void} = \frac{SeA - SeW - \frac{BA}{B_{sg}} - (DA - SaW)}{SeA - SeW - \frac{BA}{B_{sg}}} \quad \text{(Corelok method)} \tag{2-4}$$

$$\text{Maximum Specific Gravity} = \frac{DA}{SeA - (SaW + BW) - \frac{BA}{B_{sg}}} \tag{2-5}$$

$$\text{Total Air Void} = 1 - \frac{\text{Bulk Specific Gravity}}{\text{Maximum Specific Gravity}} \tag{2-6}$$

where

DA = Dry sample weight in Air (g)
BA = Bag weight in Air (g)
BW = Bag weight in Water (g)
B_{sg} = Bag Specific Gravity
SaA = Saturated sample weight in Air (g)
SaW = Saturated sample weight in Water (g)
SeA = Sealed sample weight in Air (g)
SeW = Sealed sample weight in Water (g)

Each of these methods of determining air voids has inherent measurement errors, and taken together, the two provide a useful check on the one hand, and their comparisons provide an indication of the types of errors, on the other. For example, the SSD method is subject to greater error for more open, porous mixtures. This is because the SSD method relies on being able to obtain a weight of the saturated core that still contains all of the water inside the pores of the core. However, if the mixture is open enough, the water will tend to drain out, giving a lower saturated weight and also, higher air voids. On the other hand, the core lock method will give higher air voids if the surface of the core has a lot of texture to it because the bag cannot collapse around this texture completely and therefore, this texture appears as air voids in the pavement.

Extraction and Recovery

For extraction process, a solution of 15 percent by volume of ethanol in Toluene was used to extract the asphalt binder from each sliced core. Before extraction, each core was broken into small pieces to increase contact surface with solvent. After the crushed core was washed with the solvent mixture for 20 minutes, the asphalt solution was separated from aggregate using filtration and centrifugation. This step was repeated until there was practically no asphalt remaining in the aggregate. All of the asphalt solutions from each wash were combined into one solution, and then passed to the recovery process.

In the recovery process, a Brinkman ROTOVAP apparatus was used to evaporate all solvent from the asphalt. Asphalt solution was put into the evaporator for about 80 minutes under vacuum and with a nitrogen purge to assist solvent removal. The recovered asphalt binder was then subjected to further chemical and physical analyses. Figure 2-11 shows the extraction/recovery process.

Also from Figure 2-11, the binder content for each slice is calculated as the combined weight of asphalt binder from the recovery can, the filter, and the side of rotovap column.

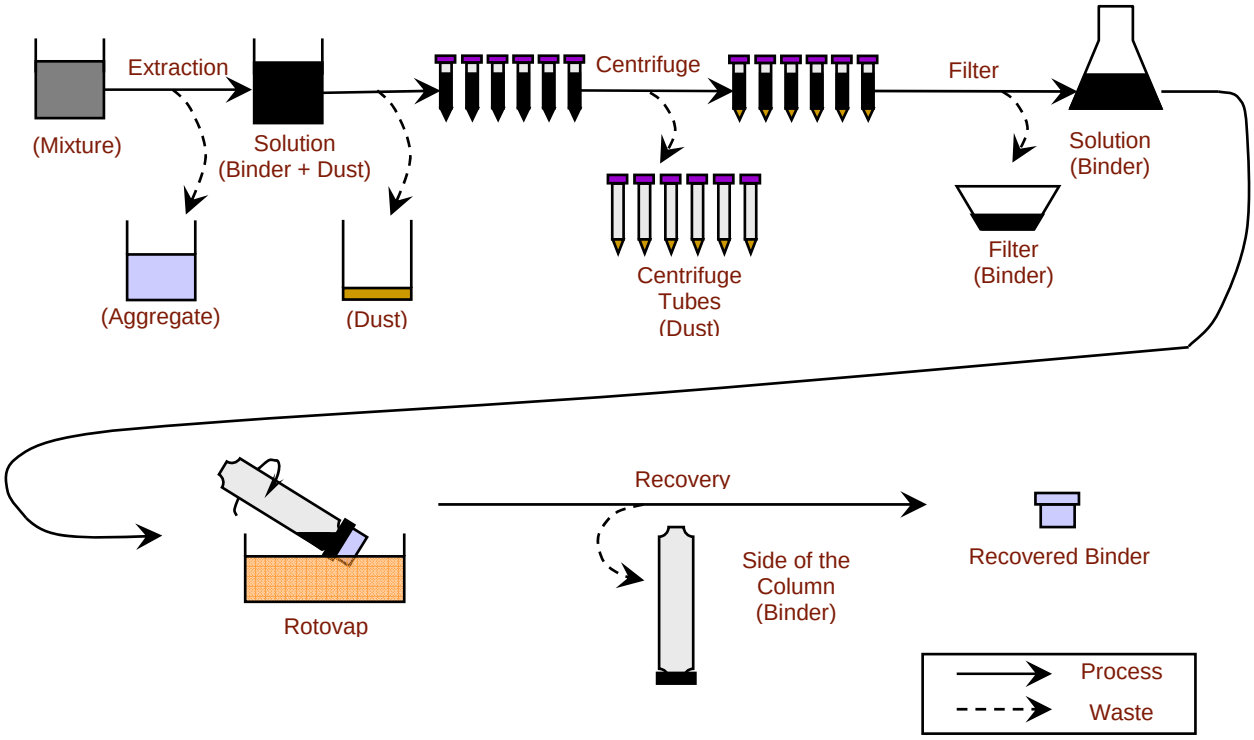

Figure 2-11. Asphalt Binder Extraction and Recovery Process.

Test Method for Binders

Dynamic Shear Rheometer (DSR)

Two types of rheological property data were obtained from dynamic shear rheometry measurements: the viscosity master curve at 60 °C and an estimated ductility of the asphalt binder. A 2.5 cm diameter parallel-plate geometry with a 500 micrometer gap was used for the measurements. To acquire the viscosity master curve at the 60 °C reference temperature, complex viscosity measurements were obtained in a controlled-stress mode by performing two frequency sweeps at 60 °C and 80 °C over a frequency range of 100 to 0.1 rad/s. Then, a shift factor was used to adjust frequency range, moduli, and viscosities of 80 °C to match with 60 °C, reference data. As a result, a single master curve with wider range of frequency at 60 °C can be constructed. After this time temperature superposition procedure, viscosity master curve at 60 °C should have a frequency range from 0.001 to 100 rad/s. At the lower end of the frequency range, the viscosity approaches a low shear rate limiting viscosity (also termed the "zero-shear" viscosity), a useful characteristic of the binder. An estimate of the binder's ductility at 15 °C and 1 cm/min extension rate can be calculated from the DSR value, G' and G" at 44.7 °C, and 10 rad/s (Ruan et al. 2003). The DSR function relationship is shown below:

$$\text{DSR Function} = \frac{G'}{\left(\eta'/G'\right)} = \frac{G'^{*}\omega}{\tan\delta} \qquad (2\text{-}7)$$

Where $\eta' = \frac{G''}{\omega}$ and $\frac{G''}{G'} = \tan\delta$

ω = Angular Frequency (rad/s)

δ = Phase Angle (degree)

Then, G' vs. (η'/G') can be plotted on the map with lines of constant ductility indicating the identified calculated ductility of each asphalt binder.

Fourier Transform-Infrared Spectrometer

The FT-IR spectrometer used in this project is a Mattson 5020 Galaxy Spectrometer. Infrared spectra of asphalt binders coated on zinc selenide prism were collected and analyzed over wavenumber of 1800 to 700 cm^{-1}. The band from 1820 and 1650 cm^{-1} is the carbonyl band, and the area under the part of the spectrum is termed the carbonyl area and indicates the level of oxidation of the binder.

Size Exclusion Chromatography (SEC)

After each recovery process, it is essential to confirm from the chromatogram that solvent was completely removed from the asphalt binder. Residual solvent present in recovered binder dramatically distorts the rheological properties of the asphalt, making it appear to be much softer than it is, in fact. Using tetrahydrofuran (THF) as a carrier fluid in size exclusion chromatography, also know as gel permeation chromatography (GPC), a toluene-based solvent can be distinctively detected. Also, any other unexpected components in the recovered binder may be observed. SEC conveniently gives a broad perspective of a binder's composition. Components that can be detected and identified from SEC, for example, are the asphaltene-rich fraction of a binder, the maltene-rich fraction, toluene, polymers, and water. Once recovered, binders are found to be free of the extracting solvent; physical properties of the binder can be confidently measured. The shape and relative size of the asphaltenes and maltenes peaks can also be used as "fingerprinting," along with other methods, to establish that different binders have been used in different pavement sections or to establish that two binders are likely the same.

In addition, SEC can be used to detect fog seal penetration in the pavement. Fog seal materials (polymer-modified asphalt and coal-tar) have unique peaks located on the chromatogram. By comparing the chromatogram of each layer, top to bottom, SEC can help determine whether fog seal material exists in any particular layer.

Test Method for Fog Seal Emulsions

Solvent Removal from Fog Seal Emulsion

The fog seal emulsions obtained from construction sites, most of the time, contain approximately 40 to 60 percent of solvent (water, oil, etc.), which was used to dilute the viscosity of the base material. In order to measure the physical properties of the fog seal base materials, the solvents must be removed from the emulsion. In this project, approximately 15 to 18 grams of fog seal emulsions in 3 oz. containers were evaporated in a laboratory oven at 60 °°C (to approximate the maximum pavement surface temperature). Weight reduction of the samples was recorded every day for 5 days as shown in Figure 2-12. According to this figure, after approximately 3 to 4 days, the weight changes are less than 1 percent compared to the previous day, which can assure that most of the solvent was evaporated. Then, the solvent-free base materials were tested with DSR and SEC, respectively.

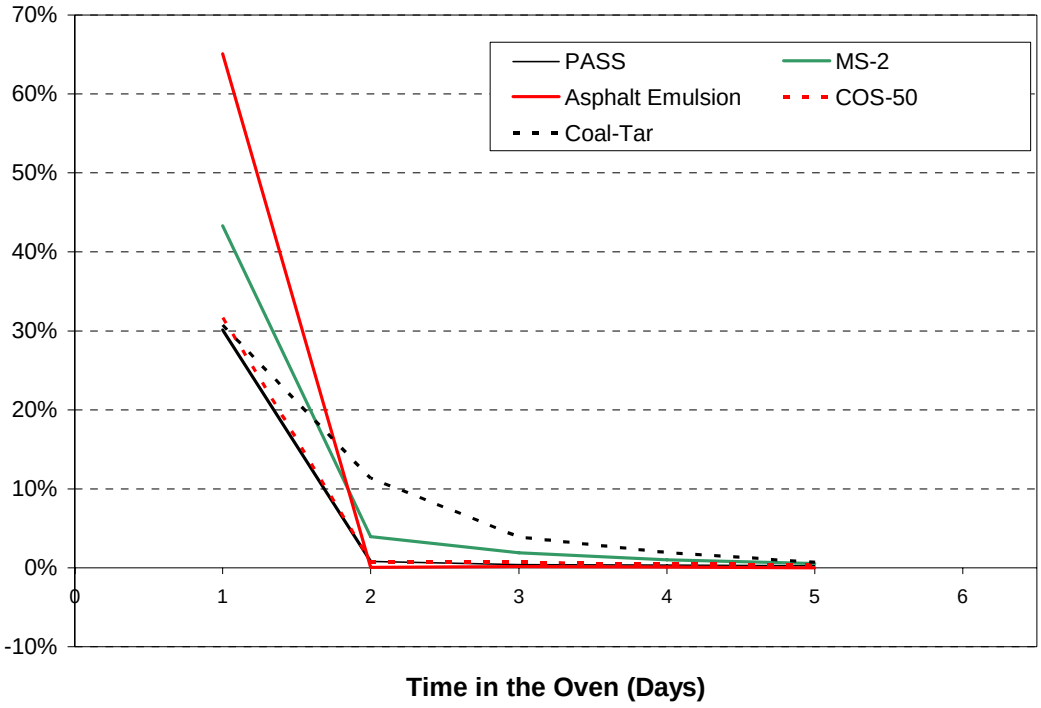

Figure 2-12. Weight Reduction of Fog Seal Emulsions.

CHAPTER 3

FOG SEAL PENETRATION AND SEALANT EFFECTIVENESS

INTRODUCTION

In Chapter 1, evidence was presented that sealants may be able to rejuvenate the binder in pavements. Figure 1-9 presented binder data from cores obtained from Texas highway 21 between Bryan and Caldwell. Binders recovered from cores obtained in 1992 and 1996 were significantly more aged or significantly harder than binders recovered from cores obtain in 2002 after a seal coat and overlay were placed in 2000. These observations were for a 2-inch layer that had 4 inches of pavement on top of it, suggesting that the sealant was able to penetrate several inches into the pavement.

Data on other pavements in Texas, obtained from LTPP cores, also suggest that seal coats may rejuvenate the binder *in situ* (Figures 1-11 and 1-12). In Figure 1-11, the solid symbols represent binder properties from cores taken approximately 10 years before the open symbols, and identical symbol shapes represent binders recovered from the same pavement. The legend indicates which pavements had seal coat treatments and the time at which the treatment was applied. Basically, in each case where there was no sealant applied between core samples, the binder moved as expected toward the upper left corner (48-2108 and 48-6086) or did not progress at all (48-3769). However, when a sealant was applied in the interim, the reverse path was taken and the binder moved in the direction of becoming softer (48-1046, 48-1056, 48-2133, and 48-9005). Figure 1-12 shows a binder's calculated ductility versus years of pavement service for the various extracted and recovered binders. Here the open symbols represent a binder's properties some time after a seal coat was placed.

While these data seem to suggest fairly strongly that sealant can penetrate into the pavement, they don't necessarily show that once the sealant has penetrated into the pores that it is absorbed by the *in situ* binder and therefore that it is effective at binder rejuvenation. These are questions that were addressed by this project.

The question of how effective a sealant might be in rejuvenating a binder can be estimated using the methodology developed by Chaffin et al. (1995) to determine the rheological properties of a blend of asphalt materials. This calculation must make certain assumptions about the application rate of the sealant, the penetration depth, the uniformity of the distribution of the sealant over that penetration depth, and absorption by the in-place binder. For this calculation, we will assume a single application rate, uniform distribution of the binder to the specified depth, and perfect absorption of the sealant by the in-place binder. Several penetration depths are used to determine several calculated scenarios as to rejuvenation effectiveness and therefore pavement life extension. Then using an approximate representative average hardening rate for binders in Texas we estimate the life extension of the binder in the pavement assuming these penetration depths, perfect absorption, and uniform rejuvenation of the in-place binder.

Table 3-1 shows these representative calculations for an application rate of 0.1 gallons of diluted emulsion per square yard using a value of 2.3 as a typical bulk specific gravity for dense-graded mixtures, and a density of asphalt binder and sealant approximately equal to that of water to provide calculations of the concentration of the rejuvenating sealant in the binder that range from 4.4 percent for 1 inch penetration up to 1.1 percent for 3 inch penetration. The next-to-last column of the table shows the ratio of the mixture binder viscosity to the original binder viscosity. Then using a typical average hardening rate in Texas pavements of 0.3 per year (Woo et al., 2006: developed and reported in project 0-4688, Chapter 5, not yet published), the final column shows the approximate life extension, for this penetration and for perfect absorption of the sealant. These calculations are based upon aged binder viscosities in the pavement having low-shear rate viscosities of 100,000, 500,000, and 1,000,000 poise at 60 °C and on the sealant being a softer asphalt material with a viscosity of 500 poise at 60 °C. We see from these calculations that a life extension of the binder of only 0.3 to 0.8 years for penetration depth of 3 to 1 inch. A significantly longer life extension of approximately 3 to 4 years is calculated (but not shown) for the binder if the penetration is only one-quarter inch.

Table 3-1. Calculations of the Hypothetical Life Extension Afforded by a Perfectly Effective Rejuvenating Fog Seal Treatment.

Penetration (in)	Sealant Conc[a] (percent)	η_{aged} (poise)	η_{blend}/η_{aged}	Est. Life Extension[a] (yrs)
1	4.4	100,000	0.84	0.6
		200,000	0.82	0.7
		500,000	0.79	0.8
2	2.3	100,000	0.89	0.4
		200,000	0.87	0.5
		500,000	0.85	0.5
3	1.5	100,000	0.924	0.3
		200,000	0.914	0.3
		500,000	0.90	0.3

[a]Based on a sealant viscosity of 500 poise, a sealant application rate of 0.1 gal diluted emulsion/yd^2, 0.5 gal original emulsion/gal diluted emulsion, 0.6 gal asphalt/gal original emulsion, a pavement bulk specific gravity of 2.3, and a pavement binder content of 5 wt percent, and a typical binder hardening rate in the pavement of 0.3/yr (actually the ln(DSR function) hardening rate, assuming approximately equal to ln(ZSV) hardening rate). It is further assumed that the rejuvenator penetrates uniformly to the depth shown and is perfectly and uniformly absorbed by aged pavement binder.

Another issue about sealants is that if they can actually do what their name applies, which is to seal the pavement against the ravages of oxygen and/or moisture, then presumably the oxidation rate of the binder would be retarded significantly, thereby extending the life of the pavement. Practically none of the data obtained on in-service pavements reported in Chapter 1 suggest that sealants can effectively retard oxidation by sealing the pavement. Nevertheless, such action by the sealant has been claimed and is conceivable.

OBJECTIVES

Within the context of the above introduction, there are two primary objectives of this chapter related directly to the penetration of sealants and whether they seal:

1. To determine if fog seals penetrate into the pavement. This objective is primarily assessed by size exclusion chromatography measurements of the binders recovered from several layers of the pavement.
2. To determine if fog treatments seal the pavement to the flow of the fluids. This objective is addressed by measuring the water permeability of the recovered cores.

The objectives related to rejuvenation of the binder by the sealant and the effects of the sealant on additional binder oxidation and binder content are addressed in Chapters 4 and 5.

METHODOLOGY

As discussed in Chapter 2, the top inch of the cores from pavements that were selected for study were sliced into one-quarter inch layers after the determination of the water permeability of the complete intact core. Then the binders from each of the one-quarter inch layers were extracted and recovered following the methodology of Chapter 2 and tested by size exclusion chromatography to determine differences between the different layers, especially, to compare the chromatogram to the type of sealant materials that were used in the pavements.

RESULTS

The Treatment Sites and Their Treatment Materials

Tables 3-2 and 3-3 summarize the sites that were studied in this project. Table 3-2 is a list of cores taken in the first year of the project (FY 2004-2005), and Table 3-3 is a list of sites cored in the second year of the project (FY 2006). In each table, the site of the core is followed with a number in parenthesis that indicates the number of cores (both untreated and treated) that were taken in each site. Also included in the table is whether the site was an airport pavement, the original construction date of the pavement, the application date of the fog seal, and the coring date. Finally, the type of fog seal treatment that was applied at each of the sites is also indicated. More details on these sites and their construction and coring were presented in Chapter 2.

Note that the fog seal materials all were either asphalt emulsions or coal-tar/rejuvenator treatments. The emulsions are designated as MS-2, PASS, COS-50, CSS-1, and SS-1. Samples of these emulsions were obtained for most of the materials with exception of the CSS-1 and the SS-1 materials. From these samples, the base materials were recovered after evaporation of water and if possible, the recovered materials were tested as to their size exclusion chromatography chromatograms and their rheological properties.

For some sites cores were obtained during both the first and second years of the project; for other sites cores were obtained in only the second year. For example, the Atlanta sites appear in Table 3-3, but not in Table 3-2 indicating that they were cored only in the second year of the

project. Also note that the Abilene site was cored more extensively than any of the other sites, as there were 18 cores obtained in the first year of the project and an additional 21 cores in the second year of the project; furthermore, this site had two types of treatments, MS-2 and PASS.

Table 3-2. Site Information for the 1st Coring of the Project.

1st Core (2004-2005)					
Site (# of cores)	**Location**	**Construction Date**	**Application Date**	**Coring Date**	**Treatment Type (# of cores)**
Abilene (18)*	SH 36	1998	2004	2004-2005	MS-2 (6), PASS (6)
Carrizo Springs (6)	Airport	1995	2004	2004-2005	Coal-Tar (3)
Fort Worth 2000 (6)	FM 4	2000	2005	2005	COS-50 (3)
Fort Worth 2003 (6)	FM 4	2003	2005	2005	COS-50 (3)
Georgetown '89 (7)	Airport	1989	1999	2004	Coal-Tar (3)
Georgetown '95 (6)	Airport	1995	1999	2004	Coal-Tar (3)
Jacksonville (6)	Airport	2004	2004	2004	Coal-Tar (3)
Lufkin (6)	Bus 59	1995	2004	2004	Coal-Tar (3)
Pleasanton (6)	Airport	1985	2004	2004	Coal-Tar (3)

* Remarks: L1 and R2 are MS-2 Treatment, L2 and R1 are PASS Treatment

Table 3-3. Site Information for the 2nd Coring of the Project.

2nd Core (2006)					
Site (# of cores)	**Location**	**Construction Date**	**Application Date**	**Coring Date**	**Treatment Type (# of cores)**
Abilene (21)*	SH 36	1998	2004	2006	MS-2 (6), PASS (6)
Atlanta CM (6)	IH 20	2001	2006	2006	CSS-1 (3)
Atlanta DG (6)	IH 20	2001	2006	2006	CSS-1 (3)
Atlanta SP (6)	IH 20	2001	2006	2006	CSS-1 (3)
Atlanta 67 (6)	US 67	2003	2004	2006	PASS (3)
Carrizo Springs (6)	Airport	1995	2004	2006	Coal-Tar (3)
Fort Worth 2000 (6)	FM 4	2000	2005	2006	COS-50 (3)
Fort Worth 2003 (6)	FM 4	2003	2005	2006	COS-50 (3)
Georgetown '89 (6)	Airport	1989	1999	2006	Coal-Tar (3)
Georgetown '95 (9)	Airport	1995	1999, 2006	2006	Coal-Tar (6)
Jacksonville (6)	Airport	2004	2004	2006	Coal-Tar (3)
Lufkin (6)	Bus 59	1995	2004	2006	Coal-Tar (3)
Odessa SH 149 (6)	SH 191	1983	2002	2006	SS-1 (3)
Odessa SH 349 (6)	SH 349	1996	2006	2006	SS-1 (3)
Pleasanton (6)	Airport	1985	2004	2006	Coal-Tar (3)
Tyler (6)	US 79	2002	2005	2006	PASS (3)

* Remarks: L1 and R2 are MS-2 Treatment, L2 and R1 are PASS Treatment

Figures 3-1 through 3-6 are SEC chromatograms of the emulsion materials. The materials were recovered from the emulsion by distilling off the water, following the procedure described in Chapter 2. The recovered materials were then tested in the SEC apparatus using standard procedures, also described in Chapter 2.

The PASS, MS-2, COS-50, and asphalt emulsion materials, to a large degree, look very much like standard asphalt materials. The typical asphalt chromatogram exhibits an asphaltenes peak that elutes between about 22 and 26 minutes, and a maltenes peak that elutes after the asphaltenes peak. The PASS material, in addition to the asphalt, contains polymer, which is seen very clearly in the prominent peak that elutes at 20 minutes. The MS-2 (Figure 3-2) and COS-50 (Figure 3-3) materials show no polymer, and the asphalt emulsion material (Figure 3-4) shows only a very minimal amount of polymer. In all of these charomatograms, there are two traces. One is the refractive index detector trace and the other is an intrinsic viscosity detector trace that is especially suited for characterizing the presence of polymer materials. Of course, even though these four materials look basically like asphalt materials, they are, nevertheless, readily distinguishable from each other through their characteristic chromatographic patterns. In addition to the asphalt in these materials, each of the traces shows three negative peaks at about 37, 40, and 41.5 minutes. These are traces of water, nitrogen, and oxygen, respectively, and exist in virtually all of the chromatograms.

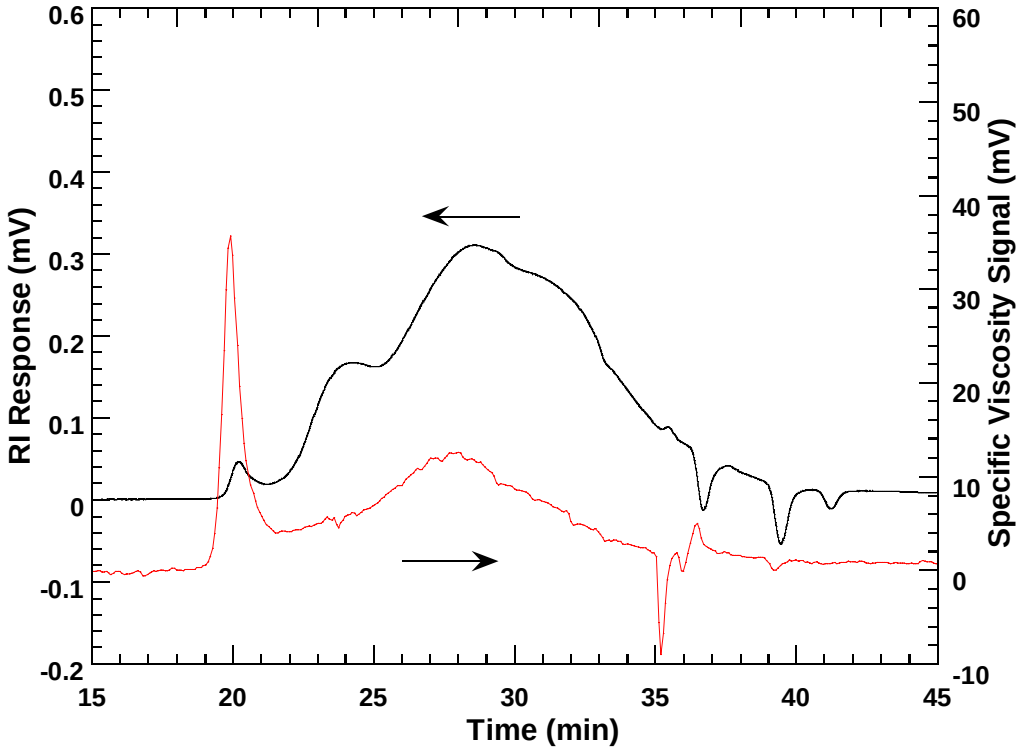

Figure 3-1. SEC Chromatogram of the Recovered PASS Fog Seal Material.

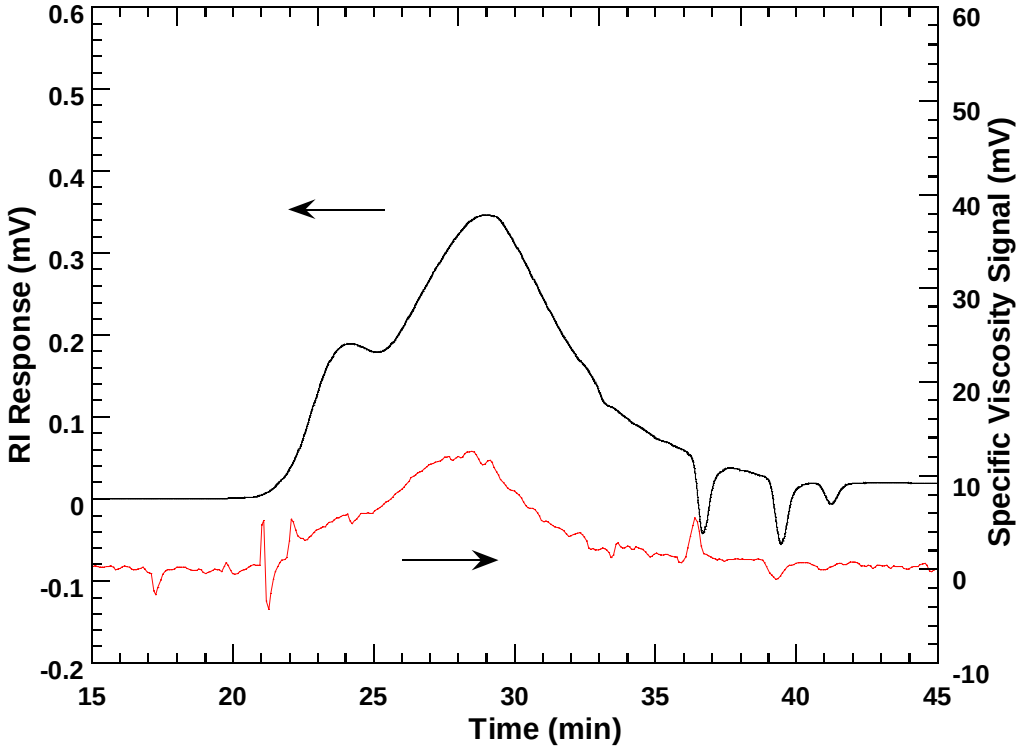

Figure 3-2. SEC Chromatogram of the Recovered MS-2 Fog Seal Material.

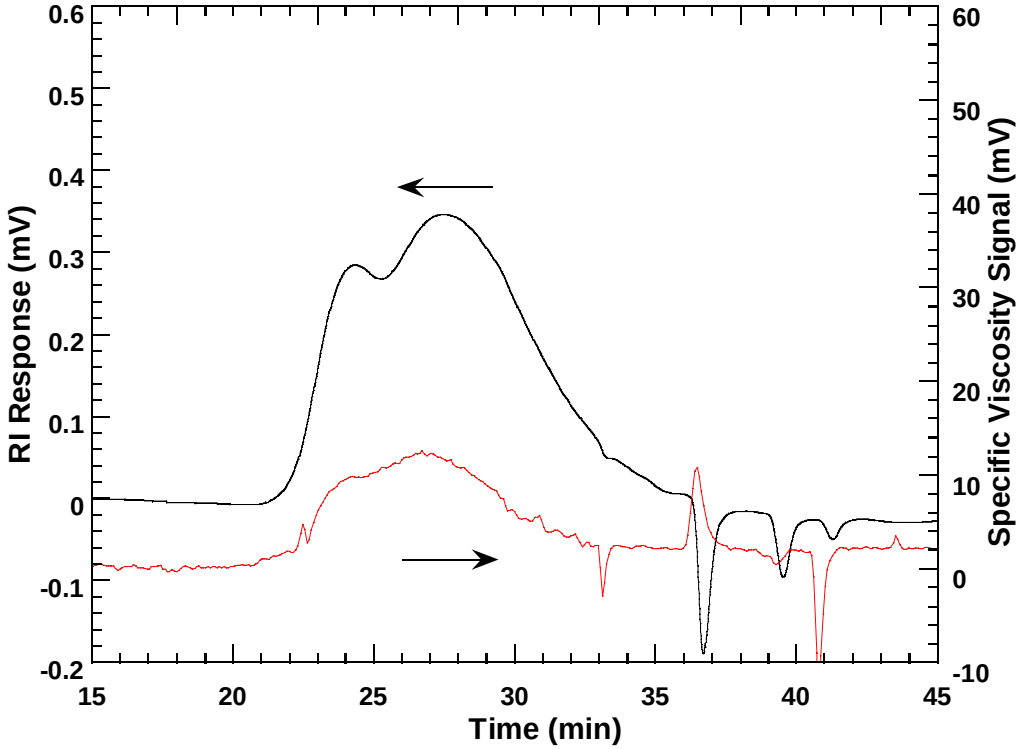

Figure 3-3. SEC Chromatogram of the Recovered COS-50 Fog Seal Material.

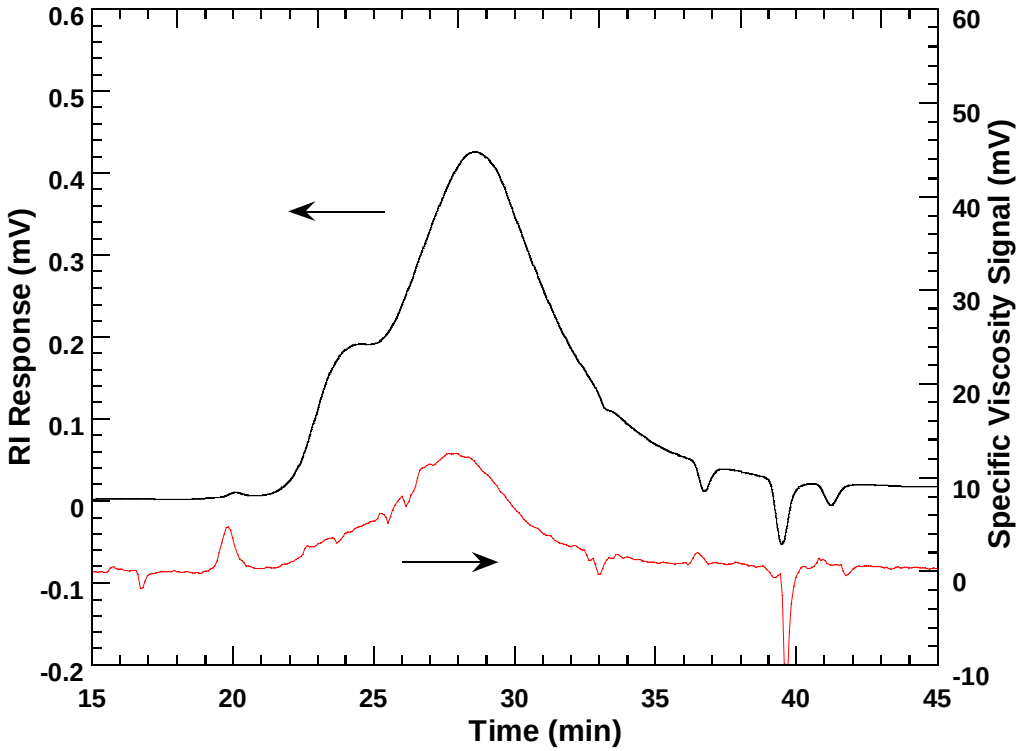

Figure 3-4. SEC Chromatogram of the Recovered Asphalt Emulsion Fog Seal Material.

The coal-tar and rejuvenator materials are decidedly different materials from the others (Figures 3-5 and 3-6). These are much lighter materials and elute beginning at about 35 minutes and ending at about 41 minutes. This establishes them as lighter components than almost any of the components in the asphalt emulsion materials, a fact that suggests that they would be much more volatile than the asphalt materials. However, because they appear at such a distinctive part of the chromatogram and have such a distinctive trace compared to the asphalt materials, they have the potential to serve as a good marker for the presence of the fog seal application and especially for its penetration below the surface into the pavement. The asphalt materials, because they look so much like asphalts, are much more difficult to distinguish from the original binder used in the pavements. Of course, if the PASS material was used over a pavement binder that did not have polymer, then the presence of the polymer in the recovered binder in the treated pavement would serve as a good indication of residual presence of the fog seal treatment. Detecting the MS-2, COS-50, and asphalt emulsion materials, however, is a much more problematic issue. One might also look for differences in the shape of the recovered binder at different layers, which may indicate the presence of the emulsion asphalt blended with the original binder.

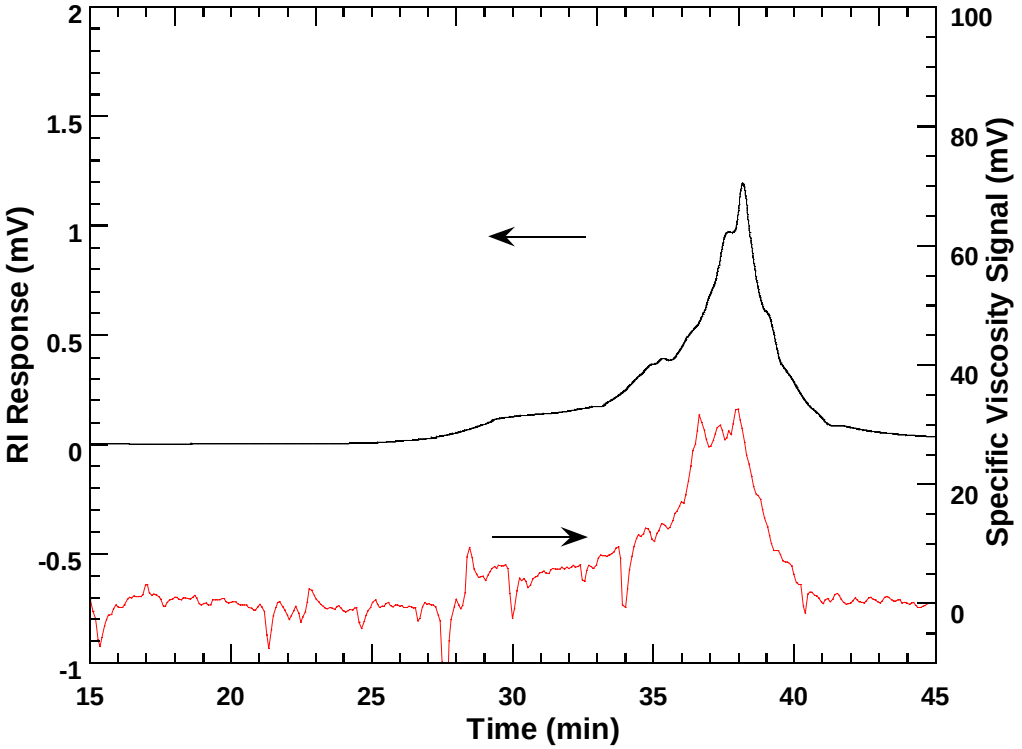

Figure 3-5. SEC Chromatogram of the Recovered Coal-tar Rejuvenating Seal Material.

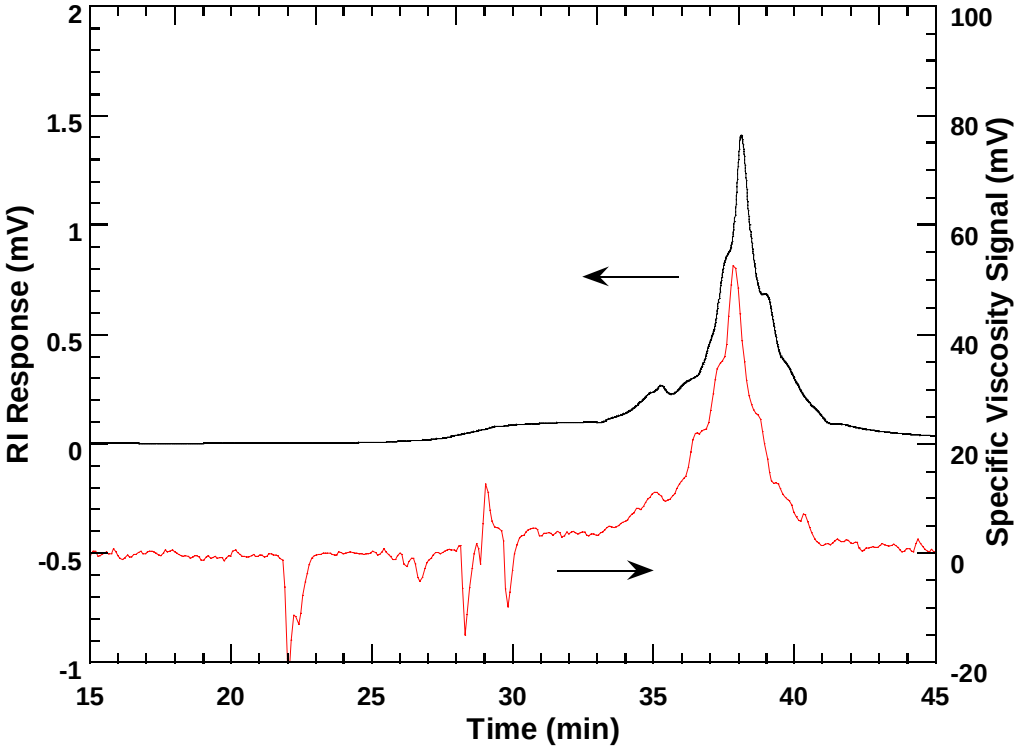

Figure 3-6. SEC Chromatogram of the Recovered Rejuvenator Material.

The Recovered Binder Chromatograms

Abilene SH 36

The Abilene site has the most number of cores of any other sites studied; additionally, treatments included two materials. As discussed previously, the PASS material is a polymer-modified asphalt material whereas the MS-2 emulsion, while still an asphalt base material, has no polymer-modifier. Furthermore, for each of the materials, there are multiple portions of the pavement, designated L1, L2, R1, and R2 (as described in Chapter 2) that were sampled in three replicates by coring. In the discussion that follows, recovered binder chromatograms are presented for cores taken from these portions of pavement, and for both untreated and treated cores. The top 1 inch of the cores was sawed into one-quarter inch slices, as described previously in Chapter 2, and the binders were extracted from the slices and then recovered and the binders tested.

Figures 3-7 through 3-14 present the chromatograms for each of the binders recovered from the Abilene slices to assess differences between treated and untreated pavements, and between the treatments. Figure 3-7 shows the chromatograms for the Abilene SH 36 L2 site; Figure 3-7a is the untreated core, replicate U3 and Figure 3-7b is the treated core, replicate T3. In each figure, there are four chromatograms for each of the two detectors (refractive index and viscosity). The treatment used in this portion of the pavement was the PASS, polymer-modified asphalt surface sealer.

The chromatograms show that there is a significant amount of polymer in each of the layers, although for the untreated core, the fourth layer shows significantly less polymer and a maltenes peak that is measurably broader than for the other three layers. Such is not the case for the treated core fourth layer where the maltenes peak has essentially the same shape and elution time to peak maximum as the other layers in the pavement, and the level of polymer is not nearly as slight as for the untreated, fourth layer. Thus the different untreated fourth layer is likely attributable to a different binder unlying that of the top inch. We further note that although there are differences in the level of polymer in the first, second, and third slices that one might consider attributing to the PASS treatment, the differences are about as great in the untreated core as they are in the treated core. Again, it should be noted that if the PASS material were present in a layer, then there likely would be a distortion of the asphalt chromatogram in that layer. This effect would be the result of the shape of the PASS asphalt chromatogram (Figure 3-1), which is significantly different from that of the paving binder. In fact, however, we note that there were no differences between the shapes of the asphalt material recovered from the treated core compared to the asphalt material recovered from the untreated core. While these are qualitative judgments, they do seem to be quite conclusive.

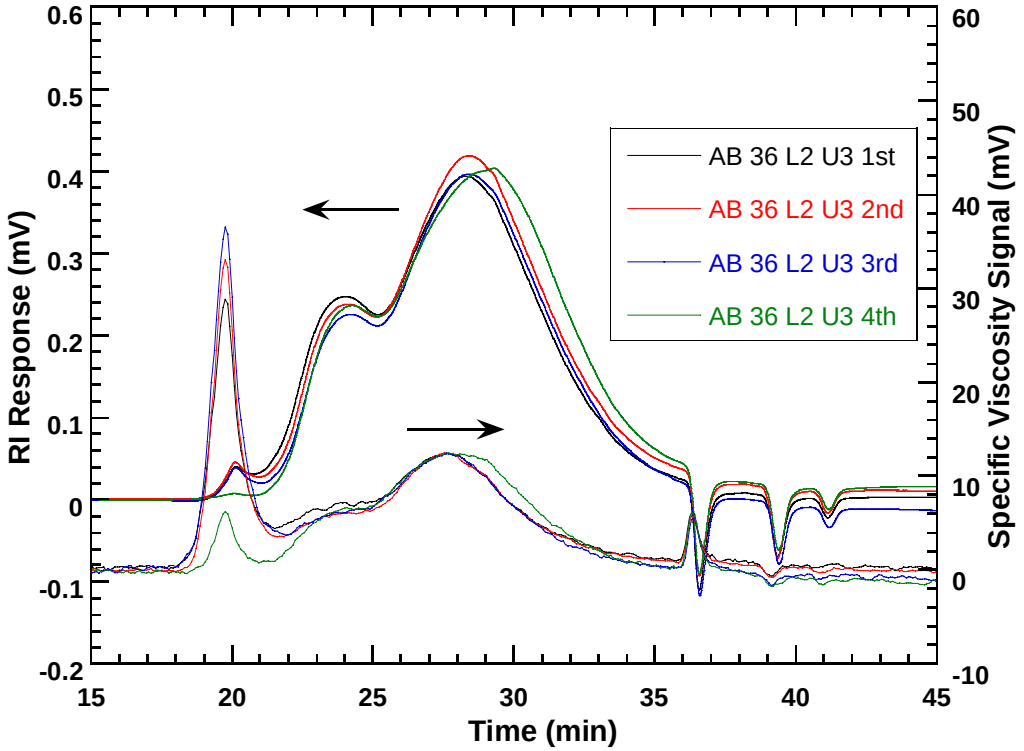

Figure 3-7a. Recovered Binder Chromatograms, Untreated Core, Abilene SH 36 L2.

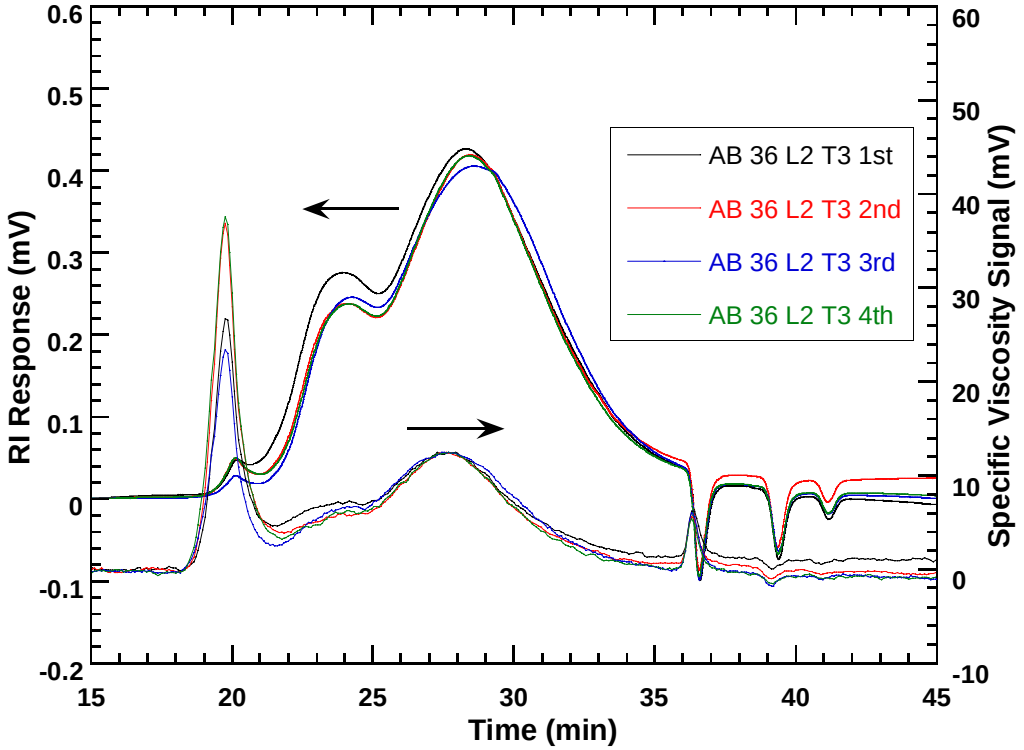

Figure 3-7b. Recovered Binder Chromatograms, PASS Treatment, Abilene SH 36 L2.

Figure 3-8 presents the chromatograms for the L2, PASS treated material second year cores. Here we note that it is the third layer that has a significantly reduced polymer content accompanied by a distinctly different shape to the maltenes peak and a different time to the peak maximum of the maltenes peak. Furthermore, it should be noted that this is true of, again, both the untreated and treated cores indicating that it is not an effect of the treatment. And again, we don't see any differences in shape of the maltenes peak as a result of the treatment nor do we see increases to the polymer content that might be attributed to the PASS treatment. Thus again, we conclude that the presence of PASS treatment cannot be detected conclusively by this chromatogram. Perhaps the treatment drained to the sides of the pavement, or perhaps it drained completely through the pavement, or at least through the top inch of the pavement and not absorbed by the binder.

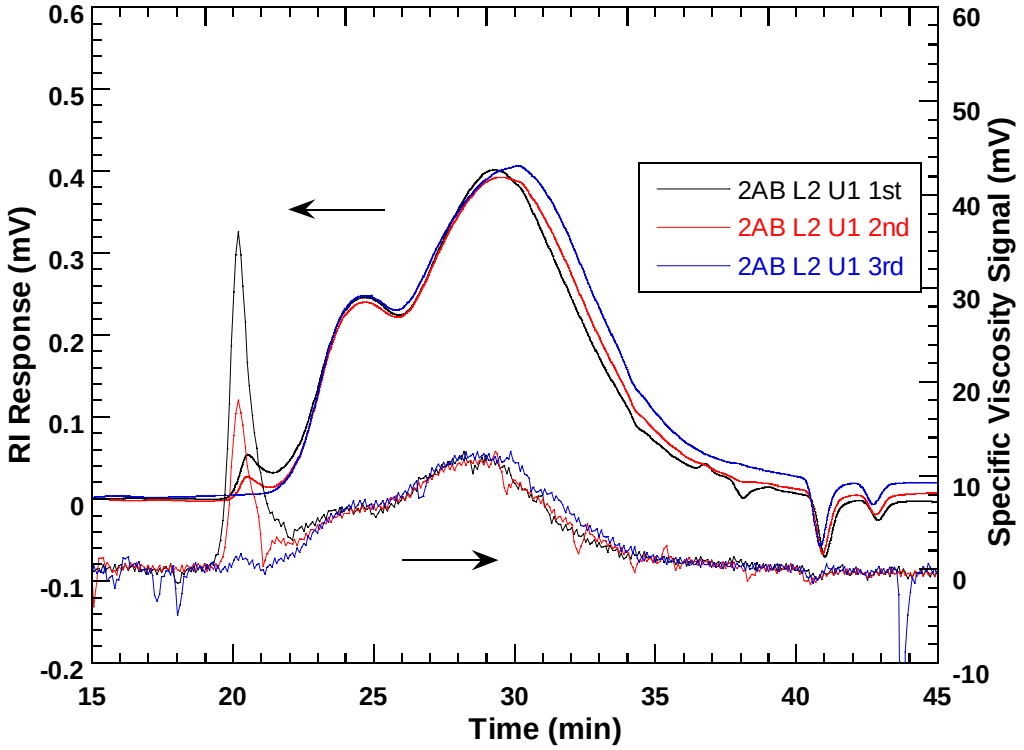

Figure 3-8a. Recovered Binder, Untreated Core, 2nd Year Abilene SH 36 L2.

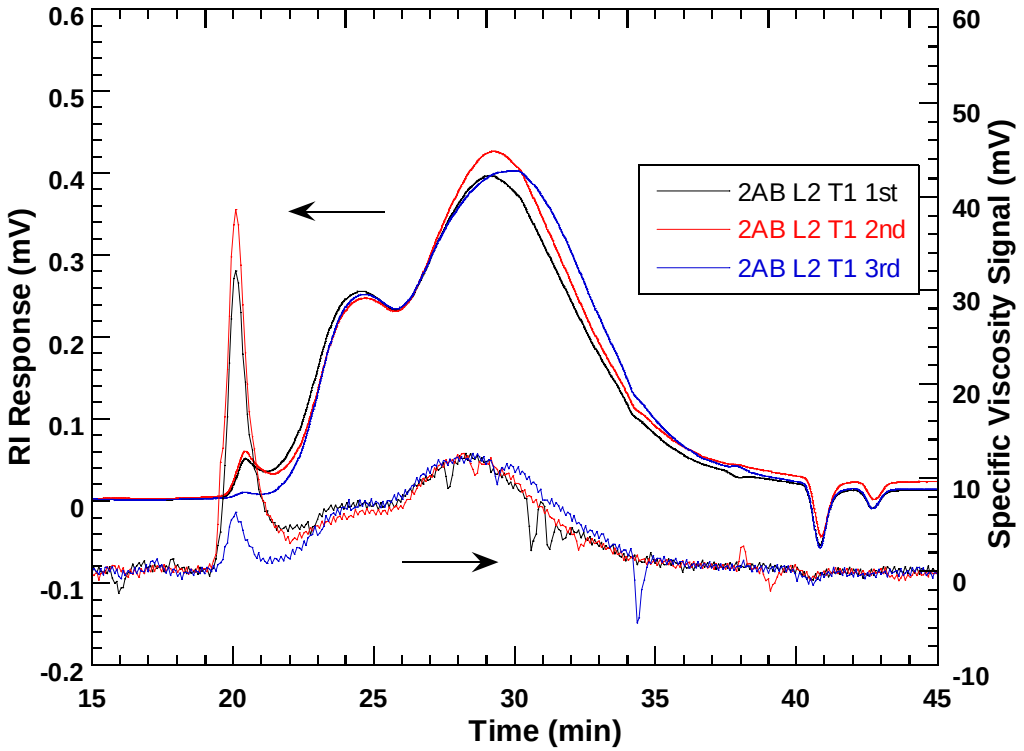

Figure 3-8b. Recovered Binder, PASS Treatment, 2nd Year Abilene SH 36 L2.

Figure 3-9a presents chromatograms for the R1 site for the first-year coring. The conclusions are similar to those for the other pairs of cores although we do see an apparent higher content of polymer in the treated core than we see in the untreated core. However, the higher polymer content is not accompanied by differences in the maltenes peak, suggesting that the higher polymer content is simply the result of the content in original binder used in the pavement. Again it is noted that the fourth layer from the surface contains no polymer and that the maltenes peak of this binder is broader with the time to the peak maximum shifted to a later time than for the other peaks.

Figure 3-10 provides the data from the same site, but for the second year of coring. The results are very similar to the first-year coring although here there are only three slices for each core, with the third slice containing very little polymer and thus comparing to the fourth slice in the first-year core. The first and second slices of these treated and untreated cores show virtually identical polymer contents. Again, we conclude from these traces that there is virtually no strong indication of the presence of the PASS treatment.

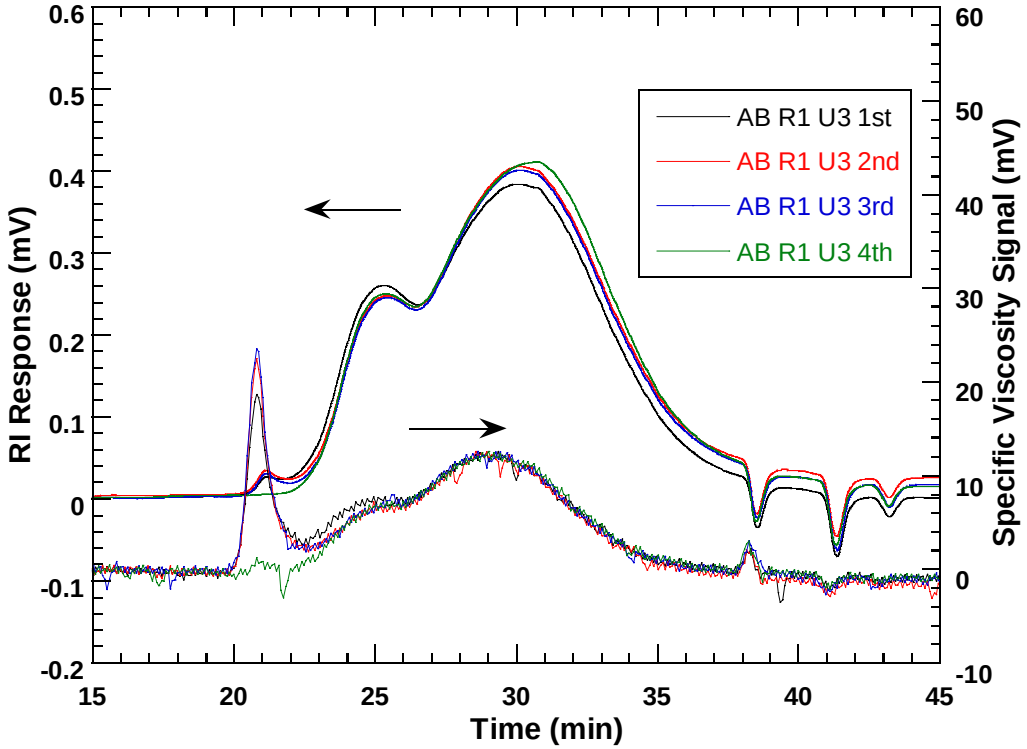

Figure 3-9a. Recovered Binder, Untreated Core, 1st Year Abilene SH 36 R1.

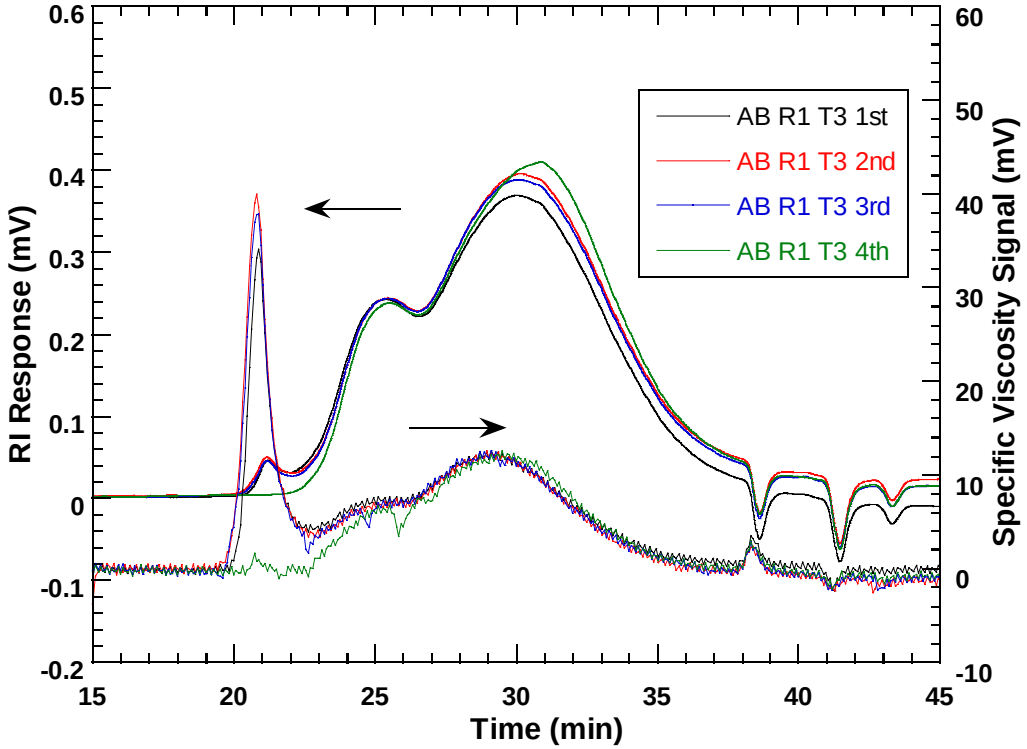

Figure 3-9b. Recovered Binder, PASS Treatment, 1st Year Abilene SH 36 R1.

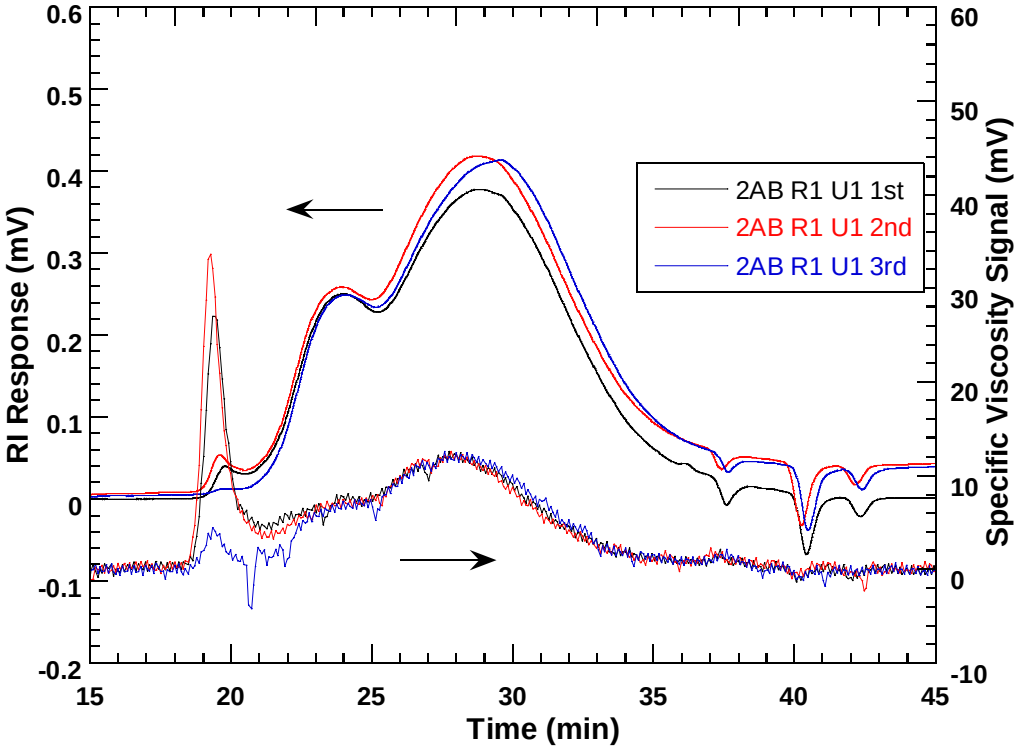

Figure 3-10a. Recovered Binder, Untreated Core, 2nd Year Abilene SH 36 R1.

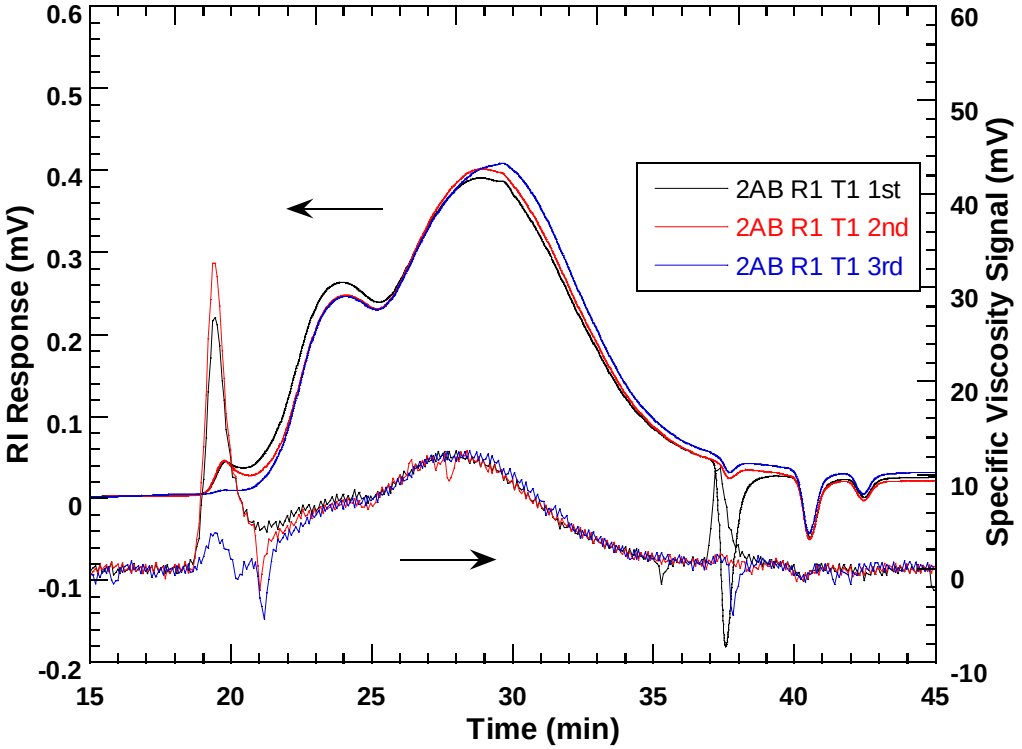

Figure 3-10b. Recovered Binder, PASS Treatment, 2nd Year Abilene SH 36 R1.

The next sets of figures address the MS-2 fog seal treatment. Figures 3-11a and 3-11b are for cores taken in the second year of the project and treated with the MS-2 emulsion. Figure 3-11a is the untreated core; Figure 3-11b is the treated core. Again the MS-2 material is basically an asphalt emulsion that contains no polymer material, as its chromatogram (Figure 3-2) looks very much like a convention asphalt material. Figure 3-11a shows chromatograms for (untreated) binders from three slices, with each binder having a significant amount of polymer in the material. Based upon typical variations between slices of the same pavement, we conclude that the polymer concentrations in each of these slices are all essentially the same. The asphaltenes and maltenes peaks also are virtually identical (accounting for the baseline shift that occurred in the analysis and carried over long past the elution of the asphalt material). In Figure 3-11b virtually identical results are seen; again the prominent polymer peaks from the intrinsic viscosity detector indicate nearly identical polymer concentrations and the asphalt peaks also overlay each other very well. From these untreated versus treated comparisons and taking into account chromatograms of the MS-2 material, we conclude that there is no definitive evidence of the fog seal treatment in any of these layers.

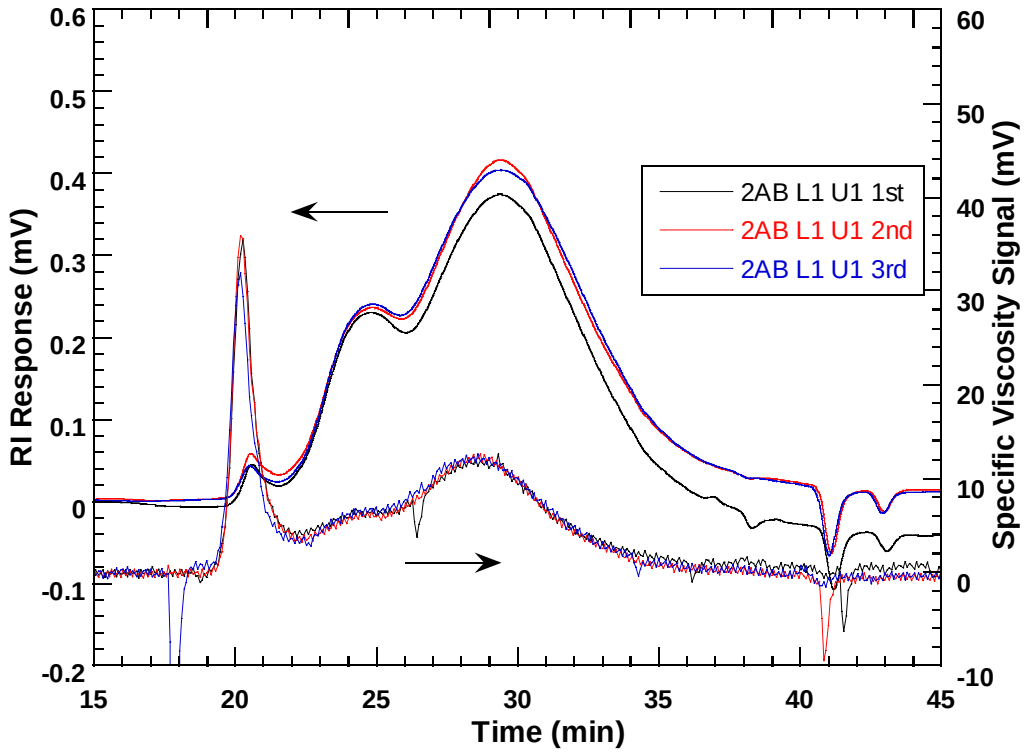

Figure 3-11a. Recovered Binder, Untreated Core, 2nd Year Abilene SH 36 L1.

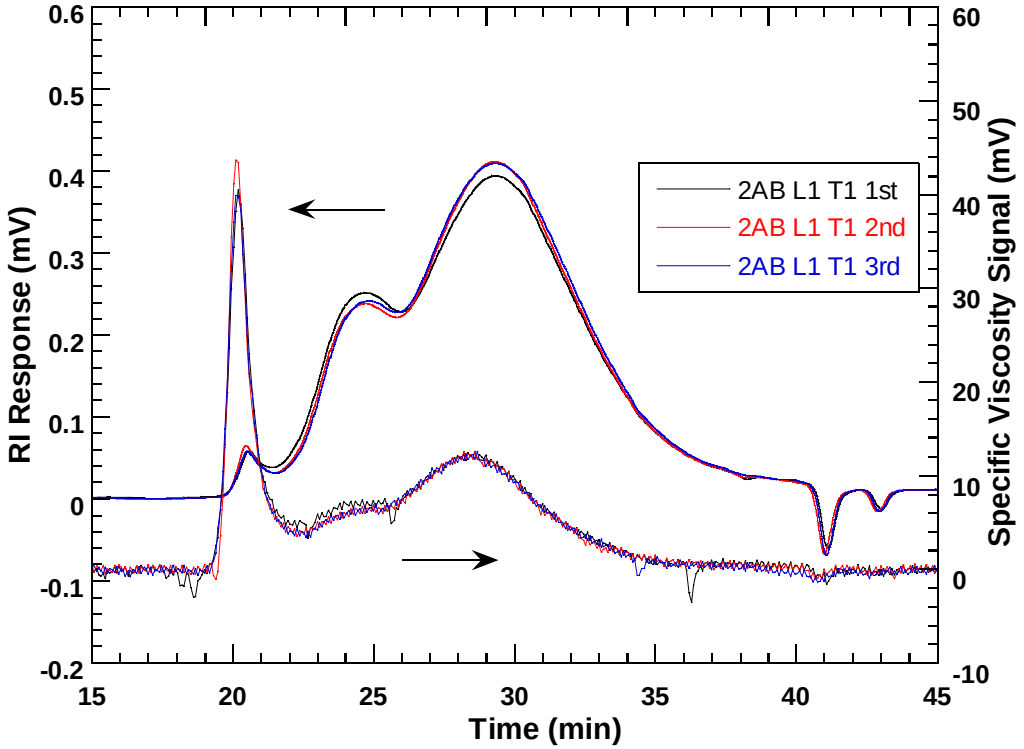

Figure 3-11b. Recovered Binder, MS-2 Treatment, 2nd Year Abilene SH 36 L1.

Figure 3-12 shows chromatograms for the second-year coring of the Abilene R2 site. Figure 3-12a illustrates the untreated core and Figure 3-12b shows the treated core. Again, the treatment was the MS-2 asphalt emulsion. For Figures 3-12a and 3-12b, an interesting feature of these cores is that the maltenes peak for the second and third slices is decidedly broader than it is for the very top or first slice. This is true of both the untreated and the treated cores. We also note that the polymer is very strong in this first slice in both the untreated and treated cores while in the third slice, it is virtually nonexistent, and it is much reduced in the second slice. These facts, taken together, suggest very strongly that the first slice (one-quarter inch thick) was a very thin overlay of a polymer-modified material. This would have been a thin overlay indeed. The second slice, also another quarter inch, appears to have some of that thin overlay together with the underlying pavement, and then the third slice apparently has none of the top overlay. Again, because both the base binder maltenes in the second and third layers are significantly different from the maltenes in the first layer and because the polymer concentrations are so different, it is logical to conclude that this first quarter inch is very different from the underlying layers. Note that the MS-2 treatment was an unmodified material and therefore the prominent polymer peaks in the first layer that appears much less prominently in the second layer would not be the result of the fog seal treatment. In fact, the fog seal treatment would have reduced the polymer concentration relative to underlying slices if it remained concentrated in that top layer. Again, the conclusion seems to be that the fog seal treatment causes no observable changes to the chromatograms of the binder in the treated core compared to the binder in the untreated core.

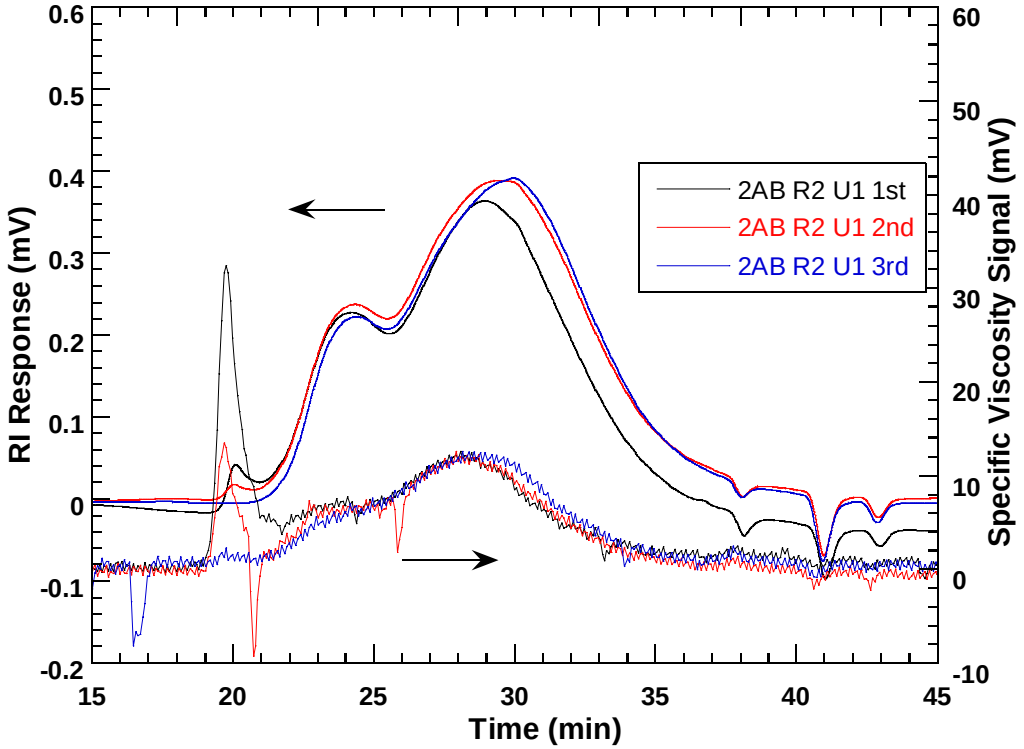

Figure 3-12a. Recovered Binder, Untreated Core, 2nd Year Abilene SH 36 R2.

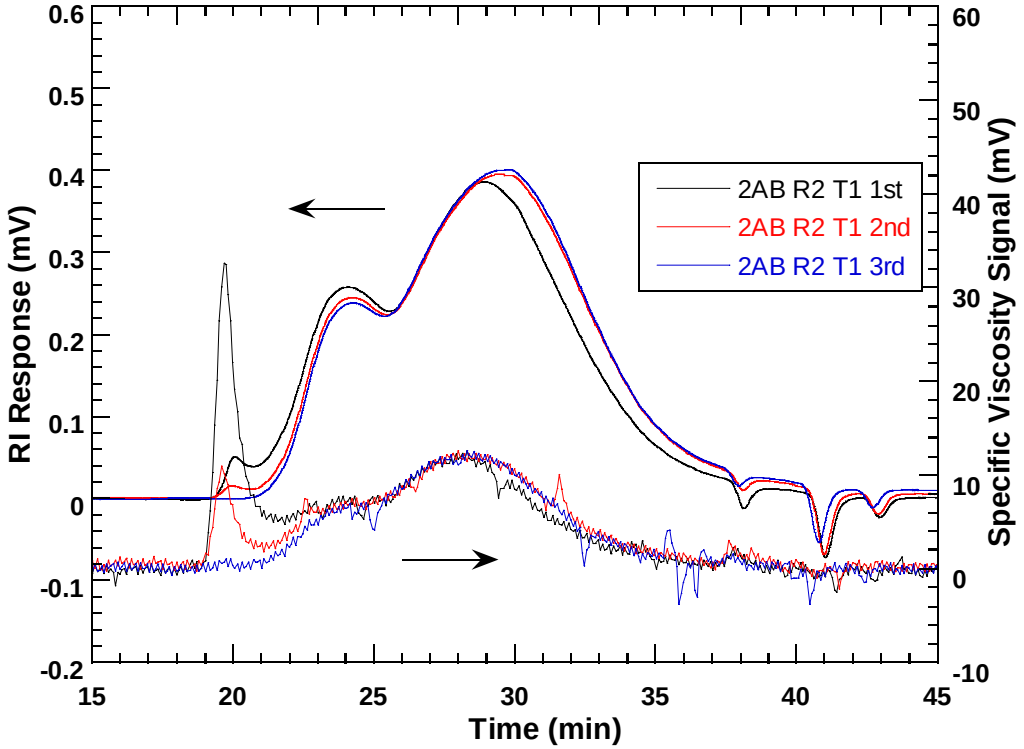

Figure 3-12b. Recovered Binder, MS-2 Treatment, 2nd Year Abilene SH 36 R2.

Figures 3-13 and 3-14 show the recovered binders in one-quarter inch slices from two separate first-year cores (not replicates) that were both treated with the MS-2 emulsion. Figure 3-13 shows four slices all with very prominent polymer peaks and also all with very similar asphalt chromatograms. Because we don't have the untreated analysis to compare to, we cannot say conclusively that there were no differences to the untreated core. Again, however, we note that the MS-2 material did not contain polymer, and if it were concentrated in any one of these particular layers, then we would expect to see that layer's polymer concentration significantly reduced below the others. Figure 3-14 is for a different core location. Note that this core was thick enough that we were able to obtain five slices, but that only the top three contained a significant amount of polymer; the fourth and fifth slices had no detectable amount of polymer. Note also that the fourth and fifth slices show definite differences in the asphalt peaks compared to the first, second, and third slices. Evidently, in this case also there was a thin overlay perhaps less than one inch that contained a polymer modifier, and the base asphalt underneath that overly had no such modifier. The base asphalt underneath the overlay also evidently was a different asphalt material, as indicated by the different chromatograms for the asphaltenes and maltenes peaks for the binder recovered from the slices. Again, we do not have an analysis of a corresponding untreated core, but certainly these data do not refute a conclusion that the fog seal treatment is virtually undetected in these chromatograms.

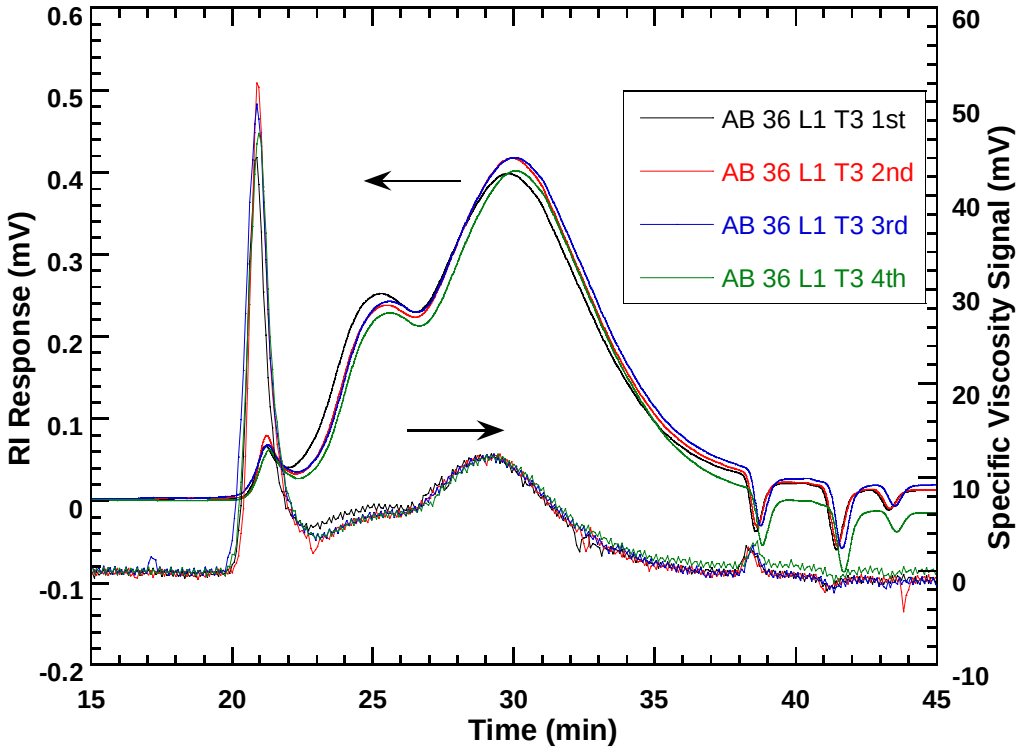

Figure 3-13. Recovered Binder, MS-2 Treatment, 1st Year Abilene SH 36 L1.

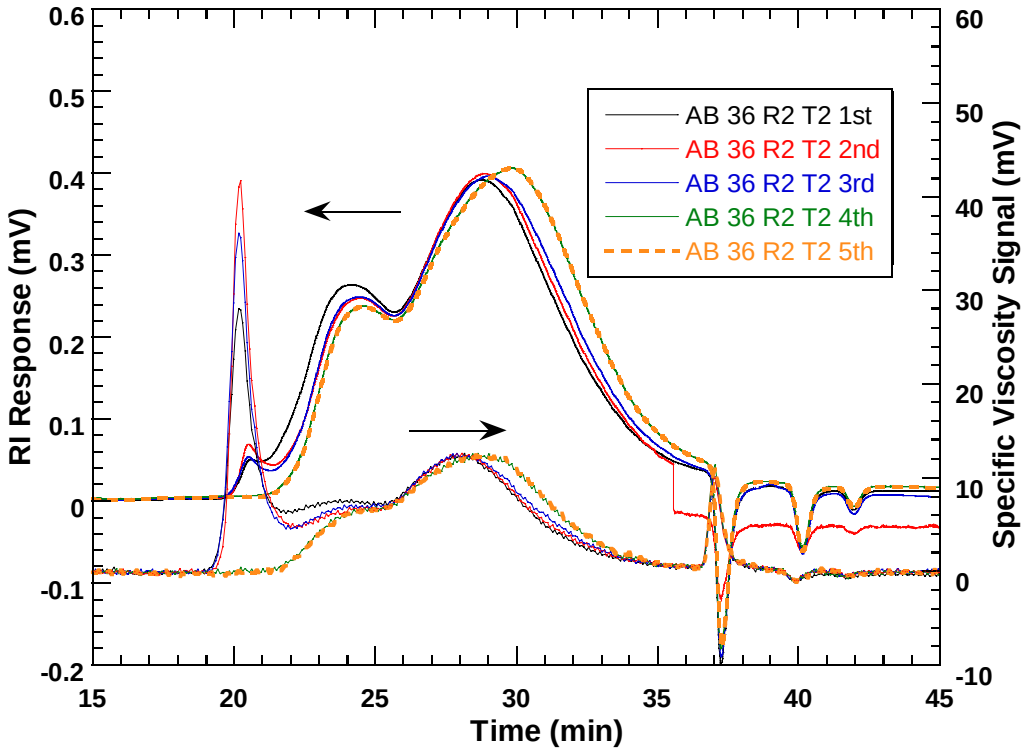

Figure 3-14. Recovered Binder, MS-2 Treatment, 1st Year Abilene SH 36 R2.

Atlanta IH 20

Figures 3-15 and 3-16 present data for the Atlanta coarse matrix mixture (IH 20 CM, Figure 3-15) and for the dense-graded mixture (IH 20 DG, Figure 3-16). Comparing Figures 3-15a (untreated core) and 3-15b (treated core), we see that there is virtually no difference between the untreated and treated cores (after accounting for the baseline shift in the untreated core between the first slice and the second and third slices). While the fog seal material that was used for the treatment was not available for testing, the fact that no differences between the untreated and treated cores is observed indicates very little, if any, of the fog seal material is present because of this treatment. This conclusion is consistent with the observations from the Abilene site presented above. Similar observations are noted from a comparison of Figures 3-16a (untreated) and 3-16b (treated) for the cores from the DG site. This site also was treated with the CSS-1 emulsion. Again, differences between layers and differences between sites that might support sealant penetration of the sealant just are not evident.

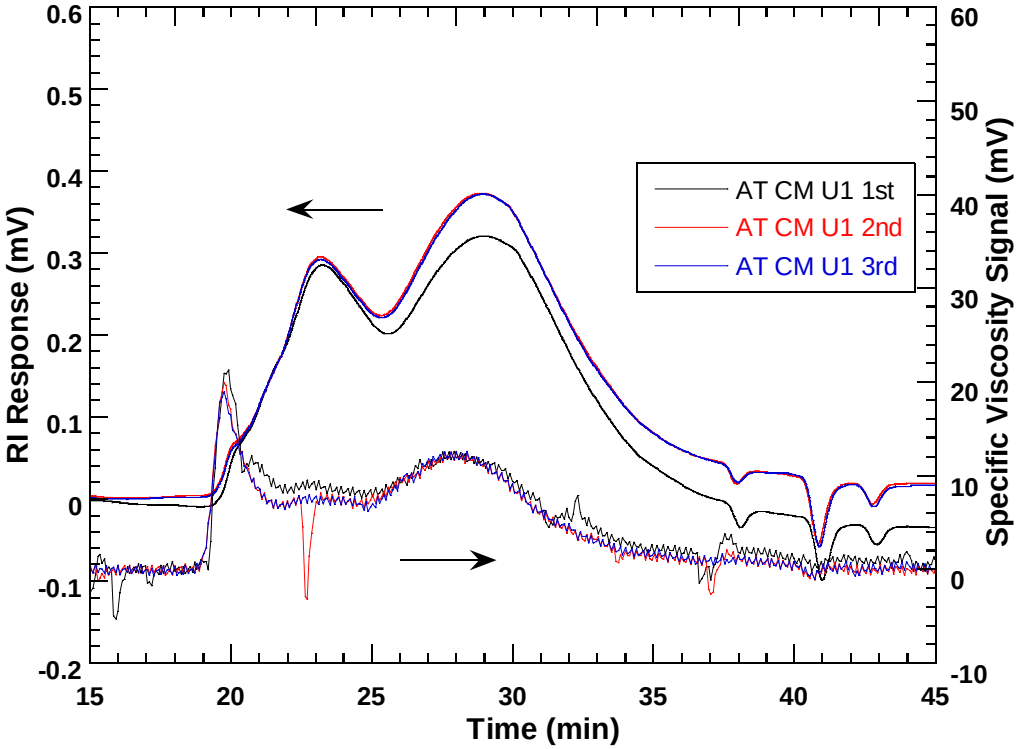

Figure 3-15a. Recovered Binder, Untreated, Atlanta IH 20 CM.

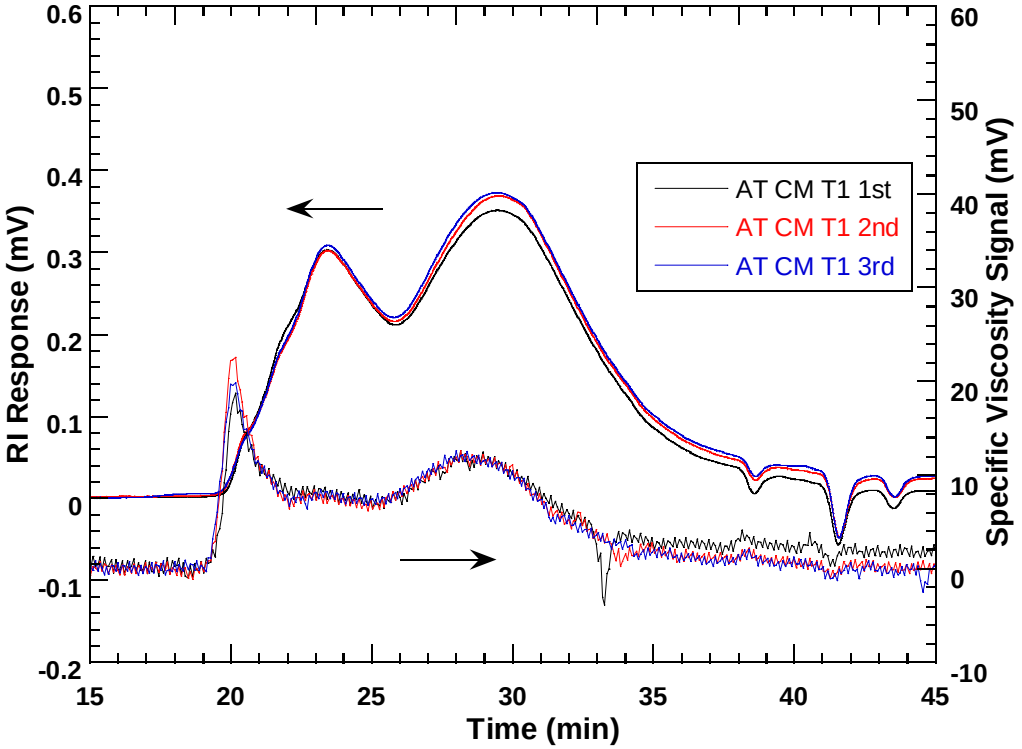

Figure 3-15b. Recovered Binder, CSS-1 Treatment, Atlanta IH 20 CM.

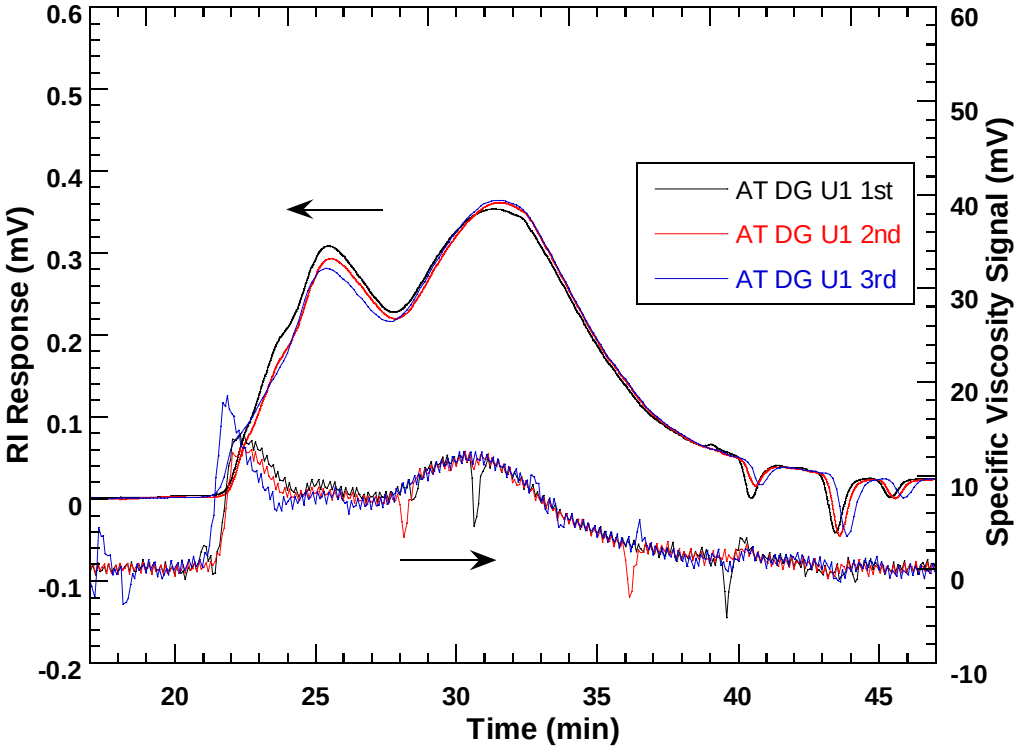

Figure 3-16a. Recovered Binder, Untreated, Atlanta IH 20 DG.

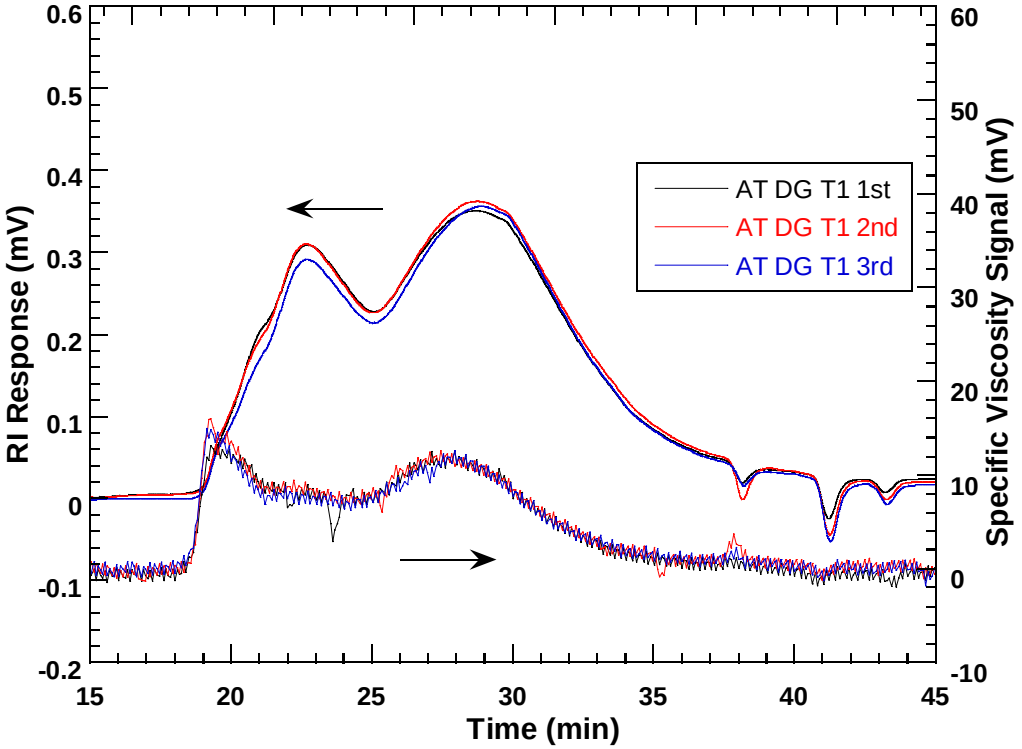

Figure 3-16b. Recovered Binder, CSS-1 Treatment, Atlanta IH 20 DG.

Atlanta US 67

Figures 3-17a and 3-17b present data for the Atlanta US 67 site. The PASS material was used for the fog seal. Again, after correcting for the baseline shift in the untreated core analyses, the first layer overlays very well with the second and third layers. Figure 3-17b shows the chromatograms for the binder from the treated core, and they match quite well the chromatograms from the untreated core (but see the first slice discussion, below). Note that the PASS treatment contains a significant amount of polymer, and if it existed to any appreciable degree in any slice, then we would expect to see a greater amount of polymer in that slice than in the treated core. However, there are no significant increases in the polymer concentration. One difference between the untreated and treated cores appears to be in the binder recovered from the first slice of the treated core, where the maltenes peak appears to have a somewhat different shape from the other slices. However, we also note that there were some time shifts in these analyses because of a leaking pump problem that may account for some of the distortions. The principal observation remains that the presence of polymer in the treated core apparently is not increased as a result of the treatment. Again, we are led to the conclusion that the treatment is not detectable to a significant degree by the SEC chromatogram.

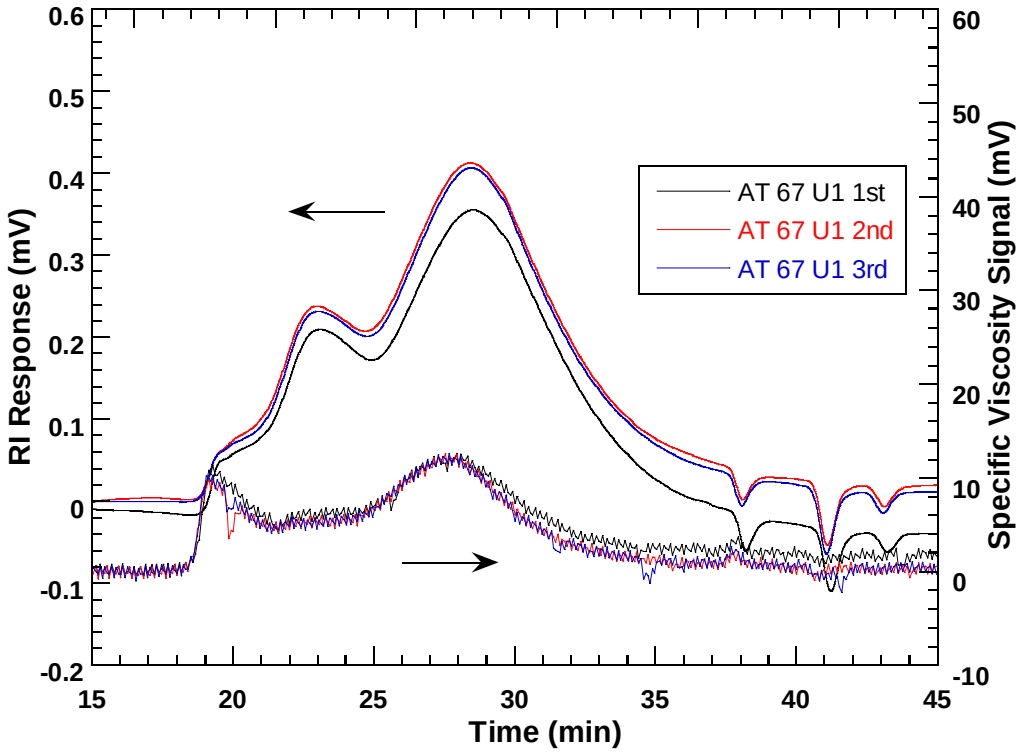

Figure 3-17a. Recovered Binder, Untreated, Atlanta US 67.

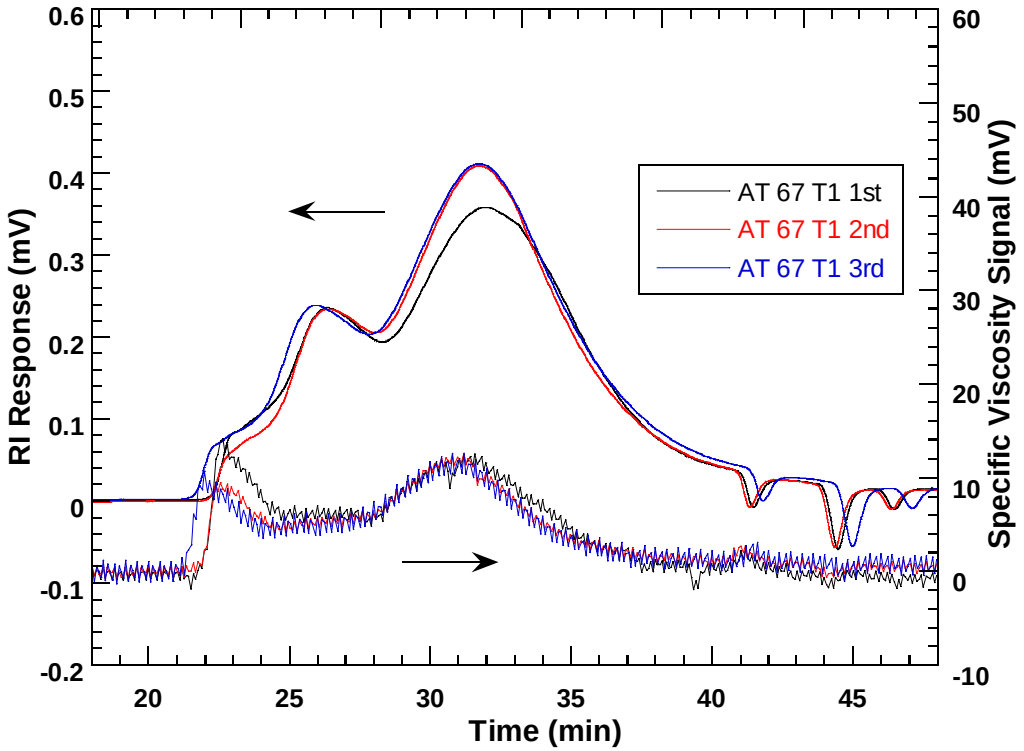

Figure 3-17b. Recovered Binder, PASS Treatment, Atlanta US 67.

Carrizo Springs Airport

Figures 3-18a and 3-18b are chromatograms for binders recovered from the Carrizo Springs Airport cores. Figure 3-18a illustrates the untreated core, and Figure 3-18b shows the treated core. At this site, a coal-tar treatment was used. As discussed earlier (Figure 3-5), the coal-tar material is a much lighter material than the asphalt in the sense of eluting at a much later time in the SEC chromatogram. The traces for the untreated core show essentially the same asphalt material in all four layers (taking into account the baseline shifts that occur in the latter part of the chromatograms). The treated binders look much the same also, with the primary exception of the first layer that shows a readily discernable amount of coal-tar, accompanied by a reduced size of the maltenes peak. The other slices of the treated core appear to be virtually unaffected by the coal-tar treatment. This pavement was constructed in 1995, and the fog seal was applied in 2004. The cores were obtained during the first year of the project.

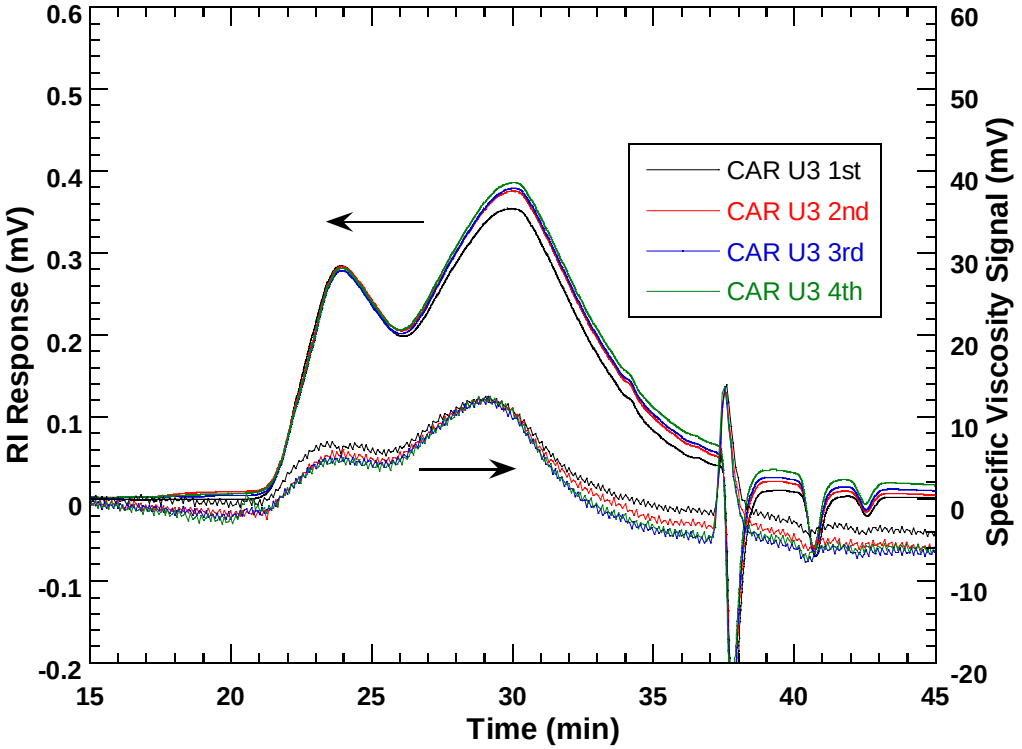

Figure 3-18a. Recovered Binder, Untreated, Carrizo Springs Airport.

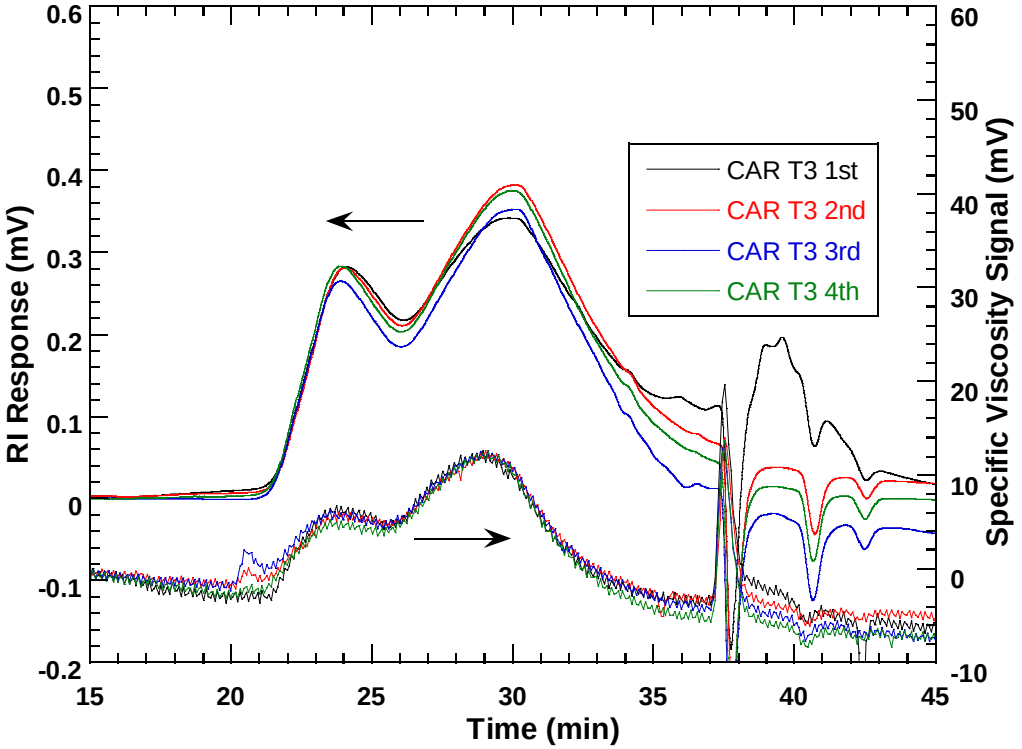

Figure 3-18b. Recovered Binder, Coal-tar Treatment, Carrizo Springs Airport.

Figures 3-19a and 3-19b show the chromatograms for the Carrizo Springs Airport cores that were obtained in the second year of the project, so these materials had an additional year of service at the time they were analyzed. Figure 3-19a, again, reflects the data from the untreated core, and there is very good reproducibility of the binders obtained from the three slices in this core in both refractive index and intrinsic viscosity detector traces. Figure 3-19b shows the chromatograms for the treated slices, and again we see the evidence of the coal-tar in the first slice, but not in the second or third slices. Otherwise, the chromatograms for each of the slices are virtually the same shape, although the third slice analysis appears to have a higher binder concentration injected into the chromatograph because both the asphaltenes and the maltenes peak are higher for this sample then for the other. It should also be noted that the coal-tar presence in this treated core is clearly at a lower concentration than it is in the core of Figure 3-18b. The reason for this difference is unknown, but it could be that the additional year of service resulted in a smaller amount of coal-tar residual in the binder, after additional weathering. Another possibility is that this particular portion of the pavement either never had, or never retained, as much treatment in the first place. There is no way to know for sure which of these possibilities is correct. The primary points to be gleaned from these results at the Carrizo Spring Airport are, first, that the fog seal treatment is clearly seen in the cores, and second that there is no evidence that they penetrated below the first quarter inch of the pavement.

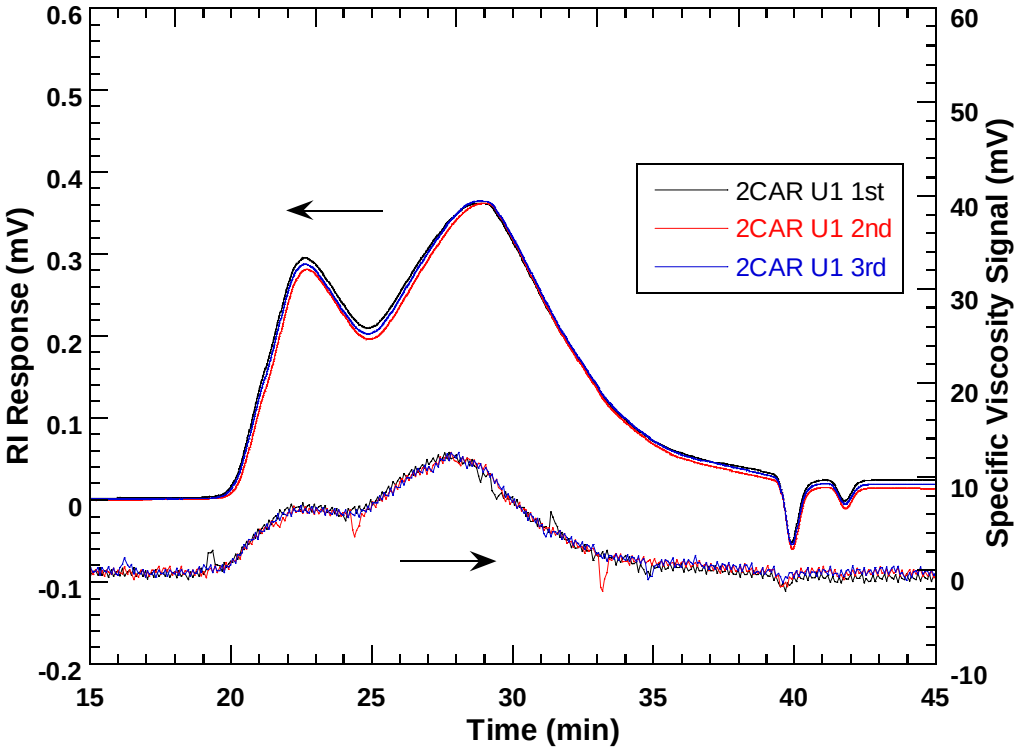

Figure 3-19a. Recovered Binder, Untreated, 2nd Year Carrizo Springs Airport.

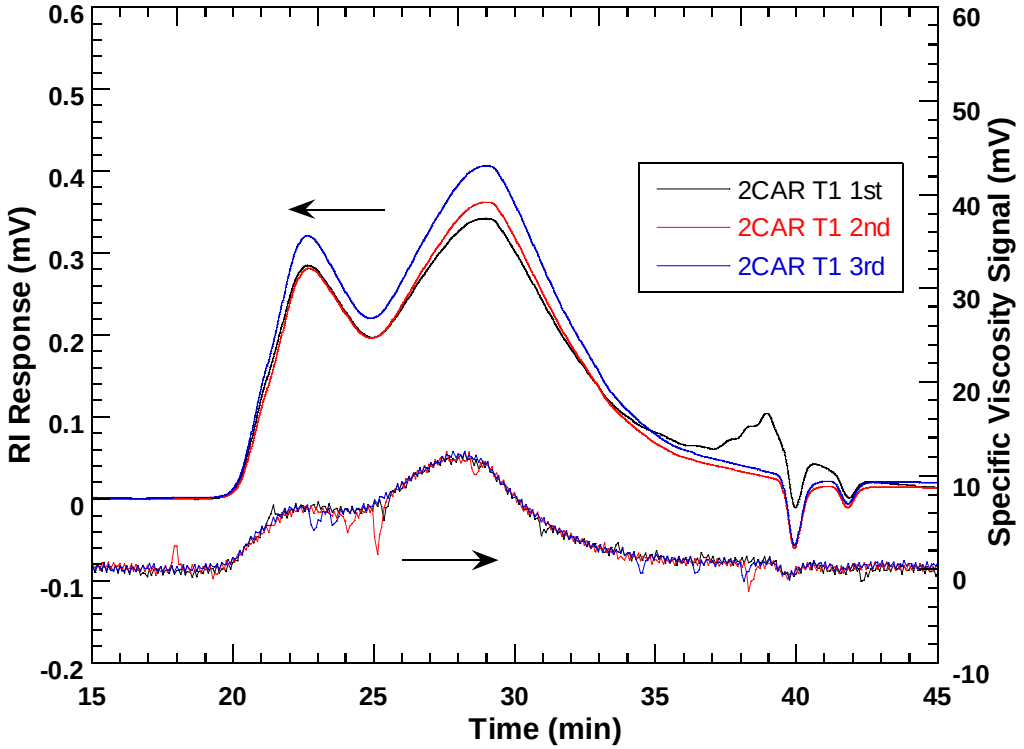

Figure 3-19b. Recovered Binder, Coal-tar Treatment, 2nd Year Carrizo Springs Airport.

Fort Worth FM 4, 2000

Figures 3-20a and 3-20b show the untreated and treated traces for the Fort Worth FM 4 pavement that was constructed in 2000 and cored in the first year of this project. These graphs show binders recovered from four slices of the pavement but it should be noted that the fourth slice had a binder that is distinctly different from the others, with the asphaltenes peak significantly smaller in size compared to the maltenes peak for this particular slice. This fourth layer also had more polymer than the other layers in both the untreated and treated cores. This pavement was treated with the COS-50 fog seal, an emulsified asphalt material that apparently had no polymer additive (Figure 3-3). Again, for this treatment as for the other asphalt emulsion treatments, SEC is unable to definitively identify the presence of the treatment in the various pavement layers. One of the features of the COS-50 asphalt material's chromatogram is that the asphaltenes and maltenes peaks are relatively close together; there is not a great deal of separation between the two. From these Fort Worth cores' chromatograms, we don't see any changes between the untreated and treated cores that would seem to suggest the presence of the COS-50 material. It should be noted, however, that the asphaltenes peak in the third slice from the treated core does seem to be relatively smaller in height than its maltenes peak, compared to the binder from the other first, second, or third slices in both the untreated and treated cores. However, because of the additional polymer that is in the third layer, this difference appears to be more due to the presence of some of the fourth layer asphalt than it does to the presence of COS-50. So again, the chromatograph is unable to produce evidence of the presence of the fog seal treatment.

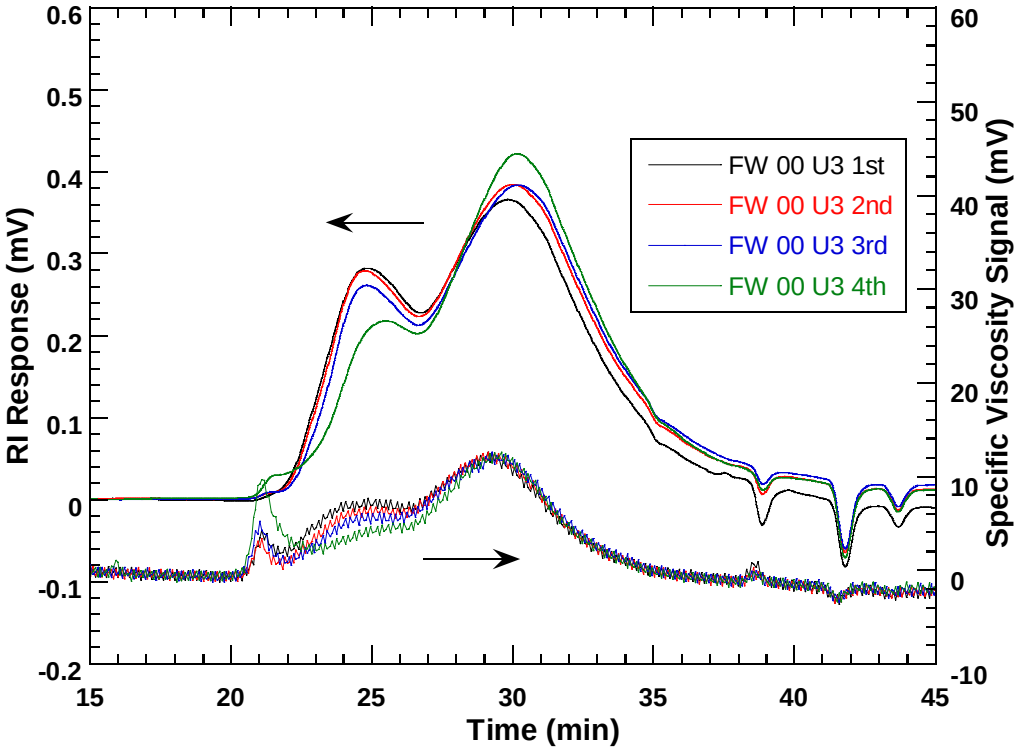

Figure 3-20a. Recovered Binder, Untreated, 1st Year Fort Worth FM 4, 2000.

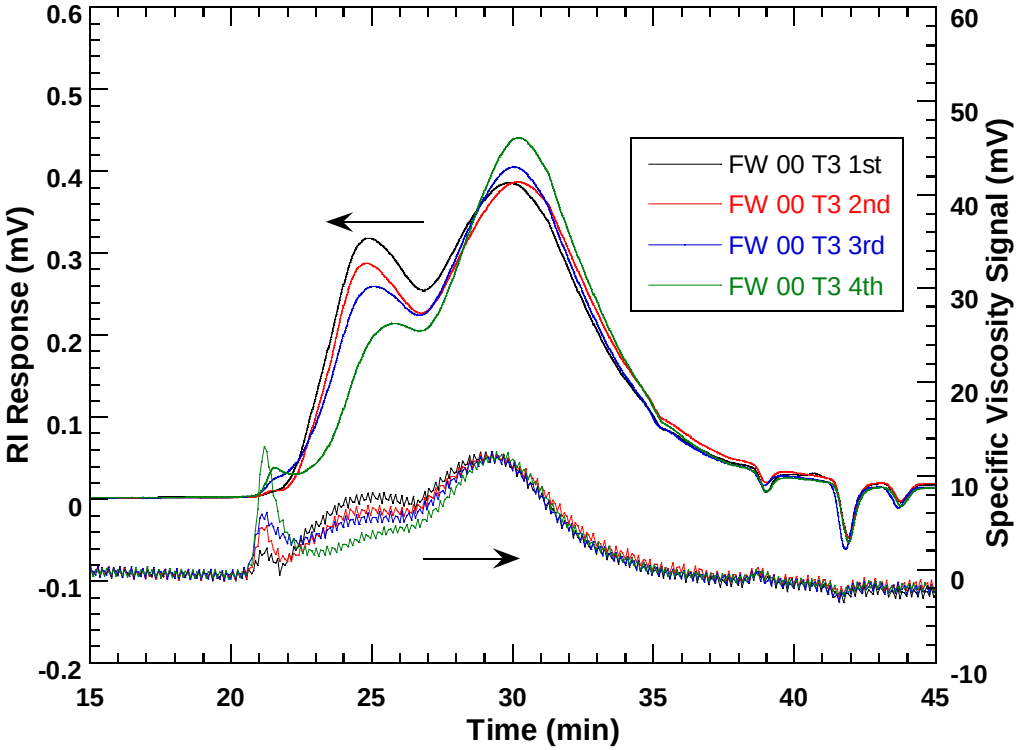

Figure 3-20b. Recovered Binder, COS-50 Treated, 1st Year Fort Worth FM 4, 2000.

This same pavement was cored in the second year of the project; Figures 3-21a and 3-21b show binder chromatograms from three slices at the top of the pavement. Again, COS-50 was the fog seal treatment. The results are very similar to the previous chromatograms in that differences between the untreated and treated cores due to the treatment cannot be identified.

Fort Worth FM 4, 2003

Another section of FM 4 in Fort Worth was constructed in 2003 and fog seal treated with COS-50 in 2005. Cores from this site were taken in the first year of the project, and the recovered binder chromatograms are shown in Figures 3-22a and 3-22b. The binder recovered from the untreated core in Figure 3-22a shows a rather interesting progression of chromatograms. Binders from slices progressively deeper into the core show a progressively smaller asphaltenes peak relative to the maltenes peak. It should also be noted that binder from the first trace has significantly more polymer than binder from any of the other slices. Binder from the slices of the treated core (Figure 3-22b) show a similar trend (allowing for the trailing baseline shift in the top slice chromatogram), but note there are only three slices represented instead of four. Also, as for the untreated cores, the polymer in the surface slice is much more evident than in the second and third slices, and the same progression in the relative size of the asphaltenes to maltenes peak is seen. Again, it is concluded that the presence of the COS-50 treatment is not discernable in the chromatogram.

Figures 3-23a and 3-23b shows untreated and treated cores from this same site, obtained in the second year of the project. No evidence of the COS-50 treatment is seen.

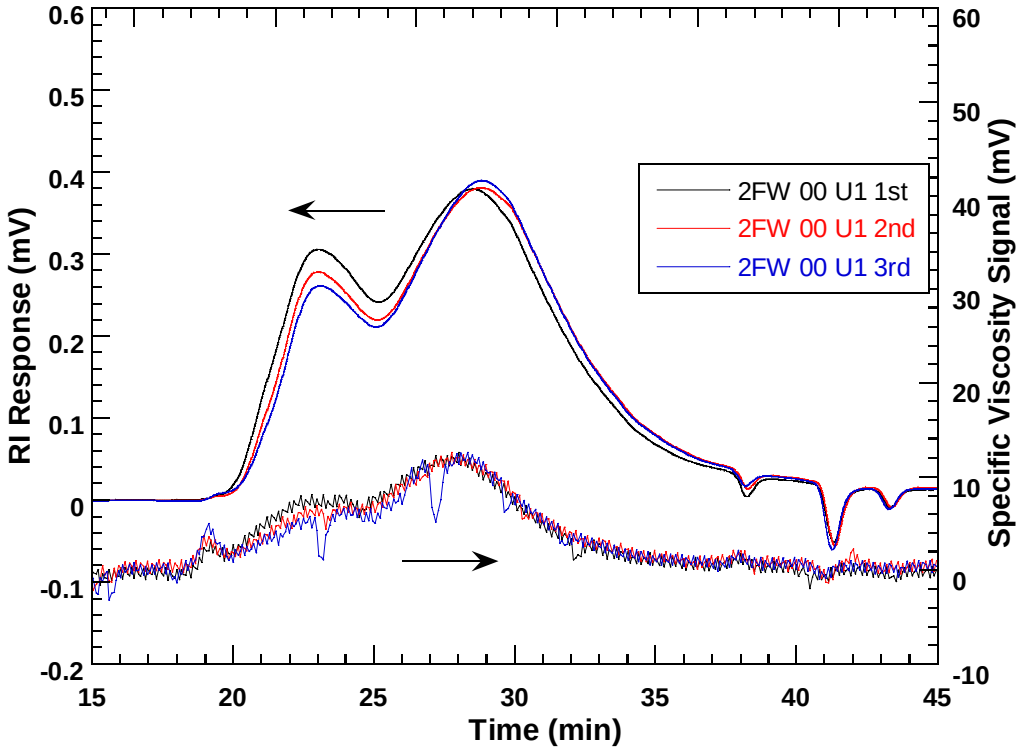

Figure 3-21a. Recovered Binder, Untreated, 2nd Year Fort Worth FM 4, 2000.

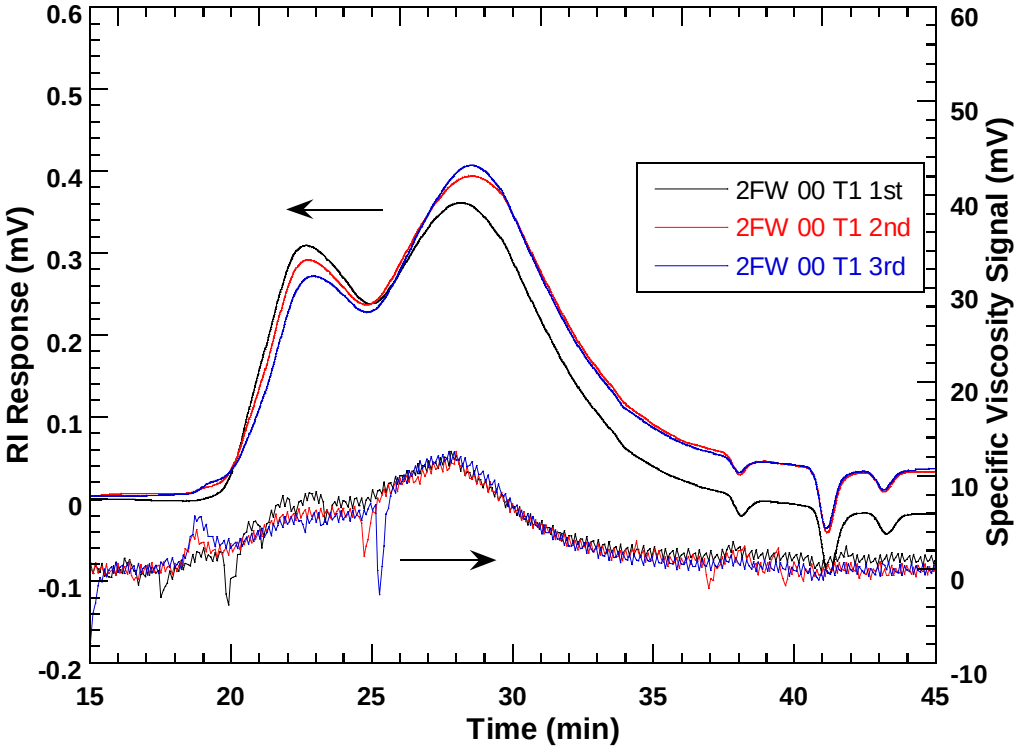

Figure 3-21b. Recovered Binder, COS-50 Treated, 2nd Year Fort Worth FM 4, 2000.

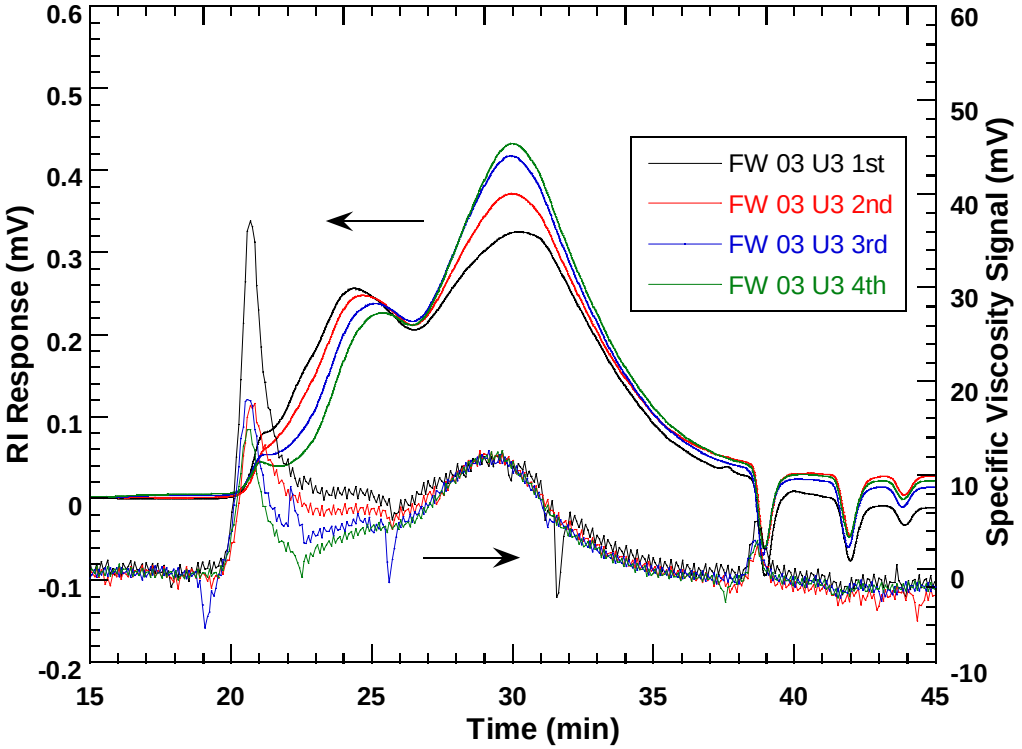

Figure 3-22a. Recovered Binder, Untreated, 1st Year Fort Worth FM 4, 2003.

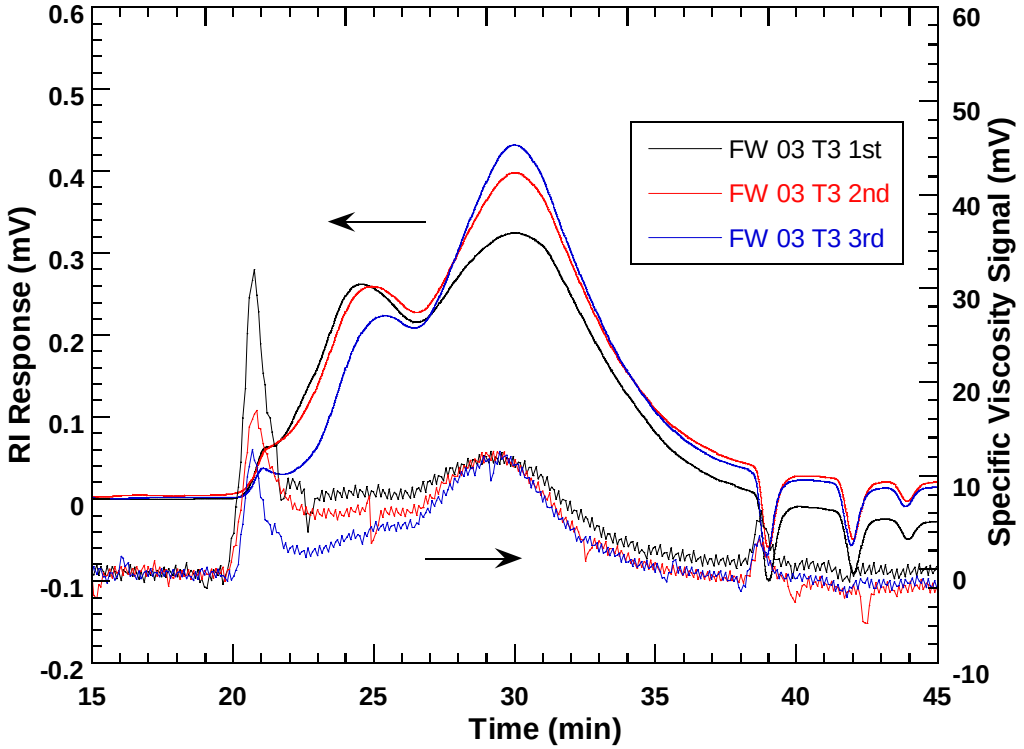

Figure 3-22b. Recovered Binder, COS-50 Treated, 1st Year Fort Worth FM 4, 2003.

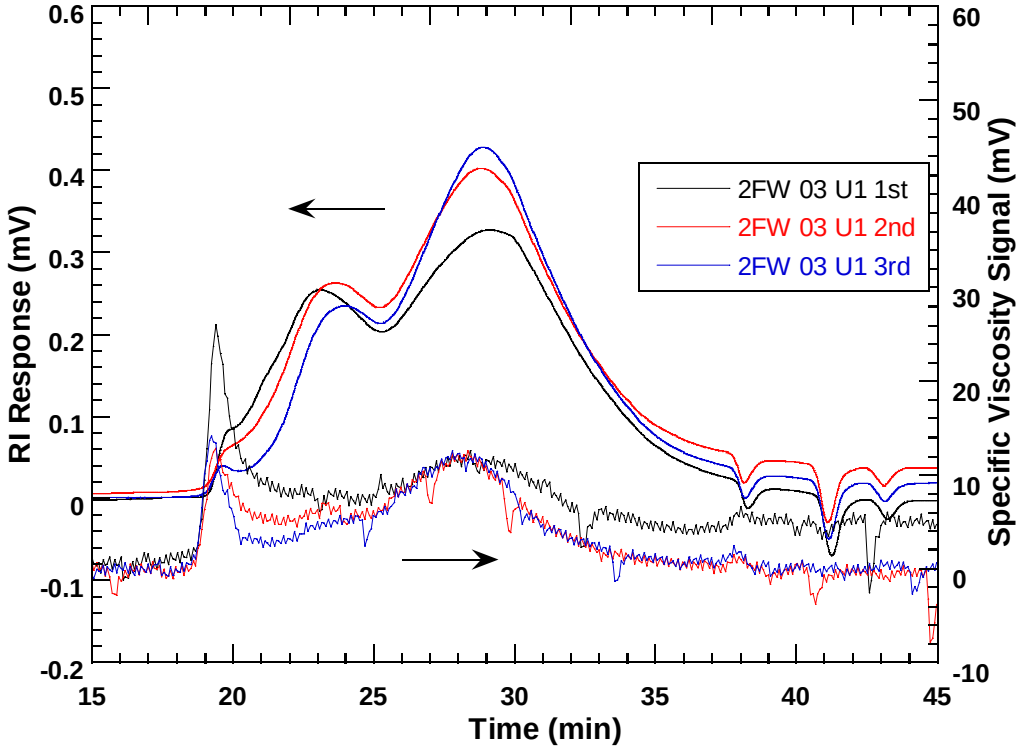

Figure 3-23a. Recovered Binder, Untreated, 2nd Year Fort Worth FM 4, 2003.

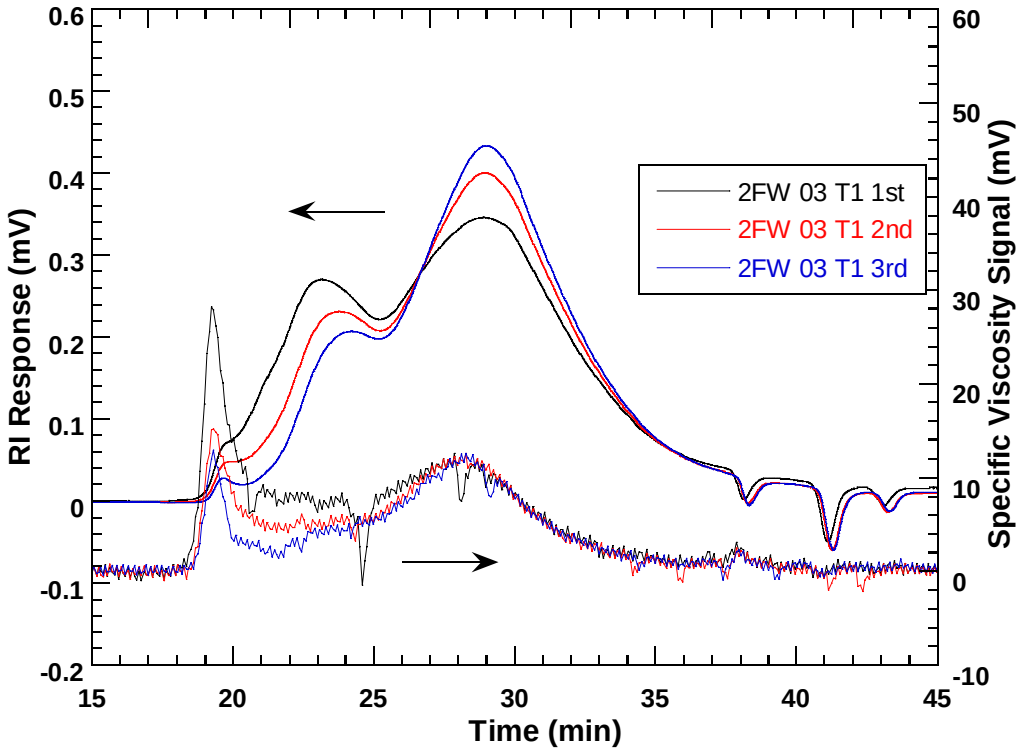

Figure 3-23b. Recovered Binder, COS-50 Treated, 2nd Year Fort Worth FM 4, 2003.

Georgetown Airport, 1989

Figures 3-24a and 3-24b show data for the Georgetown Airport site that was constructed in 1989 and fog sealed in 1999. The pavement was cored in 2004. Figure 3-24a depicts the untreated core, and Figure 3-24b shows data from the coal-tar treated core. The coal-tar material is readily seen in the binder recovered from the top slice (one-quarter inch) of the core. Besides the presence of the coal-tar material, note that the maltenes peak is reduced in this top-layer material, relative to the asphaltenes peak.

Georgetown Airport, 1995

Figures 3-25a and 3-25b show the results for a Georgetown Airport pavement constructed in 1995, treated in 1999 with EB44 coal-tar, and cored in 2004. For this pavement, the coal-tar treatment is readily seen in the first slice of the treated core, but only a very small amount is seen in a second slice and none at all in the third and fourth slices. Thus again, it appears that the treatment penetration is basically only into the top quarter inch of the pavement. Additionally, the maltenes peak is reduced in size by the treatment, as now seems typical for coal-tar treated binders.

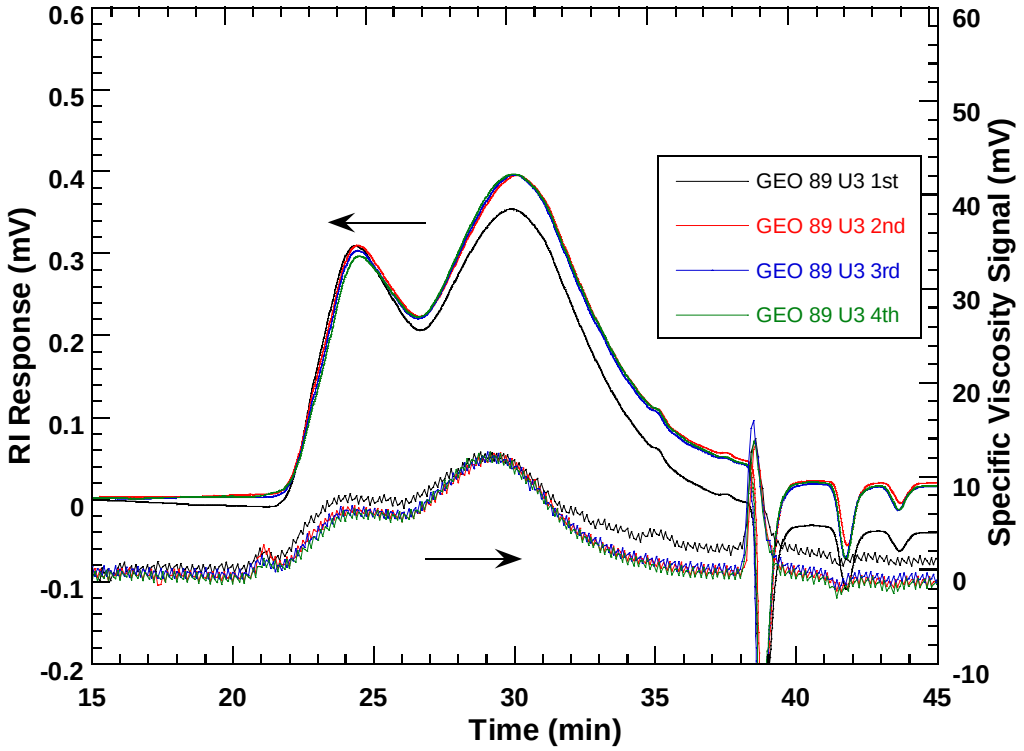

Figure 3-24a. Recovered Binder, Untreated, Georgetown Airport, 1989.

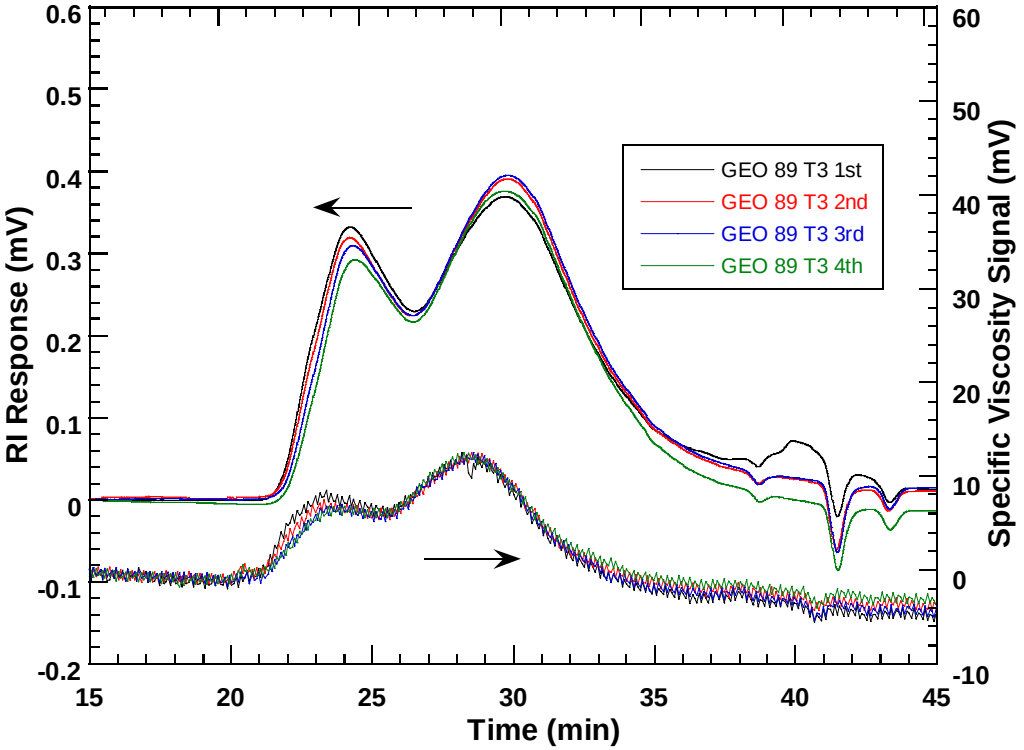

Figure 3-24b. Recovered Binder, Coal-tar Treatment, Georgetown Airport, 1989.

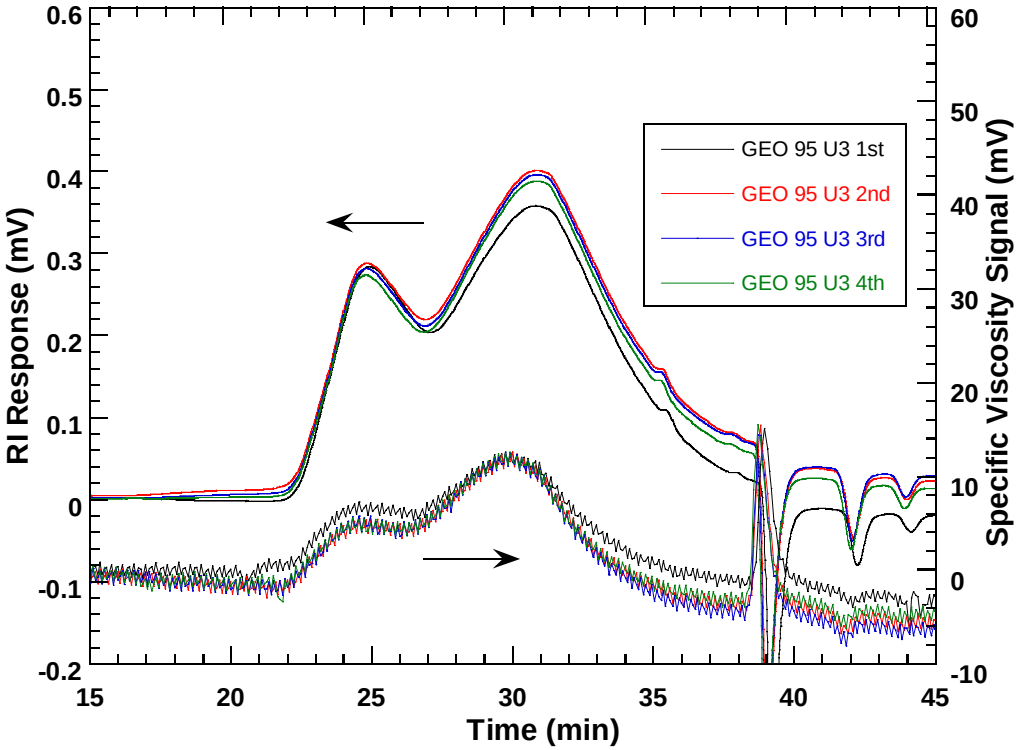

Figure 3-25a. Recovered Binder, Untreated, Georgetown, 1995.

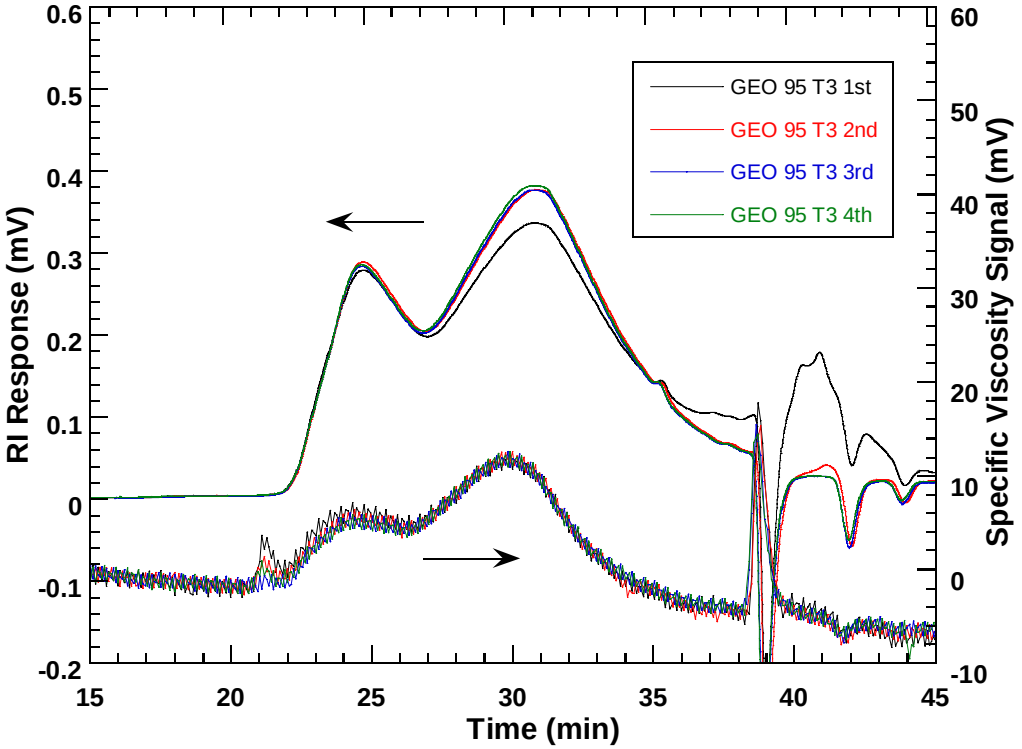

Figure 3-25b. Recovered Binder, Coal-tar Treatment, Georgetown Airport, 1995.

Jacksonville Airport

Figures 3-26a and 3-26b show chromatograms for the untreated and treated Jacksonville Airport site. The treatment material in this case was not available, but from the chromatogram of the treated core, we conclude that it was the coal-tar material. Again, comparing Figure 3-26a and 3-26b, we note that there is a very definitive evidence of a coal-tar-like material in the binder recovered from the first slice and none at all of that material in the second, third, or fourth slice binders. Again, too, the coal-tar material reduced the size of the maltenes peak in the binder recovered from the first slice of the treated core. Besides these differences in the binder of the first layer, there appear to be no discernable differences between the untreated and treated pavement chromatograms.

Figures 3-27a and 3-27b show the results from the same site, but obtained in the second year of the project. Again, we see minimal differences between the chromatograms of the asphalts, although the treated core does show the presence of the coal-tar-like material in the first layer binder. And again, the presence of the coal-tar material is accompanied by a reduction in the size of the maltenes peak for this layer. Both of these effects are less for this core obtained in the second year of the project, as they were for the Carizzo Springs airport cores.

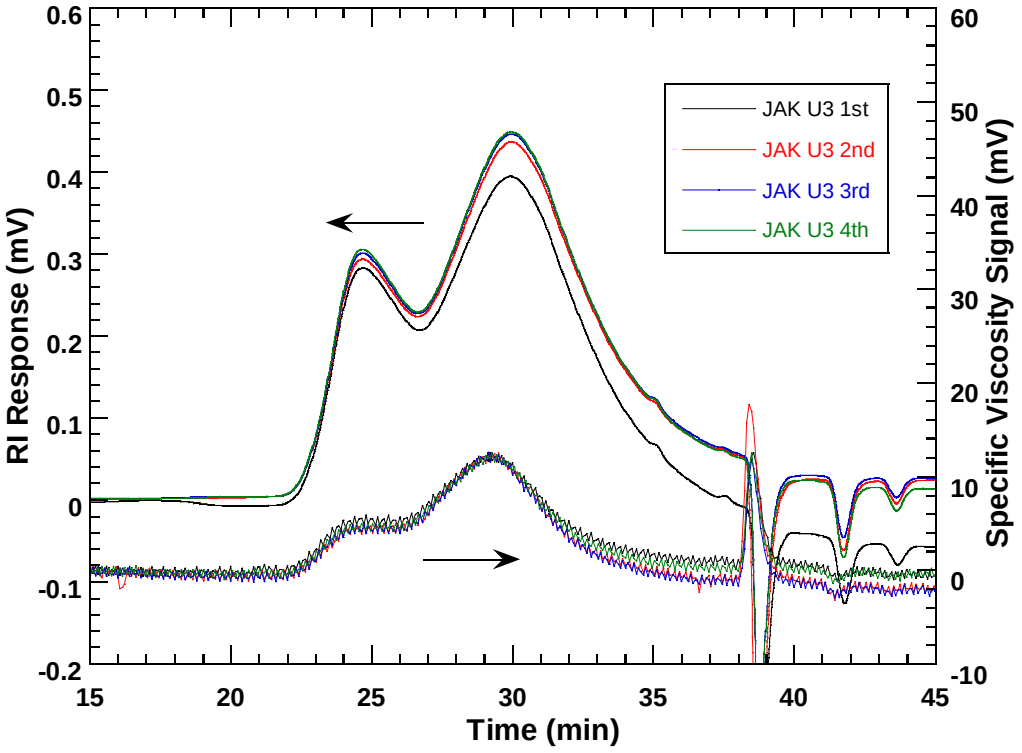

Figure 3-26a. Recovered Binder, Untreated, 1st Year Jacksonville Airport.

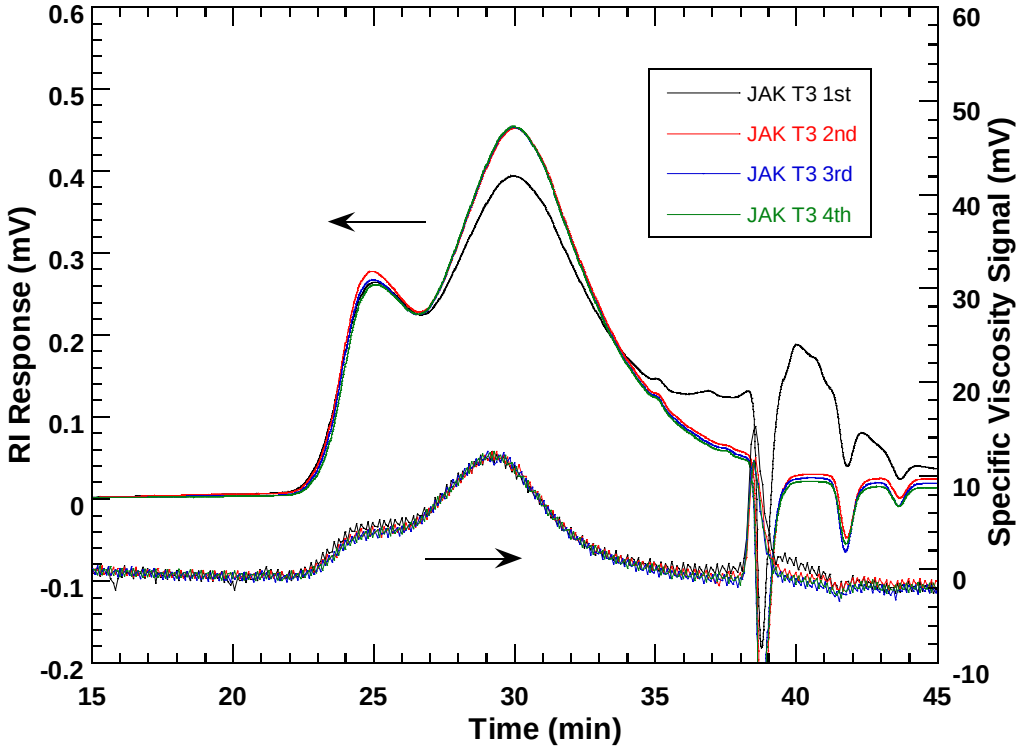

Figure 3-26b. Recovered Binder, Coal-tar Treatment, 1st Year Jacksonville Airport.

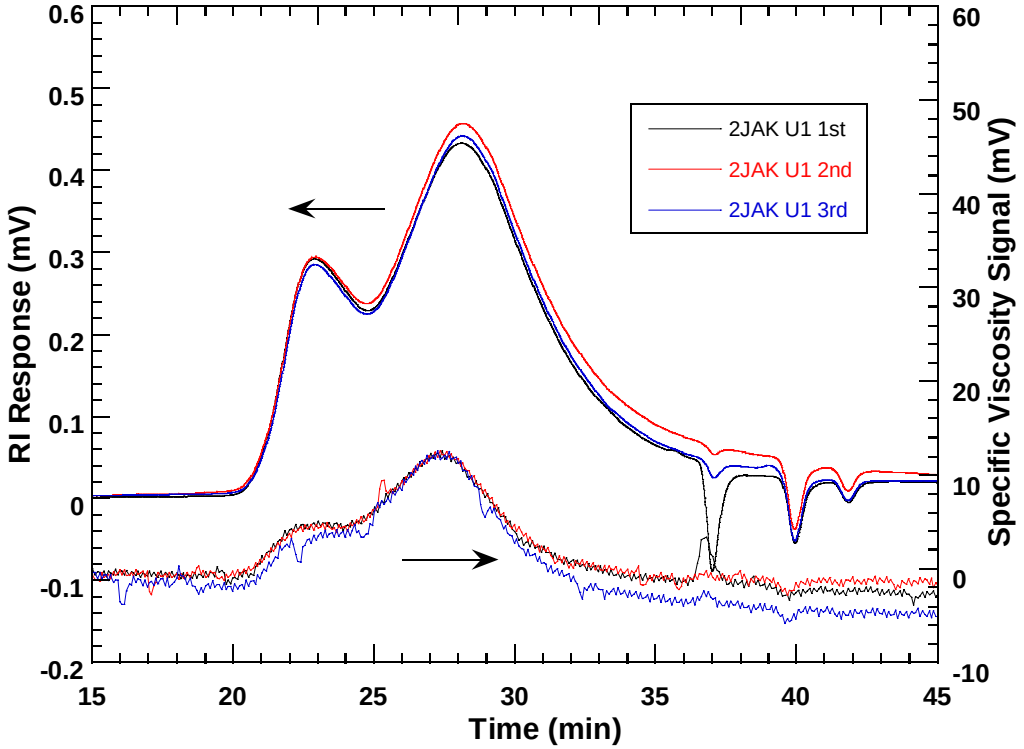

Figure 3-27a. Recovered Binder, Untreated, 2nd Year Jacksonville Airport.

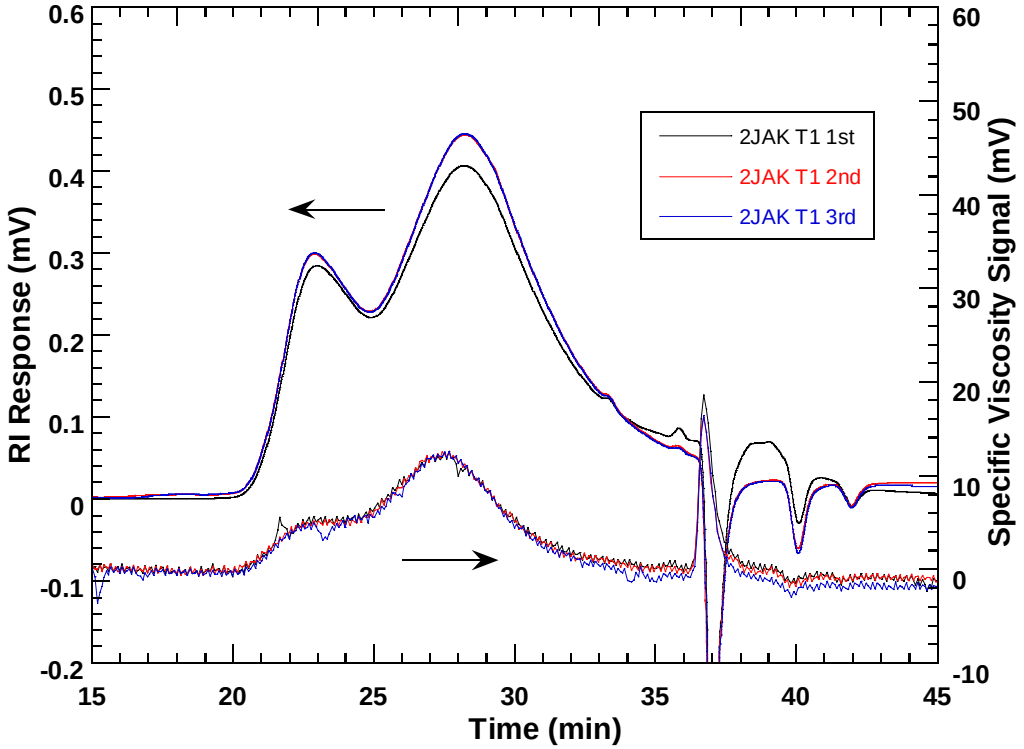

Figure 3-27b. Recovered Binder, Coal-tar Treatment, 2nd Year Jacksonville Airport.

Lufkin US 59

Figures 3-28a and 3-28b show chromatograms for the Lufkin US 59 site. A rejuvenator material (Figure 3-6), that looks much like the coal-tar material, was used for the treatment. The same observations as noted previously for the coal-tar treatments can be made for this rejuvenator material. The binder recovered from the first layer of the treated core clearly contains the rejuvenator material and the presence of the rejuvenator is accompanied by the reduction of the size of the maltenes peak relative to the asphaltenes peak. Binders from the other layers do not show any of the rejuvenator nor do they show the reduction in the maltenes peak. So again, it appears that the treatment has hardly penetrated into the pavement.

Pleasanton Airport

Figures 3-29a and 3-29b show the chromatograms for the Pleasanton Airport, treated with the coal-tar material. Again, the treated core clearly shows the evidence of the coal-tar material in the binder recovered from the first slice and this presence is accompanied by a reduction in the size of the maltenes peak. The other slices show neither the coal-tar material nor the reduction of the maltenes peak. The untreated core slices show essentially the same asphalt chromatograms with exception of the very top layer that shows an exaggerated asphaltenes peak. This exaggerated asphaltenes is most likely the result of a greater degree of oxidation in this layer compared to the others, but it is not observed in the treated core, nor has it been observed in the other chromatograms at least to this degree. Again, the conclusion appears to be that there is a minimal penetration of the coal-tar material into the pavement.

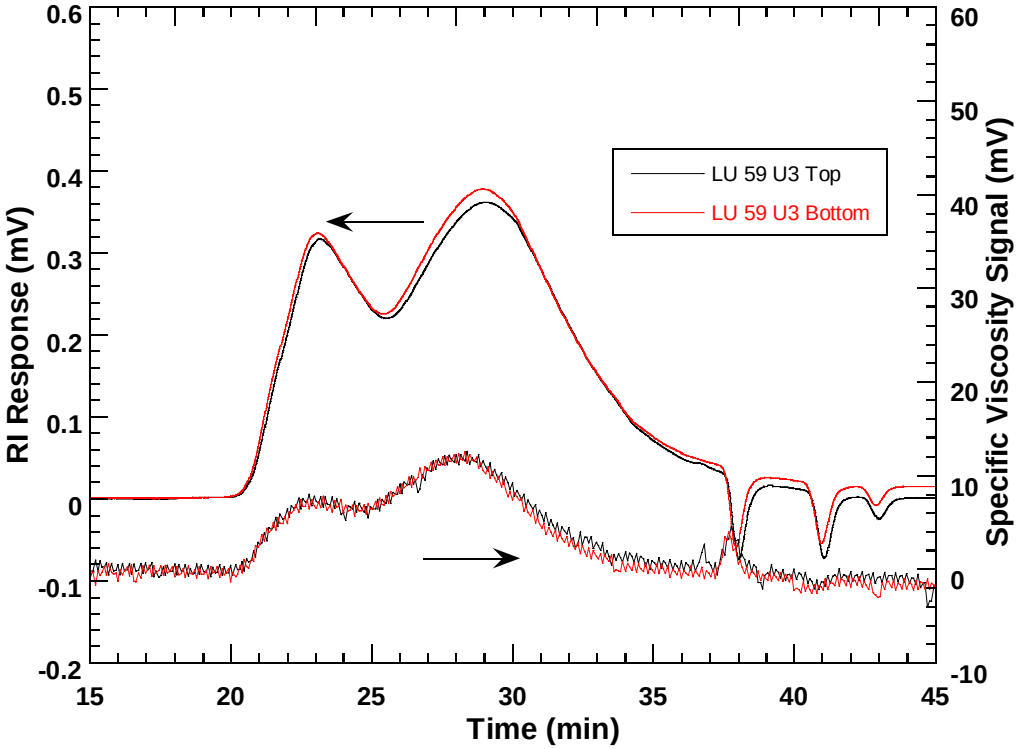

Figure 3-28a. Recovered Binder, Untreated, Lufkin BUS 59.

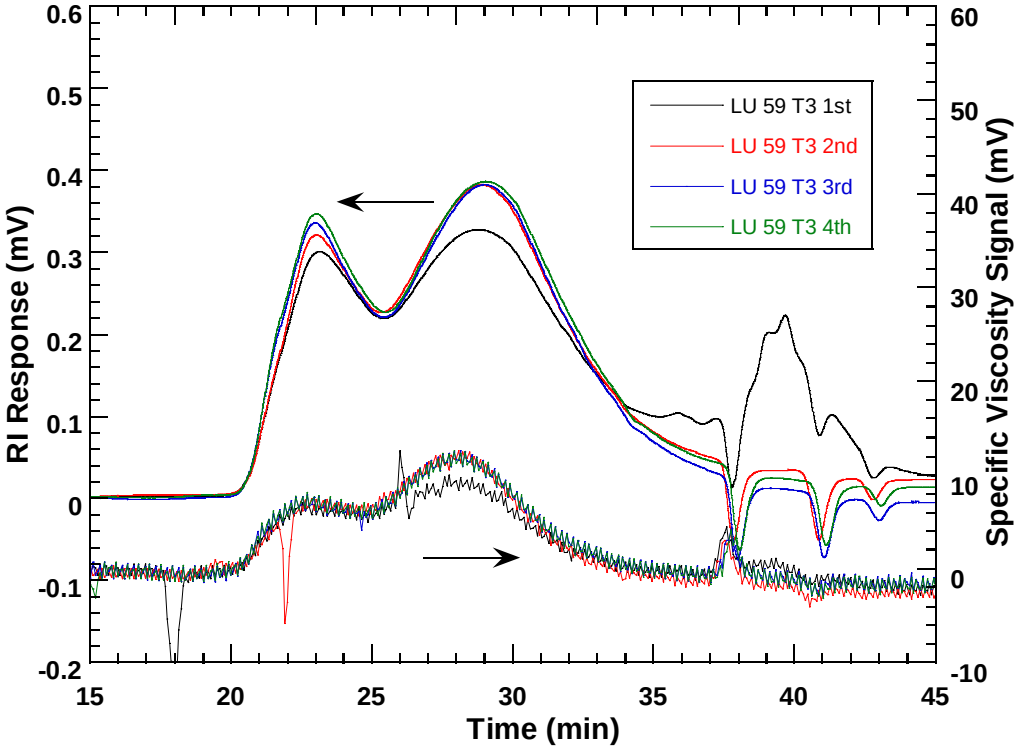

Figure 3-28b. Recovered Binder, Rejuvenator Treatment, Lufkin BUS 59.

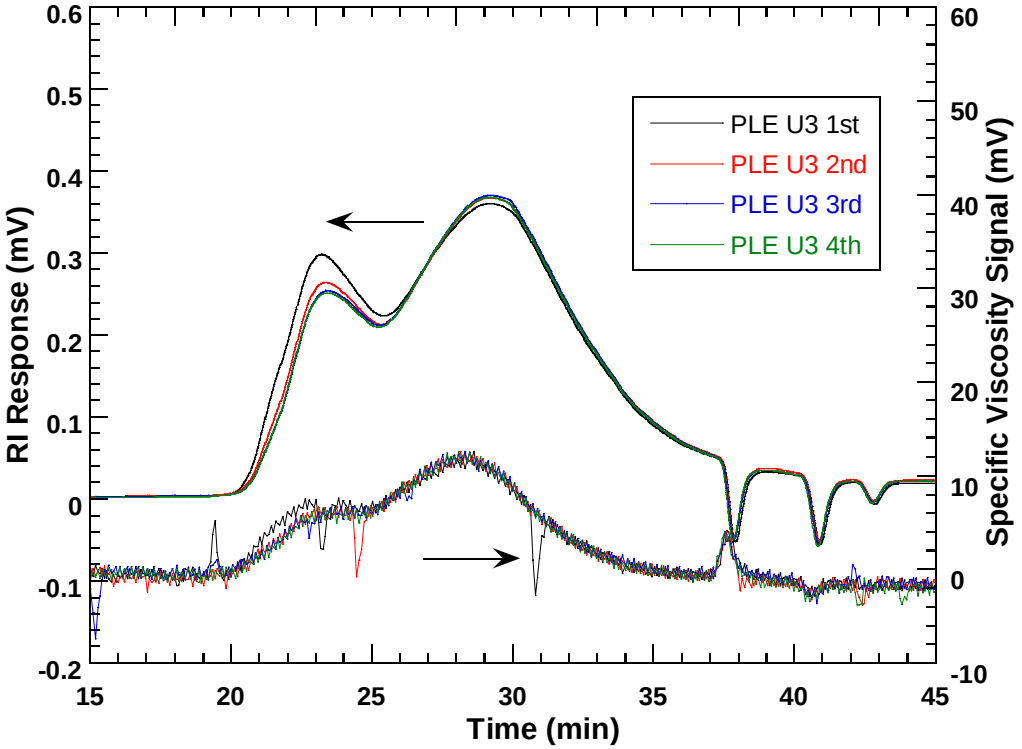

Figure 3-29a. Recovered Binder, Untreated, Pleasanton Airport.

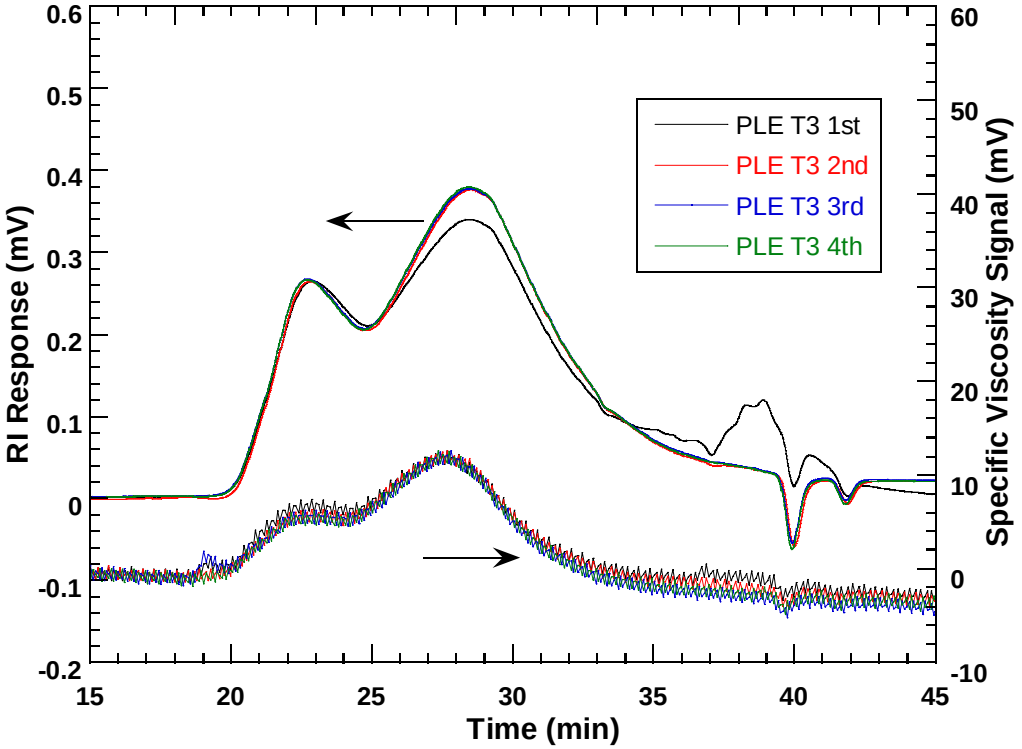

Figure 3-29b. Recovered Binder, Coal-tar Treatment, Pleasanton Airport.

Water Permeability

Water permeability values of the pavement cores were determined according to the procedure presented in Chapter 2. Data were obtained on three replicate cores for both untreated and treated sections of the pavement. Not all cores that were obtained were tested for permeability, but the great majority of them were. Tables 3-4 through 3-16 present the permeability data for the sites and core locations of this project.

Water permeabilities were measured to assess whether or not the fog seal treatments were providing any sealing of the cores to either air or moisture. Thus the comparisons that are particularly relevant are between the untreated and treated cores of the corresponding pavements at each core site. Table 3-4 shows results that are typical of all of the data. For example, for the core obtained during the second year of the project from the Abilene L1 site, we see that the untreated three replicate cores had water permeabilities that varied from 11.5 to 389.1 (10^{-6} cm/s). The corresponding treated cores range in water permeability from 91 to 116 (10^{-6} cm/s) well within the range of the three untreated cores. Similarly, for the cores obtained in the first year for the Abilene L2 site, the untreated cores range in water permeability from 2.24 to 235.9 (10^{-6} cm/s), while the treated cores range from 7.91 to 80.4 (10^{-6} cm/s). In this case, the average of the treated cores is less than the average of the untreated, but yet they fall within the range of the untreated cores, and with this small number of samples and a large standard deviation, statistically, one cannot conclude that the permeabilities of the untreated and treated cores are different, simply by comparing their mean values.

Table 3-4. Water Permeability Values of the Abilene L1 and L2 Pavement Cores.

	Condition	Replicate	PQI (g/cm^3)	k_w (10^{-6}cm/s)	Construction Year	Treatment Year	Treatment Type	Application Rate (Gal/SY)	Year Cored
1st Core Abilene L1	Untreated	U1	-	-	1998	-	-	-	-
		U2	-	-					
		U3	-	-					
	Treated	T1	-	419.9	1998	2004	MS-2	0.15	2005
		T2	-	32.9					
		T3	-	33.7					
2nd Core Abilene L1	Untreated	U1	2.80	389.1	1998	-	-	-	2006
		U2	2.46	11.8					
		U3	2.55	11.5					
	Treated	T1	2.78	113.1	1998	2004	MS-2	0.15	2006
		T2	2.47	116.1					
		T3	2.53	90.9					
1st Core Abilene L2	Untreated	U1	-	2.24	1998	-	-	-	2004
		U2	-	235.9					
		U3	-	50.6					
	Treated	T1	-	80.4	1998	2004	PASS	0.11	2004
		T2	-	7.91					
		T3	-	59.4					
2nd Core Abilene L2	Untreated	U1	2.66	174.1	1998	-	-	-	2006
		U2	2.34	208.8					
		U3	2.40	156.8					
	Treated	T1	2.50	95.5	1998	2004	PASS	0.11	2006
		T2	2.32	181.5					
		T3	2.37	8.77					

Table 3-5. Water Permeability Values of the R1 and R2 Abilene Pavement Cores.

	Condition	Replicate	PQI (g/cm^3)	k_w (10^{-6}cm/s)	Construction Year	Treatment Year	Treatment Type	Application Rate (Gal/SY)	Year Cored
1st Core Abilene R1	Untreated	U1	-	17.9	1998	-	-	-	2004
		U2	-	150.6					
		U3	-	9.46					
	Treated	T1	-	29.9	1998	2004	PASS	0.16	2004
		T2	-	0.00					
		T3	-	0.00					
2nd Core Abilene R1	Untreated	U1	2.35	31.3	1998	-	-	-	2006
		U2	2.41	595.2					
		U3	2.42	64.7					
	Treated	T1	2.37	23.3	1998	2004	PASS	0.16	2006
		T2	2.41	6.65					
		T3	2.45	36.6					
1st Core Abilene R2	Untreated	U1	-	-	1998	-	-	-	-
		U2	-	-					
		U3	-	-					
	Treated	T1	-	35.0	1998	2004	MS-2	0.15	2005
		T2	-	152.7					
		T3	-	6.49					
2nd Core Abilene R2	Untreated	U1	2.49	33.2	1998	-	-	-	2006
		U2	2.45	17.2					
		U3	2.46	15.4					
	Treated	T1	2.50	34.8	1998	2004	MS-2	0.15	2006
		T2	2.49	0.28					
		T3	2.48	175.1					

Table 3-6. Water Permeability Values of the Atlanta Pavement Cores.

	Condition	Replicate	PQI (g/cm^3)	k_w (10^{-6}cm/s)	Construction Year	Treatment Year	Treatment Type	Application Rate (Gal/SY)	Year Cored
1st Core Atlanta IH 20 CM	Untreated	U1	2.44	1759.3	2001	-	-	-	2006
		U2	2.34	1741.9					
		U3	2.31	1676.0					
	Treated	T1	-	-	2001	2006	CSS-1	0.10	2006
		T2	-	-					
		T3	-	-					
1st Core Atlanta IH 20 DG	Untreated	U1	2.79	1280.6	2001	-	-	-	2006
		U2	2.88	805.4					
		U3	3.00	1045.6					
	Treated	T1	-	-	2001	2006	CSS-1	0.10	2006
		T2	-	-					
		T3	-	-					
1st Core Atlanta IH 20 SP	Untreated	U1	3.00	0.00	2001	-	-	-	2006
		U2	3.22	8.63					
		U3	3.21	4.15					
	Treated	T1	-	-	2001	2006	CSS-1	0.10	2006
		T2	-	-					
		T3	-	-					
1st Core Atlanta US 67	Untreated	U1	2.07	168.3	2003	-	-	-	2006
		U2	2.31	149.6					
		U3	2.20	149.9					
	Treated	T1	2.01	111.8	2003	2004	PASS	0.1	2006
		T2	2.50	62.5					
		T3	2.19	529.4					

Table 3-7. Water Permeability Values of the Carrizo Springs Airport.

	Condition	Replicate	PQI (g/cm^3)	k_w (10^{-6}cm/s)	Construction Year	Treatment Year	Treatment Type	Application Rate (Gal/SY)	Year Cored
1st Core Carrizo Springs Airport	Untreated	U1	-	0.26	1995	-	-	-	2004
		U2	-	0.00					
		U3	-	0.00					
	Treated	T1	-	0.36	1995	2004	EB 44	0.055	2005
		T2	-	0.53					
		T3	-	1.18					
2nd Core Carrizo Springs Airport	Untreated	U1	2.39	23.7	1995	-	-	-	2006
		U2	2.35	11.3					
		U3	2.38	11.4					
	Treated	T1	2.40	0.00	1995	2004	EB 44	0.055	2006
		T2	2.34	8.09					
		T3	2.33	1.18					

Table 3-8. Water Permeability Values of the Fort Worth 2000 Pavement Cores.

	Condition	Replicate	PQI (g/cm^3)	k_w (10^{-6}cm/s)	Construction Year	Treatment Year	Treatment Type	Application Rate (Gal/SY)	Year Cored
1st Core Fort Worth FM 4 (2000)	Untreated	U1	-	0.69	2000	-	-	-	2005
		U2	-	0.48					
		U3	-	0.15					
	Treated	T1	-	0.45	2000	2005	COS-50	0.14	2005
		T2	-	0.65					
		T3	-	1.25					
2nd Core Fort Worth FM 4 (2000)	Untreated	U1	2.25	1.58	2000	-	-	-	2006
		U2	2.31	12.7					
		U3	2.44	199.8					
	Treated	T1	2.23	8.76	2000	2005	COS-50	0.14	2006
		T2	2.30	4.92					
		T3	2.46	11.0					

Table 3-9. Water Permeability Values of the Fort Worth 2003 Pavement Cores.

	Condition	Replicate	PQI (g/cm^3)	k_w (10^{-6}cm/s)	Construction Year	Treatment Year	Treatment Type	Application Rate (Gal/SY)	Year Cored
1st Core Fort Worth FM 4 (2003)	Untreated	U1	-	0.00	2003	-	-	-	2005
		U2	-	0.00					
		U3	-	1.60					
	Treated	T1	-	0.12	2003	2005	COS-50	0.14	2005
		T2	-	0.00					
		T3	-	0.00					
2nd Core Fort Worth FM 4 (2003)	Untreated	U1	2.30	19.8	2003	-	-	-	2006
		U2	2.49	103.0					
		U3	2.56	20.4					
	Treated	T1	2.27	0.00	2003	2005	COS-50	0.14	2006
		T2	2.51	0.00					
		T3	2.55	0.00					

Table 3-10. Water Permeability Values of the Georgetown Airport 1989 Pavement Cores.

	Condition	Replicate	PQI (g/cm^3)	k_w (10^{-6}cm/s)	Construction Year	Treatment Year	Treatment Type	Application Rate (Gal/SY)	Year Cored
1st Core Georgetown Airport (1989)	Untreated	U1	-	2.91	1989	-	-	-	2004
		U2	-	1.55					
		U3	-	1.78					
	Treated	T1	-	9.14	1989	1999	EB 44	0.05	2004
		T2	-	0.00					
		T3	-	0.00					
2nd Core Georgetown Airport (1989)	Untreated	U1	2.66	0.28	1989	-	-	-	2006
		U2	2.24	0.00					
		U3	2.64	0.39					
	Treated	T1	2.68	1.06	1989	1999	EB 44	0.05	2006
		T2	2.25	0.83					
		T3	2.64	4.57					

Table 3-11. Water Permeability Values of the Georgetown Airport 1995 Pavement Cores.

	Condition	Replicate	PQI (g/cm^3)	k_w (10^{-6}cm/s)	Construction Year	Treatment Year	Treatment Type	Application Rate (Gal/SY)	Year Cored
1st Core Georgetown Airport (1995)	Untreated	U1	-	252.5	1995	-	-	-	2004
		U2	-	208.7					
		U3	-	0.00					
	Treated	T1	-	0.00	1995	1999	EB 44	0.05	2004
		T2	-	0.00					
		T3	-	0.00					
2nd Core Georgetown Airport (1995)	Untreated	U1	2.47	0.00	1995	-	-	-	2006
		U2	2.37	4.61					
		U3	2.43	4.33					
	Treated	T1	2.43	0.00	1995	1999	EB 44	0.05	2006
		T2	2.36	0.00					
		T3	2.47	0.00					
	Treated*	T1	2.42	94.2	1995	2006	EB 44	0.05	2006
		T2	2.36	50.8					
		T3	2.47	74.2					

Table 3-12. Water Permeability Values of the Jacksonville Airport Pavement Cores.

	Condition	Replicate	PQI (g/cm^3)	k_w (10^{-6}cm/s)	Construction Year	Treatment Year	Treatment Type	Application Rate (Gal/SY)	Year Cored
1st Core Jacksonville Airport	Untreated	U1	-	14.1	2004	-	-	-	2004
		U2	-	21.5					
		U3	-	0.58					
	Treated	T1	-	0.00	2004	2004	N/A	0.05	2004
		T2	-	0.00					
		T3	-	0.01					
2nd Core Jacksonville Airport	Untreated	U1	2.37	4.96	2004	-	-	-	2006
		U2	2.42	19.0					
		U3	2.47	43.4					
	Treated	T1	2.37	59.9	2004	2005	N/A	0.05	2006
		T2	2.42	153.9					
		T3	2.49	67.3					

Table 3-13. Water Permeability Values of the Lufkin BUS 59 Pavement Cores.

	Condition	Replicate	PQI (g/cm^3)	k_w (10^{-6} cm/s)	Construction Year	Treatment Year	Treatment Type	Application Rate (Gal/SY)	Year Cored
1st Core Lufkin BUS 59	Untreated	U1	-	0.00	1995	-	-	-	2004
		U2	-	0.00					
		U3	-	0.04					
	Treated	T1	-	0.00	1995	2004	Rejuvenator	0.10	2004
		T2	-	0.00					
		T3	-	0.00					
2nd Core Lufkin BUS 59	Untreated	U1	2.39	0.97	1995	-	-	-	2006
		U2	2.51	0.39					
		U3	2.61	0.00					
	Treated	T1	2.41	7.60	1995	2004	Rejuvenator	0.10	2006
		T2	2.49	0.00					
		T3	2.65	0.00					

Table 3-14. Water Permeability Values of the Odessa SH 149 Pavement Cores.

	Condition	Replicate	PQI (g/cm^3)	k_w (10^{-6} cm/s)	Construction Year	Treatment Year	Treatment Type	Application Rate (Gal/SY)	Year Cored
1st Core Odessa SH 149	Untreated	U1	2.32	0.00	1983	-	-	-	2006
		U2	2.36	0.00					
		U3	2.47	0.00					
	Treated	T1	2.33	0.00	1983	2002	SS-1	0.09	2006
		T2	2.36	0.00					
		T3	2.46	0.00					
1st Core Odessa SH 349	Untreated	U1	2.52	0.00	1996	-	-	-	2006
		U2	2.40	0.00					
		U3	2.29	0.00					
	Treated	T1	2.55	0.00	1996	2006	SS-1	0.09	2006
		T2	2.39	0.00					
		T3	2.33	0.00					

Table 3-15. Water Permeability Values of the Pleasanton Pavement Cores.

	Condition	Replicate	PQI (g/cm^3)	k_w (10^{-6} cm/s)	Construction Year	Treatment Year	Treatment Type	Application Rate (Gal/SY)	Year Cored
1st Core Pleasanton Airport	Untreated	U1	-	0.03	1985	-	-	-	2004
		U2	-	0.00					
		U3	-	0.03					
	Treated	T1	-	0.00	1985	2004	EB 44	0.043	2004
		T2	-	0.00					
		T3	-	0.33					
2nd Core Pleasanton Airport	Untreated	U1	-	-	1985	-	-	-	-
		U2	-	-					
		U3	-	-					
	Treated	T1	2.23	0.0	1985	2004	EB 44	0.043	2006
		T2	2.21	0.0					
		T3	2.21	0.0					

Table 3-16. Water Permeability Values of the Tyler US 79 Pavement Cores.

	Condition	Replicate	PQI (g/cm^3)	k_w (10^{-6} cm/s)	Construction Year	Treatment Year	Treatment Type	Application Rate (Gal/SY)	Year Cored
1st Core Tyler US 79	Untreated	U1	2.69	1233.0	2002	-	-	-	2006
		U2	2.68	1128.7					
		U3	2.70	1099.4					
	Treated	T1	2.70	753.3	2002	2005	PASS	0.10	2006
		T2	2.71	586.0					
		T3	2.72	1010.2					

As a statistical method of assessing changes to permeability associated with the fog seal treatments, the paired t-test, also called the t-test for two correlated samples, was used (Montgomery, 2001). For this test, 1) data are matched in pairs (treated versus untreated in this case, on a site by site basis so that the only designed difference between the elements of a pair was the treatment), 2) the differences between the water permeabilities of the pair members is calculated, 3) this set of differences is then used to calculate the *t*-statistic, and 4) the *t*-test is applied using Student's *t* distribution to assess the probability that the mean difference between pairs is the result of chance.

The *t*-statistic is calculated as (*n* pairs of x_i, y_i data; $D_i = x_i, - y_i$):

$$t = \overline{D} / \sqrt{\frac{1}{n(n-1)} \sum_{i=1}^{n} (D_i - \overline{D})^2} \quad \text{where } \overline{D} \text{ is the mean difference: } \overline{D} = \frac{1}{n} \sum_{i=1}^{n} D_i \qquad (3\text{-}1)$$

Results are shown in Table 3-17 for all of the sites and all of the treatments. The replicates at a given site were averaged and then the difference between these average untreated and average treated values were used as the D_i values. The number of samples (*n*) was 25 to give 24 degrees of freedom. A mean difference in water permeability of 35 x 10^{-6} cm/s (treated cores less than treated) was obtained with a *t*-statistic of 1.90, giving a directional (one-tailed) probability that this mean difference has chance of occurrence of 3.5 percent (p=0.035).

Considering the separate treatments gave the following results: PASS ($n = 8$), $p = 0.067$; EB44 coal-tar ($n = 9$), $p = 0.28$; COS-50 ($n = 4$), $p = 0.094$. The other treatments did not have enough data to perform a meaningful calculation. These results suggest that the PASS treatment (and perhaps also the COS-50) may have some effect on decreasing the pavement permeability, and that this effect drives the *p* value for the entire data set to below 5 percent. The EB44 shows practically no probability that it is reducing permeability.

It should be noted that there is another factor besides the various treatments that may affect the pavement permeability, the passage of time. To the extent pavements tend to be plugged by debris over time, we would expect a later cored pavement to exhibit a lower permeability than an earlier cored pavement. However, this effect would not seem to bias one treatment in favor of another, the PASS in favor of the EB44, for example.

Table 3-17. Water Permeability Paired *t*-Test, All Data.

Sample	Site	Type	Water Permeability (10^{-6} cm/s) Untreated	Treated	Di		
1	2 Abilene L1	MS-2	137.44	106.68	30.76	Mean	35.16
2	Abilene L2	PASS	96.27	49.24	47.03	Standard Deviation	18.54
3	2 Abilene L2	PASS	179.87	95.28	84.59		
4	Abilene R1	PASS	59.33	9.96	49.37		
5	2Abilene R1	PASS	230.41	22.18	208.23	t	1.90
6	2 Abilene R2	MS-2	21.95	70.06	-48.12	p	0.035
7	Atlanta 67	PASS	155.93	234.56	-78.64		
8	Carrizo Springs	EB44	0.09	0.69	-0.60		
9	2 Carrizo Springs	EB44	15.44	3.09	12.35		
10	Fort Worth 2000	COS-50	0.44	0.78	-0.34		
11	2 Fort Worth 2000	COS-50	71.34	8.21	63.13		
12	Fort Worth 2003	COS-50	0.53	0.04	0.49		
13	2 Fort Worth 2003	COS-50	47.75	0.00	47.75		
14	Georgetown 1989	EB44	2.08	3.05	-0.97		
15	2 Georgetown 1989	EB44	0.22	2.15	-1.93		
16	Georgetown 1995	EB44	153.71	0.00	153.71		
17	2 Georgetown 1995	EB44	2.98	0.00	2.98		
18	Jacksonville	EB44	12.05	0.00	12.05		
19	2 Jacksonville	EB44	22.45	93.69	-71.24		
20	Lufkin	PASS	0.01	0.00	0.01		
21	2 Lufkin	PASS	0.45	2.53	-2.08		
22	Odessa 149	SS-1	0.00	0.00	0.00		
23	Odessa 349	SS-1	0.00	0.00	0.00		
24	Pleasanton	EB44	0.02	0.11	-0.09		
25	Tyler	PASS	1153.68	783.17	370.52		

SUMMARY AND CONCLUSIONS

The objective of this chapter was to determine whether or not the fog seal treatments penetrate into the pavement and if so, whether they are performing any significant sealing of the pavement. Based upon the detailed SEC chromatograms for each quarter-inch slice and measured water permeabilities, it seems clear that 1) if the fog seal is penetrating and remaining in the pavement, it is not doing so to a detectable level and 2) the permeability of the pavement is not significantly reduced. The issues of other effects of the fog seal treatment are discussed in the next chapter.

CHAPTER 4

EFFECTS OF FOG SEAL TREATMENTS ON BINDER PROPERTIES AND BINDER AGING

INTRODUCTION

In the previous chapter, cores from the various fog seal sites were examined by quarter-inch layers for the presence of the fog seal treatments. Furthermore, the water permeability of the cores was measured to determine if the treatment add a measurable effect on the pavements' permeability. The research team concluded that the fog seal treatments cannot be, definitively, detected in most of the pavement layers. However, the coal-tar treatment and the rejuvenator treatments were the exception to this general statement in that these treatments could be detected in the top quarter inch layer, but not in any others. Concerning water permeability, the fog seal treatment was not observed to have a clear impact on the permeability. Thus, in the previous chapter, the conclusion was that as far as the penetration and permeability are concerned, little or no effect of the treatments could be determined.

Of course the fact that the fog seal treatments cannot be detected in the layers of the pavement does not necessary imply that they are not effective. The ability of the detection methods to detect the treatments may just be inadequate. Therefore, the question addressed by the work of this chapter is whether, in fact, the fog seal treatments have a measurable impact on the recovered binder physical properties or on the binder aging in the pavements.

METHODOLOGY

Chapter 2 describes the methods used for the results of this chapter. Layer by layer, the binder in both untreated and treated cores from the fog seal treatment sites were extracted and recovered. Then those recovered binders were measured as to their rheology (DSR function, η^* master curves and calculated ductility) and aging (FT-IR carbonyl band – CA). Comparisons of the data for the untreated versus treated cores for the various types of treatments and pavement sites were conducted by observing DSR maps (G' versus η'/G'), Carbonyl area, DSR function hardening susceptibility, and calculated ductility. Additionally, statistical comparisons between the untreated and treated sites are reported.

RESULTS AND DISCUSSIONS

The recovered binder rheological data accompanied by the carbonyl areas are reported in Tables 4-1 through 4-17. Each table describes a specific treatment site (with the Abilene L and R sites counted as two separate sites). The rheological data include η^* at 0.1 rad/s and 60 °C, the DSR function reported measured at 44.7 °C and 10 rad/s, but reported at 15 °C and 0.005 rad/s by conversion using time-temperature superposition, and the calculated ductility (based upon the correlation of Ruan et al., 2003). Note also that for each coring, there are both untreated and treated cores, and that data are shown for the multiple slices (layers) of each core. The slices are nominally one-quarter inch thick. As described in Chapter 2, three replicates of both the untreated and treated cores were obtained at each site, but not all replicates were analyzed for

binder properties. Further analysis and discussion of these results is presented in the following pages through the DSR function maps (plot of G' versus η'/G'), hardening susceptibility calculations, and comparisons of the calculated ductility. Additionally, statistical comparisons of the calculated ductility are presented.

Table 4-1. Recovered Binder Properties for the Abilene SH 36 L1 and L2 Cores. [a]

	Replicate	layer	η* (poise) @ 60 °C 0.1 rad/s	η'/G' (s) @ 15 °C 0.005 rad/s	G' (MPa) @ 15 °C 0.005 rad/s	G'/(η'/G') (MPa/s) @ 15 °C 0.005 rad/s	Calculated Ductility (cm) -	Carbonyl Area -
	U3	1st	-	-	-	-	-	-
		2nd	-	-	-	-	-	-
1st Set		3rd	-	-	-	-	-	-
Abilene L1	T3	1st	262550	148.0	0.66774	0.0045129	2.48	-
		2nd	120880	206.8	0.35748	0.0017287	3.78	-
		3rd	217080	148.7	0.73146	0.0049181	2.38	-
	U1	1st	369380	119.4	0.74978	0.0062787	2.14	-
		2nd	155150	177.9	0.52384	0.0029445	2.99	-
		3rd	289250	120.8	0.84814	0.0070234	2.04	-
	U2	1st	307120	120.9	0.69988	0.0057897	2.22	-
		2nd	256120	131.9	0.65822	0.0049903	2.37	-
2nd Set		3rd	690860	71.5	1.30160	0.0182066	1.34	-
Alilene L1	T1	1st	370230	120.3	0.80918	0.0067258	2.08	-
		2nd	192200	162.1	0.55548	0.0034261	2.80	-
		3rd	547540	113.2	0.89858	0.0079386	1.93	-
	T2	1st	345500	127.5	0.72838	0.0057126	2.23	-
		2nd	244940	143.1	0.66484	0.0046461	2.44	-
		3rd	514760	82.5	1.29540	0.0156998	1.43	-
	U3	1st	488110	98.2	1.04100	0.0105994	1.70	1.555
		2nd	146010	195.7	0.48314	0.0024694	3.23	1.275
1st Set		3rd	337410	114.3	0.90158	0.0078887	1.94	1.331
Abilene L2	T3	1st	221010	162.8	0.61846	0.0037980	2.67	1.533
		2nd	91086	254.9	0.30442	0.0011941	4.44	1.104
		3rd	415790	87.7	1.28680	0.0146650	1.47	1.394
	U1	1st	260000	143.3	0.64532	0.0045028	2.48	-
		2nd	207050	143.2	0.80072	0.0055914	2.25	-
		3rd	145920	149.6	0.72414	0.0048421	2.40	-
	U2	1st	384280	117.1	0.81104	0.0069232	2.05	-
		2nd	200950	157.9	0.67396	0.0042671	2.54	-
2nd Set		3rd	86846	208.4	0.50010	0.0024003	3.27	-
Abilene L2	T1	1st	259220	149.6	0.67092	0.0044839	2.48	-
		2nd	148870	188.3	0.45086	0.0023939	3.27	-
		3rd	237560	123.2	0.95754	0.0077728	1.95	-
	T2	1st	242590	149.4	0.67942	0.0045470	2.47	-
		2nd	243990	139.7	0.72868	0.0052167	2.32	-
		3rd	142750	155.0	0.70338	0.0045378	2.47	-

[a] η' and G' are measured at 44.7 °C, 10 rad/s and converted by TTSP to 15 °C, 0.005 rad/s

Table 4-2. Recovered Binder Properties for the Abilene SH 36 R1 and R2 Cores. [a]

	Replicate	layer	η* (poise) @ 60 °C 0.1 rad/s	η'/G' (s) @ 15 °C 0.005 rad/s	G' (MPa) @ 15 °C 0.005 rad/s	G'/(η'/G') (MPa/s) @ 15 °C 0.005 rad/s	Calculated Ductility (cm) -	Carbonyl Area -
	U3	1st	425090	99.1	0.91202	0.0092040	1.81	-
		2nd	155620	162.7	0.73120	0.0044945	2.48	-
1st Set		3rd	213830	132.6	0.82550	0.0062235	2.15	-
Abilene R1	T3	1st	244960	137.9	0.61002	0.0044229	2.50	-
		2nd	237160	138.8	0.68938	0.0049674	2.37	-
		3rd	387680	97.8	1.10900	0.0113357	1.65	-
	U1	1st	415790	103.3	0.99738	0.0096561	1.77	-
		2nd	363730	103.0	0.89194	0.0086605	1.86	-
		3rd	144280	162.7	0.76628	0.0047106	2.43	-
	U2	1st	407320	101.4	0.91828	0.0090597	1.82	-
		2nd	428810	95.0	1.12780	0.0118739	1.62	-
2nd Set		3rd	169100	140.7	0.84640	0.0060149	2.18	-
Abilene R1	T1	1st	376870	110.1	0.93800	0.0085190	1.87	-
		2nd	318920	108.6	0.96608	0.0088951	1.84	-
		3rd	120360	175.1	0.65842	0.0037595	2.68	-
	T2	1st	369090	104.0	0.82460	0.0079324	1.93	-
		2nd	399960	96.9	0.94728	0.0097805	1.76	-
		3rd	105660	195.8	0.56900	0.0029058	3.01	-
	U2	1st	-	-	-	-	-	-
		2nd	-	-	-	-	-	-
1st Set		3rd	-	-	-	-	-	-
Abilene R2	T2	1st	672460	91.9	1.11280	0.0121091	1.60	-
		2nd	292380	128.5	0.89180	0.0069428	2.05	-
		3rd	403490	104.7	1.16860	0.0111574	1.66	-
	U1	1st	625320	89.2	1.10620	0.0124080	1.59	-
		2nd	183730	147.9	0.77932	0.0052682	2.31	-
		3rd	48292	312.2	0.23772	0.0007614	5.42	-
	U2	1st	615090	90.7	1.01606	0.0112054	1.66	-
		2nd	142610	171.0	0.68296	0.0039943	2.61	-
2nd Set		3rd	45139	300.4	0.24168	0.0008046	5.29	-
Abilene R2	T1	1st	795480	79.3	1.15720	0.0145892	1.48	-
		2nd	168710	150.1	0.69274	0.0046163	2.45	-
		3rd	88568	212.5	0.48030	0.0022602	3.36	-
	T2	1st	798450	81.6	1.06100	0.0129967	1.55	-
		2nd	74877	241.4	0.38888	0.0016108	3.90	-
		3rd	15901	607.5	0.04309	0.0000709	15.39	-

[a] η' and G' are measured at 44.7 °C, 10 rad/s and converted by TTSP to 15 °C, 0.005 rad/s

Table 4-3. Recovered Binder Properties for the Atlanta IH 20 CM Cores. [a]

	Replicate	layer	η* (poise) @ 60 °C 0.1 rad/s	η'/G' (s) @ 15 °C 0.005 rad/s	G' (MPa) @ 15 °C 0.005 rad/s	G'/(η'/G') (MPa/s) @ 15 °C 0.005 rad/s	Calculated Ductility (cm) -	Carbonyl Area -
Atlanta IH 20 CM	U1	1st	1886200	105.6	0.87602	0.0082974	1.89	-
		2nd	837260	128.5	0.69968	0.0054433	2.28	-
		3rd	748980	139.5	0.66972	0.0048020	2.41	-
	U2	1st	1783500	101.6	0.85266	0.0083953	1.88	-
		2nd	629330	148.7	0.48604	0.0032687	2.85	-
		3rd	647580	151.8	0.56948	0.0037516	2.69	-
	T1	1st	745790	142.5	0.56650	0.0039765	2.62	-
		2nd	738040	140.8	0.67632	0.0048043	2.41	-
		3rd	1090000	112.7	0.79788	0.0070782	2.03	-
	T2	1st	1504400	107.6	0.74070	0.0068814	2.06	-
		2nd	1001500	120.3	0.81866	0.0068058	2.07	-
		3rd	852270	128.3	0.71786	0.0055940	2.25	-

[a] η' and G' are measured at 44.7 °C, 10 rad/s and converted by TTSP to 15 °C, 0.005 rad/s

Table 4-4. Recovered Binder Properties for the Atlanta IH 20 DG Cores. [a]

	Replicate	layer	η* (poise) @ 60 °C 0.1 rad/s	η'/G' (s) @ 15 °C 0.005 rad/s	G' (MPa) @ 15 °C 0.005 rad/s	G'/(η'/G') (MPa/s) @ 15 °C 0.005 rad/s	Calculated Ductility (cm) -	Carbonyl Area -
Atlanta IH 20 DG	U1	1st	2373400	84.7	0.95704	0.0113055	1.65	-
		2nd	1099000	120.2	0.73168	0.0060861	2.17	-
		3rd	485730	178.9	0.43102	0.0024091	3.26	-
	U2	1st	3060100	80.7	1.03380	0.0128104	1.56	-
		2nd	1012900	129.2	0.73284	0.0056709	2.24	-
		3rd	512220	88.3	0.39318	0.0044504	2.49	-
	T1	1st	2074700	89.7	0.96692	0.0107801	1.69	-
		2nd	1752500	94.8	0.91668	0.0096729	1.77	-
		3rd	959760	128.2	0.70002	0.0054615	2.28	-
	T2	1st	2077800	96.4	1.04840	0.0108779	1.68	-
		2nd	1693700	98.5	0.89534	0.0090855	1.82	-
		3rd	1151200	120.1	0.64038	0.0053333	2.30	-

[a] η' and G' are measured at 44.7 °C, 10 rad/s and converted by TTSP to 15 °C, 0.005 rad/s

Table 4-5. Recovered Binder Properties for the Atlanta IH 20 SP Cores. [a]

	Replicate	layer	η* (poise) @ 60 °C 0.1 rad/s	η'/G' (s) @ 15 °C 0.005 rad/s	G' (MPa) @ 15 °C 0.005 rad/s	G'/(η'/G') (MPa/s) @ 15 °C 0.005 rad/s	Calculated Ductility (cm) -	Carbonyl Area -
Atlanta IH 20 SP	U1	1st	1706300	105.5	0.69292	0.0065708	2.10	-
		2nd	635160	157.1	0.50900	0.0032406	2.86	-
		3rd	180200	226.2	0.15508	0.0006856	5.67	-
	U2	1st	2131300	94.5	0.84744	0.0089666	1.83	-
		2nd	672120	150.8	0.45770	0.0030354	2.95	-
		3rd	358440	188.3	0.25116	0.0013336	4.23	-
	T1	1st	1507100	111.4	0.82980	0.0074469	1.99	-
		2nd	1278900	117.4	0.76616	0.0065277	2.10	-
		3rd	882580	136.7	0.60176	0.0044023	2.50	-
	T2	1st	1324600	112.2	0.75448	0.0067267	2.08	-
		2nd	1185300	119.5	0.73682	0.0061677	2.16	-
		3rd	928920	136.7	0.53664	0.0039269	2.63	-

[a] η' and G' are measured at 44.7 °C, 10 rad/s and converted by TTSP to 15 °C, 0.005 rad/s

Table 4-6. Recovered Binder Properties for the Atlanta US 67 Cores. [a]

	Replicate	layer	η* (poise) @ 60 °C 0.1 rad/s	η'/G' (s) @ 15 °C 0.005 rad/s	G' (MPa) @ 15 °C 0.005 rad/s	G'/(η'/G') (MPa/s) @ 15 °C 0.005 rad/s	Calculated Ductility (cm) -	Carbonyl Area -
Atlanta US 67	U1	1st	62856	327.7	0.08516	0.0002599	8.69	-
		2nd	58530	354.9	0.08859	0.0002496	8.85	-
		3rd	51932	365.1	0.07132	0.0001953	9.86	-
	U2	1st	70528	321.3	0.11212	0.0003489	7.64	-
		2nd	53257	356.1	0.08763	0.0002461	8.91	-
		3rd	65126	341.6	0.10168	0.0002976	8.19	-
	T1	1st	31275	348.6	0.03191	0.0000915	13.76	-
		2nd	58231	354.1	0.09313	0.0002630	8.65	-
		3rd	57627	351.7	0.07638	0.0002172	9.41	-
	T2	1st	198630	218.3	0.29114	0.0013335	4.23	-
		2nd	107110	275.2	0.16914	0.0006145	5.95	-
		3rd	109230	273.9	0.18948	0.0006918	5.65	-

[a] η' and G' are measured at 44.7 °C, 10 rad/s and converted by TTSP to 15 °C, 0.005 rad/s

Table 4-7. Recovered Binder Properties for the Carrizo Springs Airport Cores. [a]

	Replicate	layer	η* (poise) @ 60 °C 0.1 rad/s	η'/G' (s) @ 15 °C 0.005 rad/s	G' (MPa) @ 15 °C 0.005 rad/s	G'/(η'/G') (MPa/s) @ 15 °C 0.005 rad/s	Calculated Ductility (cm) -	Carbonyl Area -
	U3	1st	899570	111.7	0.61624	0.0055190	2.27	1.505
1st Set		2nd	216370	182.7	0.25916	0.0014183	4.12	1.298
Carrizo		3rd	180880	190.3	0.25316	0.0013303	4.24	1.234
Springs	T3	1st	4042600	52.0	1.50060	0.0288352	1.09	1.999
Airport		2nd	303470	171.7	0.36346	0.0021169	3.45	0.930
		3rd	236010	184.5	0.30800	0.0016691	3.84	1.182
	U1	1st	780050	112.3	0.64966	0.0057838	2.22	-
		2nd	317180	157.1	0.41498	0.0026409	3.13	-
		3rd	323710	156.6	0.40464	0.0025839	3.16	-
	U2	1st	1329400	91.1	0.78130	0.0085778	1.87	-
2nd Set		2nd	294550	167.5	0.33892	0.0020229	3.52	-
Carrizo		3rd	254890	177.4	0.31284	0.0017630	3.74	-
Springs	T1	1st	920540	102.2	0.74354	0.0072721	2.01	-
Airport		2nd	308890	154.1	0.34830	0.0022599	3.36	-
		3rd	380430	149.4	0.34174	0.0022881	3.34	-
	T2	1st	1452400	82.3	0.81868	0.0099465	1.75	-
		2nd	309000	153.5	0.46710	0.0030430	2.94	-
		3rd	350370	149.5	0.39176	0.0026201	3.15	-

[a] η' and G' are measured at 44.7 °C, 10 rad/s and converted by TTSP to 15 °C, 0.005 rad/s

Table 4-8. Recovered Binder Properties for the Fort Worth FM 4 (2000) Cores. [a]

	Replicate	layer	η* (poise) @ 60 °C 0.1 rad/s	η'/G' (s) @ 15 °C 0.005 rad/s	G' (MPa) @ 15 °C 0.005 rad/s	G'/(η'/G') (MPa/s) @ 15 °C 0.005 rad/s	Calculated Ductility (cm) -	Carbonyl Area -
1st Set Fort Worth FM 4 (2000)	U1	1st	-	-	-	-	-	-
		2nd	-	-	-	-	-	-
		3rd	-	-	-	-	-	-
	U2	1st	-	-	-	-	-	-
		2nd	-	-	-	-	-	-
		3rd	-	-	-	-	-	-
	U3	1st	381620	145.1	0.50398	0.0034727	2.78	-
		2nd	155690	202.8	0.29034	0.0014318	4.10	-
		3rd	59988	310.4	0.12024	0.0003874	7.29	-
	T1	1st	-	-	-	-	-	-
		2nd	-	-	-	-	-	-
		3rd	-	-	-	-	-	-
	T2	1st	-	-	-	-	-	-
		2nd	-	-	-	-	-	-
		3rd	-	-	-	-	-	-
	T3	1st	1014500	92.5	0.86926	0.0093991	1.79	-
		2nd	236220	178.5	0.38708	0.0021683	3.42	-
		3rd	95660	229.1	0.19806	0.0008644	5.12	-
2nd Set Fort Worth FM 4 (2000)	U1	1st	706550	125.6	0.66642	0.0053048	2.31	-
		2nd	140390	210.9	0.30672	0.0014543	4.08	-
		3rd	48833	285.9	0.10612	0.0003712	7.43	-
	U2	1st	823710	106.6	0.80296	0.0075352	1.98	-
		2nd	205190	183.1	0.33814	0.0018464	3.67	-
		3rd	67656	261.9	0.13478	0.0005145	6.44	-
	U3	1st	-	-	-	-	-	-
		2nd	-	-	-	-	-	-
		3rd	-	-	-	-	-	-
	T1	1st	1052000	91.6	0.91402	0.0099746	1.75	-
		2nd	228760	186.5	0.39724	0.0021301	3.45	-
		3rd	64421	262.3	0.13746	0.0005241	6.39	-
	T2	1st	1050100	94.9	0.89972	0.0094851	1.79	-
		2nd	185120	194.7	0.32154	0.0016518	3.85	-
		3rd	58434	280.3	0.12622	0.0004503	6.83	-
	T3	1st	-	-	-	-	-	-
		2nd	-	-	-	-	-	-
		3rd	-	-	-	-	-	-

[a] η' and G' are measured at 44.7 °C, 10 rad/s and converted by TTSP to 15 °C, 0.005 rad/s

Table 4-9. Recovered Binder Properties for the Fort Worth FM 4 (2003) Cores. [a]

	Replicate	layer	η* (poise) @ 60 °C 0.1 rad/s	η'/G' (s) @ 15 °C 0.005 rad/s	G' (MPa) @ 15 °C 0.005 rad/s	G'/(η'/G') (MPa/s) @ 15 °C 0.005 rad/s	Calculated Ductility (cm) -	Carbonyl Area -
1st Set Fort Worth FM 4 (2003)	U1	1st	-	-	-	-	-	-
		2nd	-	-	-	-	-	-
		3rd	-	-	-	-	-	-
	U2	1st	-	-	-	-	-	-
		2nd	-	-	-	-	-	-
		3rd	-	-	-	-	-	-
	U3	1st	464000	170.2	0.30868	0.0018140	3.70	-
		2nd	334330	170.8	0.32232	0.0018870	3.63	-
		3rd	58147	270.1	0.11410	0.0004225	7.02	-
	T1	1st	-	-	-	-	-	-
		2nd	-	-	-	-	-	-
		3rd	-	-	-	-	-	-
	T2	1st	-	-	-	-	-	-
		2nd	-	-	-	-	-	-
		3rd	-	-	-	-	-	-
	T3	1st	347080	179.8	0.32270	0.0017949	3.71	-
		2nd	289000	172.4	0.33770	0.0019584	3.58	-
		3rd	12609	500.2	0.02825	0.0000565	17.02	-
2nd Set Fort Worth FM 4 (2003)	U1	1st	477900	167.6	0.32066	0.0019138	3.61	-
		2nd	245030	172.3	0.30052	0.0017444	3.76	-
		3rd	22439	379.9	0.05860	0.0001542	10.94	-
	U2	1st	601030	164.4	0.33266	0.0020238	3.52	-
		2nd	223260	190.2	0.27232	0.0014321	4.10	-
		3rd	21087	391.6	0.04774	0.0001219	12.13	-
	U3	1st	-	-	-	-	-	-
		2nd	-	-	-	-	-	-
		3rd	-	-	-	-	-	-
	T1	1st	492590	161.9	0.33664	0.0020789	3.48	-
		2nd	75378	264.3	0.12592	0.0004764	6.66	-
		3rd	7147	601.8	0.01594	0.0000265	23.75	-
	T2	1st	536880	157.5	0.38560	0.0024486	3.24	-
		2nd	173220	199.5	0.24718	0.0012388	4.37	-
		3rd	12834	406.6	0.02836	0.0000698	15.51	-
	T3	1st	-	-	-	-	-	-
		2nd	-	-	-	-	-	-
		3rd	-	-	-	-	-	-

[a] η' and G' are measured at 44.7 °C, 10 rad/s and converted by TTSP to 15 °C, 0.005 rad/s

Table 4-10. Recovered Binder Properties for the Georgetown Airport (1989) Cores. [a]

	Replicate	layer	η* (poise) @ 60 °C 0.1 rad/s	η'/G' (s) @ 15 °C 0.005 rad/s	G' (MPa) @ 15 °C 0.005 rad/s	G'/(η'/G') (MPa/s) @ 15 °C 0.005 rad/s	Calculated Ductility (cm) -	Carbonyl Area -
1st Set Georgetown Airport (1989)	U3	1st	790130	114.0	0.81358	0.0071358	2.02	1.507
		2nd	118480	221.9	0.29498	0.0013294	4.24	1.164
		3rd	80630	259.8	0.15328	0.0005899	6.06	1.079
	T3	1st	1206800	76.2	1.13040	0.0148375	1.47	1.805
		2nd	214240	177.4	0.35942	0.0020263	3.52	1.329
		3rd	121990	222.9	0.25286	0.0011342	4.55	1.192
2nd Set Georgetown Airport (1989)	U1	1st	1507900	88.3	1.01540	0.0114974	1.64	-
		2nd	123010	221.9	0.25406	0.0011448	4.53	-
		3rd	118470	223.4	0.23918	0.0010708	4.66	-
	U2	1st	1690900	79.6	0.87482	0.0109914	1.67	-
		2nd	104340	228.7	0.19442	0.0008503	5.16	-
		3rd	62569	275.5	0.14244	0.0005170	6.42	-
	T1	1st	1542500	84.5	0.97814	0.0115763	1.64	-
		2nd	123770	221.4	0.20618	0.0009314	4.96	-
		3rd	77549	258.7	0.16742	0.0006472	5.82	-
	T2	1st	2173100	72.7	1.16880	0.0160762	1.42	-
		2nd	144630	207.1	0.27072	0.0013070	4.27	-
		3rd	122310	221.4	0.22234	0.0010045	4.80	-

[a] η' and G' are measured at 44.7 °C, 10 rad/s and converted by TTSP to 15 °C, 0.005 rad/s

Table 4-11. Recovered Binder Properties for the Georgetown Airport (1995) Cores. [a]

	Replicate	layer	η* (poise) @ 60 °C 0.1 rad/s	η'/G' (s) @ 15 °C 0.005 rad/s	G' (MPa) @ 15 °C 0.005 rad/s	G'/(η'/G') (MPa/s) @ 15 °C 0.005 rad/s	Calculated Ductility (cm) -	Carbonyl Area -
1st Set Georgetown Airport (1995)	U3	1st	965240	105.0	0.75512	0.0071934	2.02	1.498
		2nd	181930	190.8	0.30408	0.0015939	3.91	1.207
		3rd	150970	201.7	0.24604	0.0012199	4.40	1.169
	T3	1st	1422100	64.9	0.99586	0.0153463	1.45	1.815
		2nd	256470	167.3	0.39716	0.0023734	3.29	1.289
		3rd	243840	164.7	0.37316	0.0022661	3.35	1.234
2nd Set Georgetown Airport (1995)	U1	1st	371850	156.9	0.42576	0.0027143	3.10	-
		2nd	80971	246.1	0.14460	0.0005876	6.07	-
		3rd	60333	276.8	0.11452	0.0004138	7.09	-
	U2	1st	500030	140.7	0.52998	0.0037672	2.68	-
		2nd	89043	240.4	0.16408	0.0006824	5.69	-
		3rd	88002	246.5	0.17084	0.0006929	5.65	-
	T1	1st	1510400	81.0	0.95328	0.0117640	1.62	-
		2nd	433840	145.9	0.48566	0.0033290	2.83	-
		3rd	303210	163.2	0.37096	0.0022728	3.35	-
	T2	1st	2272900	74.5	1.05040	0.0141085	1.50	-
		2nd	398220	151.6	0.45634	0.0030109	2.96	-
		3rd	242610	173.7	0.32246	0.0018560	3.66	-
	T1*	1st	1334400	84.7	0.95346	0.0112511	1.66	-
		2nd	281610	170.9	0.29530	0.0017275	3.78	-
		3rd	189090	183.5	0.30020	0.0016364	3.87	-
	T2*	1st	1426400	83.8	0.94650	0.0112948	1.65	-
		2nd	235480	176.6	0.35208	0.0019938	3.55	-
		3rd	206870	179.6	0.32116	0.0017886	3.72	-

[a] η' and G' are measured at 44.7 °C, 10 rad/s and converted by TTSP to 15 °C, 0.005 rad/s

Table 4-12. Recovered Binder Properties for the Jacksonville Airport Cores. [a]

	Replicate	layer	η* (poise) @ 60 °C 0.1 rad/s	η'/G' (s) @ 15 °C 0.005 rad/s	G' (MPa) @ 15 °C 0.005 rad/s	G'/(η'/G') (MPa/s) @ 15 °C 0.005 rad/s	Calculated Ductility (cm) -	Carbonyl Area -
	U3	1st	164390	184.3	0.38792	0.0021050	3.46	1.408
1st Set		2nd	58562	284.2	0.19324	0.0006799	5.69	1.134
Jacksonville		3rd	61745	278.0	0.21472	0.0007723	5.38	1.098
Airport	T3	1st	436970	106.9	0.83726	0.0078325	1.94	1.702
		2nd	28963	394.1	0.09951	0.0002525	8.80	0.929
		3rd	20391	472.7	0.05347	0.0001131	12.54	0.800
	U1	1st	114270	206.9	0.35354	0.0017087	3.80	-
		2nd	55221	291.5	0.18108	0.0006211	5.93	-
		3rd	45784	302.7	0.15494	0.0005118	6.45	-
	U2	1st	113480	211.1	0.33018	0.0015640	3.95	-
2nd Set		2nd	57882	281.9	0.17314	0.0006142	5.95	-
Jacksonville		3rd	53273	293.8	0.18836	0.0006411	5.84	-
Airport	T1	1st	275430	145.6	0.60354	0.0041454	2.57	-
		2nd	69099	258.3	0.24572	0.0009513	4.91	-
		3rd	71689	279.5	0.22194	0.0007940	5.32	-
	T2	1st	352760	127.2	0.78138	0.0061419	2.16	-
		2nd	71116	253.0	0.24968	0.0009869	4.83	-
		3rd	71191	258.4	0.24542	0.0009496	4.92	-

[a] η' and G' are measured at 44.7 °C, 10 rad/s and converted by TTSP to 15 °C, 0.005 rad/s

Table 4-13. Recovered Binder Properties for the Lufkin BUS 59 Cores. [a]

	Replicate	layer	η* (poise) @ 60 °C 0.1 rad/s	η'/G' (s) @ 15 °C 0.005 rad/s	G' (MPa) @ 15 °C 0.005 rad/s	G'/(η'/G') (MPa/s) @ 15 °C 0.005 rad/s	Calculated Ductility (cm) -	Carbonyl Area -
	U3	1st	159280	208.5	0.30096	0.0014437	4.09	-
1st Set		2nd	261990	178.9	0.47496	0.0026552	3.13	-
Lufkin		3rd	-	-	-	-	-	-
BUS 59	T3	1st	396920	119.5	0.83934	0.0070233	2.04	-
		2nd	127470	233.9	0.24554	0.0010497	4.70	-
		3rd	241870	187.2	0.40656	0.0021715	3.42	-
	U1	1st	767840	112.6	0.87468	0.0077687	1.95	-
		2nd	164000	200.1	0.36488	0.0018234	3.69	-
		3rd	288760	161.3	0.46630	0.0028905	3.01	-
	U2	1st	1089600	96.2	0.87620	0.0091053	1.82	-
2nd Set		2nd	310130	159.1	0.52024	0.0032708	2.85	-
Lufkin		3rd	541820	125.8	0.75250	0.0059817	2.19	-
BUS 59	T1	1st	204350	182.8	0.35196	0.0019252	3.60	-
		2nd	210750	183.1	0.36366	0.0019856	3.55	-
		3rd	597050	123.5	0.76314	0.0061814	2.16	-
	T2	1st	296510	158.1	0.50882	0.0032176	2.87	-
		2nd	241000	173.1	0.45370	0.0026211	3.14	-
		3rd	396470	142.8	0.62634	0.0043876	2.51	-

[a] η' and G' are measured at 44.7 °C, 10 rad/s and converted by TTSP to 15 °C, 0.005 rad/s

Table 4-14. Recovered Binder Properties for the Odessa SH 149 Cores. [a]

	Replicate	layer	η* (poise) @ 60 °C 0.1 rad/s	η'/G' (s) @ 15 °C 0.005 rad/s	G' (MPa) @ 15 °C 0.005 rad/s	G'/(η'/G') (MPa/s) @ 15 °C 0.005 rad/s	Calculated Ductility (cm) -	Carbonyl Area -
Odessa SH 149	U1	1st	59280	282.9	0.18842	0.0006659	5.75	-
		2nd	35333	337.8	0.13264	0.0003927	7.25	-
		3rd	59228	256.3	0.26510	0.0010345	4.73	-
	U2	1st	38470	344.2	0.11294	0.0003281	7.85	-
		2nd	46071	295.9	0.17214	0.0005818	6.10	-
		3rd	52603	265.2	0.24654	0.0009297	4.96	-
	T1	1st	49228	310.9	0.15010	0.0004828	6.62	-
		2nd	42024	316.5	0.14068	0.0004445	6.87	-
		3rd	133420	174.8	0.47526	0.0027182	3.09	-
	T2	1st	61504	284.4	0.18676	0.0006567	5.78	-
		2nd	34323	340.9	0.10790	0.0003165	7.97	-
		3rd	83301	220.7	0.31088	0.0014086	4.13	-

[a] η' and G' are measured at 44.7 °C, 10 rad/s and converted by TTSP to 15 °C, 0.005 rad/s

Table 4-15. Recovered Binder Properties for the Odessa SH 349 Cores. [a]

	Replicate	layer	η* (poise) @ 60 °C 0.1 rad/s	η'/G' (s) @ 15 °C 0.005 rad/s	G' (MPa) @ 15 °C 0.005 rad/s	G'/(η'/G') (MPa/s) @ 15 °C 0.005 rad/s	Calculated Ductility (cm) -	Carbonyl Area -
Odessa SH 349	U1	1st	13634	517.8	0.02292	0.0000443	18.94	-
		2nd	116640	198.7	0.44624	0.0022462	3.37	-
		3rd	134760	179.8	0.48686	0.0027075	3.10	-
	U2	1st	19724	445.6	0.03742	0.0000840	14.29	-
		2nd	293770	124.7	0.86702	0.0069535	2.05	-
		3rd	184210	162.0	0.51488	0.0031785	2.89	-
	T1	1st	36527	361.9	0.10314	0.0002850	8.35	-
		2nd	51192	285.4	0.22170	0.0007767	5.37	-
		3rd	46099	304.5	0.16690	0.0005481	6.26	-
	T2	1st	17991	476.7	0.03113	0.0000653	15.96	-
		2nd	93448	218.0	0.35120	0.0016108	3.90	-
		3rd	56594	278.1	0.23078	0.0008298	5.22	-

[a] η' and G' are measured at 44.7 °C, 10 rad/s and converted by TTSP to 15 °C, 0.005 rad/s

Table 4-16. Recovered Binder Properties for the Pleasanton Airport Cores. [a]

	Replicate	layer	η* (poise) @ 60 °C 0.1 rad/s	η'/G' (s) @ 15 °C 0.005 rad/s	G' (MPa) @ 15 °C 0.005 rad/s	G'/(η'/G') (MPa/s) @ 15 °C 0.005 rad/s	Calculated Ductility (cm) -	Carbonyl Area -
1st Set Pleasanton Airport	U3	1st	321790	165.5	0.42332	0.0025577	3.18	1.203
		2nd	40917	329.7	0.07858	0.0002383	9.03	0.805
		3rd	18239	430.0	0.03333	0.0000775	14.81	0.645
	T3	1st	2051100	76.3	0.91082	0.0119345	1.61	1.366
		2nd	155790	211.8	0.21972	0.0010374	4.73	0.990
		3rd	124980	219.0	0.22292	0.0010180	4.77	0.957
	U1	1st	-	-	-	-	-	-
		2nd	-	-	-	-	-	-
		3rd	-	-	-	-	-	-
	U2	1st	-	-	-	-	-	-
2nd Set Pleasanton Airport		2nd	-	-	-	-	-	-
		3rd	-	-	-	-	-	-
	T1	1st	1055800	108.8	0.73324	0.0067367	2.08	-
		2nd	176090	200.3	0.26320	0.0013143	4.26	-
		3rd	128100	215.1	0.21536	0.0010014	4.80	-
	T2	1st	1356700	98.4	0.76246	0.0077513	1.95	-
		2nd	156370	203.1	0.24982	0.0012302	4.39	-
		3rd	135670	210.6	0.21524	0.0010218	4.76	-

[a] η' and G' are measured at 44.7 °C, 10 rad/s and converted by TTSP to 15 °C, 0.005 rad/s

Table 4-17. Recovered Binder Properties for the Tyler US 79 Cores. [a]

	Replicate	layer	η* (poise) @ 60 °C 0.1 rad/s	η'/G' (s) @ 15 °C 0.005 rad/s	G' (MPa) @ 15 °C 0.005 rad/s	G'/(η'/G') (MPa/s) @ 15 °C 0.005 rad/s	Calculated Ductility (cm) -	Carbonyl Area -
Tyler US 79	U1	1st	2008400	116.9	0.64078	0.0054820	2.27	-
		2nd	492840	189.0	0.25632	0.0013563	4.20	-
		3rd	440750	197.8	0.22548	0.0011398	4.54	-
	U2	1st	2592600	103.2	0.85716	0.0083050	1.89	-
		2nd	534150	188.2	0.27072	0.0014384	4.10	-
		3rd	428190	200.9	0.19908	0.0009908	4.82	-
	T1	1st	2590800	99.6	0.81124	0.0081409	1.91	-
		2nd	568700	181.5	0.28150	0.0015506	3.96	-
		3rd	553310	181.7	0.28272	0.0015562	3.96	-
	T2	1st	1981400	114.7	0.69816	0.0060855	2.17	-
		2nd	529270	184.7	0.25966	0.0014061	4.14	-
		3rd	461200	187.0	0.21538	0.0011517	4.52	-

[a] η' and G' are measured at 44.7 °C, 10 rad/s and converted by TTSP to 15 °C, 0.005 rad/s

Dynamic Complex Viscosity Master Curves of the Fog Seal Materials

The recovered fog seal asphalt materials were analyzed for their rheological properties. Dynamic complex viscosity master curves, at 60 °C and for low frequencies, are shown in Appendix F, Figure F-1. The PASS, MS-2, and asphalt emulsion materials are much like conventional viscosity-graded AC-10 to AC-20 asphalts, having viscosities that range from 1000, to nearly 3000, poise. The COS-50 material is significantly harder, 30,000 poise.

DSR Function Maps

Figures 4-1 to 4-19 present the DSR maps for each of the treatment sites. Each map presents data for one site including data for both the first and second year of the project if those data were obtained, and for both the untreated and treated cores. Note again that there are four figures for the Abilene site, two for the L1 and L2 sites, and two for the R1 and R2 sites, because both the PASS and the MS-2 treatments were tested on this pavement.

Figure 4-1 presents the data for the Abilene SH 36 L1 site. The DSR map is the map of G' versus η'/G' (both values determined at 44.7 °C and 10 rad/s, but converted by time-temperature superposition to values at 15 °C and 0.005 rad/s because of the correlation discovered by Ruan et al. (2003) between these DSR properties and the ductility of unmodified binders). On the DSR map, this correlation is shown by the curved dash lines for each calculated ductility as a function of G' and η'/G'. Generally, it should be noted that as a binder ages, it moves from the lower right corner of this graph toward the upper left corner. The exact starting point and the specific direction of the path depend on each individual binder, but that general path is observed, nevertheless. As such, the movement of the binder across this map toward the top left corner provides an excellent method for tracking the impact on binder oxidation.

In Figure 4-1, the data obtained from the core in the first year of the project are shown in solid symbols, and the data obtained from the core in the second year of the project are shown as open symbols. Additionally, data for the various replicates (both the untreated and treated cores) and for the various layers are shown. It should be noted that this pavement was constructed in 1998, and the fog seal treatment was placed in 2004. As a matter of convenience, the location of the various points on this graph will be referred to by their calculated ductility coordinates rather than the DSR values. The first year core binder recovered from the three layers ranges in calculated ductility from about 2.5 to 4 cm with the less-aged 4 cm ductility being indicated for the second slice, while the first and third slices have essentially equal calculated ductilities near 2.5 cm. This was a treated core and there was no untreated core sample binder to compare with it. The second-year data include two untreated core replicates and two treated replicates. Considering all of the second-year data, the calculated ductilities range from something less then 2 cm up to a value of 3 cm. The third slice of both the untreated and the treated cores have the hardest binders, having ductilities less than 2 cm. At the other extreme, the two softest materials are the second slices of one of the untreated cores, but also one of the treated cores. The binder properties for the other slices clustered between a value of 2 and 2.5 cm. Given that we see both untreated and treated recovered binder properties at both of the extremes and clustering of both the untreated and treated binders in between these extremes, we conclude that for MS-2 treatment at this site, a clear effect of the fog seal effect is not evident.

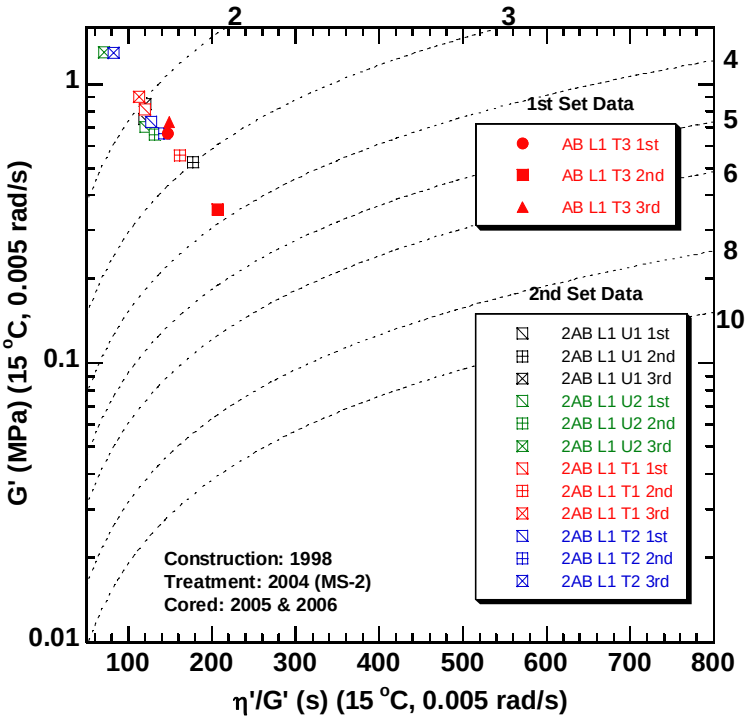

Figure 4-1. DSR Map for Binders Recovered from the Abilene SH 36 L1 Cores.

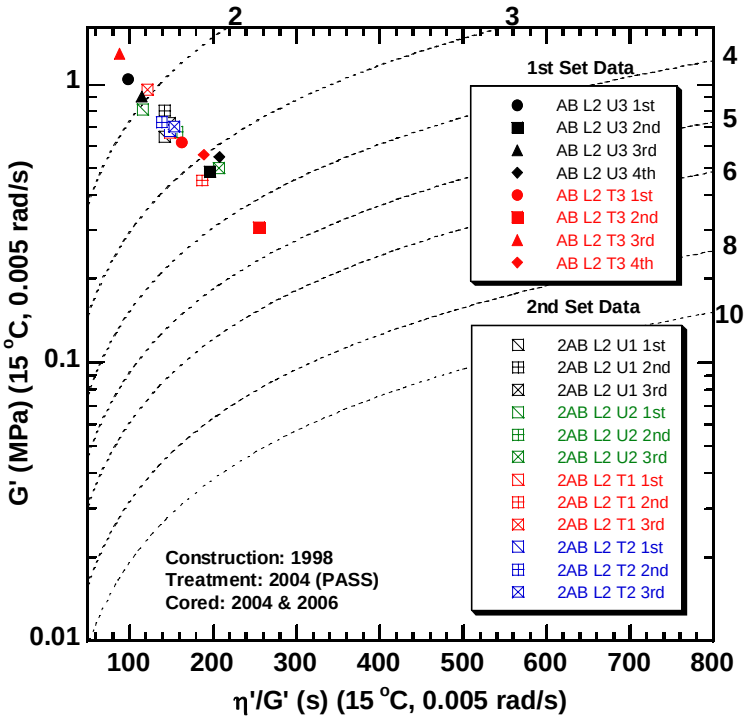

Figure 4-2. DSR Map for Binders Recovered from the Abilene SH 36 L2 Cores.

Figure 4-2 presents data for the Abilene L2 site, treated with the PASS fog seal material. Both untreated and treated replicates were obtained in both the first and second year of the project. Again, the solid symbols are for the first-year cores, and the open symbols are for the second-year cores. For the binder properties obtained from the first-year cores, a fairly wide range in the calculated ductility is obtained, and it should be noted that both the hardest and the softest materials obtained from the first-year cores are from treated cores; the third slice of the treated core is the hardest (lowest ductility), and the second slice of the treated core is the softest (highest ductility). Further, there appear to be inconsistent differences between untreated and treated cores. Considering the top slices, the untreated binder is stiffer than the treated binder, with a calculated ductility less than 2 cm, while the treated first layer has a calculated ductility of nearly 3 cm. Comparing the second slices, again the treated binder is softer than the untreated as the second slice untreated binder ductility is close to 3 cm (but greater than 3 cm) while the second slice treated value is about 4.5 cm. The third layer, however, doesn't fit this patern as the treated layer is actually stiffer than the untreated layer; the treated third layer ductility is about 1.5 cm, while the untreated third layer is right at 2 cm. Finally, considering the fourth layer, both the untreated and treated binders have calculated ductilities very close to 3 cm. In summary, a conclusion about the effect of the fog seal treatment seems to be unwarranted by these data.

The second-year data are even less conclusive in that the range of the data is considerably tighter (from 2 to a little more than 3 cm), and there is a very tight cluster of most of the data points. The extremes of the range are marked by two binders at 2 cm, one of which is an untreated first layer and the other a treated third layer, and two other binders at a little over 3 cm, one of which is an untreated third layer and the other a treated second layer. Again, the inconsistent comparisons between untreated and treated cores leads to a conclusion that the fog seal treatment has not made a significant difference in the binder properties either by rejuvenating the binder or by retarding the effect of oxidation. It should be noted that with the fog seal placed in 2004, the first-year core would not be expected to show any effect of the treatment with respect to aging, although we might expect to see a rejuvenation effect if a fog seal treatment were present to a significant degree in the treated core slices. Again, a conclusion to that effect does not seem possible.

Figure 4-3 presents the data for both the first and second year for the Abilene SH 36 R1 site at which the PASS fog seal treatment was used. In this case, we see a relatively small range of calculated ductilities for all the recovered binders with the exception of the first year treated fourth layer. That binder has a calculated ductility of over 5 cm; all of the others range from about 1.5 to 3 cm. Again, it is difficult to discern with any confidence a specific pattern that would suggest the treatment is effective and rejuvenates the binder. Furthermore, over the duration of the project, it is difficult to discern from measurements of these slices, that hardening of the binder has occurred, whether in untreated or treated cores.

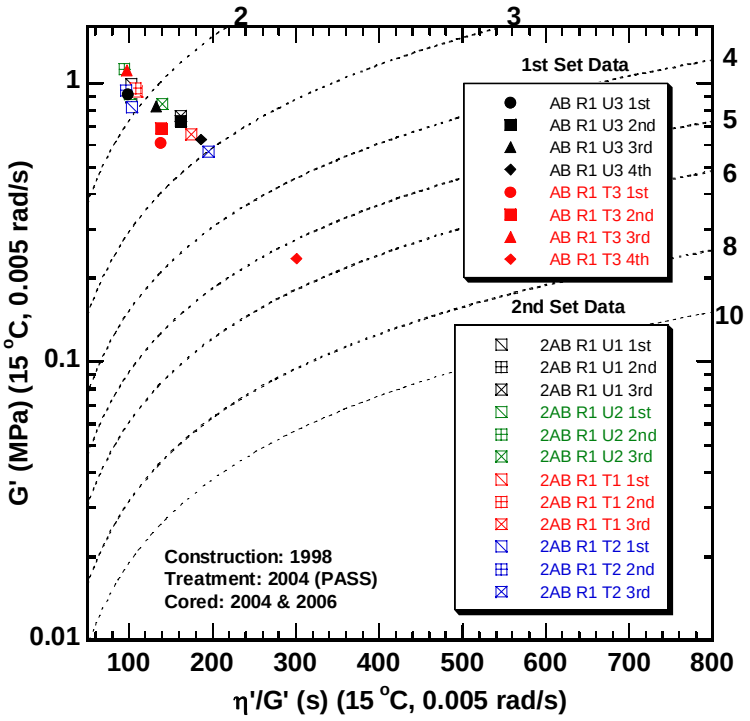

Figure 4-3. DSR Map for Binders Recovered from the Abilene SH 36 R1 Cores.

Figure 4-4 shows the final set of data for the Abilene site. In this case, the first year coring data are for the treated pavement only, while the second-year coring contains data for both the untreated and treated cores. The fog seal treatment in this case was the MS-2 material that, it should be recalled from the discussion in Chapter 3, has the appearance of unmodified emulsified asphalt. These data show a much wider span of calculated ductility than any of the previous data in that the softest binder, which is the third layer from a treated core of the second year, is well over 10 cm, while the stiffest binders are well under 2 cm. The five first-year core slices range from about 1.5 to 5 cm which is also about the same range for the second year recovered binders, with the exception of the previously mentioned binder that has a calculated ductility of well over 10 cm. Looking further at the first-year core data, we see that the first three layers cluster together fairly closely and then the fourth and fifth layers lie together near 5 cm. Here it should be noted that in Chapter 3, Figure 3-14 presented SEC chromatograms for these binders, and it was observed that the fourth and fifth layers represented a different base binder that had no polymer compared to the first three layers. Therefore, the fact that these two binders in the fourth and fifth layers are softer than the first through third layers is most certainly the result of these differences in the binders rather than the results of the fog seal treatment. Looking at the second year data, a similar effect appears to be playing a role in that, referring to Figure 3-12b and 3-12a, it is seen that the first layer of the U1 and T1 cores is a binder that has the significant amount of polymer whereas the second and third layers have significantly reduced amounts, in fact the third layer has virtually no polymer. Also, the maltenes peak of the second and third layer binders appears to have a significantly higher amount of a larger molecular size material in that their peaks and trailing edges are shifted well to the right of those for the first layer binders. Both the lack of polymer (or a significantly reduced amount) and the presence of smaller molecular size material would result in a softer material. And, in this case, as we go from

the first layer to the third layer in both U1 and T1 samples (Figure 4-4), ductility increases from about 1.5 to 2.5 cm (first and second layers) to 3.3 to 5.5 cm (third layer) from the first to the second to the third layers. Again, these differences are most likely the result of differences in the original binder rather than any effect of the MS-2 fog seal treatment, based upon the SEC chromatogram. So again, the data appear to argue against a major rejuvenating effect of the fog seal treatment as well as any retardation of the aging (although the effect of aging is impossible to discern because of the overwhelming apparent effect of the different base binder in the various cores and the various layers).

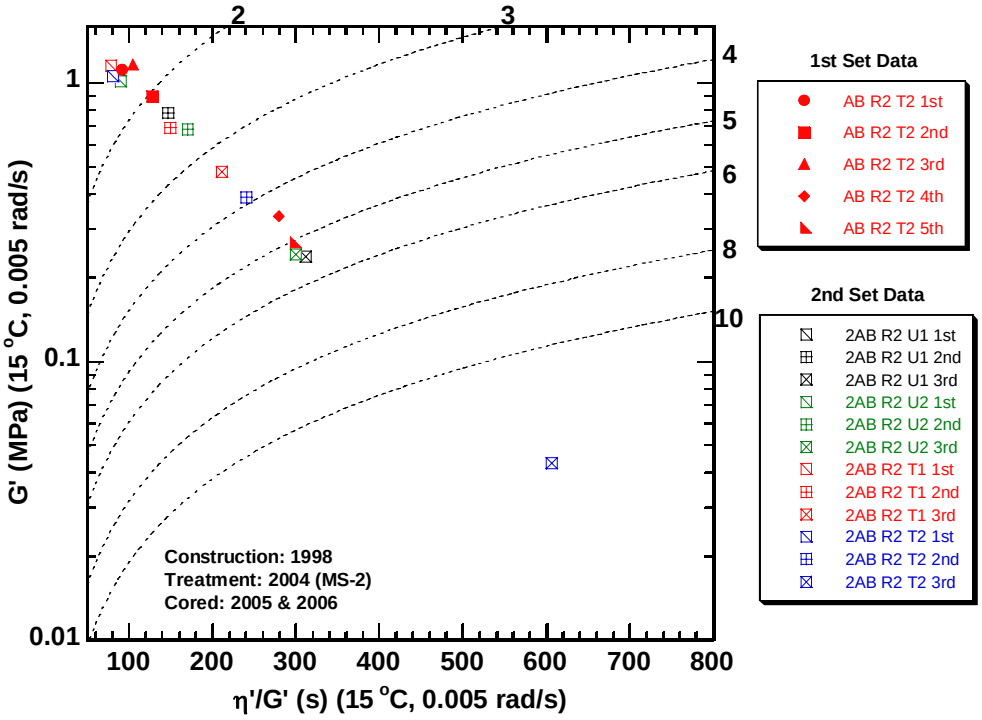

Figure 4-4. DSR Map for Binders Recovered from the Abilene SH 36 R2 Cores.

Figure 4-5 is a DSR map for the Atlanta 67 site. The data shown are for cores taken at the second year of the project, but this pavement was constructed in 2001 with the fog seal application in 2006 and so therefore, it became a possible site only in 2006. The SEC chromatograms for the U1 and T1 cores were given in Figures 3-17a and 3-17b. Referring back to these chromatograms, we noted that differences between the three layers in an untreated site appear to be very minimal (correcting for the baseline shift in the first layer sample at the trailing edge of the chromatogram), while for the treated cores the first layer appears to be significantly different in that even though the asphaltenes peak is the same height as the second and third layers, the maltenes peak is not. This difference would not appear to be due to the PASS fog seal material in as much as the presence of the polymer from the PASS treatment is not evident at all in this first layer material. Thus, it would seem that this top layer binder is just a different binder for some reason. Referring now to the DSR map, we see that the untreated cores, the first, second and third layers, fall relatively close together between 8 and 10 cm calculated ductilities. Likewise, for the U2 materials, the first, second, and third layer binders, are all very similar with ductilities near 8 cm or somewhat above, and the T1 binders layers clustered together quite well

except for the first layer which is definitely out of line with the other materials, consistent with the fact that the SEC chromatogram is different for the binder from this layer. For the T2 core, the first, second, and third layers are not as close together with the first layer binder falling away from the second and third. However, it should be noted that three of these layers taken together lie significantly away from the other binders. Again, this is almost certainly an indication that the T2 site itself is different from the T1 or even the U1 and U2 sites rather than their differences being the result of the PASS treatment. So, there are differences between some of the cores and between different layers, but these differences are almost certainly attributable to factors other than the fog seal treatment.

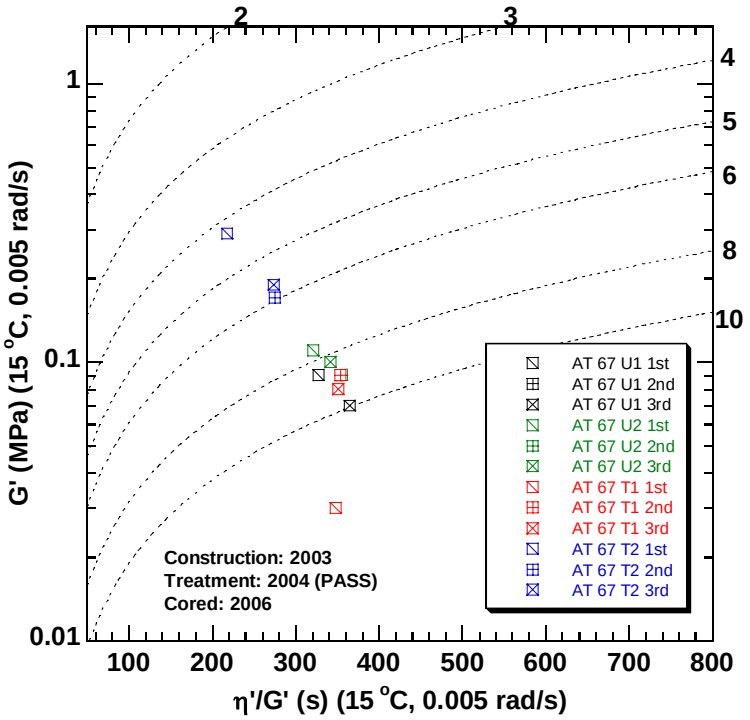

Figure 4-5. DSR Map for Binders Recovered from the Atlanta US 67 Cores.

Figure 4-6 presents the DSR map for the Atlanta IH 20 Coarse Matrix high binder material. There are two replicate untreated cores and two replicate treated cores for which each has three binders from three layers. In this case, all of the binders fall quite close together, between 2 and 3 cm ductility. It is very difficult to say that there are any differences between either of the untreated replicates or between the treated replicates or even between the untreated and the treated. The biggest difference is between the first layer of the U2 core and the second and third layers of the U2 core. The reason for this difference is unclear and is not evident from the chromatogram, Figure 3-15a. Considering the T1 data, it is perhaps significant to note that the first layer binder shows a higher ductility than either the second or third (although whether these are significant differences is questionable). Based upon the chromatogram (Figure 3-15b), it's hard to see that there are major differences between the first, second, and third layers that would suggest different DSR function values for these materials. Again, the conclusion seems warranted that any effect of the fog seal treatment, in this case is a cationic slow set (CSS-1) emulsion, is minimal.

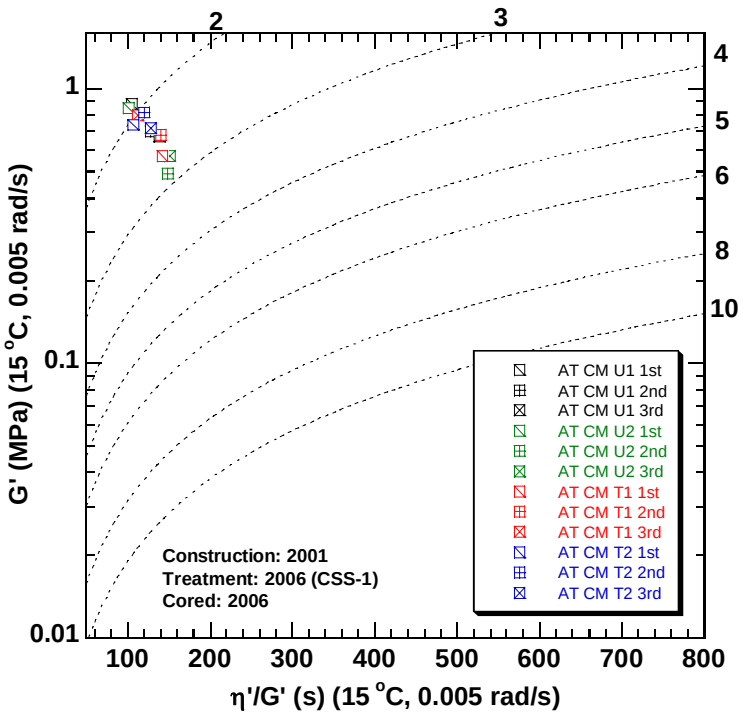

Figure 4-6. DSR Map for Binders Recovered from the Atlanta IH 20 CM Cores.

Figure 4-7 shows the DSR function data for the Atlanta IH 20 dense-graded pavement. Again, there appear to be very minimal differences between the untreated and treated binders recovered from these cores. There does seem to be somewhat more range in the calculated ductilities for the U1 core slices (the calculated ductilities range from something less than 2 cm to something little over 3 cm), and the third slice binder of the U2 core lies off track with the others, which would seem to suggest that this third layer could be largely a different binder. However, we don't have the chromatograms of this material and therefore, can't verify it in that way. Nevertheless, these two "outliers" are both for the untreated materials and therefore, do not provide evidence that the fog seal treatment benefits the pavement.

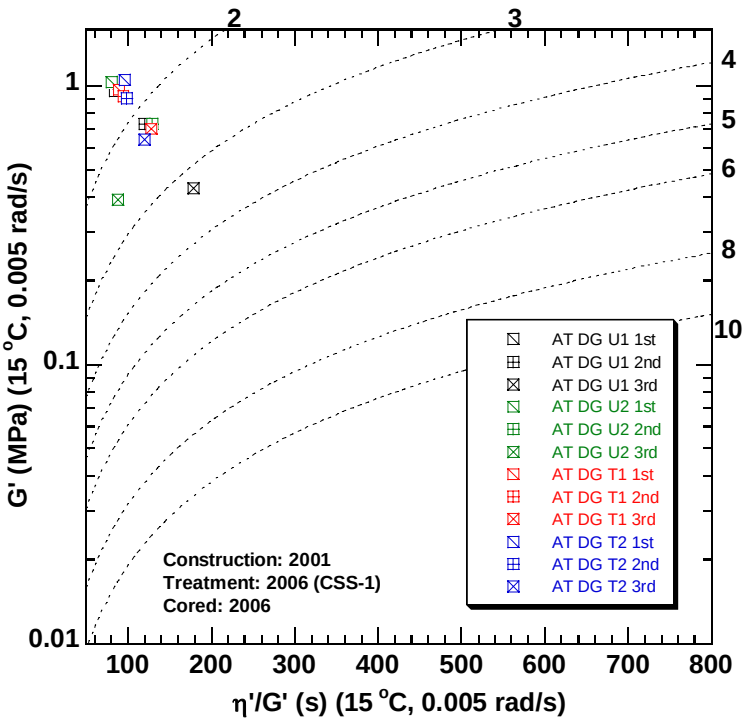

Figure 4-7. DSR Map for Binders Recovered from the Atlanta IH 20 DG Cores.

Figure 4-8 presents data for Atlanta IH 20 Superpave pavement. Here the two untreated replicates have binders from the three layers that spread out across the DSR map, providing the calculated ductility that ranges from 2 cm up to 6 cm. By comparison, the binders recovered from the treated cores are all fairly tightly clustered and range from 2 cm to less than 3 cm. The broader range for the untreated cores could possibly be due to progression toward a different binder deeper into the pavement, but without the SEC chromatograms this conclusion is only conjecture. Nevertheless, it would seem to hold again that the fog seal treatment, which again was the CSS-1 emulsion, had virtually no rejuvenating effect on the in-place binder.

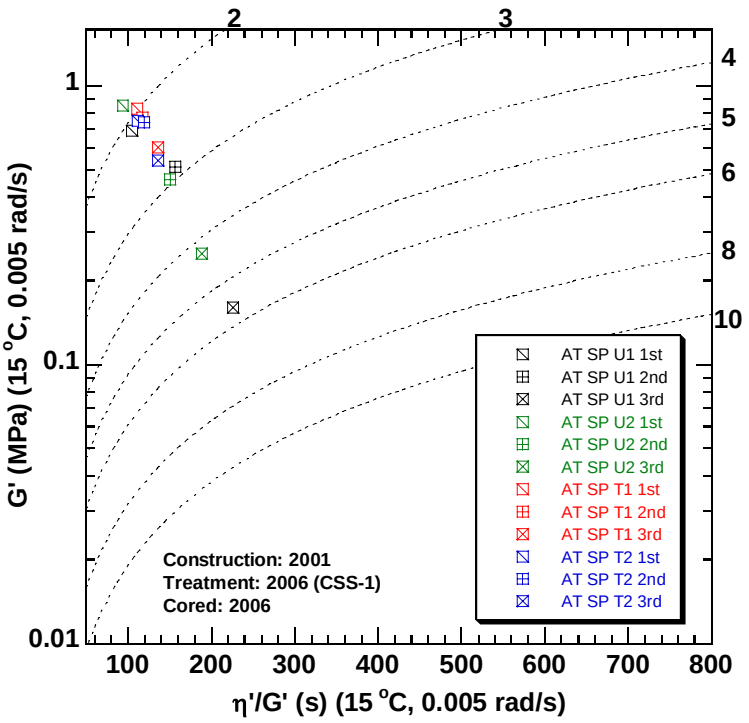

Figure 4-8. DSR Map for Binders Recovered from the Atlanta IH 20 SP Cores.

Figure 4-9 presents the data for the Carrizo Springs site, which was treated with the EB44 coal-tar material. Four cores were obtained in the first and second year of the project. The first-year data are the solid black and red symbols, and the second year data are the open symbols. Here we note that the first layer of the treated core from the first year is the hardest of any other materials, significantly harder than the other three layers from this core. The first layer calculated ductility is close to 1 cm while second, third, and fourth calculated ductilities are in the range of 3.5 to 4 cm. Note that the untreated layer binders range from a value greater than 2 cm (first layer) to values in excess of 4 cm (layers 2, 3, and 4). So, for both of these cores (untreated and treated), obtained in the first year of the project, the first quarter inch is significantly harder than the others, but also the treated pavement binders, especially the first layer, is notably harder (lower calculated ductility) than the untreated binder.

Looking at the core data obtained in the second year of the project, we do not see such large differences, although in each case, the first layer is notably harder than the second and third layers. In fact, for these second-year data, the first layer calculated ductilities are fairly close to 2 cm, while the second and third layers are all uniformly between 3 and 4 cm. It would not be unexpected to see a harder material in the top quarter inch as this would represent the higher level of aging that occurs at the hardest portion of the pavement. However, this effect has not been observed to such a degree in the other pavements. In any case, there does not appear to be a rejuvenation effect of the EB44 treatment, nor does there seem to be any beneficial effect of the treatment on subsequent aging of the binder; differences between untreated and treated materials that would suggest an improvement in aging just do not appear to exist.

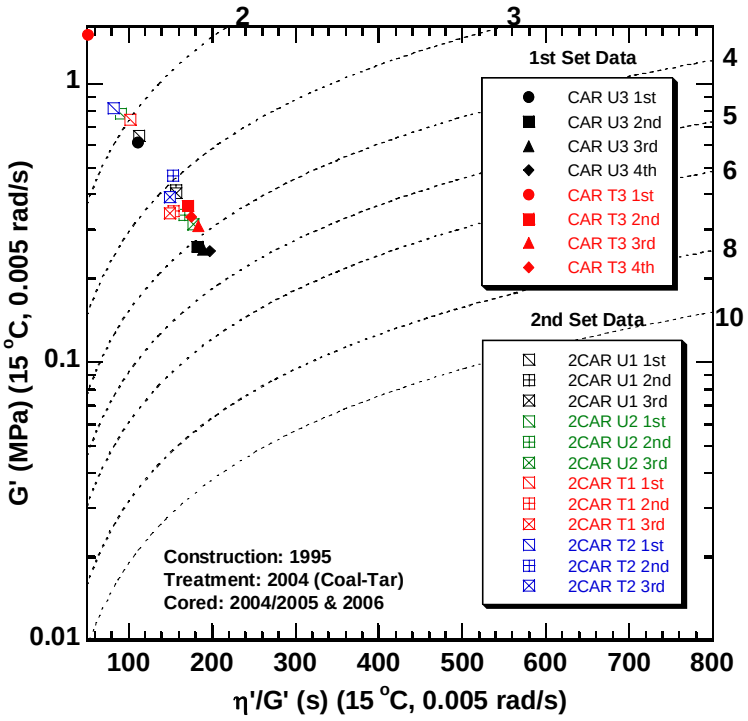

Figure 4-9. DSR Map for Binders Recovered from the Carrizo Springs Airport Cores.

Figure 4-10 shows the DSR map data for the Fort Worth FM 4 pavement that was placed in 2000 and treated in 2005. Data for both corings obtained in the first year and second year are shown, and the results display an extreme span across the DSR map. In fact, this span is covered by the single core, the treated core obtained in the first year, with the first layer binder having a calculated ductility of about 2 cm while the fourth layer data point is almost to the bottom of the DSR map and well off the calculated ductility scale. Similarly, the untreated core from this first year ranged from the value of 3 cm to a value that was well off the ductility scale, but not as far down the map as the treated layer. The second-year data show an extreme range also, but not nearly as much as the first year data. This pavement was treated with the COS-50 fog seal material. This extreme range in data across the DSR map is certainly the result of different binder materials in different slices of the pavement.

The SEC chromatograms are shown in 3-20a for the untreated U3 core and in Figure 3-20b for the treated T3 core. As discussed in Chapter 3, there appears to be a gradient in binder type with depth into the pavement. The first layer for both the untreated and treated cores has a fairly high asphaltenes peak relative to the maltenes peak, while the fourth layer has a much lower asphaltenes peak, again relative to the maltenes peak. The second and the third layers vary proportionally between these two extremes. A smaller asphaltenes peak relative to the maltenes peak (everything else being equal) would provide a softer material, and a higher asphaltenes peak would provide a harder material. Additionally, the fourth layer and even the third layer to some degree has a small amount of polymer, but this appears to not change the conclusion about the direction of the binder hardness, as indicated by the SEC chromatograms. So again, it appears that differences, in this case, even extreme differences between the binder properties at the different layers in the cores, cannot be attributed to the COS-50 fog seal

material, but to this rather interesting gradient concentration in the pavement base asphalt material. This span across the DSR map carries over to the cores in the second year as well, in that the first layer for each core is near the 2 cm ductility line. The second layer is close to the 4 cm ductility line, and the third layer is close to the ductility of 7 cm. These are very interesting results, but apparently not at all related to the fog seal treatment. The chromatograms for the second-year cores are shown in Figures 3-21a and 3-21b. Interestingly, and consistent with the DSR map, while they show similar trends in chromatograms in terms of relative concentration between asphaltenes and maltenes, the differences are not nearly present to the extent they are in the first-year data.

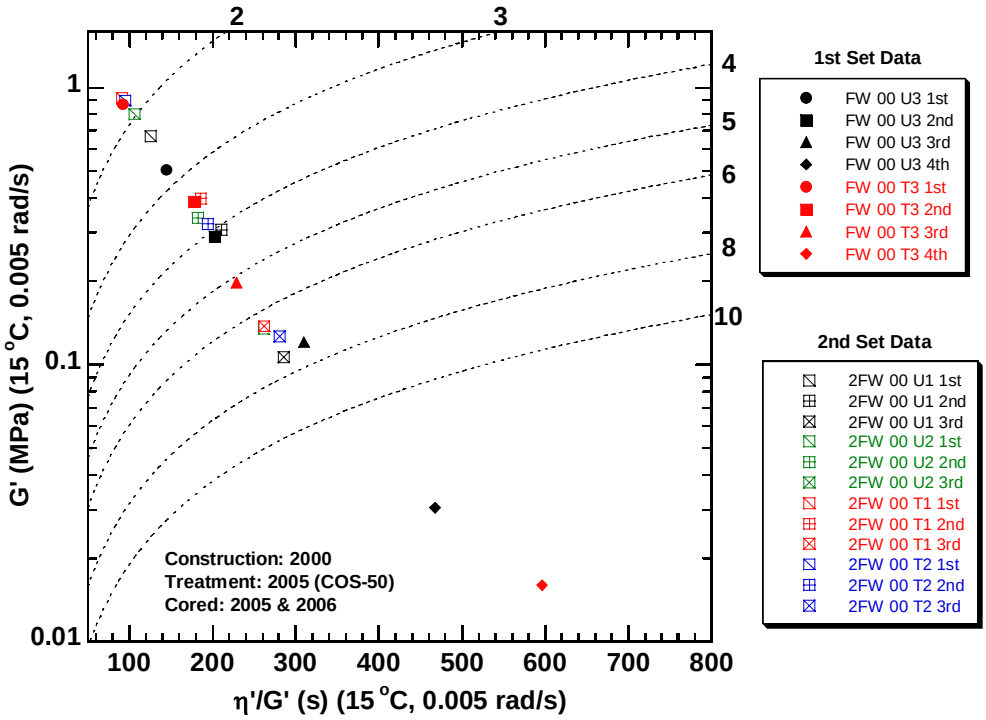

Figure 4-10. DSR Map for Binders Recovered from the Fort Worth FM 4 (2000) Cores.

Figure 4-11 presents the data for the Fort Worth FM 4 pavement that was placed in 2003. These data are much like the pavement placed in 2000 in that again there is an extreme span of the DSR function value across the DSR map. For the cores obtained in the first year, the first and second layer binders give calculated ductilities of almost 4 cm while the third layer untreated binders give a calculated ductility of 7 cm, and the third layer treated binders give the calculated ductility that is well in excess of 10 cm. There is also a fourth layer binder from the untreated core, and its ductility matches the third layer treated core, well in excess of 10 cm. The second year data show an even greater span than the first year data. The first and second layer calculated ductilities are clustered around 4 cm, and the third layer values range from something well exceeding 10 cm to near the bottom of the map. The chromatograms for these cores are shown in Figures 3-22a and 3-22b for the cores obtained in the first year and Figures 3-23a and 3-23b for the cores obtained in the second year. Again, we note the extreme extent to which these chromatograms do not overlay each other and again, there is a gradient change in the relative

concentration of the asphaltenes to maltenes as slices are taken deeper into the pavement. Again, the binder obtained from the first layer has relatively more asphaltenes and less maltenes whereas binders obtained from deeper into the pavement have relatively less asphaltenes and relatively more maltenes. In addition, there is a gradient decrease in the polymer peak for binders that are deeper below the surface of the pavement. Both of these trends would suggest a softer binder for layers that are deeper into the pavement, consistent with the DSR map value shown in Figure 4-11. Again, it is impossible to argue that there is an effect of the fog seal treatment toward softening the binder or that there is an effect on aging of the binder as a result of the fog seal treatment.

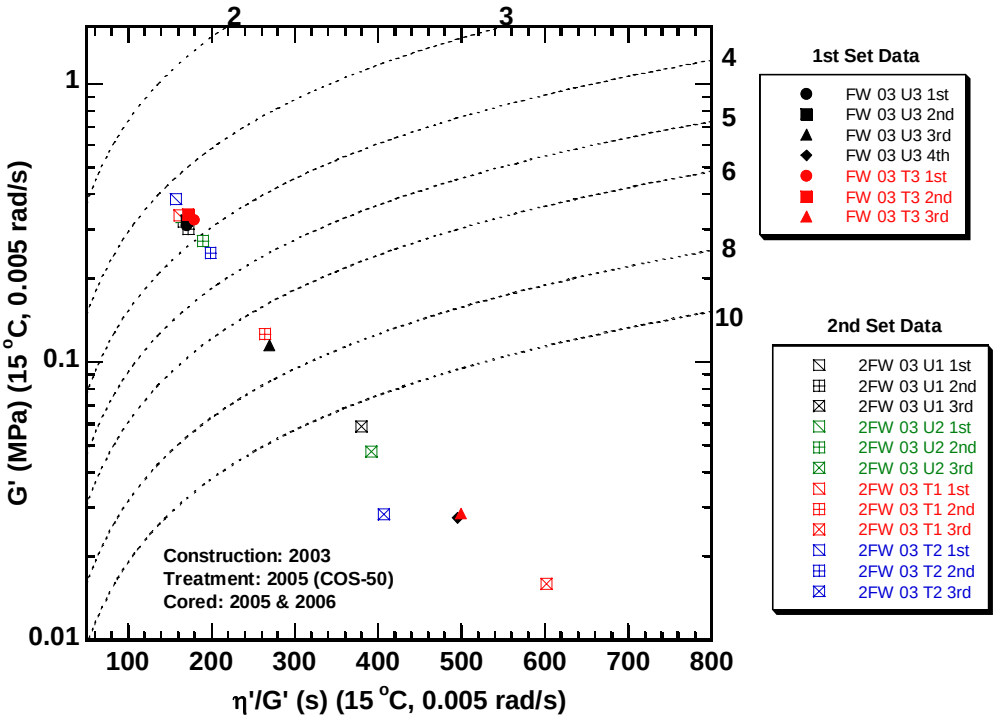

Figure 4-11. DSR Map for Binders Recovered from the Fort Worth FM 4 (2003) Cores.

Figure 4-12 presents data for the Georgetown pavement that was constructed in 1989. The fog seal treatment was applied in 1999, and cores obtained in both the first year and second year of the project are shown. Looking at this DSR map, we see a cluster of data points from the top slices in the neighborhood of 2 cm and below for both the untreated and treated cores and for the cores obtained in the first year and the second year of the project. Furthermore, we see data obtained in the other layers of the core that are significantly higher in the calculated ductility, ranging from about 3.5 to 6 cm. Interestingly, as was the case for Carrizo Springs pavement, we see in this case also that the top layers are notably separated from the other layers in binder stiffness. Notably, the treatment material at this site was also EB44 coal-tar material as it was in Carrizo Springs. In the layers below the top quarter inch, it appears that researchers can form no firm conclusion about the effect of EB44 in as much as the U2 untreated recovered binder in both the first year data U3 core and the second year data U2 core provides the softest materials whereas the treated material (first year T3, second T1 and T2 materials) provides the harder materials. However, the differences, while significant from the experimental viewpoint, are

probably not related to the EB44 treatment, but rather to the differences in the *in situ* binder. Concerning the chromatograms and in the context of DSR function map, it appears notable that the first layer chromatograms in both the untreated and treated cores have more relative asphaltenes compared to maltenes than the other layers, consistent with the first layers being stiffer materials. Again, this added stiffness could be due to a more accelerated aging at the harder surface of the pavement, but nevertheless it is not something we have seen to this degree in the other pavements with the exception of the Carrizo Springs.

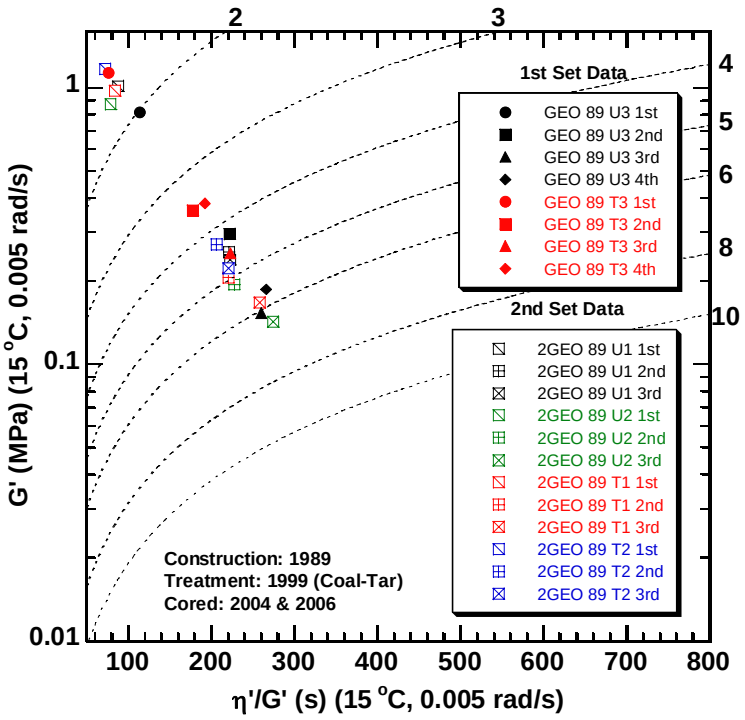

Figure 4-12. DSR Map for Binders Recovered from the Georgetown Airport (1989) Cores.

Figure 4-13 provides the DSR data for the Georgetown pavement that was constructed in 1995. Again, data for cores obtained in both the first year and the second year of the project are shown. These results are very consistent with the Georgetown1989 data in that again the first layer binders are clustered together at 2 cm or below while the binder data from other layers are spread across the map from the calculated ductility of 3 cm up to nearly 8 cm. Beyond that, the layers from each core tend to be clustered fairly close to each other so the differences are likely to be more due to the inherent properties of the *in situ* base binder rather than the EB44 treatment. The chromatograms for the site were presented in Figure 3-25a and 3-25b and again, the layers (for U3 and T3 sites) virtually overlay each other with the exception of the top layer, which has a relatively greater amount of the asphaltenes. A result is again consistent with this top layer having the significantly lower calculated ductility values.

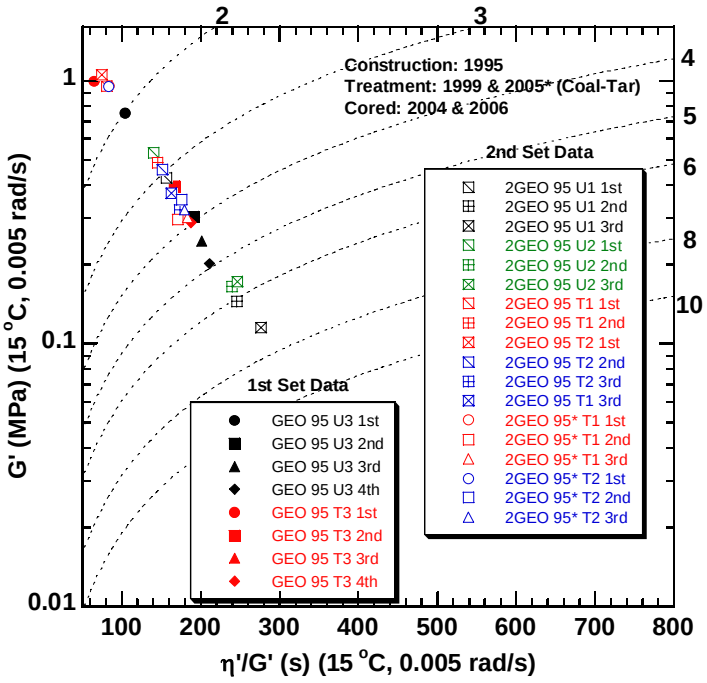

Figure 4-13. DSR Map for Binders Recovered from the Georgetown (1995) Cores.

Figure 4-14 presents the data for the Jacksonville Airport locations for cores obtained in both the first year and second year of the project. This is another case where the recovered binder's calculated ductility values span a wide range across the DSR function map. In fact, the first year cores defined the extreme of this range with the first layer of the treated core having a calculated ductility of about 2 cm and the third and fourth layers of this treated core being something in excess of 10 cm. The second layer is much closer to the third and fourth with a ductility about 9 cm. The second year core data covered a significantly smaller range, but also began at the value of 2 cm for the first layer of the T2 treated core and extended up to the value between 6 and 7 cm for the third layer of the untreated core. The first year untreated core first layer is significantly separated from the second, third, and fourth layer data with it having a calculated ductility of about 3.5 cm while the second, third, and fourth layers are closer to 6 cm. Interestingly, for the second year cores, the first layers of the treated cores, T1 and T2, are significantly stiffer than the first layers of the untreated cores, U1 and U2. The treated cores' calculated ductilities are between 2 and 2.5 cm, approximately, while the untreated ones are much closer to 4 cm. So here again, this is another pavement where the top layers, regardless of whether they are untreated or treated, appear to be significantly stiffer than the next lower layers. Based upon SEC chromatograms (Figures 3-26a, b and Figures 3-27a, b), the treatment material appears to be the coal-tar material. But again, in this case, the clear conclusion seems to be that the wide range of binder stiffness in the untreated versus treated pavements is more the result of the underlying base binder than it is the treatment material. In fact, if there is any effect of the treatment material, it would appear to be to stiffen the binder rather than to soften it. The chromatographic data indicate that the treatment material exists primarily in the top layer while the DSR function data indicate that it is the top layer that is significantly stiffer than binder from the other layers. This question is addressed later in this chapter in statistical comparisons of the treatments and layers.

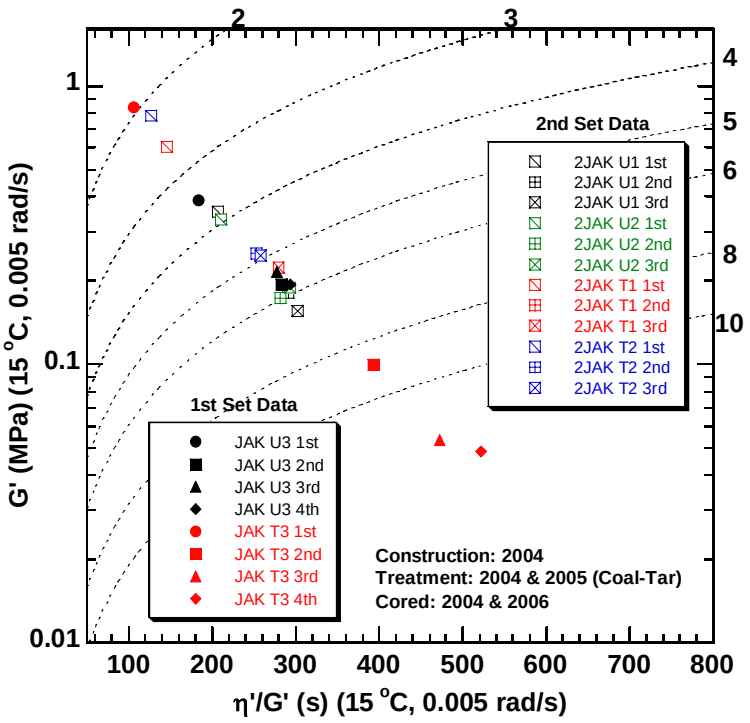

Figure 4-14. DSR Map for Binders Recovered from the Jacksonville Airport Cores.

Figure 4-15 provides data for the Lufkin BUS 59 site from cores obtained in both the first and second year of the project. This site was treated with a rejuvenator material that appears to be much like a coal-tar material, based upon its SEC chromatogram. For these data, we see that the untreated binders from the U1 core fall between 3 and 4 cm calculated ductility, U2 between 4 and 5 cm, and U3 between 3 and 4 cm. However, the results are not necessarily consistent with the top layer being the harder layer, as the reverse is true for U1 and for U3. The treated core, the solid red symbols, spans a range of 2 cm to 5 cm, which is nearly the extreme of this entire data set. Again, however, the order is not perfectly top to bottom, as the first layer is indeed the stiffest, but then the next stiffest is the fourth layer followed by the third then followed by the second which is the softest. The data from the core obtained in the second year show a smaller range in ductilities, from 2 cm to nearly 4 cm. Again, the order of stiffness of various layers is not entirely consistent; while the top layers of U1 and U2 cores are the stiffest, the next stiffest is the third layer of the T1 treated core and the T3 untreated core, then followed by the third layer of the T2 treated core and so on. The softest binders are the second layers of the U1 untreated and the T1 treated cores and accompanied by the third layer of the T1 treated core. The order of these particular samples is hard to justify base upon the chromatograms, because the differences between the different traces seem to be very small. We are then left with no clear trend in the data, but no great discrepancies from one to the other either in terms of a wide range in calculated ductilities, which there is not.

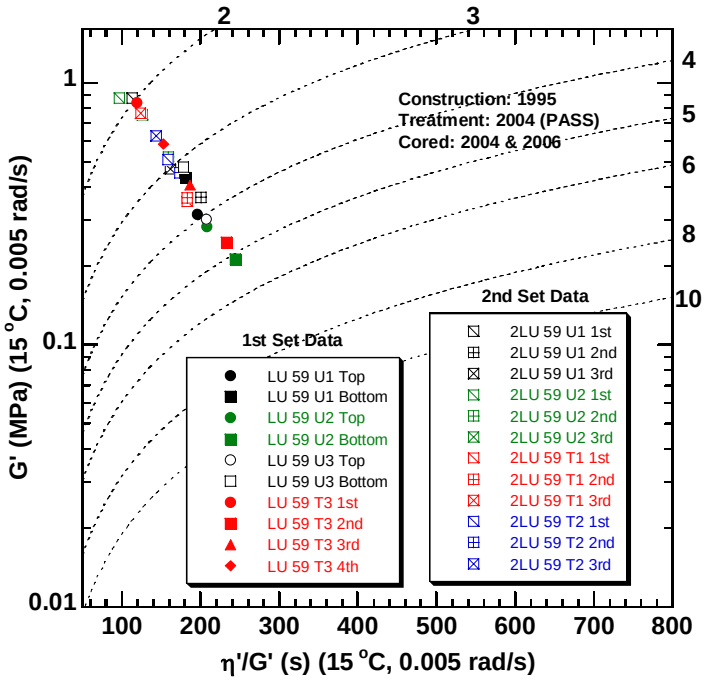

Figure 4-15. DSR Map for Binders Recovered from the Lufkin BUS 59 Cores.

Figure 4-16 presents the data for the Pleasanton Airport from both the first year and the second year of the project. Here again, a rather wide range in calculated ductilities from below 2 cm up to well above 10 cm is observed. However, there are some clear comparisons between the data in that for the first year cores, the top layer in both the untreated and the treated case is significantly harder than the lower layers. For example, the U3 core first layer has the calculated ductility of 3 cm, whereas the second, third, and fourth layers range from 9 cm to well above 10 cm. Additionally, the first year treated core has the first layer calculated ductility that is less than 2 cm and the second, third, and fourth layer calculated ductilities that are close to 5 cm. These are quite significant differences and represent real differences in binder properties. These second year data show similar differences although not to the same extreme. For both the T1 and T2 cores, the first layers show the calculated ductility of about 2 cm, while the second and third layers in each case show ductilities of about 4.5 cm.

Comparing these results to the SEC chromatograms (Figures 3-29a and 3-29b) provides some confirmation of these results. The first layer chromatogram for the U3 core (Figures 3-29a) shows a significantly higher level of asphaltenes compare to the other three layers and this corresponds well to the lower calculated ductility for the same recovered binder. These chromatograms are both for the first year data; the second year chromatogram data are not available. For the T3 cores (Figure 3-29b) the first layer shows an asphaltenes peak that is higher relative to the maltenes peak than the other materials. It also shows the coal-tar EB44 material in the first layer. This is another example where the EB44 material is used and is clearly detected in the first layers and these layers' stiffnesses are significantly greater than the other layers in the cores. However, it should be noted again that the binder recovered from the untreated cores at this same site also were stiffer than the binder recovered from the other layers. These issues will be discussed later in this chapter in the section on statistical comparisons.

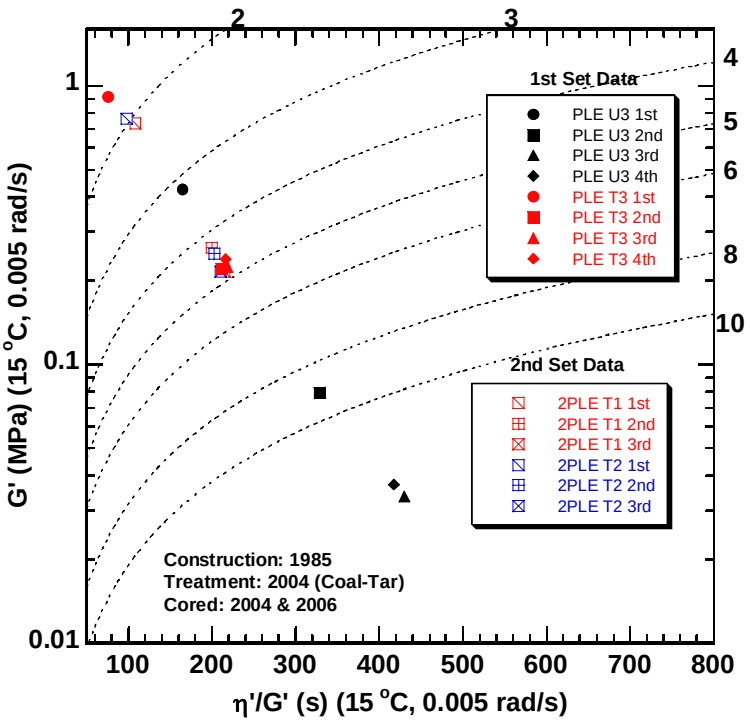

Figure 4-16. DSR Map for Binders Recovered from the Pleasanton Airport Cores.

Figure 4-17 presents the data for Odessa SH 149. The chromatograms of this site are not available, but there is an interesting observation with these recovered binders in that for each of the cores, the third layer is stiffer than the other two, while the second layer is the softest of the three with the exception of the U2 core for which the first layer is the softest (calculated ductility of 8 cm), the second layer, the next softest, with the calculated ductility of 6 cm, and the third layer, the hardest, with the ductility of 5 cm. Also, there appears to be no particular correlation between untreated and treated pavements.

Figure 4-18 presents the DSR map data for the Odessa SH 349 site. These binder properties also form a very wide range across the DSR map, the extreme limits of which are established by the two untreated cores with the very softest binder being the first layer of the U1 core. Meanwhile, the treated cores, T1 and T2, lie in the middle of this extreme range. For each of the four cores in this figure, the four softest binders are from the very top layers recovered from the two untreated and two treated cores. While the chromatograms are not available for this site, this unusual behavior of the very wide span of stiffnesses for the recovered binders and the fact that the top layers are the softest of the recovered binders, are almost certainly the result of an unusual pattern to the *in situ* base binder used in this site, much as it was for the Fort Worth site.

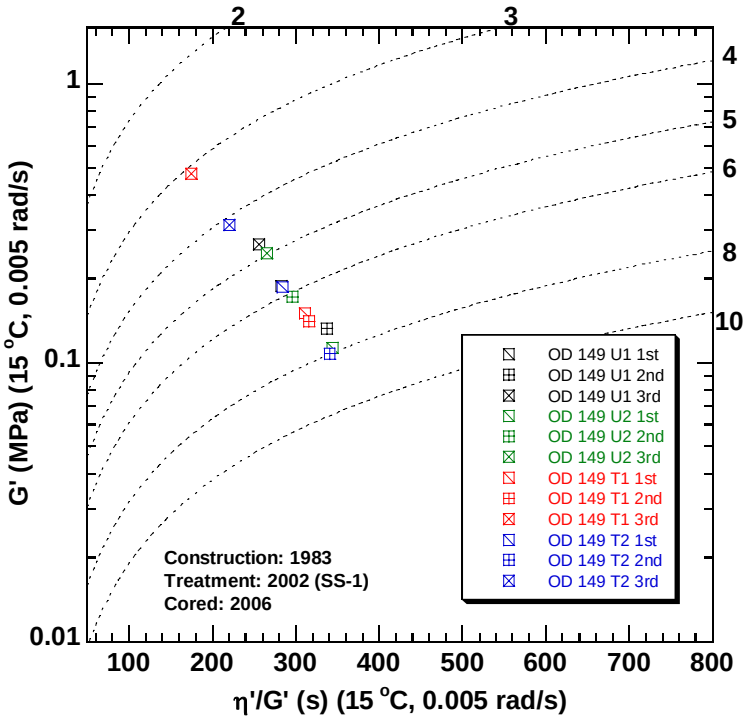

Figure 4-17. DSR Map for Binders Recovered from the Odessa SH 149 Cores.

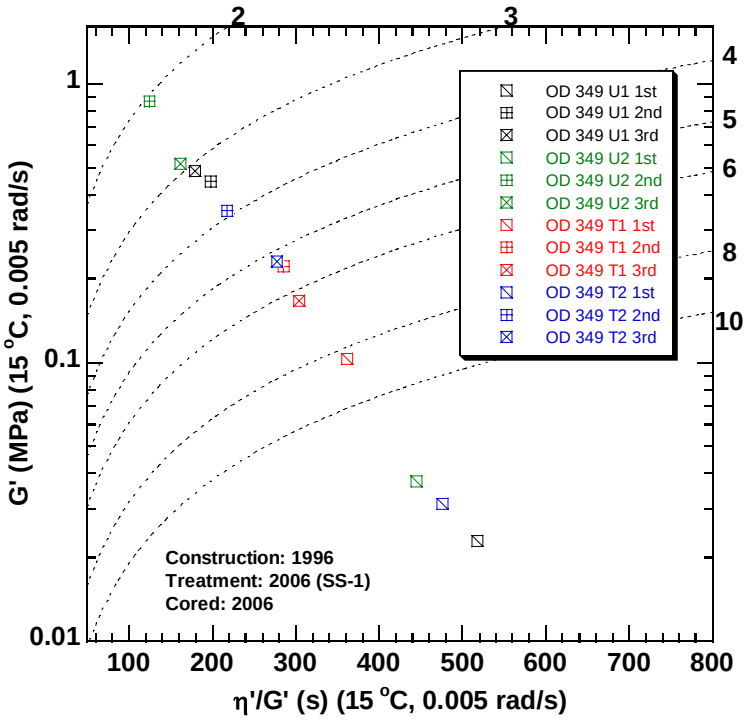

Figure 4-18. DSR Map for Binders Recovered from the Odessa SH 349 Cores.

Figure 4-19 provides the data for the Tyler site that used the PASS fog seal material. At this site, all four of the first layer binders are the stiffest materials and clustered around the ductility of 2 cm while all of the other layers clustered together between the ductility of 4 and 5 cm. Thus, here the binder behavior is much more reasonable, with the top quarter inch being notably more aged than the others, but with no apparent significant differences between the untreated and treated binders in any other cores. We do not have the chromatograms for these binders, but it appears unlikely that there are any particular surprises between the different binders used in these cores.

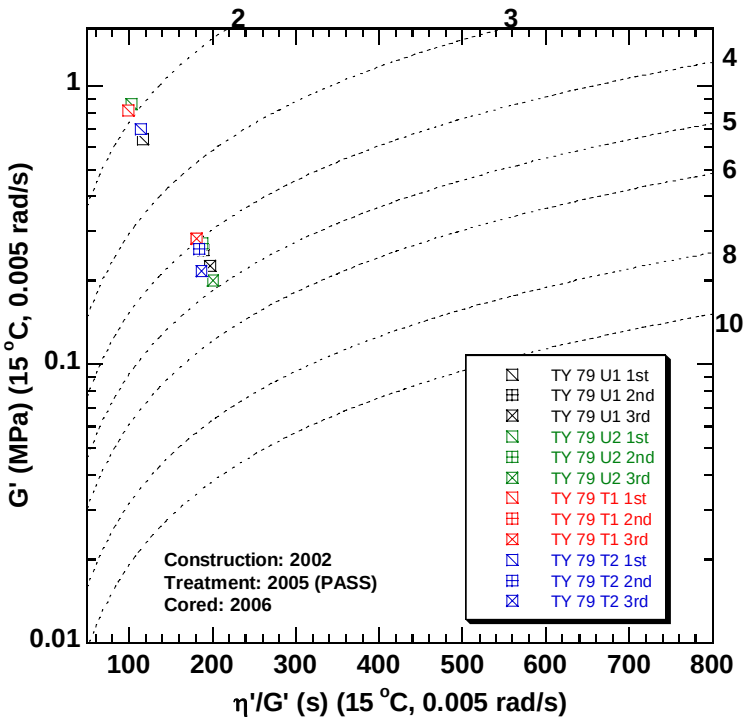

Figure 4-19. DSR Map for Binders Recovered from the Tyler US 79 Cores.

Oxidative Aging – Carbonyl Area

Figures 4-20 through 4-25 compare the carbonyl levels in recovered binders from untreated and treated cores at several different sites. The data are limited, as infrared spectroscopy measurements were not made on all of the recovered binders. Figure 4-20, is the Abilene SH 36 site that was treated with the PASS fog seal material. The other sites are the various airport sites which were treated with the coal-tar or rejuvenator materials. Consequently, the conclusions that can be made are quite limited; however, an idea of the extent to which the treatment might affect binder oxidation can be obtained.

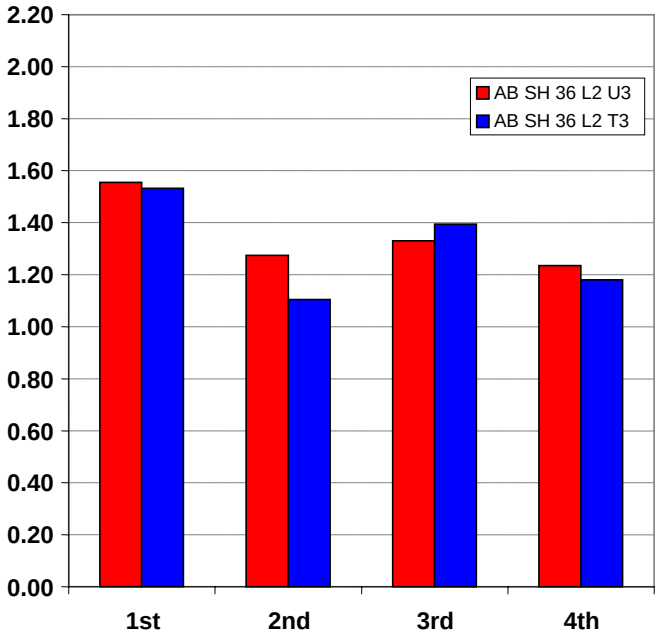

Figure 4-20. Carbonyl Content for Abilene SH 36 L2 Recovered Binders.

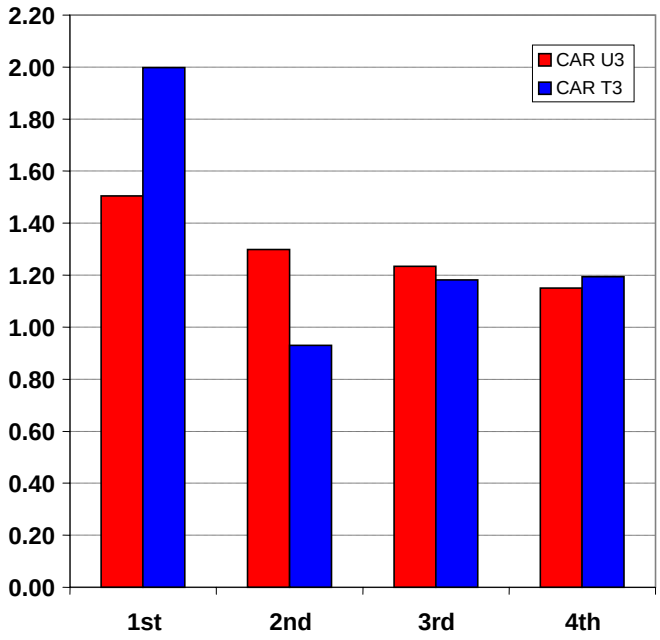

Figure 4-21. Carbonyl Content for Carrizo Springs Airport Recovered Binders.

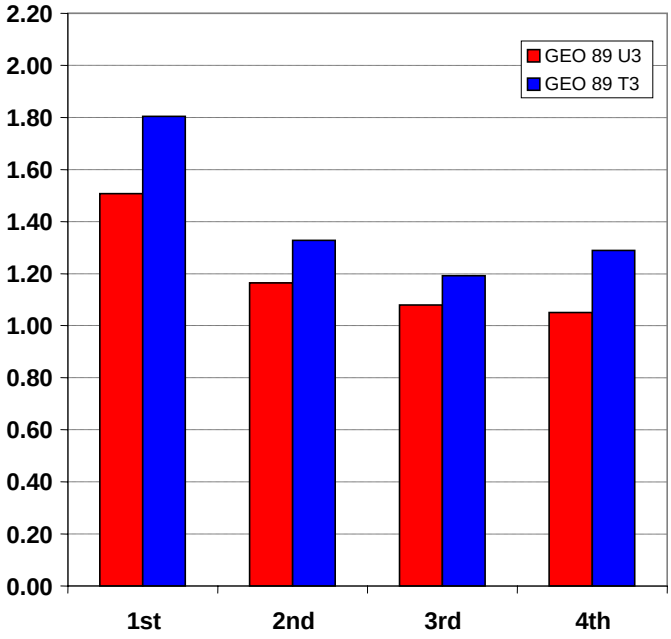

Figure 4-22. Carbonyl Content for Georgetown Airport (1989) Recovered Binders.

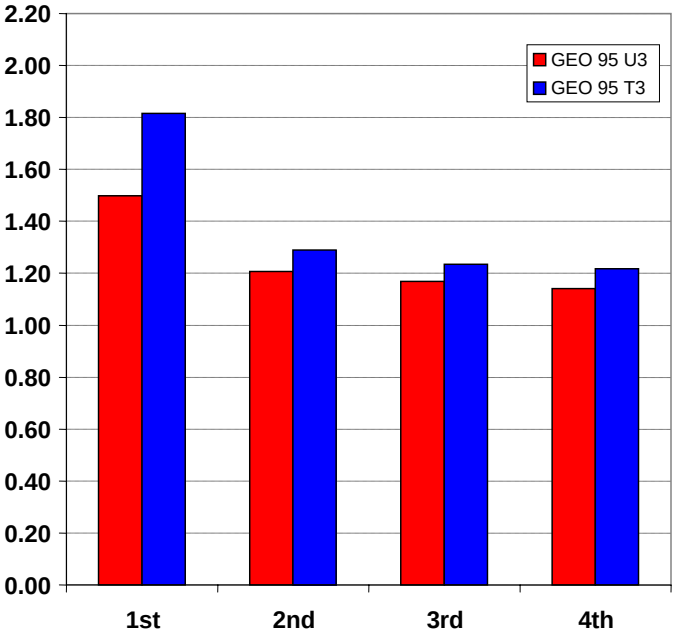

Figure 4-23. Carbonyl Content for Georgetown Airport (1995) Recovered Binders.

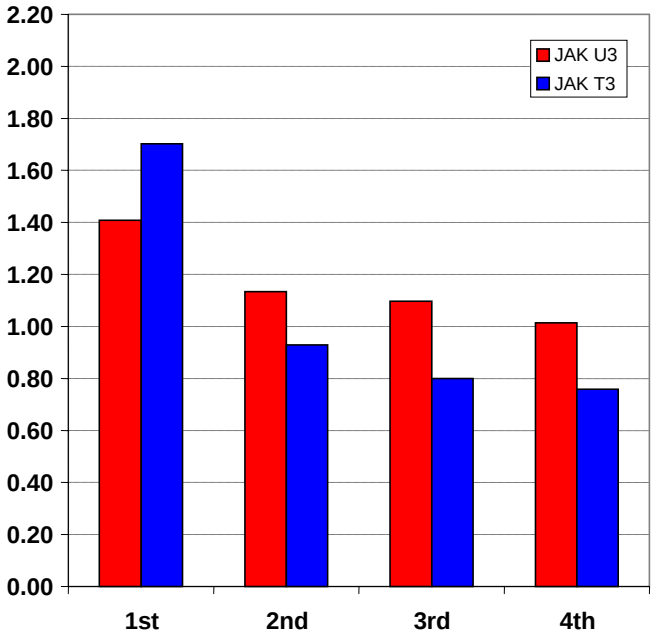

Figure 4-24. Carbonyl Content for Jacksonville Airport Recovered Binders.

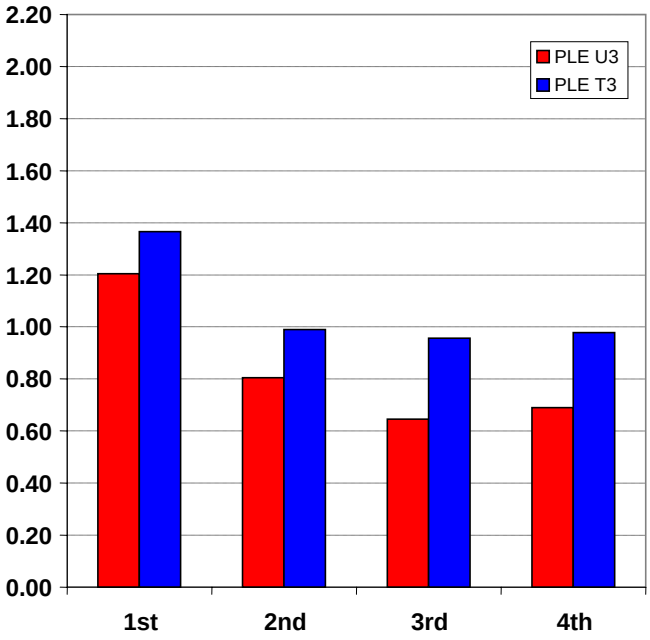

Figure 4-25. Carbonyl Content for Pleasanton Airport Recovered Binders.

Concerning the PASS treated material, Figure 4-20, we see that there is no clear difference between the untreated and treated recovered binders, and this conclusion is true regardless of the depth of the layer into the core. For some of the layers, the untreated binder carbonyl area, CA, is greater than for the corresponding treated binder (layer 1, 2, and 4) and for the other layers, the reverse is true. However, the differences are relatively minor and certainly cannot be attributed to any effects of the fog seal treatment.

The rest of the figures are for coal-tar type treatments. While some of the differences between the untreated and treated binders look significantly greater than they were for the PASS treatment, the differences do not appear to occur with sufficient order as to provide conclusive indication of a trend in the effect of treatment on the binders' carbonyl area. Complicating this conclusion is the fact that the coal-tar material cannot be recovered and tested for either its original carbonyl area or for its response to oxidative aging. The Carrizo Springs site (Figure 4-21) is an interesting example in that the binder recovered from the first layer shows the treated binder to have a notably greater CA than the untreated binder, but for the second layer, the reverse is true (although to the lesser degree) and for the third and fourth layers, the CA values are close enough to be called the same. Whether the seemingly large difference in the first layer is due to the effect of the treatment or an initially high CA in that layer or some other reasons not related to the treatment is not known. For both of the Georgetown 1989 and 1995 sites, the top layer (first layer) also shows the treated binder to be a notably higher in carbonyl area than the untreated binder and the other layers show considerably less difference, but the interesting fact at these two sites is that for each layer tested, the CA of the treated binder is greater than the CA of the corresponding untreated binder. However, the differences are relatively small especially for the Georgetown 1995 site (Figure 4-23) and thus it cannot be stated that there is any effect of the treatment. Again, this is a coal-tar treatment. At the Jacksonville site (Figure 4-24) , again the first layer treated binder shows a higher CA than does the untreated site, but the other layers, 2 through 4, have CA values for the untreated binders that are greater than for the treated.

The data for the Pleasanton site are shown in Figure 4-25. This is another case where all the treated binders have CA values in excess of the untreated values, although for the first layer, the differences are not as great as they were for the Carrizo Springs or Georgetown sites or even for the Jacksonville site. The fact that for the preponderance of the sites, the treated binders have higher carbonyl areas than the untreated is interesting, but as stated previously, the limited data and the inconsistency of this result prevent a conclusion as of the effect of the treatment to within any reasonable degree of certainty. It should also be observed that the time of coring relative to the treatment is different for some of these sites. For the Abilene site, the application date was 2004, and the cores were taken beginning in 2004 and extending into 2005. Similar timing exists for the Carrizo Springs Airport site. However, for the Georgetown sites the applications were made in 1999, and coring occurred 5 years later in 2004 so for those two sites, there were some significant delays between the treatment and the coring. It is conceivable that this delay had an effect on the treated binder aging. However, from the data, it is certainly not clear that it is true. The Jacksonville and Pleasanton sites had the treatments applied in 2004, and the cores were obtained shortly after the treatments, also in 2004. For those cases, where the cores were obtained fairly soon after the treatments, enough time did not elapse for the treatments to have had an effect on the aging, either to accelerate the aging or to retard the aging, perhaps through

blocking access of oxygen. It is conceivable at these sites that the treatment would have altered the measured CA to the extent the blending of the treatment material with the *in situ* binder brought about a composition change that affects the carbonyl content. However, again, the data are inconclusive as to whether any of these factors might have played a role in the data.

Hardening Susceptibility

Figures 4-26 through 4-29 present hardening susceptibility comparisons for those binders where infrared measurements of carbonyl content were made. The hardening susceptibility is an indication of the extent to which a binder hardens in the response to oxidation, with the oxidation measured by the area under the carbonyl band of the infrared spectrum. In these figures, η_0*, the low shear rate limiting dynamic viscosity, is used to represent binder stiffness and as a binder ages it hardens, resulting in an increase in this η_0*. Thus a plot of log η_0* versus carbonyl area generally provides a straight line that represents hardening that occurs in response to oxidation, and the slope of this line is termed the hardening susceptibility. In these graphs, the hardening data are obtained site-by-site and core-by-core from the recovered binder obtained from the layers in each core. Thus they do not represent controlled laboratory experiments of binder aging, but rather they simply represent the aging that occurred under the oxidation conditions in the pavement. As a consequence, the data points are not spread out over a very broad range in either η_0* or carbonyl area and therefore these correlating statistics related to the hardening susceptibility slope are generally quite poor.

Figure 4-26 provides the data for the Abilene L2 site. In this case, in particular, there is a fair degree of scatter among the data points even though we saw fairly good agreement between the carbonyl area values for the untreated and treated binders. Referring back to the chromatograms for this site (Figures 3-7a and 3-7b), we noted that there are enough differences in the chromatograms that suggest that the binder is not uniform through the pavement and in fact the fourth layer binder, which has a very small amount of polymer in the untreated core, is a decidedly different binder, and its maltenes peak also has a broader tail to it. The scatter in the data points produces a low degree of confidence in the hardening susceptibility values and thus prevents a conclusion as to whether the untreated and treated values are different.

Figure 4-27 shows the hardening susceptibility data for the Carrizo Springs untreated and treated cores. While the slopes of these two data sets look significantly different, we should note that for both the untreated and treated binders, the values of the η_0* obtained from layers 2, 3, and 4 are essentially all the same and even their carbonyl values are in very close agreement. Therefore, the hardening susceptibility values are established almost entirely by the first layer data points and thus the fact that the treated binder shows an exceptionally higher carbonyl area plays an important role in the lower hardening susceptibility slope obtained from this treated core. Consequently, it is difficult to say with any certainty that there is a difference between the untreated and treated hardening susceptibilities.

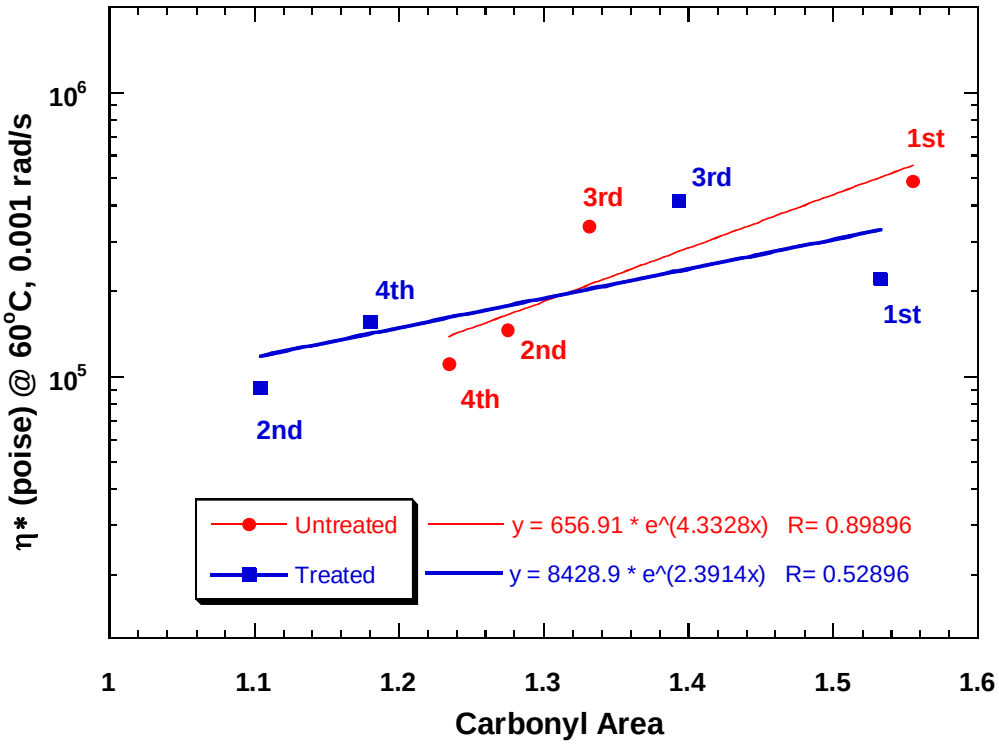

Figure 4-26. Hardening Susceptibility Comparison for the Abilene SH 36 L2 Site.

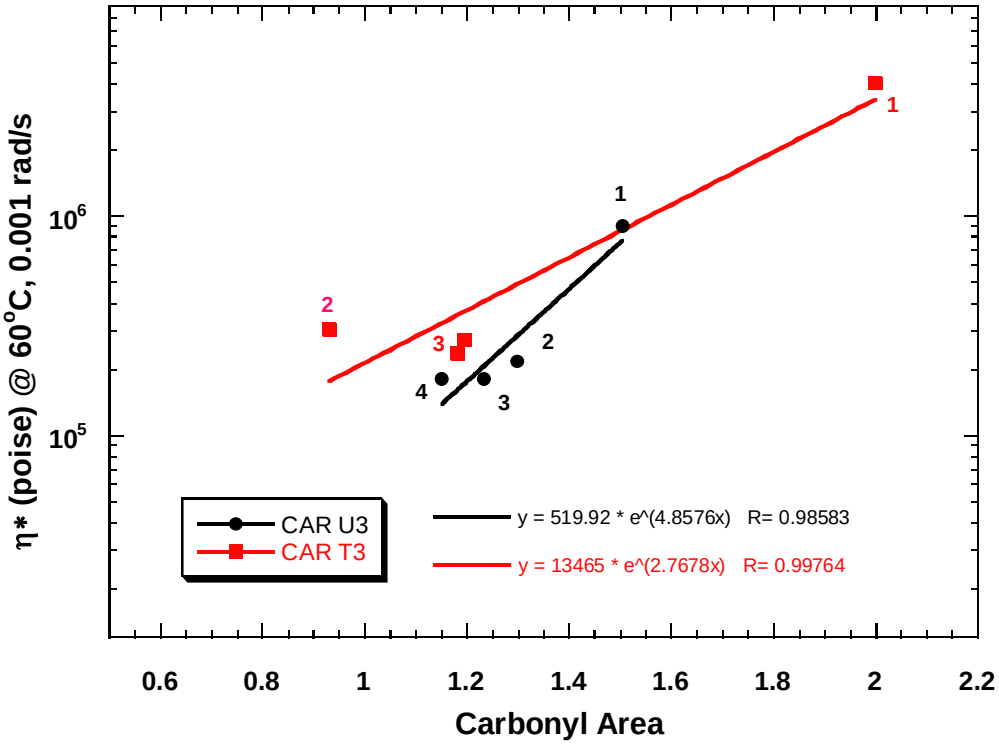

Figure 4-27. Hardening Susceptibility Comparison for the Carrizo Springs Airport Site.

Similar statements can be made for the Georgetown 1989 and 1995 sites (Figure 4-28), although the results appear to be more consistent. Nevertheless it should be noted that any experimental error in the top layer data could change the result significantly. Nevertheless, both 1989 and 1995 sites show an untreated hardening susceptibility in a range of 5 to 5.5, whereas the treated hardening susceptibility is in the range of 3 to 3.5. These results might suggest that the treatment has resulted in a lower hardening susceptibility and therefore a binder that it is less susceptible to the effects of oxidative aging. However, it should be stated that this is a very tentative statement and cannot be a firm conclusion without acquiring substantially more data.

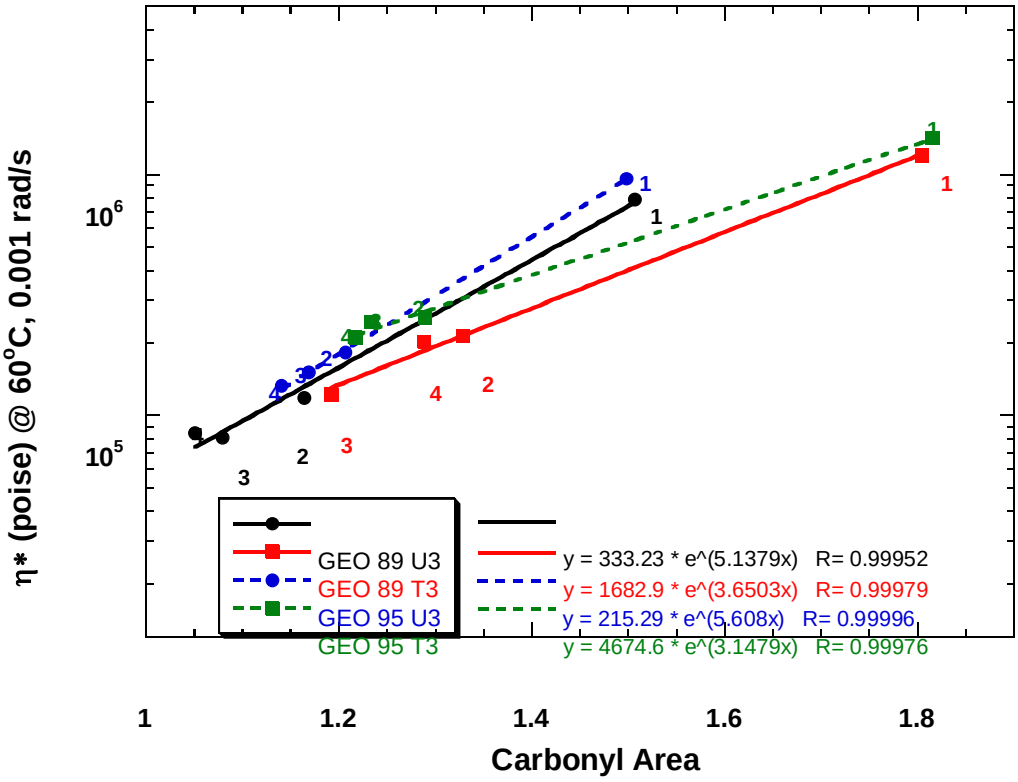

Figure 4-28. Hardening Susceptibility Comparison for the Georgetown Airport Sites.

Figure 4-29 shows the data from the Jacksonville Airport site and in this case one would have to conclude that there is no hardening susceptibility difference between the untreated and treated binders.

Because of the uncertainty and the difficulty of making firm determinations of the effect of the treatments on hardening susceptibility, obtaining further data for these types of comparisons was placed as a low priority item for the project.

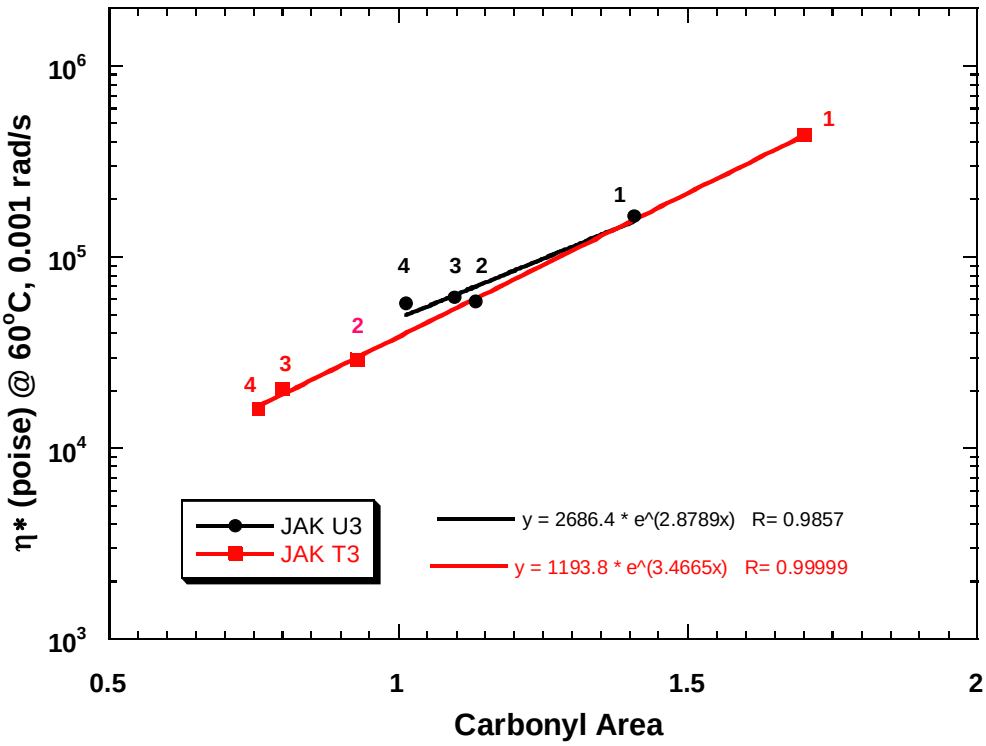

Figure 4-29. Hardening Susceptibility Comparison for the Jacksonville Airport Site.

Binder Rheology – Calculated Ductility

Rheological data for the binders recovered from the various pavement slices at each of the core locations were presented in Tables 4-1 through 4-17, and the data were shown graphically in the DSR maps on Figures 4-1 through 4-19. These results were discussed in the context of mostly qualitative differences between the layers for the untreated versus treated binders; quantifying the data directly was not presented in detail. In this section, the binder rheology is compared directly, and statistical calculations are presented to support the conclusions.

Figures 4-30 through 4-38 show the calculated ductility values (at 15 °C, 1 cm/min) of the various core slices at each of the locations. In each figure, the ductilities are compared layer by layer so that all of the first layer binders at a given location are compared, untreated versus treated. Then all of the second layer binders are compared, again untreated versus treated, and then the third layer binders are compared. This comparison is intended to focus more directly on the untreated versus treated binders, as differences having to do with oxidation at different levels in the pavement are reduced as are differences having to do with some of the gradation of binder at different levels that became apparent from viewing the SEC chromatograms. The calculated ductility is used to measure binder stiffnesses based on the correlation of Ruan et al. (2003). The DSR function values could be used just as well, because the correlation is a direct correlation between ductility and the DSR function. However, the ductility is probably a number that most people are more familiar with than the DSR function, and thus it was chosen in this work as a property for comparing the rheological stiffness of the binders.

Figure 4-30 presents the data for the Abilene SH 36 L1 and L2 sites. The first layer binders from the L1 site (second-year cores only) show quite consistent calculated ductilities of just over 2 cm and no differences between untreated and treated binders. By contrast, the second slices from the L2 site show considerably more variability, and include data obtained in the first year of the project, for which the untreated calculated ductility is a little over 3 cm whereas the treated ductility is about 4.5 cm. Considering all of the second-year cores, untreated binder ductilities range from about 2.1 to 2.5 cm versus treated binder ductilities that range from about 2.2 to 3.2 cm. Viewing all of these data, a pattern is not clear.

In Figure 4-31, the Abilene R1 and R2 sites are shown, and the striking feature of the R1 site is that all of the calculated ductilities from all three layers and for both the untreated and treated cores lie in a range of 2 to 3 cm. The uniformity of the values is quite striking. At the R2 site, such uniformity does not exist at all because the first layer data are all in very good agreement under 2 cm, whereas the third layer calculated ductilities range from 5 up to a high of about 15 cm for one of the treated cores. The point here is that the measurements show significant differences between the different layers and probably between the untreated and treated layers as well.

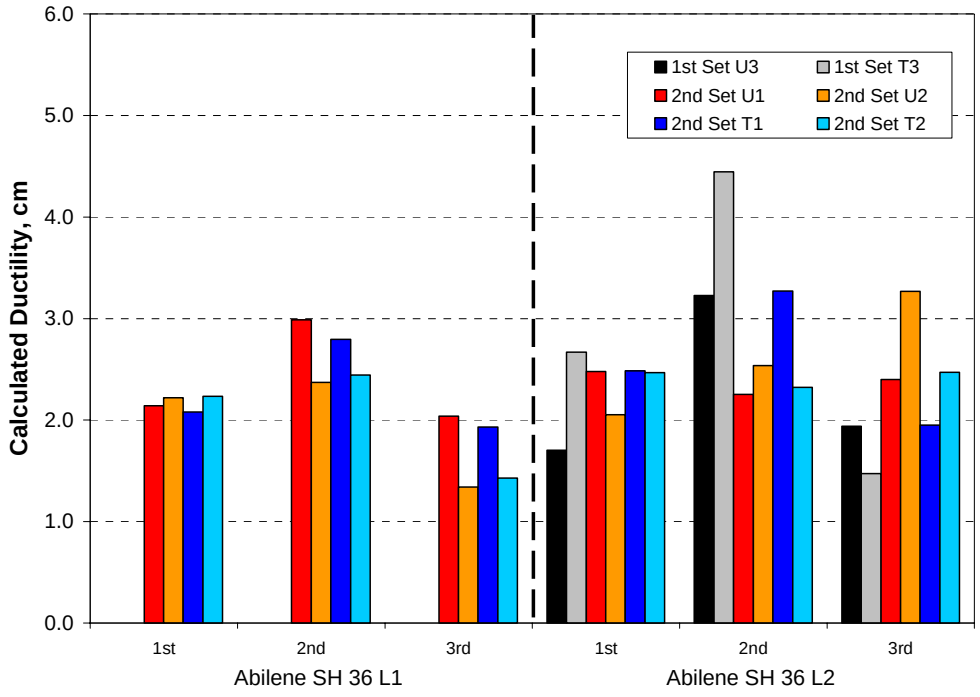

Figure 4-30. Abilene SH 36 L Series Calculated Ductility Comparison by Layer.

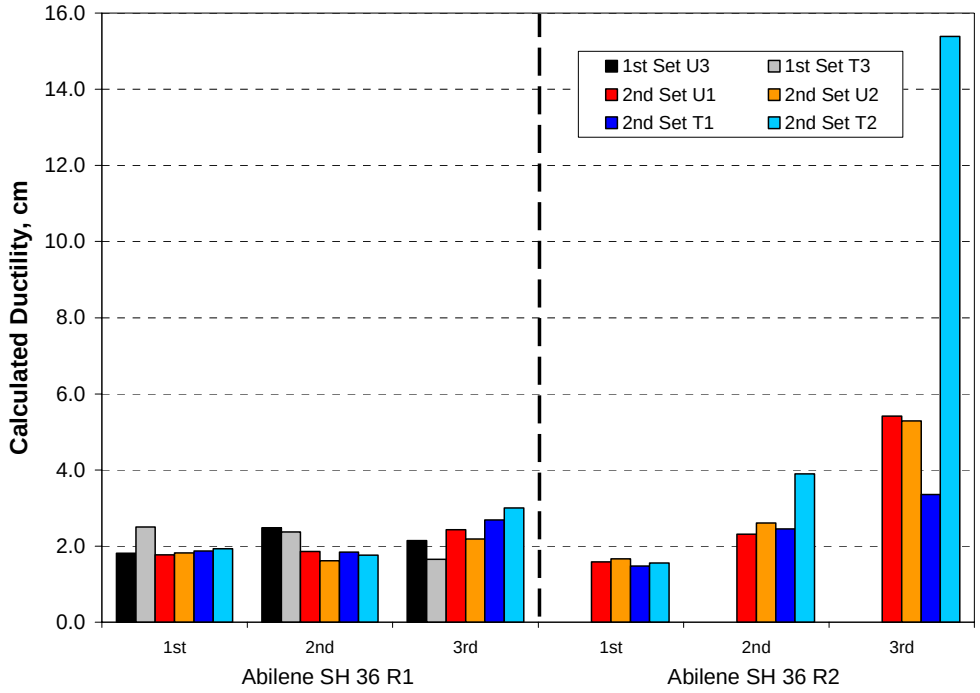

Figure 4-31. Abilene SH 36 R Series Calculated Ductility Comparison by Layer.

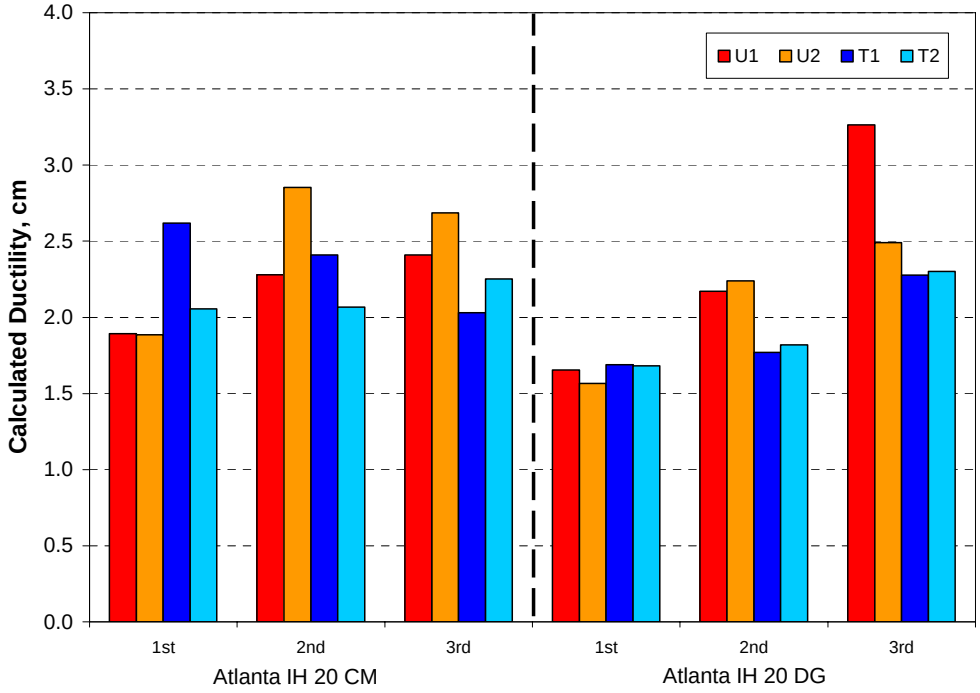

Figure 4-32. Atlanta IH 20 CM and DG Calculated Ductility Comparison by Layer.

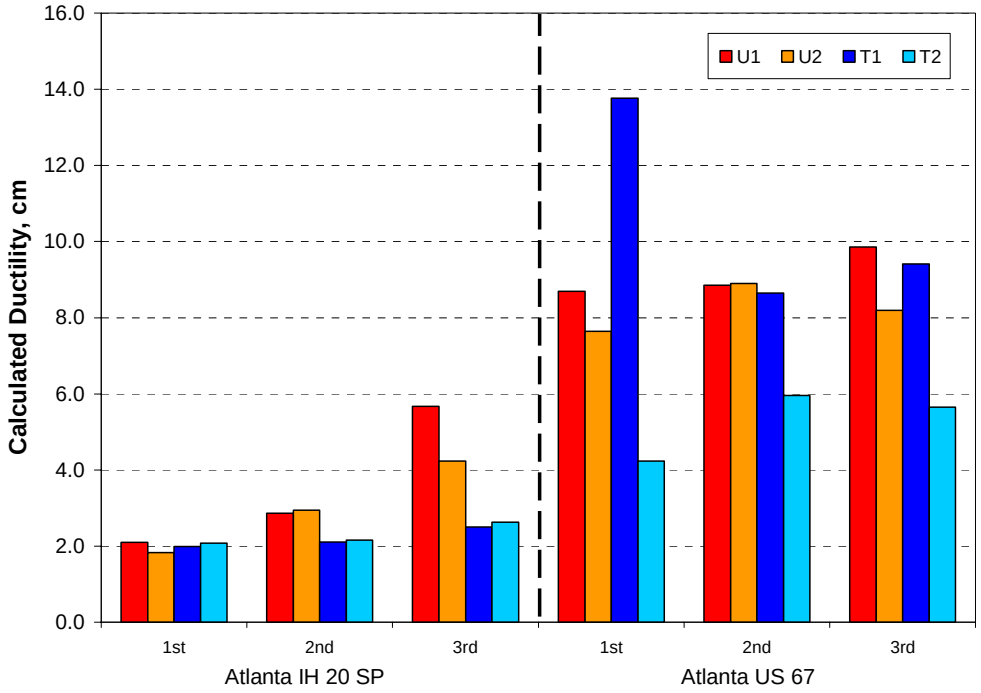

Figure 4-33. Atlanta IH 20 SP and US 67 Calculated Ductility Comparison by Layer.

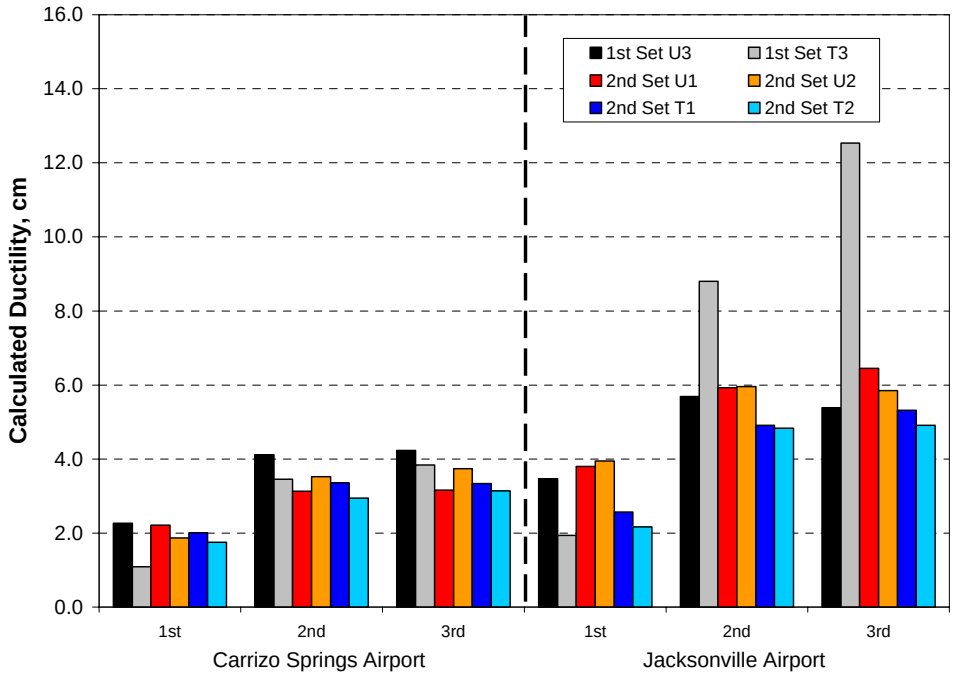

Figure 4-34. Carrizo Springs and Jacksonville Airports Calculated Ductility Comparisons by Layer.

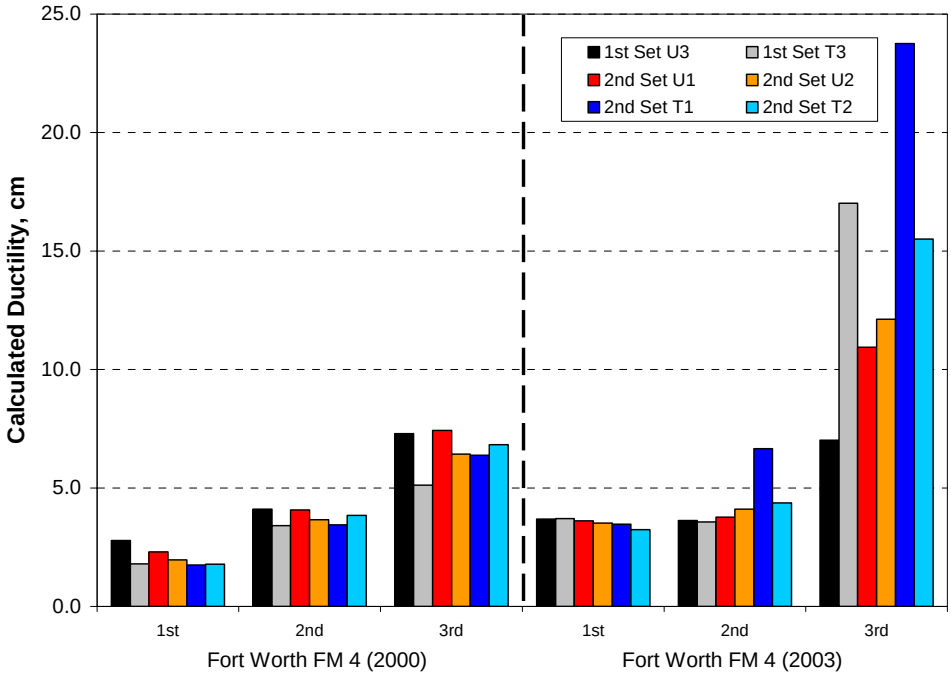

Figure 4-35. Fort Worth FM 4 (2000) and (2003) Calculated Ductility Comparison by Layer.

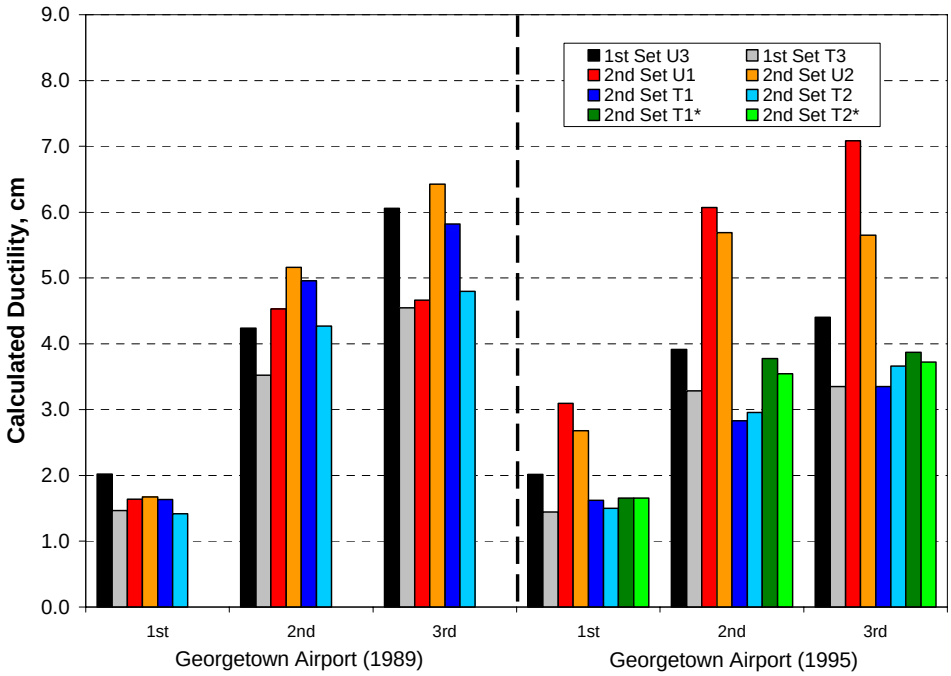

Figure 4-36. Georgetown Airport (1989) and (1995) Calculated Ductility Comparison by Layer.

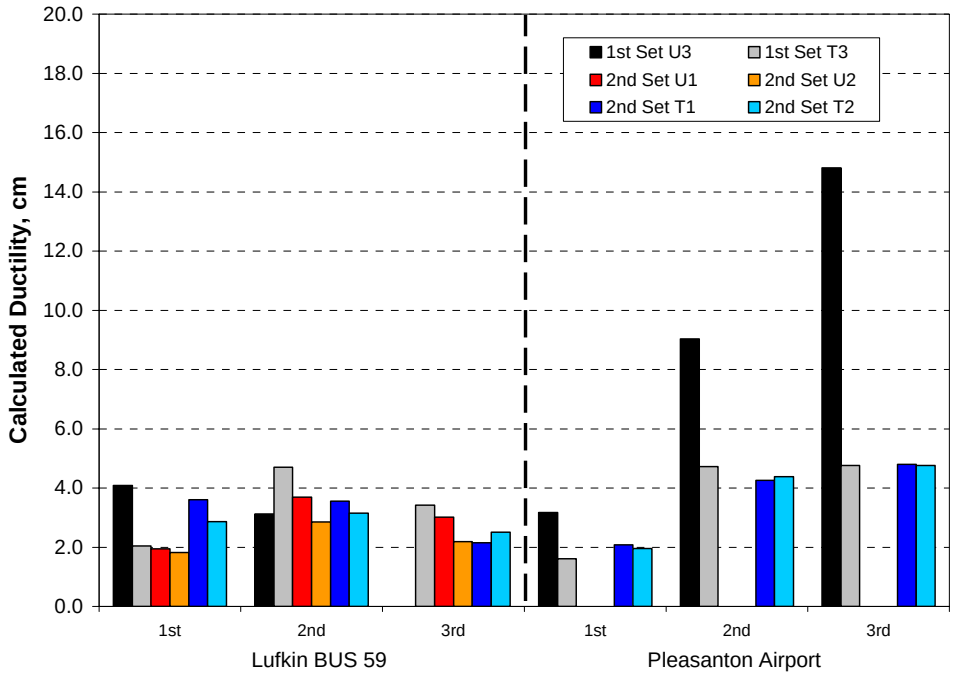

Figure 4-37. Lufkin BUS 59 and Pleasanton Airport Calculated Ductility Comparison by Layer.

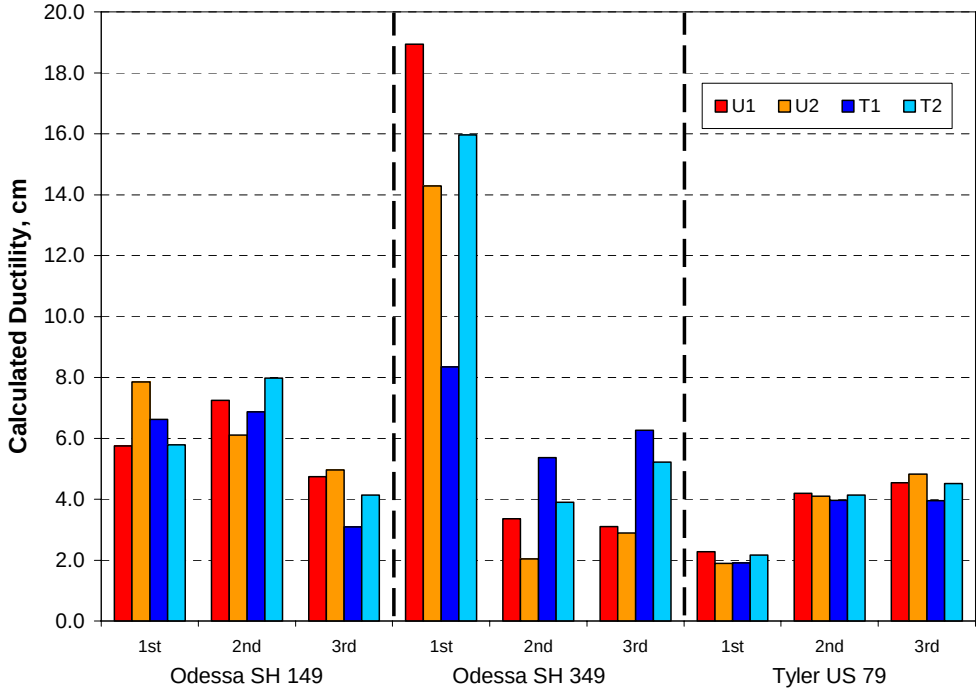

Figure 4-38. Odessa SH 149, SH 349, and Tyler US 79 Calculated Ductility Comparison by Layer.

Without going through each figure in great detail, a few highlights will be noted and then further discussion will be made within a context of statistical comparisons.

Figure 4-34 shows data for the Carrizo Springs and Jacksonville Airports and the interesting result here is that at the Jacksonville Airport, the second and third layers of the core obtained in the first year of the project show interesting and significant differences between the untreated and the treated cores. For the second layer, the untreated binder has a calculated ductility of about 6 cm, whereas the treated value is nearly 9 cm, and the third layer untreated value is about 5.5 cm and the treated is about 12.5 cm. These differences are quite large within the context of normal ductility measurement variability. The treatments used at these general aviation airports were coal-tar type materials.

Figure 4-36 shows results for the Georgetown Airport sites. And again, significant differences between the untreated and treated cores are evident. At the Georgetown Airport 1995 site, the cores obtained in the second year of the project, uniformly, show the untreated cores with notably higher calculated ductilities than the corresponding treated core calculated ductilities. The reasons for these differences are not known, but they appear to be quite significant.

Figure 4-37 tells a similar story, this time for the Pleasanton Airport. The cores obtained in the first year of the project again show the untreated core calculated ductilities in the top layer significantly higher than the corresponding treated core calculated ductilities. All of these pavements were treated with the coal-tar type materials as opposed to asphalt emulsion fog seals.

Other comparisons of the calculated ductility data are not nearly as compelling. One exception is the Fort Worth pavements, shown in Figure 4-35. Here, there is good uniformity for each layer of the FM 4 2000 core; the first layer ductilities are all quite low, around 2.5 cm, then the second layer ductilities are all quite uniform and somewhat higher, and then the third layers also are fairly uniform, and higher still, above 5 cm ductility. Similarly, the FM 4 constructed in 2003 has a notably softer binder in the third layer and harder in the first. These results are consistent with the qualitative observations of the SEC chromatograms where these sites in particular exhibited gradient changes in the binder chromatograms with increasing depth into the pavement. These gradient changes are manifested in the calculated ductility data by increases in ductility with increasing pavement depth.

Statistical Comparisons of the Calculated Ductility Values

The previous discussions were largely qualitative, whether they were discussions of the calculated ductility, or discussions of the DSR maps, or discussions of the SEC chromatograms. In this section, further comparisons of the rheology of the binders obtained from the various slices and from the various sites are made for the purpose of making more objective and quantitative comparisons.

Statistical comparisons are made beginning with simple comparisons of all of the calculated ductilities for all of the slices and all of the pavement sites. The values from multiple replicates, layer by layer, were averaged for both the untreated and treated cores. Thus, at each site, a single average value was determined for the calculated ductility on a layer-by-layer basis and for the untreated versus treated cores. Then, with these untreated and treated values, each site and each layer was considered as a paired set from which were calculated differences between the untreated and treated ductilities. These "before" and "after" values were then used in a number of "paired *t*-test" statistical analyses to assess the effect of the treatment on the binder rheology. Again, it should be noted that the calculated ductility values are numbers that were determined simply to represent the rheology of the binder, including both the viscous and elastic nature of the binder and that has been observed to correlate well to binder ductility for unmodified binders. A number of paired *t*-test analyses were determined by grouping the data in different ways. The comparisons included groupings by:

- all sites, all layers, and all treatments (all data);
- all layers grouped by treatments (e.g., all PASS data);
- all treatments grouped by layers (e.g., all top slice data); and
- groups by treatment and by layer (e.g., all PASS top slice data).

The null hypothesis (H_0) used in this study was *"there is no difference between the calculated ductility values of the treated and untreated asphalt binder"*. This null hypothesis will be rejected if the level of confidence of the data set is lower than 0.05 (5%), which means that there are significant differences between the treated and untreated data. In addition, since the ductility values of treated binders can be greater or smaller than those of the untreated ones, non-directional analysis was used to detect the difference in both increasing and decreasing direction.

Thus each of these comparisons is more detailed as to assessing the effects of treatment type. The pairing of the data layer-by-layer and untreated versus treated allowed calculations to be made that eliminated, at least to a large degree, the inherent variability that occurred from site-to-site and layer-to-layer as a result of different binders, different aging rates, and different treatments.

Table 4-18 presents the data for all of the sites and all of the layers together with the statistical calculations. Note again that at each site and for each layer, there is a single number reported for the untreated cores and a single number for the treated cores. Each of these numbers is an average of the results obtained for replicate cores obtained from each site. The layer-by-layer identities are preserved, however. In all, there are 86 samples reported in this table. For each of these samples, there is an untreated data point paired with the treated value. The difference between these untreated and treated values provides a variable D_i which is used for the statistical calculations. From these 86 values, a *t*-statistic is calculated as described in Chapter 3 (Equation 3-1). Then with this t statistic, the student's *t* distribution provides a level of significance for the possibility that these differences between the untreated and treated measurements occurred purely by chance (Montgomery, 2001). In Table 4-18, the mean difference between the untreated and treated calculated ductilities is 0.2 cm, the *t* statistic is 0.82, and the level of significance for non-directional test is 0.42, meaning that there is a 42 percent chance that the mean difference occurred by chance. Thus, the data as a whole do not support a conclusion that the treatments affect binder rheology.

Table 4-18. Paired t-test, All Samples (n=86).

Site	Layer	Average Calculated Ductility (cm)		Sample	D_i
		Untreated	Treated		
2nd Set Abilene L1	1st	2.18	2.15	1	0.03
	2nd	2.68	2.62	2	0.06
	3rd	1.69	1.68	3	0.01
1st Set Abilene L2	1st	1.70	2.67	4	-0.97
	2nd	3.23	4.44	5	-1.22
	3rd	1.94	1.47	6	0.46
2nd Set Abilene L2	1st	2.26	2.48	7	-0.21
	2nd	2.40	2.80	8	-0.40
	3rd	2.83	2.21	9	0.63
1st Set Abilene R1	1st	1.81	2.50	10	-0.69
	2nd	2.48	2.37	11	0.11
	3rd	2.15	1.65	12	0.50
2nd Set Abilene R1	1st	1.80	1.90	13	-0.11
	2nd	1.74	1.80	14	-0.06
	3rd	2.31	2.84	15	-0.54
2nd Set Abilene R2	1st	1.62	1.52	16	0.11
	2nd	2.46	3.17	17	-0.71
	3rd	5.35	9.38	18	-4.02
Atlanta IH 20 CM	1st	1.89	2.34	19	-0.45
	2nd	2.57	2.24	20	0.33
	3rd	2.55	2.14	21	0.41
Atlanta IH 20 DG	1st	1.61	1.68	22	-0.08
	2nd	2.21	1.80	23	0.41
	3rd	2.88	2.29	24	0.59
Atlanta IH 20 SP	1st	1.96	2.03	25	-0.07
	2nd	2.91	2.13	26	0.77
	3rd	4.95	2.57	27	2.39
Atlanta US 67	1st	8.17	9.00	28	-0.83
	2nd	8.88	7.30	29	1.58
	3rd	9.02	7.53	30	1.49
1st Set Carrizo Springs	1st	2.27	1.09	31	1.17
	2nd	4.12	3.45	32	0.67
	3rd	4.24	3.84	33	0.40
2nd Set Carrizo Springs	1st	2.04	1.88	34	0.17
	2nd	3.33	3.15	35	0.18
	3rd	3.45	3.24	36	0.21
1st Set Fort Worth FM 4 (2000)	1st	2.78	1.79	37	0.99
	2nd	4.10	3.42	38	0.68
	3rd	7.29	5.12	39	2.17
2nd Set Fort Worth FM 4 (2000)	1st	2.14	1.77	40	0.37
	2nd	3.87	3.65	41	0.22
	3rd	6.93	6.61	42	0.33
1st Set Fort Worth FM 4 (2003)	1st	3.70	3.71	43	-0.02
	2nd	3.63	3.58	44	0.06
	3rd	7.02	17.02	45	-10.00
2nd Set Fort Worth FM 4 (2003)	1st	3.57	3.36	46	0.21
	2nd	3.93	5.52	47	-1.58
	3rd	11.53	19.63	48	-8.10

Table 4-18. Paired t-test, All Samples (n=86) (Cont'd).

Site	Layer	Average Calculated Ductility (cm)		Sample	D_i
		Untreated	Treated		
1st Set Georgetown Airport (1989)	1st	2.02	1.47	49	0.56
	2nd	4.24	3.52	50	0.72
	3rd	6.06	4.55	51	1.52
2nd Set Georgetown Airport (1989)	1st	1.66	1.53	52	0.13
	2nd	4.84	4.61	53	0.23
	3rd	5.54	5.31	54	0.24
1st Set Georgetown Airport (1995)	1st	2.02	1.45	55	0.57
	2nd	3.91	3.29	56	0.63
	3rd	4.40	3.35	57	1.05
2nd Set Georgetown Airport (1995)	1st	2.89	1.56	58	1.33
	2nd	5.88	2.89	59	2.98
	3rd	6.37	3.50	60	2.86
	1st	2.89	1.66	61	1.23
	2nd	5.88	3.66	62	2.22
	3rd	6.37	3.79	63	2.57
1st Set Jacksonville Airport	1st	3.46	1.94	64	1.52
	2nd	5.69	8.80	65	-3.11
	3rd	5.38	12.54	66	-7.15
2nd Set Jacksonville Airport	1st	3.87	2.37	67	1.51
	2nd	5.94	4.87	68	1.07
	3rd	6.15	5.12	69	1.03
1st Set Lufkin BUS 59	1st	4.09	2.04	70	2.05
	2nd	3.13	4.70	71	-1.58
2nd Set Lufkin BUS 59	1st	1.88	3.24	72	-1.35
	2nd	3.27	3.35	73	-0.08
	3rd	2.60	2.33	74	0.27
Odessa SH 149	1st	6.80	6.20	75	0.60
	2nd	6.67	7.42	76	-0.74
	3rd	4.85	3.61	77	1.23
Odessa SH 349	1st	16.62	12.16	78	4.46
	2nd	2.71	4.63	79	-1.93
	3rd	2.99	5.74	80	-2.74
1st Set Pleasanton Airport	1st	3.18	1.61	81	1.56
	2nd	9.03	4.73	82	4.30
	3rd	14.81	4.77	83	10.04
Tyler US 79	1st	2.08	2.04	84	0.04
	2nd	4.15	4.05	85	0.10
	3rd	4.68	4.24	86	0.44
				Sum	18.01
				M_d	0.21
				SSD	475.17
				Variance	5.59
				σ	0.25
				t	0.82
				Level of significance for Non-Directional Test	**0.41**

Table 4-19 presents the comparable calculation for all three layers, but only for those sites that were treated with the PASS fog seal material. In this case, the *t* statistic was -0.08 (the minus means that treated material on average had a higher ductility than the untreated material). The level of significance of the non-directional test was 94 percent probability that this difference occurred by chance which again means that no conclusion can be drawn about the effect of the treatment and in fact we would have to say that there is no significant difference between the untreated and treated layers for this PASS treatment.

Table 4-19. Paired t-test, All PASS Samples (n=23).

Site	Layer	Average Calculated Ductility (cm)		Sample	D_i
		Untreated	Treated		
1st Set Abilene L2	1st	1.70	2.67	1	-0.97
	2nd	3.23	4.44	2	-1.22
	3rd	1.94	1.47	3	0.46
2nd Set Abilene L2	1st	2.26	2.48	4	-0.21
	2nd	2.40	2.80	5	-0.40
	3rd	2.83	2.21	6	0.63
1st Set Abilene R1	1st	1.81	2.50	7	-0.69
	2nd	2.48	2.37	8	0.11
	3rd	2.15	1.65	9	0.50
2nd Set Abilene R1	1st	1.80	1.90	10	-0.11
	2nd	1.74	1.80	11	-0.06
	3rd	2.31	2.84	12	-0.54
Atlanta US 67	1st	8.17	9.00	13	-0.83
	2nd	8.88	7.30	14	1.58
	3rd	9.02	7.53	15	1.49
1st Set Lufkin BUS 59	1st	4.09	2.04	16	2.05
	2nd	3.13	4.70	17	-1.58
2nd Set Lufkin BUS 59	1st	1.88	3.24	18	-1.35
	2nd	3.27	3.35	19	-0.08
	3rd	2.60	2.33	20	0.27
Tyler US 79	1st	2.08	2.04	21	0.04
	2nd	4.15	4.05	22	0.10
	3rd	4.68	4.24	23	0.44
				Sum	-0.36
				M_d	-0.02
				SSD	18.49
				Variance	0.84
				σ	0.19
				t	-0.08
				Level of significance for Non-Directional Test	**0.94**

Table 4-20 shows the comparable table for the EB44 coal-tar material. In this case, we see that the *t* statistic is 2.29, and the level of significance is 0.03. Thus, we can say that there is a 3 percent probability that the difference between the untreated and treated binders was a chance occurrence. This is a fairly low probability, and thus we would be justified in saying that the EB44 material did affect the calculated ductility of the binder in the direction of producing a stiffer binder, that is to say that the treated binder, on average, is significantly stiffer than the untreated material. Again, this calculation includes all of the top three layers of this pavement.

Table 4-20. Paired t-test, All EB44 Type Samples (n=30).

Site	Layer	Average Calculated Ductility (cm)		Sample	D_i
		Untreated	Treated		
1st Set Carrizo Springs	1st	2.27	1.09	1	1.17
	2nd	4.12	3.45	2	0.67
	3rd	4.24	3.84	3	0.40
2nd Set Carrizo Springs	1st	2.04	1.88	4	0.17
	2nd	3.33	3.15	5	0.18
	3rd	3.45	3.24	6	0.21
1st Set Georgetown Airport (1989)	1st	2.02	1.47	7	0.56
	2nd	4.24	3.52	8	0.72
	3rd	6.06	4.55	9	1.52
2nd Set Georgetown Airport (1989)	1st	1.66	1.53	10	0.13
	2nd	4.84	4.61	11	0.23
	3rd	5.54	5.31	12	0.24
1st Set Georgetown Airport (1995)	1st	2.02	1.45	13	0.57
	2nd	3.91	3.29	14	0.63
	3rd	4.40	3.35	15	1.05
2nd Set Georgetown Airport (1995)	1st	2.89	1.56	16	1.33
	2nd	5.88	2.89	17	2.98
	3rd	6.37	3.50	18	2.86
	1st	2.89	1.66	19	1.23
	2nd	5.88	3.66	20	2.22
	3rd	6.37	3.79	21	2.57
1st Set Jacksonville Airport	1st	3.46	1.94	22	1.52
	2nd	5.69	8.80	23	-3.11
	3rd	5.38	12.54	24	-7.15
2nd Set Jacksonville Airport	1st	3.87	2.37	25	1.51
	2nd	5.94	4.87	26	1.07
	3rd	6.15	5.12	27	1.03
1st Set Pleasanton Airport	1st	3.18	1.61	28	1.56
	2nd	9.03	4.73	29	4.30
	3rd	14.81	4.77	30	10.04
				Sum	32.39
				Md	1.08
				SSD	193.41
				Variance	6.67
				σ	0.47
				t	2.29
				Level of significance for Non-Directional Test	**0.03**

Table 4-21 shows the result for the COS-50 material. In this case, again, there is no statistical strength for claiming an effect of the COS-50 treatment. We must conclude that there is no statistical difference between untreated and treated binders included in this data set.

Table 4-21. Paired t-test, All COS-50 Samples (n=12).

Site	Layer	Average Calculated Ductility (cm)		Sample	D_i
		Untreated	Treated		
1st Set	1st	2.78	1.79	1	0.99
Fort Worth	2nd	4.10	3.42	2	0.68
FM 4 (2000)	3rd	7.29	5.12	3	2.17
2nd Set	1st	2.14	1.77	4	0.37
Fort Worth	2nd	3.87	3.65	5	0.22
FM 4 (2000)	3rd	6.93	6.61	6	0.33
1st Set	1st	3.70	3.71	7	-0.02
Fort Worth	2nd	3.63	3.58	8	0.06
FM 4 (2003)	3rd	7.02	17.02	9	-10.00
2nd Set	1st	3.57	3.36	10	0.21
Fort Worth	2nd	3.93	5.52	11	-1.58
FM 4 (2003)	3rd	11.53	19.63	12	-8.10
				Sum	-14.66
				M_d	-1.22
				SSD	156.57
				Variance	14.23
				σ	1.09
				t	-1.12
				Level of significance for Non-Directional Test	**0.29**

The next set of tables considered the same data, but one layer at the time. We noted before that there appears to be very little evidence of penetration of the fog seal material into the pavement, or at least beyond the top layer of the pavement; the coal-tar material was detected in the top layer, but not at all in the lower layers. Thus, it is reasonable to suspect that there may be quantifiable differences between the layers.

Table 4-22 presents that data for all of the treatment sites and all of the treatment material, but for only the first layer binders. This data set consists of 29 samples and provides the *t* statistic of 2.28 for a level of significance of 0.03. Thus, this calculation provides strong support for the hypothesis that there are differences between the untreated and treated binders in the first layers for all of these sites taken as a group.

Table 4-22. Paired t-test, All Data, Top Layer (n=29).

Sample	Average Calculated Ductility (cm)		D_i
	Untreated	Treated	
1	2.18	2.15	0.03
2	1.70	2.67	-0.97
3	2.26	2.48	-0.21
4	1.81	2.50	-0.69
5	1.80	1.90	-0.11
6	1.62	1.52	0.11
7	1.89	2.34	-0.45
8	1.61	1.68	-0.08
9	1.96	2.03	-0.07
10	8.17	9.00	-0.83
11	2.27	1.09	1.17
12	2.04	1.88	0.17
13	2.78	1.79	0.99
14	2.14	1.77	0.37
15	3.70	3.71	-0.02
16	3.57	3.36	0.21
17	2.02	1.47	0.56
18	1.66	1.53	0.13
19	2.02	1.45	0.57
20	2.89	1.56	1.33
21	2.89	1.66	1.23
22	3.46	1.94	1.52
23	3.87	2.37	1.51
24	4.09	2.04	2.05
25	1.88	3.24	-1.35
26	6.80	6.20	0.60
27	16.62	12.16	4.46
28	3.18	1.61	1.56
29	2.08	2.04	0.04
		Sum	13.83
		M_d	0.48
		SSD	35.61
		Variance	1.27
		σ	0.21
		t	2.28
Level of significance for Non-Directional Test			**0.03**

Table 4-23 provides the same analysis for the second layer, but here the level of significance is now 0.45, a much higher value that does not support a conclusion of differences between the untreated and treated binders. Similarly, Table 4-24 provides the data for the third layer and in this case, the statistical comparison is even weaker as there is basically almost 93 percent chance that this small difference in the mean that is observed is a result of chance. Thus, these three tables that review the data layer-by-layer show that whatever differences there are in the entire data set between untreated and treated binders, they primarily occurred in the top layer, consistent with the qualitative judgments observed previously.

Table 4-23. Paired t-test, All Data, Second Layer (n=29).

Sample	Average Calculated Ductility (cm)		D_i
	Untreated	Treated	
1	2.68	2.62	0.06
2	3.23	4.44	-1.22
3	2.40	2.80	-0.40
4	2.48	2.37	0.11
5	1.74	1.80	-0.06
6	2.46	3.17	-0.71
7	2.57	2.24	0.33
8	2.21	1.80	0.41
9	2.91	2.13	0.77
10	8.88	7.30	1.58
11	4.12	3.45	0.67
12	3.33	3.15	0.18
13	4.10	3.42	0.68
14	3.87	3.65	0.22
15	3.63	3.58	0.06
16	3.93	5.52	-1.58
17	4.24	3.52	0.72
18	4.84	4.61	0.23
19	3.91	3.29	0.63
20	5.88	2.89	2.98
21	5.88	3.66	2.22
22	5.69	8.80	-3.11
23	5.94	4.87	1.07
24	3.13	4.70	-1.58
25	3.27	3.35	-0.08
26	6.67	7.42	-0.74
27	2.71	4.63	-1.93
28	9.03	4.73	4.30
29	4.15	4.05	0.10
		Sum	5.90
		M_d	0.20
		SSD	58.71
		Variance	2.10
		σ	0.27
		t	0.76
Level of significance for Non-Directional Test			**0.45**

Table 4-24. Paired t-test, All Data, Third Layer (n=28).

Sample	Average Calculated Ductility (cm)		D_i
	Untreated	Treated	
1	1.69	1.68	0.01
2	1.94	1.47	0.46
3	2.83	2.21	0.63
4	2.15	1.65	0.50
5	2.31	2.84	-0.54
6	5.35	9.38	-4.02
7	2.55	2.14	0.41
8	2.88	2.29	0.59
9	4.95	2.57	2.39
10	9.02	7.53	1.49
11	4.24	3.84	0.40
12	3.45	3.24	0.21
13	7.29	5.12	2.17
14	6.93	6.61	0.33
15	7.02	17.02	-10.00
16	11.53	19.63	-8.10
17	6.06	4.55	1.52
18	5.54	5.31	0.24
19	4.40	3.35	1.05
20	6.37	3.50	2.86
21	6.37	3.79	2.57
22	5.38	12.54	-7.15
23	6.15	5.12	1.03
24	2.60	2.33	0.27
25	4.85	3.61	1.23
26	2.99	5.74	-2.74
27	14.81	4.77	10.04
28	4.68	4.24	0.44
		Sum	-1.72
		M_d	-0.06
		SSD	376.71
		Variance	13.95
		σ	0.71
		t	-0.09
		Level of significance for Non-Directional Test	**0.93**

The final collection of tables assesses each treatment material on a layer-by-layer basis. Thus, there is a much smaller data set in each case, but on the other hand, the calculations are sharply focused on a particular treatment and layer. Tables 4-25a to 4-25c provide the calculation for the PASS treatment in the first, second, and third layer, respectively. All layers of this material do not support the suggestion of differences between the untreated and treated cores since all of the levels of significance are exceed 0.05.

Table 4-25a. Paired t-test, PASS Treatment, First Layer (n=8).

Average Calculated Ductility (cm)		Sample	D_i
Untreated	Treated		
1.70	2.67	1	-0.97
2.26	2.48	2	-0.21
1.81	2.50	3	-0.69
1.80	1.90	4	-0.11
8.17	9.00	5	-0.83
4.09	2.04	6	2.05
1.88	3.24	7	-1.35
2.08	2.04	8	0.04
		Sum	-2.07
		M_d	-0.26
		SSD	7.67
		Variance	1.10
		σ	0.37
		t	-0.70
		1st Layer's Level of significance for Non-Directional Test	**0.51**

Table 4-25b. Paired t-test, PASS Treatment, Second Layer (n=8).

Average Calculated Ductility (cm)		Sample	D_i
Untreated	Treated		
3.23	4.44	1	-1.22
2.40	2.80	2	-0.40
2.48	2.37	3	0.11
1.74	1.80	4	-0.06
8.88	7.30	5	1.58
3.13	4.70	6	-1.58
3.27	3.35	7	-0.08
4.15	4.05	8	0.10
		Sum	-1.55
		M_d	-0.19
		SSD	6.34
		Variance	0.91
		σ	0.34
		t	-0.58
		2nd Layer's Level of significancefor Non-Directional Test	**0.58**

Table 4-25c. Paired t-test, PASS Treatment, Third Layer (n=7).

Average Calculated Ductility (cm)		Sample	D_i
Untreated	Treated		
1.94	1.47	1	0.46
2.83	2.21	2	0.63
2.15	1.65	3	0.50
2.31	2.84	4	-0.54
9.02	7.53	5	1.49
2.60	2.33	6	0.27
4.68	4.24	7	0.44
		Sum	3.25
		M_d	0.46
		SSD	2.13
		Variance	0.36
		σ	0.23
		t	2.06
		3rd Layer's Level of significance for Non-Directional Test	**0.09**

Tables 4-26a through 4-26c show the same calculations, but for the EB44 material. In this case, in the first layer, we see a very low level of significance of approximately 0.00 percent. This calculation suggests very strongly that there is a very low probability that this difference observed between the untreated and treated binders is a chance occurrence. Thus, we conclude that the EB44 is doing something to harden that top layer in the pavement. We noted earlier in the discussion in Chapter 3 of the chromatograms of sites treated with this material that the top layer maltenes peak appears to be reduced in size compared to the asphaltenes peak in that top layer, but it is not reduced in the other layers of the pavement. These chromatograms together with this statistical calculation suggest that perhaps the coal-tar material, which is a very light organic material, may actually be dissolving some of the lighter materials of the asphalt in the pavement, thereby reducing the resins in the binder relative to the asphaltenes and producing a stiffer binder. At this point, this scenario is conjecture, but it is supported by both the chromatograms and these statistical calculated ductility comparisons.

Table 4-26b provides the second layer data and here, the level of significance is a higher value of 0.15 and a third layer is higher still (Table 4-26c), at a value of 0.36. Evidently, the biggest effect of the EB44 material occurs in the first layer and then a greatly reduced effect carried over through the second and third layers.

Table 4-26a. Paired t-test, EB44 Treatment, First Layer (n=10).

Average Calculated Ductility (cm)		Sample	D_i
Untreated	Treated		
2.27	1.09	1	1.17
2.04	1.88	2	0.17
2.02	1.47	3	0.56
1.66	1.53	4	0.13
2.02	1.45	5	0.57
2.89	1.56	6	1.33
2.89	1.66	7	1.23
3.46	1.94	8	1.52
3.87	2.37	9	1.51
3.18	1.61	10	1.56
		Sum	9.75
		M_d	0.97
		SSD	2.86
		Variance	0.32
		σ	0.18
		t	5.47
		1st Layer's Level of significance for Non-Directional Test	**0.00**

Table 4-26b. Paired t-test, EB44 Treatment, Second Layer (n=10).

Average Calculated Ductility (cm)		Sample	D_i
Untreated	Treated		
4.12	3.45	1	0.67
3.33	3.15	2	0.18
4.24	3.52	3	0.72
4.84	4.61	4	0.23
3.91	3.29	5	0.63
5.88	2.89	6	2.98
5.88	3.66	7	2.22
5.69	8.80	8	-3.11
5.94	4.87	9	1.07
9.03	4.73	10	4.30
		Sum	9.88
		M_d	0.99
		SSD	34.82
		Variance	3.87
		σ	0.62
		t	1.59
		2nd Layer's Level of significance for Non-Directional Test	**0.15**

Table 4-26c. Paired t-test, EB44 Treatment, Third Layer (n=10).

Average Calculated Ductility (cm)		Sample	D_i
Untreated	Treated		
4.24	3.84	1	0.40
3.45	3.24	2	0.21
6.06	4.55	3	1.52
5.54	5.31	4	0.24
4.40	3.35	5	1.05
6.37	3.50	6	2.86
6.37	3.79	7	2.57
5.38	12.54	8	-7.15
6.15	5.12	9	1.03
14.81	4.77	10	10.04
		Sum	12.76
		M_d	1.28
		SSD	155.14
		Variance	17.24
		σ	1.31
		t	0.97
		3rd Layer's Level of significance for Non-Directional Test	**0.36**

Tables 4-27a through 4-27c provide calculations for COS-50 material. Note that here there are only four samples for comparison which by itself reduces the statistical certainty in any calculation. In these tables, the level of significance for the first layer is shown to be 0.17, the second layer 0.78, and the third layer 0.29. Thus, the conclusion is that there is no statistical support for claiming that there are differences between the untreated and treated calculated ductility values.

Table 4-27a. Paired t-test, COS-50 Treatment, First Layer (n=4).

Average Calculated Ductility (cm)		Sample	Di
Untreated	Treated		
2.78	1.79	1	0.99
2.14	1.77	2	0.37
3.70	3.71	3	-0.02
3.57	3.36	4	0.21
		Sum	1.55
		M_d	0.39
		SSD	0.55
		Variance	0.18
		σ	0.21
		t	1.80
		1st Layer's Level of significance for Non-Directional Test	**0.17**

Table 4-27b. Paired t-test, COS-50 Treatment, Second Layer (n=4).

Average Calculated Ductility (cm)		Sample	Di
Untreated	Treated		
4.10	3.42	1	0.68
3.87	3.65	2	0.22
3.63	3.58	3	0.06
3.93	5.52	4	-1.58
		Sum	-0.62
		M_d	-0.15
		SSD	2.94
		Variance	0.98
		σ	0.49
		t	-0.31
		2nd Layer's Level of significance for Non-Directional Test	**0.78**

Table 4-27c. Paired t-test, COS-50 Treatment, Third Layer (n=4).

Average Calculated Ductility (cm)		Sample	Di
Untreated	Treated		
7.29	5.12	1	2.17
6.93	6.61	2	0.33
7.02	17.02	3	-10.00
11.53	19.63	4	-8.10
		Sum	-15.59
		M_d	-3.90
		SSD	109.50
		Variance	36.50
		σ	3.02
		t	-1.29
		3rd Layer's Level of significance for Non-Directional Test	**0.29**

Thus, based on all of these calculations, we conclude that most of the effects on the binder rheology occur on the first slices of the pavement (top quarter inch) and that most of this effect is related to the EB44 (coal-tar) treatment and that the effect is to harden the binder rather than to soften it, as one might have been suspected. The other treatment materials, it may be concluded, cause very little, if any, changes to the binder rheology.

SUMMARY AND CONCLUSIONS

The objectives of the work presented in this chapter were to investigate the effects of the fog seal treatments on the *in situ* binder. The effects that were primarily of interest were possible rejuvenation of the binder and possible effects to retard the binder aging in the pavement. The latter effects could occur in principle because of changes to the binder chemistry or because of restricting the transport of oxygen to the binder. To investigate these effects, the binders were recovered from quarter inch slices from the top inch of the cores, and then the binders were analyzed as to their rheology (dynamic viscous and elastic properties) and in some cases, their oxidation as represented by the carbonyl band of the FT-IR spectrum. Based on these investigations, the following conclusions are proposed.

- Generally, no clear effect of the fog seal treatments on the DSR map plots of binder recovered from the several slices of the pavement was observed. By comparing the DSR map to SEC chromatograms, the differences between the untreated and treated slices seem more likely due to original binder variability with depth than to the fog seal treatments. The one exception seems to be for the coal-tar treatments that appear to harden the top layer.
- Generally, over the year or so time frame over which cores were obtained for this project, only minimal differences in the recovered binder hardening were observed. Thus, accurate hardening rates could not be obtained for the binders recovered from the pavements.
- An effect of the fog seal treatments on hardening susceptibility was not observed.
- A paired *t*-test statistical analysis of recovered binder stiffnesses shows that practically the only significant effect on the rheology of the *in situ* binder was by the EB44 coal-tar type material, that it stiffens the binder, and that this effect is primarily restricted to the top quarter inch or so of the pavement.

These conclusions are entirely consistent with the conclusions of Chapter 3 related to the penetration and the sealing effectiveness of the various treatments.

CHAPTER 5

THE EFFECT OF ACCESSIBLE AIR VOIDS ON BINDER PROPERTIES AND AGING

INTRODUCTION

The earlier chapters in this report provided the results of extensive and detailed studies of the effect of fog seals on pavement and binder properties such as water permeability, binder rheology, and oxidative aging. The conclusion in all of these areas is that the fog seal treatments have very little, if any, positive effects on the binder properties, binder rheology, pavement permeability, or binder aging. There are some indications that the water permeability can be reduced by certain fog seal treatments, but the impact of this reduction on binder aging or other binder properties appears to be minimal. In fact, it was reported in Chapter 4 that apparently the coal-tar treatments actually stiffen the binders in the top portion of the pavement, stiffening which may result in premature cracking of the binder, although such cracking has not been documented in this project.

As a result of the various analyses that have been conducted layer-by-layer on the pavement and recovered binders, data exist to evaluate the effect of other parameters besides fog seal treatment on binder properties and aging. Specifically, the objective of this chapter is to assess the effects, if any, of the accessible (interconnected) air voids and of binder content on binder aging. When the accessible air voids in a pavement are reduced, it might be expected that oxygen transport to the binder is also reduced and therefore, that binder aging would be slowed. Similarly, to the extent an increased binder content results in a thicker binder film, the transport of oxygen throughout the binder could be reduced. Either of these effects conceivably could result in a reduction in hardening rates of binder in pavements.

METHODOLOGY

As described in Chapter 2, the pavement cores were sliced into nominal quarter inch layers through the top inch of the pavement. Then for each of the slices, the total air voids and the accessible air voids were determined. Additionally, the binder in each of these slices was extracted and recovered to provide the binder content and measurement of the binder's DSR properties provided values for binder stiffness. The binder rheology was then assessed for each core as to its correlation to accessible air voids and binder content.

RESULTS AND DISCUSSION

The bulk core properties are provided for each layer and for each site in Tables 5-1 through 5-17. Reported for both the untreated and treated cores and layer-by-layer are the core bulk specific gravity, the maximum specific gravity, the total air voids, the accessible (interconnected) air voids, and the binder content. Note that not all of the data are reported for each of the slices. Also note that two methods were used for determining the air voids: the saturated surface-dry method (SSD, ASTM D 2041-91) and the Corelok (ASTM D 6752-03, ASTM D 6857-03) methods, see Chapter 2.

Table 5-1. Properties of the Abilene L1 and L2 Cores.

	Replicate	layer	Bulk S.G. SSD	Bulk S.G. Corelok	Maximum S.G.	Total A.V. SSD	Total A.V. Corelok	Accessible A.V. SSD	Accessible A.V. Corelok	Binder Content
	U3	1st	-	-	-	-	-	-	-	-
		2nd	-	-	-	-	-	-	-	-
1st Core		3rd	-	-	-	-	-	-	-	-
Abilene L1	T3	1st	2.27	2.05	2.54	10.84	19.28	6.35	14.57	5.06
		2nd	2.26	2.13	2.54	10.76	16.20	7.54	12.25	5.09
		3rd	2.25	2.09	2.51	10.48	16.83	7.64	13.25	5.37
	U1	1st	2.26	2.11	2.44	7.61	13.66	7.84	12.89	3.72
		2nd	2.25	2.15	2.44	8.00	11.99	7.54	10.61	4.40
		3rd	2.23	2.14	2.45	9.10	12.58	8.87	11.08	4.28
	U2	1st	2.22	2.11	2.47	10.12	14.47	10.37	13.01	3.79
		2nd	2.22	2.11	2.47	10.27	14.69	9.47	12.50	4.09
2nd Core		3rd	2.22	2.11	2.47	10.14	14.51	9.64	12.56	4.69
Abilene L1	T1	1st	2.22	2.07	2.45	9.36	15.49	8.39	13.47	4.55
		2nd	2.23	2.10	2.47	9.94	14.96	9.04	12.80	4.40
		3rd	2.23	2.06	2.48	10.15	16.96	9.58	15.01	4.35
	T2	1st	2.22	2.09	2.45	9.49	14.77	9.46	13.33	4.37
		2nd	2.21	2.06	2.46	10.21	16.20	9.87	14.36	5.05
		3rd	2.21	2.11	2.46	10.09	14.48	9.95	12.78	4.60
	U3	1st	-	-	-	-	-	-	-	4.22
		2nd	-	-	-	-	-	-	-	5.38
1st Core		3rd	-	-	-	-	-	-	-	4.90
Abilene L2	T3	1st	-	-	-	-	-	-	-	4.88
		2nd	-	-	-	-	-	-	-	5.42
		3rd	-	-	-	-	-	-	-	5.30
	U1	1st	2.20	2.07	2.45	10.00	15.61	10.65	14.46	4.07
		2nd	2.22	2.14	2.47	10.00	13.54	10.14	12.03	4.96
		3rd	2.24	2.11	2.50	10.69	15.55	8.68	12.44	3.84
	U2	1st	2.21	2.02	2.47	10.55	18.37	10.71	16.79	3.89
		2nd	2.22	2.03	2.43	8.69	16.74	9.39	16.02	4.64
2nd Core		3rd	2.26	2.21	2.47	8.55	10.76	7.88	9.05	4.35
Abilene L2	T1	1st	2.21	2.04	2.45	9.48	16.64	8.81	14.80	4.54
		2nd	2.23	2.09	2.44	8.70	14.48	7.75	12.62	4.82
		3rd	2.24	2.17	2.48	9.60	12.58	8.72	10.48	4.63
	T2	1st	2.20	2.04	2.44	9.94	16.60	7.82	13.66	4.17
		2nd	2.23	2.02	2.46	9.29	17.94	8.40	16.04	4.69
		3rd	2.26	2.21	2.49	9.29	11.41	8.60	9.50	4.13

Table 5-2. Properties of the Abilene R1 and R2 Cores.

	Replicate	layer	Bulk S.G.		Maximum	Total A.V.		Accessible A.V.		Binder
			SSD	Corelok	S.G.	SSD	Corelok	SSD	Corelok	Contents
	U3	1st	2.33	2.14	2.57	8.95	16.36	4.45	11.89	4.14
		2nd	2.32	2.15	2.54	8.77	15.17	5.26	11.43	4.86
1st Core		3rd	2.28	2.16	2.51	8.98	13.84	6.99	11.14	4.96
Abilene R1	T3	1st	2.29	2.07	2.51	8.76	17.57	4.96	13.74	4.68
		2nd	2.29	2.01	2.55	10.00	21.16	5.54	16.78	5.32
		3rd	2.27	2.09	2.52	10.04	17.02	7.41	13.71	5.15
	U1	1st	2.25	2.02	2.48	9.26	18.50	8.16	16.49	3.99
		2nd	2.23	2.05	2.46	9.30	16.81	8.66	15.05	4.36
		3rd	2.28	2.25	2.48	8.34	9.50	7.38	7.62	4.79
	U2	1st	2.26	2.07	2.46	8.14	15.85	6.52	13.68	3.94
		2nd	2.26	2.07	2.47	8.48	16.18	7.12	14.12	4.08
2nd Core		3rd	2.30	2.25	2.50	7.93	9.82	6.86	7.96	3.89
Abilene R1	T1	1st	2.24	2.04	2.46	8.78	17.07	7.45	14.98	4.17
		2nd	2.22	2.08	2.45	9.47	15.29	8.77	13.41	4.30
		3rd	2.28	2.26	2.48	7.87	8.90	6.50	6.80	4.65
	T2	1st	2.25	2.08	2.46	8.22	15.18	4.72	11.58	4.30
		2nd	2.24	2.09	2.45	8.48	14.76	7.97	13.26	4.51
		3rd	2.31	2.28	2.46	5.81	7.11	3.73	4.80	4.97
	U2	1st	-	-	-	-	-	-	-	-
		2nd	-	-	-	-	-	-	-	-
1st Core		3rd	-	-	-	-	-	-	-	-
Abilene R2	T2	1st	-	-	-	-	-	-	-	4.72
		2nd	-	-	-	-	-	-	-	4.60
		3rd	-	-	-	-	-	-	-	5.68
	U1	1st	2.22	1.97	2.48	10.48	20.46	10.66	18.95	3.65
		2nd	2.42	2.16	2.46	1.77	12.06	9.01	17.31	4.31
		3rd	2.27	2.12	2.44	6.86	13.02	0.45	7.04	4.96
	U2	1st	2.17	1.90	2.48	12.34	23.42	5.19	16.74	3.78
		2nd	2.23	2.17	2.45	9.06	11.35	8.61	9.68	5.06
2nd Core		3rd	2.28	2.27	2.45	6.92	7.13	5.46	5.14	5.02
Abilene R2	T1	1st	2.21	1.98	2.46	10.24	19.76	10.33	18.26	4.34
		2nd	2.24	2.16	2.46	8.73	12.16	7.71	10.18	5.07
		3rd	2.27	2.21	2.44	6.90	9.44	5.49	7.54	5.50
	T2	1st	2.23	1.98	2.48	10.10	20.16	9.44	18.24	3.62
		2nd	2.30	2.25	2.45	6.11	8.06	4.20	5.88	5.35
		3rd	2.29	2.27	2.38	3.84	4.66	2.02	2.78	7.05

Table 5-3. Properties of the Atlanta IH 20 CM Cores.

	Replicate	layer	Bulk S.G.		Maximum	Total A.V.		Accessible A.V.		Binder
			SSD	Corelok	S.G.	SSD	Corelok	SSD	Corelok	Contents
	U1	1st	2.26	1.88	2.48	8.80	24.00	10.69	24.00	2.92
		2nd	2.33	2.13	2.42	3.79	11.76	0.54	8.78	3.66
		3rd	2.28	2.14	2.28	0.00	5.89	6.49	11.56	3.55
	U2	1st	2.27	1.99	2.48	8.68	19.68	7.25	17.62	3.50
1st Core		2nd	2.24	2.12	2.42	7.45	12.47	5.04	9.75	4.48
Atlanta		3rd	2.27	2.15	2.44	6.89	11.96	6.59	10.95	4.29
IH 20 CM	T1	1st	2.25	2.05	2.41	6.81	14.96	7.54	14.72	3.71
		2nd	2.29	2.09	2.49	8.14	16.10	6.57	13.96	3.71
		3rd	2.32	2.07	2.49	6.81	16.56	5.39	14.82	3.59
	T2	1st	2.29	1.98	2.45	6.78	19.41	5.71	17.99	3.60
		2nd	2.29	2.13	2.48	7.73	14.31	6.33	12.34	3.63
		3rd	2.29	2.16	2.45	6.87	12.03	6.03	10.62	3.68

Table 5-4. Properties of the Atlanta IH 20 DG Cores.

	Replicate	layer	Bulk S.G.		Maximum	Total A.V.		Accessible A.V.		Binder
			SSD	Corelok	S.G.	SSD	Corelok	SSD	Corelok	Contents
	U1	1st	2.26	2.09	2.47	8.46	15.44	9.11	14.74	3.31
		2nd	2.33	2.23	2.50	7.12	10.87	6.26	9.37	4.11
		3rd	2.29	2.18	2.48	7.56	11.94	6.38	10.13	3.94
	U2	1st	2.28	2.06	2.51	9.31	18.15	7.93	15.92	3.48
1st Core		2nd	2.30	2.22	2.52	8.63	12.01	6.11	8.94	3.49
Atlanta		3rd	2.31	2.23	2.48	6.98	10.15	5.66	8.32	4.26
IH 20 DG	T1	1st	2.30	2.07	2.50	8.04	17.13	6.20	14.86	3.35
		2nd	2.28	2.17	2.49	8.47	12.66	7.22	10.59	3.59
		3rd	2.32	2.20	2.51	7.41	12.21	5.23	9.68	3.18
	T2	1st	2.29	2.04	2.49	8.02	18.13	6.73	16.27	3.77
		2nd	2.31	2.17	2.49	7.37	12.88	6.23	11.16	3.46
		3rd	2.32	2.21	2.50	7.08	11.77	5.95	10.09	3.66

Table 5-5. Properties of the Atlanta IH 20 SP Cores.

	Replicate	layer	Bulk S.G.		Maximum	Total A.V.		Accessible A.V.		Binder
			SSD	Corelok	S.G.	SSD	Corelok	SSD	Corelok	Contents
	U1	1st	2.34	2.20	2.53	7.51	13.02	5.52	10.62	3.44
		2nd	2.38	2.38	2.53	6.06	6.03	3.66	3.38	3.82
		3rd	2.37	2.34	2.52	5.96	7.06	3.85	4.70	4.40
	U2	1st	2.33	2.22	2.51	7.12	11.45	7.01	10.52	4.06
1st Core		2nd	2.36	2.30	2.52	6.19	8.72	4.76	6.92	4.31
Atlanta		3rd	2.35	2.32	2.50	6.24	7.46	5.46	6.16	4.20
IH 20 SP	T1	1st	2.35	2.11	2.53	7.01	16.34	5.54	13.96	3.99
		2nd	2.36	2.26	2.59	8.95	12.88	5.86	9.44	4.00
		3rd	2.38	2.28	2.54	6.39	10.48	4.65	8.38	4.15
	T2	1st	2.31	2.12	2.52	8.26	15.60	7.44	14.52	3.90
		2nd	2.35	2.25	2.53	6.84	10.90	5.96	9.33	3.85
		3rd	2.35	2.27	2.54	7.46	10.43	5.98	8.44	3.77

Table 5-6. Properties of the Atlanta US 67 Cores.

	Replicate	layer	Bulk S.G.		Maximum	Total A.V.		Accessible A.V.		Binder
			SSD	Corelok	S.G.	SSD	Corelok	SSD	Corelok	Contents
	U1	1st	2.26	2.19	2.43	7.06	9.96	6.30	8.54	4.04
		2nd	2.28	2.26	2.43	6.27	6.96	5.34	5.52	4.69
		3rd	2.28	2.25	2.43	6.16	7.23	5.74	6.23	4.64
	U2	1st	2.24	2.19	2.43	7.66	9.76	5.21	6.88	4.11
1st Core		2nd	2.27	2.26	2.45	7.32	7.66	5.38	5.21	4.35
Atlanta		3rd	2.27	2.26	2.44	6.85	7.28	5.85	5.68	4.69
US 67	T1	1st	2.27	2.22	2.45	7.32	9.15	5.18	6.57	4.40
		2nd	2.24	2.21	2.46	8.80	10.07	6.09	6.74	4.70
		3rd	2.24	2.23	2.45	8.60	8.90	7.40	6.75	4.58
	T2	1st	2.26	2.20	2.43	6.93	9.39	5.75	7.67	3.90
		2nd	2.28	2.22	2.42	6.11	8.49	5.42	7.30	4.45
		3rd	2.28	2.22	2.43	6.22	8.71	6.22	8.05	4.24

Table 5-7. Properties of the Carrizo Springs Airport Cores.

	Replicate	layer	Bulk S.G.		Maximum	Total A.V.		Accessible A.V.		Binder
			SSD	Corelok	S.G.	SSD	Corelok	SSD	Corelok	Contents
	U3	1st	2.31	2.30	2.59	10.80	11.23	5.06	5.05	4.38
1st Core		2nd	2.34	2.40	2.57	9.21	6.82	3.91	1.09	5.08
Carrizo		3rd	2.34	2.32	2.50	6.25	7.18	0.23	1.22	5.21
Springs	T3	1st	2.26	2.22	2.61	13.39	14.85	5.35	6.44	5.30
Airport		2nd	2.30	2.32	2.56	10.37	9.50	5.78	4.26	5.23
		3rd	2.31	2.32	2.57	9.96	9.74	4.40	3.81	5.05
	U1	1st	2.28	2.22	2.49	8.56	10.77	7.31	8.64	4.61
		2nd	2.32	2.31	2.46	5.87	6.36	4.79	4.87	4.86
		3rd	2.30	2.31	2.49	7.40	7.13	4.72	4.04	4.66
	U2	1st	2.28	2.21	2.51	8.83	11.80	7.61	9.64	4.48
2nd Core		2nd	2.32	2.31	2.49	6.76	7.32	4.68	4.85	4.41
Carrizo		3rd	2.32	2.32	2.47	5.99	6.12	4.37	4.15	4.45
Springs	T1	1st	2.29	2.28	2.46	6.68	7.29	5.98	5.96	4.60
Airport		2nd	2.33	2.34	2.48	6.08	5.51	3.98	3.11	4.83
		3rd	2.33	2.35	2.45	4.79	3.89	3.17	2.07	4.76
	T2	1st	2.27	2.25	2.48	8.73	9.46	7.77	7.46	4.20
		2nd	2.31	2.31	2.46	6.13	6.12	3.89	3.60	4.73
		3rd	2.32	2.33	2.46	5.83	5.40	3.79	3.08	4.72

Table 5-8. Properties of the Fort Worth FM 4 (2000) Cores.

	Replicate	layer	Bulk S.G.		Maximum	Total A.V.		Accessible A.V.		Binder
			SSD	Corelok	S.G.	SSD	Corelok	SSD	Corelok	Contents
	U1	1st	2.32	1.91	2.43	4.43	21.56	6.12	22.40	-
		2nd	2.24	2.08	2.25	0.40	7.65	3.63	10.42	-
		3rd	2.17	2.09	2.14	0.00	2.60	3.88	7.10	-
	U2	1st	2.33	1.85	2.55	8.76	27.70	2.04	22.31	-
		2nd	2.22	2.03	2.38	6.57	14.63	4.59	12.47	-
		3rd	2.17	2.05	2.31	5.94	11.18	3.78	8.89	-
	U3	1st	2.12	1.81	2.55	16.95	28.82	4.76	18.02	5.21
1st Core		2nd	2.18	2.01	2.34	6.71	14.03	5.21	12.19	9.61
Fort Worth		3rd	2.14	2.03	2.29	6.65	11.34	5.68	9.87	10.18
FM 4	T1	1st	2.27	1.87	2.50	9.34	25.07	7.73	22.89	-
(2000)		2nd	2.19	2.05	2.34	6.15	12.30	4.42	10.35	-
		3rd	2.13	2.08	2.23	4.55	6.91	3.63	5.77	-
	T2	1st	2.30	1.91	2.48	7.49	23.20	6.81	21.96	-
		2nd	2.22	2.01	2.37	6.31	15.20	4.03	12.87	-
		3rd	2.09	2.03	2.22	5.68	8.40	4.80	7.14	-
	T3	1st	2.26	1.94	2.45	7.54	20.60	5.46	18.35	5.69
		2nd	2.22	2.01	2.39	6.89	15.81	4.94	13.65	8.09
		3rd	2.12	2.03	2.23	5.11	8.93	3.22	6.92	13.77
	U1	1st	2.29	1.97	2.45	6.58	19.82	4.69	17.85	6.13
		2nd	2.24	2.03	2.36	5.20	14.00	2.99	11.83	8.37
		3rd	2.15	2.12	2.25	4.13	5.74	1.87	3.46	11.99
	U2	1st	2.32	1.95	2.46	5.52	20.68	5.48	20.20	4.94
		2nd	2.25	2.07	2.36	4.72	12.28	2.41	10.05	9.20
		3rd	2.18	2.13	2.27	3.90	5.97	1.80	3.85	10.66
	U3	1st	2.30	1.92	2.47	7.05	22.36	4.28	19.76	-
2nd Core		2nd	2.16	2.06	2.36	8.29	12.61	2.06	6.59	-
Fort Worth		3rd	2.17	2.08	2.28	4.95	8.76	2.85	6.60	-
FM 4	T1	1st	2.25	1.97	2.39	5.95	17.80	5.25	16.75	9.38
(2000)		2nd	2.19	2.06	2.31	5.35	10.80	4.04	9.28	9.07
		3rd	2.12	2.07	2.22	4.44	6.70	3.02	5.15	11.54
	T2	1st	2.26	1.95	2.36	4.21	17.49	5.55	18.17	6.95
		2nd	2.21	2.05	2.34	5.39	12.57	3.74	10.80	8.37
		3rd	2.10	2.07	2.24	6.01	7.74	0.67	2.48	11.25
	T3	1st	2.23	1.86	2.41	7.46	23.06	1.59	18.14	-
		2nd	2.19	2.09	2.31	5.10	9.52	3.48	7.76	-
		3rd	2.10	2.05	2.22	5.58	7.73	3.32	5.32	-

Table 5-9. Properties of the Fort Worth FM 4 (2003) Cores.

	Replicate	layer	Bulk S.G.		Maximum	Total A.V.		Accessible A.V.		Binder
			SSD	Corelok	S.G.	SSD	Corelok	SSD	Corelok	Contents
	U1	1st	2.10	2.00	2.20	4.60	9.23	2.36	7.00	-
		2nd	2.19	2.13	2.27	3.86	6.35	0.93	3.47	-
		3rd	2.34	2.24	2.56	8.38	12.54	3.36	7.55	-
	U2	1st	2.03	1.84	2.26	10.14	18.38	1.78	10.73	-
		2nd	2.02	1.98	2.07	2.49	4.40	0.59	2.54	-
		3rd	2.36	2.23	2.48	4.73	10.15	2.43	7.88	-
	U3	1st	2.15	1.96	2.28	5.55	13.99	1.93	10.63	14.93
1st Core		2nd	2.07	2.01	2.18	5.09	7.95	1.20	4.16	15.71
Fort Worth		3rd	2.36	2.28	2.49	4.98	8.11	1.66	4.84	6.80
FM 4	T1	1st	2.11	1.96	2.16	2.42	9.42	2.11	9.06	-
(2003)		2nd	2.11	2.08	2.19	3.77	5.36	0.95	2.57	-
		3rd	2.36	2.28	2.49	5.17	8.55	2.91	6.21	-
	T2	1st	2.12	1.94	2.23	5.15	13.22	0.21	8.71	-
		2nd	2.12	2.08	2.17	2.34	4.13	0.37	2.19	-
		3rd	2.36	2.29	2.48	4.62	7.55	2.10	5.03	-
	T3	1st	2.19	2.09	2.22	1.66	6.08	1.26	5.68	13.58
		2nd	2.16	2.15	2.25	3.75	4.46	1.78	2.44	12.36
		3rd	2.38	2.24	2.51	5.14	10.62	3.20	8.61	4.33
	U1	1st	2.14	1.97	2.24	4.19	11.94	2.92	10.62	13.08
		2nd	2.16	2.17	2.26	4.34	4.20	0.88	0.72	12.74
		3rd	2.41	2.37	2.51	4.15	5.77	2.35	3.91	4.14
	U2	1st	2.20	1.96	2.33	5.28	15.58	3.80	14.02	9.21
		2nd	2.18	2.16	2.24	2.86	3.63	1.57	2.30	12.16
		3rd	2.39	2.34	2.50	4.49	6.60	2.69	4.70	4.18
	U3	1st	2.10	2.00	2.17	3.35	7.84	2.01	6.49	-
2nd Core		2nd	2.30	2.21	2.40	4.28	8.08	1.59	5.44	-
Fort Worth		3rd	2.32	2.11	2.49	6.96	15.35	4.12	12.48	-
FM 4	T1	1st	2.09	2.03	2.16	3.42	6.04	1.60	4.22	15.45
(2003)		2nd	2.21	2.20	2.29	3.69	3.99	2.07	2.29	10.10
		3rd				-	-	-	-	4.05
	T2	1st	2.06	2.01	2.11	2.68	4.89	1.36	3.56	16.48
		2nd	2.21	2.20	2.28	3.08	3.53	1.16	1.59	10.54
		3rd	2.41	2.21	2.57	6.13	14.00	3.66	11.51	3.00
	T3	1st	2.05	1.95	2.12	3.45	7.92	1.29	5.83	-
		2nd	2.04	2.01	2.08	2.21	3.60	0.66	2.06	-
		3rd	2.39	2.25	2.53	5.44	11.02	3.70	9.14	-

Table 5-10. Properties of the Georgetown Airport (1989) Cores.

	Replicate	layer	Bulk S.G.		Maximum	Total A.V.		Accessible A.V.		Binder
			SSD	Corelok	S.G.	SSD	Corelok	SSD	Corelok	Contents
	U3	1st	2.19	2.12	2.50	12.69	15.30	10.95	11.71	5.18
1st Core		2nd	2.31	2.27	2.47	6.84	8.23	3.25	4.50	6.43
Georgetown		3rd	2.31	2.22	2.39	3.39	7.13	0.07	3.94	6.53
Airport	T3	1st	2.26	2.13	2.47	8.51	13.68	7.49	11.79	5.55
(1989)		2nd	2.32	2.27	2.51	7.58	9.56	4.31	6.02	5.65
		3rd	2.32	2.27	2.47	6.08	8.26	3.55	5.56	5.70
	U1	1st	2.21	2.09	2.49	11.10	16.17	10.46	13.86	4.59
		2nd	2.31	2.27	2.46	6.30	7.93	3.85	5.24	5.60
		3rd	2.34	2.32	2.48	5.65	6.44	2.05	2.79	6.13
	U2	1st	2.21	2.06	2.49	11.00	17.19	10.45	15.00	4.37
2nd Core		2nd	2.29	2.28	2.45	6.27	6.96	3.86	4.30	5.71
Georgetown		3rd	2.34	2.33	2.42	3.05	3.51	1.40	1.83	6.41
Airport	T1	1st	2.23	2.10	2.49	10.67	15.89	8.95	12.99	4.60
(1989)		2nd	2.31	2.31	2.45	5.67	6.00	3.08	3.24	5.22
		3rd	2.31	2.29	2.46	6.17	7.11	3.58	4.31	5.32
	T2	1st	2.22	2.07	2.51	11.46	17.53	9.24	14.12	4.94
		2nd	2.30	2.30	2.44	5.64	5.71	3.52	3.36	5.54
		3rd	2.31	2.29	2.46	5.85	6.82	2.81	3.67	6.03

Table 5-11. Properties of the Georgetown Airport (1995) Cores.

	Replicate	layer	Bulk S.G.		Maximum	Total A.V.		Accessible A.V.		Binder
			SSD	Corelok	S.G.	SSD	Corelok	SSD	Corelok	Contents
	U3	1st	2.23	2.14	2.54	12.02	15.64	8.67	11.19	5.19
1st Core		2nd	2.28	2.25	2.38	4.27	5.45	6.08	6.59	5.65
Georgetown		3rd	2.29	2.24	2.54	9.85	11.69	5.63	6.99	5.32
Airport	T3	1st	2.16	2.15	2.43	10.94	11.61	9.52	8.70	6.19
(1995)		2nd	2.25	2.28	2.59	12.92	11.99	7.03	5.16	5.70
		3rd	2.23	2.22	2.52	11.69	11.96	6.76	6.24	5.97
	U1	1st	2.25	2.16	2.47	9.25	12.89	2.54	6.33	4.68
		2nd	2.30	2.29	2.46	6.65	7.05	4.32	4.39	5.41
		3rd	2.32	2.32	2.44	4.91	4.87	2.46	2.30	5.77
	U2	1st	2.24	2.15	2.49	10.33	13.89	8.71	11.09	4.87
		2nd	2.26	2.25	2.46	7.82	8.53	6.46	6.44	5.19
		3rd	2.28	2.27	2.46	7.38	7.63	5.33	5.07	5.59
	T1	1st	2.22	2.19	2.45	9.38	10.52	7.59	7.77	5.49
2nd Core		2nd	2.28	2.28	2.48	7.96	8.14	5.32	5.00	5.39
Georgetown		3rd	2.29	2.29	2.47	7.43	7.26	4.62	4.06	5.63
Airport	T2	1st	2.21	2.00	2.44	9.47	17.98	0.62	9.95	5.40
(1995)		2nd	2.29	2.29	2.45	6.40	6.62	4.82	4.63	5.60
		3rd	2.32	2.31	2.45	5.61	5.84	3.59	3.59	5.69
	T1*	1st	2.24	2.13	2.44	8.34	12.91	7.84	11.42	5.47
		2nd	2.27	2.25	2.49	8.45	9.40	6.71	6.89	4.73
		3rd	2.27	2.27	2.47	8.19	8.34	6.25	5.71	5.40
	T2*	1st	2.22	2.16	2.45	9.39	11.82	8.94	10.06	4.76
		2nd	2.27	2.24	2.46	7.81	8.81	6.32	6.63	5.44
		3rd	2.31	2.29	2.48	6.98	7.82	4.94	5.36	4.73

Table 5-12. Properties of the Jacksonville Airport Cores.

	Replicate	layer	Bulk S.G.		Maximum	Total A.V.		Accessible A.V.		Binder
			SSD	Corelok	S.G.	SSD	Corelok	SSD	Corelok	Contents
	U3	1st	2.27	2.17	2.51	9.29	13.56	6.74	10.37	5.89
1st Core		2nd	2.33	2.26	2.44	4.48	7.48	1.93	4.94	7.48
Jacksonville		3rd	2.28	2.26	2.47	7.43	8.20	4.97	5.32	6.72
Airport	T3	1st	2.29	2.24	2.46	6.73	8.78	2.54	4.56	7.37
		2nd	2.35	2.32	2.45	3.82	5.37	1.49	3.04	6.74
		3rd	2.36	2.32	2.46	4.08	5.42	2.04	3.34	6.65
	U1	1st	2.28	2.19	2.50	8.80	12.21	8.18	10.51	5.50
		2nd	2.32	2.25	2.47	6.08	8.93	4.08	6.69	6.37
		3rd	2.30	2.24	2.47	6.87	9.24	4.48	6.56	6.43
	U2	1st	2.29	2.22	2.50	8.51	11.23	7.48	9.28	5.62
2nd Core		2nd	2.32	2.27	2.48	6.56	8.44	5.14	6.58	6.20
Jacksonville		3rd	2.33	2.30	2.47	5.98	7.04	5.02	5.64	6.39
Airport	T1	1st	2.23	2.14	2.45	9.02	12.65	8.76	11.14	5.76
		2nd	2.26	2.24	2.46	8.27	8.95	7.19	6.98	6.16
		3rd	2.26	2.22	2.46	8.40	9.74	7.75	8.08	6.09
	T2	1st	2.24	2.17	2.49	9.91	12.82	8.33	10.14	6.16
		2nd	2.24	2.20	2.47	9.04	10.70	8.03	8.63	6.20
		3rd	2.24	2.19	2.26	0.82	3.10	7.80	8.89	6.48

Table 5-13. Properties of the Lufkin BUS 59 Cores.

	Replicate	layer	Bulk S.G.		Maximum	Total A.V.		Accessible A.V.		Binder
			SSD	Corelok	S.G.	SSD	Corelok	SSD	Corelok	Contents
	U3	1st	-	-	-	-	-	-	-	3.89
1st Core		2nd	-	-	-	-	-	-	-	4.31
Lufkin		3rd	-	-	-	-	-	-	-	
BUS 59	T3	1st	-	-	-	-	-	-	-	4.50
		2nd	-	-	-	-	-	-	-	4.36
		3rd	-	-	-	-	-	-	-	4.20
	U1	1st	2.30	2.22	2.55	9.66	12.95	8.71	10.79	3.19
		2nd	2.29	2.25	2.56	10.31	12.11	8.04	8.79	4.06
		3rd	2.29	2.21	2.53	9.55	12.85	8.32	10.52	3.77
	U2	1st	2.32	2.21	2.56	9.33	13.44	8.01	11.12	3.21
2nd Core		2nd	2.30	2.23	2.58	10.72	13.52	8.13	9.91	3.53
Lufkin		3rd	2.29	2.23	2.52	9.27	11.76	7.00	8.72	3.69
BUS 59	T1	1st	2.30	2.28	2.50	8.04	8.91	6.26	6.46	3.88
		2nd	2.31	2.29	2.49	7.16	8.23	5.86	6.34	3.94
		3rd	2.28	2.19	2.47	7.71	11.31	7.83	10.40	4.48
	T2	1st	2.33	2.31	2.51	7.06	7.87	4.86	5.25	3.17
		2nd	2.32	2.31	2.51	7.40	7.80	5.62	5.47	3.93
		3rd	2.31	2.28	2.51	7.90	9.31	6.81	7.44	3.70

Table 5-14. Properties of the Odessa SH 149 Cores.

	Replicate	layer	Bulk S.G.		Maximum	Total A.V.		Accessible A.V.		Binder
			SSD	Corelok	S.G.	SSD	Corelok	SSD	Corelok	Contents
	U1	1st	2.14	2.03	2.11	0.00	3.77	0.86	6.05	11.38
		2nd	2.31	2.24	2.36	2.14	4.77	0.00	2.39	5.88
		3rd	2.35	2.35	2.43	3.27	3.23	0.67	0.62	4.95
	U2	1st	2.15	2.01	2.24	3.94	10.49	1.50	8.17	9.94
1st Core		2nd	2.30	2.29	2.34	1.91	2.31	0.64	1.04	6.60
Odessa		3rd	2.34	2.34	2.42	3.27	3.10	1.39	1.18	4.50
SH 149	T1	1st	2.13	2.00	2.22	3.87	9.98	2.07	8.21	11.00
		2nd	2.32	2.32	2.35	1.53	1.25	0.41	0.12	5.97
		3rd	2.32	2.32	2.43	4.56	4.41	2.10	1.86	4.62
	T2	1st	2.12	2.03	2.19	3.18	7.32	1.50	5.67	11.40
		2nd	2.32	2.34	2.36	1.83	1.12	0.71	0.00	5.86
		3rd	2.33	2.34	2.41	3.53	3.06	1.18	0.68	4.74

Table 5-15. Properties of the Odessa SH 349 Cores.

	Replicate	layer	Bulk S.G.		Maximum	Total A.V.		Accessible A.V.		Binder
			SSD	Corelok	S.G.	SSD	Corelok	SSD	Corelok	Contents
	U1	1st	2.10	2.02	2.17	3.39	6.93	1.92	5.45	8.95
		2nd	2.28	2.24	2.39	4.86	6.27	3.09	4.35	5.48
		3rd	2.27	2.24	2.40	5.26	6.64	3.45	4.65	5.76
	U2	1st	2.05	1.91	2.10	2.32	9.15	1.76	8.57	9.13
1st Core		2nd	2.27	2.20	2.44	6.93	9.91	4.69	7.35	5.00
Odessa		3rd	2.21	2.18	2.27	2.74	4.26	2.43	3.84	8.03
SH 349	T1	1st	2.16	2.01	2.26	4.38	11.22	2.34	9.23	10.85
		2nd	2.35	2.35	2.41	2.33	2.45	0.55	0.67	4.58
		3rd	2.30	2.29	2.32	1.04	1.18	0.81	0.93	6.42
	T2	1st	2.11	2.02	2.17	2.68	6.98	1.08	5.43	8.79
		2nd	2.31	2.30	2.23	0.00	0.00	1.30	1.92	5.91
		3rd	2.29	2.25	2.39	4.21	5.83	1.17	2.81	7.05

Table 5-16. Properties of Pleasanton Airport Cores.

	Replicate	layer	Bulk S.G.		Maximum	Total A.V.		Accessible A.V.		Binder
			SSD	Corelok	S.G.	SSD	Corelok	SSD	Corelok	Contents
	U3	1st	2.29	2.17	2.39	4.28	9.18	4.37	8.94	5.93
1st Core		2nd	2.34	2.38	2.45	4.21	2.54	1.76	0.00	6.30
Pleasanton		3rd	2.35	2.33	2.42	2.81	3.99	1.26	2.42	6.11
Airport	T3	1st	2.26	2.16	2.44	7.23	11.30	4.37	8.24	6.77
		2nd	2.30	2.16	2.49	7.76	13.18	5.06	10.20	5.53
		3rd	2.29	2.23	2.46	7.04	9.39	3.93	6.08	5.76
	U1	1st	-	-	-	-	-	-	-	-
		2nd	-	-	-	-	-	-	-	-
		3rd	-	-	-	-	-	-	-	-
	U2	1st	-	-	-	-	-	-	-	-
2nd Core		2nd	-	-	-	-	-	-	-	-
Pleasanton		3rd	-	-	-	-	-	-	-	-
Airport	T1	1st	2.24	2.19	2.42	7.31	9.50	5.22	6.98	6.54
		2nd	2.31	2.27	2.44	5.53	7.24	3.65	5.15	5.27
		3rd	2.32	2.30	2.45	5.34	6.12	3.06	3.68	5.05
	T2	1st	2.24	2.19	2.41	7.16	9.22	4.87	6.56	6.00
		2nd	2.31	2.26	2.45	5.77	7.91	3.40	5.38	5.12
		3rd	2.32	2.28	2.48	6.69	8.03	0.95	2.36	5.07

Table 5-17. Properties of Tyler US 79 Cores.

	Replicate	layer	Bulk S.G.		Maximum	Total A.V.		Accessible A.V.		Binder
			SSD	Corelok	S.G.	SSD	Corelok	SSD	Corelok	Contents
	U1	1st	2.30	2.17	2.55	9.98	14.77	8.30	12.07	2.90
		2nd	2.34	2.24	2.54	7.81	11.93	6.23	9.77	3.83
		3rd	2.36	2.28	2.52	6.65	9.78	5.51	8.15	3.50
	U2	1st	2.32	2.16	2.57	10.03	15.95	9.99	14.36	3.01
1st Core		2nd	2.34	2.24	2.55	8.10	12.13	6.66	10.00	3.67
Tyler		3rd	2.35	2.26	2.52	6.79	10.29	6.45	9.26	3.90
US 79	T1	1st	2.31	2.20	2.56	9.84	13.99	9.41	12.16	3.54
		2nd	2.32	2.26	2.55	8.90	11.27	8.32	9.55	3.37
		3rd	2.33	2.27	2.52	7.42	9.93	7.80	9.28	3.24
	T2	1st	2.33	2.21	2.54	8.47	13.26	8.21	11.91	3.16
		2nd	2.35	2.28	2.54	7.62	10.29	6.42	8.41	3.59
		3rd	2.37	2.31	2.52	6.09	8.28	5.89	7.47	3.60

Binder rheology measurements were reported earlier in Tables 4-1 through 4-17. The binder rheology η* master curves are presented in Appendix F from Figure F-2 through Figure F-30. The air voids results are presented in Appendix G from Figure G-1 through Figure G-28b, and the data on binder content are presented graphically in Appendix H, Figures H-1 through H-19. The air voids results are presented two ways in these figures. The first comparison is in

Figures G-1 through G-9 in which the accessible air voids in each figure are for a particular site, but are grouped according to layer so that all of the first-layer binders (untreated, treated, first year, second year) are compared side by side as bar graphs; all of the second-layer binders are compared side by side; and the third-layer binders are compared side by side. The second comparison presents the accessible air voids in one figure and the total air void in another figure for each site, but also the layers in each core are compared directly to each other. Thus the first, second and third layers for one core are compared to each other, side by side, and then they are compared to each other for another core and so on. Again, this latter comparison is done for both the accessible air voids and the total air voids in Figures G-10a through G-28b. For the binder contents in Appendix H, the results are compared layer-by-layer for each core.

Figures 5-1 and 5-2 are comparisons of the DSR function to the accessible air voids for all the sites, and all slices. Figure 5-1 presents the DSR function versus accessible air voids, with each site identified. Note that the range of accessible air voids is from nearly 0 percent to approximately 11 percent, a surprisingly wide range, with many data points at each value within this range. The DSR function, of course, increases as the binder stiffens with aging. Therefore, if accessible air voids is a factor in aging, we might expect the DSR function would tend to be less where there is low accessible air voids and higher where accessible air voids are higher. However, there is so much scatter to the data in Figure 5-1, that such a correlation is not evident.

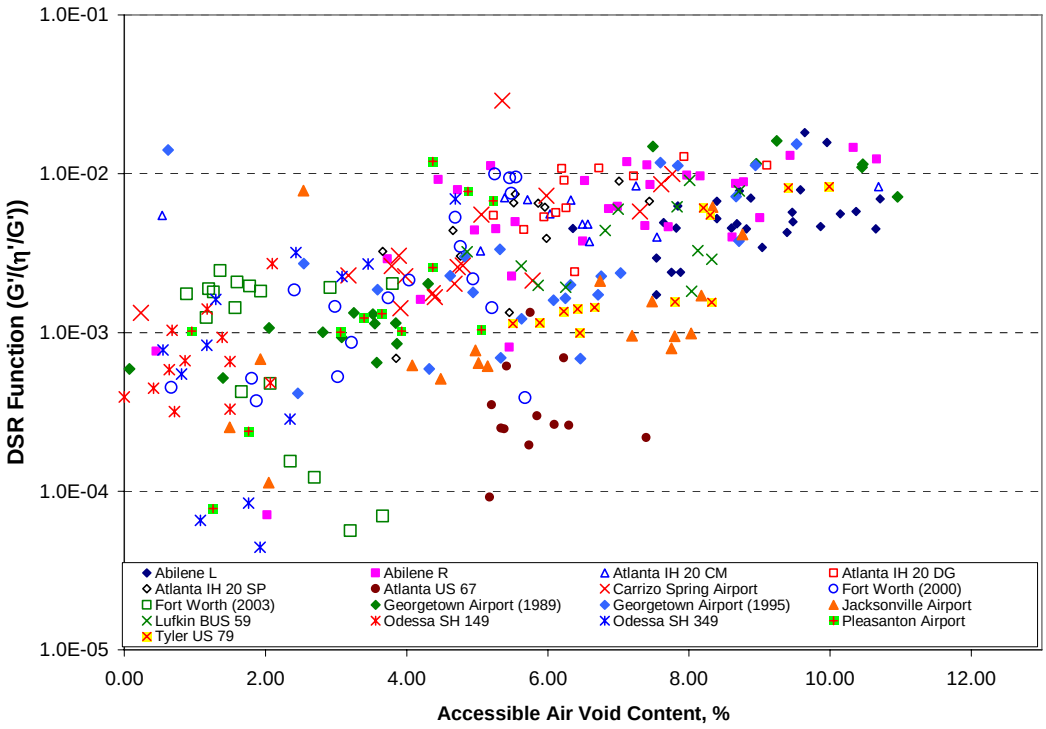

Figure 5-1. DSR Function versus Accessible Air Voids Content for All Cores and Sites.

Figure 5-2 shows the data in a different way. This is a plot of the DSR function versus service life of the pavement with the data categorized by the accessible air voids level. Low accessible air voids (less then 3 percent) are identified by green diamond symbols, moderate accessible air voids (between 3 and 6 percent) are indicated by blue squares, and high accessible air voids (greater than 6 percent) are indicated by red triangles. In this figure, it is seen that binders that were in the portions of the pavements having low accessible air voids tended to be lower in binder stiffness throughout the service life of the pavement than those associated with high accessible air voids. Moderate accessible air voids appear to be in between. The separation appears better at longer service times and very few of the high accessible air voids slices contained binders with low DSR function values. From these results, one might infer that lower accessible air voids can contribute to lower binder hardening rates.

Figure 5-3 presents a similar comparison to Figure 5-2, except for binder content. In this case the green symbols are low binder content, blue symbols are moderate binder content and red symbols are high binder content. In this case, there appears to be much less, or no correlation, between binder content and DSR function.

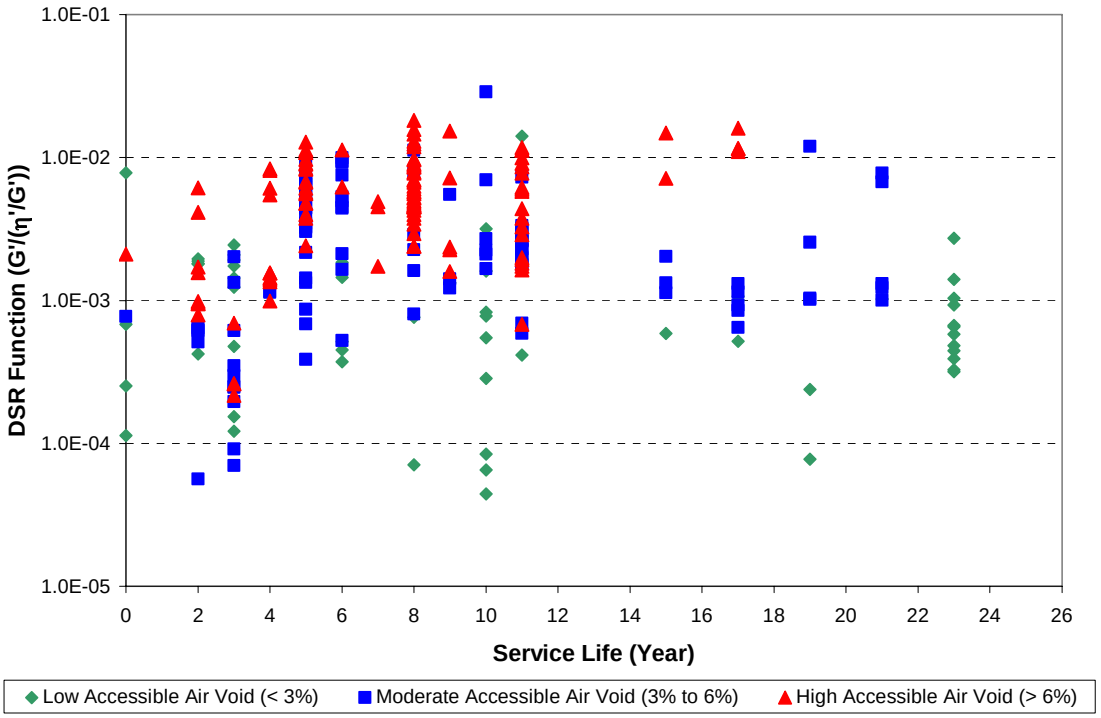

Figure 5-2. DSR Function versus Service Life for Three Accessible Air Voids Intervals.

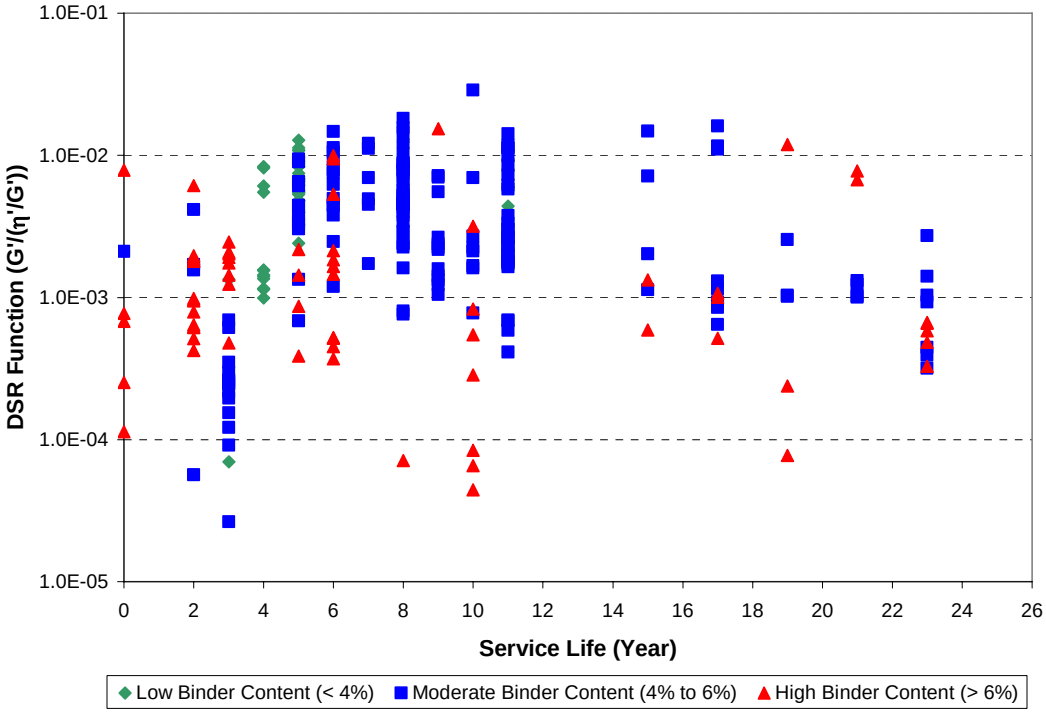

Figure 5-3. DSR Function versus Service Life for Three Binder Content Intervals.

CONCLUSIONS

The results of this chapter are weak because the data were not designed specifically to address the effects of air voids or binder content, and therefore can provide only qualitative results. Nevertheless, they support previous work, that the aging rates of asphalt binders are affected by accessible air voids, especially at very low levels.

CHAPTER 6

SUMMARY AND CONCLUSIONS

BACKGROUND

With the Performance Grading of asphalts, the asphalt industry has a better understanding of the additives and agents available and the performance characteristics when used in the department's more traditional surfacing treatments, i.e., thin asphalt concrete overlays and one course surface treatment. Due to the increased use of fog seal as a tool to better maintain our roadways, it has become apparent that fog seal material can be improved. Limited field trials have been conducted on fog seal products that are designed as maltene rejuvenators. Because different materials affect the performance of a fog seal and the rejuvenating properties on the existing pavement, the purpose of this project was to determine which asphalts and additives are best suited to TxDOT's needs.

This work was conducted for the purpose of assessing the effectiveness of fog seal treatments as an aid to highway maintenance managers in making sound decisions for fog seal treatments. Specifically, the objectives of this project were:

- to evaluate the physical and durability properties of fog seal binders;
- to determine whether or not the fog seal treatments penetrate into the pavement and if so, whether they are performing any significant sealing of the pavement;
- to investigate the effects of the fog seal treatments on the *in situ* binder; possible rejuvenation of the binder and possible effects to retard the binder aging; and
- to review the data of this project to assess the effects of air voids or binder content on binder aging in pavements.

METHODOLOGY

Multiple pavements were sampled by taking three replicate cores of both treated and untreated sections. Multiple types of treatements were included in the study, and the pavements included both highways and general aviation airports. During the first year of the project, cores were obtained from nine sites, giving a total of 67 cores; in the second year, 16 sites produced 114 cores. The second year cores included the nine sites cored in the first year, giving two sets of cores that spanned at least one year of pavement service for those nine sites. The treatments included a polymer modified asphalt surface sealer (PASS), an asphalt emulsion, COS-50 emulsion, a medium set resin emulsion (MS-2), a cationic slow set emulsion (CSS-1), a slow set emulsion, and EB44 and rejuvenator coal-tar materials.

The original fog seal materials were analyzed as to their size exclusion chromatography (SEC) chromatograms and their viscosity master curves. The chromatograms were used to assess the type of material and general molecular size distribution. Prior to analysis, the water was removed from the emulsion by distillation. The chromatograms were used to assist in determining to what extent the treatments might have penetrated into the pavement.

To assess the effects of the treatment materials, researchers assessed the whole cores by two methods: 1) measuring water permeability (to evaluate possible reductions in permeability due to the sealing treatments), and 2) measuring the susceptibility to permanent deformation using the asphalt pavement analyzer.

Then replicate cores (that had not been subjected to the APA) were sawed into one-quarter inch slices through the top inch of the core and the slices individually analyzed. The thin slices were used to increase the likelihood of detecting the presence of the treatment materials and their effects on the original pavement binder. Each slice was analyzed for total air voids, accessible air voids, and the binder in each slice was extracted and recovered to give binder content and then analyzed for oxidative aging and rheology, and to search for the presence of fog seal material.

RESULTS

The fog seal materials studied in this project were of two basic kinds, based upon their size exclusion chromatography chromatograms: asphalt emulsions and coal-tar type materials (a light, primarily aromatic, hydrocarbon material). The asphalt materials were both polymer modified (PASS) and unmodified (MS-2, asphalt emulsion, COS-50). These base materials typically were 1,000 to 3,000 poise (low shear rate limiting viscosity at 60 °C), approximately AC-10 to AC-30 viscosity grade, but one was quite high, at 30,000 poise.

Based upon the detailed SEC chromatograms that were measured on binder extracted from quarter inch slices of the top inch of the pavement and based upon measured water permeabilities, the conclusion seems clear that if the fog seal is penetrating into the pavement, it is not doing so to a detectable level (it is either draining off the side of the pavement or it is draining through the pavement and away from the top surface of the pavement) and that the permeability of the pavement is not significantly reduced. Furthermore, APA tests did not show any softening of the pavements by the treatments.

Several possible effects of the fog seal treatments on the pavement and its *in situ* binder were evaluated. The effects of the treatments that were primarily of interest were rejuvenation of the binder and retardation of binder aging. The latter effects, in principle, could occur because of changes to the binder chemistry or because of restricting the transport of oxygen to the binder. Based on these investigations, the following conclusions were reached.

- Generally, no clear effect of the fog seal treatments on the DSR map plots of binder recovered from the several slices of the pavement was observed. By comparing the DSR map to SEC chromatograms, the differences between the untreated and treated slices seem more likely due to original binder variability with depth than to the fog seal treatments. The one exception seems to be for the coal-tar treatments, which appear to harden the top layer.
- Generally, over the year or so time frame over which cores were obtained for this project, only minimal differences in the recovered binder hardening were observed. Thus, accurate hardening rates could not be obtained for the binders recovered from the pavements.

- An effect of the fog seal treatments on hardening susceptibility was not observed.
- A paired *t*-test statistical analysis of recovered binder stiffnesses shows that practically the only significant effect on the rheology of the *in situ* binder was by the EB44 coal-tar type material, that it stiffens the binder, and that this effect is primarily restricted to the top quarter inch or so of the pavement.

In addition to the above results, the effect of air voids, and accessible or interconnected air voids in particular, on binder oxidation were investigated. The results are only qualitative because of the nature of the experimental data. Nevertheless, they support previous work, that the aging rates of asphalt binders are decreased by very low accessible air voids.

CONCLUSIONS

Effects of fog seals on pavement durability appear to be minimal, with respect to binder rejuvenation or sealing. Cosmetic effects or possibly protecting against shelling or raveling remain as possible benefits, although they were not assessed by this project. In response to this work, engineers should reassess the cost-benefit balance of fog seal treatments.

REFERENCES

Asphalt Emulsion Manufacturer's Association, "Recommended Performance Guidelines," AEMA, Washington, D.C., 1990.

The Asphalt Institute, "A Basic Asphalt Emulsion Manual," Manual Series No. 16, Lexington, Kentucky, 1999a.

The Asphalt Institute, "A Basic Asphalt Emulsion Manual," Manual Series No. 19, Lexington, Kentucky, 1999b.

ASTM D 2041. Standard Test Method for Theoretical Maximum Specific Gravity and Density of Bituminous Paving Mixtures. 1994 Annual Book of ASTM Standards, 04.03, ASTM, Easton, Maryland, 1991, pp. 177-183.

ASTM D 6752. Standard Test Method for Bulk Specific Gravity and Density of Compacted Bituminous Mixtures Using Automatic Vacuum Sealing Method. 2006 Annual Book of ASTM Standards, 04.03, ASTM, West Conshohocken, Pennsylvania, 2003, pp. 840-843.

ASTM D 6857. Standard Test Method for Maximum Specific Gravity and Density of Bituminous Paving Mixtures Using Automatic Vacuum Sealing Method. 2006 Annual Book of ASTM Standards, 04.03, ASTM, West Conshohocken, Pennsylvania, 2003, pp. 862-866.

Booth, E. H. S., R. Gaughan, G. Holleran. "Some Uses of Bitumen Emulsions in SA and NSW," *Proceedings, Australian Road Research Board*, March 1988, pp. 387-401.

Brown E. R., "Preventive Maintenance of Asphalt Concrete Pavements," NCAT Report No. 88-1, 1988.

California Department of Transportation (CADOT), "Fog Seal Guidelines," Caltrans Division of Maintenance, October 2003.

Carpenter, S. H. and J. R. Wolosick. "Modifier Influence in the Characterization of Hot-Mix Recycled Material," *Transportation Research Record 777*, Transportation Research Board, National Research Council, Washington, D.C., 1980, pp. 15-22.

Chaffin, J.M., R. R. Davison, C. J. Glover, and J. A. Bullin. *"Viscosity Mixing Rules for Asphalt Recycling"* Transportation Research Record No. 1507, Transportation Research Board – National Research Council, 1995, pp.78-85.

Davison, R. R., J. A. Bullin, C. J. Glover, J. M. Chaffin, G. D. Peterson, K. M. Lunsford, D. Linzey, M. Liu, and M. A. Ferry. "Verification of an Asphalt Aging Test and Development of Superior Recycling Agents and Asphalt." Report FHWA/TX-94/1314-1F, Texas Transportation Institute and Chemical Dept., Texas A&M University, College Station, Texas, 1994.

Estakhri, C. K. and H. Agarwal. “Effectiveness of Fog Seals and Rejuvenators for Bituminous Pavement Surfaces,” Research Report 1156-1F, Project No. 1156, Texas Transportation Institute, College Station, 1991.

Federal Aviation Administration (FAA), “Engineering Brief No. 44: Coal-Tar Sealer/Rejuvenator,” November 1989.

Glover, C. J. and T. J. Freeman. *Guidelines on the Use of Fog Seals and Rejuvenator Seals.* TxDOT Product 0-5091-P1, Texas Transportation Institute, College Station, Texas, 2007.

Heydorn, A., “Applying Solvent-Based Sealers,” *Pavement*, January 1998, pp. 19-24.

Hicks, R. G. and G. Holleran. “Purpose and Use of Fog Seal and Rejuvenators,” Sealer Binder Workshop, Foundation for Pavement Preservation, Federal Highway Administration, March 2002.

Highway Research Board, *National Cooperative Highway Research Program Synthesis of Highway Practice 14: Skid Resistance*. Highway Research Board, National Academy of Sciences, Washington, D.C., 1972.

Jayawickrama, P. W. and B. Thomas. “Correction of Field Skid Measurements for Seasonal Variations in Texas,” *Transportation Research Record 1639*, Transportation Research Board, National Research Council, Washington, D.C., 1998, pp. 147-154.

Jemison, H. B., B. L. Burr, R. R. Davison, J. A. Bullin, and C. J. Glover. “Application and Use of the ATR, FTIR Method to Asphalt Aging Studies,” *Fuel Sci. Technol. Int*. 10, 1992, pp. 795-808.

Minnesota Department of Transportation (MNDOT), “Asphalt Pavement Maintenance: Field Handbook,” Manual No. 2001-05, Minnesota Local Road Research Board, April 2001.

Montgomery, D. C., “Design and Analysis of Experiments,” 5th edition, John Wiley & Sons, Inc., New York, New York, 2001.

Noureldin, A. S. and L. E. Wood. “Rejuvenator Diffusion in Binder Film for Hot-Mix Recycled Asphalt Pavement,” *Transportation Research Record*, Vol. 1115, 1987, pp. 51-61.

Outcalt, W., “SHRP Chip Seal,” Report No. CDOT-DTD-R-2001-20, Colorado Department of Transportation Research Branch, December 2001.

Ruan, Y., R. R. Davison, and C. J. Glover. “An Investigation of Asphalt Durability: Relationships between Ductility and Rheological Properties for Unmodified Asphalts,” *Petroleum Science and Technology*, Vol. 21, Nos. 1-2, 2003, pp. 231-254.

Stroup-Gardiner, M., D. E. Newcomb, J. A. Epps, and G. L. Paulsen. "Laboratory Test Methods and Field Correlations for Predicting the Performance of Chip Seals," *Asphalt Emulsions, ASTM STP 1079*, H. W. Muncy, Ed., American Society for Testing and Materials, Philadelphia, 1990, pp. 2-19.

Texas Department of Transportation (TXDOT), "Maintenance Operation Manual," Revised September 2005.

Texas State Department of Highways and Public Transportation, "Manual of Testing Procedures," Volume 2, TEX 436-A, January 1983.

Transport Research Board, "Asphalt Emulsion Technology," *Transport Research Circular*, Number E-C102, August 2006, pp. 1-15.

Western Emulsion, Inc., "PASS®," http://www.westernemulsions.com/pass/pass.html, 2002.

Whorlow, R. W., *Rheological Techniques*, Third edition, Intl. Specialized Book Service Inc., December 2005.

Woo, W., E. Ofori-Abebresse, A. Chowdhury, J. Hilbrich, Z. Kraus, M. A. Epps, and C. J. Glover, "Polymer Modified Asphalt Durability in Pavements," Report FHWA/TX-07-0-4688-1, Texas Transportation Institute, The Texas A&M University System, College Station, Texas, 2006 (Not Yet Published).

APPENDIX A

RESULTS OF FOG SEAL QUESTIONNAIRE

RESULTS OF FOG SEAL QUESTIONNAIRE

QUESTIONNAIRE RESULTS

The following tables represent the questions and results of the questionnaire that was completed by calling each of the TxDOT districts, divisions, other states, and industry representatives.

Table A-1. General Use of Treatments.

Responder	Do you use fog seals or Rejuvenators
Abilene	Fog
Amarillo	Both
Austin	Fog with Rejuv
Atlanta	Both
Beaumont	No
Brownwood	Fog
Bryan	Fog
Childress	Mostly fog
Corpus Christi	No
Dallas	Both
Fort Worth	Fog
Houston	No
Laredo	No
Lubbock1	Mostly fog
Lubbock2	Fog
Lufkin	Mostly fog
Odessa	Fog
Paris	Both
Pharr	Fog
San Angelo	Fog
San Antonio	Fog
Tyler	Both
Waco	Not Really
Wichita Falls	Fog
Yoakum	Very little
Aviation1	Both
Aviation2	Rejuv
Maintenance Division	Both
Oklahoma	Fog
Lousiana	No
Asphalt Institute	Fog -yes, Rejuv-maybe

Table A-2. Extent of Use of Treatments.

Responder	How much do you use?	
	Fog	Rejuvenator
Abilene	Somewhat, varies across district	No
Amarillo	Some	New
Austin	Yes	Some
Atlanta	Lots last year. Fog program	Fair amount
Beaumont	-	-
Brownwood	Little	Experimental
Bryan	Some, first year	-
Childress	Some	None
Corpus Christi	-	-
Dallas	Some	Little
Fort Worth	Little	Experimental only
Houston	-	-
Laredo	-	-
Lubbock1	Fair amount	Experiment
Lubbock2	Lots	Tried them
Lufkin	Moderate	Experiments
Odessa	Quite a lot	None
Paris	Lots	Little
Pharr	Quite a bit 2,000,000 SY	None
San Angelo	Some	-
San Antonio	Little	-
Tyler	Quite a bit	Just a little
Waco	None	Small spots
Wichita Falls	Little	-
Yoakum	Very little	Occasionally
Aviation1	Routinely	Routinely
Aviation2	No more	Extensively
Maintenance Division	Lot, 23.8million sy	Not a lot, mostly experiments
Oklahoma	6.5million sy	-

Table A-3. Trend of Usage.

Responder	Do you use more or less than you used to	
	More	Less
Abilene	-	Yes
Amarillo	-	Yes
Austin	Recently	-
Atlanta	Yes because of rock loss and fog seal program	-
Beaumont	-	Yes
Brownwood	-	Less
Bryan	First year	-
Childress	-	Yes
Corpus Christi	-	-
Dallas	Yes	-
Fort Worth	-	Less
Houston	-	-
Laredo	-	-
Lubbock1	-	Slightly
Lubbock2	Slowly increase	-
Lufkin	Somewhat more	-
Odessa	-	Less
Paris	Less on SC, more on HMAC	-
Pharr	About same	-
San Angelo	-	Less
San Antonio	-	-
Tyler	-	Less than a long time ago
Waco	Just not much	-
Wichita Falls	-	Lots
Yoakum	Neither	-
Aviation1	Yes	-
Aviation2	-	Far less
Maintenance Division	Slight increase last 5 years	-

Table A-4. Reasons for Not Using Treatments.

Responder	Why not			
	Skid	Never used	Don't think they work	Other
Abilene	-		Some	Pavement Marking
Amarillo	-			Bleeding
Austin	Yes			Traffic volume
Atlanta	-			Pavement marking
Beaumont	-		Didn't see benefit	
Brownwood	-			Doing better job on seal coats so less need
Bryan	-	Yes		
Childress	Yes			Traffic complaints
Corpus Christi	Yes	Yes		River gravel doesn't absorb
Dallas	-	-	Yes	
Fort Worth	-	-		Not using emulsion seal coats
Houston	-	Yes		
Laredo	-	-		Use seal coat instead
Lubbock1	-	-		
Lubbock2	Reju	-	Wonder	
Lufkin	-	-	Yes	
Odessa	-	-		Austin sees fog as corrective rather than preventive, less money to go around
Paris	-	-		Flushing
Pharr	No	-		
San Angelo	-	-		Change in supervisors, but newer folks don't know about them
San Antonio	-	-		Only for shelling
Tyler	Yes	-	Yes	Used to fog all seal coat roads
Waco	-	Yes		Didn't think seal coat was in bad shape
Wichita Falls	-	-		Using less plant mix seal
Yoakum	-	Yes		Only shelling
Aviation1	-	-		
Aviation2	-	-		Fog susceptible to UV, streaky
Maintenance Division	-	-		Use anytime needed, some concern on high volume roads
Oklahoma	-	-		Not sure
Louisiana	-	Yes		
Asphalt Institute	Rejuv	Yes	Yes	Can be messy

Table A-5. Fog Seal Use and Rates.

Responder	Fog			
	HMAC Type	HMAC RATE	Seal Coat Type	Seal Coat Rate
Abilene	Diluted 60% MS2, 40% water	0.15gals/sy	Diluted 60% MS2, 40% water	0.15gal/sy
Amarillo	CRS1 or 2	Residual .05-06	-	-
Austin				
Atlanta	Diluted 70-30 or 50-50 SS-1	0.10 -0.15gal/sy	Diluted 70-30 or 50-50 SS-1	0.10-0.15gal/sy
Beaumont				
Brownwood	No, use seal coat	-	Emulsion 60-40, or 80-20	0.10gal/sy
Bryan	CSS-1h	0.08gal/sy	On patches	
Childress	MS-2 or CSS-1h	0.05-0.07gal/sy	MS-2 or CSS-1h	0.1 gal/sy
Corpus Christi				
Dallas	Shoulders		-	
Fort Worth	-	-	MS-1 or MS-2	0.08-0.10gal/sy
Houston				
Laredo				
Lubbock1	CRS, or MS	-	CRS, or MS	Varies
Lubbock2	MS-2,SS-1,moving to CSS1h	0.10-0.12gal/sy	MS-2, SS-1,moving to CSS1h	0.15 gal/sy
Lufkin	Rarely		SS1, CSS1	0.08-0.10gal/sy
Odessa			SS-1	0.12-0.15gal/sy
Paris	50-50 MS-1	0.06-0.12gal/sy	50-50 MS-1	0.1 gal/sy
Pharr	SS1-4, 40%emuls	0.1gal/sy	SS1-h	0.1 gal/sy
San Angelo	-		60-40, or 70-30 diluted MS-2	0.20-0.25gal/sy
San Antonio			60-40, 70-30 MS-2	
Tyler				
Waco	-	-	-	-
Wichita Falls	CSS, CRS, MS	0.05-0.07gal/sy	CSS, CRS, MS	0.08-0.10gal/sy
Yoakum	-	-	Diluted CRS-2	-
Aviation1	CRS2, Coal Tar w/sand	.05-.065 gal/sy	-	-
Aviation2	P627 coal tar + sand	.35/pass, 2 coats	-	-

Table A-6. Rejuvenator Use and Rates.

Responder	Rejuvenator			
	HMAC Type	HMAC RATE	Seal Coat Type	Seal Coat Rate
Abilene	-	-	-	-
Amarillo	PASS	.08-.10	-	-
Austin	PASS		PASS	
Atlanta	PASS	0.1	PASS	0.1
Beaumont				
Brownwood				
Bryan				
Childress	-	-	-	-
Corpus Christi				
Dallas	PASS	.10-.15		
Fort Worth	-	-	-	-
Houston				
Laredo				
Lubbock1	Golden Bear		-	
Lubbock2	-	-	-	-
Lufkin	Experimental			
Odessa				
Paris	PASS	0.08	-	-
Pharr	-	-	-	-
San Angelo	-	-	-	-
San Antonio	-	-	-	-
Tyler	CMS+rejuv		-	
Waco	-	-	Not sure	
Wichita Falls	-	-	-	-
Yoakum	Can't remember		-	-
Aviation1	Coal tar rejuv (EB44)	.05-.07 gal/sy	-	-

Table A-7. Application Rates and Cost.

Responder	How do you determine application Rate			Approx Cost
	Trial	Experience	Other	
Abilene		Yes	Maintenance supervisor	in-house
Amarillo			Manufacturer	
Austin			Manufacturer	
Atlanta		Yes	Manufacturer	
Beaumont				
Brownwood		Yes		don't know
Bryan			Manufacturer	
Childress		Yes		
Corpus Christi				
Dallas		Yes		
Fort Worth			Maintenance Supervisor	
Houston				
Laredo				
Lubbock1		Yes		
Lubbock2	Test shot			$0.09/sy
Lufkin	Yes			
Odessa		Yes		
Paris	HMAC	Seal coat		$.75-1.00
Pharr			Maintenance supervisor	$0.10/SY
San Angelo		Yes		
San Antonio		Yes		
Tyler		Of district seal coat crew		
Waco				
Wichita Falls	Sometimes		Maintenance Supervisor	
Yoakum		Yes		
Aviation1	Test 3 rates, pick			approx $0.80-$1.00/SY
Aviation2		Yes	Specification range	$1/SY
Maintenance Division				$0.15/sy statewide

Table A-8. Reasons for Treatment.

Responder	What are you trying to correct					
	Shelling seal coat	Seal pavement	Loss of fines/ravel	Rejuvenate	Preventive	On new seal coat/Other
Abilene	Yes	Yes	Yes	-	Yes	Only if agg loss
Amarillo			Yes	Yes		Reduce cracking
Austin	Yes	Yes	Yes	Yes	Yes - PM program	
Atlanta		Yes	Yes	Yes	Yes	
Beaumont						
Brownwood	Yes			On shoulder	Yes	Only when season is late
Bryan			Yes		Yes	Sweeten patches
Childress	Yes	Yes	Yes			
Corpus Christi						
Dallas		After milling, before next layer				Freshen patches
Fort Worth	Yes	-	Yes	-	-	Only emuls seal coat
Houston						
Laredo						
Lubbock1	Yes	Yes	Lots on edges		Working on it	
Lubbock2	Yes	Yes	Yes			Yes between seal coats
Lufkin	Yes	-	-	-	-	Yes
Odessa	Yes			Yes		Oxidized
Paris		Yes	Yes	Yes	Yes	
Pharr	Yes	Yes	Yes	Yes	-	-
San Angelo	Yes			Yes		
San Antonio	Yes					
Tyler	Yes	Yes	Some	Experimental	Yes	With emuls seal coat
Waco				Yes		
Wichita Falls	Yes	Yes	Yes	Yes	Only in past	Sometimes
Yoakum	Yes		Yes			
Aviation1	-	Yes	Yes	Yes		Fuel/oil proof
Aviation2		Yes	Yes	Yes	Yes	
Maintenance Division	Yes	Yes	Yes	Yes	Yes	Some do
Asphalt Institute	Yes	Yes	Yes			Yes

Table A-9. Reasons for Not Using Treatment.

Responder	When do you NOT use them	What surface preparation beforehand
Abilene	No rules	Sweep surface clean
Amarillo	No	Sweep
Austin	High traffic, skid worries	Sweep surface clean
Atlanta	Not HMAC with river gravel	Sweep surface clean
Beaumont	All	
Brownwood	Not in urban areas	Sweep clean
Bryan		Road clean
Childress	High traffic volume	Sweep
Corpus Christi	AC doesn't absorb	
Dallas	Not used globally	Sweep
Fort Worth	All other cases	Sweep
Houston		
Laredo	Seal coat works better and crews don't have experience	
Lubbock1	Bleeding pavement	Sweep
Lubbock2	Not within city limits	Sweep
Lufkin	Used on shelling	Sweep
Odessa	Open graded FC	Sweep
Paris	When ready for seal coat	Sweep
Pharr	Urban, heavy traffic	Sweep
San Angelo	Urban settings, high ADT, or flushed	Sweep, patching a year beforehand
San Antonio	High traffic	Sweep
Tyler	Urban areas	Sweep
Waco	When surface is flushed	Sweep
Wichita Falls	Avoid urban, foot traffic	Sweep
Yoakum	High volume	Sweep
Aviation1	If too badly aged, skid worries on high speed areas	Sweep/clean, rout cracks, seal afterwards
Aviation2		Sweep
Maintenance Division	High traffic	Sweep surface clean
Oklahoma		
Louisiana		
Asphalt Institute	Rutted, low air voids, fine texture	

Table A-10. Opening to Traffic.

Responder	How long before opening	How do you determine
Abilene	2-3 hours	Visual
Amarillo	45min-1.5 hours for rejuv. longer in cooler weather	Visual, touch, drive
Austin	2-4 hours	Visual, touch, drive
Atlanta	Varies 2-3 hours	Visual, touch, drive
Beaumont		
Brownwood	Depends on weather	Visual, touch, drive
Bryan	30 min	Visual and touch
Childress	3-4 hours for MS2, 1-2 for CSS	Drive
Corpus Christi		
Dallas	Depends on weather, when tracking stops	Visual
Fort Worth	Usually 1 hour	Drive
Houston		
Laredo		
Lubbock1	Varies widely	Visual, touch, drive
Lubbock2	Varies with material CSS1h faster, within 2-3 hours	Visual, touch, drive
Lufkin	Varies, 15-20min	Visual, touch
Odessa	0.5 - 1 hour	Weather report
Paris	Fog - 1 hour Rejuv – longer	Visual and drive
Pharr	30-45 min	Visual
San Angelo	30min-1 hour	Visual, break and walk on it
San Antonio	3-4 hours +, depending on weather	Visual, touch, drive
Tyler	Varies	Visual, drive
Waco		
Wichita Falls	Varies	Visual, touch
Yoakum	Max 1 hour	Drive
Aviation1	At least 48 hours	Touch/feel
Aviation2	When dry. 2 days?	
Maintenance Division	4 hours or as long as possible	Drive

Table A-11. Application Suggestions.

Responder	Application suggestions	Problems encountered
Abilene	Routine common sense	Only with mis-application
Amarillo		Need experienced people, heated water didn't help
Austin	Use less, need cure time	Skid is biggest concern, some pick up
Atlanta	Err on light side	
Beaumont		
Brownwood	Stay on low side and be careful of cool, humid, days	On cold, humid days way too long to open to traffic, covering up stripping
Bryan	Humid overcast is bad, less is better, two distributors worked well	Some tracking
Childress	Stay on low side	Some bad asphalt
Corpus Christi		
Dallas	Keep rates low, use two passes, can always add more later	Tracking, covers pavement markers
Fort Worth	Get rate right, guess low	Opened too quickly
Houston		
Laredo		
Lubbock1	Good, dry weather, can always add second coat, so first can be low, Keep traffic off until ready	Wind blowing it onto other lanes, bad material, rain before set
Lubbock2	Be willing to adjust rates throughout project. Just do it.	Be sure to dilute, re-check order. Inconsistent material, especially with pre-diluted. Quality control.
Lufkin	Start on low side	None
Odessa	Can always add more, use heater tank	Some bad emulsions
Paris	Go 500', make first shot a little light. Use rubber tired roller, right away, to force material into pavement and cracks. Will streak, but seals better.	Watch for foaming
Pharr	Used lots on shoulders or pavement edge. Make sure it is properly use	Some oil on cars
San Angelo	Err on light side, experienced maintenance supervisor	No, works well
San Antonio	Critical for maint section to drive roads after cold spell. If shelling, must be there right away or rock is gone. Don't apply in heat of summer	Re-striping, paint doesn't stick, surface is slick. Long time to cure
Tyler	Don't use more than twice on same section	apparent skid problems
Waco		
Wichita Falls	Better to use too little than too much	Some tracking, pick up
Yoakum	Less is better	Shot too much
Aviation1	Better too little than too much!	If adjacent pavements are different, need individual application rates
Aviation2	Rollers	
Maintenance Division	Start low	
Asphalt Institute	Better too little than too much, can always add more	When application rate too high

APPENDIX B

DESCRIPTION OF TEST SITES IN THE FOG/REJUVENATOR STUDY

DESCRIPTION OF TEST SITES IN THE FOG/REJUVENATOR STUDY

ABILENE, SH 36

The site in Abilene is on both lanes of the divided highway, both directions of State Highway (SH) 36 near the airport, from the airport entrance road north and west to FM 18. The porous friction course (PFC) surface was constructed in 1998 over an existing hot-mix asphalt concrete (HMAC) surface. The site was selected as part of an experiment to evaluate the PASS (CMS1-P) rejuvenating seal. The southbound, outside lane, designated R1, and the northbound, inside lane, designated L2, were sealed with the PASS rejuvenating emulsion at 0.16 and 0.11 Gal/SY, respectively, on 11/10/2004. The target rate was 0.10 Gal/SY. The high rate for the R1 lane resulted in sand being spread on the site to reduce the amount of excess material on the surface. That same day the first attempt to apply the standard treatment, MS-2, was made but had to be cancelled due to equipment problems. The MS-2 fog seal was placed on lanes R2 and L1 on 12/16/2004 at 0.15 Gal/SY of 60-40 dilution. Some skid testing has been done on this site, but the site was seal coated not long after the second round of coring.

The designations for this site are:

ABL SH 36 L1 MS2	ABL SH 36 L1 Untreated
ABL SH 36 L2 PASS	ABL SH 36 L2 Untreated
ABL SH 36 R1 PASS	ABL SH 36 R1 Untreated
ABL SH 36 R2 MS2	ABL SH 36 R2 Untreated

Figures B-1 through B-14 illustrate the pre-treatment conditions, application, and 15 months post-treatment conditions.

Figure B-1. Abilene, SH 36 L2 Location.

Figure B-2. Abilene, SH 36 R1 Location.

Figure B-3. Abilene, SH 36 L2, Untreated Surface, Close-up (2004).

Figure B-4. Abilene, SH 36 R1, Untreated Surface, Close-up (2004).

Figure B-5. Abilene, SH 36 L1, Untreated Surface Close-up (2006).

Figure B-6. Abilene, SH 36 L2 Untreated Surface Close-up (2006).

Figure B-7. Abilene, SH 36 R1, Untreated Surface Close-up (2006).

Figure B-8. Abilene, SH 36 R2, Untreated Surface Close-up (2006).

Figure B-9. Abilene, SH 36 R1, PASS Treatment (2004).

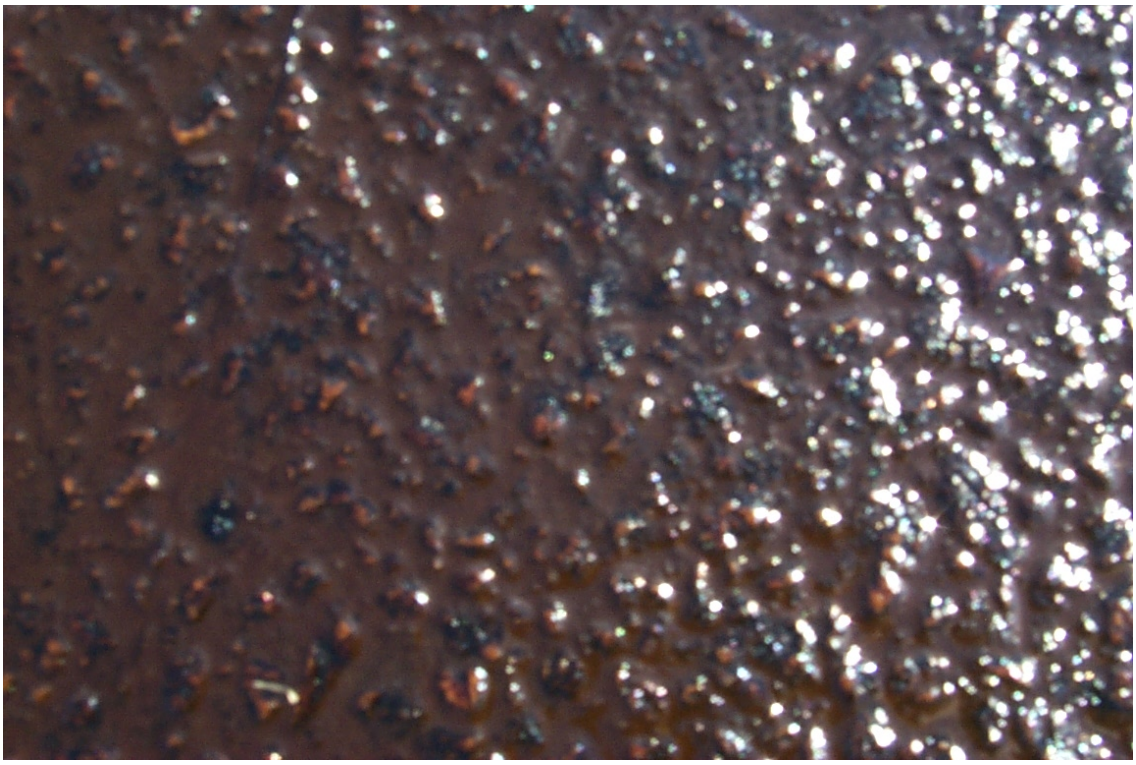

Figure B-10. Abilene, SH 36 R1, PASS Treatment Close-up (2004).

Figure B-11. Abilene, SH 36 L1, MS-2 Treatment Close-up (2006).

Figure B-12. Abilene, SH 36 L2, PASS Treatment Close-up (2006).

Figure B-13. Abilene, SH 36 R1, PASS Treatment Close-up (2006).

Figure B-14. Abilene, SH 36 R2, MS-2 Treatment Close-up (2006).

ATLANTA, IH20

This site is in the Atlanta District along Interstate 20 near Marshall, Texas, and the overpass of FM3251, from reference marker (RM) 613 to RM 610. There are three consecutive sections that were part of research project 4203, "Strategic Study for Resolving Hot Mix Related Issues" (Chowdhury, Bhasin, Button 2003) and includes sections with coarse-matrix, high binder (CMHB), dense graded (DG), and Superpave (SP) HMAC surfaces. Originally, this site was to receive a rejuvenator but instead received a fog seal with a 50/50 blend of cationic slow set (CSS-1) emulsion at 0.10 Gal/SY. The surfaces were placed in 2001, and the seal was placed in April 2006.

The site was overlaid not long after coring. The designations for this site are ATL IH20 CM, ATL IH20 DG, and ATL IH20 SP. A problem with the digital camera resulted in no pictures for this site.

ATLANTA, US67

This Atlanta District site is on US67, just east of the intersection with US259, near Omaha, Texas. This site was sealed with the PASS rejuvenator seal, 50/50 blend, at 0.10 Gal/SY. The surface was placed in November 2003, and the seal was placed in December 2004.

The designation for this site is ATL US67. A problem with the digital camera resulted in no pictures for this site.

CARRIZO SPRINGS AIRPORT

The HMAC surface of the Carrizo Springs Airport (120 miles southwest of San Antonio) was placed in 1995 and has been showing signs of surface deterioration. In October 2004, the surface was sealed with an EB 44 Coal-Tar sealer (coal-tar sealer with rejuvenator) at 0.14 Gal/SY. The designations for this site are CarrizU and CarrizT.

Figures B-15 through B-18 illustrate the pre-treatment conditions, 4 months post treatment, and 18 months pre- and post-treatment conditions.

Figure B-15. Carrizo Springs Airport, Untreated Surface Close-up (2004).

Figure B-16. Carrizo Springs Airport, EB 44 Treated Close-up (2005).

Figure B-17. Carrizo Springs Airport, Untreated Surface Close-up (2006).

Figure B-18. Carrizo Springs Airport, EB 44 Treated Close-up (2006).

FORT WORTH, FM 4

This site is on FM 4 in Hood County, near Thorp Springs, from RM 312+0.1 to RM 310+0.6. There are two test sections here because TxDOT selected a site where an older seal coat met a newer seal coat in order to test the experimental COS-50 treatment. On the southeast side of the bridge over Robinson Creek, the pavement is from 2003. On the northwest side, it was placed in 2000. Both sides received the same treatment, in the K6 lane only. The 2003 section received 0.10 Gal/SY while the older, more oxidized 2000 section received 0.14 Gal/SY. After the treatment, the 2003 section remained slick for several hours. This was partly due to the overcast, cool conditions, but the 2000 section did not seem to be as affected. The treatment was placed in February 2005.

Figures B-19 through B-26 illustrate the pre-treatment conditions, post treatment, and 13 months pre- and post-treatment conditions.

The site designations are:

FtW FM4 00 for the older section whose surface was placed in the year 2000.

FtW FM4 03 for the newer section whose surface was placed in the year 2003.

Figure B-19. Fort Worth, FM 4, 2000, Untreated Surface (2005).

Figure B-20. Fort Worth, FM 4, 2000, Treated COS-50 Close-up (2005).

Figure B-21. Fort Worth, FM 4, 2000, Untreated Surface Close-up (2006).

Figure B-22. Fort Worth, FM 4, 2000, Treated COS-50 Close-up (2006).

Figure B-23. Fort Worth, FM 4, 2003, Untreated Surface Close-up (2005).

Figure B-24. Fort Worth, FM 4, 2003, Treated COS-50 Close-up (2005).

Figure B-25. Fort Worth, FM 4, 2003, Untreated Surface Close-up (2006).

Figure B-26. Fort Worth, FM 4, 2003, Treated COS-50 Close-up (2006).

GEORGETOWN AIRPORT

The HMAC taxiway and runway surfaces near the 29 end of runway 11-29 at the Georgetown airport (30 miles north of Austin) were placed in 1989 and 1995. Most of the pavement was sealed with an EB 44 coal-tar sealer (coal-tar sealer with rejuvenator) at 0.05 Gal/SY in 1999, but the runway (1995) was sealed with the EB 44 coal-tar sealer at 0.05 Gal/SY in July 2005. The test sections are designated:

GEO89U	built in 1989, unsealed
GEO89T	built in 1989, sealed 1999
GEO95U	built in 1995, unsealed
GEO95T	built in 1995, sealed 1999
GEO95*U	built in 1995, unsealed
GEO95*T	built in 1995, sealed 2006

Figures B-27 through B-37 illustrate the pre-treatment conditions, 5 and 7 year post treatment, and 9 months post treatment conditions for the recently sealed section.

Figure B-27. Georgetown Airport, 1989, Untreated Close-up (2004).

Figure B-28. Georgetown Airport, 1989, Treated Close-up (2004).

Figure B-29. Georgetown Airport, 1989, Treated (2004).

Figure B-30. Georgetown Airport, 1989, Untreated Close-up (2006).

Figure B-31. Georgetown Airport, 1989, Treated Close-up (2006).

Figure B-32. Georgetown Airport, 1995, Untreated Close-up (2004).

Figure B-33. Georgetown Airport, 1995, Treated Close-up (2004).

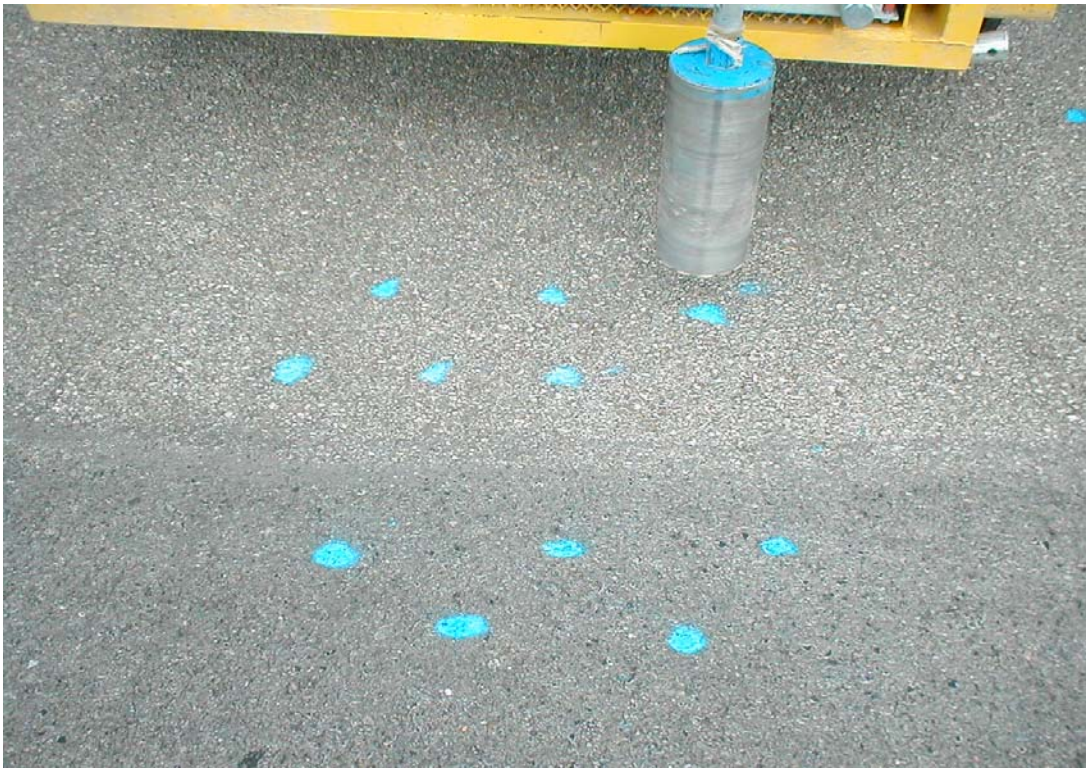

Figure B-34. Georgetown Airport, 1995, Untreated and Treated (2006).

Figure B-35. Georgetown Airport, 1995, Untreated Close-up (2006).

Figure B-36. Georgetown Airport, 1995, Treated Close-up (2006).

Figure B-37. Georgetown Airport, 1995*, Treated 2005 Close-up (2006).

JACKSONVILLE AIRPORT

The HMAC surface of the Cherokee County airport, outside Jacksonville (120 miles southeast of Dallas) was placed in June 2004. In July 2004, the surface was sealed with an EB 44 coal-tar sealer (coal-tar sealer with rejuvenator) at 0.05 Gal/SY and cored two months later. The designations for this site are JacksU and JacksT.

Figures B-38 through B-40 illustrate the pre-treatment conditions, two months post treatment, and 18 months pre- and post-treatment conditions.

A problem with the digital camera resulted in no pictures for this site in 2006.

Figure B-38. Jacksonville Airport, Untreated 2004 (2004).

Figure B-39. Jacksonville Airport, Treated 2004 Close-up (2004).

Figure B-40. Jacksonville Airport, Treated 2004 (2004).

LUFKIN, BUS59

The site is on Bus 59 just north of the TxDOT district office, in the southbound lanes. The PASS rejuvenator was placed in October 2004 as part of a demonstration on the HMAC pavement that was constructed in 1995.

Figures B-41 through B-44 illustrate the pre-treatment conditions, 1 month post treatment, and 15 months pre- and post-treatment conditions. A problem with the digital camera resulted in no pictures for this site in 2006. The site designations are LUF BUS59U and LUF BUS59T.

Figure B-41. Lufkin BUS59 Southbound, Treated Location (2004).

Figure B-42. Lufkin BUS59 Southbound, Treated 2004 Close-up (2004).

Figure B-43. Lufkin BUS59 Southbound, Treated 2004 (2004).

ODESSA WB FR SH 191

The site is on the westbound frontage road for SH 191 between Midland and Odessa, just west of SH 158. The SS-1 emulsion was placed in November 2002 as part of a routine seal on a pavement constructed in 1983.

Figures B-44 through B-47 illustrate the pre-treatment condition and 41 months post treatment condition. Due to a mistake by the coring person, the site designations are ODE 149U and ODE149T rather than the highway designation 191.

Figure B-44. Odessa Westbound Frontage Road, SH191, Untreated 1983 Close-up (2006).

Figure B-45. Odessa Westbound Frontage Road, SH191, Treated 2002, Close-up (2006).

ODESSA SH 349

The site is southbound on SH 349 just south of Midland. The SS-1 emulsion was placed in February 2006 as part of a routine seal on a pavement constructed in 1996.

Figures B-46 through B-47 illustrate the pre-treatment condition and 2 months post treatment condition. The site designations are ODE 349U and ODE 349T.

Figure B-46. Odessa SH349 Southbound, Untreated 1996, Close-up (2006).

Figure B-47. Odessa SH349 Southbound, Treated 2006, Close-up (2006).

PLEASANTON AIRPORT

The HMAC surface of the Pleasanton airport, outside Jacksonville (35 miles south of San Antonio) was placed in 1985. In August 2004 the surface was sealed with an EB 44 coal-tar sealer (coal-tar sealer with rejuvenator) at 0.043 Gal/SY. Originally, only the runway ends were sealed, but the rate was high and had to be sanded and swept. This area was not tested.

Sometime after the first coring visit in 2004, the entire airport was sealed. There were no areas remaining that did not receive the seal, so there are no "U" cores from 2006. The designations for this site are PleasU and PleasT.

Figures B-48 through B-52 illustrate the pre-treatment conditions, two months post treatment, and 18 months pre- and post-treatment conditions.

Figure B-48. Pleasanton Airport, Untreated 1985, Close-up (2004).

Figure B-49. Pleasanton Airport Application 2004 (2004).

Figure B-50. Pleasanton Airport Treated 2004 (2004).

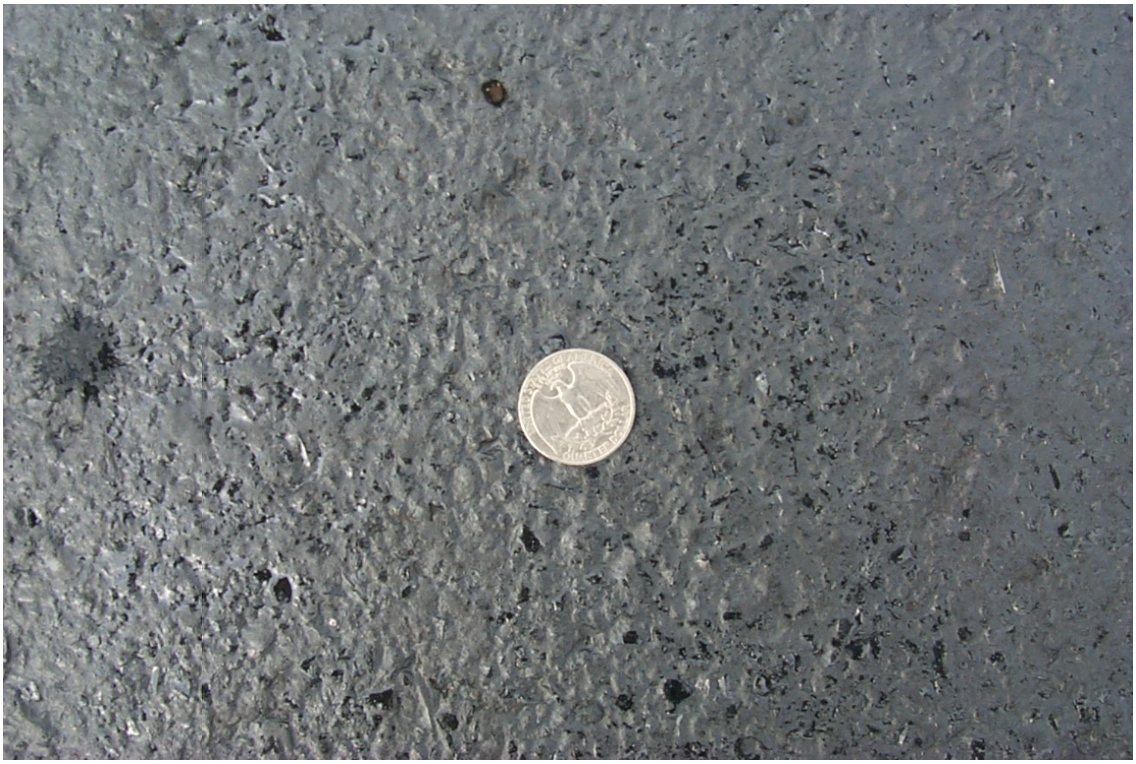

Figure B-51. Pleasanton Airport, Treated 2004, Close-up (2004).

Figure B-52. Pleasanton Airport, Treated 2004, Close-up (2006).

TYLER, US79

This Tyler District site is on the east bound shoulder of US79, just northeast of Jacksonville at RM 360+1.85. This site was sealed with the PASS rejuvenator seal, 50/50 blend, at 0.10 Gal/SY. The surface was placed in 2002, and the seal was placed in March 2005. The coring visit was after a recent rain and although the untreated areas were still wet from absorbed water, the treated area looked dry.

The designation for this site is TYL US79. A problem with the digital camera resulted in no pictures for this site.

APPENDIX C

RESULTS OF FIELD PQI TESTING AND LABORATORY PERMEABILITY TESTING

RESULTS OF FIELD PQI TESTING AND LABORATORY PERMEABILITY TESTING

PQI AND AIR VOID TESTING

The procedures for PQI and permeability testing were described in Chapter 2. The following figures document the results of those tests. There was no PQI testing done until late in 2005, so the figures describing results for 2005 do not have many results. Typically, for sites cored in 2005, only one treated and one untreated core were sliced and tested for air voids.

Figures C-1 through C-5 illustrate the PQI results, where PQI tests were conducted. The untreated and treated locations are shown as different symbols on the same plot. Ideally, all symbols would be at exactly the same point, but some variation was expected.

Figures C-6 through C-24 illustrate the permeability of the specimens tested with the air voids values displayed on each of the bar graphs.

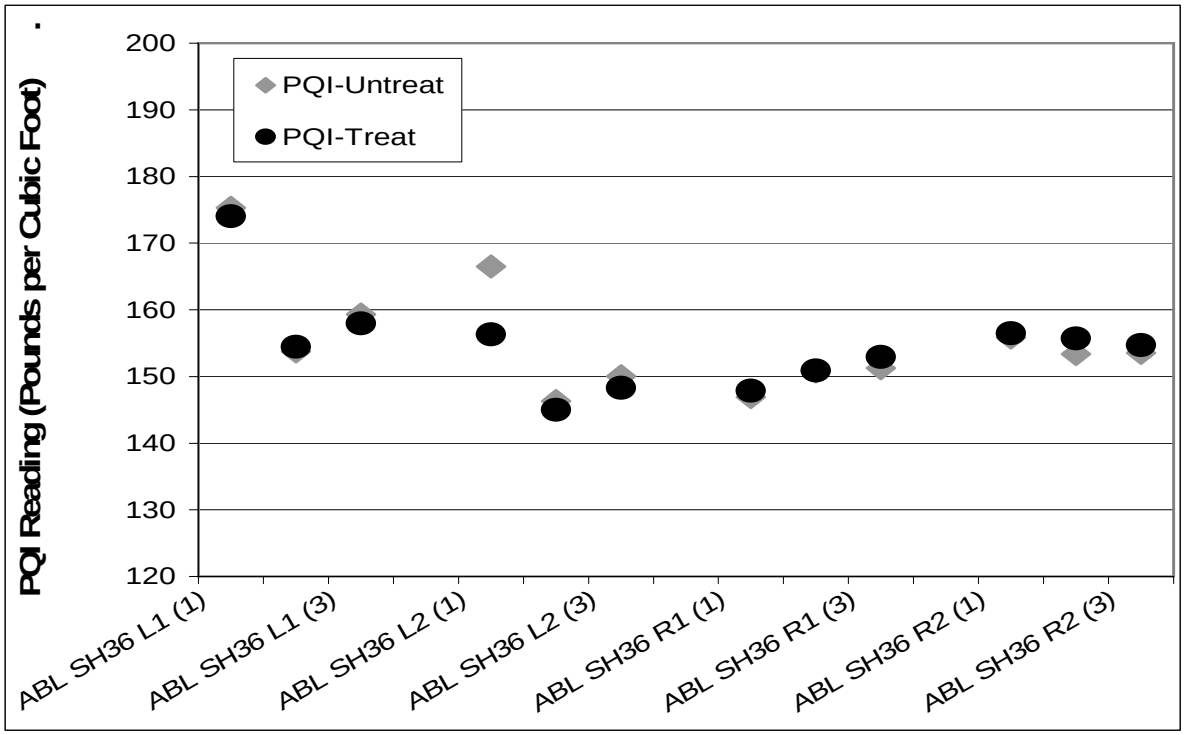

Figure C-1. PQI Readings for Abilene Sites.

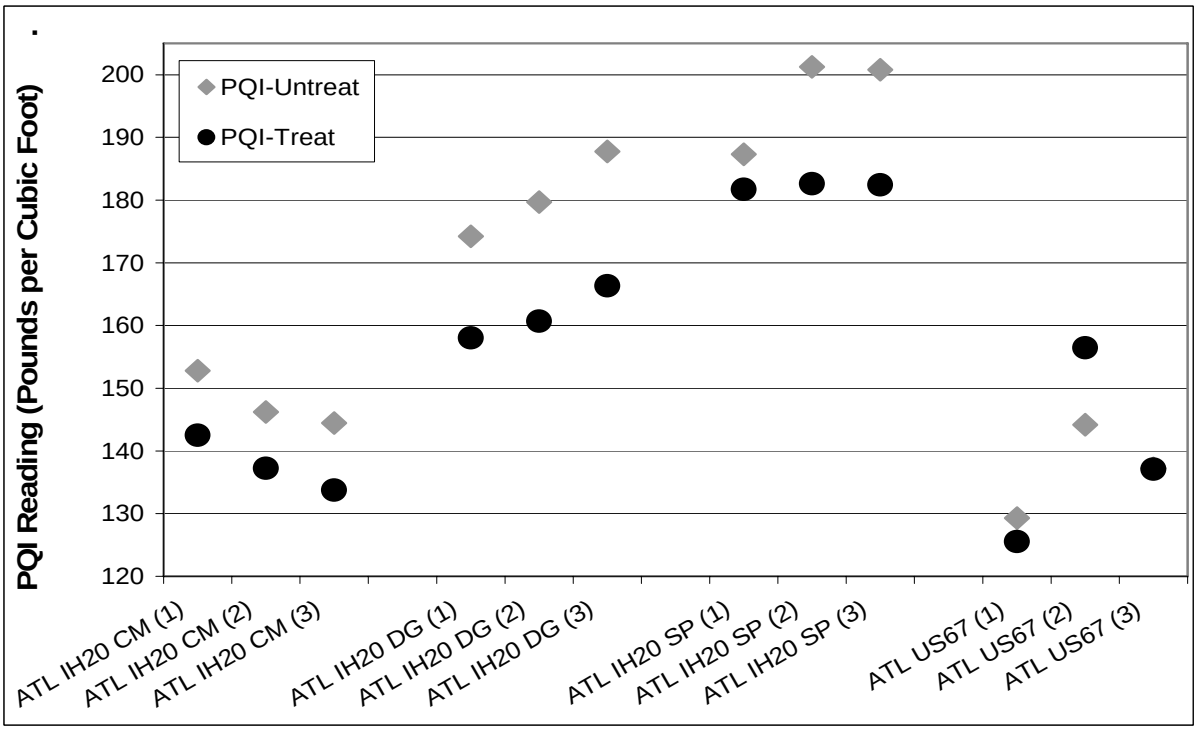

Figure C-2. PQI Readings for Atlanta Sites.

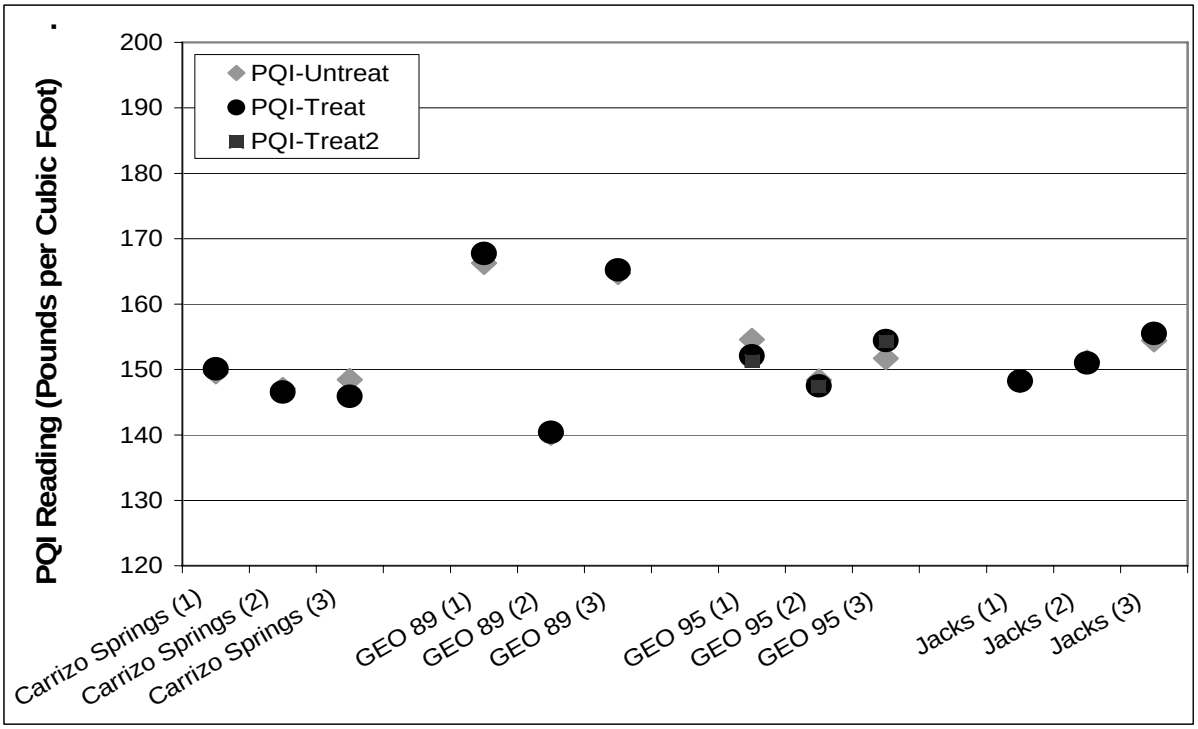

Figure C-3. PQI Readings for Carrizo Springs and Georgetown Airport Sites.

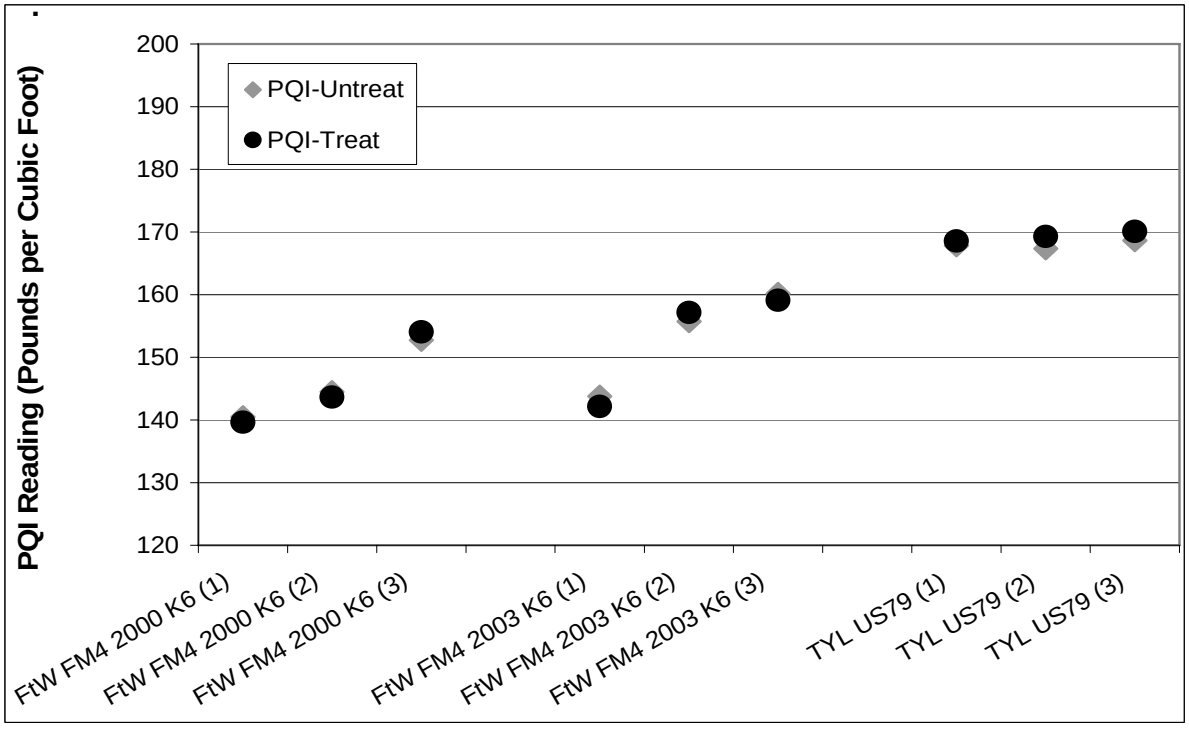

Figure C-4. PQI Readings for Fort Worth and Tyler Sites.

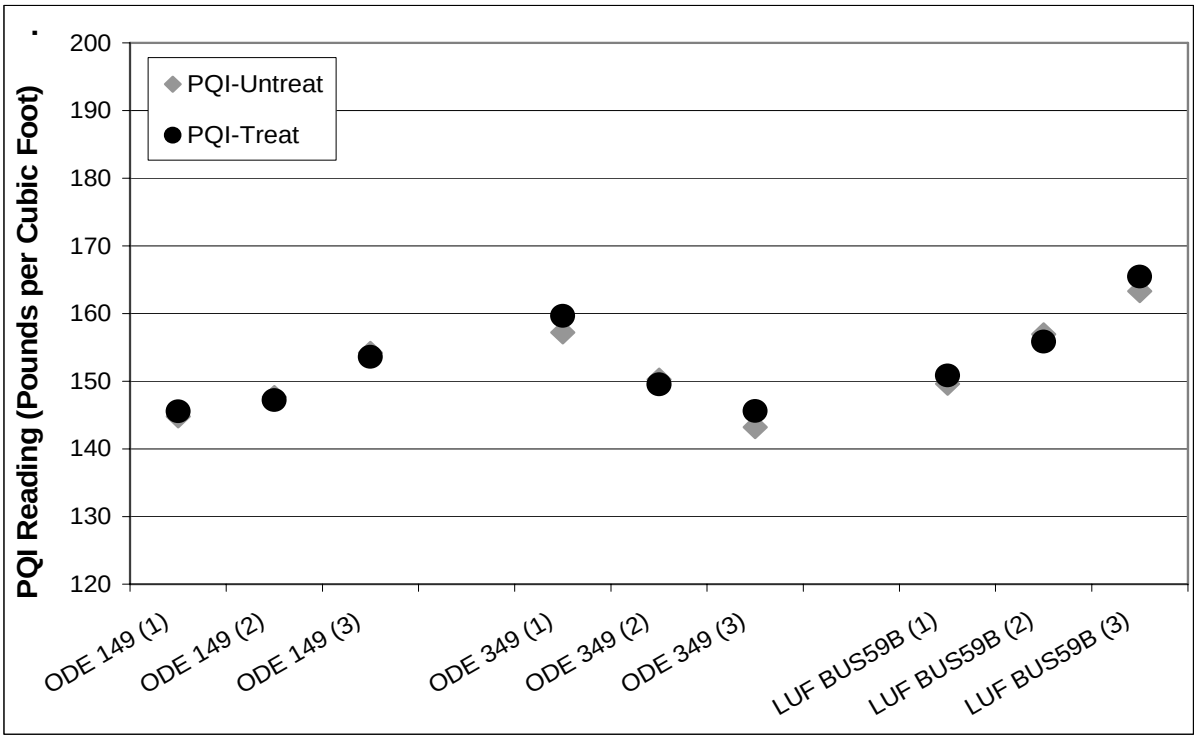

Figure C-5. PQI Readings for Odessa and Lufkin Sites.

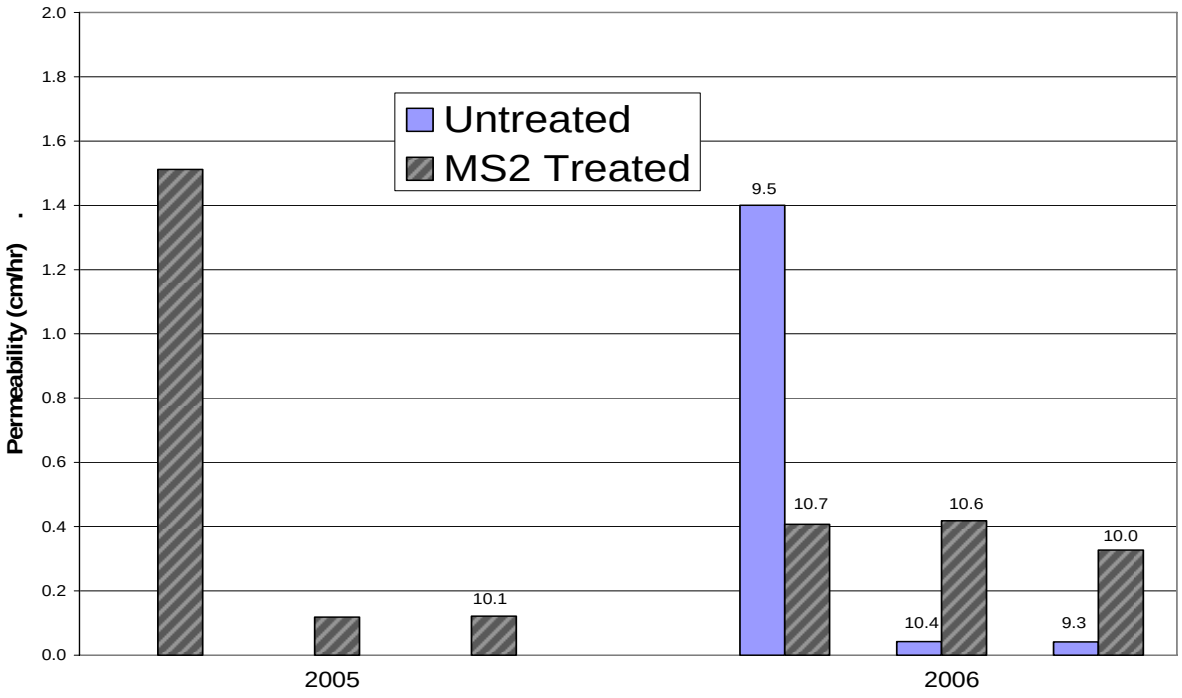

Figure C-6. Permeability and Air Voids for Abilene Lane L1 Sites.

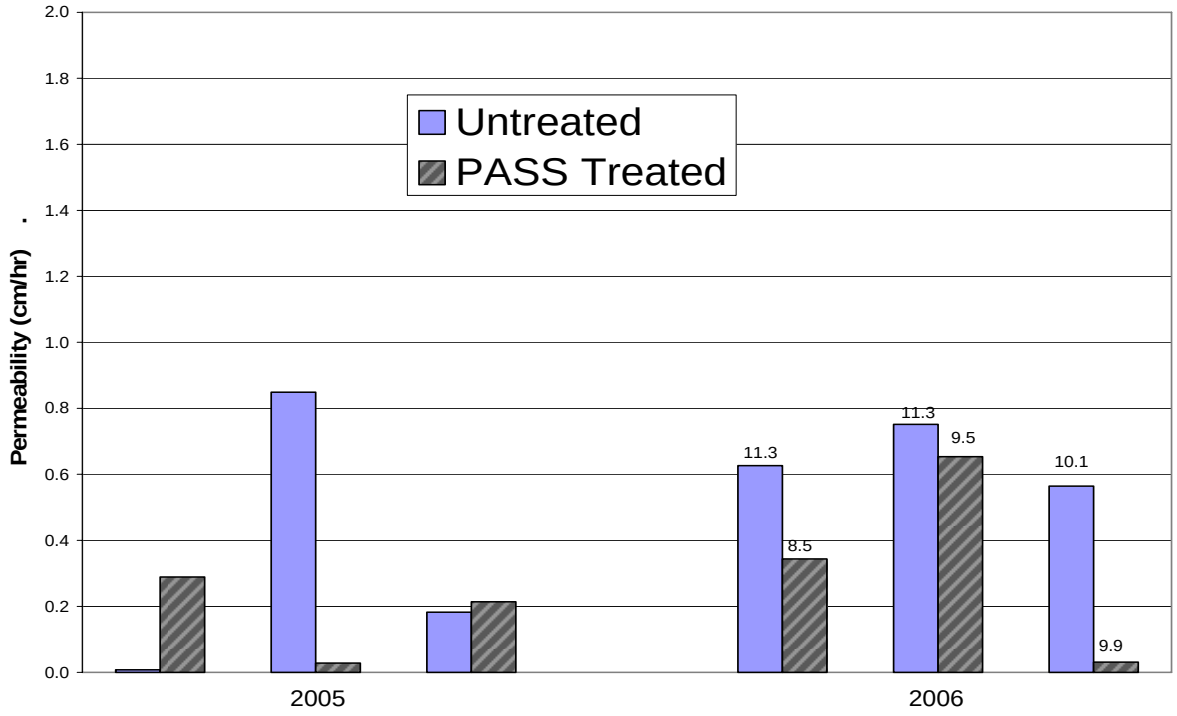

Figure C-7. Permeability and Air Voids for Abilene L2 Sites.

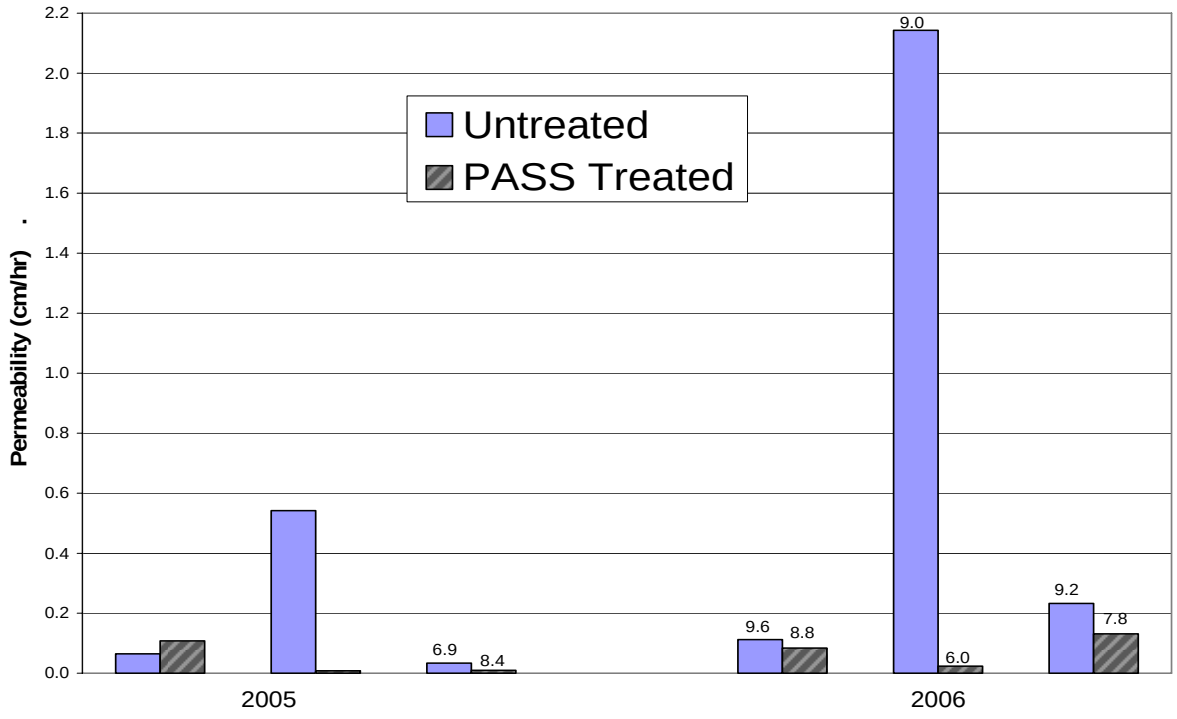

Figure C-8. Permeability and Air Voids for Abilene R1 Sites.

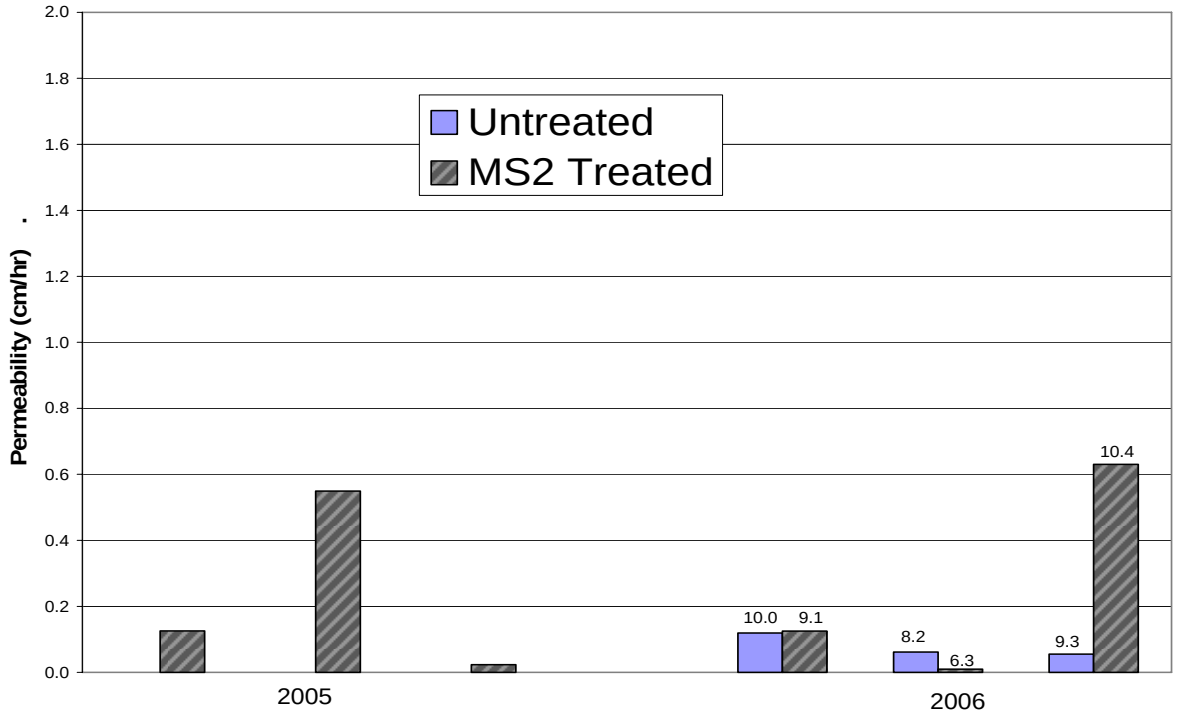

Figure C-9. Permeability and Air Voids for Abilene R2 Sites.

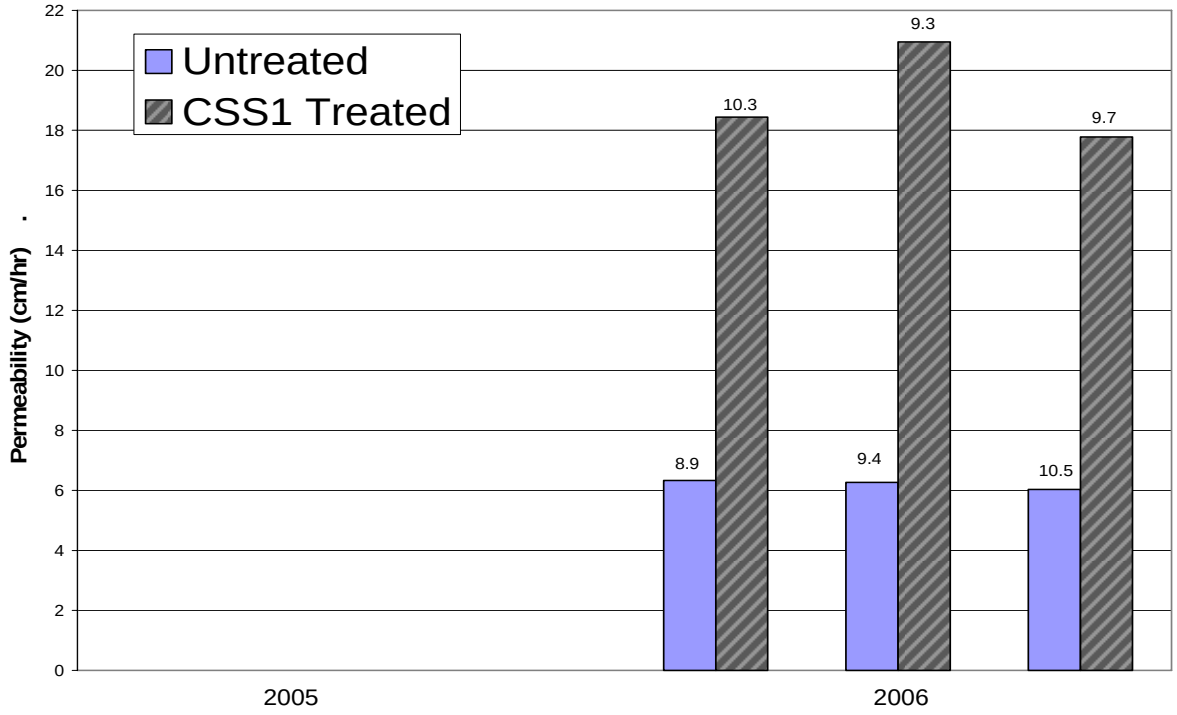

Figure C-10. Permeability and Air Voids for Atlanta IH20 CM Site.

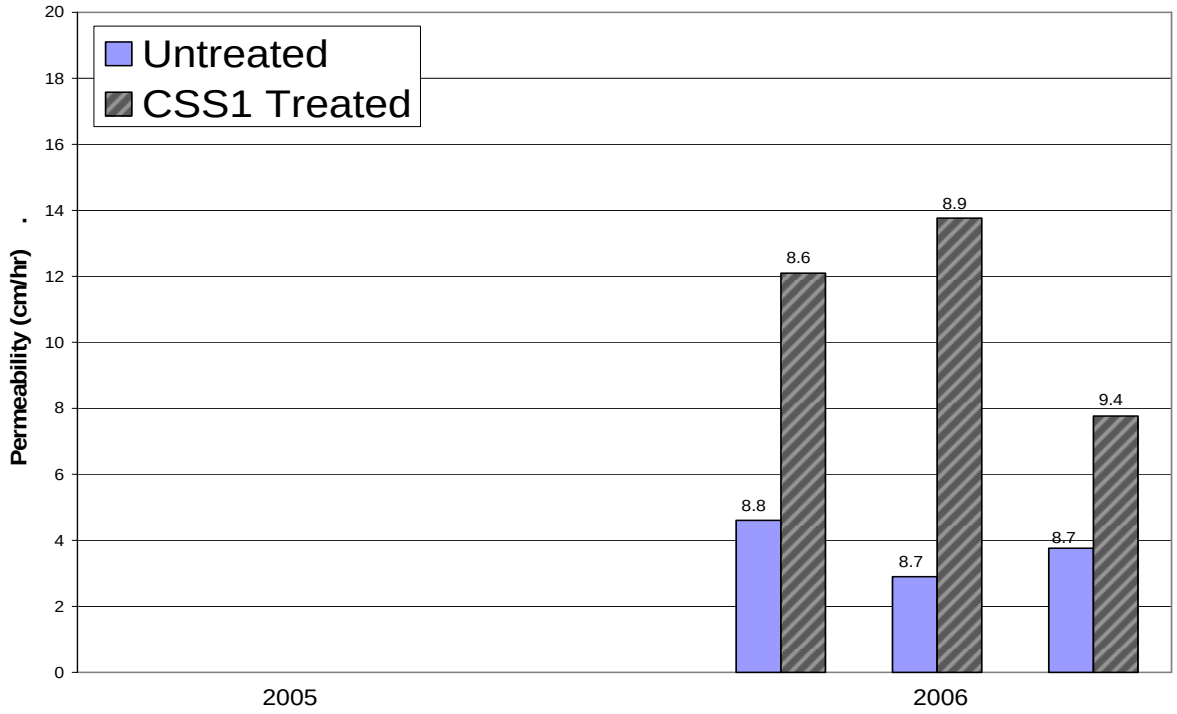

Figure C-11. Permeability and Air Voids for Atlanta DG Site.

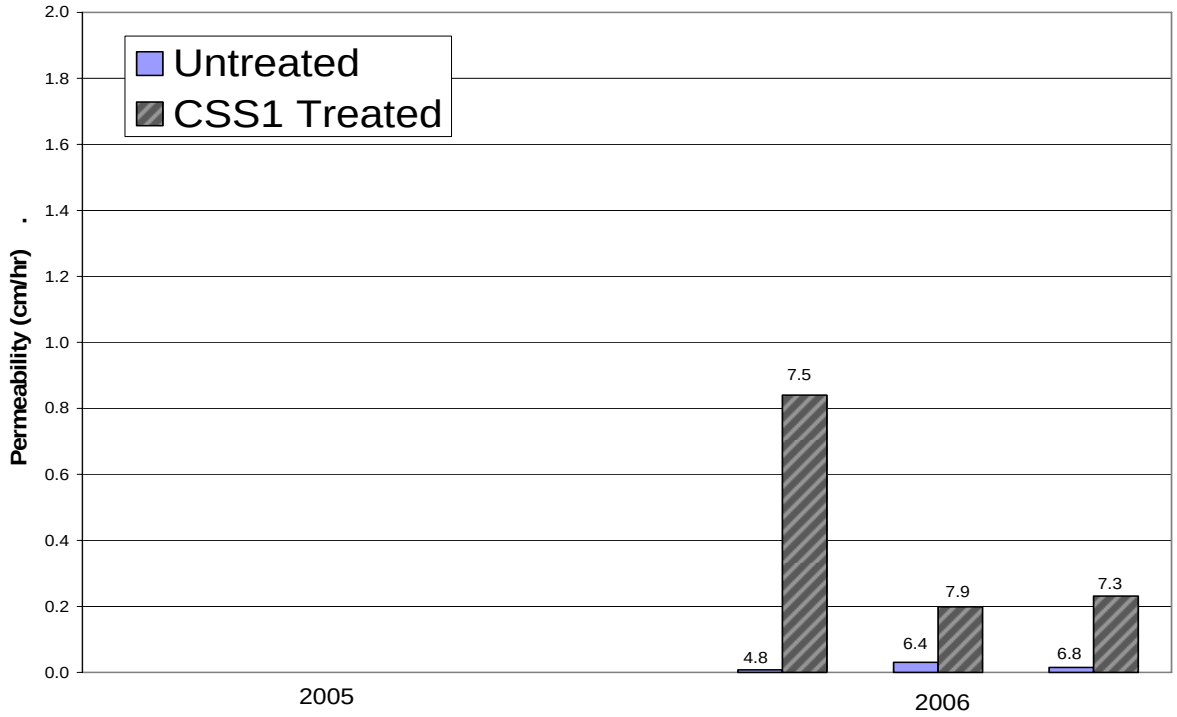

Figure C-12. Permeability and Air Voids for Atlanta SP Site.

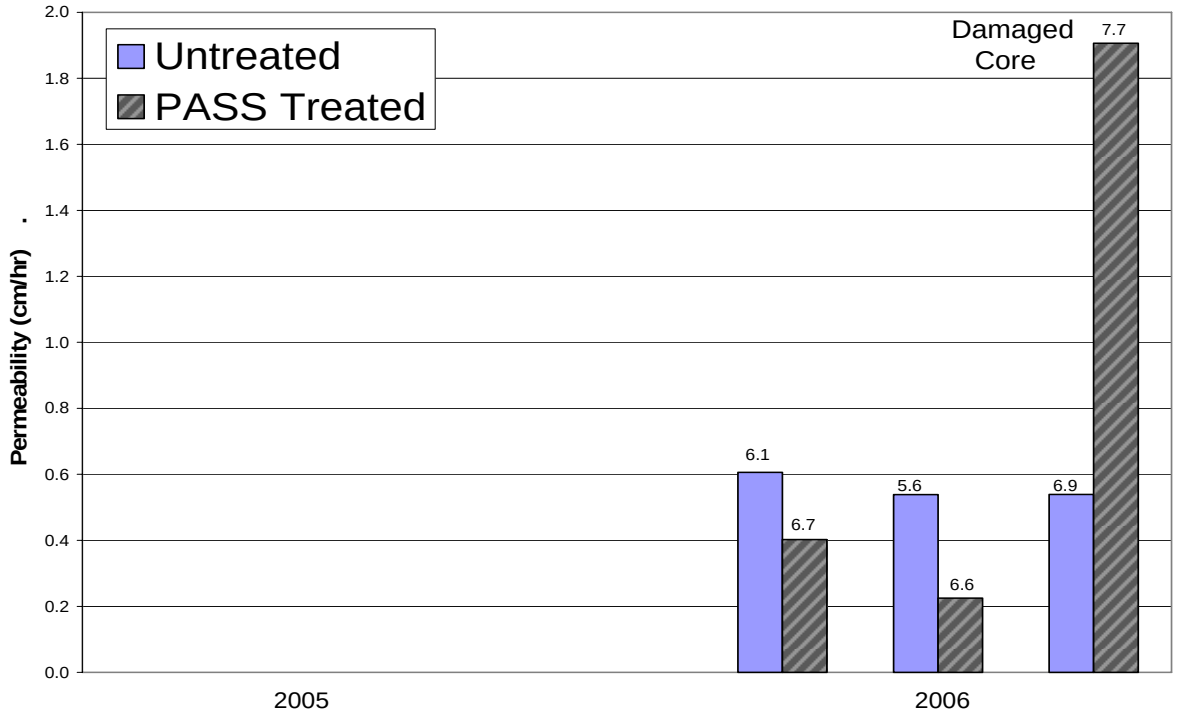

Figure C-13. Permeability and Air Voids for Atlanta US67 Site.

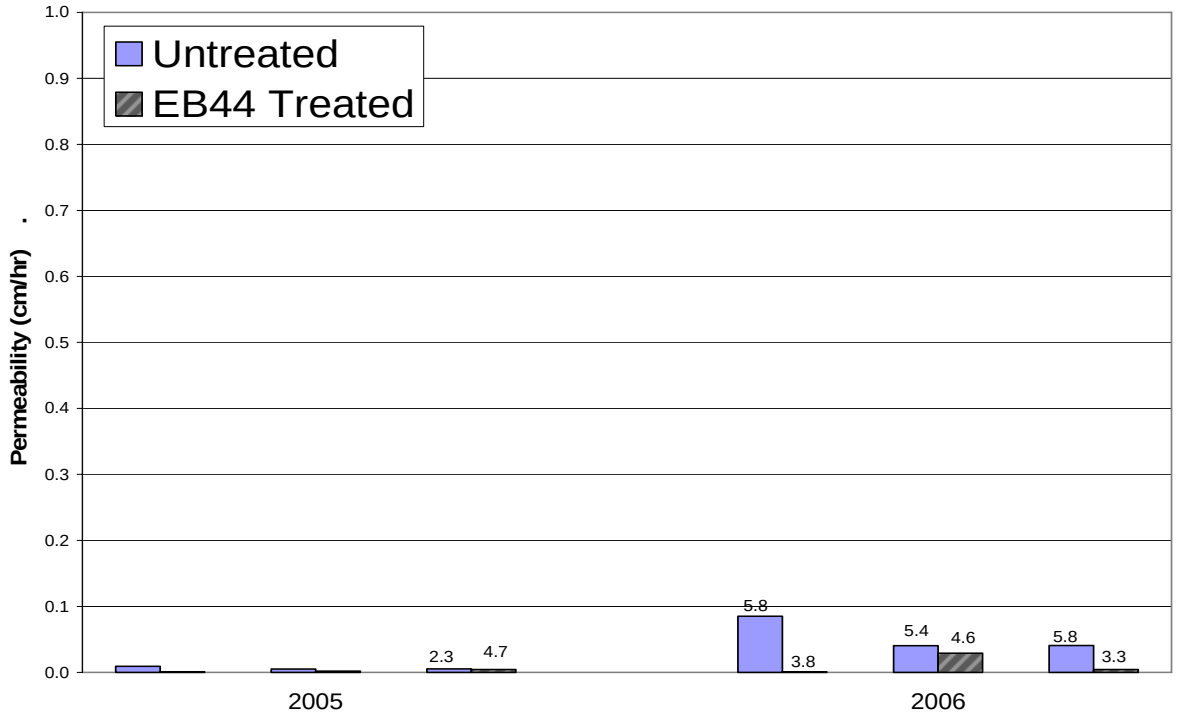

Figure C-14. Permeability and Air Voids for Carrizo Springs Airport.

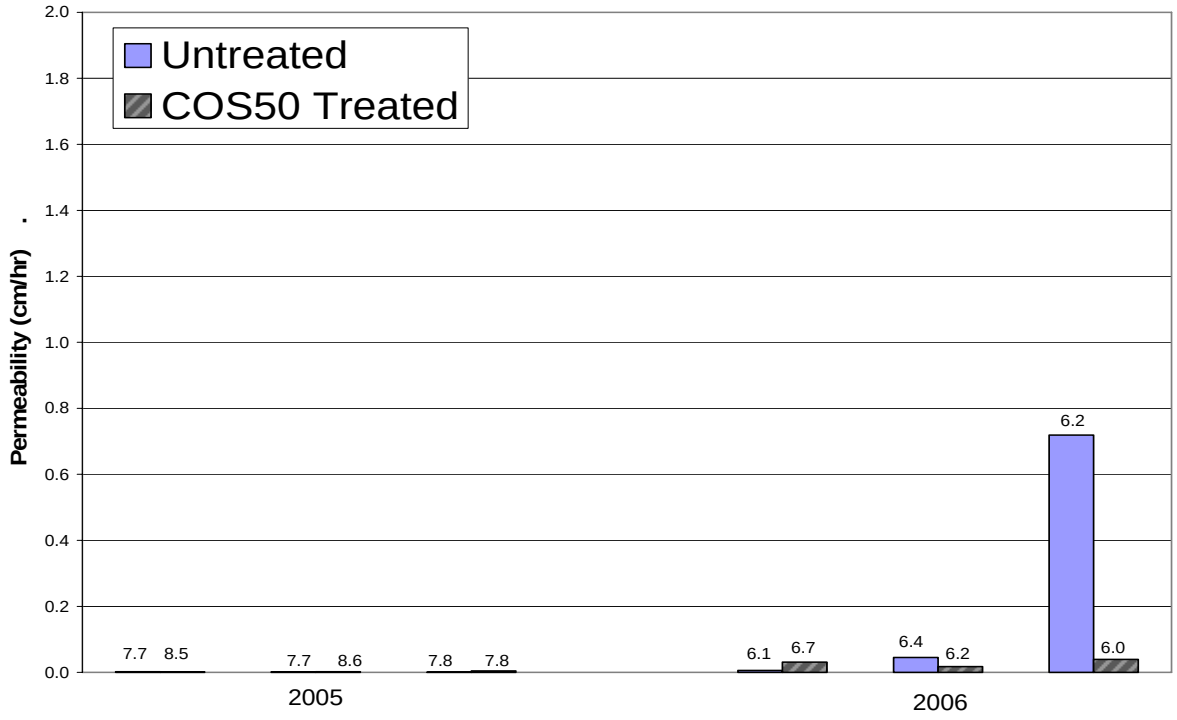

Figure C-15. Permeability and Air Voids for Fort Worth FM 4 (2000) Site.

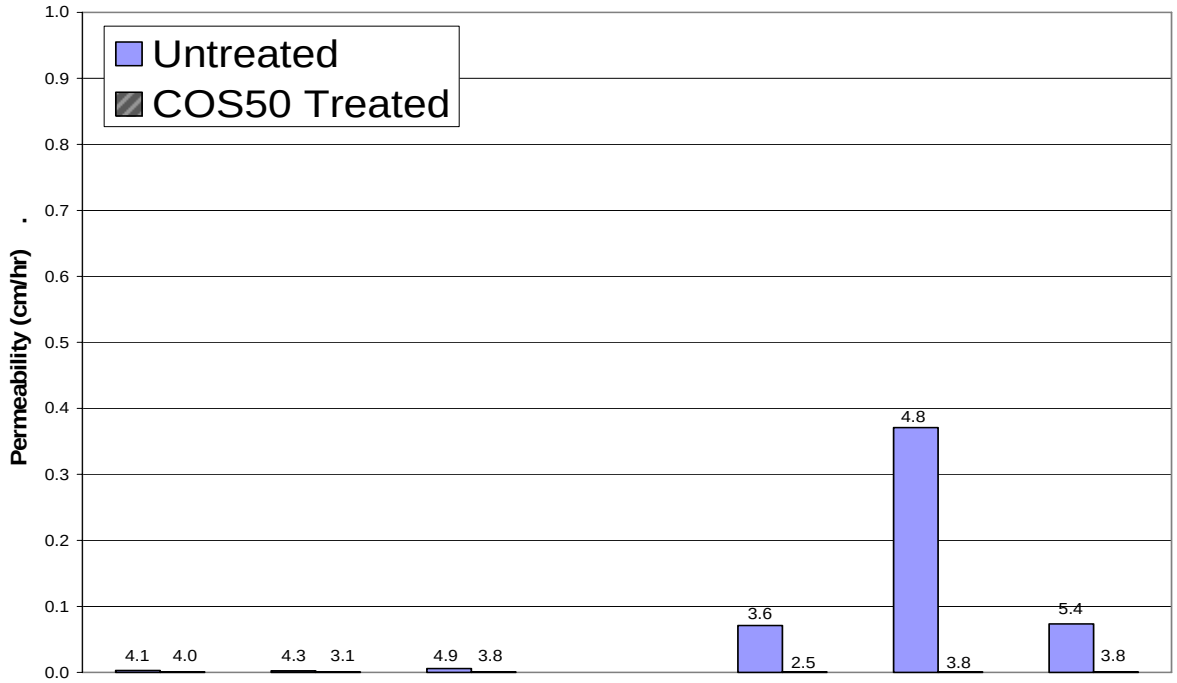

Figure C-16. Permeability and Air Voids for Fort Worth FM 4 (2003) Site.

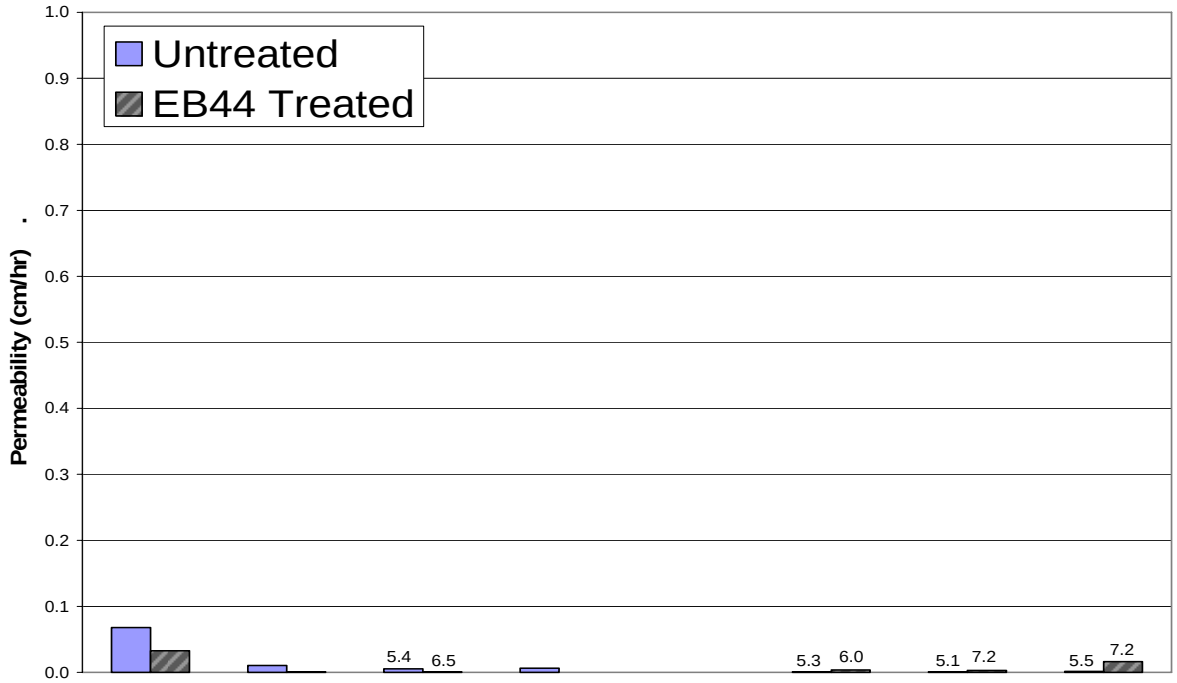

Figure C-17. Permeability and Air Voids for Georgetown Airport (1989) Site.

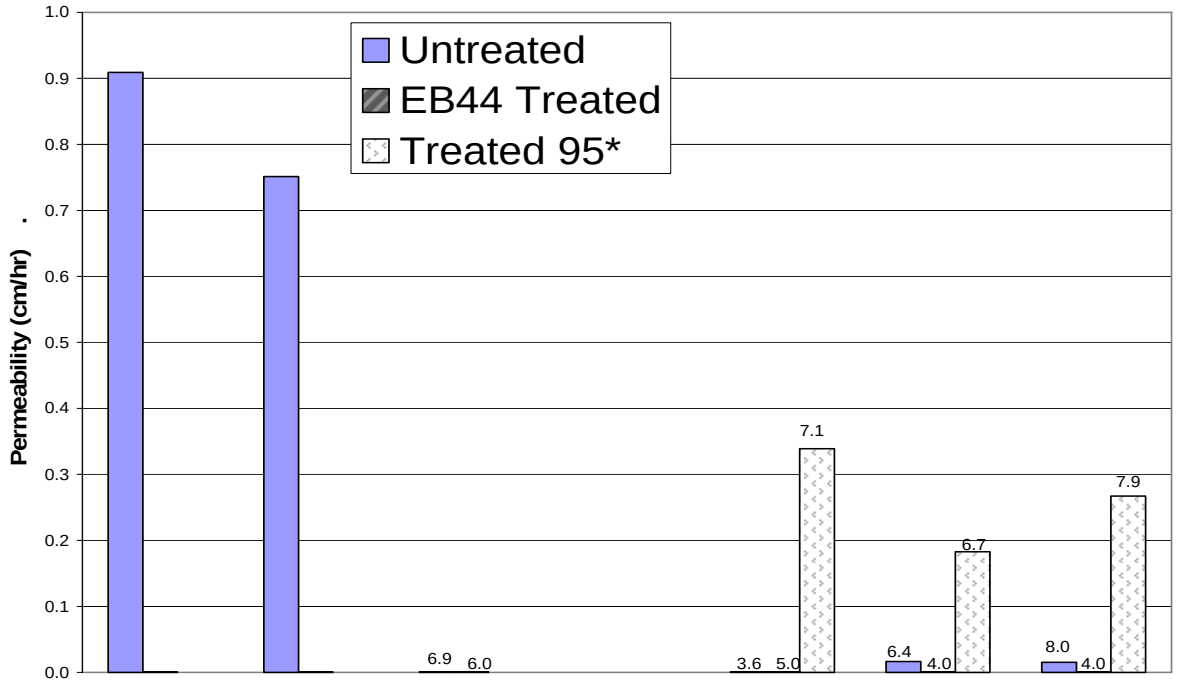

Figure C-18. Permeability and Air Voids for Georgetown Airport (1995) Site.

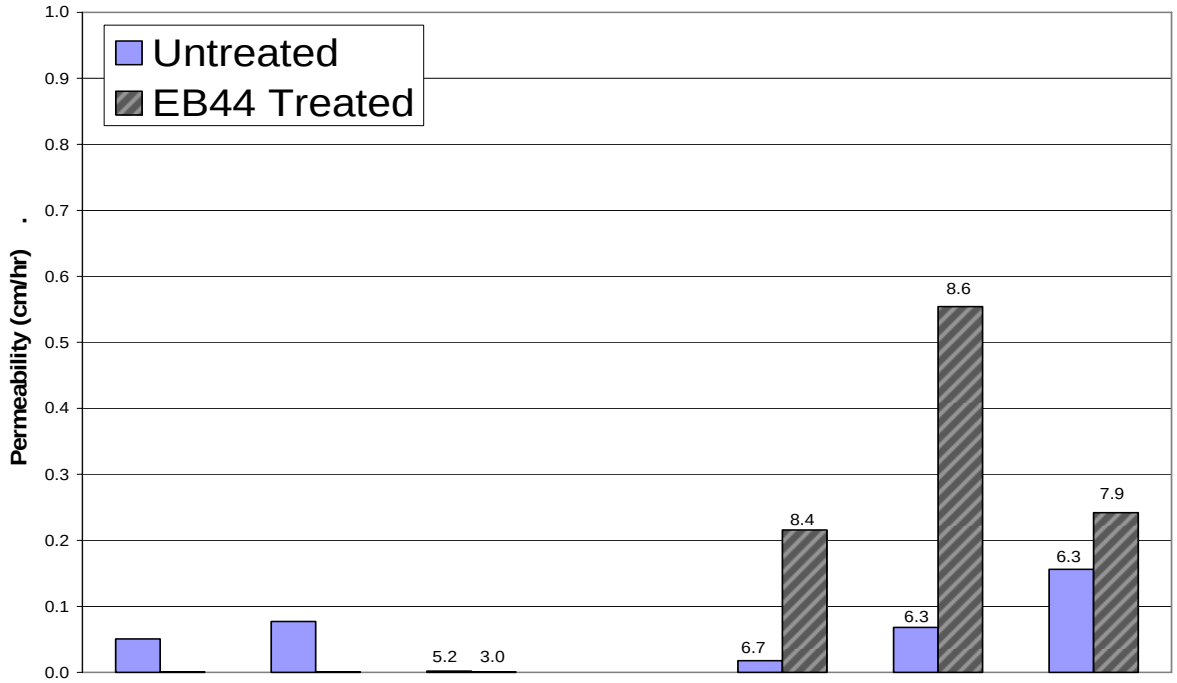

Figure C-19. Permeability and Air Voids for Jacksonville Airport Site.

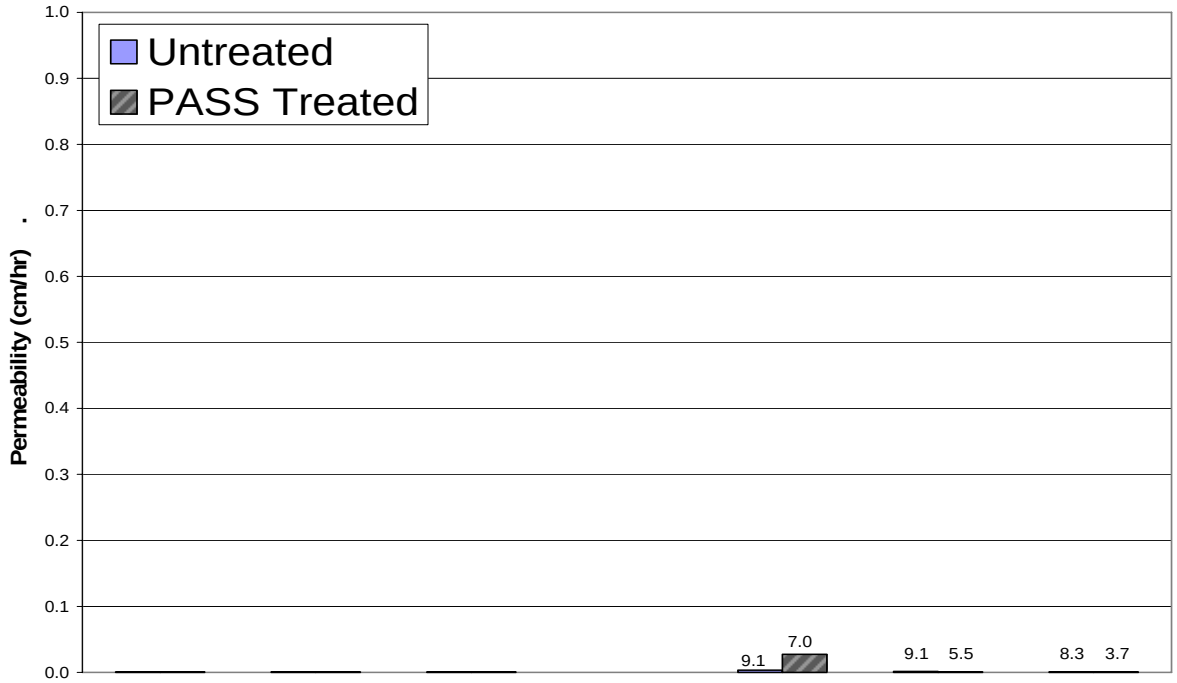

Figure C-20. Permeability and Air Voids for Lufkin BUS59 Sites.

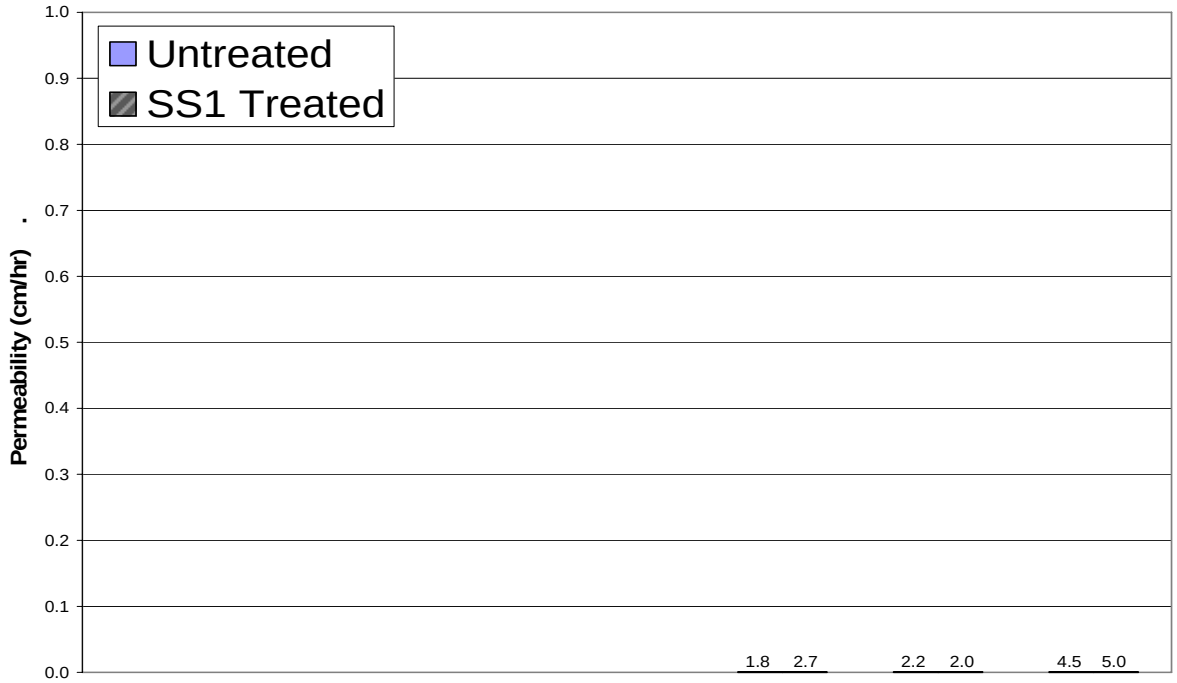

Figure C-21. Permeability and Air Voids for Odessa SH149 Site.

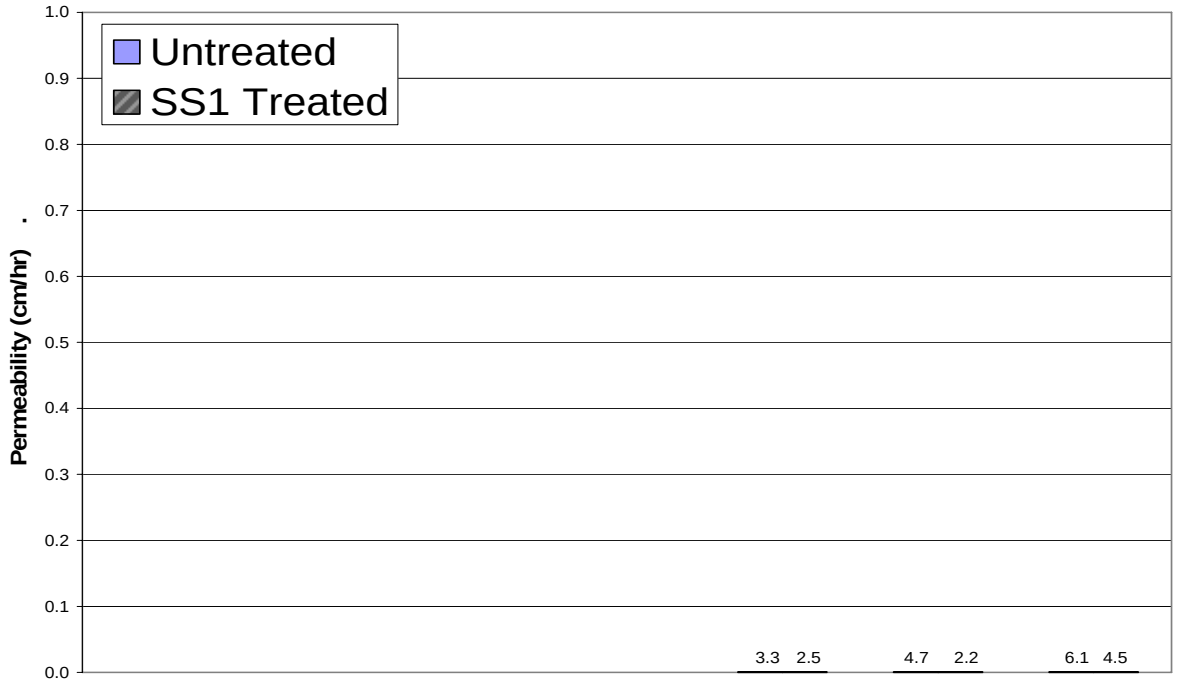

Figure C-22. Permeability and Air Voids for SH349 Site.

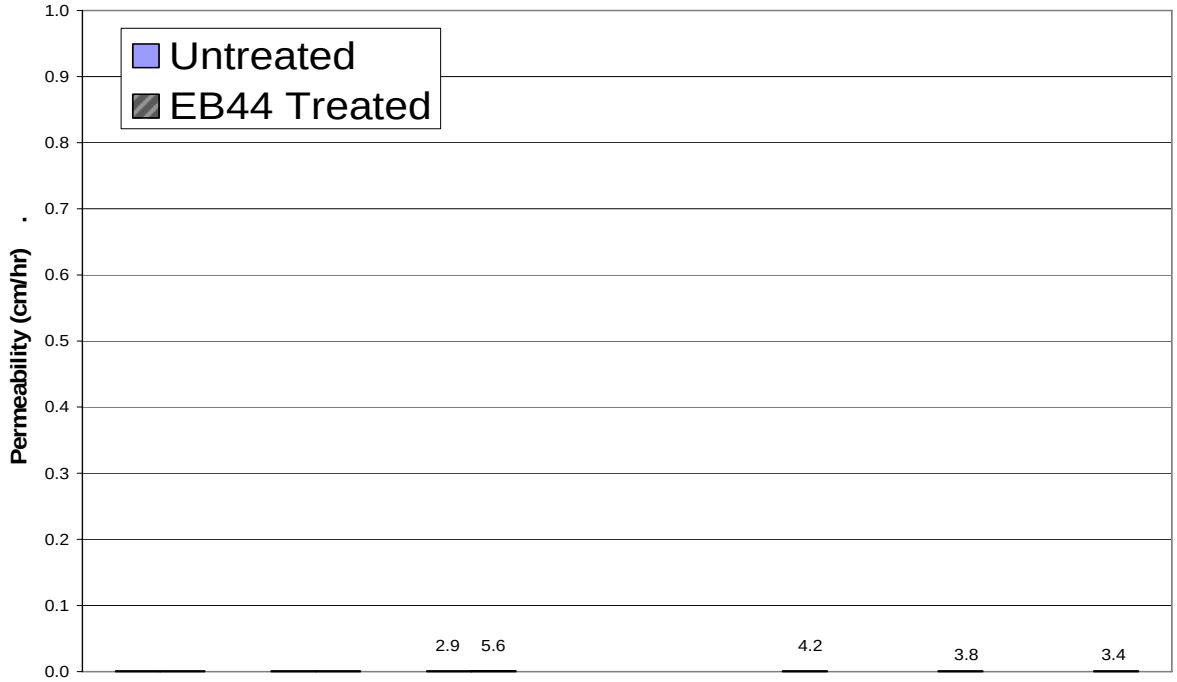

Figure C-23. Permeability and Air Voids for Pleasanton Airport Site.

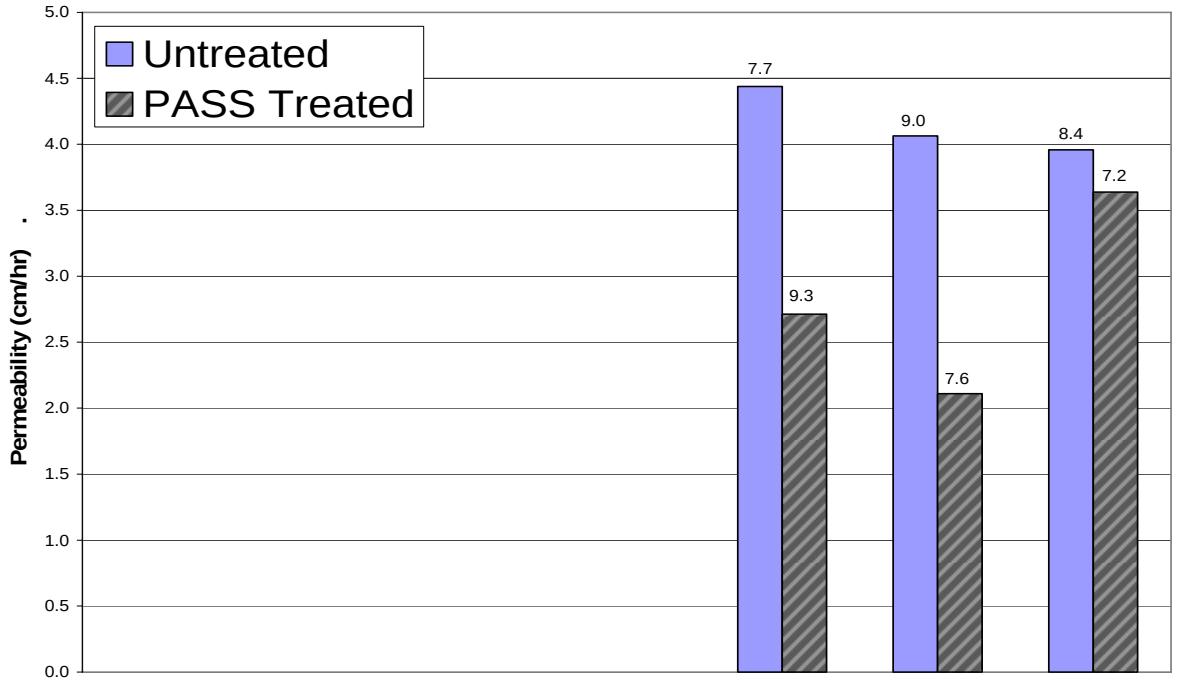

Figure C-24. Permeability and Air Voids for Tyler US79 Site.

APPENDIX D

RESULTS OF THE LABORATORY TESTING FOR AIR VOIDS, SLICE THICKNESSES, AND ESTIMATED DEPTH OF SAMPLES

RESULTS OF LABORATORY TESTING FOR AIR VOIDS, SLICE THICKNESSES AND ESTIMATED DEPTH OF SAMPLES

LABORATORY TESTING FOR AIR VOIDS

Chapter 2 describes the procedures for air voids testing. The following figures document the results of those tests. Typically, for sites cored in 2005, only one treated and one untreated core were sliced and tested for air voids.

Figures D-1 through D-28 illustrate the laboratory measured air voids and where PQI tests were conducted, the resulting values are also plotted on the secondary Y-axis. There was no PQI testing done until late in 2005, so most of the figures describing results for 2005 do not have any results. The designations for the various sites have been abbreviated so that the labels along the X-axis use less space. Tables D-1 through D-28 list the designations and the estimated slice thickness. This thickness was computed from the mass and average bulk specific gravity for the slice. Due to losses of material during the coring process and other possible losses of mass, the thicknesses and depth to the bottom of the slice can only be considered approximate.

Table D-1. Figure Designation and Slice Thickness for Abilene SH36 L1 2005 Cores.

Figure Designation	Site	Estimated Slice Thickness (in.)	Estimated Depth (in.)
L1 (05) MS2 T1-3-1	AB SH36 L1 MS2 (2005) T1-3, Slice 1	0.16	0.16
L1 (05) MS2 T1-3-2	AB SH36 L1 MS2 (2005) T1-3, Slice 2	0.15	0.45
L1 (05) MS2 T1-3-3	AB SH36 L1 MS2 (2005) T1-3, Slice 3	0.20	0.80
L1 (05) MS2 T1-3-4	AB SH36 L1 MS2 (2005) T1-3, Slice 4	0.12	1.07
R1 (05) U1-3-1	AB SH36 R1 (2005) U1-3, Slice 1	0.12	0.12
R1 (05) U1-3-2	AB SH36 R1 (2005) U1-3, Slice 2	0.17	0.43
R1 (05) U1-3-3	AB SH36 R1 (2005) U1-3, Slice 3	0.20	0.78
R1 (05) U1-3-4	AB SH36 R1 (2005) U1-3, Slice 4	0.14	1.07
R1 (05) Pass T1-3-1	AB SH36 R1 PASS (2005) T1-3, Slice 1	0.18	0.18
R1 (05) Pass T1-3-2	AB SH36 R1 PASS (2005) T1-3, Slice 2	0.10	0.42
R1 (05) Pass T1-3-3	AB SH36 R1 PASS (2005) T1-3, Slice 3	0.19	0.77
R1 (05) Pass T1-3-4	AB SH36 R1 PASS (2005) T1-3, Slice 4	0.13	1.04

Table D-2. Figure Designation and Slice Thickness for Abilene SH36 L1 2006 Cores.

Figure Designation	Site	Estimated Slice Thickness (in.)	Estimated Depth (in.)
L1 (06) U2-1-1	ABL SH36 L1 (2006) U2-1, Slice 1	0.27	0.27
L1 (06) U2-1-2	ABL SH36 L1 (2006) U2-1, Slice 2	0.24	0.65
L1 (06) U2-1-3	ABL SH36 L1 (2006) U2-1, Slice 3	0.27	1.07
L1 (06) U2-1-4	ABL SH36 L1 (2006) U2-1, Slice 4	0.26	1.48
L1 (06) U2-2-1	ABL SH36 L1 (2006) U2-2, Slice 1	0.31	0.31
L1 (06) U2-2-2	ABL SH36 L1 (2006) U2-2, Slice 2	0.25	0.70
L1 (06) U2-2-3	ABL SH36 L1 (2006) U2-2, Slice 3	0.19	1.04
L1 (06) U2-2-4	ABL SH36 L1 (2006) U2-2, Slice 4	0.21	1.40
L1 (06) U2-3-1	ABL SH36 L1 (2006) U2-3, Slice 1	0.30	0.30
L1 (06) U2-3-2	ABL SH36 L1 (2006) U2-3, Slice 2	0.19	0.64
L1 (06) U2-3-3	ABL SH36 L1 (2006) U2-3, Slice 3	0.18	0.96
L1 (06) U2-3-4	ABL SH36 L1 (2006) U2-3, Slice 4	0.19	1.30
L1 (06) MS2 T2-1-1	ABL SH36 L1 MS2 (2006) T2-1, Slice 1	0.26	0.26
L1 (06) MS2 T2-1-2	ABL SH36 L1 MS2 (2006) T2-1, Slice 2	0.23	0.63
L1 (06) MS2 T2-1-3	ABL SH36 L1 MS2 (2006) T2-1, Slice 3	0.25	1.02
L1 (06) MS2 T2-1-4	ABL SH36 L1 MS2 (2006) T2-1, Slice 4	0.25	1.43
L1 (06) MS2 T2-2-1	ABL SH36 L1 MS2 (2006) T2-2, Slice 1	0.33	0.33
L1 (06) MS2 T2-2-2	ABL SH36 L1 MS2 (2006) T2-2, Slice 2	0.25	0.72
L1 (06) MS2 T2-2-3	ABL SH36 L1 MS2 (2006) T2-2, Slice 3	0.23	1.10
L1 (06) MS2 T2-2-4	ABL SH36 L1 MS2 (2006) T2-2, Slice 4	0.21	1.46
L1 (06) MS2 T2-3-1	ABL SH36 L1 MS2 (2006) T2-3, Slice 1	0.33	0.33
L1 (06) MS2 T2-3-2	ABL SH36 L1 MS2 (2006) T2-3, Slice 2	0.27	0.75
L1 (06) MS2 T2-3-3	ABL SH36 L1 MS2 (2006) T2-3, Slice 3	0.25	1.15
L1 (06) MS2 T2-3-4	ABL SH36 L1 MS2 (2006) T2-3, Slice 4	0.26	1.56

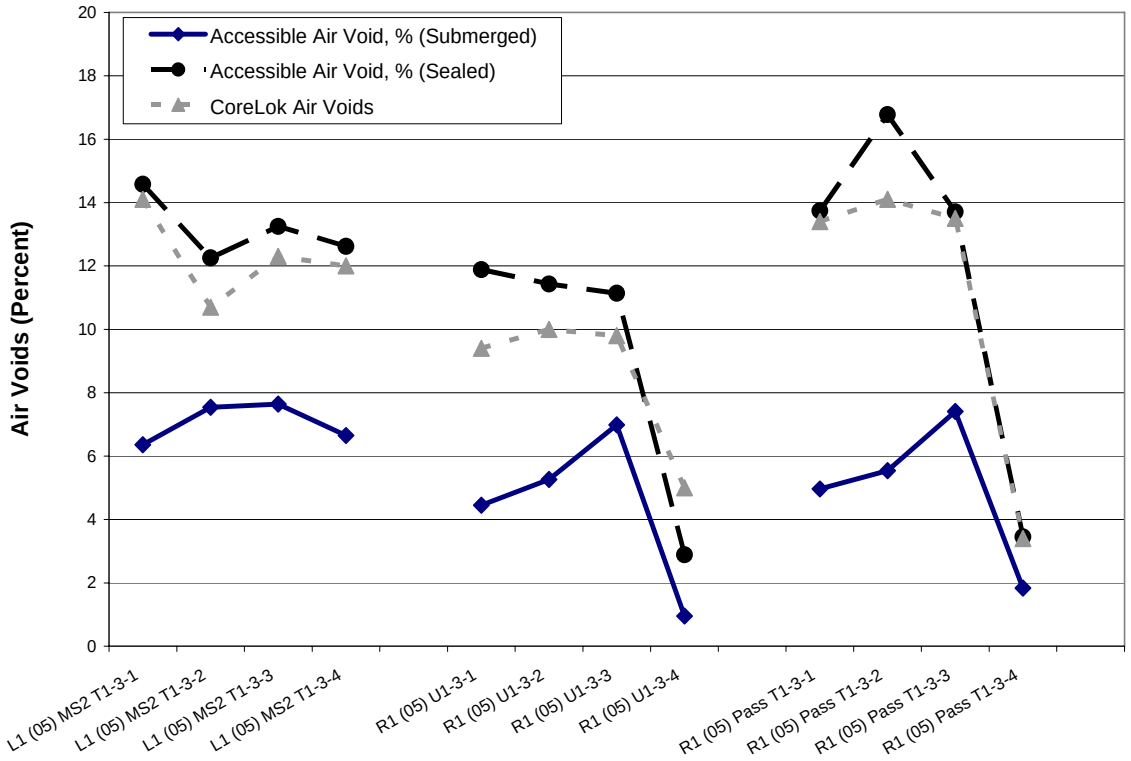

Figure D-1. Abilene SH 36, L1, 2005 Cores.

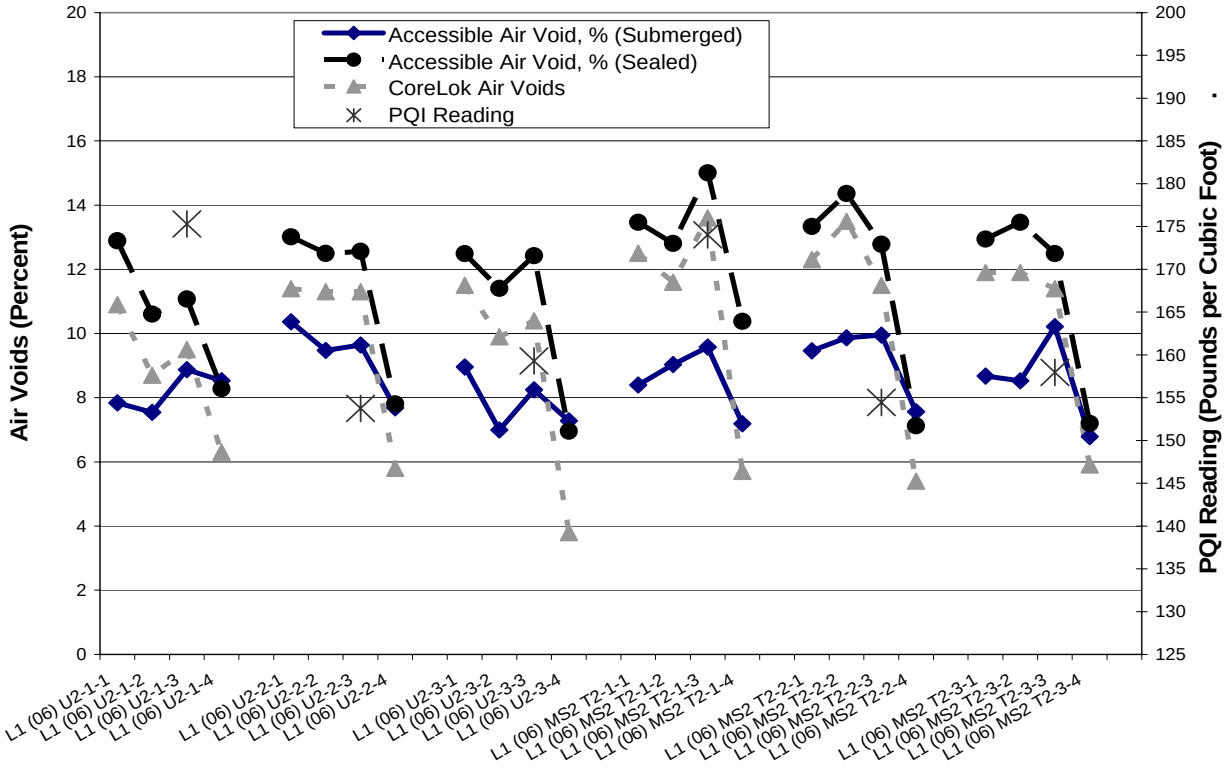

Figure D-2. Abilene SH 36, L1, 2006 Cores.

Table D-3. Figure Designation and Slice Thickness for Abilene SH36 L2 2006 Cores.

Figure Designation	Site	Estimated Slice Thickness (in.)	Estimated Depth (in.)
L2 (06) U2-1-1	ABL SH36 L2 (2006) U2-1, Slice 1	0.39	0.39
L2 (06) U2-1-2	ABL SH36 L2 (2006) U2-1, Slice 2	0.27	0.81
L2 (06) U2-1-3	ABL SH36 L2 (2006) U2-1, Slice 3	0.26	1.21
L2 (06) U2-1-4	ABL SH36 L2 (2006) U2-1, Slice 4	0.25	1.61
L2 (06) U2-2-1	ABL SH36 L2 (2006) U2-2, Slice 1	0.37	0.37
L2 (06) U2-2-2	ABL SH36 L2 (2006) U2-2, Slice 2	0.30	0.81
L2 (06) U2-2-3	ABL SH36 L2 (2006) U2-2, Slice 3	0.35	1.31
L2 (06) U2-2-4	ABL SH36 L2 (2006) U2-2, Slice 4	0.29	1.74
L2 (06) U2-3-1	ABL SH36 L2 (2006) U2-3, Slice 1	0.40	0.40
L2 (06) U2-3-2	ABL SH36 L2 (2006) U2-3, Slice 2	0.30	0.86
L2 (06) U2-3-3	ABL SH36 L2 (2006) U2-3, Slice 3	0.29	1.29
L2 (06) U2-3-4	ABL SH36 L2 (2006) U2-3, Slice 4	0.33	1.76
L2 (06) Pass T2-1-1	ABL SH36 L2 Pass (2006) T2-1, Slice 1	0.31	0.31
L2 (06) Pass T2-1-2	ABL SH36 L2 Pass (2006) T2-1, Slice 2	0.27	0.74
L2 (06) Pass T2-1-3	ABL SH36 L2 Pass (2006) T2-1, Slice 3	0.30	1.18
L2 (06) Pass T2-1-4	ABL SH36 L2 Pass (2006) T2-1, Slice 4	0.32	1.65
L2 (06) Pass T2-2-1	ABL SH36 L2 Pass (2006) T2-2, Slice 1	0.37	0.37
L2 (06) Pass T2-2-2	ABL SH36 L2 Pass (2006) T2-2, Slice 2	0.29	0.81
L2 (06) Pass T2-2-3	ABL SH36 L2 Pass (2006) T2-2, Slice 3	0.30	1.25
L2 (06) Pass T2-2-4	ABL SH36 L2 Pass (2006) T2-2, Slice 4	0.33	1.73
L2 (06) Pass T2-3-1	ABL SH36 L2 Pass (2006) T2-3, Slice 1	0.39	0.39
L2 (06) Pass T2-3-2	ABL SH36 L2 Pass (2006) T2-3, Slice 2	0.30	0.84
L2 (06) Pass T2-3-3	ABL SH36 L2 Pass (2006) T2-3, Slice 3	0.30	1.28
L2 (06) Pass T2-3-4	ABL SH36 L2 Pass (2006) T2-3, Slice 4	0.31	1.74

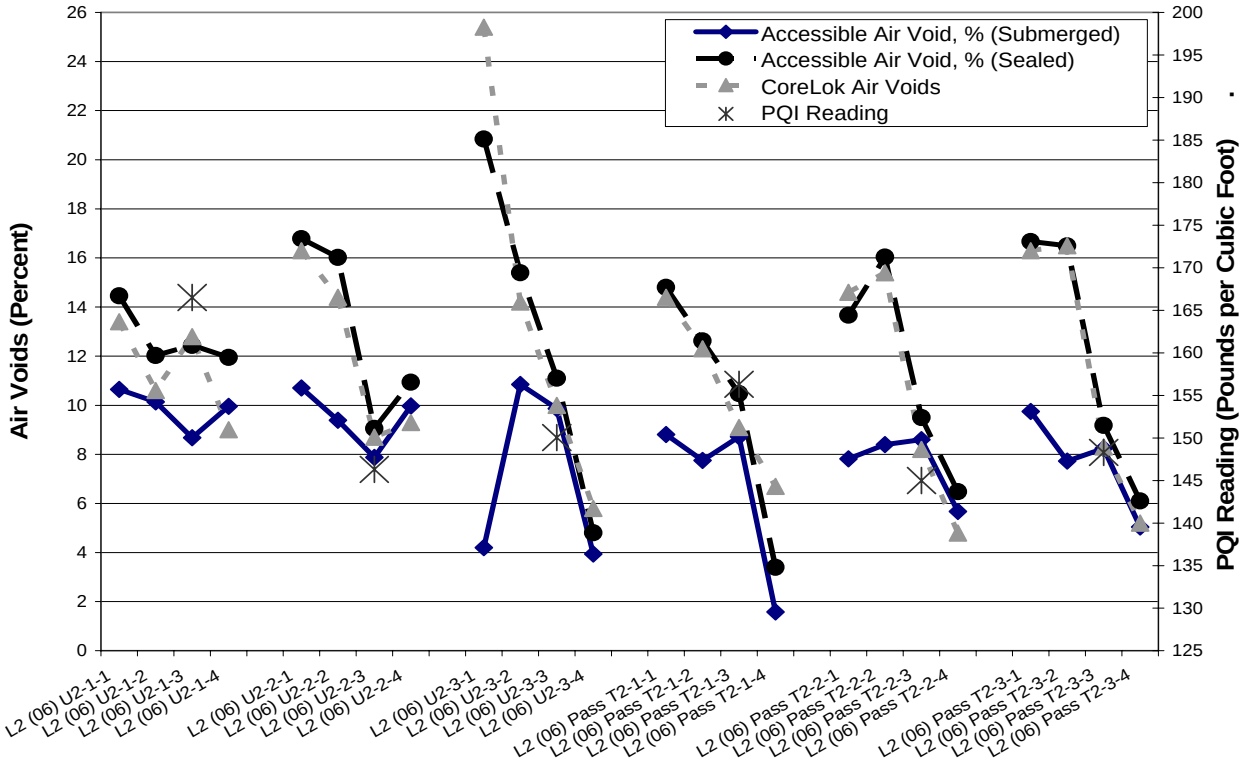

Figure D-3. Abilene SH 36, L2, 2006 Cores.

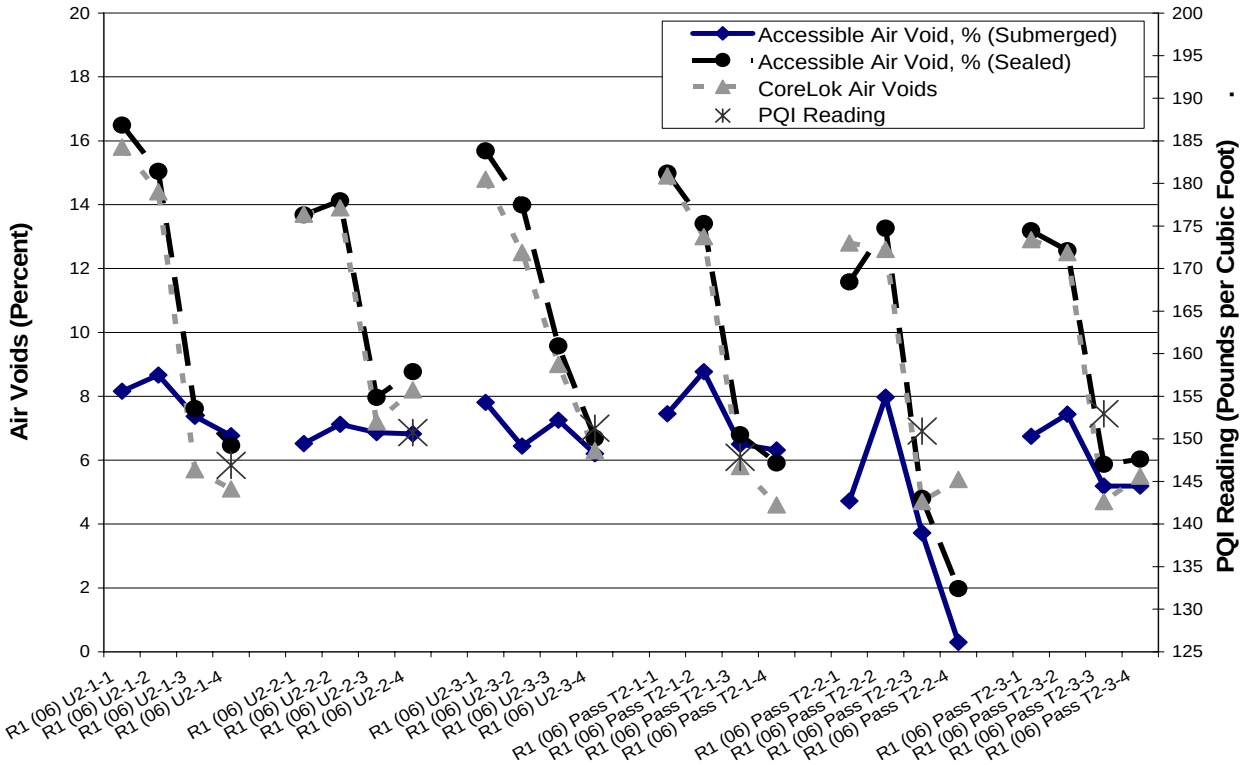

Figure D-4. Abilene SH 36, R1, 2006 Cores.

Table D-4. Figure Designation and Slice Thickness for Abilene SH36 R1 2006 Cores.

Figure Designation	Site	Estimated Slice Thickness (in.)	Estimated Depth (in.)
R1 (06) U2-1-1	ABL SH36 R1 (2006) U2-1, Slice 1	0.25	0.25
R1 (06) U2-1-2	ABL SH36 R1 (2006) U2-1, Slice 2	0.30	0.70
R1 (06) U2-1-3	ABL SH36 R1 (2006) U2-1, Slice 3	0.25	1.10
R1 (06) U2-1-4	ABL SH36 R1 (2006) U2-1, Slice 4	0.26	1.51
R1 (06) U2-2-1	ABL SH36 R1 (2006) U2-2, Slice 1	0.34	0.34
R1 (06) U2-2-2	ABL SH36 R1 (2006) U2-2, Slice 2	0.31	0.79
R1 (06) U2-2-3	ABL SH36 R1 (2006) U2-2, Slice 3	0.31	1.25
R1 (06) U2-2-4	ABL SH36 R1 (2006) U2-2, Slice 4	0.34	1.74
R1 (06) U2-3-1	ABL SH36 R1 (2006) U2-3, Slice 1	0.25	0.25
R1 (06) U2-3-2	ABL SH36 R1 (2006) U2-3, Slice 2	0.16	0.55
R1 (06) U2-3-3	ABL SH36 R1 (2006) U2-3, Slice 3	0.29	0.99
R1 (06) U2-3-4	ABL SH36 R1 (2006) U2-3, Slice 4	0.29	1.42
R1 (06) Pass T2-1-1	ABL SH36 R1 Pass (2006) T2-1, Slice 1	0.31	0.31
R1 (06) Pass T2-1-2	ABL SH36 R1 Pass (2006) T2-1, Slice 2	0.32	0.78
R1 (06) Pass T2-1-3	ABL SH36 R1 Pass (2006) T2-1, Slice 3	0.27	1.20
R1 (06) Pass T2-1-4	ABL SH36 R1 Pass (2006) T2-1, Slice 4	0.24	1.58
R1 (06) Pass T2-2-1	ABL SH36 R1 Pass (2006) T2-2, Slice 1	0.29	0.29
R1 (06) Pass T2-2-2	ABL SH36 R1 Pass (2006) T2-2, Slice 2	0.30	0.74
R1 (06) Pass T2-2-3	ABL SH36 R1 Pass (2006) T2-2, Slice 3	0.32	1.20
R1 (06) Pass T2-2-4	ABL SH36 R1 Pass (2006) T2-2, Slice 4	0.30	1.65
R1 (06) Pass T2-3-1	ABL SH36 R1 Pass (2006) T2-3, Slice 1	0.35	0.35
R1 (06) Pass T2-3-2	ABL SH36 R1 Pass (2006) T2-3, Slice 2	0.34	0.84
R1 (06) Pass T2-3-3	ABL SH36 R1 Pass (2006) T2-3, Slice 3	0.31	1.29
R1 (06) Pass T2-3-4	ABL SH36 R1 Pass (2006) T2-3, Slice 4	0.32	1.76

Table D-5. Figure Designation and Slice Thickness for Abilene SH36 R2 2006 Cores.

Figure Designation	Site	Estimated Slice Thickness (in.)	Estimated Depth (in.)
R2 (06) U2-1-1	ABL SH36 R2 (2006) U2-1, Slice 1	0.33	0.33
R2 (06) U2-1-2	ABL SH36 R2 (2006) U2-1, Slice 2	0.26	0.74
R2 (06) U2-1-3	ABL SH36 R2 (2006) U2-1, Slice 3	0.31	1.20
R2 (06) U2-1-4	ABL SH36 R2 (2006) U2-1, Slice 4	0.30	1.65
R2 (06) U2-2-1	ABL SH36 R2 (2006) U2-2, Slice 1	0.34	0.34
R2 (06) U2-2-2	ABL SH36 R2 (2006) U2-2, Slice 2	0.33	0.82
R2 (06) U2-2-3	ABL SH36 R2 (2006) U2-2, Slice 3	0.22	1.19
R2 (06) U2-2-4	ABL SH36 R2 (2006) U2-2, Slice 4	0.24	1.57
R2 (06) U2-3-1	ABL SH36 R2 (2006) U2-3, Slice 1	0.35	0.35
R2 (06) U2-3-2	ABL SH36 R2 (2006) U2-3, Slice 2	0.27	0.77
R2 (06) U2-3-3	ABL SH36 R2 (2006) U2-3, Slice 3	0.25	1.17
R2 (06) U2-3-4	ABL SH36 R2 (2006) U2-3, Slice 4	0.24	1.56
R2 (06) MS2 T2-1-1	ABL SH36 R2 MS2 (2006) T2-1, Slice 1	0.32	0.32
R2 (06) MS2 T2-1-2	ABL SH36 R2 MS2 (2006) T2-1, Slice 2	0.30	0.77
R2 (06) MS2 T2-1-3	ABL SH36 R2 MS2 (2006) T2-1, Slice 3	0.29	1.21
R2 (06) MS2 T2-1-4	ABL SH36 R2 MS2 (2006) T2-1, Slice 4	0.34	1.70
R2 (06) MS2 T2-2-1	ABL SH36 R2 MS2 (2006) T2-2, Slice 1	0.35	0.35
R2 (06) MS2 T2-2-2	ABL SH36 R2 MS2 (2006) T2-2, Slice 2	0.26	0.76
R2 (06) MS2 T2-2-3	ABL SH36 R2 MS2 (2006) T2-2, Slice 3	0.29	1.19
R2 (06) MS2 T2-2-4	ABL SH36 R2 MS2 (2006) T2-2, Slice 4	0.35	1.69
R2 (06) MS2 T2-3-1	ABL SH36 R2 MS2 (2006) T2-3, Slice 1	0.35	0.35
R2 (06) MS2 T2-3-2	ABL SH36 R2 MS2 (2006) T2-3, Slice 2	0.30	0.79
R2 (06) MS2 T2-3-3	ABL SH36 R2 MS2 (2006) T2-3, Slice 3	0.28	1.22
R2 (06) MS2 T2-3-4	ABL SH36 R2 MS2 (2006) T2-3, Slice 4	0.16	1.53

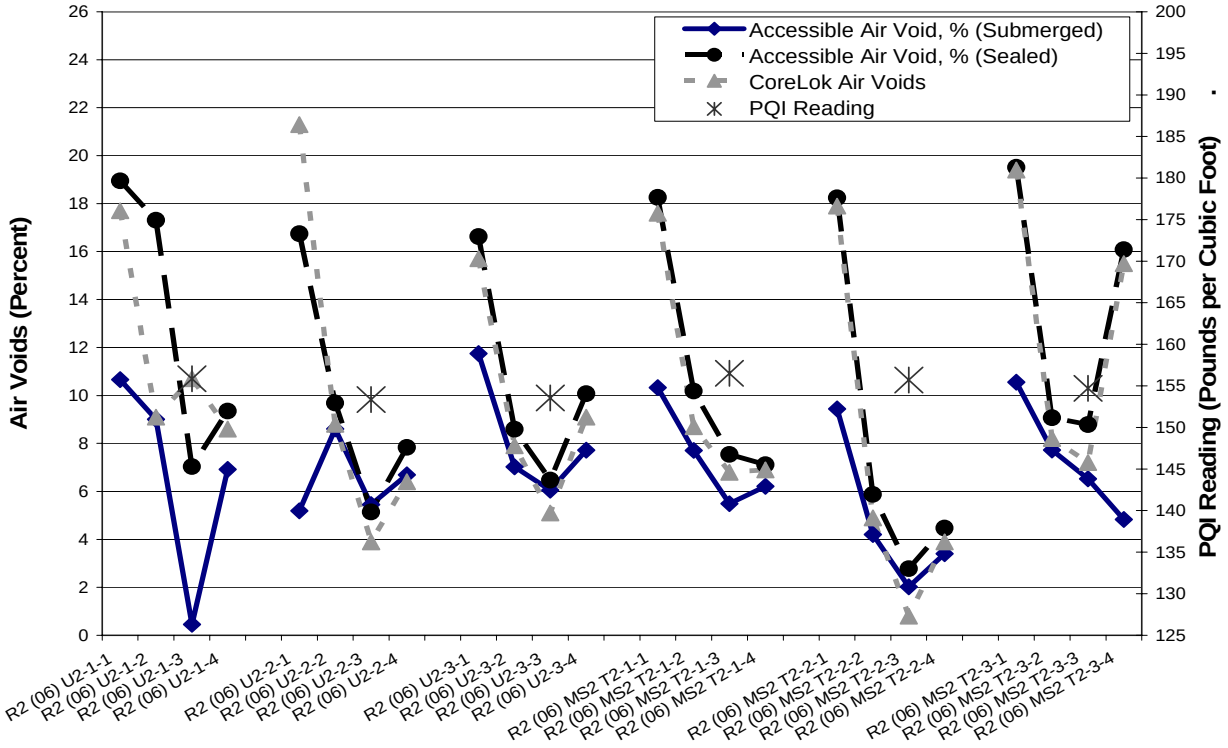

Figure D-5. Abilene SH 36, R2, 2006 Cores.

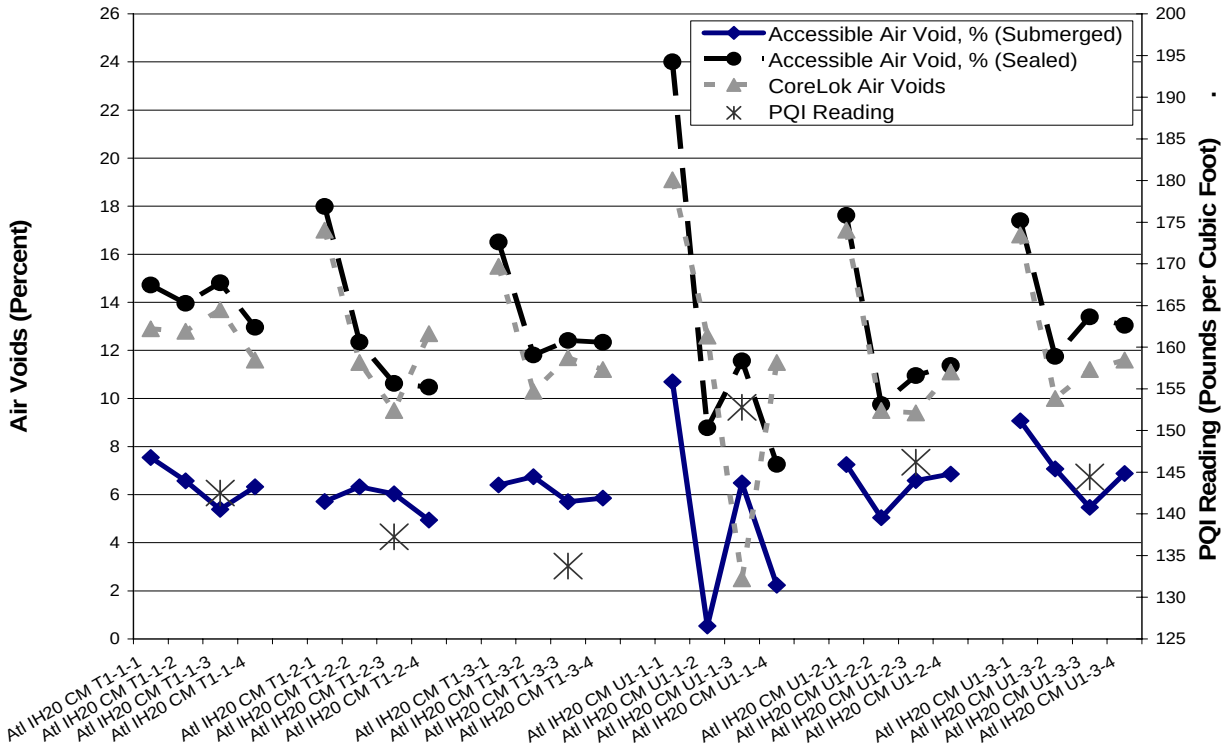

Figure D-6. Atlanta IH 20, Coarse-Matrix High-Binder, 2006 Cores.

Table D-6. Figure Designation and Slice Thickness for Atlanta IH20 CM 2006 Cores.

Figure Designation	Site	Estimated Slice Thickness (in.)	Estimated Depth (in.)
Atl IH20 CM T1-1-1	ATL IH20 CM (2006) T1, Slice 1	0.32	0.32
Atl IH20 CM T1-1-2	ATL IH20 CM (2006) T1, Slice 2	0.21	0.68
Atl IH20 CM T1-1-3	ATL IH20 CM (2006) T1, Slice 3	0.22	1.05
Atl IH20 CM T1-1-4	ATL IH20 CM (2006) T1, Slice 4	0.23	1.42
Atl IH20 CM T1-2-1	ATL IH20 CM (2006) T2, Slice 1	0.27	0.27
Atl IH20 CM T1-2-2	ATL IH20 CM (2006) T2, Slice 2	0.22	0.63
Atl IH20 CM T1-2-3	ATL IH20 CM (2006) T2, Slice 3	0.25	1.03
Atl IH20 CM T1-2-4	ATL IH20 CM (2006) T2, Slice 4	0.28	1.46
Atl IH20 CM T1-3-1	ATL IH20 CM (2006) T3, Slice 1	0.29	0.29
Atl IH20 CM T1-3-2	ATL IH20 CM (2006) T3, Slice 2	0.22	0.66
Atl IH20 CM T1-3-3	ATL IH20 CM (2006) T3, Slice 3	0.20	1.00
Atl IH20 CM T1-3-4	ATL IH20 CM (2006) T3, Slice 4	0.22	1.37
Atl IH20 CM U1-1-1	ATL IH20 CM (2006) U1, Slice 1	0.25	0.25
Atl IH20 CM U1-1-2	ATL IH20 CM (2006) U1, Slice 2	0.22	0.61
Atl IH20 CM U1-1-3	ATL IH20 CM (2006) U1, Slice 3	0.28	1.04
Atl IH20 CM U1-1-4	ATL IH20 CM (2006) U1, Slice 4	0.29	1.48
Atl IH20 CM U1-2-1	ATL IH20 CM (2006) U2, Slice 1	0.27	0.27
Atl IH20 CM U1-2-2	ATL IH20 CM (2006) U2, Slice 2	0.26	0.67
Atl IH20 CM U1-2-3	ATL IH20 CM (2006) U2, Slice 3	0.29	1.11
Atl IH20 CM U1-2-4	ATL IH20 CM (2006) U2, Slice 4	0.33	1.59
Atl IH20 CM U1-3-1	ATL IH20 CM (2006) U3, Slice 1	0.30	0.30
Atl IH20 CM U1-3-2	ATL IH20 CM (2006) U3, Slice 2	0.28	0.73
Atl IH20 CM U1-3-3	ATL IH20 CM (2006) U3, Slice 3	0.28	1.15
Atl IH20 CM U1-3-4	ATL IH20 CM (2006) U3, Slice 4	0.30	1.60

Table D-7. Figure Designation and Slice Thickness for Atlanta IH20 DG 2006 Cores.

Figure Designation	Site	Estimated Slice Thickness (in.)	Estimated Depth (in.)
Atl IH20 DG T1-1-1	ATL IH20 DG (2006) T1, Slice 1	0.20	0.20
Atl IH20 DG T1-1-2	ATL IH20 DG (2006) T1, Slice 2	0.22	0.57
Atl IH20 DG T1-1-3	ATL IH20 DG (2006) T1, Slice 3	0.20	0.92
Atl IH20 DG T1-1-4	ATL IH20 DG (2006) T1, Slice 4	0.11	1.18
Atl IH20 DG T1-2-1	ATL IH20 DG (2006) T2, Slice 1	0.21	0.21
Atl IH20 DG T1-2-2	ATL IH20 DG (2006) T2, Slice 2	0.25	0.60
Atl IH20 DG T1-2-3	ATL IH20 DG (2006) T2, Slice 3	0.24	0.99
Atl IH20 DG T1-2-4	ATL IH20 DG (2006) T2, Slice 4	0.22	1.36
Atl IH20 DG T1-3-1	ATL IH20 DG (2006) T3, Slice 1	0.21	0.21
Atl IH20 DG T1-3-2	ATL IH20 DG (2006) T3, Slice 2	0.24	0.60
Atl IH20 DG T1-3-3	ATL IH20 DG (2006) T3, Slice 3	0.22	0.97
Atl IH20 DG T1-3-4	ATL IH20 DG (2006) T3, Slice 4	0.18	1.29
Atl IH20 DG U1-1-1	ATL IH20 DG (2006) U1, Slice 1	0.35	0.35
Atl IH20 DG U1-1-2	ATL IH20 DG (2006) U1, Slice 2	0.23	0.72
Atl IH20 DG U1-1-3	ATL IH20 DG (2006) U1, Slice 3	0.27	1.14
Atl IH20 DG U1-1-4	ATL IH20 DG (2006) U1, Slice 4	0.24	1.52
Atl IH20 DG U1-2-1	ATL IH20 DG (2006) U2, Slice 1	0.29	0.29
Atl IH20 DG U1-2-2	ATL IH20 DG (2006) U2, Slice 2	0.24	0.68
Atl IH20 DG U1-2-3	ATL IH20 DG (2006) U2, Slice 3	0.26	1.09
Atl IH20 DG U1-2-4	ATL IH20 DG (2006) U2, Slice 4	0.30	1.53
Atl IH20 DG U1-3-1	ATL IH20 DG (2006) U3, Slice 1	0.32	0.32
Atl IH20 DG U1-3-2	ATL IH20 DG (2006) U3, Slice 2	0.24	0.71
Atl IH20 DG U1-3-3	ATL IH20 DG (2006) U3, Slice 3	0.22	1.08
Atl IH20 DG U1-3-4	ATL IH20 DG (2006) U3, Slice 4	0.27	1.49

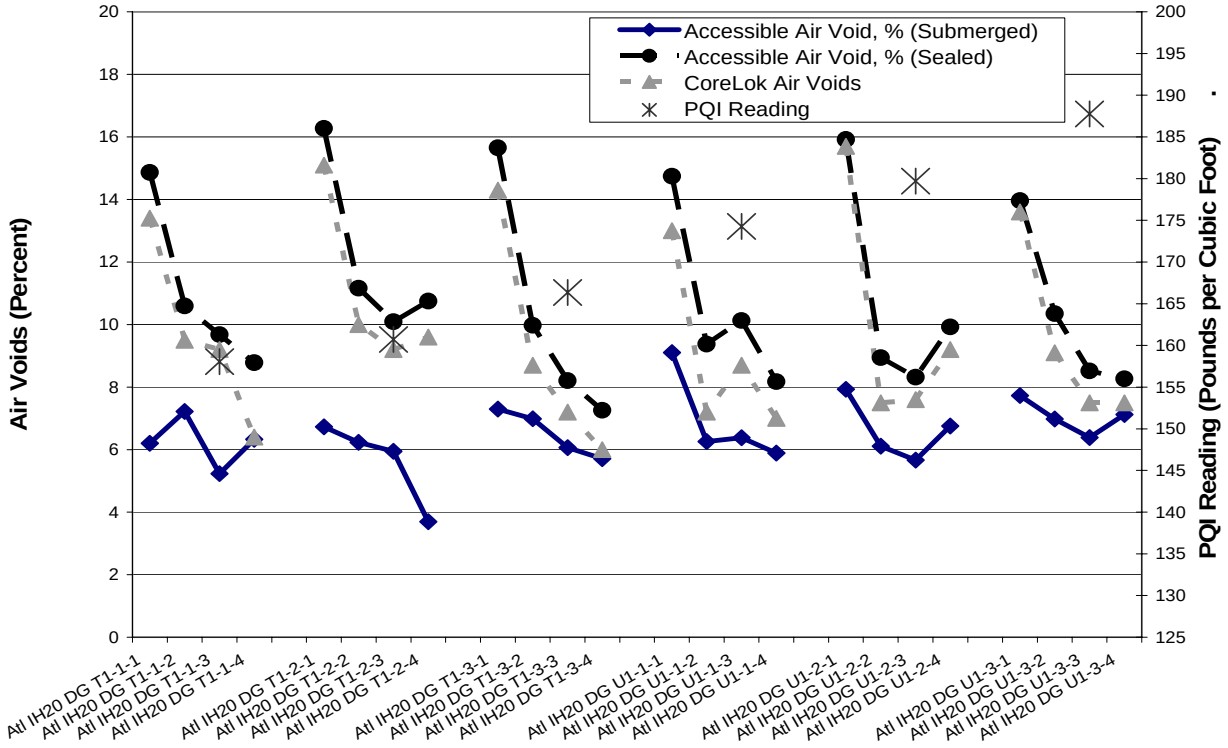

Figure D-7. Atlanta IH 20, Dense Graded, 2006 Cores.

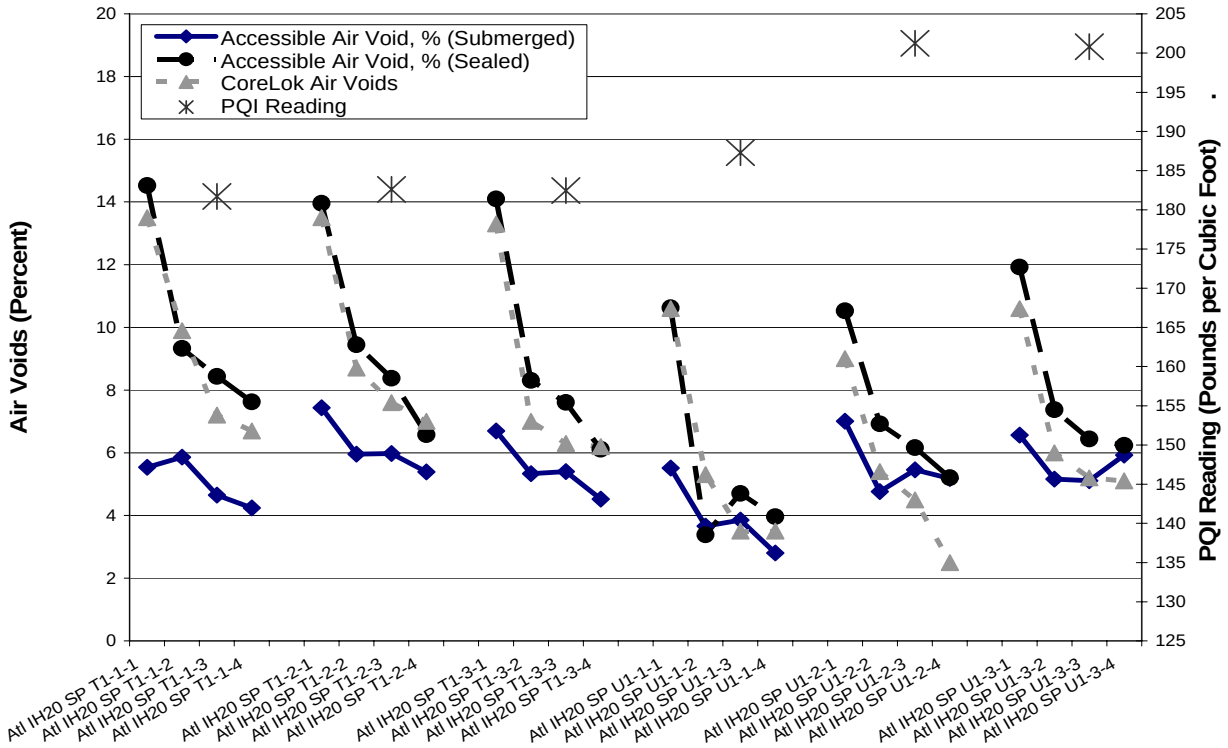

Figure D-8. Atlanta IH 20, Superpave, 2006 Cores.

Table D-8. Figure Designation and Slice Thickness for Atlanta IH20 SP 2006 Cores.

Figure Designation	Site	Estimated Slice Thickness (in.)	Estimated Depth (in.)
Atl IH20 SP T1-1-1	ATL IH20 SP (2006) T1, Slice 1	0.22	0.22
Atl IH20 SP T1-1-2	ATL IH20 SP (2006) T1, Slice 2	0.23	0.60
Atl IH20 SP T1-1-3	ATL IH20 SP (2006) T1, Slice 3	0.19	0.93
Atl IH20 SP T1-1-4	ATL IH20 SP (2006) T1, Slice 4	0.16	1.24
Atl IH20 SP T1-2-1	ATL IH20 SP (2006) T2, Slice 1	0.30	0.30
Atl IH20 SP T1-2-2	ATL IH20 SP (2006) T2, Slice 2	0.32	0.77
Atl IH20 SP T1-2-3	ATL IH20 SP (2006) T2, Slice 3	0.26	1.18
Atl IH20 SP T1-2-4	ATL IH20 SP (2006) T2, Slice 4	0.28	1.60
Atl IH20 SP T1-3-1	ATL IH20 SP (2006) T3, Slice 1	0.24	0.24
Atl IH20 SP T1-3-2	ATL IH20 SP (2006) T3, Slice 2	0.21	0.60
Atl IH20 SP T1-3-3	ATL IH20 SP (2006) T3, Slice 3	0.22	0.97
Atl IH20 SP T1-3-4	ATL IH20 SP (2006) T3, Slice 4	0.25	1.37
Atl IH20 SP U1-1-1	ATL IH20 SP (2006) U1, Slice 1	0.34	0.34
Atl IH20 SP U1-1-2	ATL IH20 SP (2006) U1, Slice 2	0.22	0.70
Atl IH20 SP U1-1-3	ATL IH20 SP (2006) U1, Slice 3	0.26	1.11
Atl IH20 SP U1-1-4	ATL IH20 SP (2006) U1, Slice 4	0.25	1.50
Atl IH20 SP U1-2-1	ATL IH20 SP (2006) U2, Slice 1	0.32	0.32
Atl IH20 SP U1-2-2	ATL IH20 SP (2006) U2, Slice 2	0.25	0.73
Atl IH20 SP U1-2-3	ATL IH20 SP (2006) U2, Slice 3	0.31	1.18
Atl IH20 SP U1-2-4	ATL IH20 SP (2006) U2, Slice 4	0.21	1.53
Atl IH20 SP U1-3-1	ATL IH20 SP (2006) U3, Slice 1	0.29	0.29
Atl IH20 SP U1-3-2	ATL IH20 SP (2006) U3, Slice 2	0.23	0.66
Atl IH20 SP U1-3-3	ATL IH20 SP (2006) U3, Slice 3	0.25	1.06
Atl IH20 SP U1-3-4	ATL IH20 SP (2006) U3, Slice 4	0.28	1.49

Table D-9. Figure Designation and Slice Thickness for Atlanta US67 2006 Cores.

Figure Designation	Site	Estimated Slice Thickness (in.)	Estimated Depth (in.)
Atl US67 T1-1-1	ATL US67 (2006) T1, Slice 1	0.25	0.25
Atl US67 T1-1-2	ATL US67 (2006) T1, Slice 2	0.24	0.63
Atl US67 T1-1-3	ATL US67 (2006) T1, Slice 3	0.26	1.04
Atl US67 T1-1-4	ATL US67 (2006) T1, Slice 4	0.27	1.45
Atl US67 T1-2-1	ATL US67 (2006) T2, Slice 1	0.28	0.28
Atl US67 T1-2-2	ATL US67 (2006) T2, Slice 2	0.24	0.67
Atl US67 T1-2-3	ATL US67 (2006) T2, Slice 3	0.24	1.06
Atl US67 T1-2-4	ATL US67 (2006) T2, Slice 4	0.22	1.43
Atl US67 T1-3-1	ATL US67 (2006) T3, Slice 1	0.33	0.33
Atl US67 T1-3-2	ATL US67 (2006) T3, Slice 2	0.32	0.79
Atl US67 T1-3-3	ATL US67 (2006) T3, Slice 3	0.20	1.14
Atl US67 T1-3-4	ATL US67 (2006) T3, Slice 4	0.23	1.52
Atl US67 U1-1-1	ATL US67 (2006) U1, Slice 1	0.32	0.32
Atl US67 U1-1-2	ATL US67 (2006) U1, Slice 2	0.28	0.74
Atl US67 U1-1-3	ATL US67 (2006) U1, Slice 3	0.27	1.16
Atl US67 U1-1-4	ATL US67 (2006) U1, Slice 4	0.28	1.58
Atl US67 U1-2-1	ATL US67 (2006) U2, Slice 1	0.39	0.39
Atl US67 U1-2-2	ATL US67 (2006) U2, Slice 2	0.24	0.78
Atl US67 U1-2-3	ATL US67 (2006) U2, Slice 3	0.17	1.10
Atl US67 U1-2-4	ATL US67 (2006) U2, Slice 4	0.22	1.46
Atl US67 U1-3-1	ATL US67 (2006) U3, Slice 1	0.33	0.33
Atl US67 U1-3-2	ATL US67 (2006) U3, Slice 2	0.26	0.74
Atl US67 U1-3-3	ATL US67 (2006) U3, Slice 3	0.22	1.11
Atl US67 U1-3-4	ATL US67 (2006) U3, Slice 4	0.23	1.49

Table D-10. Figure Designation and Slice Thickness for Carrizo Springs Airport 2005 Cores.

Figure Designation	Site	Estimated Slice Thickness (in.)	Estimated Depth (in.)
Carriz (05) T1-3-1	Carriz (2005) T1-3, Slice 1	0.13	0.13
Carriz (05) T1-3-2	Carriz (2005) T1-3, Slice 2	0.22	0.50
Carriz (05) T1-3-3	Carriz (2005) T1-3, Slice 3	0.19	0.83
Carriz (05) T1-3-4	Carriz (2005) T1-3, Slice 4	0.24	1.22
Carriz (05) U1-3-1	Carriz (2005) U1-3, Slice 1	0.19	0.19
Carriz (05) U1-3-2	Carriz (2005) U1-3, Slice 2	0.18	0.51
Carriz (05) U1-3-3	Carriz (2005) U1-3, Slice 3	0.29	0.95
Carriz (05) U1-3-4	Carriz (2005) U1-3, Slice 4	0.19	1.29

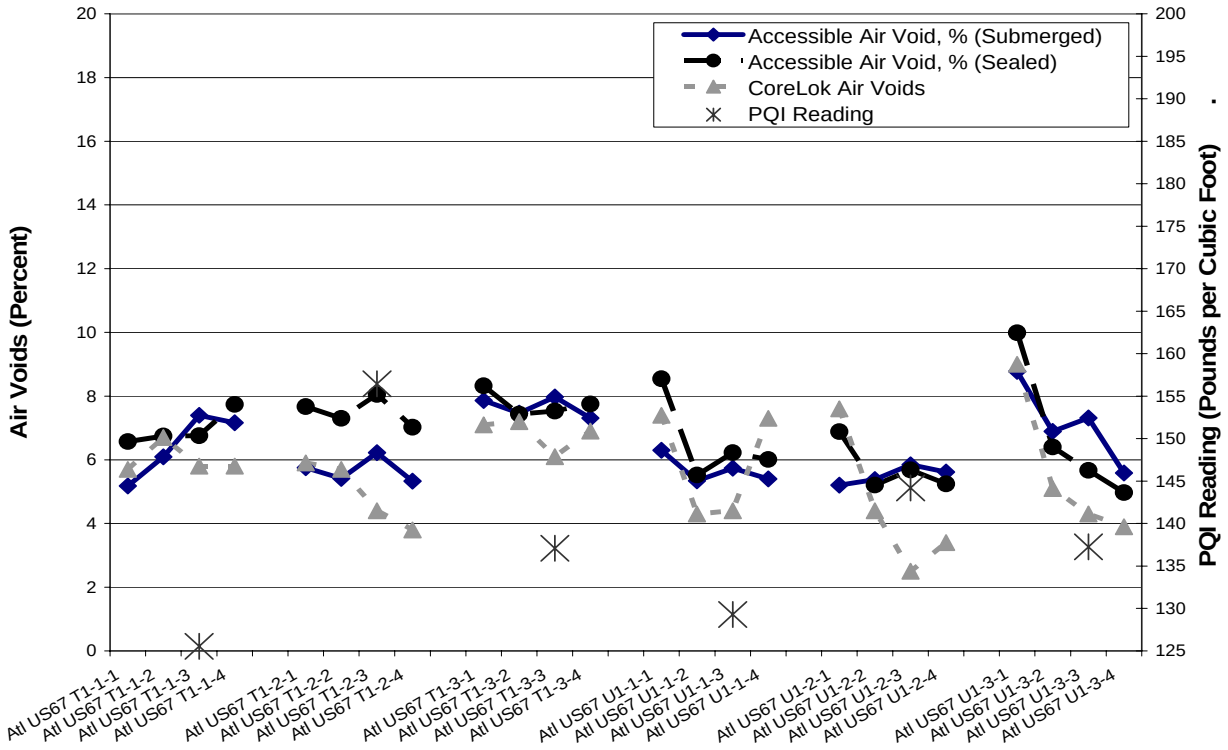

Figure D-9. Atlanta US67, 2006 Cores.

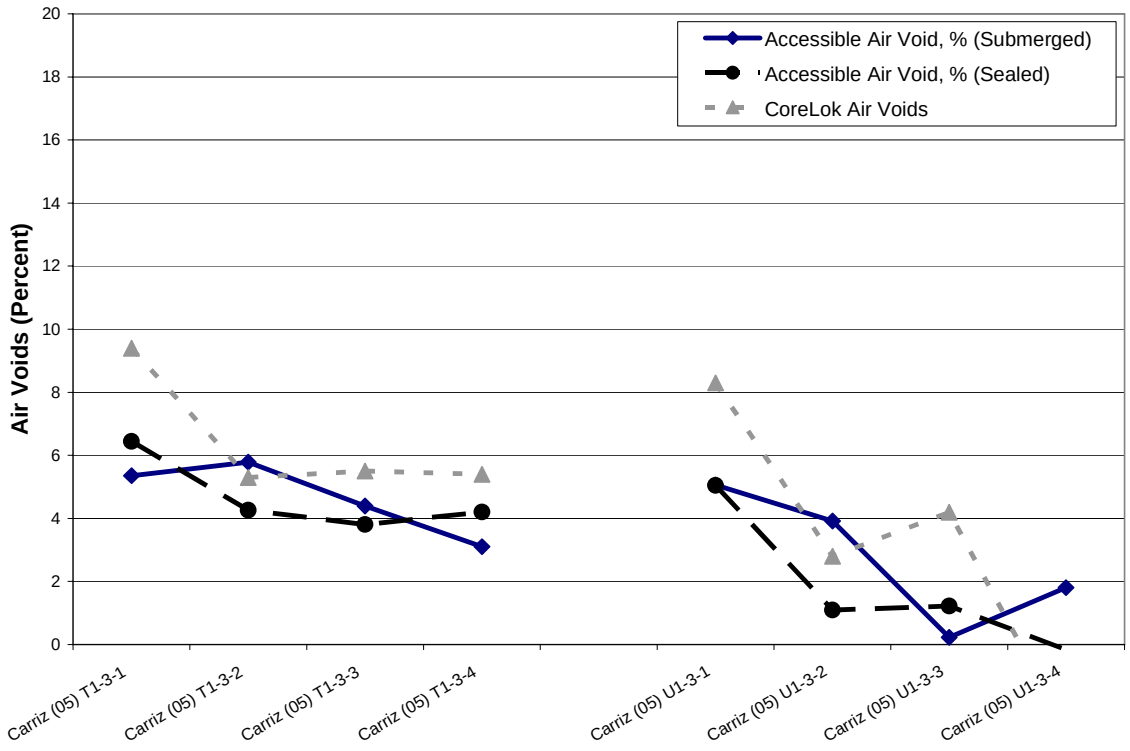

Figure D-10. Carrizo Springs Airport, 2005 Cores.

Table D-11. Figure Designation and Slice Thickness for Carrizo Springs Airport 2006 Cores.

Figure Designation	Site	Estimated Slice Thickness (in.)	Estimated Depth (in.)
Carriz (06) T2-1-1	Carriz (2006) T2-1, Slice 1	0.33	0.33
Carriz (06) T2-1-2	Carriz (2006) T2-1, Slice 2	0.27	0.75
Carriz (06) T2-1-3	Carriz (2006) T2-1, Slice 3	0.27	1.17
Carriz (06) T2-1-4	Carriz (2006) T2-1, Slice 4	0.25	1.56
Carriz (06) T2-2-1	Carriz (2006) T2-2, Slice 1	0.22	0.22
Carriz (06) T2-2-2	Carriz (2006) T2-2, Slice 2	0.23	0.59
Carriz (06) T2-2-3	Carriz (2006) T2-2, Slice 3	0.30	1.04
Carriz (06) T2-2-4	Carriz (2006) T2-2, Slice 4	0.31	1.49
Carriz (06) T2-3-1	Carriz (2006) T2-3, Slice 1	0.20	0.20
Carriz (06) T2-3-2	Carriz (2006) T2-3, Slice 2	0.24	0.59
Carriz (06) T2-3-3	Carriz (2006) T2-3, Slice 3	0.25	0.99
Carriz (06) T2-3-4	Carriz (2006) T2-3, Slice 4	0.21	1.34
Carriz (06) U2-1-1	Carriz (2006) U2-1, Slice 1	0.33	0.33
Carriz (06) U2-1-2	Carriz (2006) U2-1, Slice 2	0.26	0.73
Carriz (06) U2-1-3	Carriz (2006) U2-1, Slice 3	0.25	1.13
Carriz (06) U2-1-4	Carriz (2006) U2-1, Slice 4	0.30	1.58
Carriz (06) U2-2-1	Carriz (2006) U2-2, Slice 1	0.25	0.25
Carriz (06) U2-2-2	Carriz (2006) U2-2, Slice 2	0.26	0.66
Carriz (06) U2-2-3	Carriz (2006) U2-2, Slice 3	0.28	1.08
Carriz (06) U2-2-4	Carriz (2006) U2-2, Slice 4	0.32	1.54
Carriz (06) U2-3-1	Carriz (2006) U2-3, Slice 1	0.27	0.27
Carriz (06) U2-3-2	Carriz (2006) U2-3, Slice 2	0.34	0.76
Carriz (06) U2-3-3	Carriz (2006) U2-3, Slice 3	0.28	1.19
Carriz (06) U2-3-4	Carriz (2006) U2-3, Slice 4	0.32	1.65

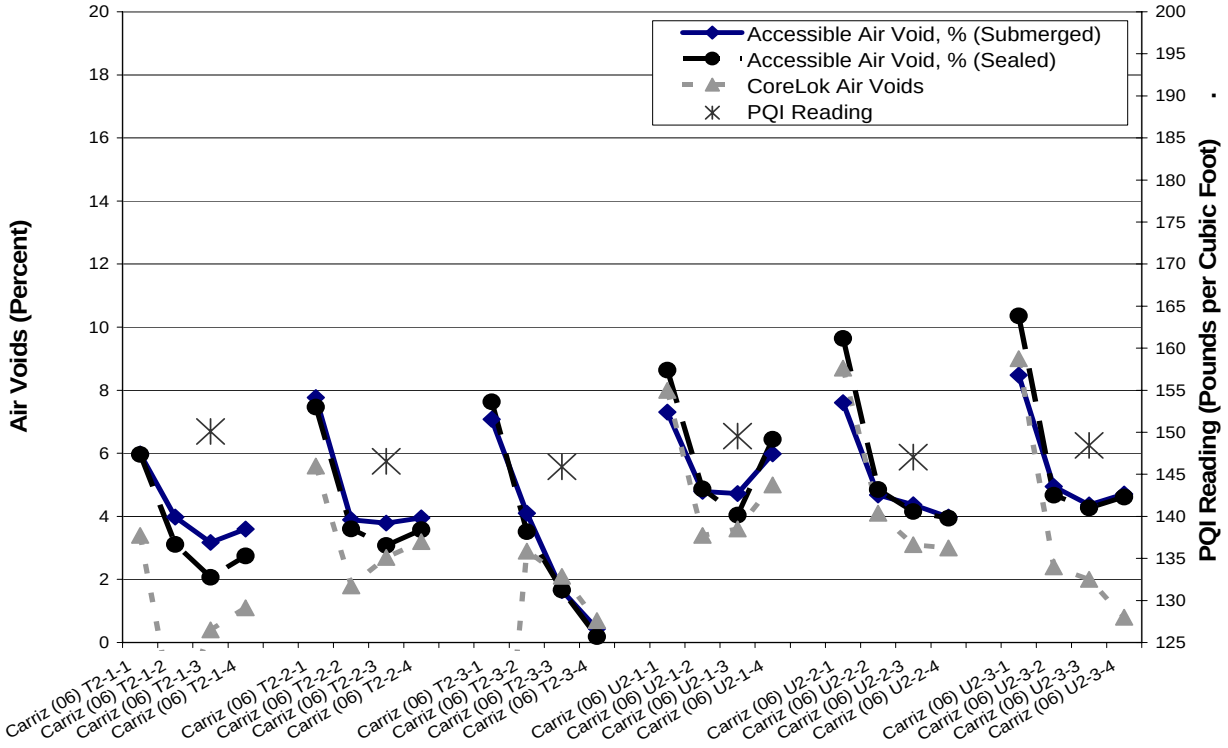

Figure D-11. Carrizo Springs Airport, 2006 Cores.

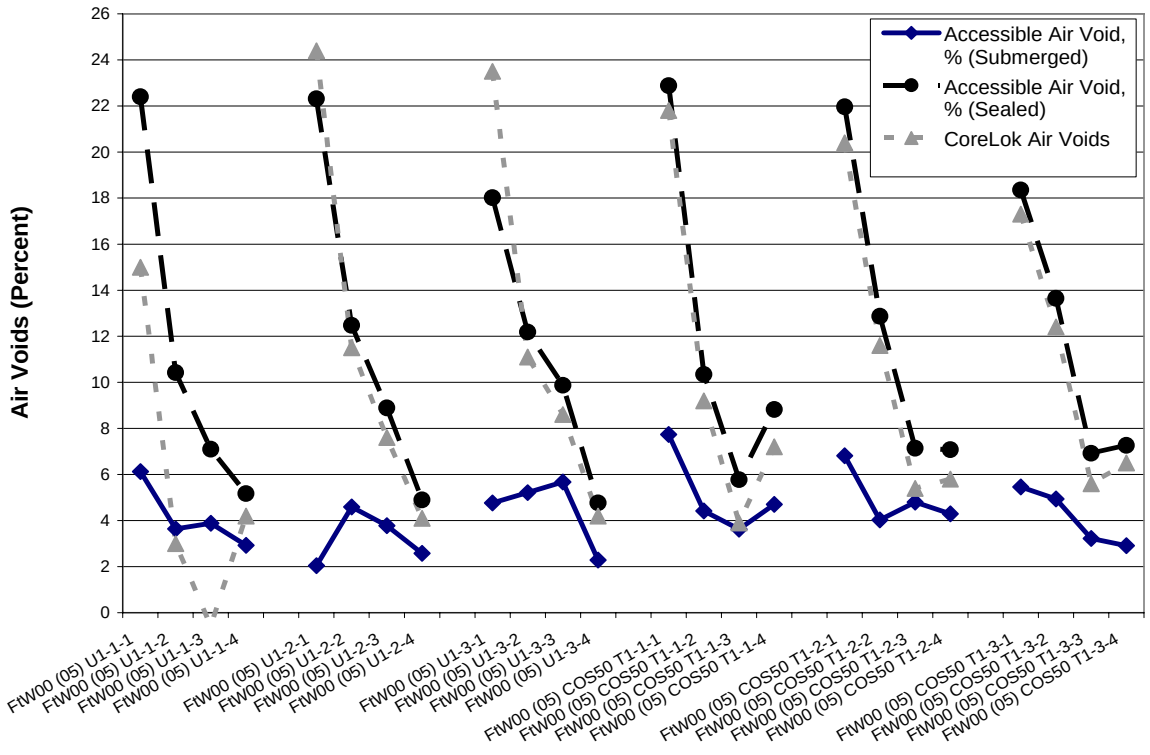

Figure D-12. Fort Worth, FM4 (2000), 2005 Cores.

Table D-12. Figure Designation and Slice Thickness for Fort Worth FM 4 (2000) 2005 Cores.

Figure Designation	Site	Estimated Slice Thickness (in.)	Estimated Depth (in.)
FtW00 (05) U1-1-1	FtW FM4 2000 K6 (2005) U1-1, Slice 1	0.09	0.09
FtW00 (05) U1-1-2	FtW FM4 2000 K6 (2005) U1-1, Slice 2	0.20	0.44
FtW00 (05) U1-1-3	FtW FM4 2000 K6 (2005) U1-1, Slice 3	0.30	0.89
FtW00 (05) U1-1-4	FtW FM4 2000 K6 (2005) U1-1, Slice 4	0.56	1.59
FtW00 (05) U1-2-1	FtW FM4 2000 K6 (2005) U1-2, Slice 1	0.18	0.18
FtW00 (05) U1-2-2	FtW FM4 2000 K6 (2005) U1-2, Slice 2	0.25	0.57
FtW00 (05) U1-2-3	FtW FM4 2000 K6 (2005) U1-2, Slice 3	0.24	0.96
FtW00 (05) U1-2-4	FtW FM4 2000 K6 (2005) U1-2, Slice 4	0.46	1.57
FtW00 (05) U1-3-1	FtW FM4 2000 K6 (2005) U1-3, Slice 1	0.09	0.09
FtW00 (05) U1-3-2	FtW FM4 2000 K6 (2005) U1-3, Slice 2	0.27	0.51
FtW00 (05) U1-3-3	FtW FM4 2000 K6 (2005) U1-3, Slice 3	0.39	1.04
FtW00 (05) U1-3-4	FtW FM4 2000 K6 (2005) U1-3, Slice 4	0.40	1.60
FtW00 (05) COS50 T1-1-1	FtW FM4 2000 K6 COS50 (2005) T1-1, Slice 1	0.20	0.20
FtW00 (05) COS50 T1-1-2	FtW FM4 2000 K6 COS50 (2005) T1-1, Slice 2	0.26	0.61
FtW00 (05) COS50 T1-1-3	FtW FM4 2000 K6 COS50 (2005) T1-1, Slice 3	0.31	1.07
FtW00 (05) COS50 T1-1-4	FtW FM4 2000 K6 COS50 (2005) T1-1, Slice 4	0.29	1.50
FtW00 (05) COS50 T1-2-1	FtW FM4 2000 K6 COS50 (2005) T1-2, Slice 1	0.24	0.24
FtW00 (05) COS50 T1-2-2	FtW FM4 2000 K6 COS50 (2005) T1-2, Slice 2	0.23	0.61
FtW00 (05) COS50 T1-2-3	FtW FM4 2000 K6 COS50 (2005) T1-2, Slice 3	0.32	1.08
FtW00 (05) COS50 T1-2-4	FtW FM4 2000 K6 COS50 (2005) T1-2, Slice 4	0.38	1.60
FtW00 (05) COS50 T1-3-1	FtW FM4 2000 K6 COS50 (2005) T1-3, Slice 1	0.27	0.27
FtW00 (05) COS50 T1-3-2	FtW FM4 2000 K6 COS50 (2005) T1-3, Slice 2	0.25	0.67
FtW00 (05) COS50 T1-3-3	FtW FM4 2000 K6 COS50 (2005) T1-3, Slice 3	0.28	1.10
FtW00 (05) COS50 T1-3-4	FtW FM4 2000 K6 COS50 (2005) T1-3, Slice 4	0.31	1.55

Table D-13. Figure Designation and Slice Thickness for Fort Worth FM 4 (2000) 2006 Cores.

Figure Designation	Site	Estimated Slice Thickness (in.)	Estimated Depth (in.)
FtW00 (06) U2-1-1	FtW FM4 2000 K6 (2006) U2-1, Slice 1	0.30	0.30
FtW00 (06) U2-1-2	FtW FM4 2000 K6 (2006) U2-1, Slice 2	0.20	0.64
FtW00 (06) U2-1-3	FtW FM4 2000 K6 (2006) U2-1, Slice 3	0.25	1.04
FtW00 (06) U2-1-4	FtW FM4 2000 K6 (2006) U2-1, Slice 4	0.36	1.55
FtW00 (06) U2-2-1	FtW FM4 2000 K6 (2006) U2-2, Slice 1	0.27	0.27
FtW00 (06) U2-2-2	FtW FM4 2000 K6 (2006) U2-2, Slice 2	0.16	0.57
FtW00 (06) U2-2-3	FtW FM4 2000 K6 (2006) U2-2, Slice 3	0.22	0.94
FtW00 (06) U2-2-4	FtW FM4 2000 K6 (2006) U2-2, Slice 4	0.35	1.43
FtW00 (06) U2-3-1	FtW FM4 2000 K6 (2006) U2-3, Slice 1	0.20	0.20
FtW00 (06) U2-3-2	FtW FM4 2000 K6 (2006) U2-3, Slice 2	0.14	0.48
FtW00 (06) U2-3-3	FtW FM4 2000 K6 (2006) U2-3, Slice 3	0.24	0.88
FtW00 (06) U2-3-4	FtW FM4 2000 K6 (2006) U2-3, Slice 4	0.21	1.23
FtW00 (06) COS50 T2-1-1	FtW FM4 2000 K6 COS50 (2006) T2-1, Slice 1	0.28	0.28
FtW00 (06) COS50 T2-1-2	FtW FM4 2000 K6 COS50 (2006) T2-1, Slice 2	0.27	0.70
FtW00 (06) COS50 T2-1-3	FtW FM4 2000 K6 COS50 (2006) T2-1, Slice 3	0.21	1.06
FtW00 (06) COS50 T2-1-4	FtW FM4 2000 K6 COS50 (2006) T2-1, Slice 4	0.31	1.51
FtW00 (06) COS50 T2-2-1	FtW FM4 2000 K6 COS50 (2006) T2-2, Slice 1	0.26	0.26
FtW00 (06) COS50 T2-2-2	FtW FM4 2000 K6 COS50 (2006) T2-2, Slice 2	0.24	0.65
FtW00 (06) COS50 T2-2-3	FtW FM4 2000 K6 COS50 (2006) T2-2, Slice 3	0.24	1.03
FtW00 (06) COS50 T2-2-4	FtW FM4 2000 K6 COS50 (2006) T2-2, Slice 4	0.32	1.50
FtW00 (06) COS50 T2-3-1	FtW FM4 2000 K6 COS50 (2006) T2-3, Slice 1	0.40	0.40
FtW00 (06) COS50 T2-3-2	FtW FM4 2000 K6 COS50 (2006) T2-3, Slice 2	0.27	0.81
FtW00 (06) COS50 T2-3-3	FtW FM4 2000 K6 COS50 (2006) T2-3, Slice 3	0.20	1.16
FtW00 (06) COS50 T2-3-4	FtW FM4 2000 K6 COS50 (2006) T2-3, Slice 4	0.31	1.62

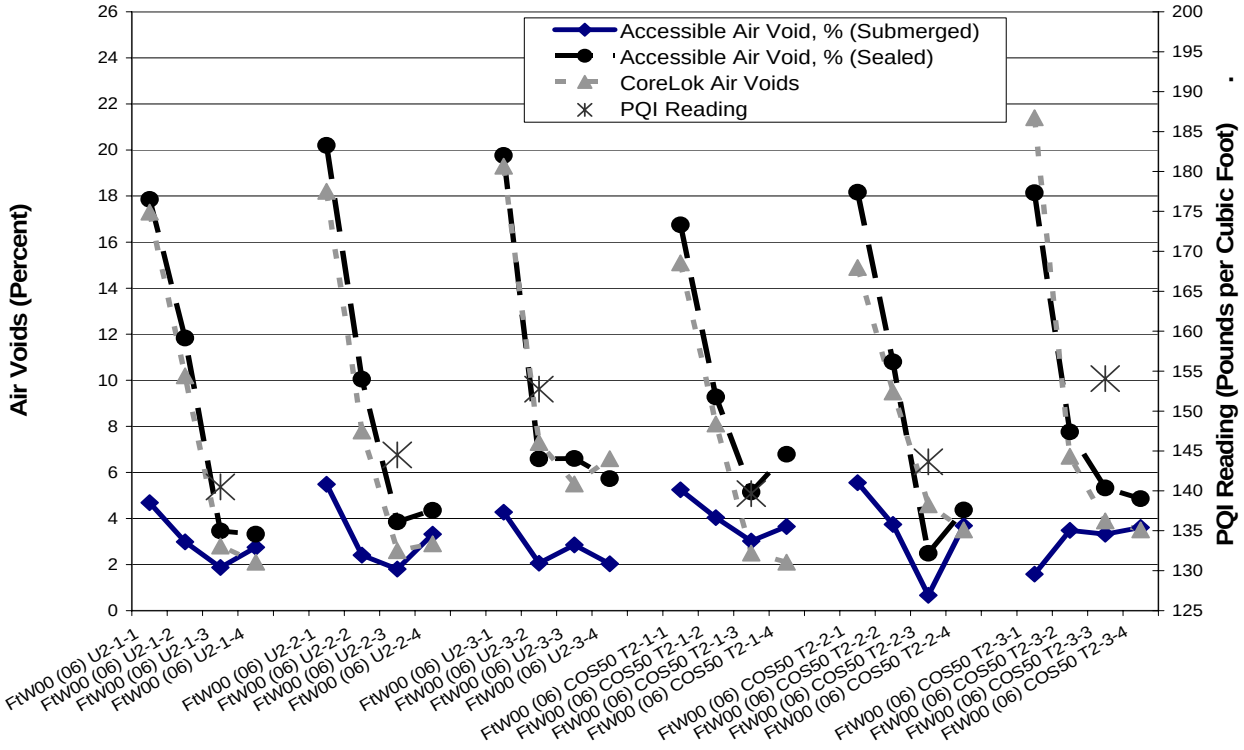

Figure D-13. Fort Worth, FM4 (2000), 2006 Cores.

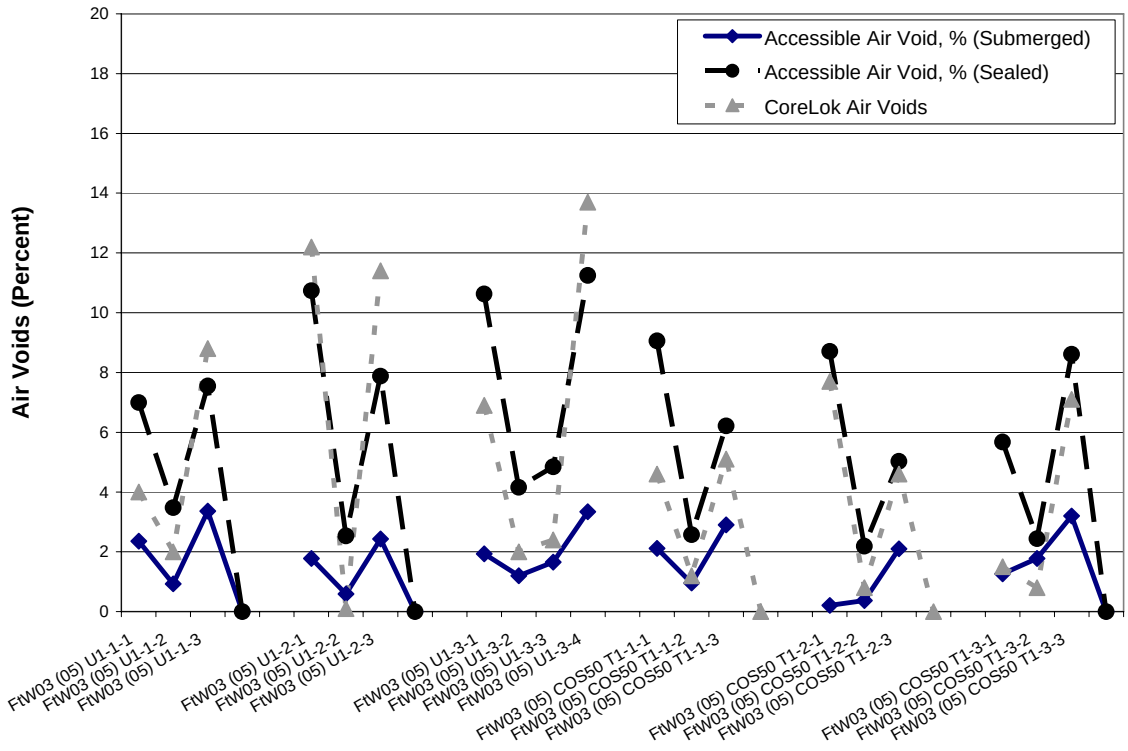

Figure D-14. Fort Worth, FM4 (2003), 2005 Cores.

Table D-14. Figure Designation and Slice Thickness for Fort Worth FM 4 (2003) 2005 Cores.

Figure Designation	Site	Estimated Slice Thickness (in.)	Estimated Depth (in.)
FtW03 (05) U1-1-1	FtW FM4 2003 K6 (2005) U1-1, Slice 1	0.16	0.16
FtW03 (05) U1-1-2	FtW FM4 2003 K6 (2005) U1-1, Slice 2	0.20	0.51
FtW03 (05) U1-1-3	FtW FM4 2003 K6 (2005) U1-1, Slice 3	0.19	0.84
FtW03 (05) U1-1-4	FtW FM4 2003 K6 (2005) U1-1, Slice 4	x	x
FtW03 (05) U1-2-1	FtW FM4 2003 K6 (2005) U1-2, Slice 1	0.10	0.10
FtW03 (05) U1-2-2	FtW FM4 2003 K6 (2005) U1-2, Slice 2	0.19	0.43
FtW03 (05) U1-2-3	FtW FM4 2003 K6 (2005) U1-2, Slice 3	0.22	0.80
FtW03 (05) U1-2-4	FtW FM4 2003 K6 (2005) U1-2, Slice 4	x	x
FtW03 (05) U1-3-1	FtW FM4 2003 K6 (2005) U1-3, Slice 1	0.11	0.11
FtW03 (05) U1-3-2	FtW FM4 2003 K6 (2005) U1-3, Slice 2	0.14	0.40
FtW03 (05) U1-3-3	FtW FM4 2003 K6 (2005) U1-3, Slice 3	0.14	0.68
FtW03 (05) U1-3-4	FtW FM4 2003 K6 (2005) U1-3, Slice 4	0.14	0.97
FtW03 (05) COS50 T1-1-1	FtW FM4 2003 K6 COS50 (2005) T1-1, Slice 1	0.16	0.16
FtW03 (05) COS50 T1-1-2	FtW FM4 2003 K6 COS50 (2005) T1-1, Slice 2	0.19	0.50
FtW03 (05) COS50 T1-1-3	FtW FM4 2003 K6 COS50 (2005) T1-1, Slice 3	0.25	0.89
FtW03 (05) COS50 T1-1-4	FtW FM4 2003 K6 COS50 (2005) T1-1, Slice 4	x	x
FtW03 (05) COS50 T1-2-1	FtW FM4 2003 K6 COS50 (2005) T1-2, Slice 1	0.11	0.11
FtW03 (05) COS50 T1-2-2	FtW FM4 2003 K6 COS50 (2005) T1-2, Slice 2	0.24	0.50
FtW03 (05) COS50 T1-2-3	FtW FM4 2003 K6 COS50 (2005) T1-2, Slice 3	0.28	0.93
FtW03 (05) COS50 T1-2-4	FtW FM4 2003 K6 COS50 (2005) T1-2, Slice 4	x	x
FtW03 (05) COS50 T1-3-1	FtW FM4 2003 K6 COS50 (2005) T1-2, Slice 1	0.19	0.19
FtW03 (05) COS50 T1-3-2	FtW FM4 2003 K6 COS50 (2005) T1-3, Slice 2	0.25	0.58
FtW03 (05) COS50 T1-3-3	FtW FM4 2003 K6 COS50 (2005) T1-3, Slice 3	0.25	0.98
FtW03 (05) COS50 T1-3-4	FtW FM4 2003 K6 COS50 (2005) T1-3, Slice 4	x	x

Table D-15. Figure Designation and Slice Thickness for Fort Worth FM 4 (2003) 2006 Cores.

Figure Designation	Site	Estimated Slice Thickness (in.)	Estimated Depth (in.)
FtW03 (06) U1-1-1	FtW FM4 2003 K6 (2006) U2-1, Slice 1	0.27	0.27
FtW03 (06) U1-1-2	FtW FM4 2003 K6 (2006) U2-1, Slice 2	0.10	0.52
FtW03 (06) U1-1-3	FtW FM4 2003 K6 (2006) U2-1, Slice 3	0.21	0.88
FtW03 (06) U1-1-4	FtW FM4 2003 K6 (2006) U2-1, Slice 4	x	x
FtW03 (06) U1-2-1	FtW FM4 2003 K6 (2006) U2-2, Slice 1	0.25	0.25
FtW03 (06) U1-2-2	FtW FM4 2003 K6 (2006) U2-2, Slice 2	0.19	0.59
FtW03 (06) U1-2-3	FtW FM4 2003 K6 (2006) U2-2, Slice 3	0.24	0.97
FtW03 (06) U1-2-4	FtW FM4 2003 K6 (2006) U2-2, Slice 4	x	x
FtW03 (06) U1-3-1	FtW FM4 2003 K6 (2006) U2-3, Slice 1	0.33	0.33
FtW03 (06) U1-3-2	FtW FM4 2003 K6 (2006) U2-3, Slice 2	0.15	0.63
FtW03 (06) U1-3-3	FtW FM4 2003 K6 (2006) U2-3, Slice 3	0.14	0.91
FtW03 (06) U1-3-4	FtW FM4 2003 K6 (2006) U2-3, Slice 4	x	x
FtW03 (06) COS50 T2-1-1	FtW FM4 2003 K6 COS50 (2005) T1-3, Slice 1	0.22	0.22
FtW03 (06) COS50 T2-1-2	FtW FM4 2003 K6 COS50 (2005) T1-3, Slice 2	0.23	0.59
FtW03 (06) COS50 T2-1-3	FtW FM4 2003 K6 COS50 (2006) T2-1, Slice 3	x	x
FtW03 (06) COS50 T2-1-4	FtW FM4 2003 K6 COS50 (2006) T2-1, Slice 4	x	x
FtW03 (06) COS50 T2-2-1	FtW FM4 2003 K6 COS50 (2006) T2-1, Slice 1	0.20	0.20
FtW03 (06) COS50 T2-2-2	FtW FM4 2003 K6 COS50 (2006) T2-1, Slice 2	0.20	0.55
FtW03 (06) COS50 T2-2-3	FtW FM4 2003 K6 COS50 (2006) T2-1, Slice 3	0.19	0.89
FtW03 (06) COS50 T2-2-4	FtW FM4 2003 K6 COS50 (2006) T2-2, Slice 4	x	x
FtW03 (06) COS50 T2-3-1	FtW FM4 2003 K6 COS50 (2006) T2-2, Slice 1	0.18	0.18
FtW03 (06) COS50 T2-3-2	FtW FM4 2003 K6 COS50 (2006) T2-2, Slice 2	0.17	0.50
FtW03 (06) COS50 T2-3-3	FtW FM4 2003 K6 COS50 (2006) T2-2, Slice 3	0.24	0.89
FtW03 (06) COS50 T2-3-4	FtW FM4 2003 K6 COS50 (2006) T2-2, Slice 4	x	x

Table D-16. Figure Designation and Slice Thickness for Georgetown Airport (1989) 2005 Cores.

Figure Designation	Site	Estimated Slice Thickness (in.)	Estimated Depth (in.)
Geo 89 (05) T1-3-1	GEO 89 (2005) T1-3, Slice 1	0.21	0.21
Geo 89 (05) T1-3-2	GEO 89 (2005) T1-3, Slice 2	0.15	0.51
Geo 89 (05) T1-3-3	GEO 89 (2005) T1-3, Slice 3	0.23	0.89
Geo 89 (05) T1-3-4	GEO 89 (2005) T1-3, Slice 4	0.22	1.25
Geo 89 (05) U1-3-1	GEO 89 (2005) U1-3, Slice 1	0.21	0.21
Geo 89 (05) U1-3-2	GEO 89 (2005) U1-3, Slice 2	0.18	0.54
Geo 89 (05) U1-3-3	GEO 89 (2005) U1-3, Slice 3	0.32	1.00
Geo 89 (05) U1-3-4	GEO 89 (2005) U1-3, Slice 4	0.19	1.34

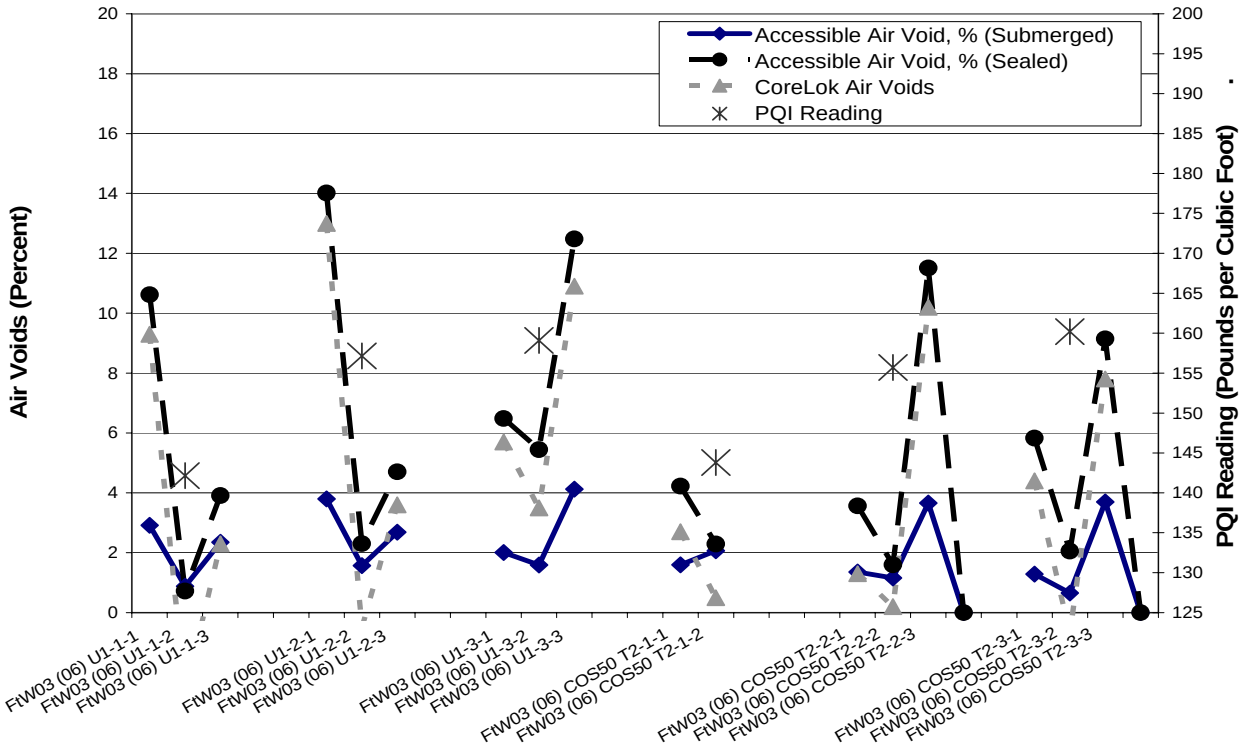

Figure D-15. Fort Worth, FM4 (2003), 2006 Cores.

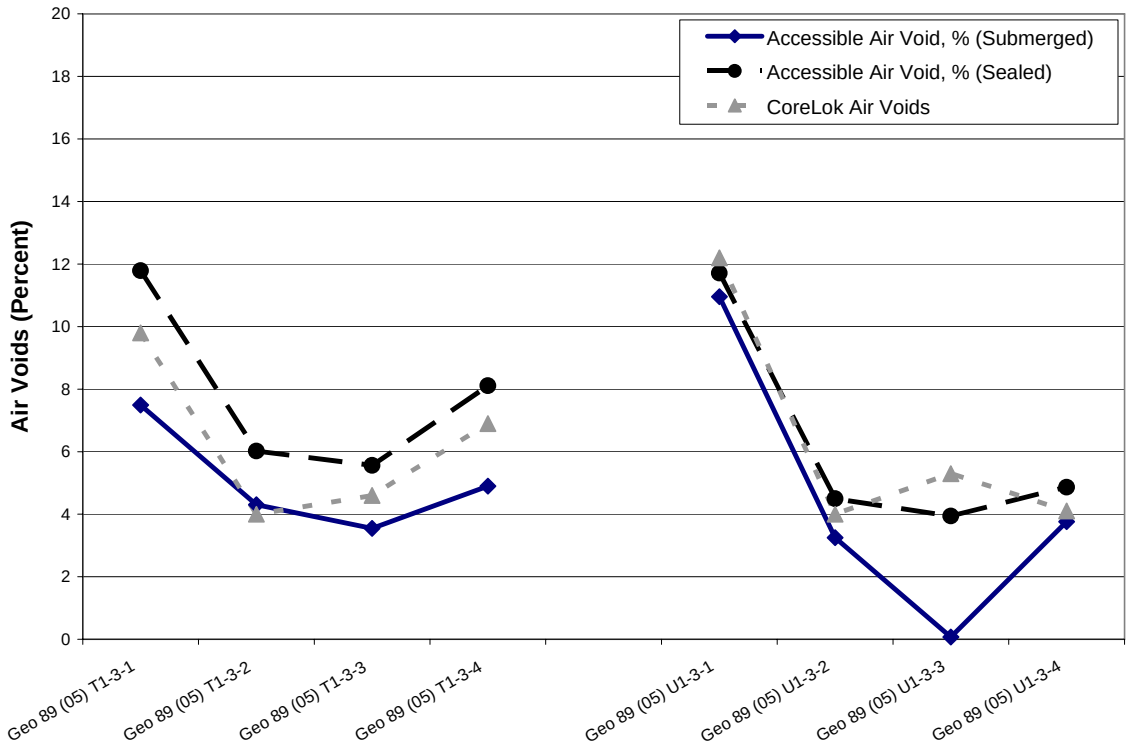

Figure D-16. Georgetown Airport (1989), 2005 Cores.

Table D-17. Figure Designation and Slice Thickness for Georgetown Airport (1989) 2006 Cores.

Figure Designation	Site	Estimated Slice Thickness (in.)	Estimated Depth (in.)
Geo 89 (06) T2-1-1	GEO 89 (2006) T2-1, Slice 1	0.21	0.21
Geo 89 (06) T2-1-2	GEO 89 (2006) T2-1, Slice 2	0.19	0.55
Geo 89 (06) T2-1-3	GEO 89 (2006) T2-1, Slice 3	0.19	0.89
Geo 89 (06) T2-1-4	GEO 89 (2006) T2-1, Slice 4	x	x
Geo 89 (06) T2-2-1	GEO 89 (2006) T2-2, Slice 1	0.15	0.15
Geo 89 (06) T2-2-2	GEO 89 (2006) T2-2, Slice 2	0.20	0.50
Geo 89 (06) T2-2-3	GEO 89 (2006) T2-2, Slice 3	0.16	0.80
Geo 89 (06) T2-2-4	GEO 89 (2006) T2-2, Slice 4	0.35	1.30
Geo 89 (06) T2-3-1	GEO 89 (2006) T2-3, Slice 1	0.23	0.23
Geo 89 (06) T2-3-2	GEO 89 (2006) T2-3, Slice 2	0.21	0.59
Geo 89 (06) T2-3-3	GEO 89 (2006) T2-3, Slice 3	0.25	0.98
Geo 89 (06) T2-3-4	GEO 89 (2006) T2-3, Slice 4	0.27	1.40
Geo 89 (06) U2-1-1	GEO 89 (2006) U2-1, Slice 1	0.20	0.20
Geo 89 (06) U2-1-2	GEO 89 (2006) U2-1, Slice 2	0.19	0.54
Geo 89 (06) U2-1-3	GEO 89 (2006) U2-1, Slice 3	0.13	0.81
Geo 89 (06) U2-1-4	GEO 89 (2006) U2-1, Slice 4	0.14	1.10
Geo 89 (06) U2-2-1	GEO 89 (2006) U2-2, Slice 1	0.20	0.20
Geo 89 (06) U2-2-2	GEO 89 (2006) U2-2, Slice 2	0.20	0.55
Geo 89 (06) U2-2-3	GEO 89 (2006) U2-2, Slice 3	0.18	0.88
Geo 89 (06) U2-2-4	GEO 89 (2006) U2-2, Slice 4	0.22	1.24
Geo 89 (06) U2-3-1	GEO 89 (2006) U2-3, Slice 1	0.16	0.16
Geo 89 (06) U2-3-2	GEO 89 (2006) U2-3, Slice 2	0.17	0.48
Geo 89 (06) U2-3-3	GEO 89 (2006) U2-3, Slice 3	0.14	0.76
Geo 89 (06) U2-3-4	GEO 89 (2006) U2-3, Slice 4	0.14	1.05

Table D-18. Figure Designation and Slice Thickness for Georgetown Airport (1995) 2005 Cores.

Figure Designation	Site	Estimated Slice Thickness (in.)	Estimated Depth (in.)
Geo 95 (05) T1-3-1	GEO 95 (2005) T1-3, Slice 1	0.24	0.24
Geo 95 (05) T1-3-2	GEO 95 (2005) T1-3, Slice 2	0.08	0.47
Geo 95 (05) T1-3-3	GEO 95 (2005) T1-3, Slice 3	0.13	0.74
Geo 95 (05) T1-3-4	GEO 95 (2005) T1-3, Slice 4	0.27	1.16
Geo 95 (05) U1-3-1	GEO 95 (2005) U1-3, Slice 1	0.21	0.21
Geo 95 (05) U1-3-2	GEO 95 (2005) U1-3, Slice 2	0.15	0.50
Geo 95 (05) U1-3-3	GEO 95 (2005) U1-3, Slice 3	0.17	0.82
Geo 95 (05) U1-3-4	GEO 95 (2005) U1-3, Slice 4	0.20	1.17

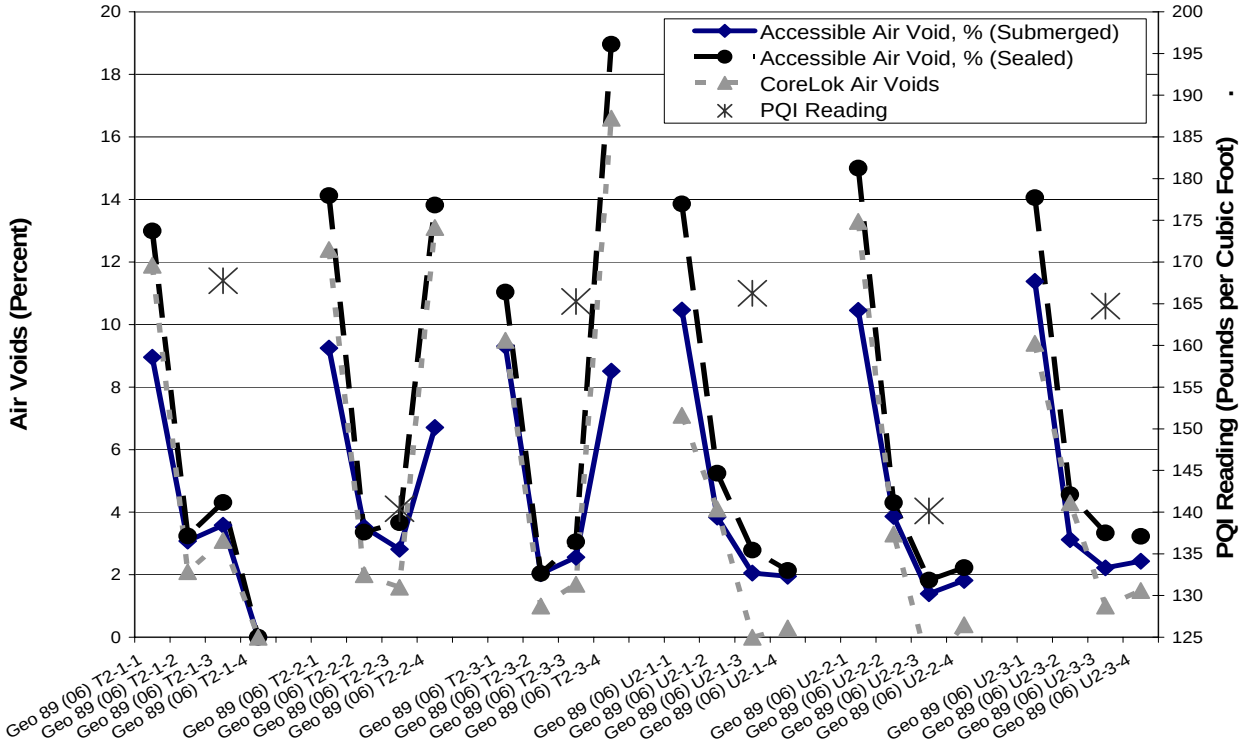

Figure D-17. Georgetown Airport (1989), 2006 Cores.

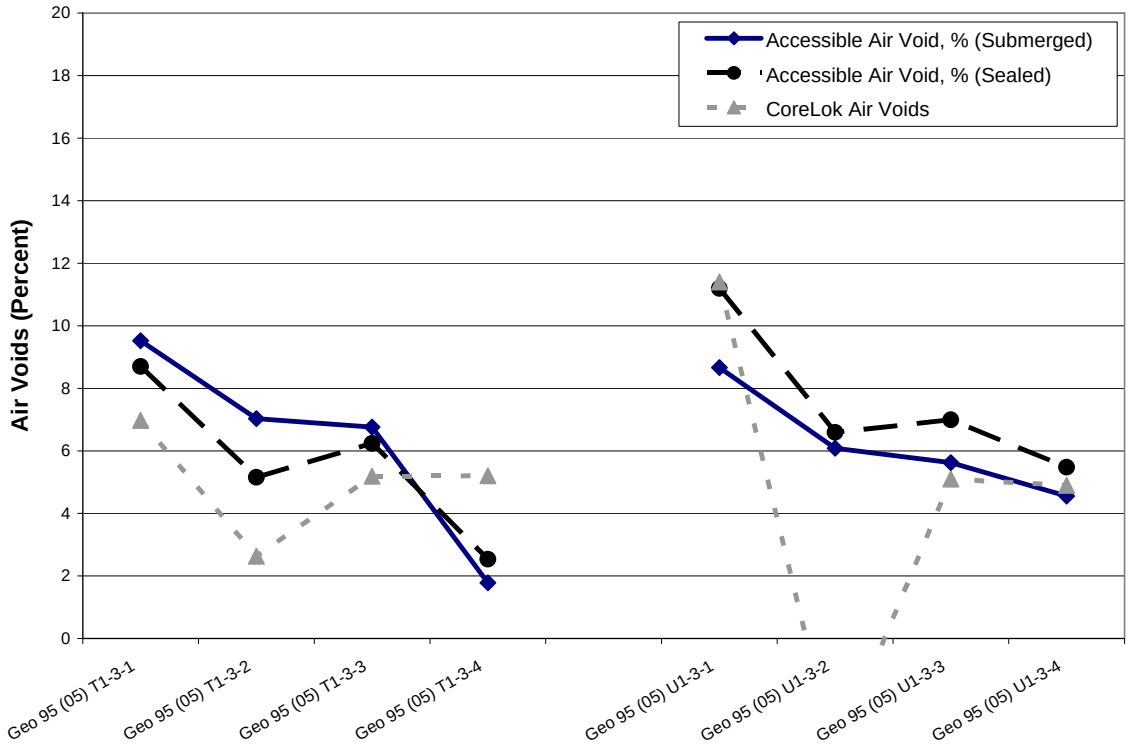

Figure D-18. Georgetown Airport (1995), 2005 Cores.

Table D-19. Figure Designation and Slice Thickness for Georgetown Airport (1995) 2006 Cores.

Figure Designation	Site	Estimated Slice Thickness (in.)	Estimated Depth (in.)
Geo 95 (06) T2-1-1	GEO 95 (2006) T2-1, Slice 1	0.20	0.20
Geo 95 (06) T2-1-2	GEO 95 (2006) T2-1, Slice 2	0.16	0.51
Geo 95 (06) T2-1-3	GEO 95 (2006) T2-1, Slice 3	0.20	0.85
Geo 95 (06) T2-1-4	GEO 95 (2006) T2-1, Slice 4	0.19	1.19
Geo 95 (06) T2-2-1	GEO 95 (2006) T2-2, Slice 1	0.26	0.26
Geo 95 (06) T2-2-2	GEO 95 (2006) T2-2, Slice 2	0.26	0.66
Geo 95 (06) T2-2-3	GEO 95 (2006) T2-2, Slice 3	0.22	1.03
Geo 95 (06) T2-2-4	GEO 95 (2006) T2-2, Slice 4	0.17	1.35
Geo 95 (06) T2-3-1	GEO 95 (2006) T2-3, Slice 1	0.20	0.20
Geo 95 (06) T2-3-2	GEO 95 (2006) T2-3, Slice 2	0.17	0.52
Geo 95 (06) T2-3-3	GEO 95 (2006) T2-3, Slice 3	0.18	0.85
Geo 95 (06) T2-3-4	GEO 95 (2006) T2-3, Slice 4	0.24	1.24
Geo 95 (06) U2-1-1	GEO 95 (2006) U2-1, Slice 1	0.22	0.22
Geo 95 (06) U2-1-2	GEO 95 (2006) U2-1, Slice 2	0.19	0.55
Geo 95 (06) U2-1-3	GEO 95 (2006) U2-1, Slice 3	0.16	0.86
Geo 95 (06) U2-1-4	GEO 95 (2006) U2-1, Slice 4	0.16	1.17
Geo 95 (06) U2-2-1	GEO 95 (2006) U2-2, Slice 1	0.20	0.20
Geo 95 (06) U2-2-2	GEO 95 (2006) U2-2, Slice 2	0.22	0.57
Geo 95 (06) U2-2-3	GEO 95 (2006) U2-2, Slice 3	0.22	0.94
Geo 95 (06) U2-2-4	GEO 95 (2006) U2-2, Slice 4	0.15	1.24
Geo 95 (06) U2-3-1	GEO 95 (2006) U2-3, Slice 1	0.20	0.20
Geo 95 (06) U2-3-2	GEO 95 (2006) U2-3, Slice 2	0.19	0.53
Geo 95 (06) U2-3-3	GEO 95 (2006) U2-3, Slice 3	0.17	0.85
Geo 95 (06) U2-3-4	GEO 95 (2006) U2-3, Slice 4	0.16	1.16

Table D-20. Figure Designation and Slice Thickness for Georgetown Airport (1995*) 2006 Cores.

Figure Designation	Site	Estimated Slice Thickness (in.)	Estimated Depth (in.)
Geo 95* (06) T2-1-1	GEO 95* (2006) T1, Slice 1	0.26	0.26
Geo 95* (06) T2-1-2	GEO 95* (2006) T1, Slice 2	0.18	0.59
Geo 95* (06) T2-1-3	GEO 95* (2006) T1, Slice 3	0.17	0.91
Geo 95* (06) T2-1-4	GEO 95* (2006) T1, Slice 4	0.18	1.24
Geo 95* (06) T2-2-1	GEO 95* (2006) T2, Slice 1	0.30	0.30
Geo 95* (06) T2-2-2	GEO 95* (2006) T2, Slice 2	0.20	0.65
Geo 95* (06) T2-2-3	GEO 95* (2006) T2, Slice 3	0.22	1.01
Geo 95* (06) T2-2-4	GEO 95* (2006) T2, Slice 4	0.25	1.40
Geo 95* (06) T2-3-1	GEO 95* (2006) T3, Slice 1	0.24	0.24
Geo 95* (06) T2-3-2	GEO 95* (2006) T3, Slice 2	0.23	0.62
Geo 95* (06) T2-3-3	GEO 95* (2006) T3, Slice 3	0.23	1.00
Geo 95* (06) T2-3-4	GEO 95* (2006) T3, Slice 4	0.24	1.38

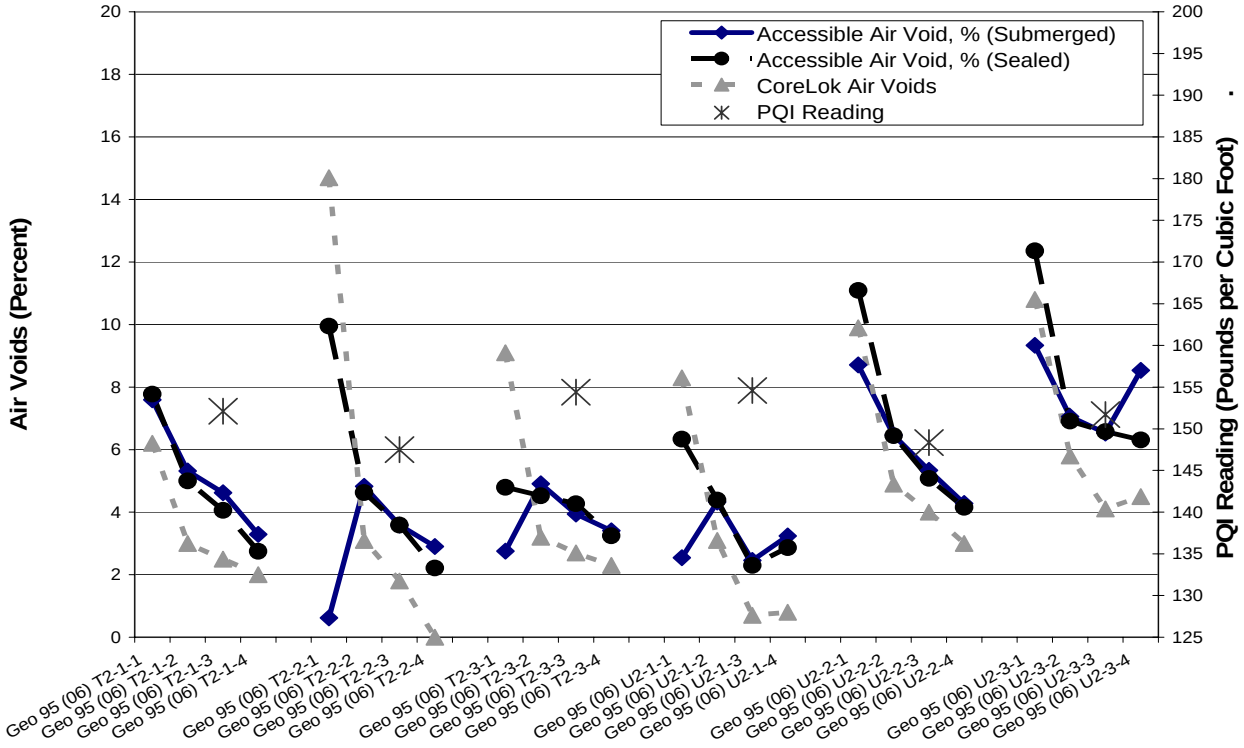

Figure D-19. Georgetown Airport (1995), 2006 Cores.

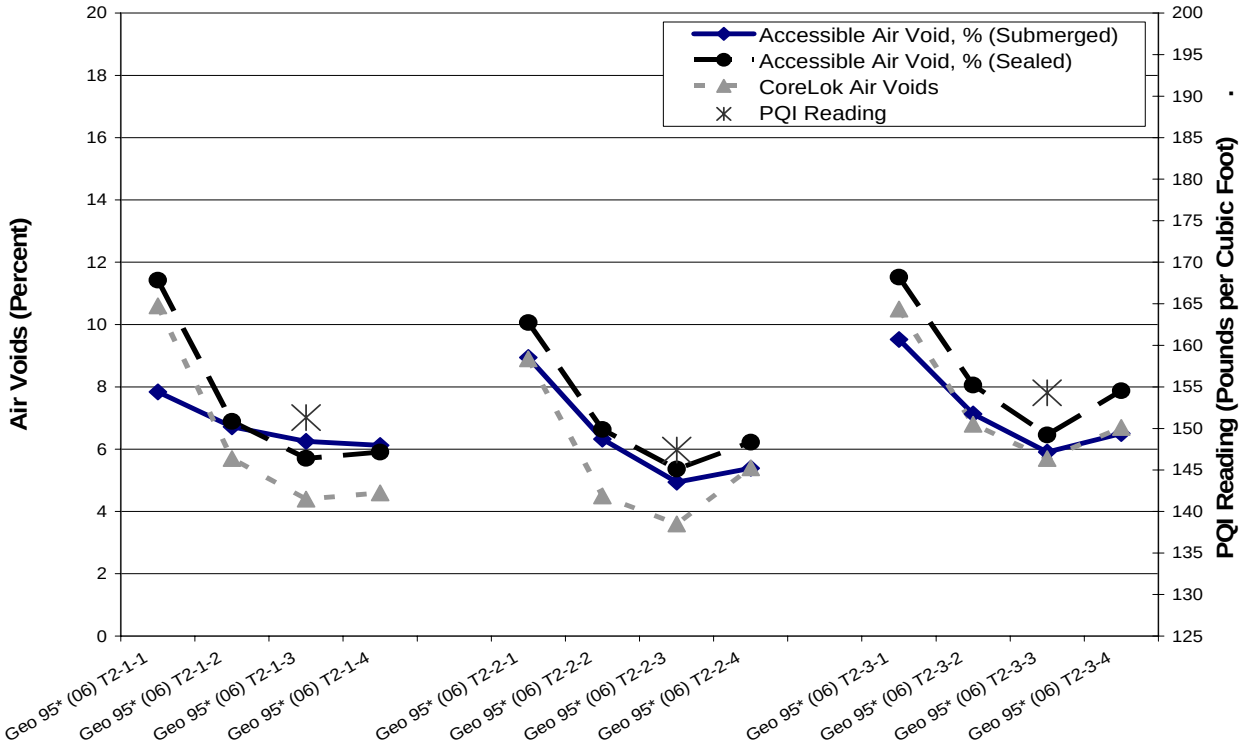

Figure D-20. Georgetown Airport (1995*), 2006 Cores.

Table D-21. Figure Designation and Slice Thickness for Jacksonville Airport 2005 Cores.

Figure Designation	Site	Estimated Slice Thickness (in.)	Estimated Depth (in.)
Jacks (05) T1-1-1	Jacks (2005) T1-3, Slice 1	0.12	0.12
Jacks (05) T1-1-2	Jacks (2005) T1-3, Slice 2	0.26	0.53
Jacks (05) T1-1-3	Jacks (2005) T1-3, Slice 3	0.24	0.92
Jacks (05) T1-1-4	Jacks (2005) T1-3, Slice 4	0.19	1.25
Jacks (05) U1-1-1	Jacks (2005) U1-3, Slice 1	0.17	0.17
Jacks (05) U1-1-2	Jacks (2005) U1-3, Slice 2	0.23	0.54
Jacks (05) U1-1-3	Jacks (2005) U1-3, Slice 3	0.18	0.87
Jacks (05) U1-1-4	Jacks (2005) U1-3, Slice 4	0.23	1.25

Table D-22. Figure Designation and Slice Thickness for Jacksonville Airport 2006 Cores.

Figure Designation	Site	Estimated Slice Thickness (in.)	Estimated Depth (in.)
Jacks (06) T2-1-1	Jacks (2006) T2-1, Slice 1	0.23	0.23
Jacks (06) T2-1-2	Jacks (2006) T2-1, Slice 2	0.25	0.63
Jacks (06) T2-1-3	Jacks (2006) T2-1, Slice 3	0.27	1.05
Jacks (06) T2-1-4	Jacks (2006) T2-1, Slice 4	0.25	1.45
Jacks (06) T2-2-1	Jacks (2006) T2-2, Slice 1	0.23	0.23
Jacks (06) T2-2-2	Jacks (2006) T2-2, Slice 2	0.28	0.66
Jacks (06) T2-2-3	Jacks (2006) T2-2, Slice 3	0.30	1.10
Jacks (06) T2-2-4	Jacks (2006) T2-2, Slice 4	0.23	1.48
Jacks (06) T2-3-1	Jacks (2006) T2-3, Slice 1	0.29	0.29
Jacks (06) T2-3-2	Jacks (2006) T2-3, Slice 2	0.27	0.72
Jacks (06) T2-3-3	Jacks (2006) T2-3, Slice 3	0.26	1.13
Jacks (06) T2-3-4	Jacks (2006) T2-3, Slice 4	0.23	1.51
Jacks (06) U2-1-1	Jacks (2006) U2-1, Slice 1	0.25	0.25
Jacks (06) U2-1-2	Jacks (2006) U2-1, Slice 2	0.21	0.61
Jacks (06) U2-1-3	Jacks (2006) U2-1, Slice 3	0.25	1.00
Jacks (06) U2-1-4	Jacks (2006) U2-1, Slice 4	0.33	1.48
Jacks (06) U2-2-1	Jacks (2006) U2-2, Slice 1	0.24	0.24
Jacks (06) U2-2-2	Jacks (2006) U2-2, Slice 2	0.23	0.62
Jacks (06) U2-2-3	Jacks (2006) U2-2, Slice 3	0.23	1.00
Jacks (06) U2-2-4	Jacks (2006) U2-2, Slice 4	0.26	1.41
Jacks (06) U2-3-1	Jacks (2006) U2-3, Slice 1	0.36	0.36
Jacks (06) U2-3-2	Jacks (2006) U2-3, Slice 2	0.26	0.76
Jacks (06) U2-3-3	Jacks (2006) U2-3, Slice 3	0.28	1.19
Jacks (06) U2-3-4	Jacks (2006) U2-3, Slice 4	0.18	1.52

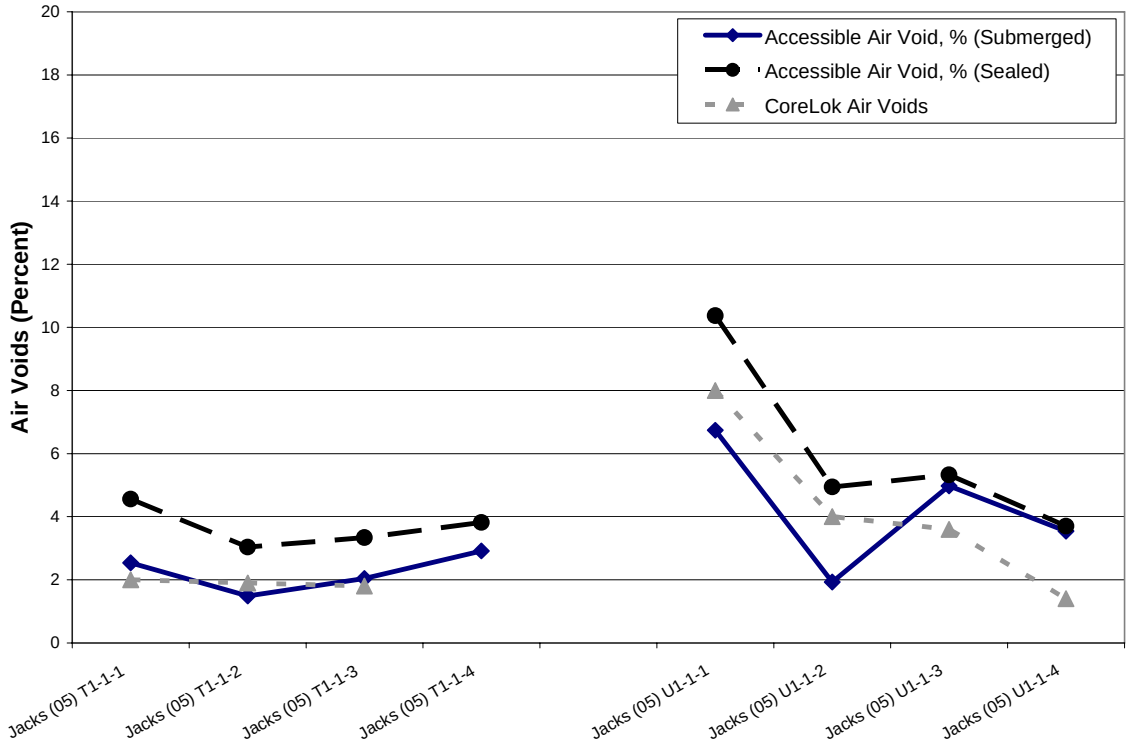

Figure D-21. Jacksonville Airport, 2005 Cores.

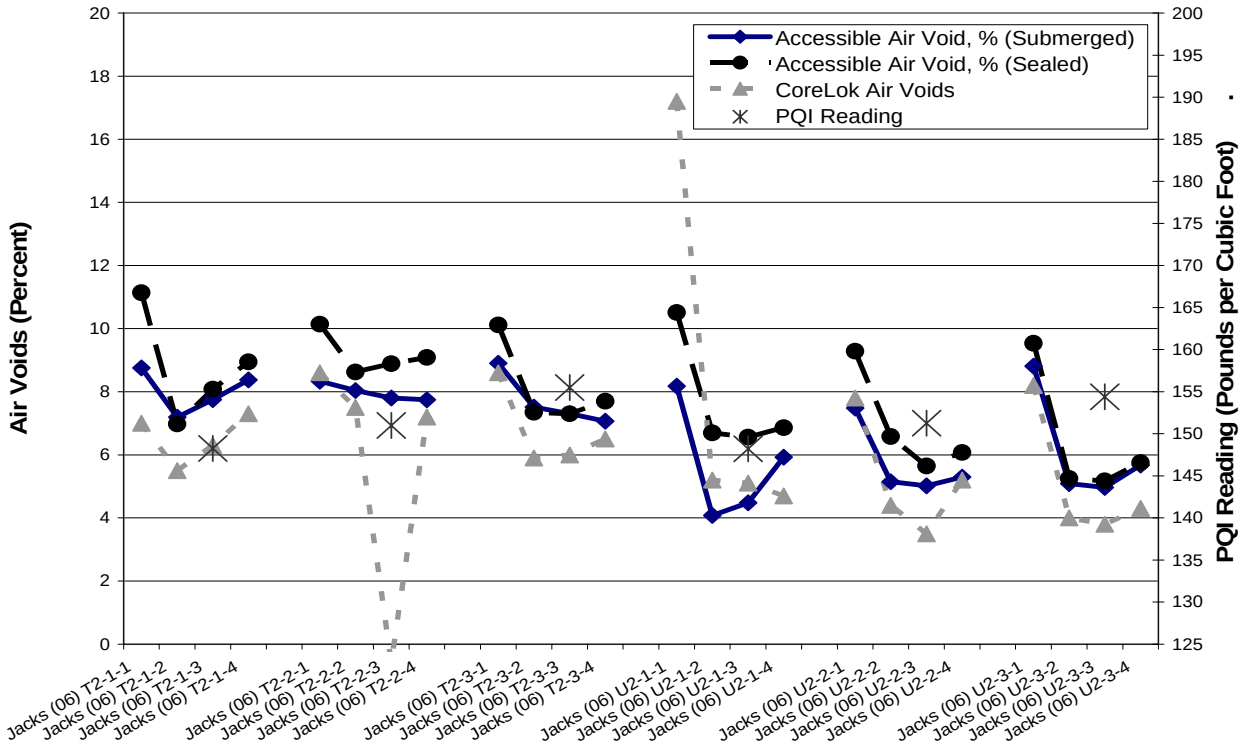

Figure D-22. Jacksonville Airport, 2006 Cores.

Table D-23. Figure Designation and Slice Thickness for Lufkin BUS 59 2006 Cores.

Figure Designation	Site	Estimated Slice Thickness (in.)	Estimated Depth (in.)
LufBus59 (06) T2-1-1	LUF BUS59B (2006) T2-1, Slice 1	0.42	0.42
LufBus59 (06) T2-1-2	LUF BUS59B (2006) T2-1, Slice 2	0.33	0.89
LufBus59 (06) T2-1-3	LUF BUS59B (2006) T2-1, Slice 3	0.29	1.33
LufBus59 (06) T2-1-4	LUF BUS59B (2006) T2-1, Slice 4	0.27	1.75
LufBus59 (06) T2-2-1	LUF BUS59B (2006) T2-2, Slice 1	0.34	0.34
LufBus59 (06) T2-2-2	LUF BUS59B (2006) T2-2, Slice 2	0.27	0.76
LufBus59 (06) T2-2-3	LUF BUS59B (2006) T2-2, Slice 3	0.27	1.17
LufBus59 (06) T2-2-4	LUF BUS59B (2006) T2-2, Slice 4	0.26	1.58
LufBus59 (06) T2-3-1	LUF BUS59B (2006) T2-3, Slice 1	0.32	0.32
LufBus59 (06) T2-3-2	LUF BUS59B (2006) T2-3, Slice 2	0.23	0.70
LufBus59 (06) T2-3-3	LUF BUS59B (2006) T2-3, Slice 3	0.26	1.11
LufBus59 (06) T2-3-4	LUF BUS59B (2006) T2-3, Slice 4	0.28	1.54
LufBus59 (06) U2-1-1	LUF BUS59B (2006) U2-1, Slice 1	0.26	0.26
LufBus59 (06) U2-1-2	LUF BUS59B (2006) U2-1, Slice 2	0.16	0.57
LufBus59 (06) U2-1-3	LUF BUS59B (2006) U2-1, Slice 3	0.19	0.90
LufBus59 (06) U2-1-4	LUF BUS59B (2006) U2-1, Slice 4	0.10	1.15
LufBus59 (06) U2-2-1	LUF BUS59B (2006) U2-2, Slice 1	0.22	0.22
LufBus59 (06) U2-2-2	LUF BUS59B (2006) U2-2, Slice 2	0.20	0.57
LufBus59 (06) U2-2-3	LUF BUS59B (2006) U2-2, Slice 3	0.21	0.93
LufBus59 (06) U2-2-4	LUF BUS59B (2006) U2-2, Slice 4	0.19	1.26
LufBus59 (06) U2-3-1	LUF BUS59B (2006) U2-3, Slice 1	0.28	0.28
LufBus59 (06) U2-3-2	LUF BUS59B (2006) U2-3, Slice 2	0.21	0.64
LufBus59 (06) U2-3-3	LUF BUS59B (2006) U2-3, Slice 3	0.19	0.97
LufBus59 (06) U2-3-4	LUF BUS59B (2006) U2-3, Slice 4	x	x

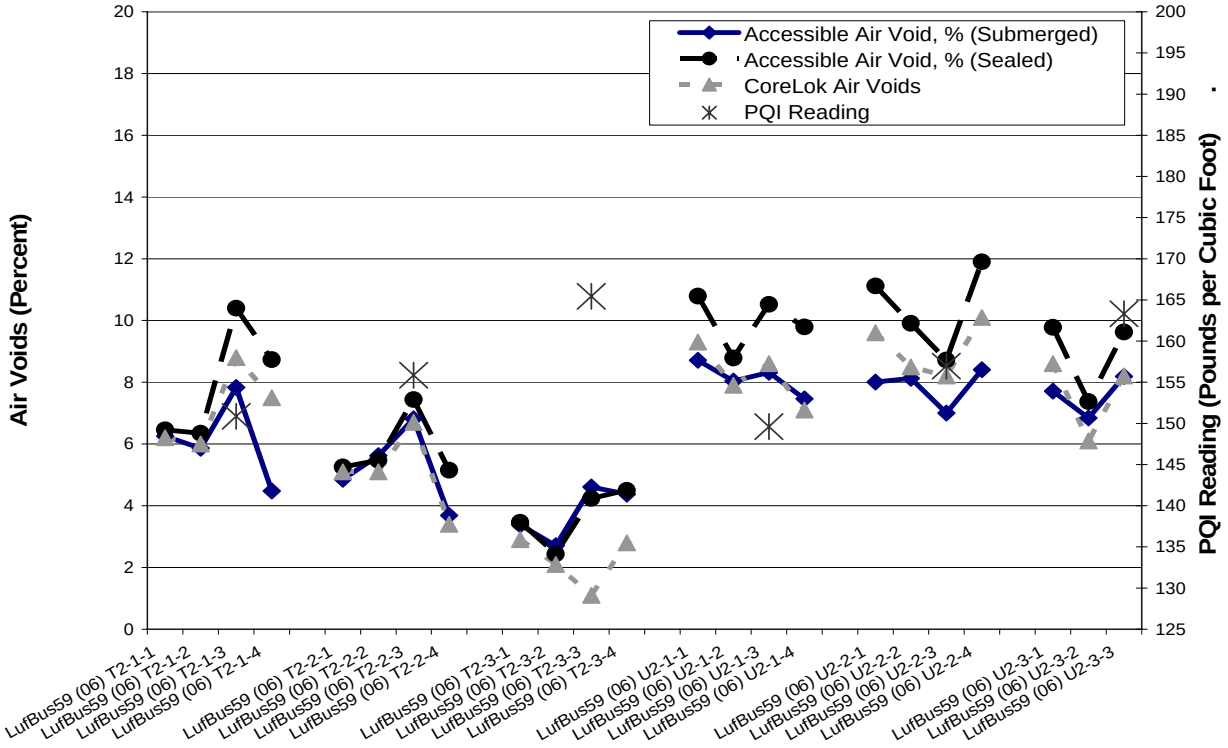

Figure D-23. Lufkin BUS59B, 2006 Cores.

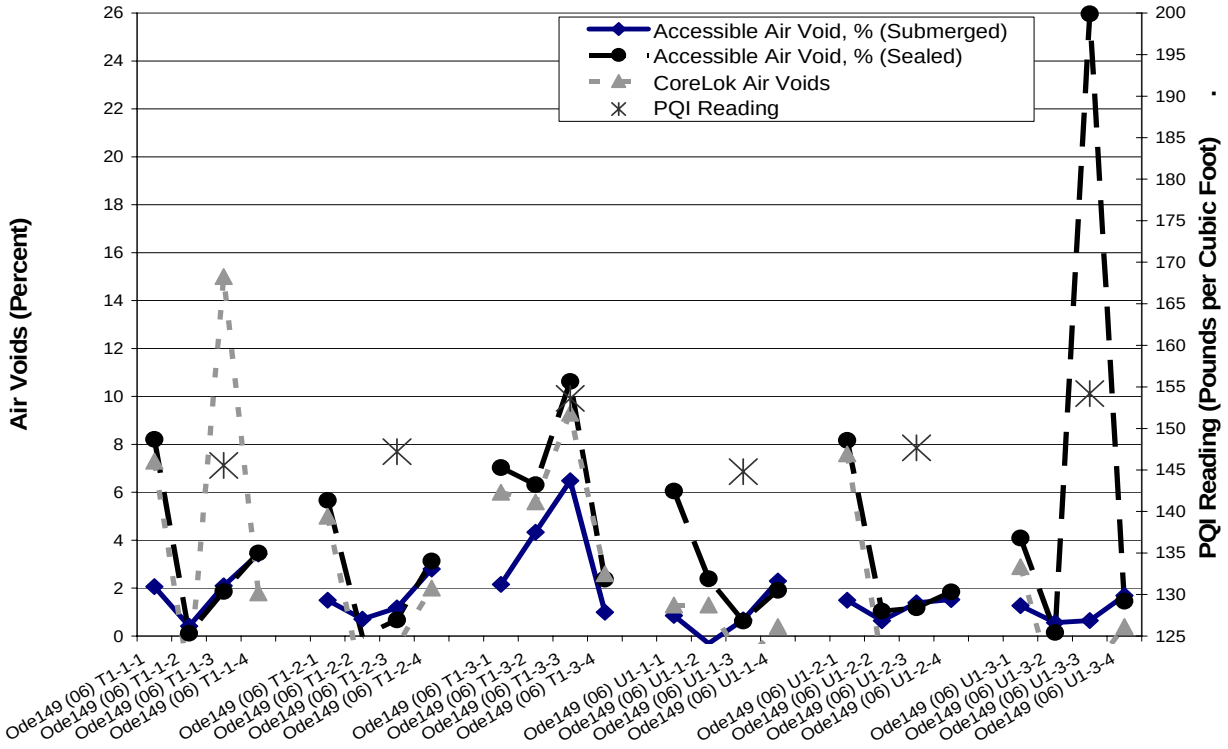

Figure D-24. Odessa SH149, 2006 Cores.

Table D-24. Figure Designation and Slice Thickness for Odessa SH 149 2006 Cores.

Figure Designation	Site	Estimated Slice Thickness (in.)	Estimated Depth (in.)
Ode149 (06) T1-1-1	ODE 149 (2006) T1, Slice 1	0.29	0.29
Ode149 (06) T1-1-2	ODE 149 (2006) T1, Slice 2	0.27	0.71
Ode149 (06) T1-1-3	ODE 149 (2006) T1, Slice 3	0.22	1.08
Ode149 (06) T1-1-4	ODE 149 (2006) T1, Slice 4	0.22	1.45
Ode149 (06) T1-2-1	ODE 149 (2006) T2, Slice 1	0.35	0.35
Ode149 (06) T1-2-2	ODE 149 (2006) T2, Slice 2	0.26	0.75
Ode149 (06) T1-2-3	ODE 149 (2006) T2, Slice 3	0.25	1.15
Ode149 (06) T1-2-4	ODE 149 (2006) T2, Slice 4	0.24	1.53
Ode149 (06) T1-3-1	ODE 149 (2006) T3, Slice 1	0.34	0.34
Ode149 (06) T1-3-2	ODE 149 (2006) T3, Slice 2	0.23	0.72
Ode149 (06) T1-3-3	ODE 149 (2006) T3, Slice 3	0.23	1.10
Ode149 (06) T1-3-4	ODE 149 (2006) T3, Slice 4	0.23	1.47
Ode149 (06) U1-1-1	ODE 149 (2006) U1, Slice 1	0.32	0.32
Ode149 (06) U1-1-2	ODE 149 (2006) U1, Slice 2	0.23	0.69
Ode149 (06) U1-1-3	ODE 149 (2006) U1, Slice 3	0.20	1.04
Ode149 (06) U1-1-4	ODE 149 (2006) U1, Slice 4	0.21	1.40
Ode149 (06) U1-2-1	ODE 149 (2006) U2, Slice 1	0.25	0.25
Ode149 (06) U1-2-2	ODE 149 (2006) U2, Slice 2	0.25	0.65
Ode149 (06) U1-2-3	ODE 149 (2006) U2, Slice 3	0.20	0.99
Ode149 (06) U1-2-4	ODE 149 (2006) U2, Slice 4	0.20	1.34
Ode149 (06) U1-3-1	ODE 149 (2006) U3, Slice 1	0.26	0.26
Ode149 (06) U1-3-2	ODE 149 (2006) U3, Slice 2	0.24	0.64
Ode149 (06) U1-3-3	ODE 149 (2006) U3, Slice 3	0.24	1.03
Ode149 (06) U1-3-4	ODE 149 (2006) U3, Slice 4	0.22	1.40

Table D-25. Figure Designation and Slice Thickness for Odessa SH 349 2006 Cores.

Figure Designation	Site	Estimated Slice Thickness (in.)	Estimated Depth (in.)
Ode349 (06) T1-1-1	ODE 349 (2006) T1, Slice 1	0.21	0.21
Ode349 (06) T1-1-2	ODE 349 (2006) T1, Slice 2	0.29	0.64
Ode349 (06) T1-1-3	ODE 349 (2006) T1, Slice 3	0.28	1.07
Ode349 (06) T1-1-4	ODE 349 (2006) T1, Slice 4	0.21	1.43
Ode349 (06) T1-2-1	ODE 349 (2006) T2, Slice 1	0.32	0.32
Ode349 (06) T1-2-2	ODE 349 (2006) T2, Slice 2	0.25	0.72
Ode349 (06) T1-2-3	ODE 349 (2006) T2, Slice 3	0.18	1.04
Ode349 (06) T1-2-4	ODE 349 (2006) T2, Slice 4	0.19	1.38
Ode349 (06) T1-3-1	ODE 349 (2006) T3, Slice 1	0.29	0.29
Ode349 (06) T1-3-2	ODE 349 (2006) T3, Slice 2	0.19	0.62
Ode349 (06) T1-3-3	ODE 349 (2006) T3, Slice 3	0.19	0.95
Ode349 (06) T1-3-4	ODE 349 (2006) T3, Slice 4	0.27	1.37
Ode349 (06) U1-1-1	ODE 349 (2006) U1, Slice 1	0.36	0.36
Ode349 (06) U1-1-2	ODE 349 (2006) U1, Slice 2	0.25	0.75
Ode349 (06) U1-1-3	ODE 349 (2006) U1, Slice 3	0.26	1.16
Ode349 (06) U1-1-4	ODE 349 (2006) U1, Slice 4	0.27	1.58
Ode349 (06) U1-2-1	ODE 349 (2006) U2, Slice 1	0.34	0.34
Ode349 (06) U1-2-2	ODE 349 (2006) U2, Slice 2	0.22	0.70
Ode349 (06) U1-2-3	ODE 349 (2006) U2, Slice 3	0.18	1.04
Ode349 (06) U1-2-4	ODE 349 (2006) U2, Slice 4	0.29	1.47
Ode349 (06) U1-3-1	ODE 349 (2006) U3, Slice 1	0.32	0.32
Ode349 (06) U1-3-2	ODE 349 (2006) U3, Slice 2	0.21	0.68
Ode349 (06) U1-3-3	ODE 349 (2006) U3, Slice 3	0.21	1.04
Ode349 (06) U1-3-4	ODE 349 (2006) U3, Slice 4	0.23	1.41

Table D-26. Figure Designation and Slice Thickness for Pleasanton Airport 2005 Cores.

Figure Designation	Site	Estimated Slice Thickness (in.)	Estimated Depth (in.)
Pleas (05) T1-3-1	Pleas (2005) T1-3, Slice 1	0.15	0.15
Pleas (05) T1-3-2	Pleas (2005) T1-3, Slice 2	0.15	0.45
Pleas (05) T1-3-3	Pleas (2005) T1-3, Slice 3	0.19	0.78
Pleas (05) T1-3-4	Pleas (2005) T1-3, Slice 4	0.16	1.09
Pleas (05) U1-3-1	Pleas (2005) U1-3, Slice 1	0.20	0.20
Pleas (05) U1-3-2	Pleas (2005) U1-3, Slice 2	0.20	0.54
Pleas (05) U1-3-3	Pleas (2005) U1-3, Slice 3	0.31	1.00
Pleas (05) U1-3-4	Pleas (2005) U1-3, Slice 4	0.22	1.37

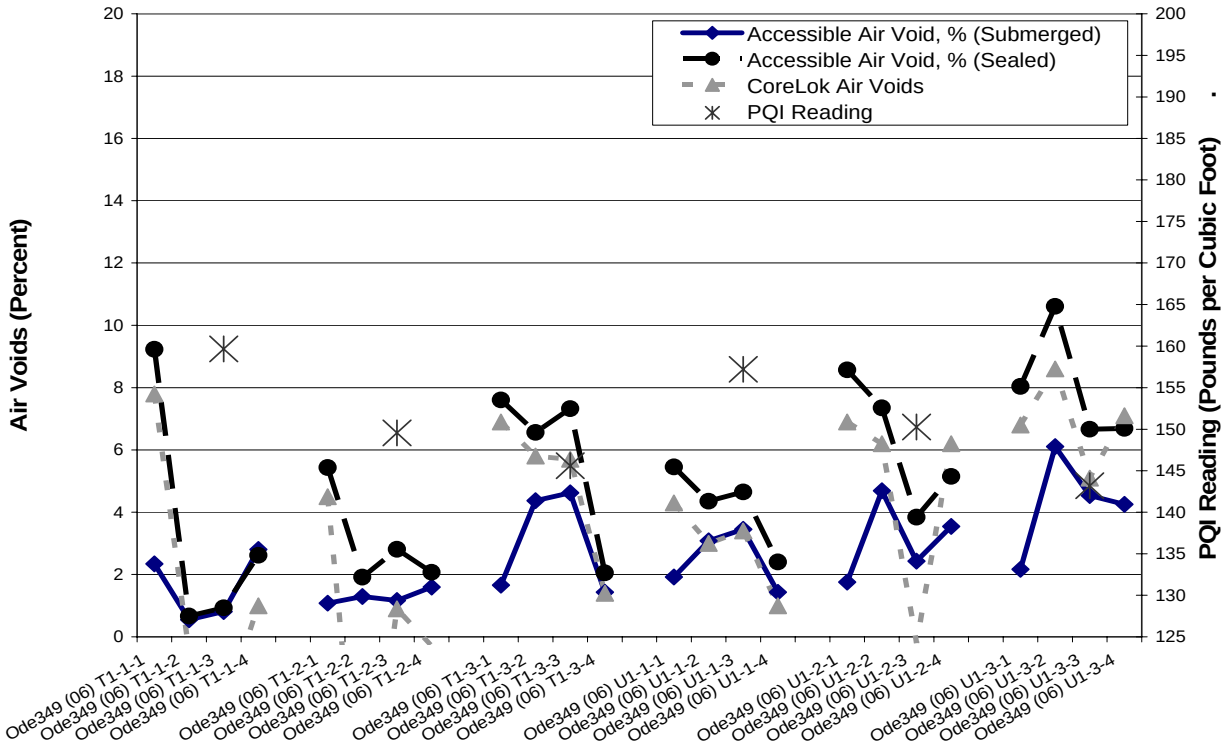

Figure D-25. Odessa SH349, 2006 Cores.

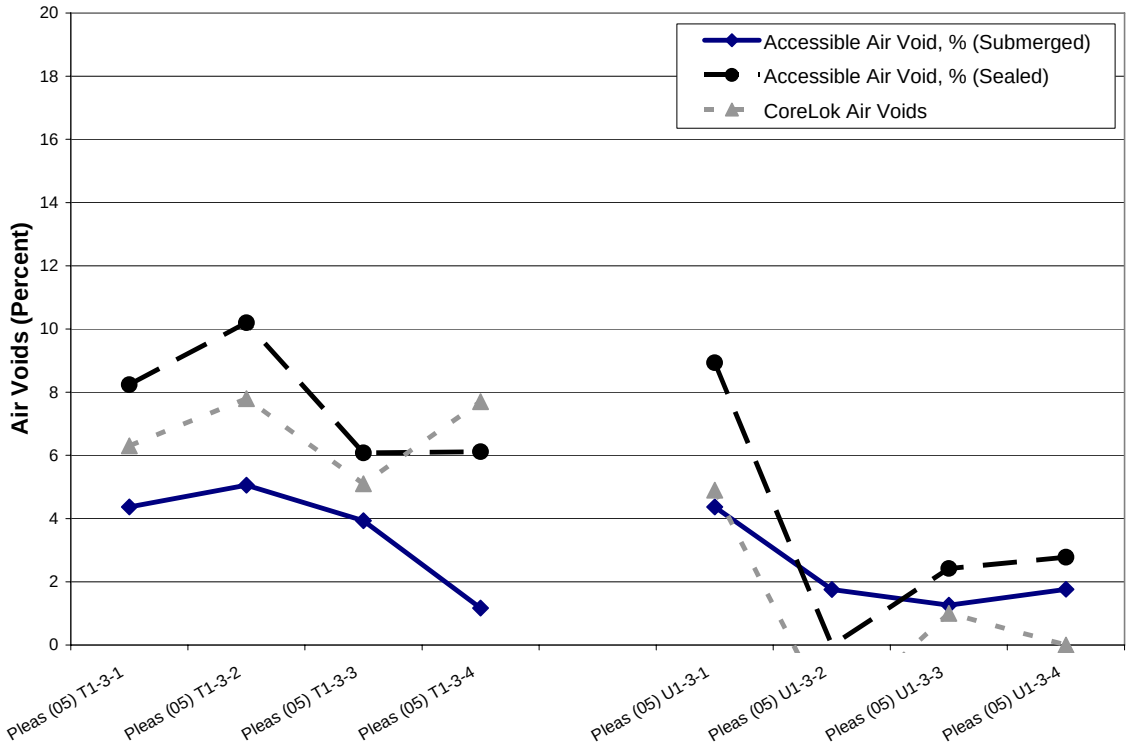

Figure D-26. Pleasanton Airport, 2005 Cores.

Table D-27. Figure Designation and Slice Thickness for Pleasanton Airport 2006 Cores.

Figure Designation	Site	Estimated Slice Thickness (in.)	Estimated Depth (in.)
Pleas (06) T2-1-1	Pleas (2006) T2-1, Slice 1	0.24	0.24
Pleas (06) T2-1-2	Pleas (2006) T2-1, Slice 2	0.25	0.64
Pleas (06) T2-1-3	Pleas (2006) T2-1, Slice 3	0.22	1.00
Pleas (06) T2-1-4	Pleas (2006) T2-1, Slice 4	0.20	1.35
Pleas (06) T2-2-1	Pleas (2006) T2-2, Slice 1	0.26	0.26
Pleas (06) T2-2-2	Pleas (2006) T2-2, Slice 2	0.19	0.60
Pleas (06) T2-2-3	Pleas (2006) T2-2, Slice 3	0.14	0.90
Pleas (06) T2-2-4	Pleas (2006) T2-2, Slice 4	0.15	1.19
Pleas (06) T2-3-1	Pleas (2006) T2-3, Slice 1	0.26	0.26
Pleas (06) T2-3-2	Pleas (2006) T2-3, Slice 2	0.25	0.65
Pleas (06) T2-3-3	Pleas (2006) T2-3, Slice 3	0.18	0.98
Pleas (06) T2-3-4	Pleas (2006) T2-3, Slice 4	0.19	1.32

Table D-28. Figure Designation and Slice Thickness for Tyler US79 2006 Cores.

Figure Designation	Site	Estimated Slice Thickness (in.)	Estimated Depth (in.)
Tyl US79 (06) T1-1-1	TYL US79 (2006) T1, Slice 1	0.31	0.31
Tyl US79 (06) T1-1-2	TYL US79 (2006) T1, Slice 2	0.21	0.67
Tyl US79 (06) T1-1-3	TYL US79 (2006) T1, Slice 3	0.31	1.13
Tyl US79 (06) T1-1-4	TYL US79 (2006) T1, Slice 4	0.30	1.57
Tyl US79 (06) T1-2-1	TYL US79 (2006) T2, Slice 1	0.32	0.32
Tyl US79 (06) T1-2-2	TYL US79 (2006) T2, Slice 2	0.29	0.75
Tyl US79 (06) T1-2-3	TYL US79 (2006) T2, Slice 3	0.27	1.17
Tyl US79 (06) T1-2-4	TYL US79 (2006) T2, Slice 4	0.31	1.62
Tyl US79 (06) T1-3-1	TYL US79 (2006) T3, Slice 1	0.35	0.35
Tyl US79 (06) T1-3-2	TYL US79 (2006) T3, Slice 2	0.23	0.73
Tyl US79 (06) T1-3-3	TYL US79 (2006) T3, Slice 3	0.27	1.14
Tyl US79 (06) T1-3-4	TYL US79 (2006) T3, Slice 4	0.34	1.63
Tyl US79 (06) U1-1-1	TYL US79 (2006) U1, Slice 1	0.34	0.34
Tyl US79 (06) U1-1-2	TYL US79 (2006) U1, Slice 2	0.27	0.75
Tyl US79 (06) U1-1-3	TYL US79 (2006) U1, Slice 3	0.26	1.16
Tyl US79 (06) U1-1-4	TYL US79 (2006) U1, Slice 4	0.26	1.57
Tyl US79 (06) U1-2-1	TYL US79 (2006) U2, Slice 1	0.25	0.25
Tyl US79 (06) U1-2-2	TYL US79 (2006) U2, Slice 2	0.25	0.65
Tyl US79 (06) U1-2-3	TYL US79 (2006) U2, Slice 3	0.25	1.05
Tyl US79 (06) U1-2-4	TYL US79 (2006) U2, Slice 4	0.26	1.45
Tyl US79 (06) U1-3-1	TYL US79 (2006) U3, Slice 1	0.28	0.28
Tyl US79 (06) U1-3-2	TYL US79 (2006) U3, Slice 2	0.29	0.72
Tyl US79 (06) U1-3-3	TYL US79 (2006) U3, Slice 3	0.26	1.12
Tyl US79 (06) U1-3-4	TYL US79 (2006) U3, Slice 4	0.28	1.54

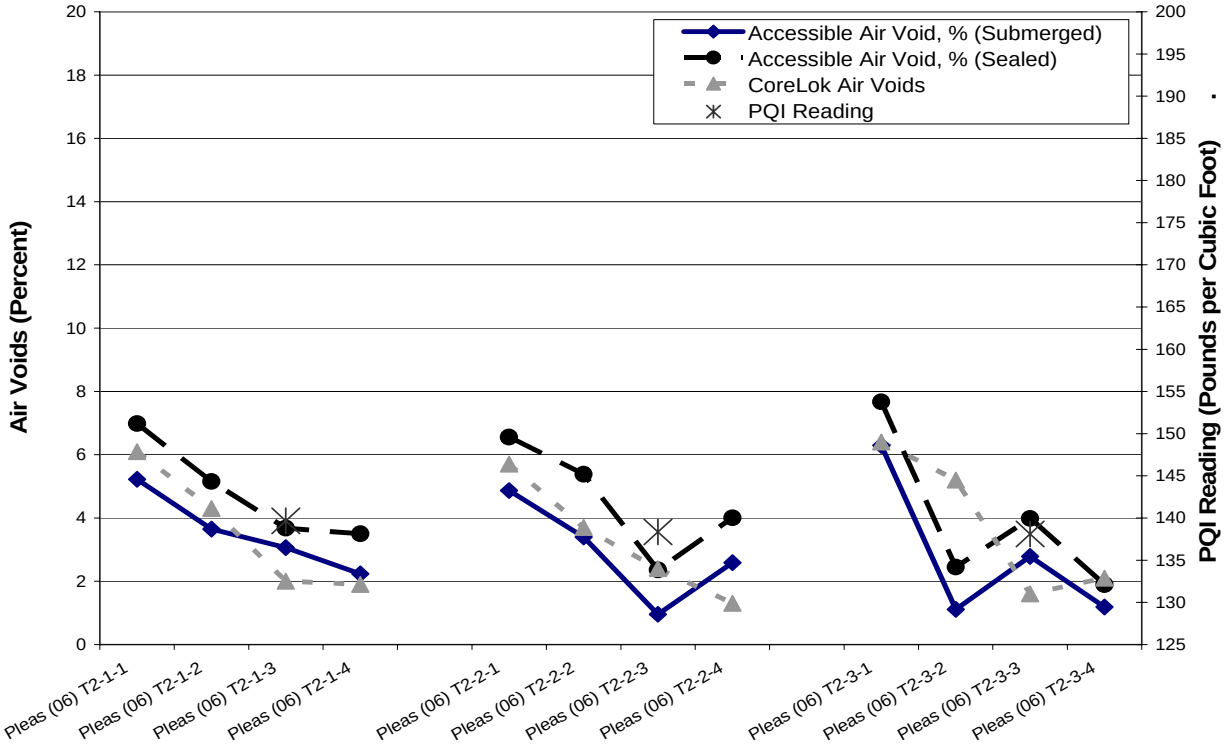

Figure D-27. Pleasanton Airport, 2006 Cores.

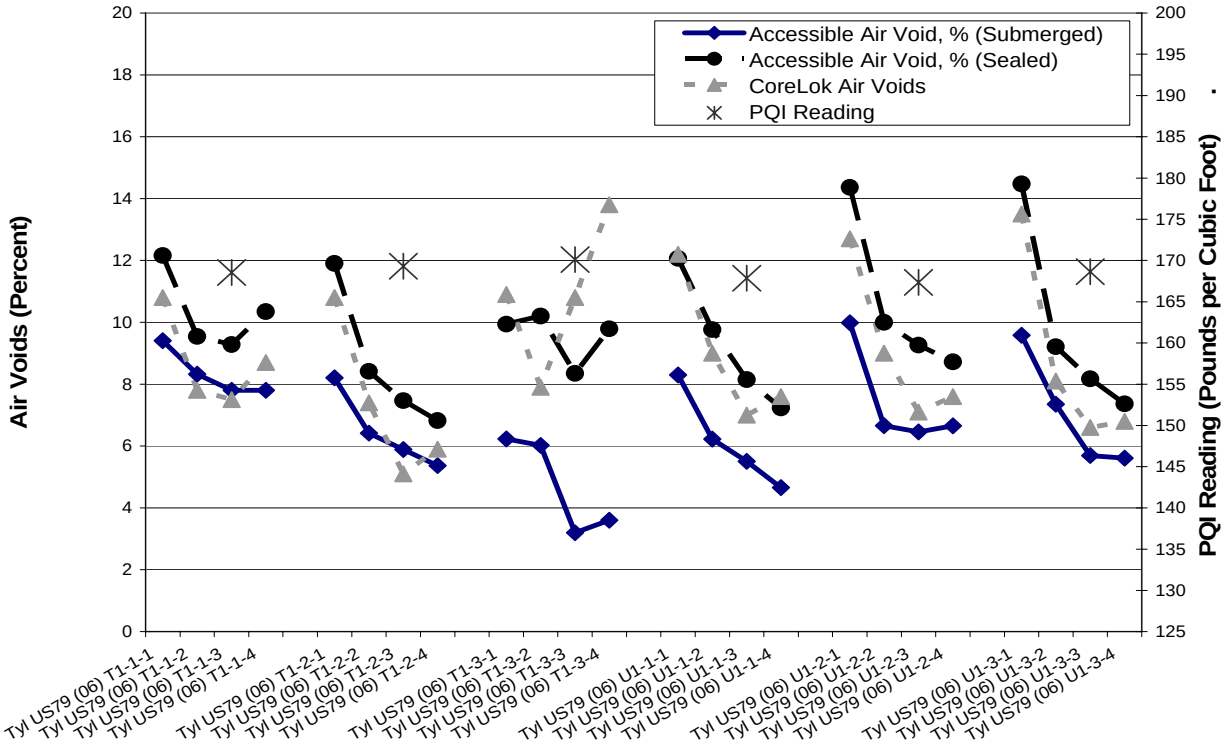

Figure D-28. Tyler US79, 2006 Cores.

APPENDIX E

ASPHALT PAVEMENT ANALYZER (APA)

LABORATORY TESTING RESULTS

ASPHALT PAVEMENT ANALYZER LABORATORY TESTING RESULTS

ASPHALT PAVEMENT ANALYZER LABORATORY TESTING

The purpose of conducting APA tests was to ensure that the rejuvenator and fog seal did not soften the surface so much that rutting would occur. The following graphs illustrate that no appreciable softening occurred.

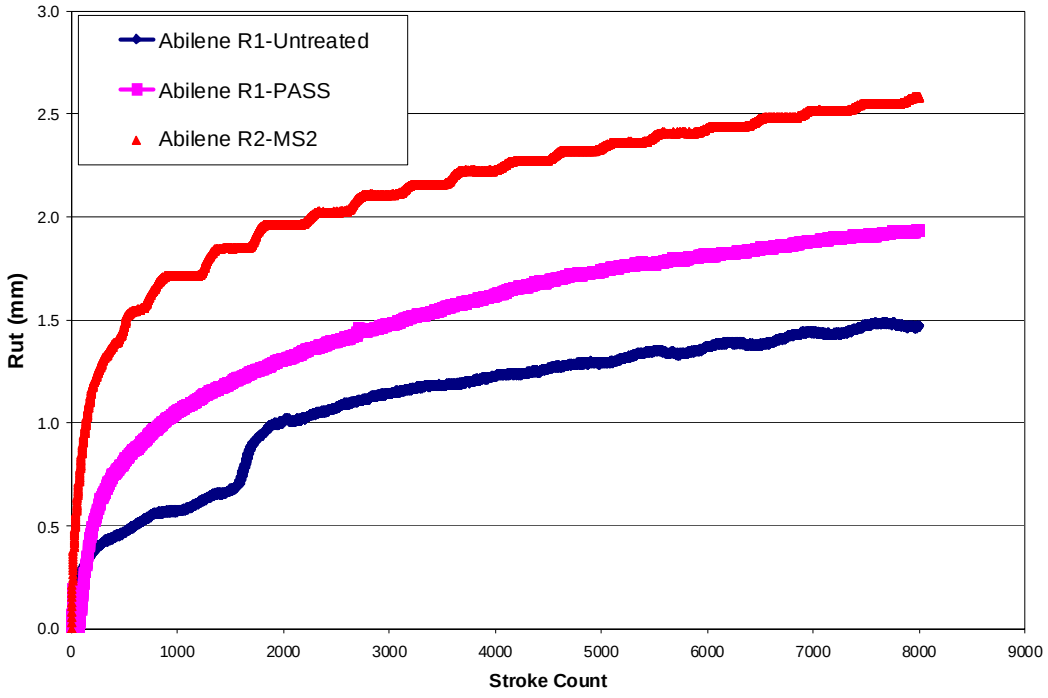

Figure E-1. Asphalt Pavement Analyzer Results for Abilene R1 and R2.

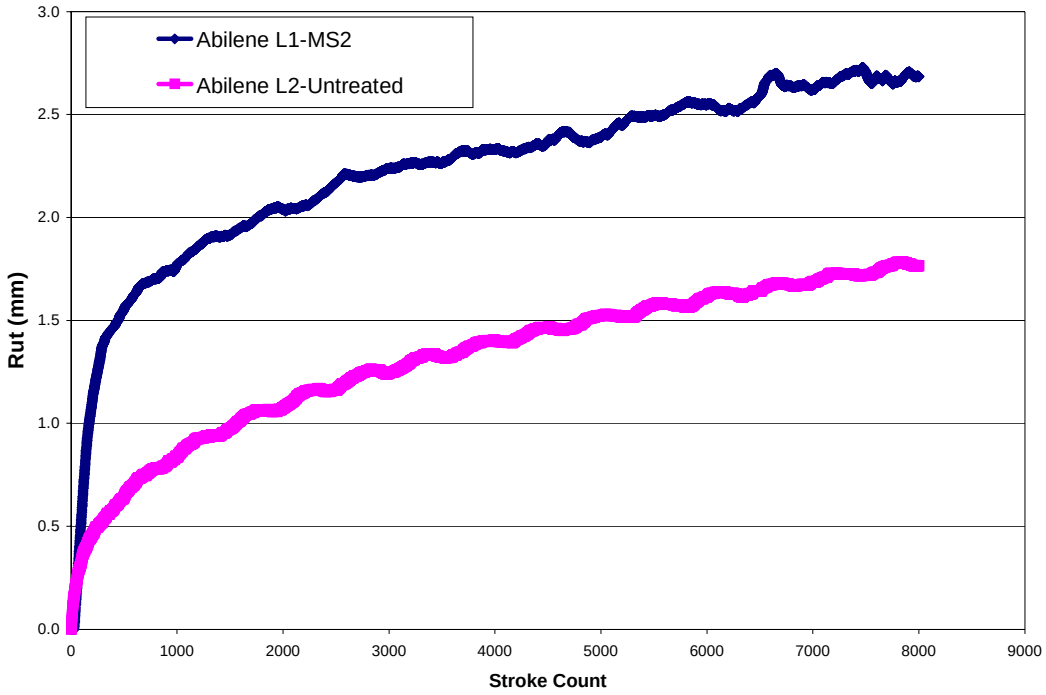

Figure E-2. Asphalt Pavement Analyzer Results for Abilene L1 and L2.

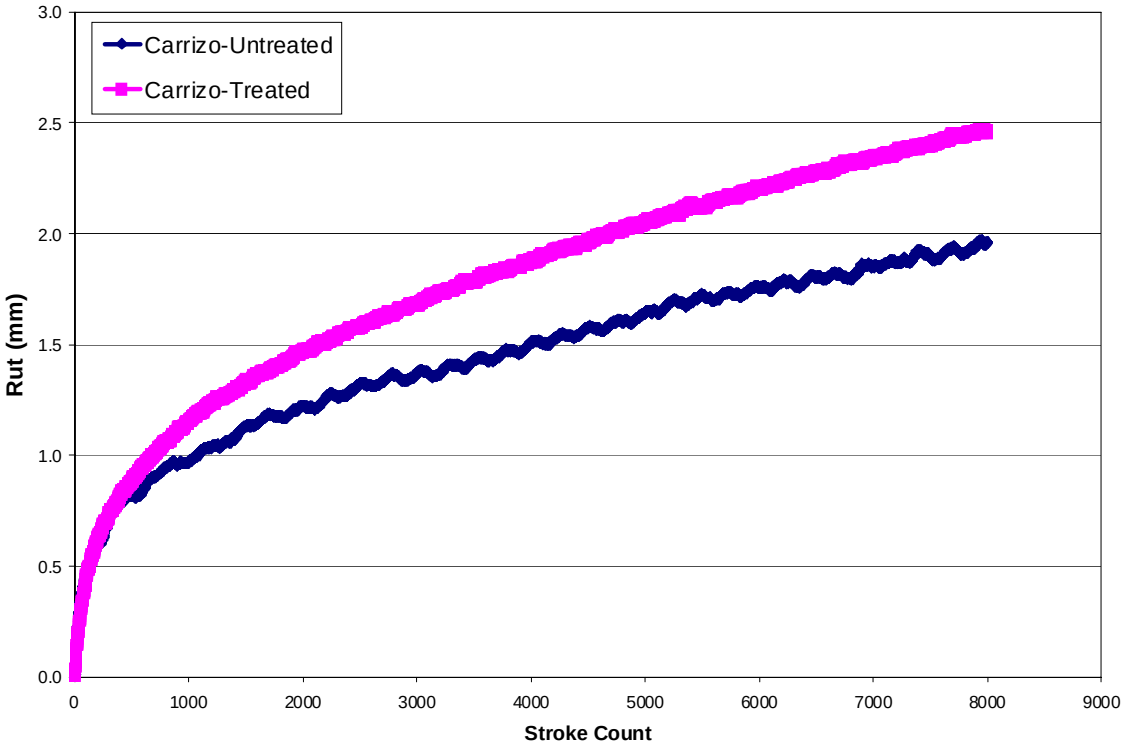

Figure E-3. Asphalt Pavement Analyzer Results for Carrizo Springs.

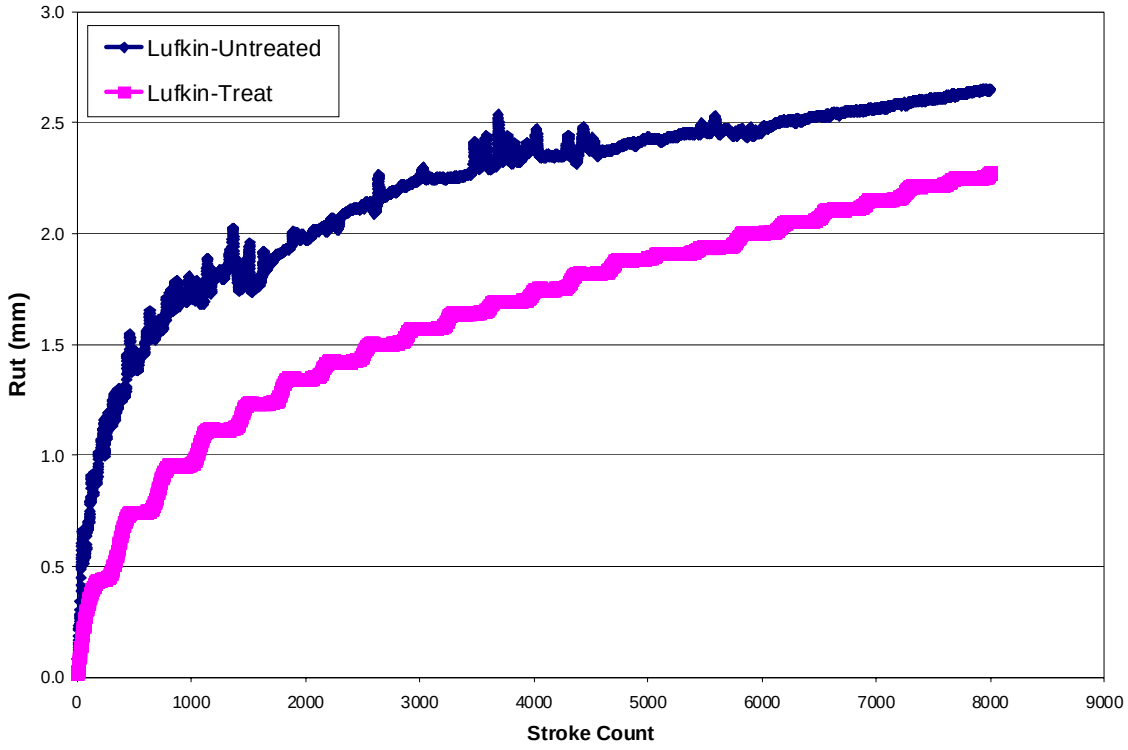

Figure E-4. Asphalt Pavement Analyzer Results for Lufkin BUS 59.

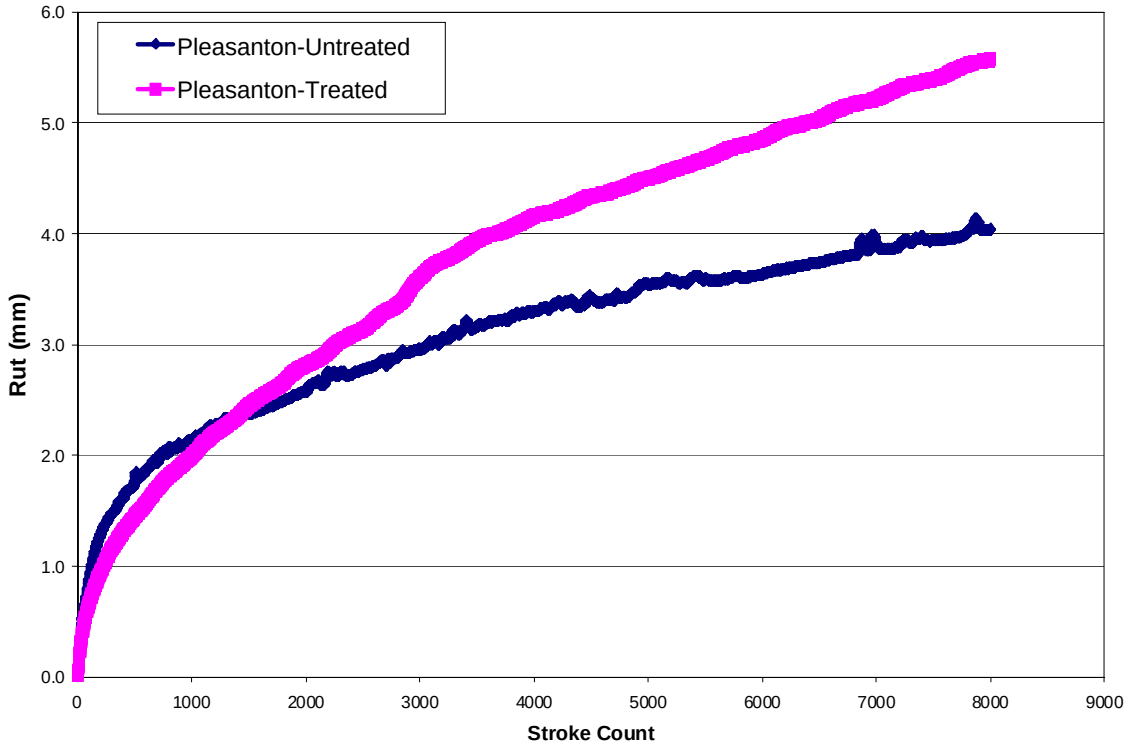

Figure E-5. Asphalt Pavement Analyzer Results for Pleasanton Airport.

APPENDIX F

VISCOSITY MASTER CURVES OF BASE MATERIALS

FROM FOG SEAL EMULSIONS

AND RECOVERED ASPHALT BINDERS

FROM TEST SITES (BY LAYER)

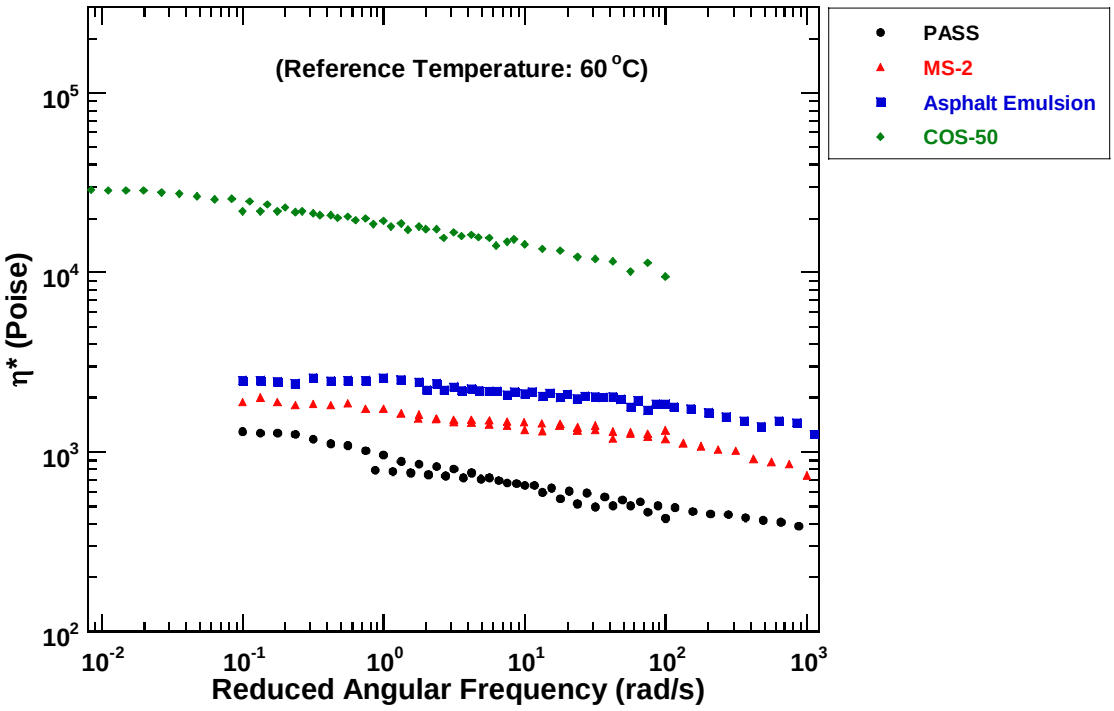

Figure F-1. Complex Viscosity Master Curves for Base Materials of Fog Seal Emulsions.

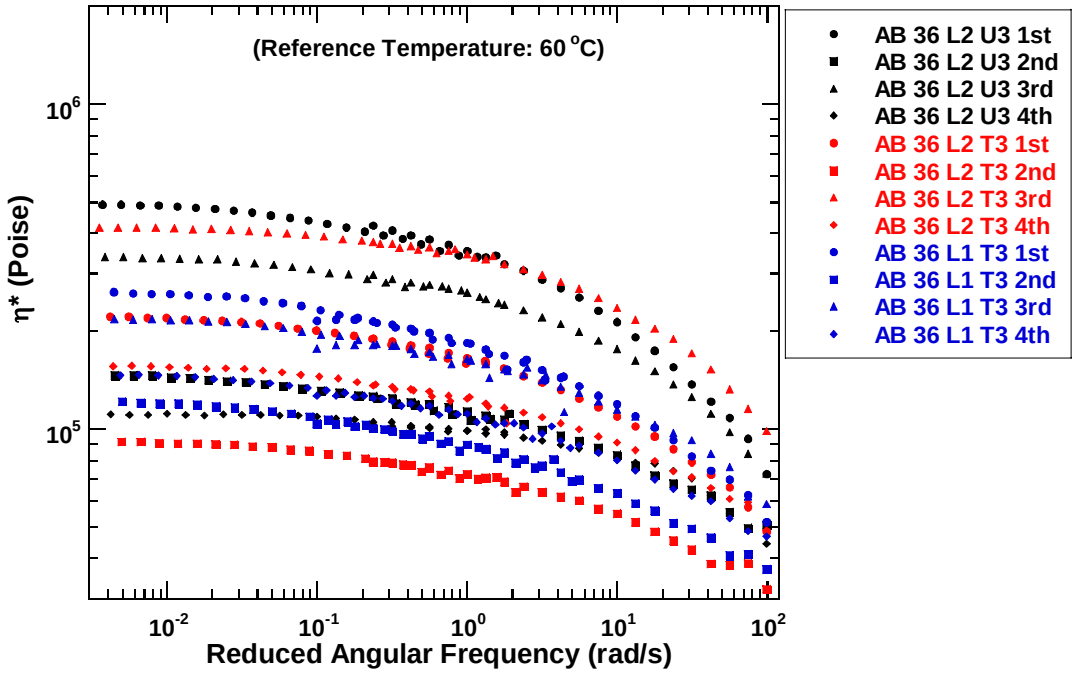

Figure F-2. Complex Viscosity Master Curves
Abilene SH 36 L1 T3, Abilene SH 36 L2 U3 and T3.

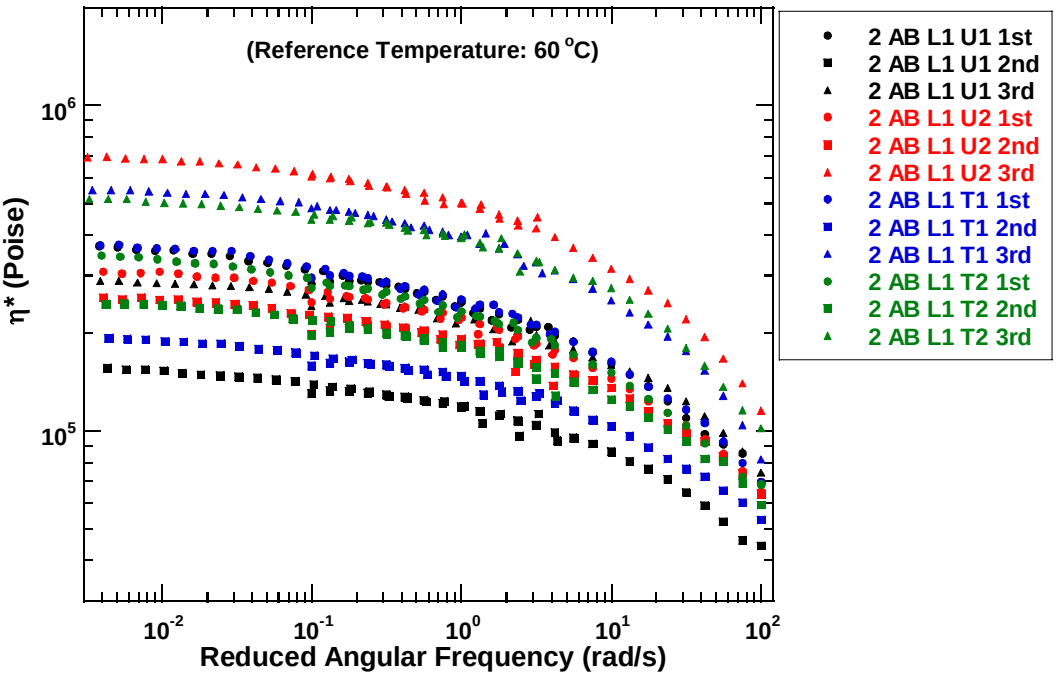

Figure F-3. Complex Viscosity Master Curves 2nd Set Abilene SH 36 L1 U1, U2, T1, and T2.

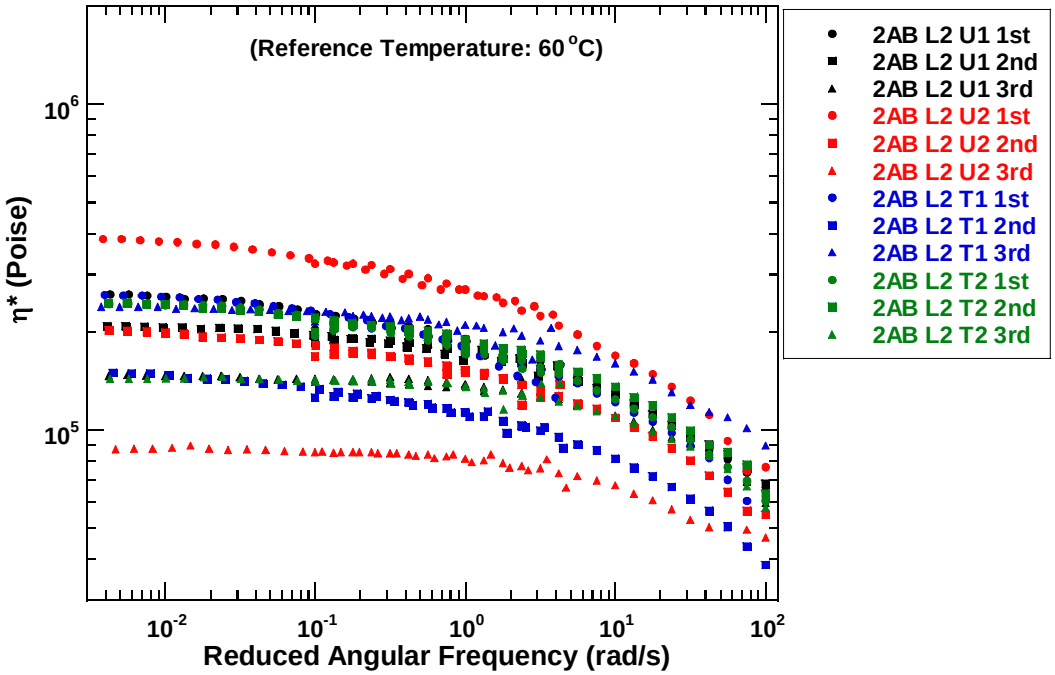

Figure F-4. Complex Viscosity Master Curves 2nd Set Abilene SH 36 L2 U1, U2, T1, and T2.

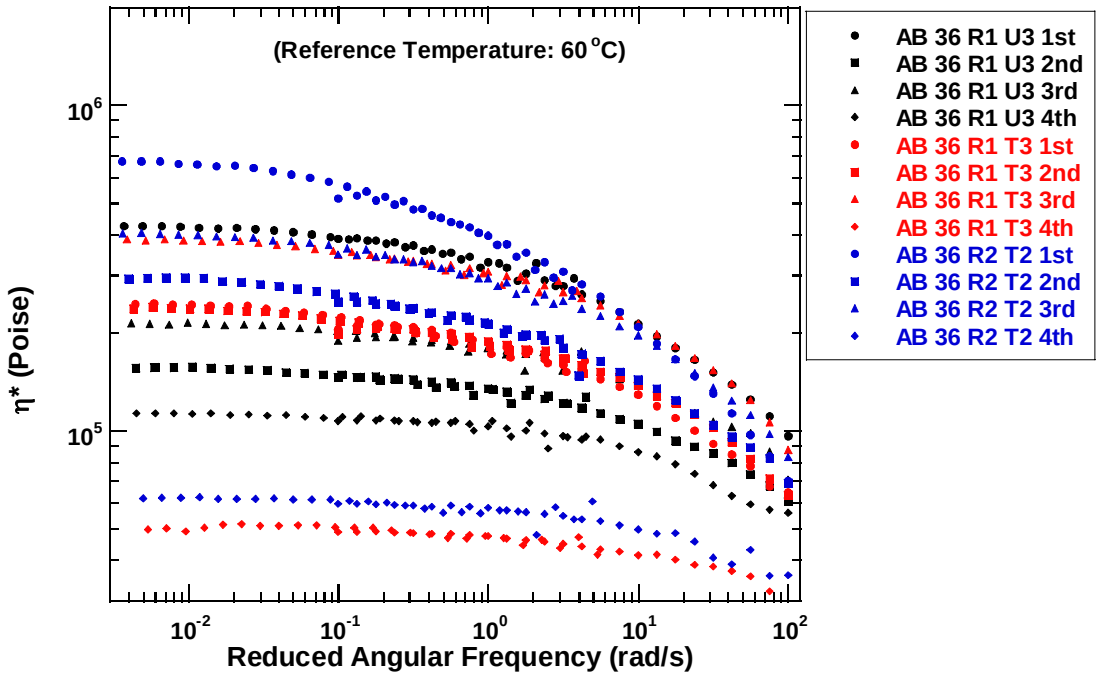

Figure F-5. Complex Viscosity Master Curves
Abilene SH 36 R1 U3 and T3, Abilene SH 36 R2 T2.

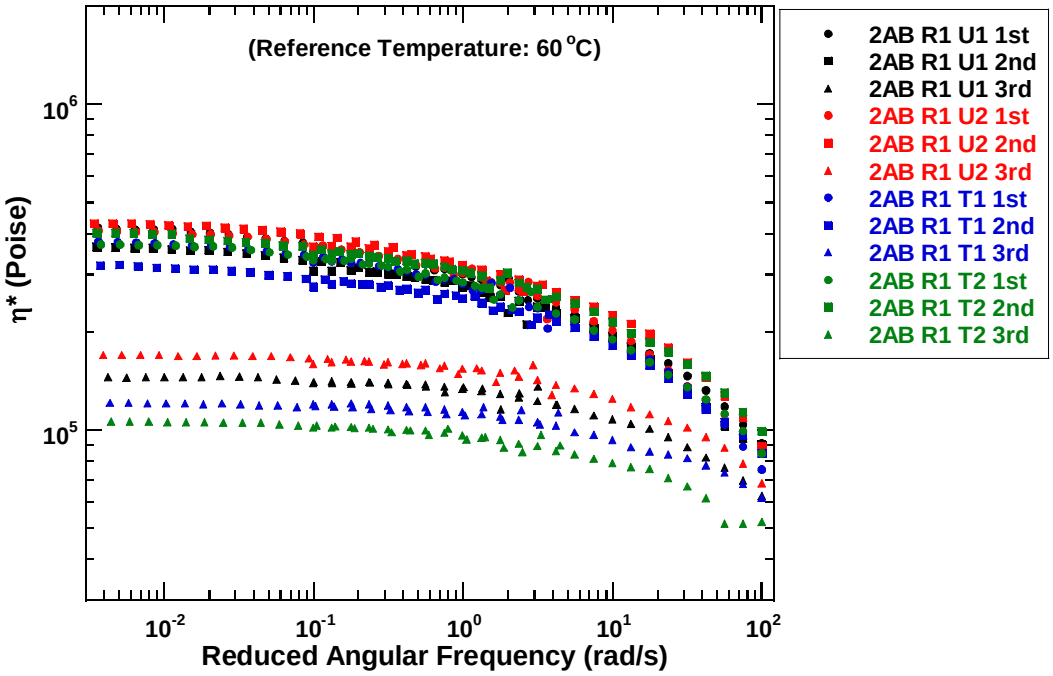

Figure F-6. Complex Viscosity Master Curves
2nd Set Abilene SH 36 R1 U1, U2, T1, and T2.

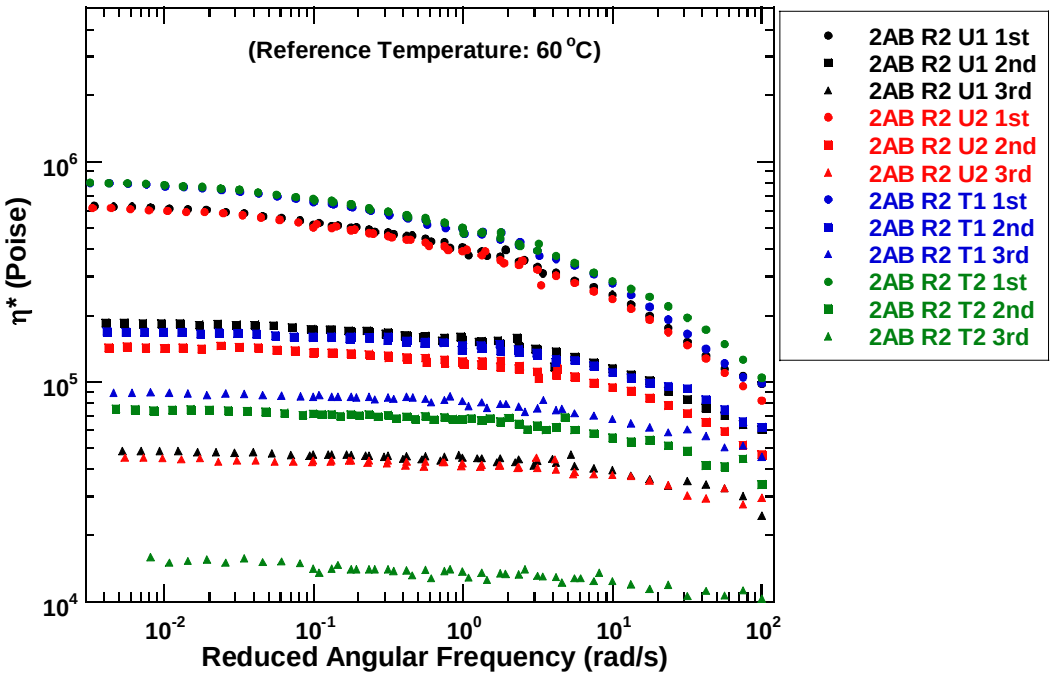

Figure F-7. Complex Viscosity Master Curves 2nd Set Abilene SH 36 R2 U1, U2, T1, and T2.

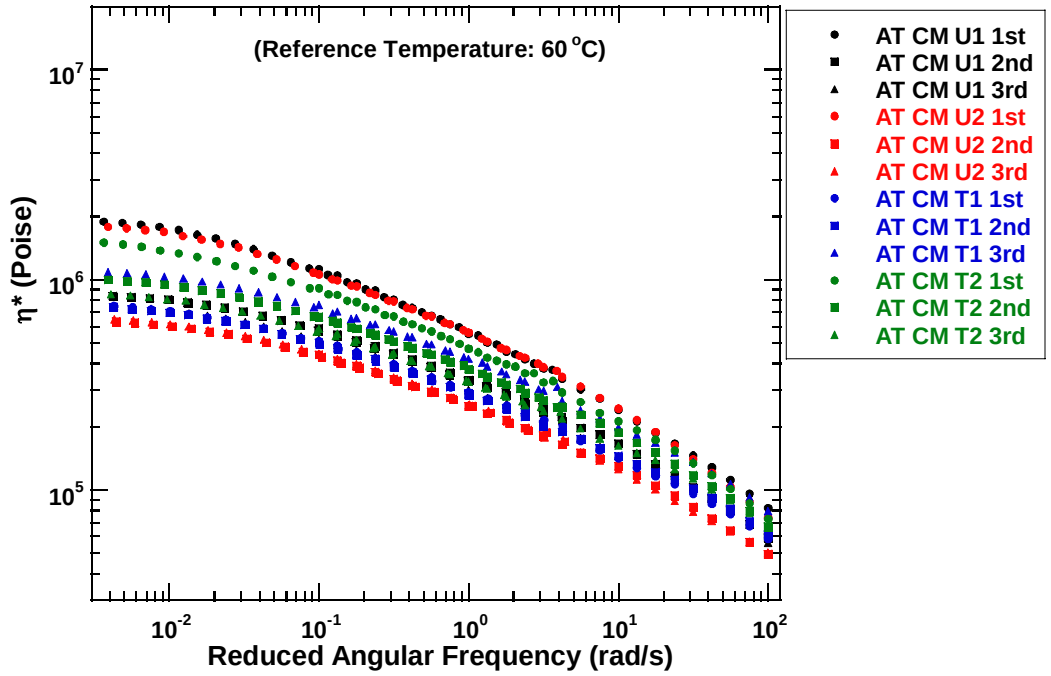

Figure F-8. Complex Viscosity Master Curves Atlanta IH 20 CM U1, U2, T1, and T2.

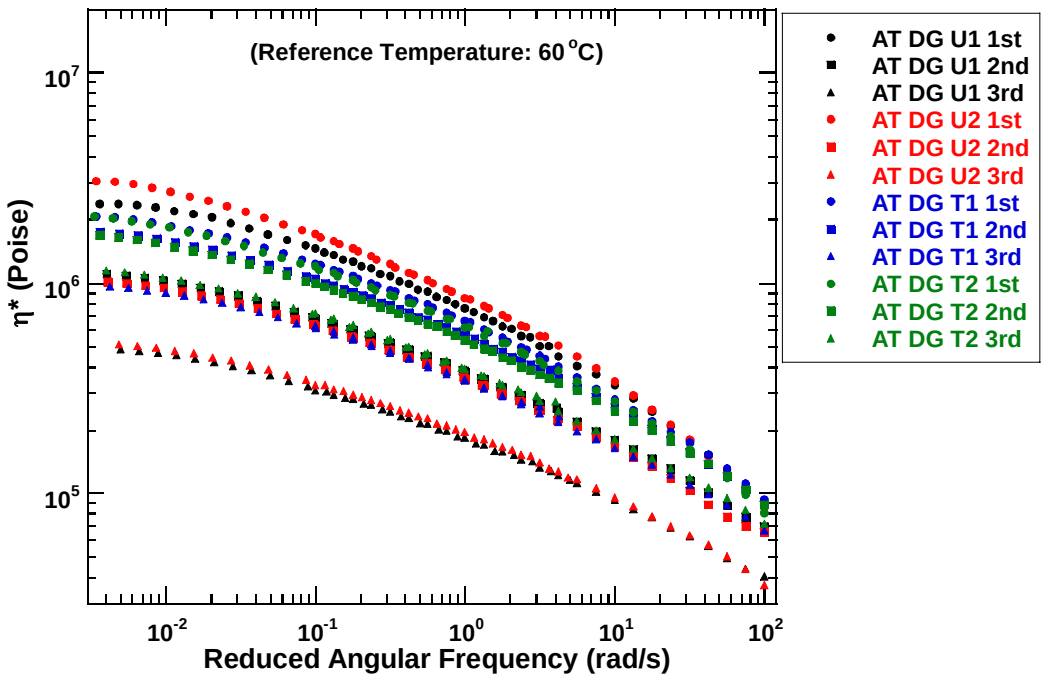

Figure F-9. Complex Viscosity Master Curves Atlanta IH 20 DG U1, U2, T1, and T2.

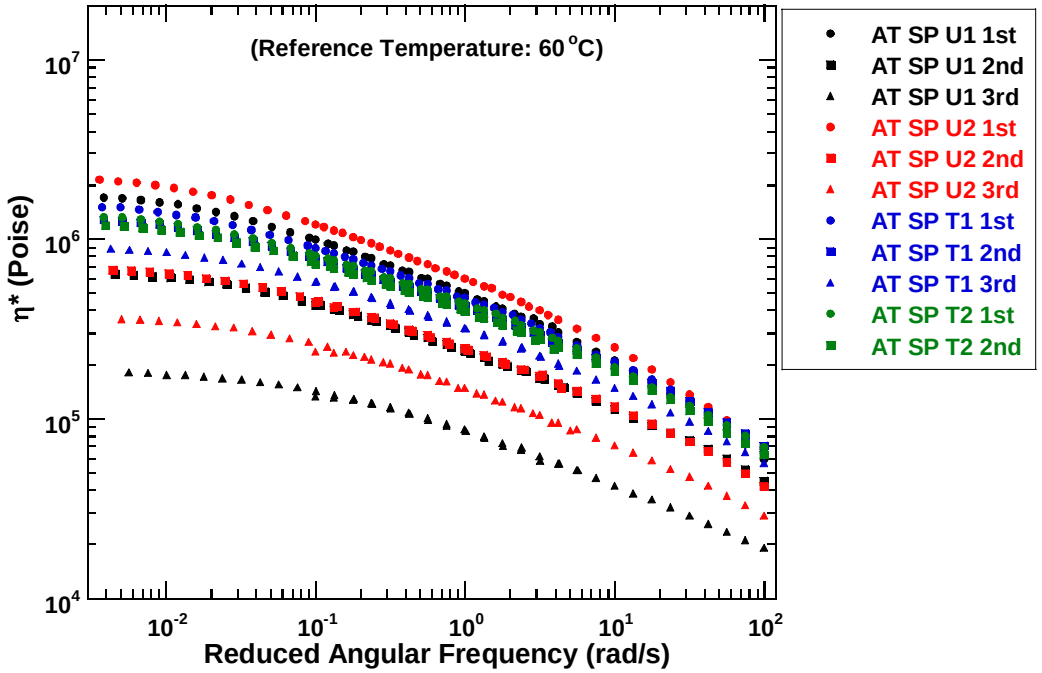

Figure F-10. Complex Viscosity Master Curves Atlanta IH 20 SP U1, U2, T1, and T2.

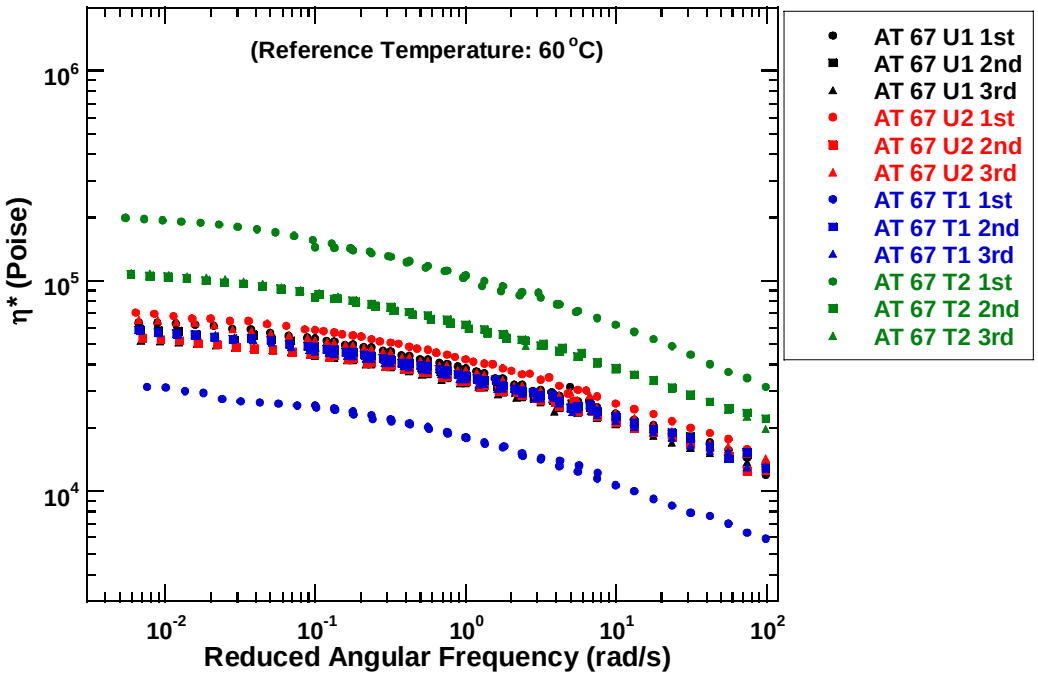

Figure F-11. Complex Viscosity Master Curves
Atlanta US 67 U1, U2, T1, and T2.

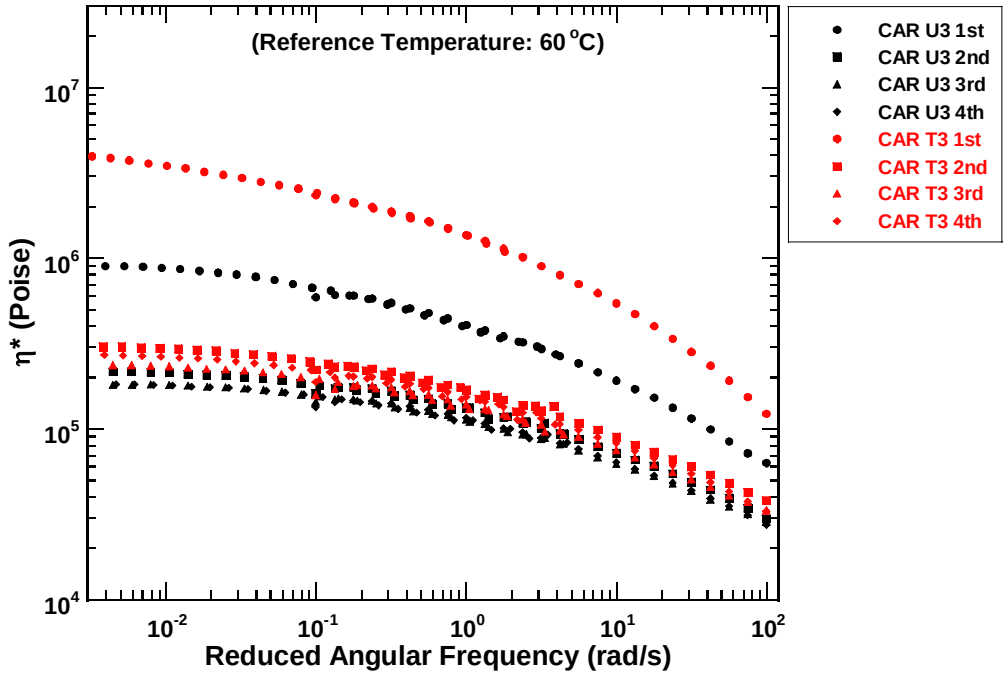

Figure F-12. Complex Viscosity Master Curves
Carrizo Springs Airport U3 and T3.

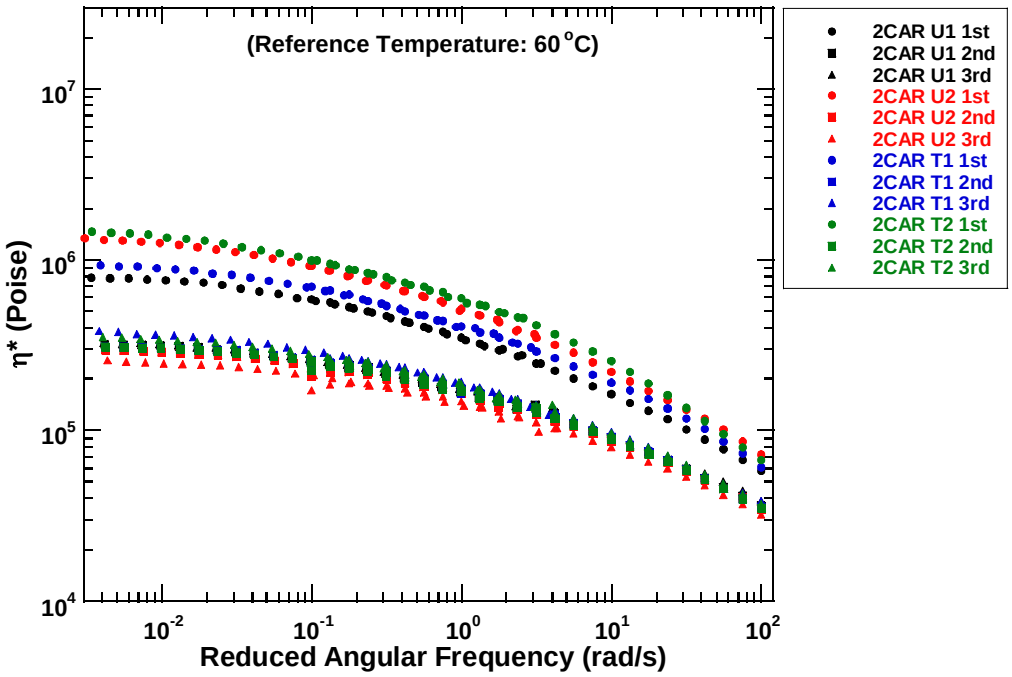

Figure F-13. Complex Viscosity Master Curves
2nd Set Carrizo Springs Airport U1, U2, T1, and T2.

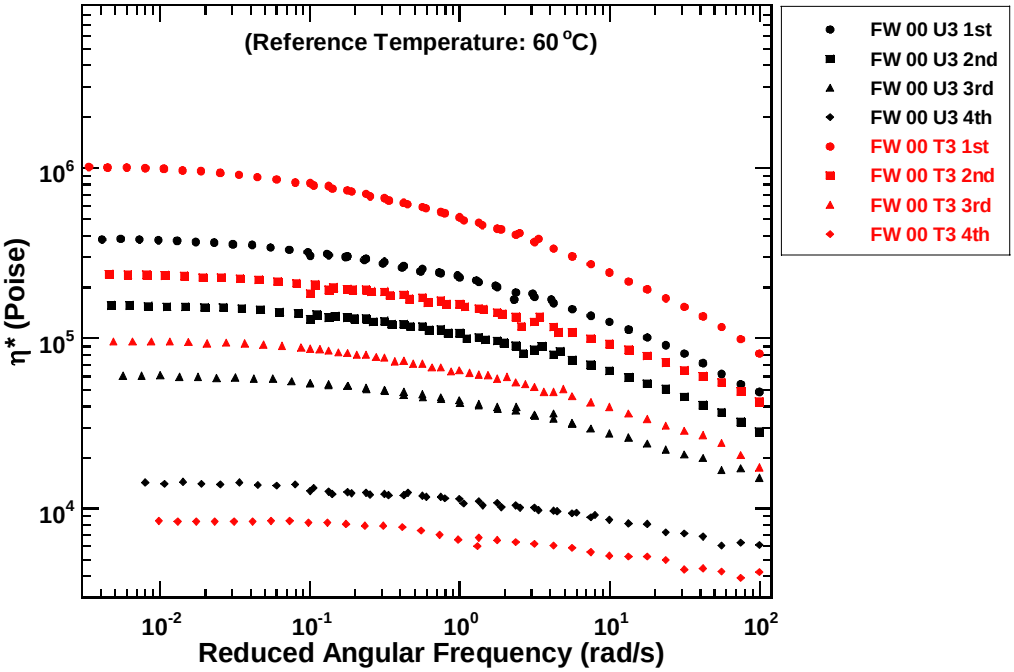

Figure F-14. Complex Viscosity Master Curves
Fort Worth FM 4 (2000) U3 and T3.

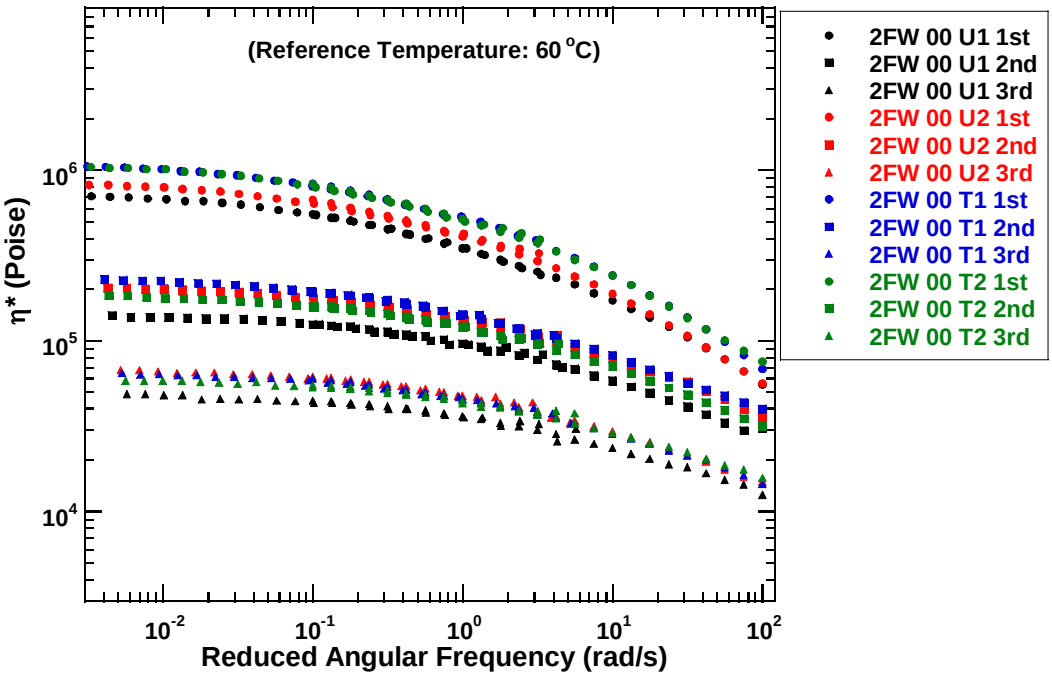

Figure F-15. Complex Viscosity Master Curves
2nd Set Fort Worth FM 4 (2000) U1, U2, T1, and T2.

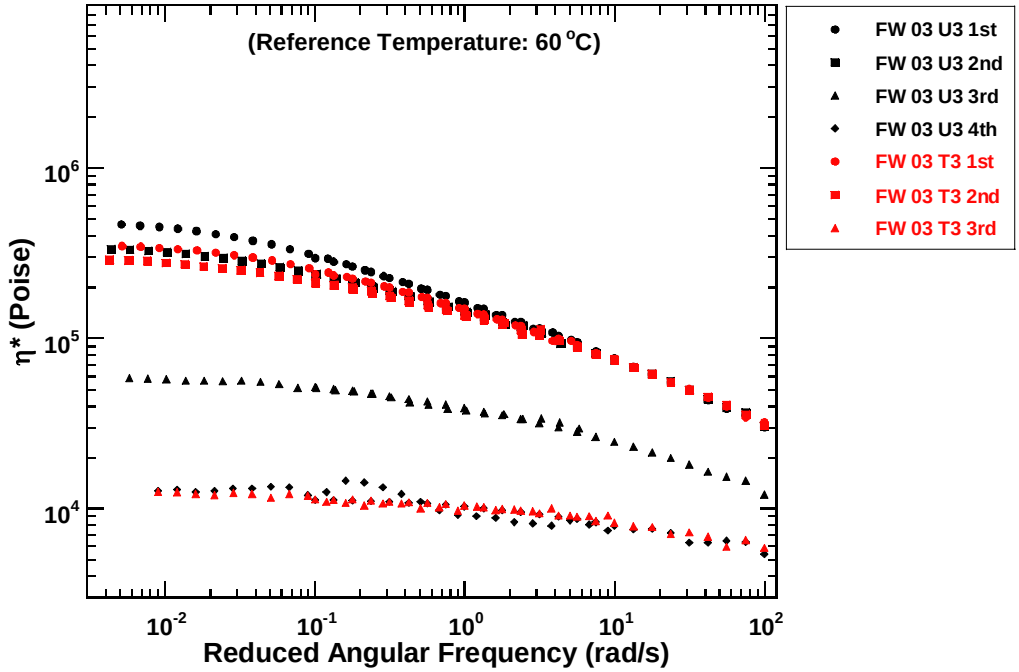

Figure F-16. Complex Viscosity Master Curves
Fort Worth FM 4 (2003) U3 and T3.

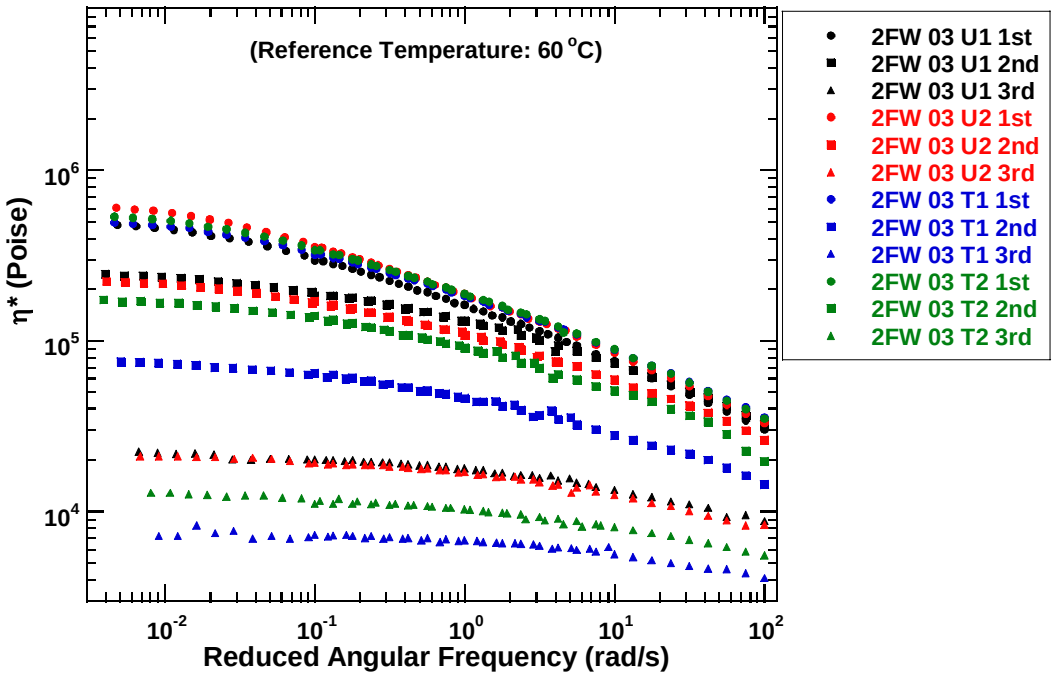

Figure F-17. Complex Viscosity Master Curves
2nd Set Fort Worth FM 4 (2003) U1, U2, T1, and T2.

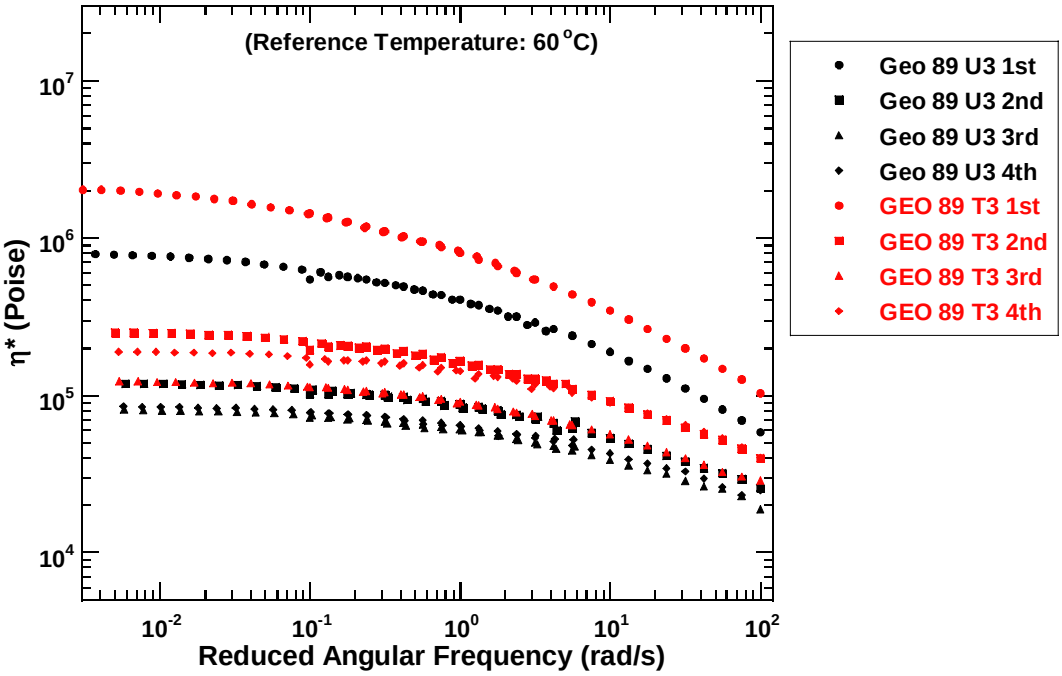

Figure F-18. Complex Viscosity Master Curves
Georgetown Airport (1989) U3 and T3.

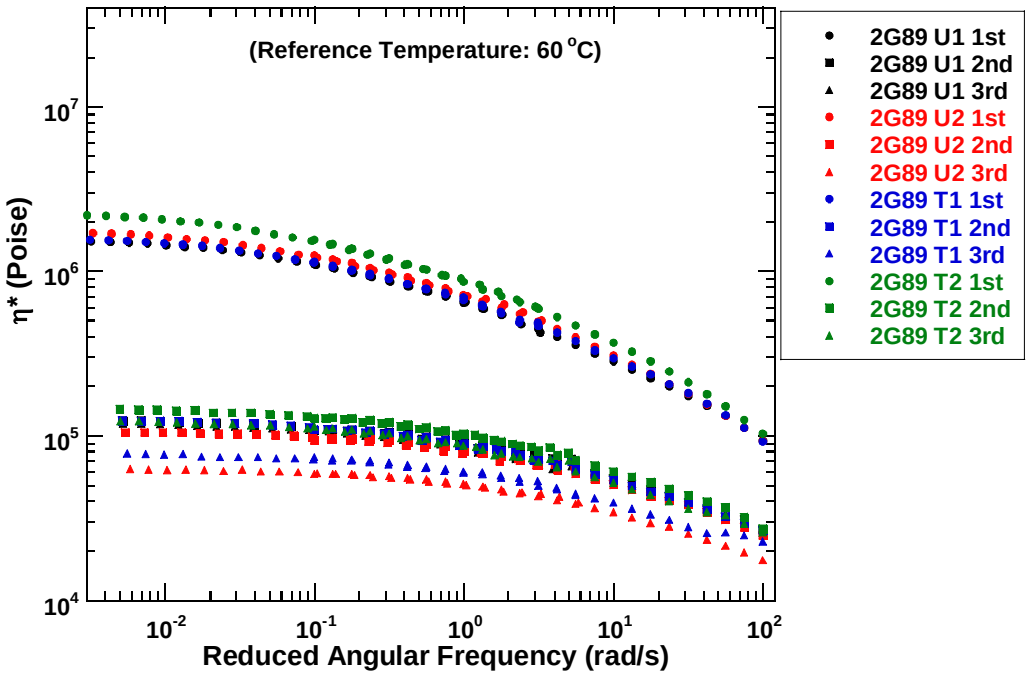

Figure F-19. Complex Viscosity Master Curves
2nd Set Georgetown Airport (1989) U1, U2, T1, and T2.

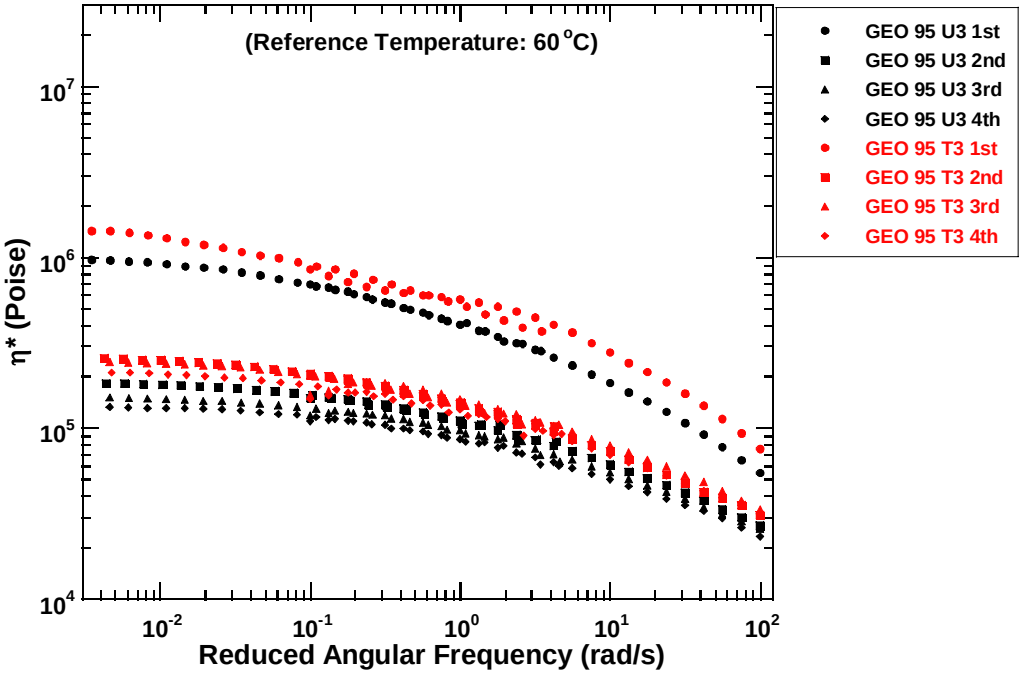

Figure F-20. Complex Viscosity Master Curves
Georgetown Airport (1995) U3 and T3.

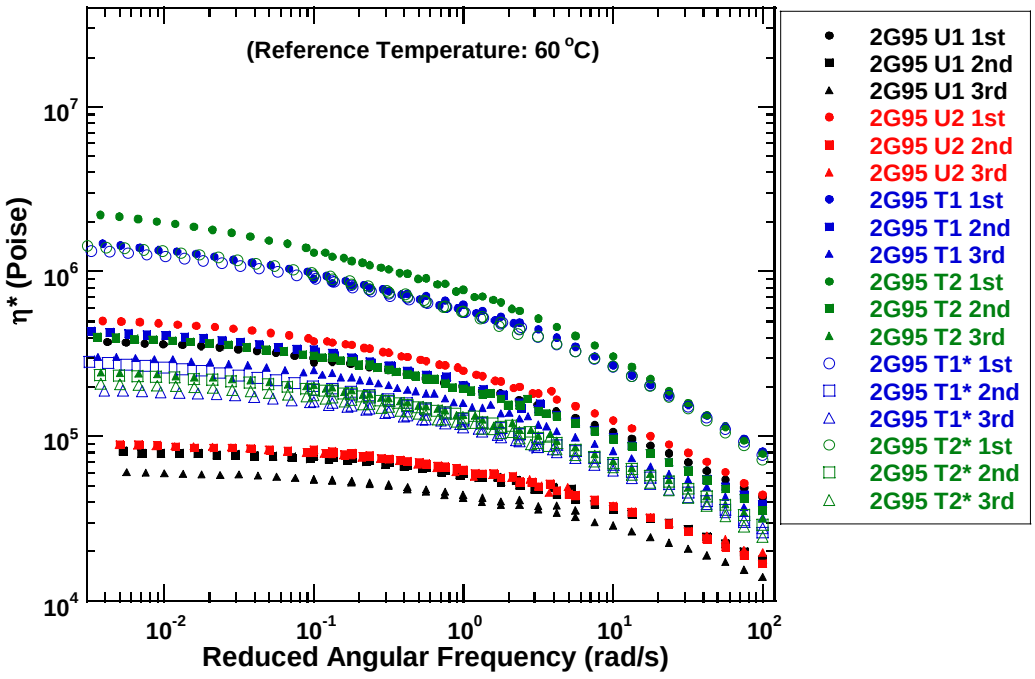

Figure F-21. Complex Viscosity Master Curves
2nd Set Georgetown Airport (1995) U1, U2, T1, T2, T1*, and T2*.

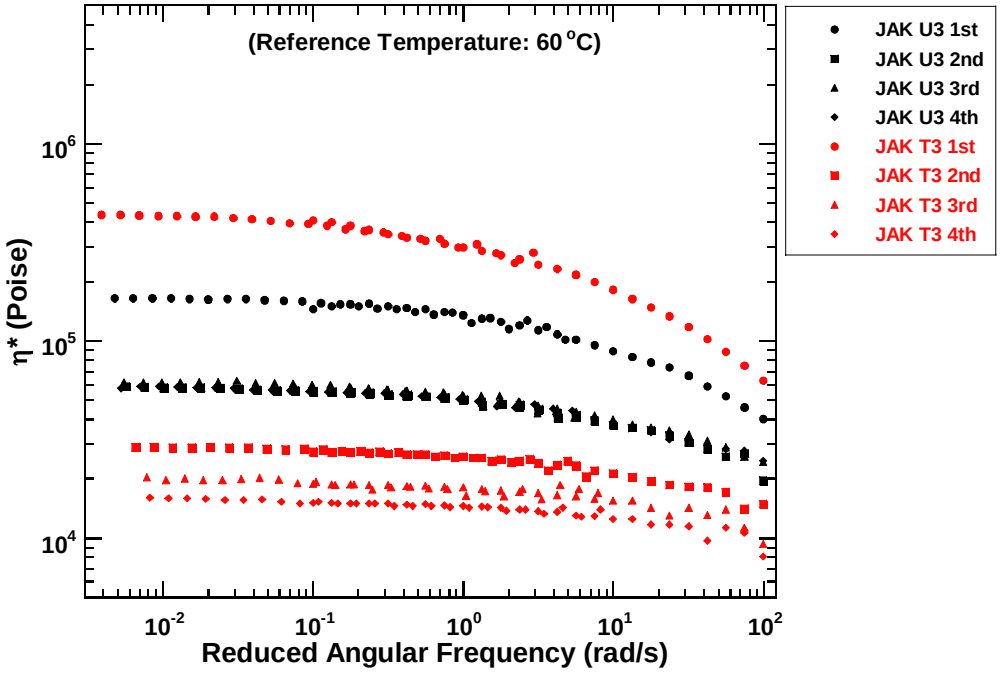

Figure F-22. Complex Viscosity Master Curves
Jacksonville Airport U3 and T3.

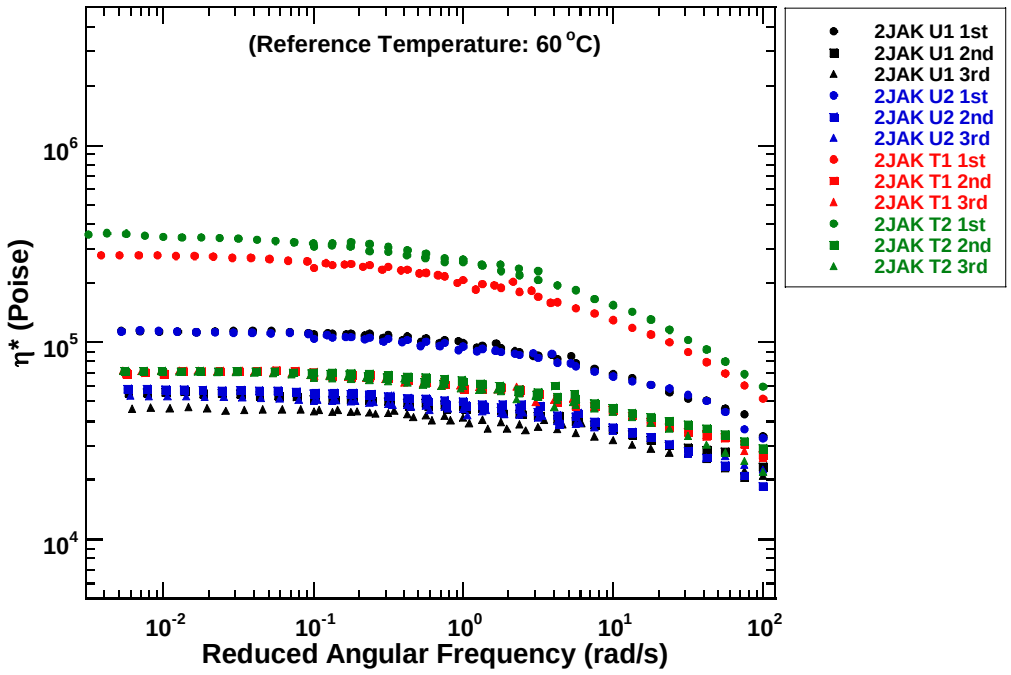

Figure F-23. Complex Viscosity Master Curves
2nd Set Jacksonville Airport U1, U2, T1, and T2.

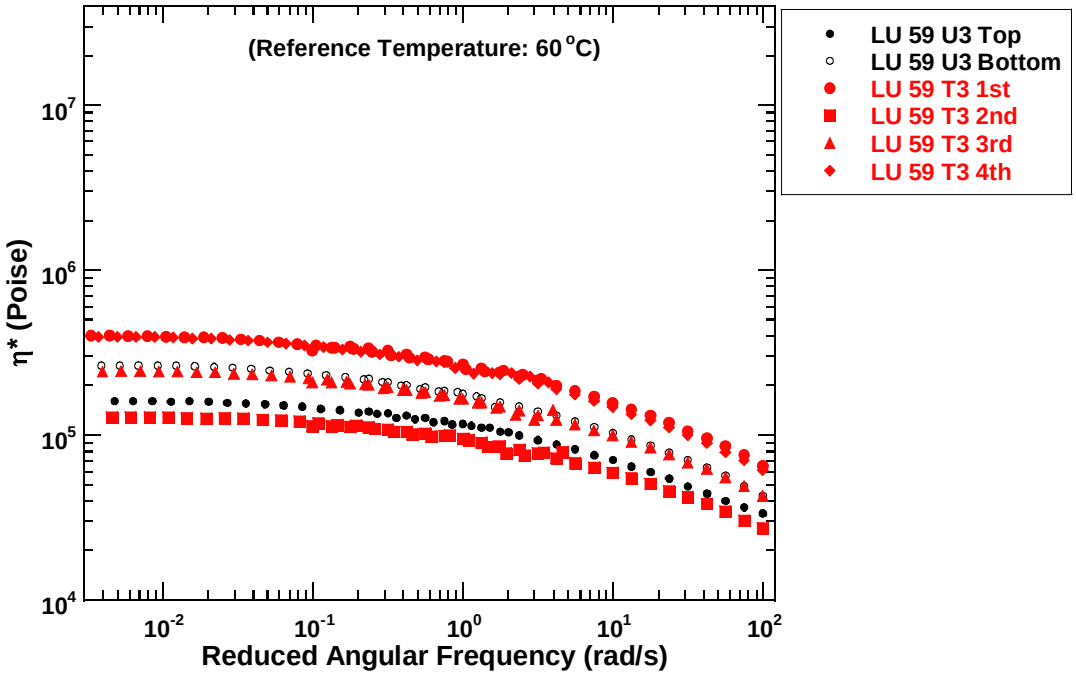

Figure F-24. Complex Viscosity Master Curves
Lufkin BUS 59 U3 and T3.

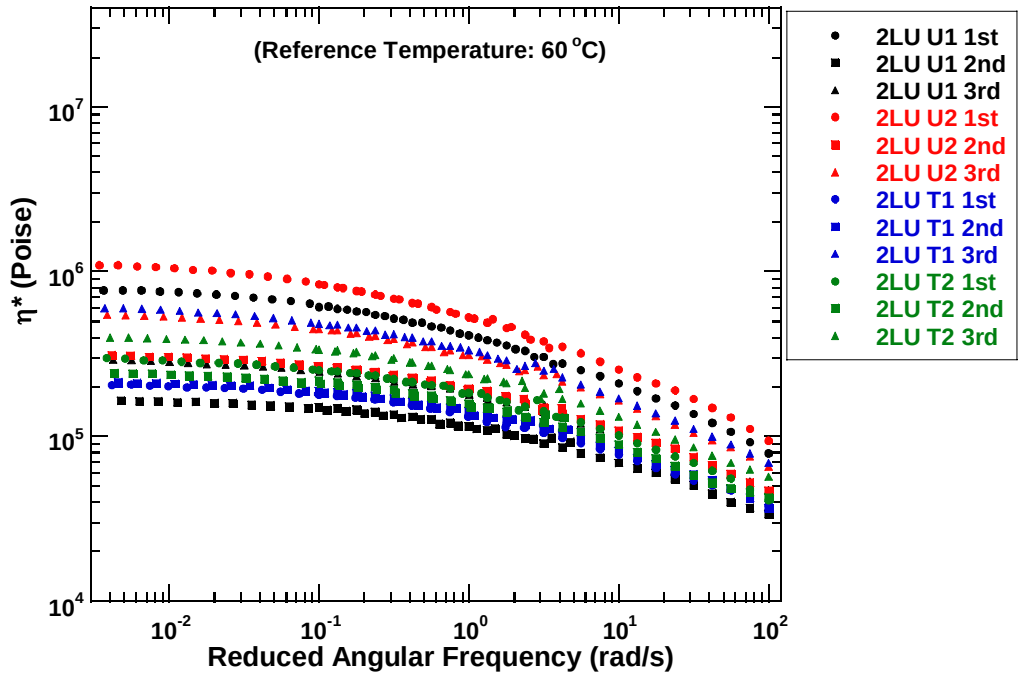

Figure F-25. Complex Viscosity Master Curves
2nd Set Lufkin BUS 59 U1, U2, T1, and T2.

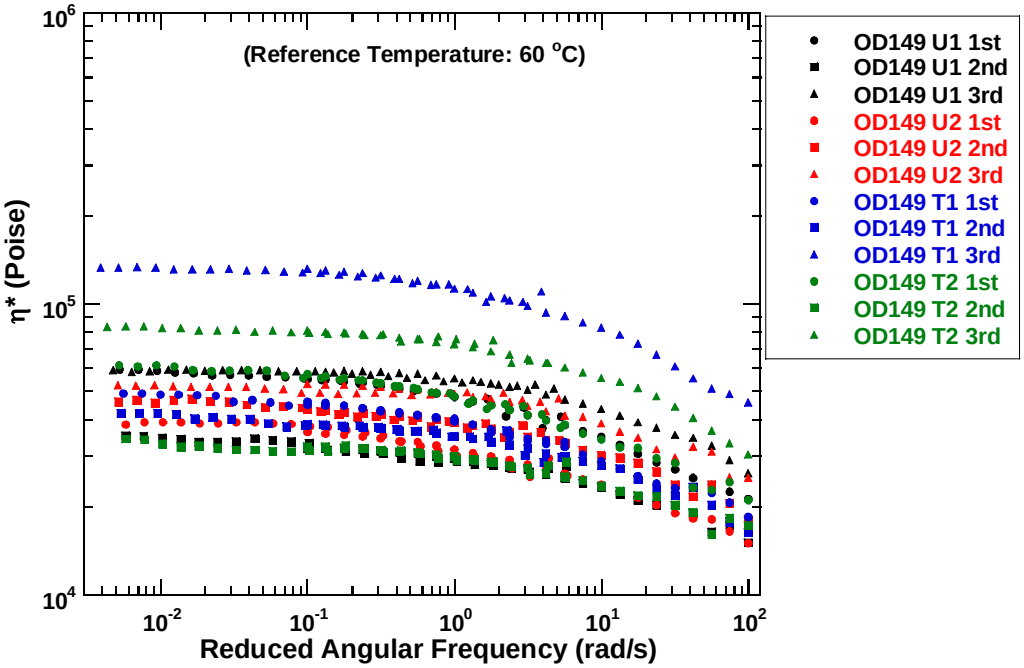

Figure F-26. Complex Viscosity Master Curves
Odessa SH 149 U1, U2, T1, and T2.

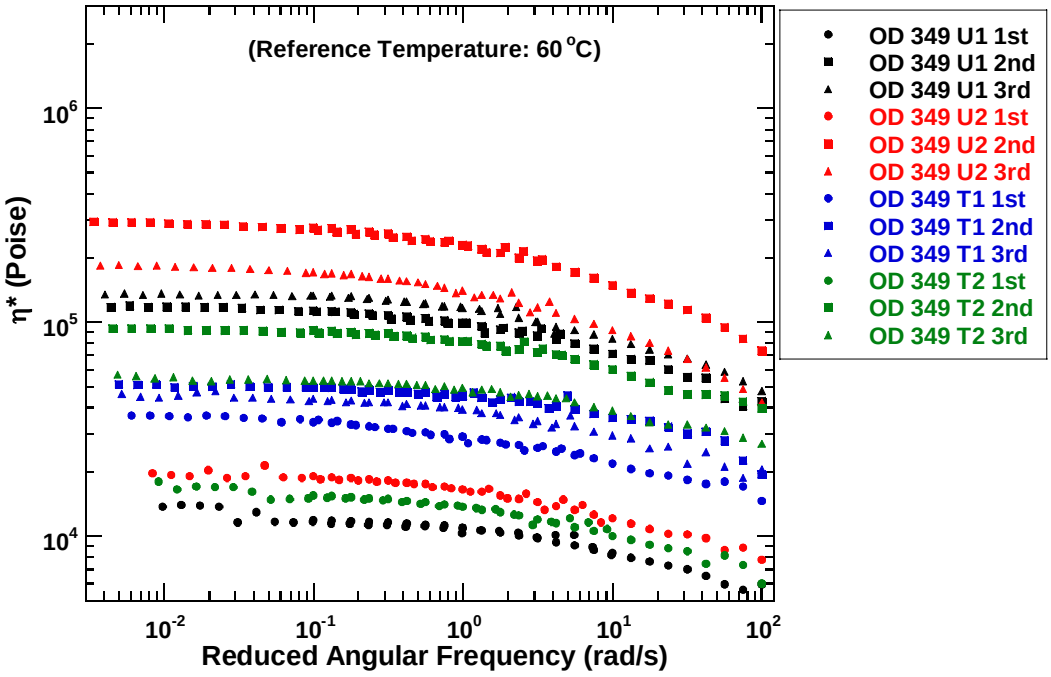

Figure F-27. Complex Viscosity Master Curves
Odessa SH 349 U1, U2, T1, and T2.

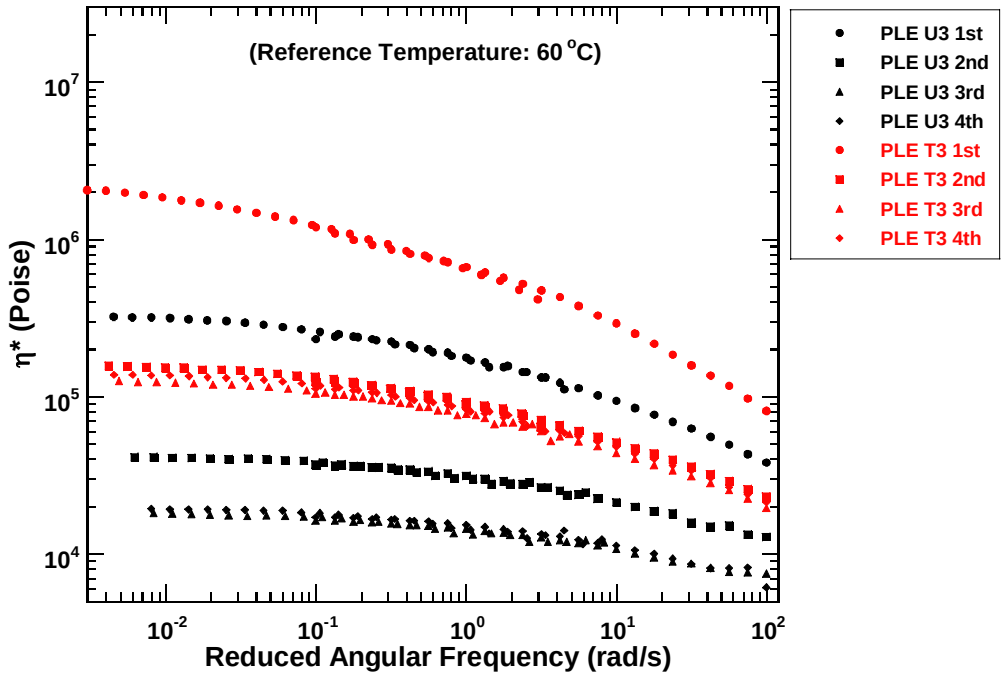

Figure F-28. Complex Viscosity Master Curves
Pleasanton Airport U3 and T3.

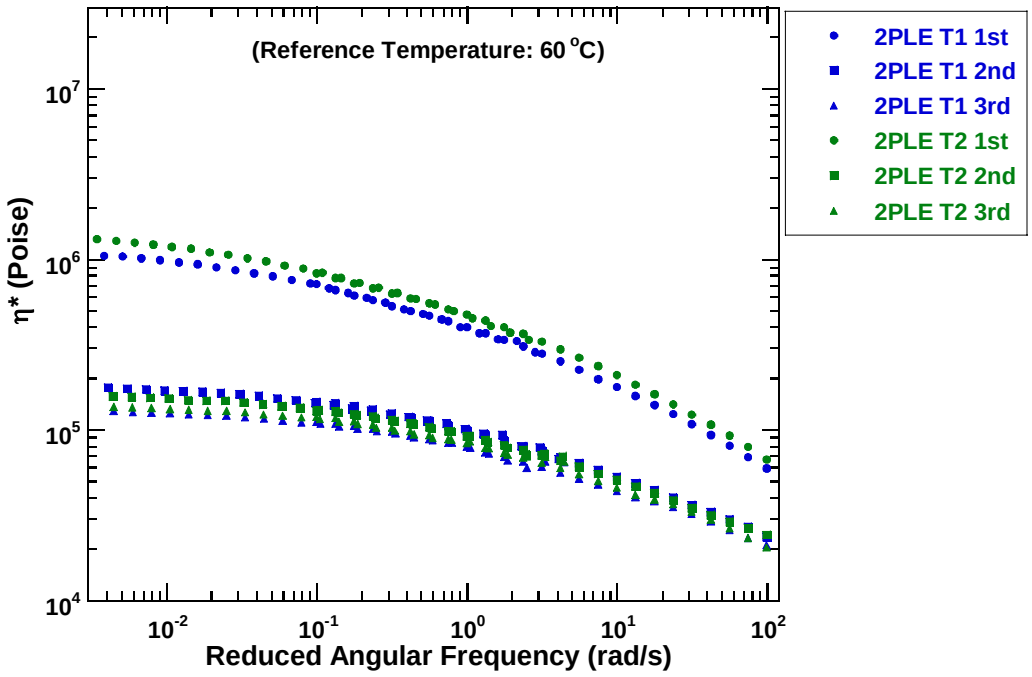

Figure F-29. Complex Viscosity Master Curves
2nd Set Pleasanton Airport T1 and T2.

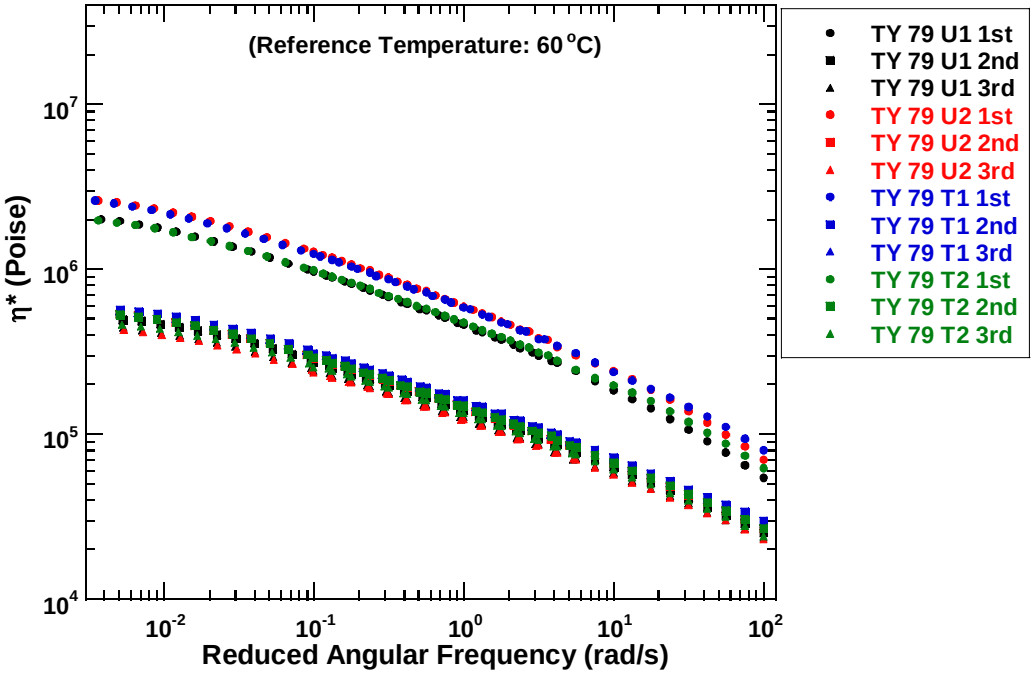

Figure F-30. Complex Viscosity Master Curves
Tyler US 79 U1, U2, T1, and T2.

APPENDIX G

ACCESSIBLE AIR VOIDS DATA COMPARISON BY LAYERS

AND

ACCESSIBLE/TOTAL AIR VOIDS DATA COMPARISON BY TEST SITES

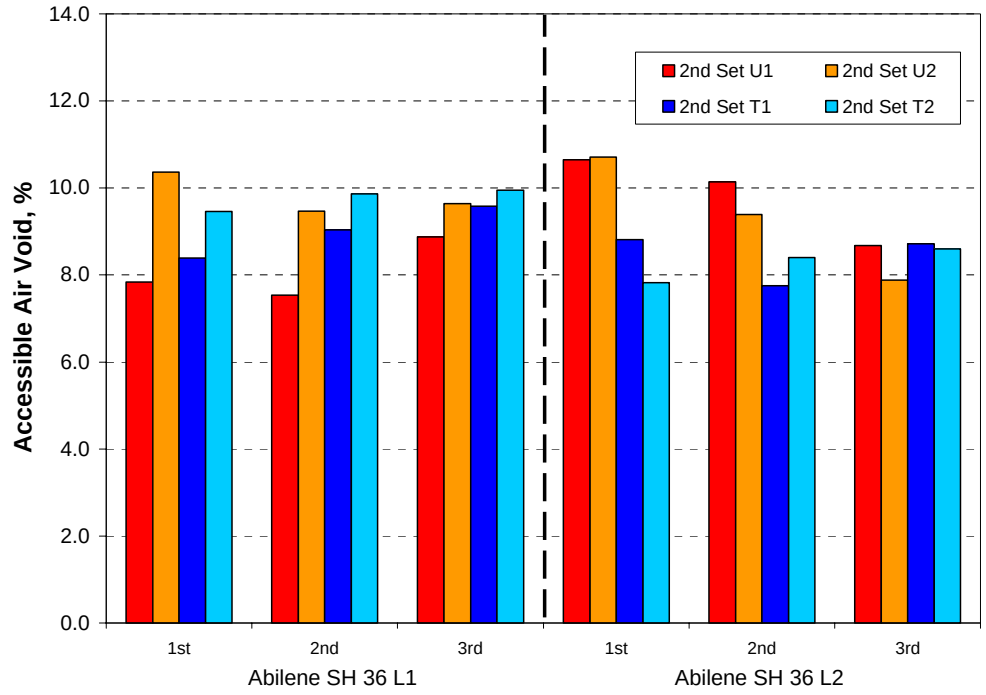

Figure G-1. Abilene SH 36 L Series Accessible Air Void Comparison by Layers.

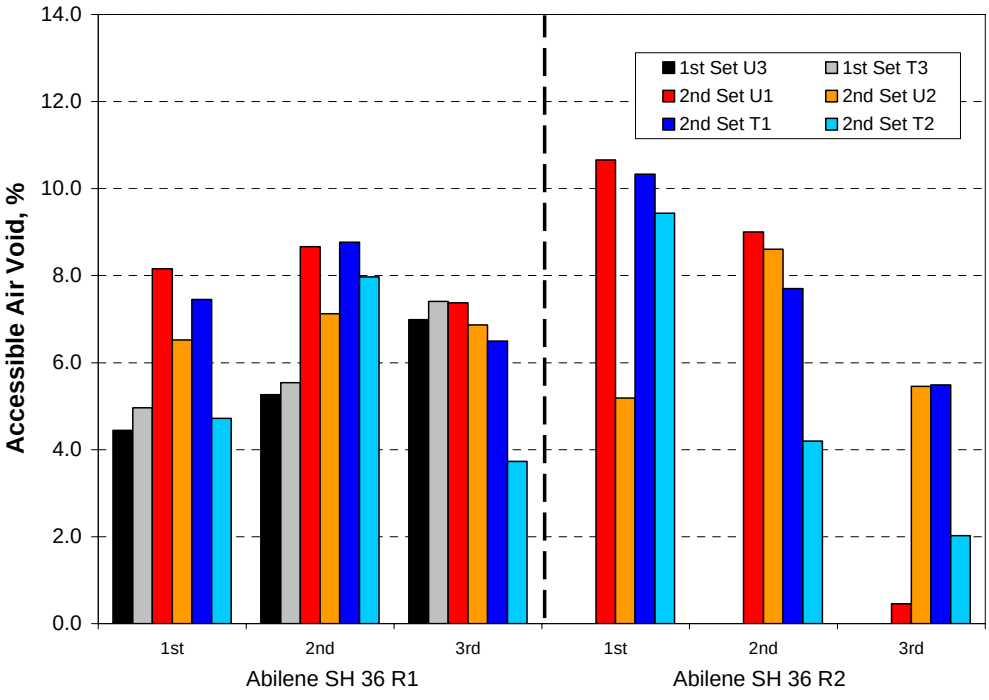

Figure G-2. Abilene SH 36 R Series Accessible Air Void Comparison by Layers.

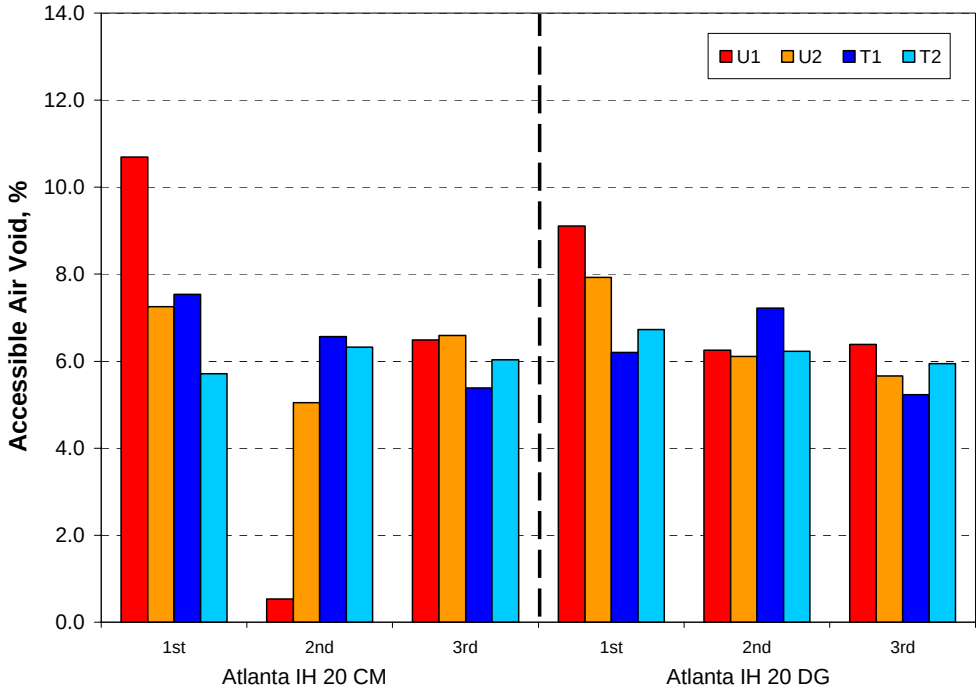

Figure G-3. Atlanta IH 20 CM and DG Accessible Air Void Comparison by Layers.

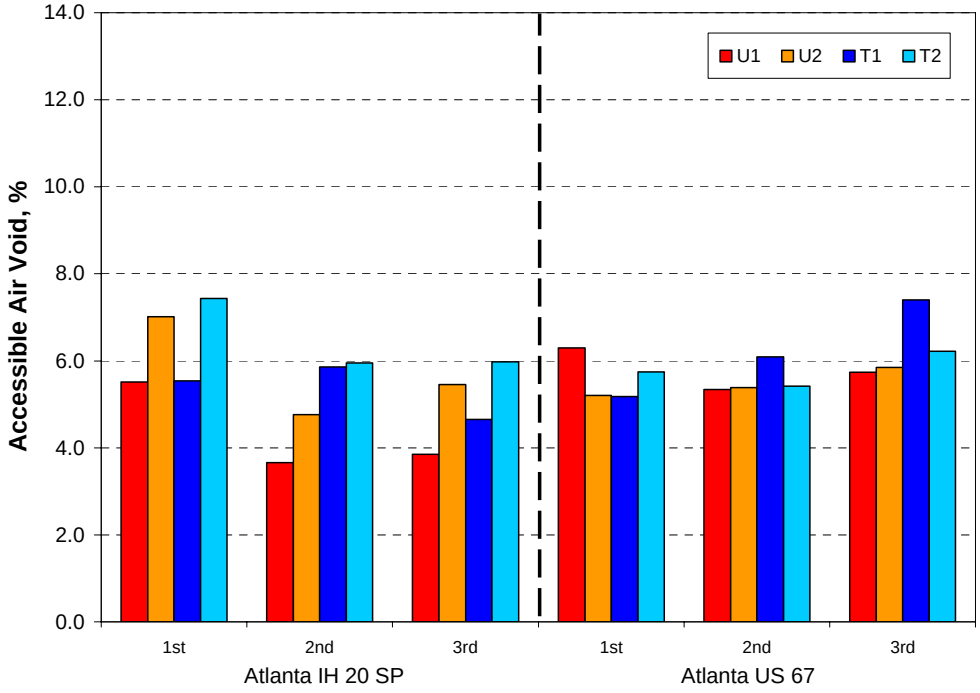

Figure G-4. Atlanta IH 20 SP and Atlanta US 67 Accessible Air Void Comparison by Layers.

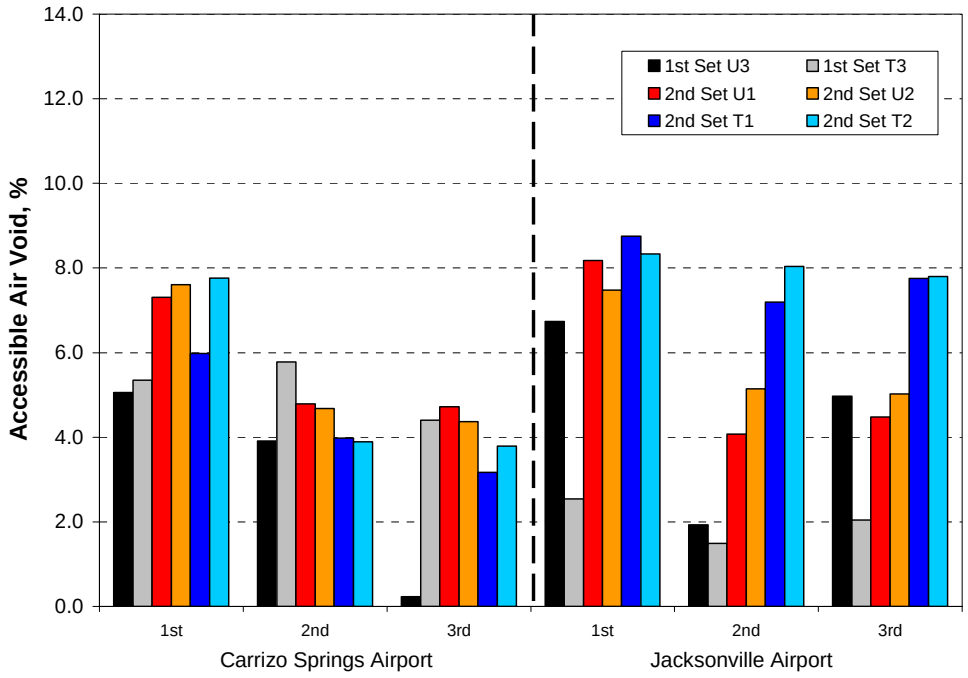

Figure G-5. Carrizo Springs Airport and Jacksonville Airport Accessible Air Void Comparison by Layers.

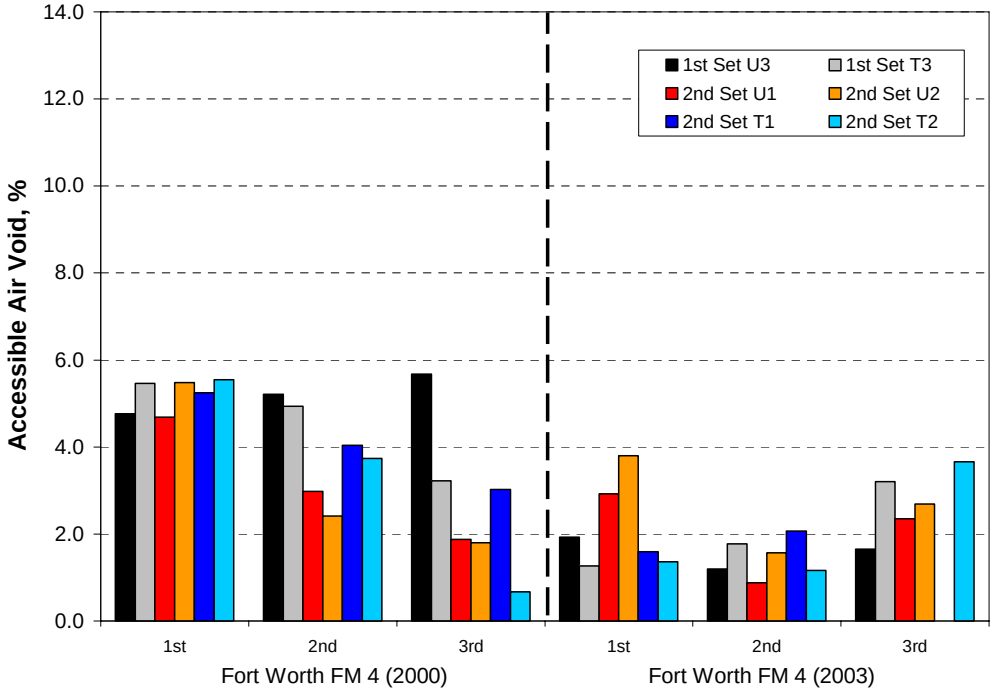

Figure G-6. Fort Worth FM 4 (2000) and (2003) Accessible Air Void Comparison by Layers.

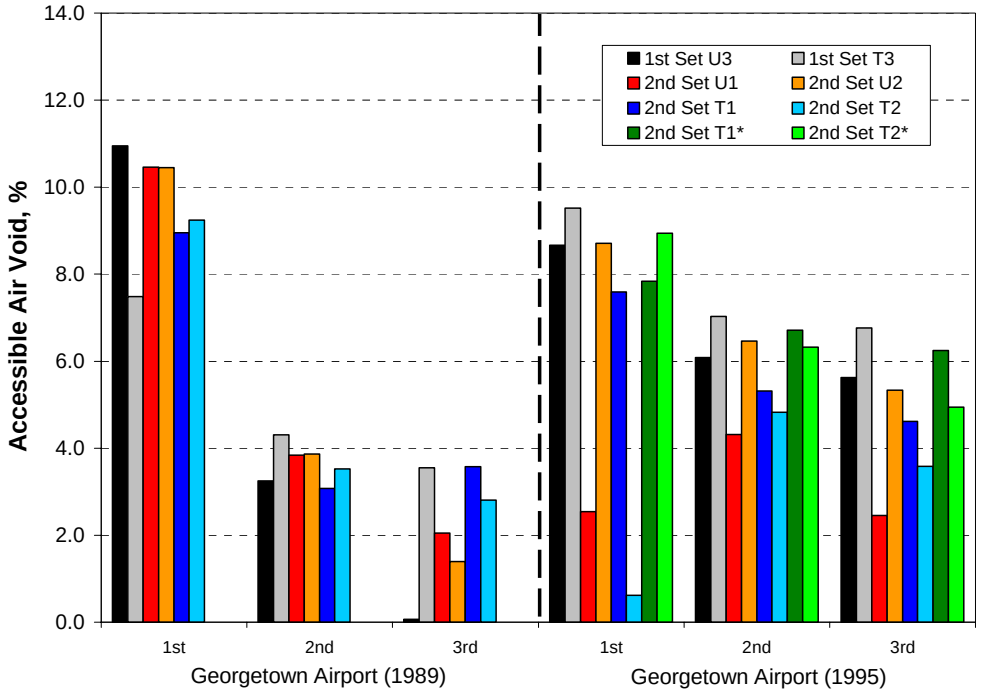

Figure G-7. Georgetown Airport (1989) and (1995) Accessible Air Void Comparison by Layers.

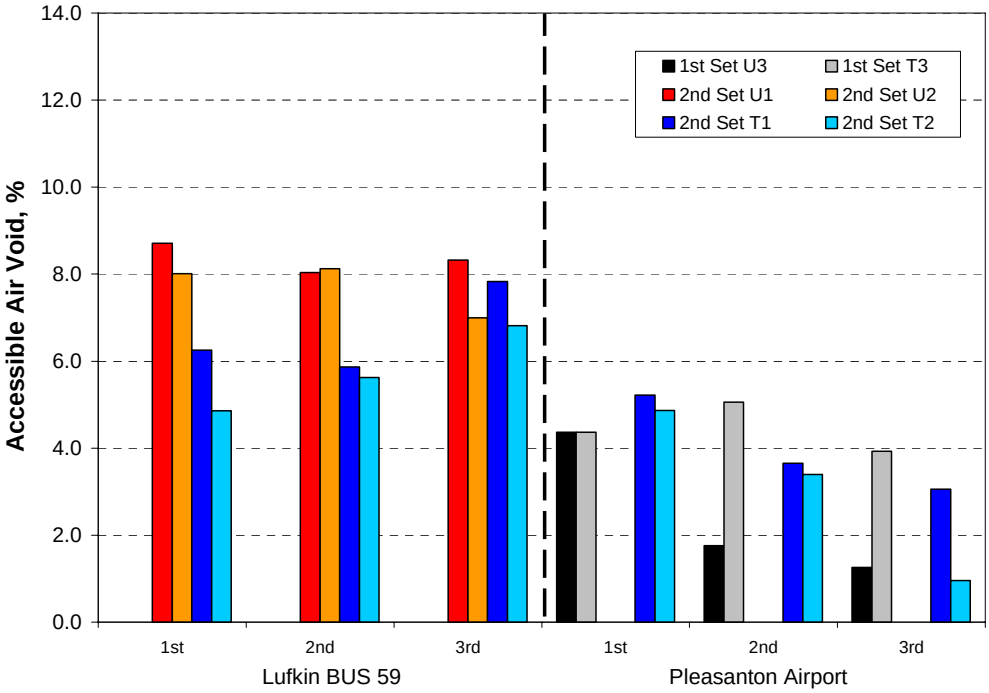

Figure G-8. Lufkin BUS 59 and Pleasanton Airport Accessible Air Void Comparison by Layers.

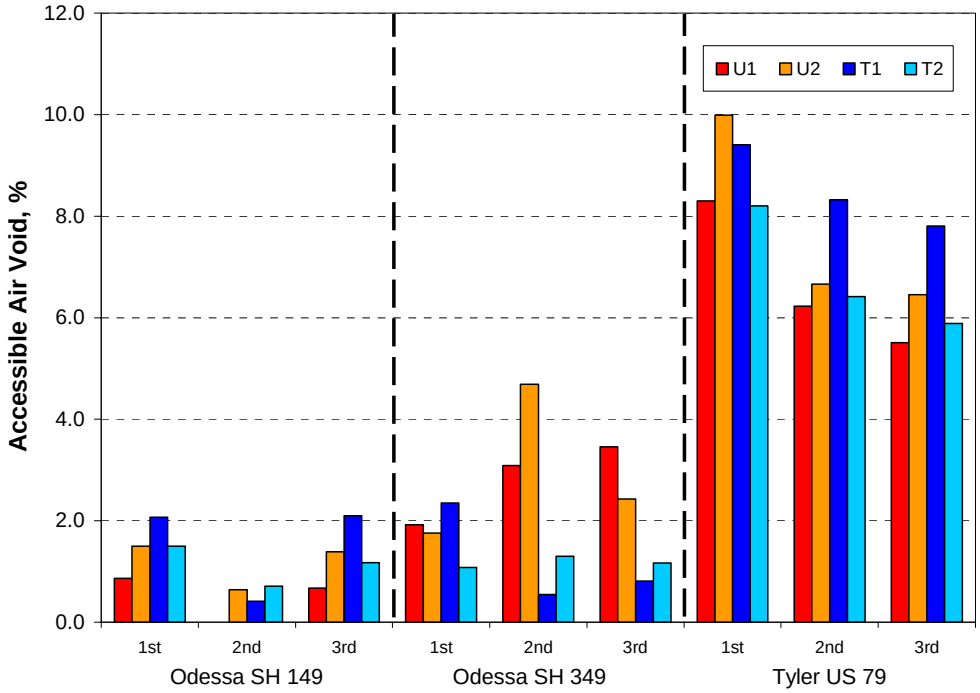

Figure G-9. Odessa SH 149, SH 349, and Tyler US 79 Accessible Air Void Comparison by Layers.

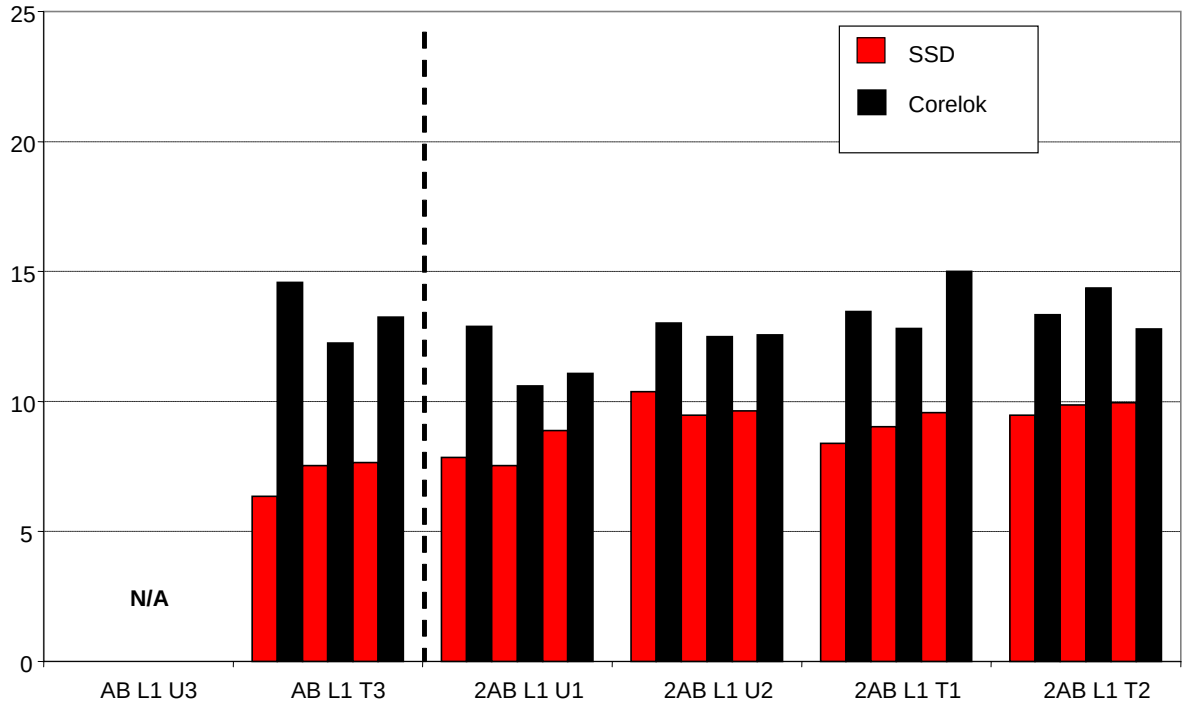

Figure G-10a. Accessible Air Void of 1st and 2nd Set Abilene SH 36 L1, %.

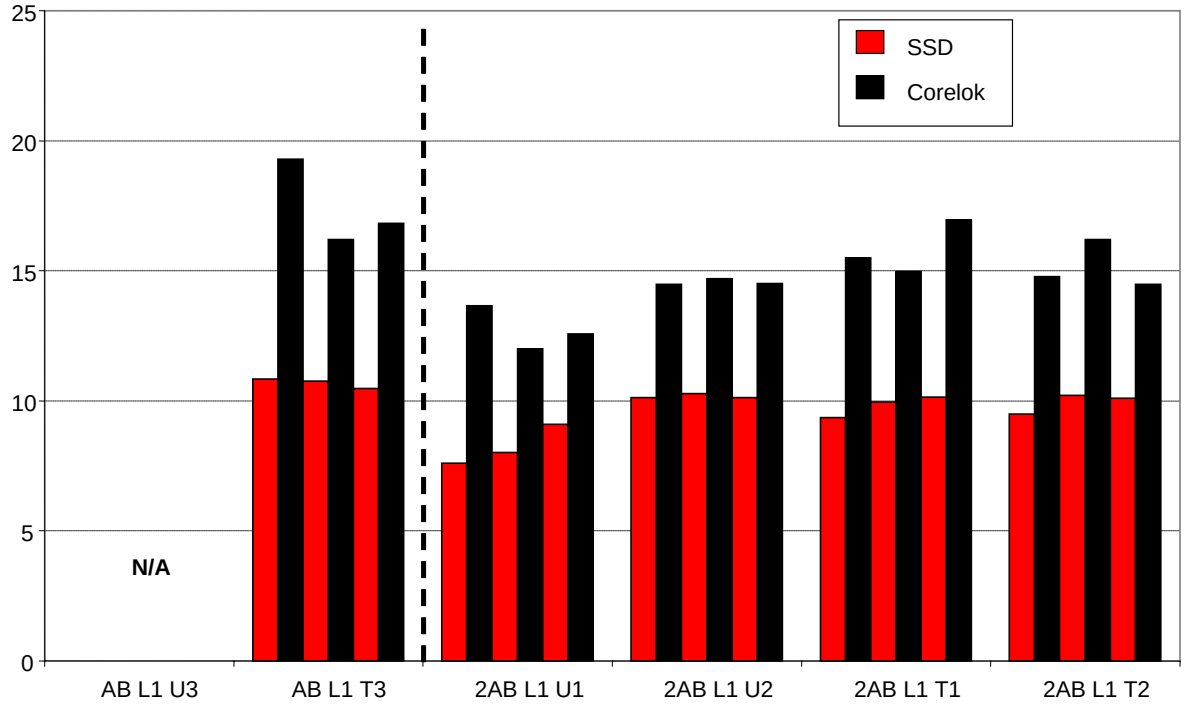

Figure G-10b. Total Air Void of 1st and 2nd Set Abilene SH 36 L1, %.

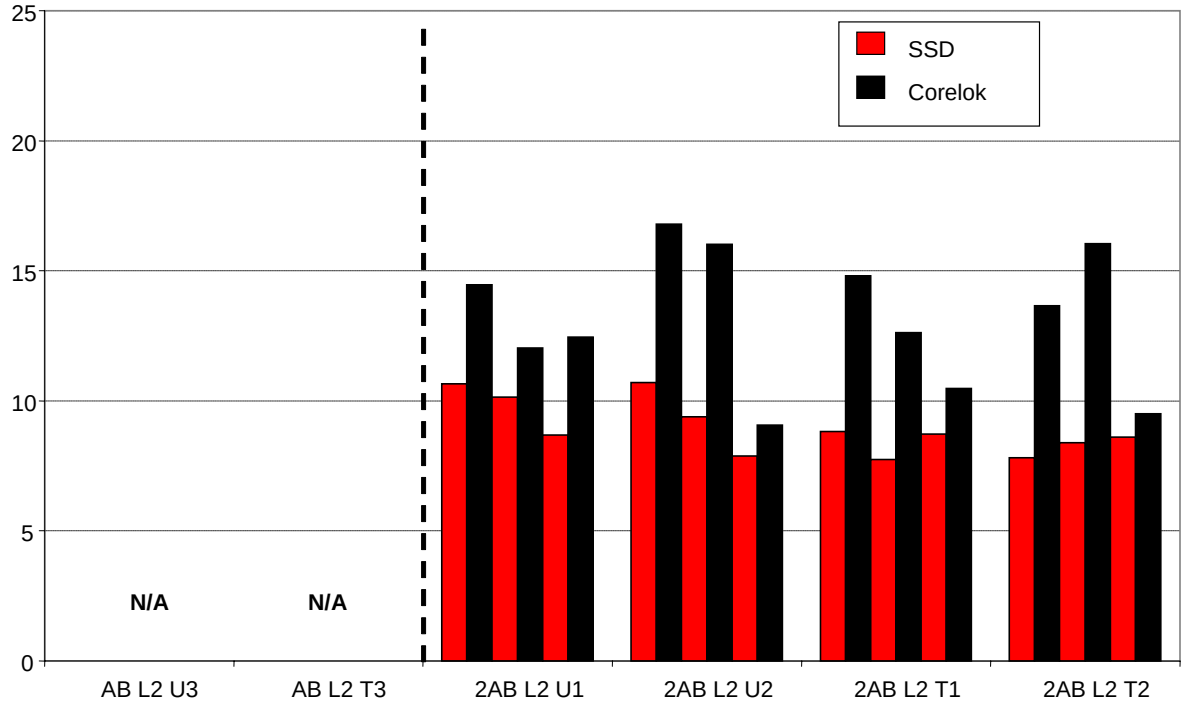

Figure G-11a. Accessible Air Void of 2nd Set Abilene SH 36 L2, %.

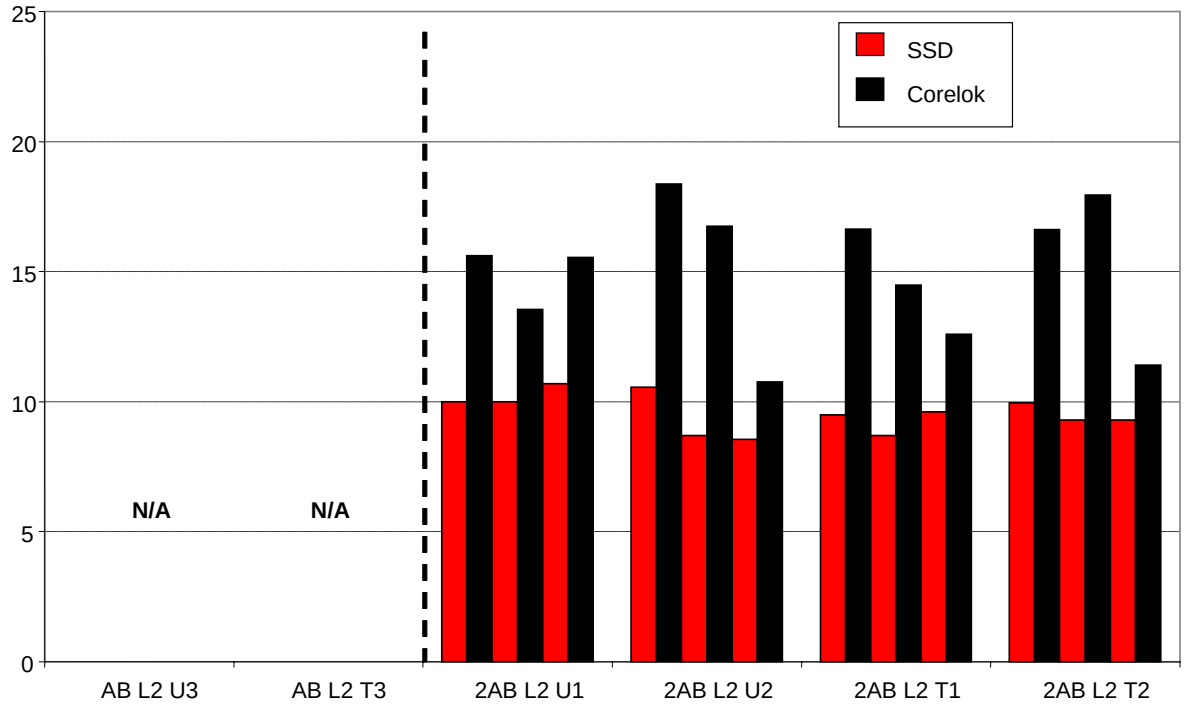

Figure G-11b. Total Air Void of and 2nd Set Abilene SH 36 L2, %.

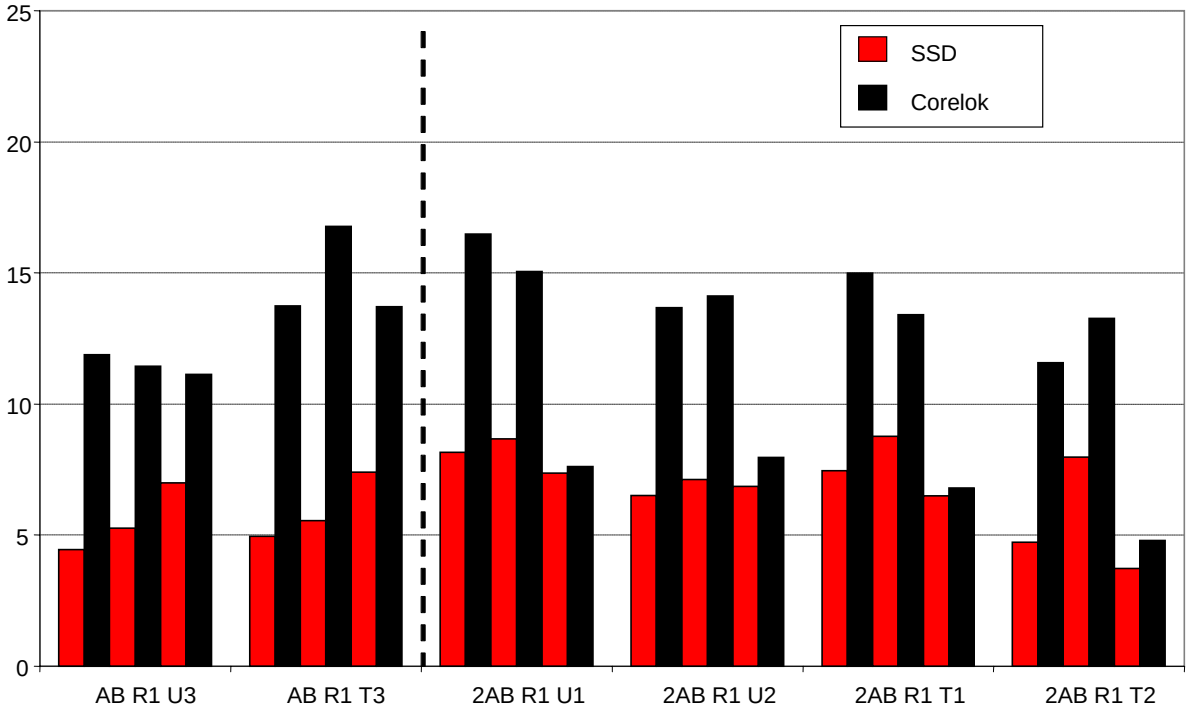

Figure G-12a. Accessible Air Void of 1st and 2nd Set Abilene SH 36 R1, %.

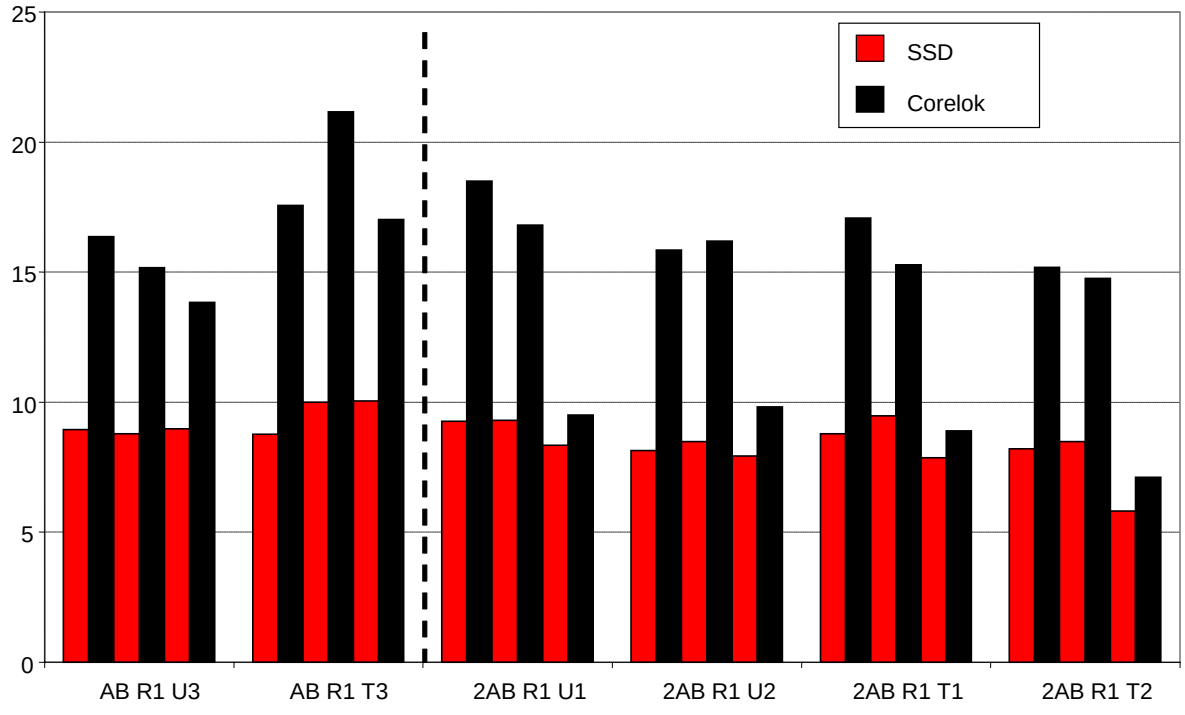

Figure G-12b. Total Air Void of 1st and 2nd Set Abilene SH 36 R1, %.

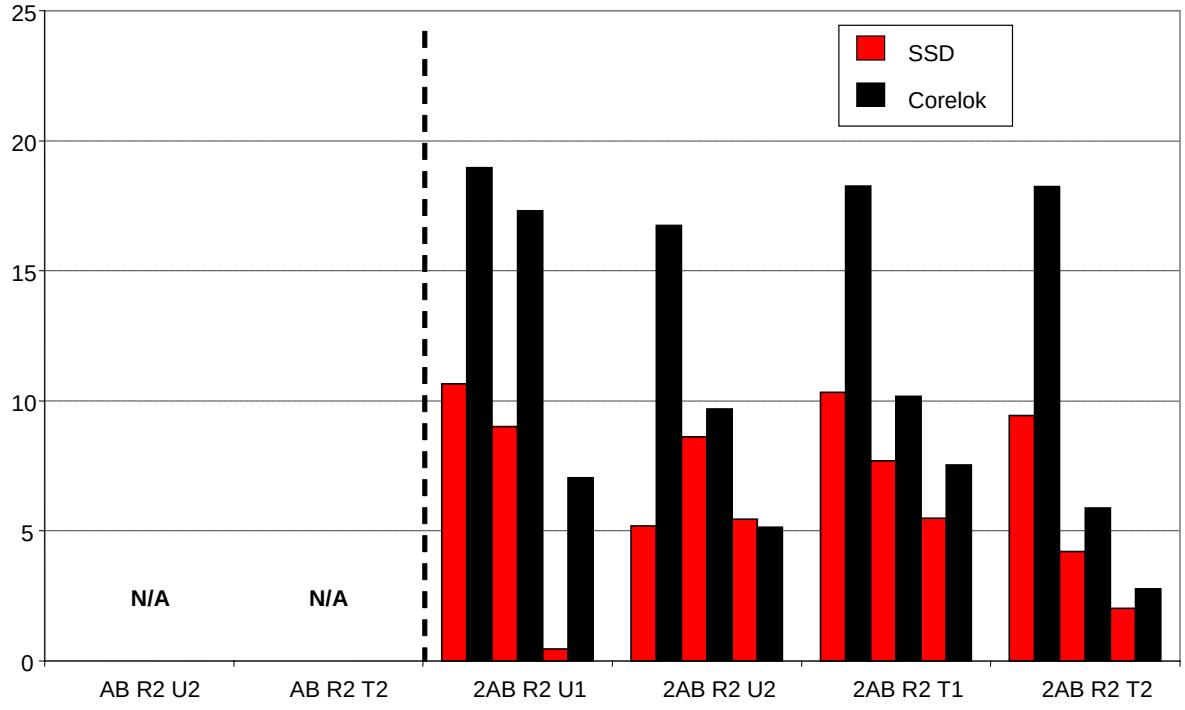

Figure G-13a. Accessible Air Void of 2nd Set Abilene SH 36 R2, %.

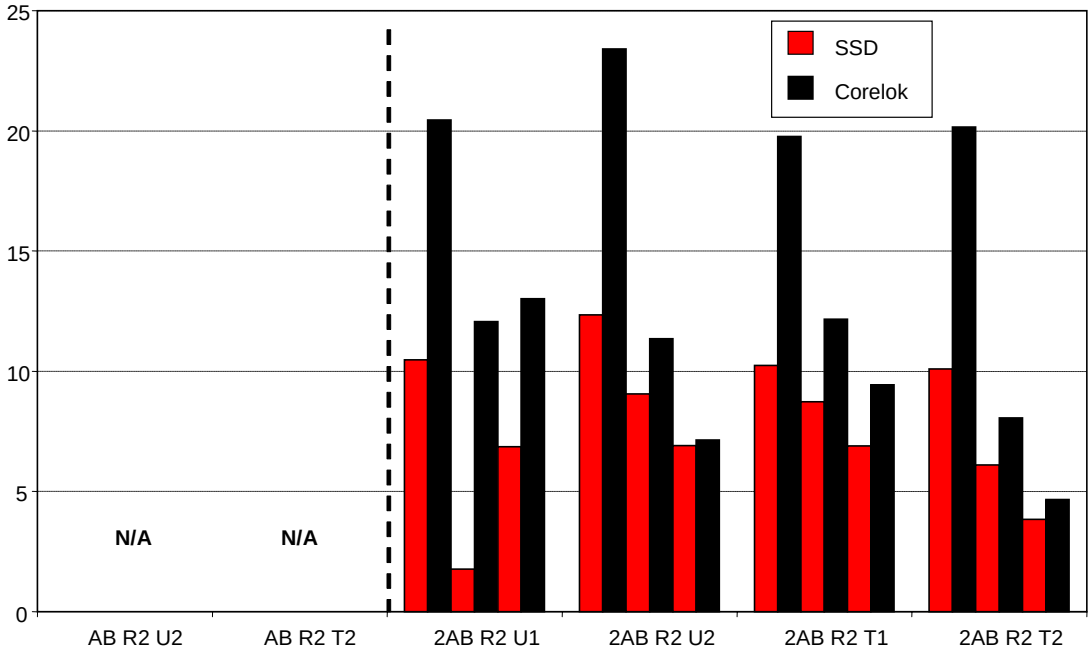

Figure G-13b. Total Air Void of 2nd Set Abilene SH 36 R2, %.

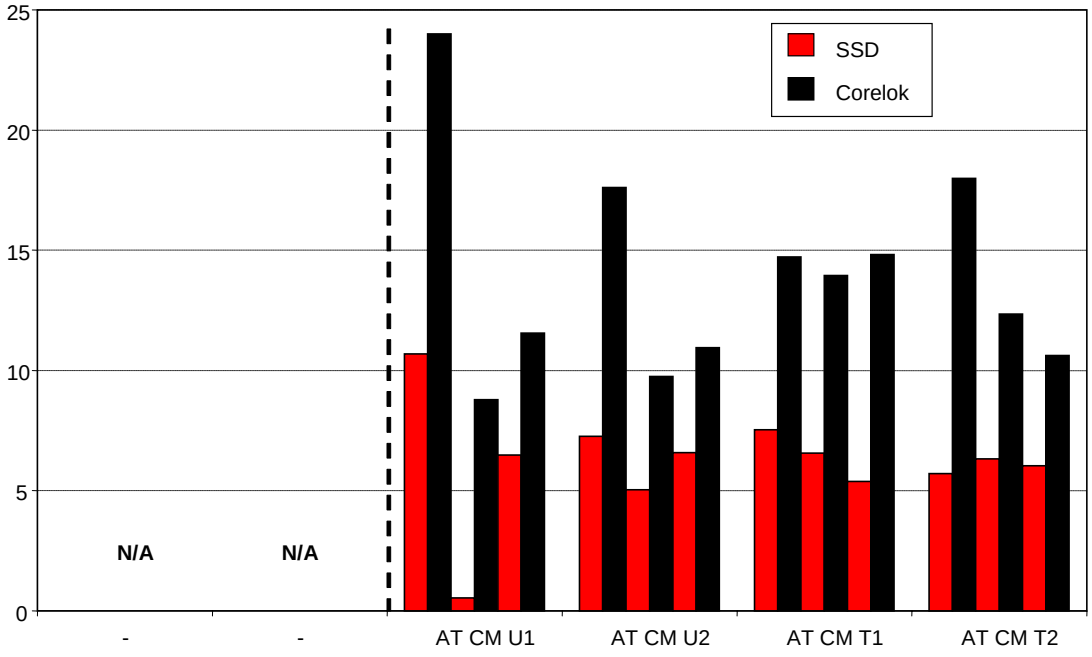

Figure G-14a. Accessible Air Void of Atlanta IH 20 CM, %.

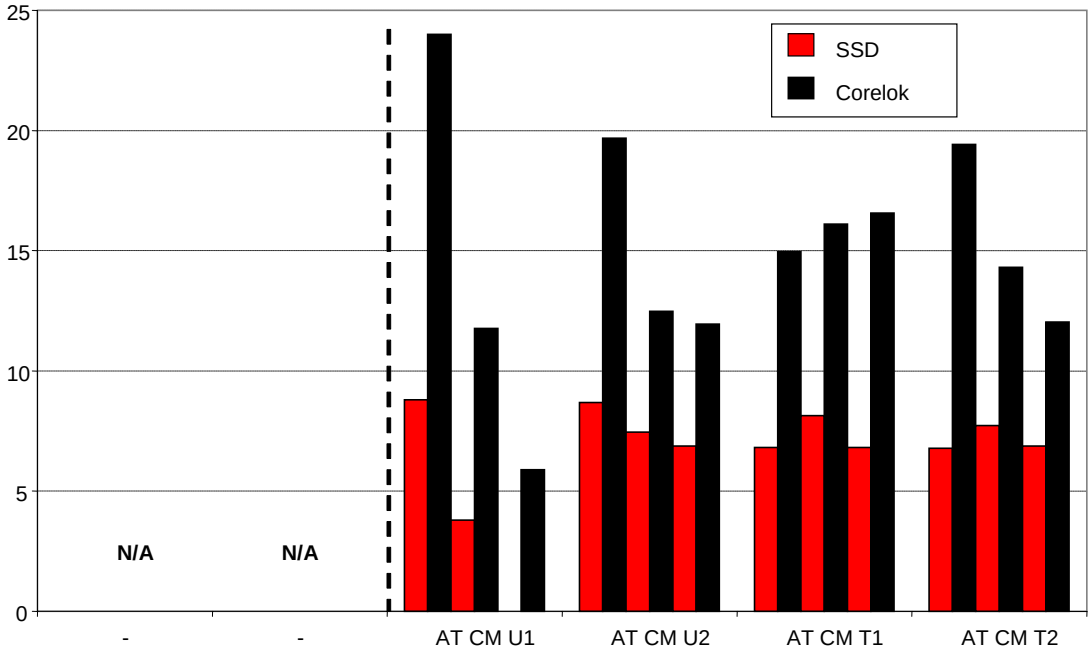

Figure G-14b Total Air Void of Atlanta IH 20 CM, %.

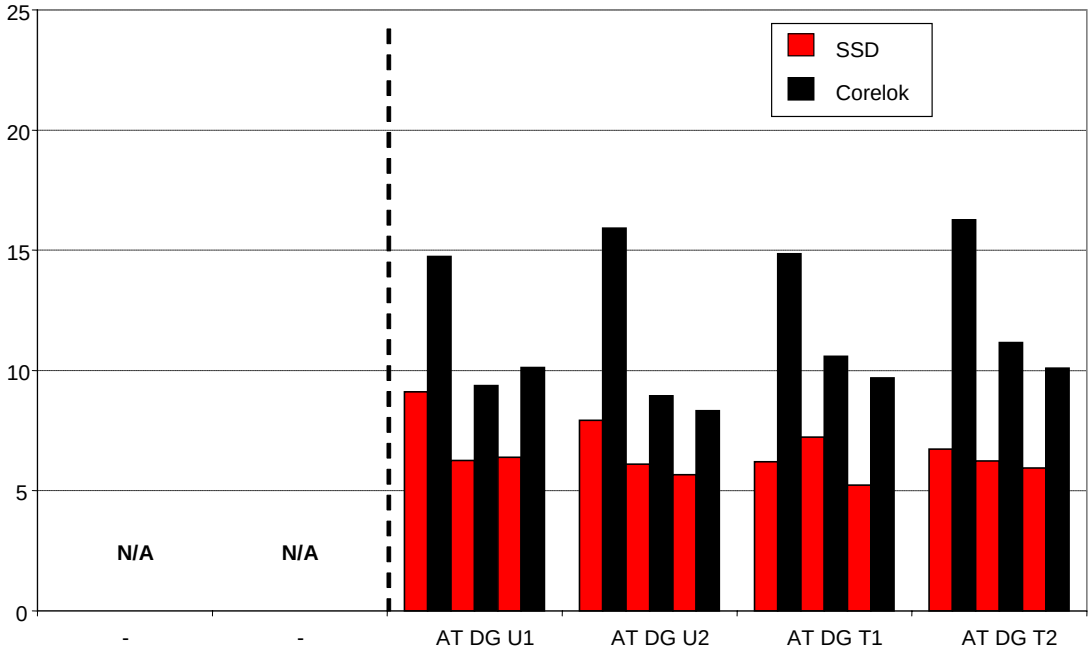

Figure G-15a. Accessible Air Void of Atlanta IH 20 DG, %.

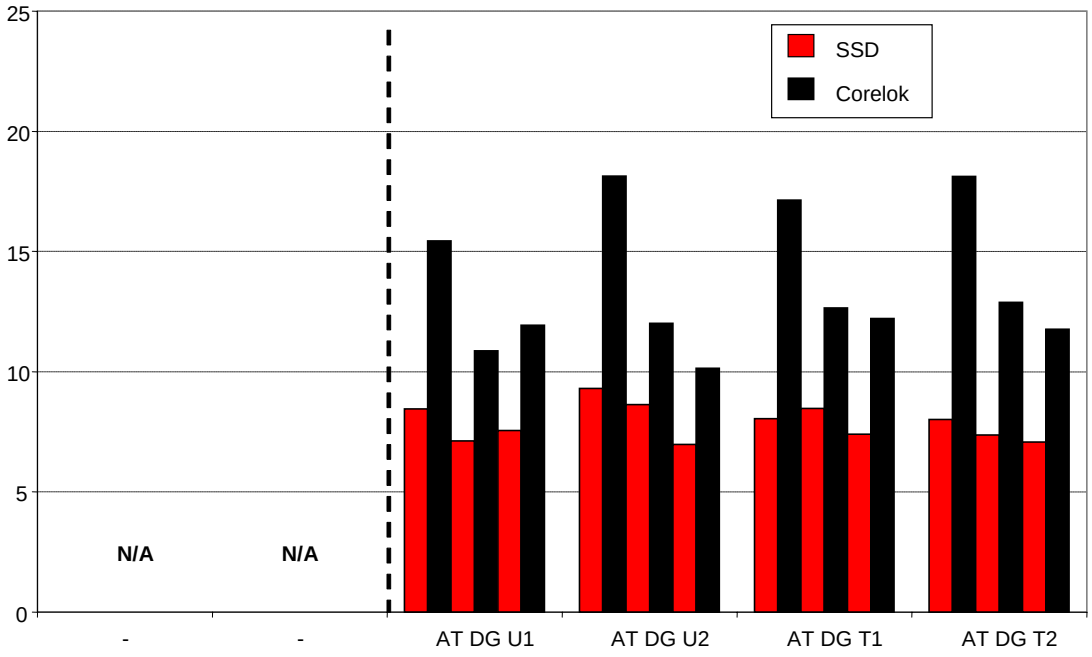

Figure G-15b. Total Air Void of Atlanta IH 20 DG, %.

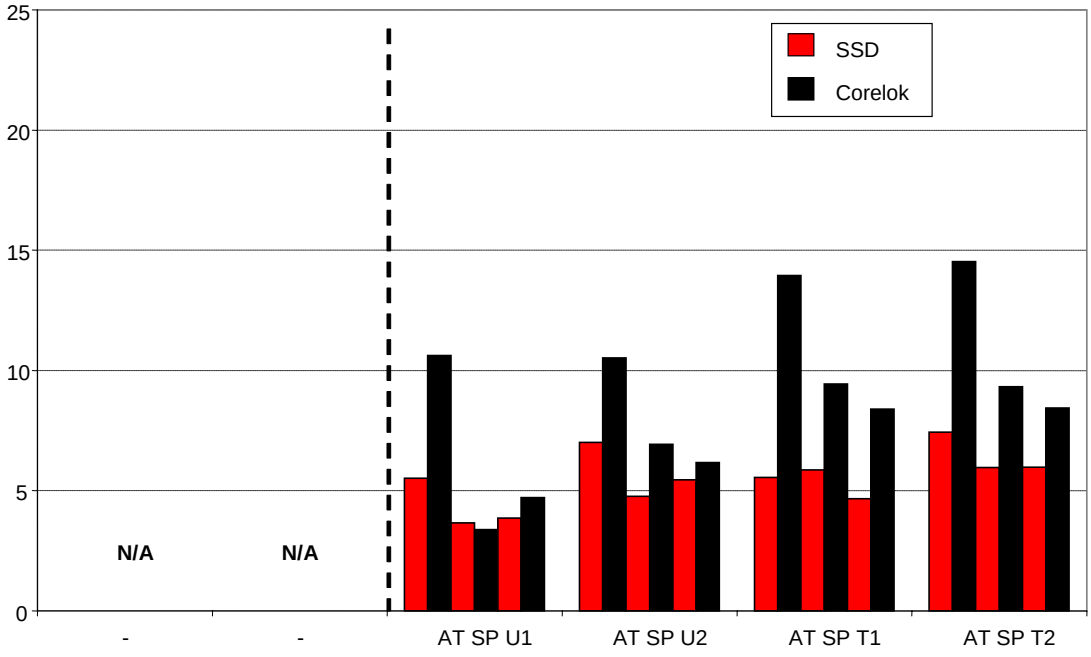

Figure G-16a. Accessible Air Void of Atlanta IH 20 SP, %.

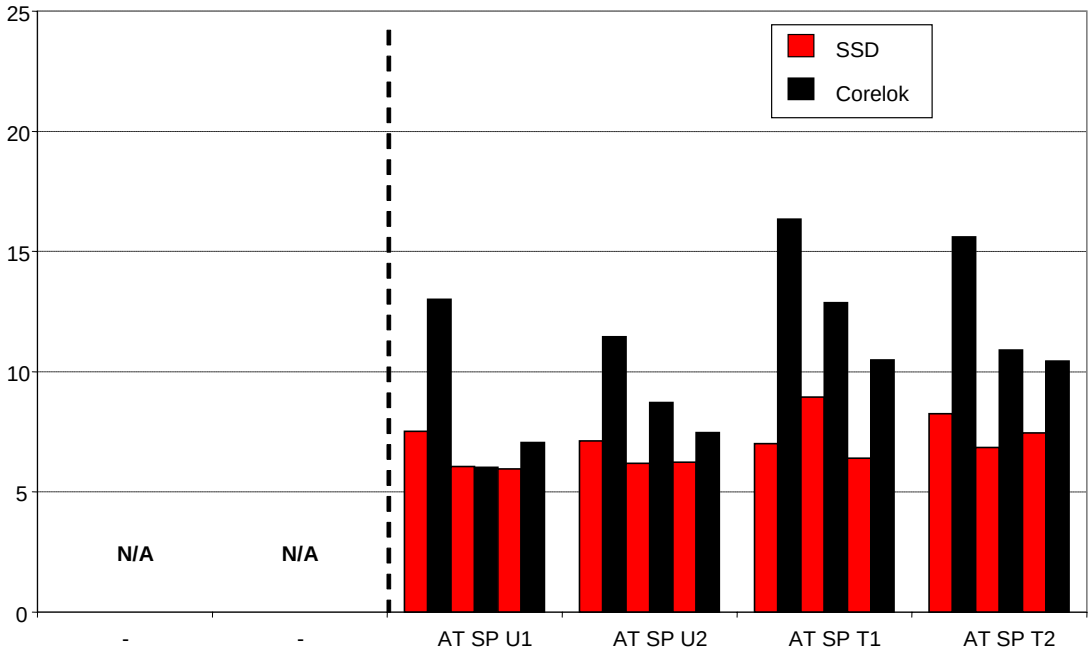

Figure G-16b. Total Air Void of Atlanta IH 20 SP, %.

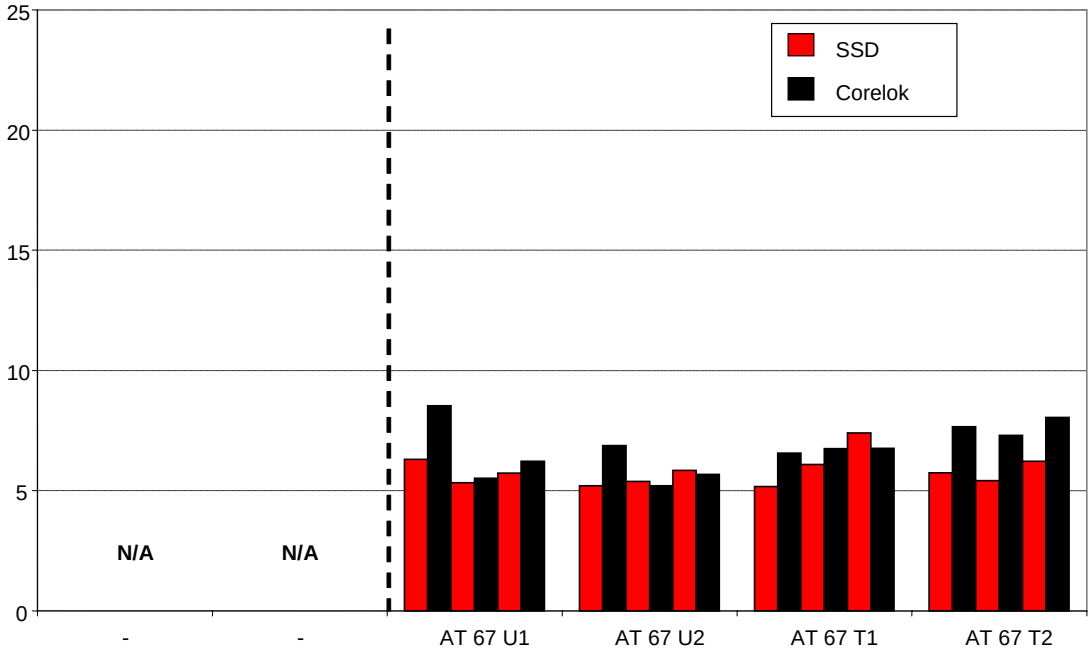

Figure G-17a. Accessible Air Void of Atlanta US 67, %.

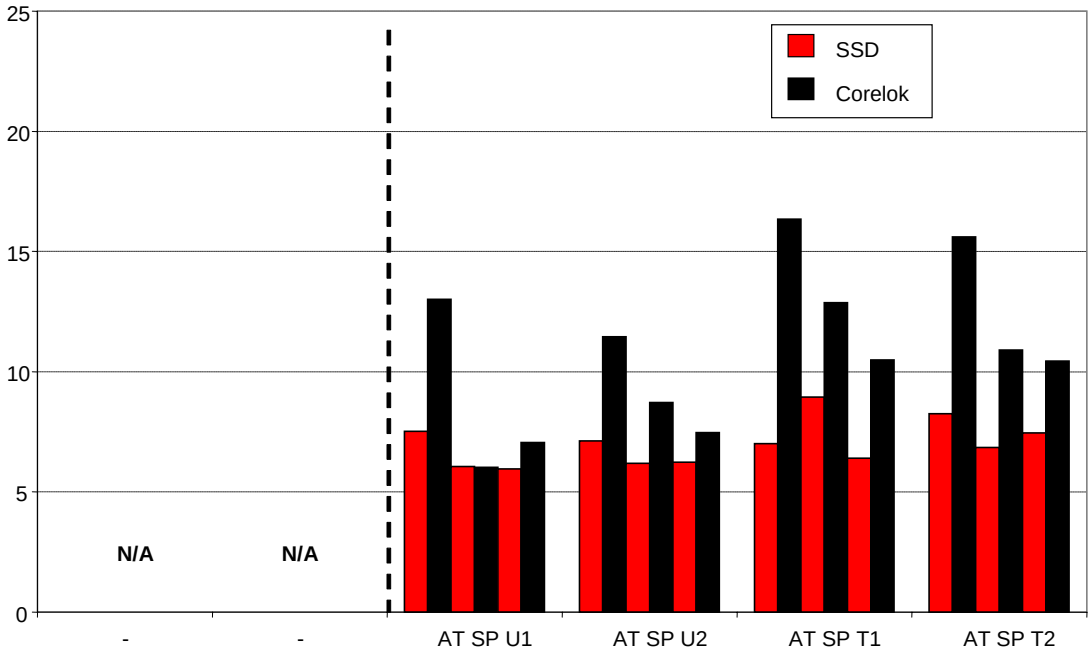

Figure G-17b. Total Air Void of Atlanta US 67, %.

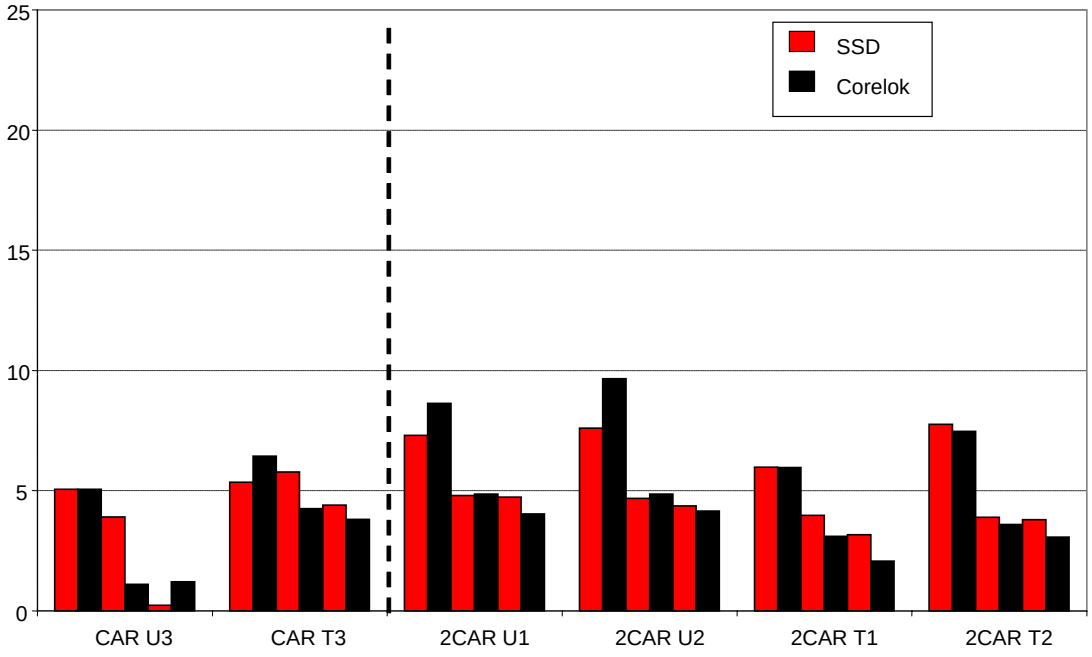

Figure G-18a. Accessible Air Void of 1st and 2nd Set Carrizo Springs Airport, %.

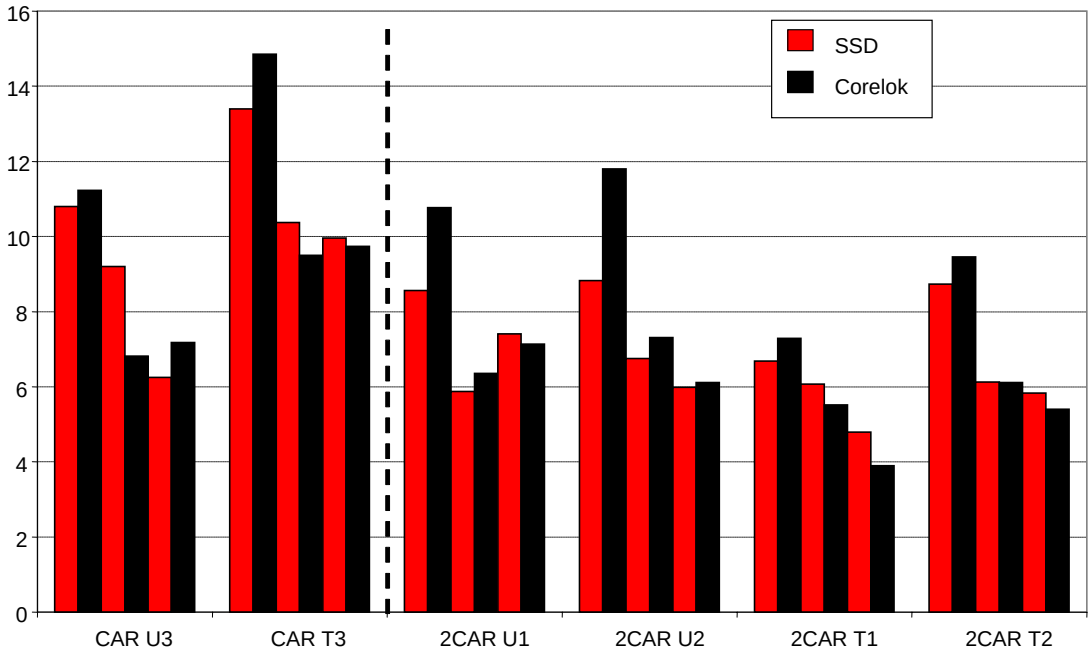

Figure G-18b. Total Air Void of 1st and 2nd Set Carrizo Springs Airport, %.

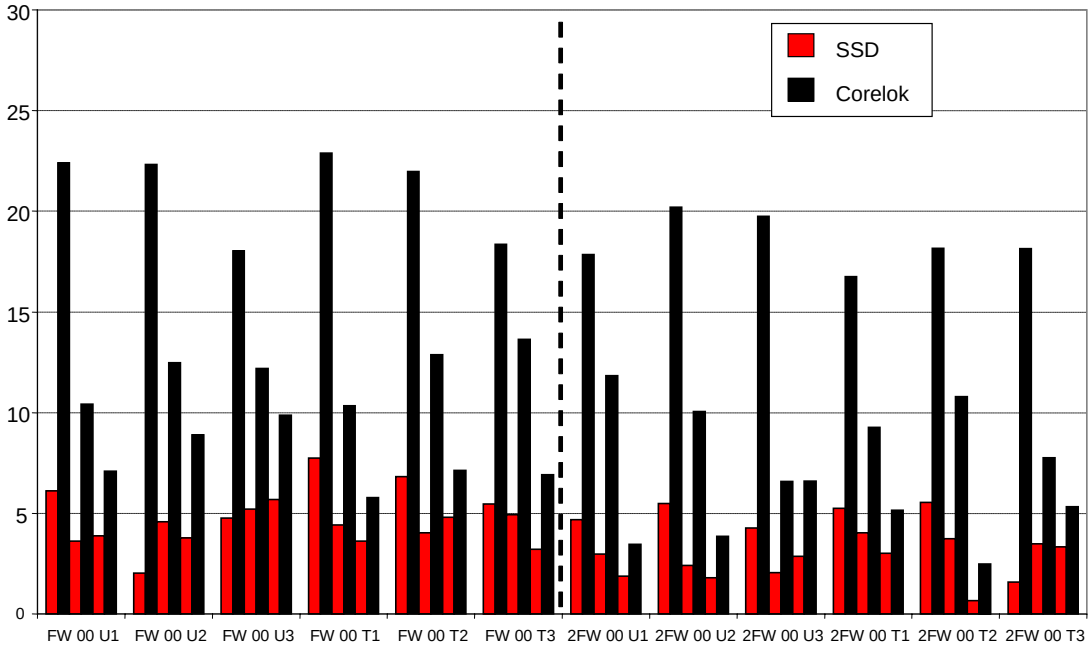

Figure G-19a. Accessible Air Void of 1st and 2nd Set Fort Worth FM 4 (2000), %.

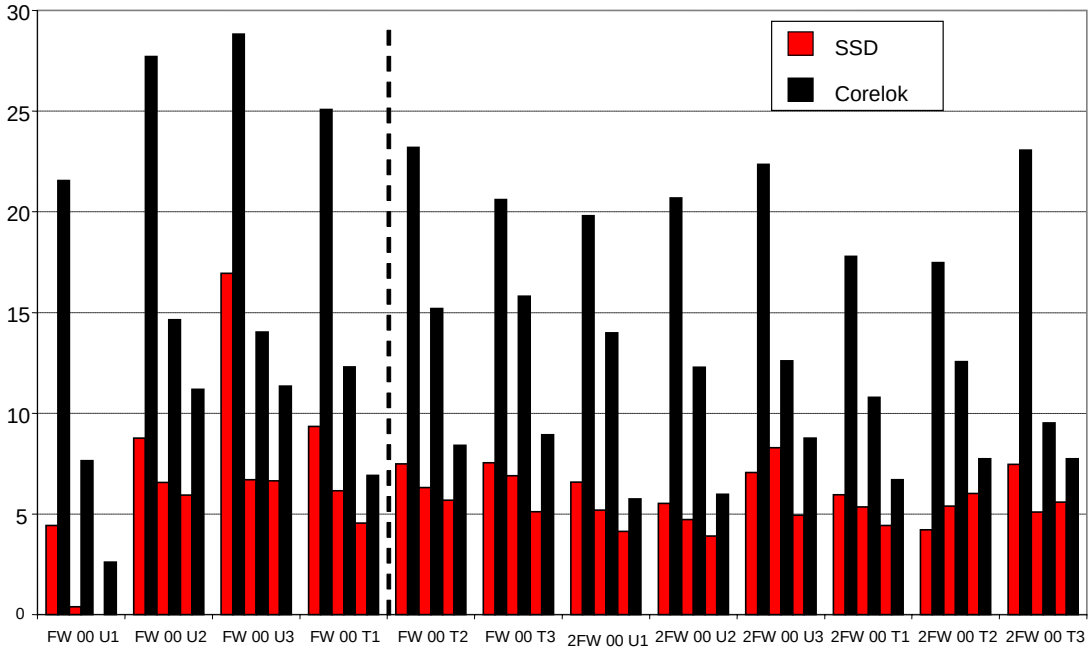

Figure G-19b. Total Air Void of 1st and 2nd Set Fort Worth FM 4 (2000), %.

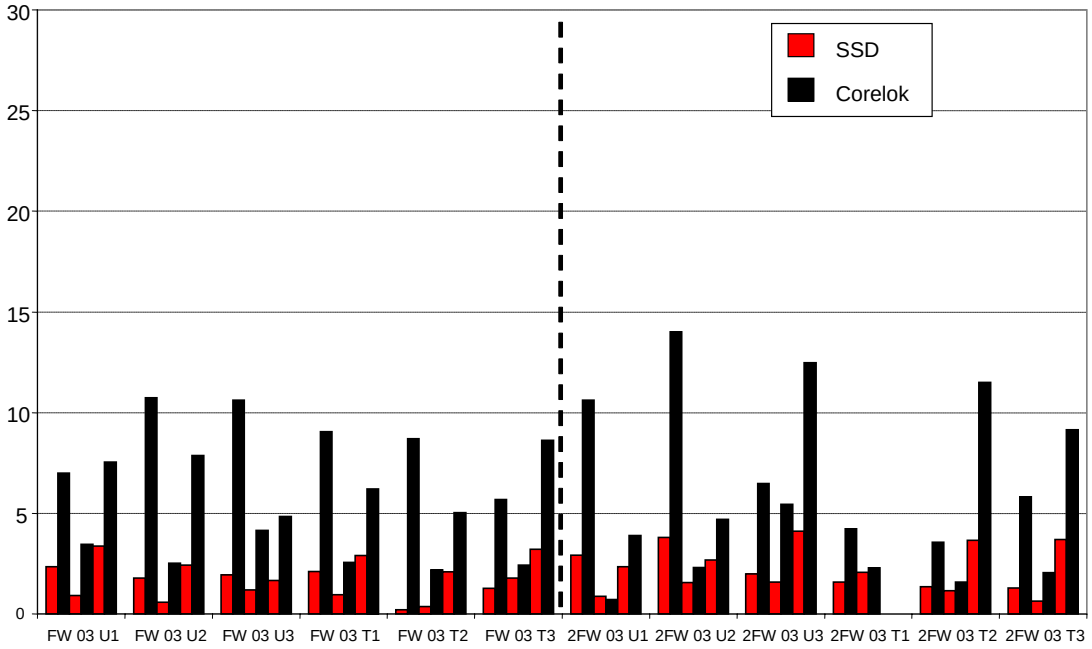

Figure G-20a. Accessible Air Void of 1st and 2nd Set Fort Worth FM 4 (2003), %.

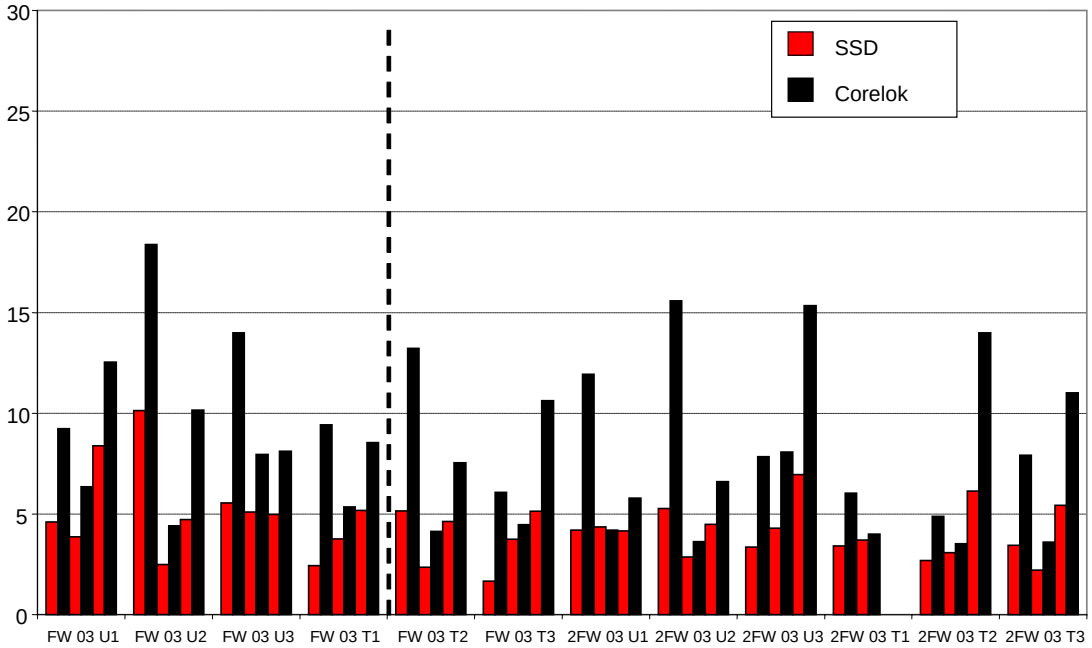

Figure G-20b. Total Air Void of 1st and 2nd Set Fort Worth FM 4 (2003), %.

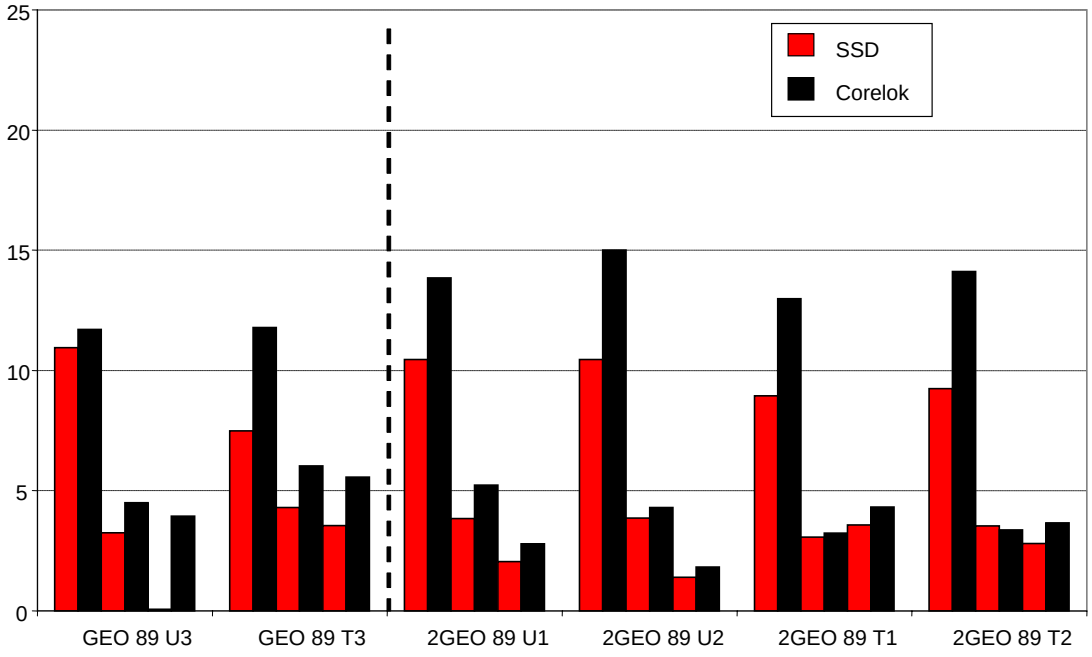

Figure G-21a. Accessible Air Void of 1st and 2nd Set Georgetown Airport (1989), %.

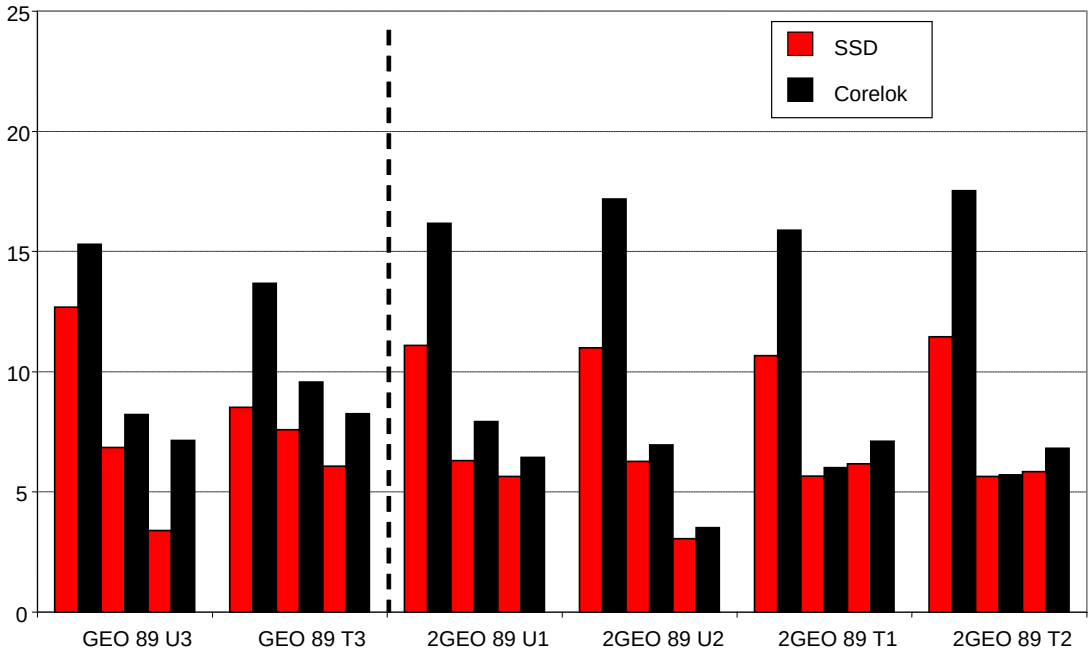

Figure G-21b. Total Air Void of 1st and 2nd Set Georgetown Airport (1989), %.

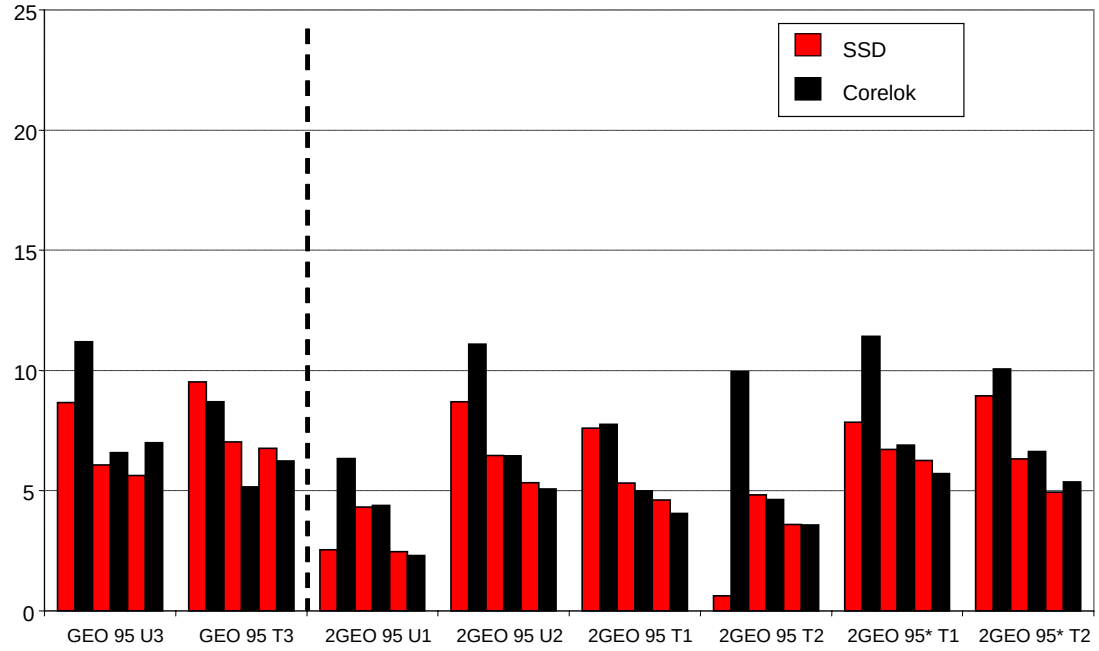

Figure G-22a. Accessible Air Void of 1st and 2nd Set Georgetown Airport (1995), %.

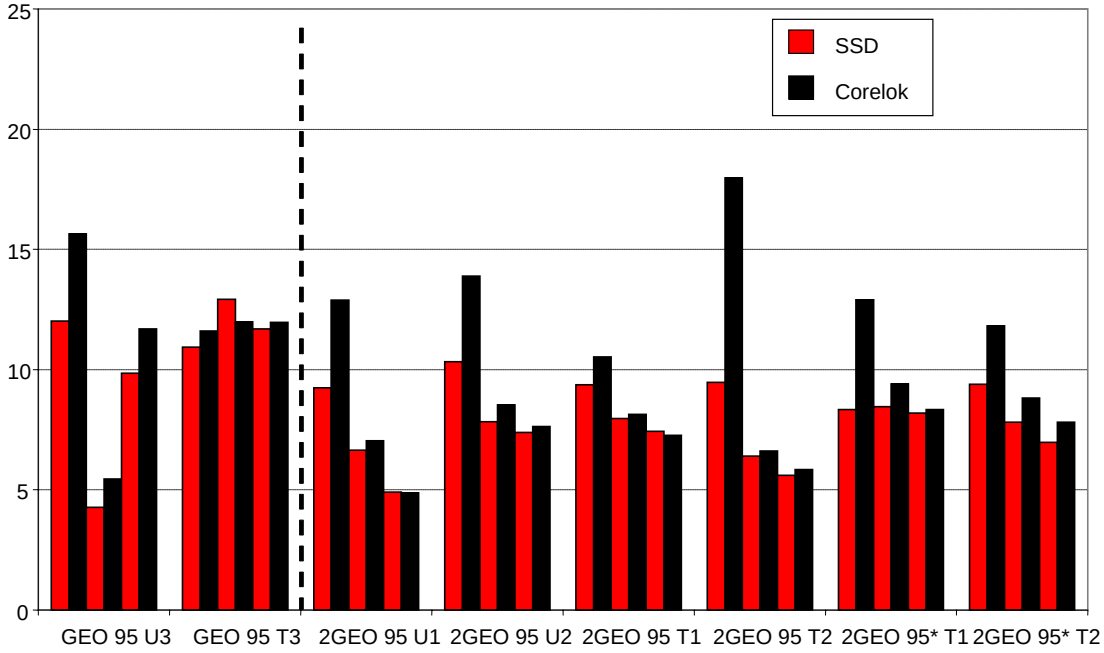

Figure G-22b. Total Air Void of 1st and 2nd Set Georgetown Airport (1995), %.

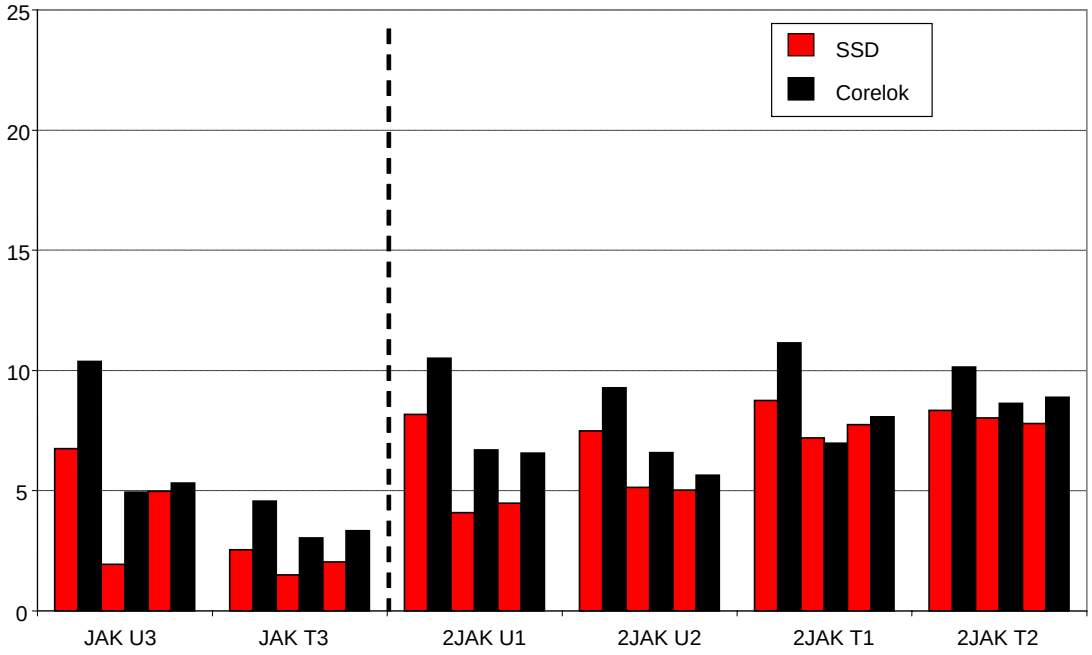

Figure G-23a. Accessible Air Void of 1st and 2nd Set Jacksonville Airport, %.

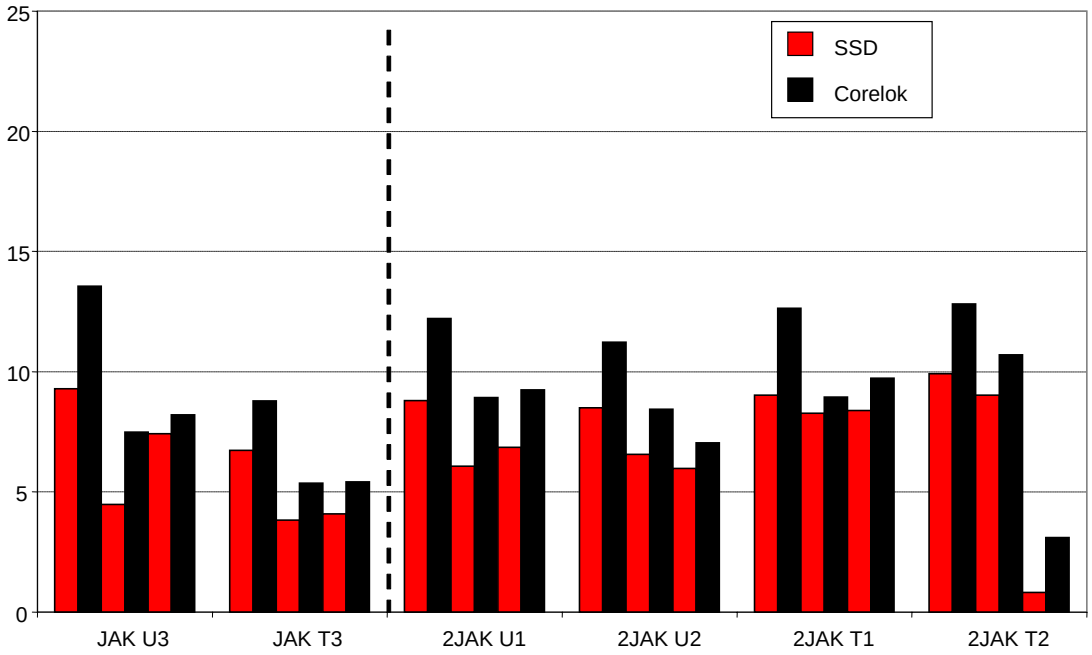

Figure G-23b. Total Air Void of 1st and 2nd Set Jacksonville Airport, %.

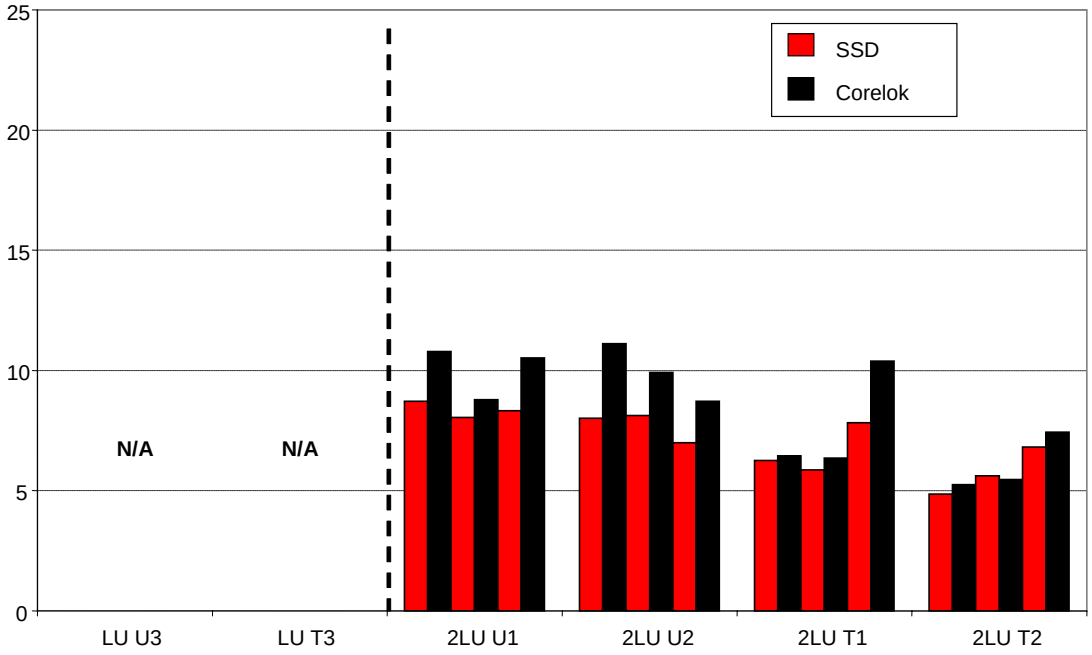

Figure G-24a. Accessible Air Void of 2nd Set Lufkin BUS 59, %.

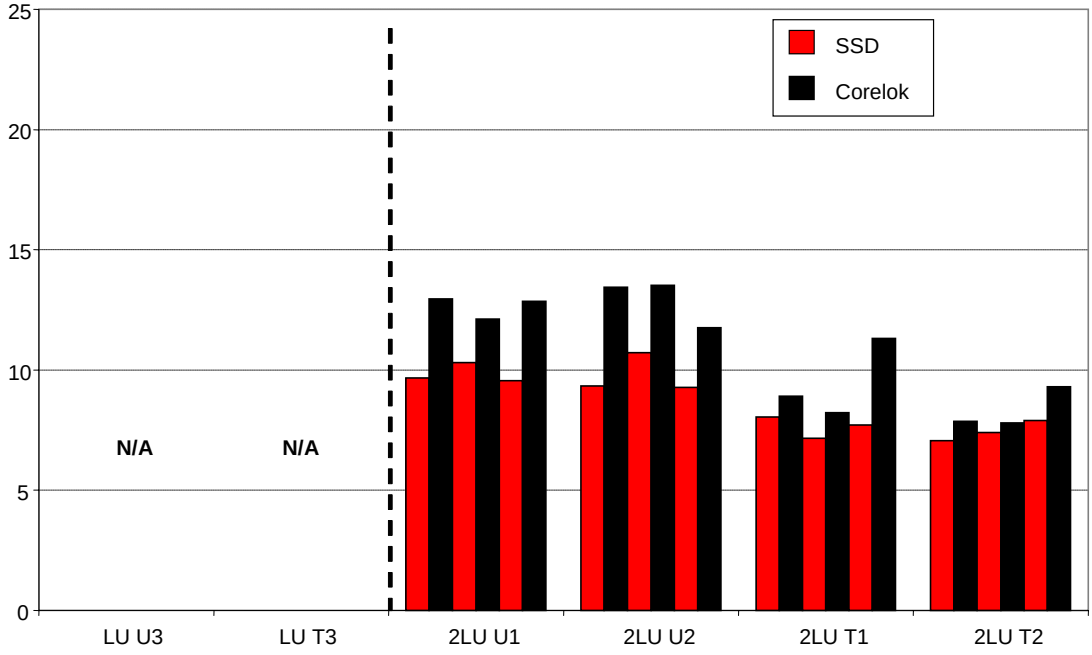

Figure G-24b. Total Air Void of 2nd Set Lufkin BUS 59, %.

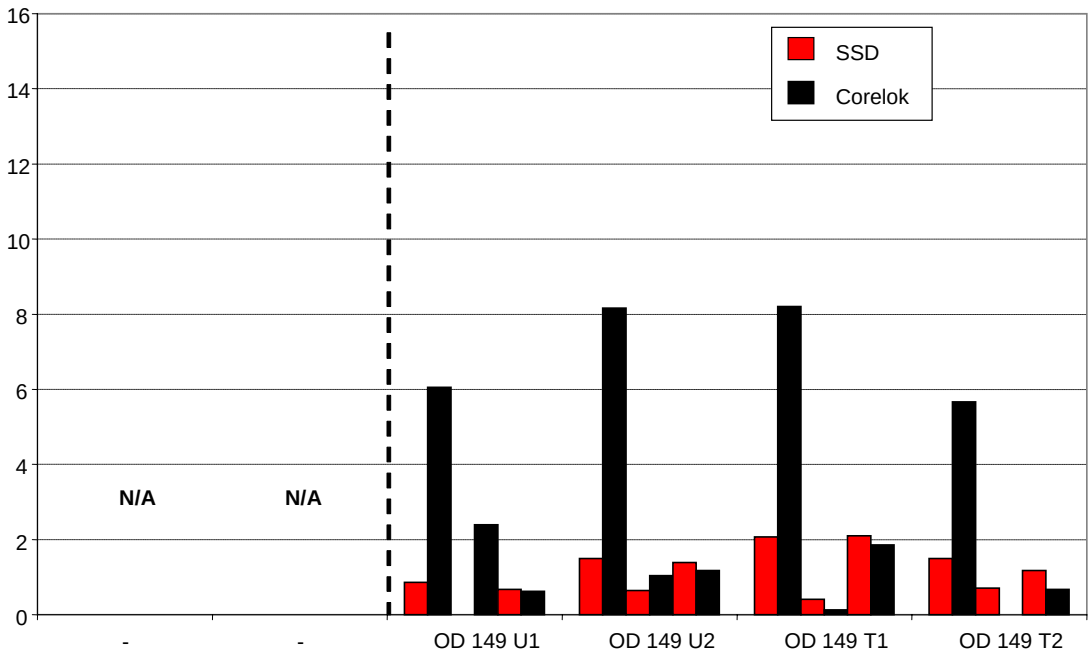

Figure G-25a. Accessible Air Void of Odessa SH 149, %.

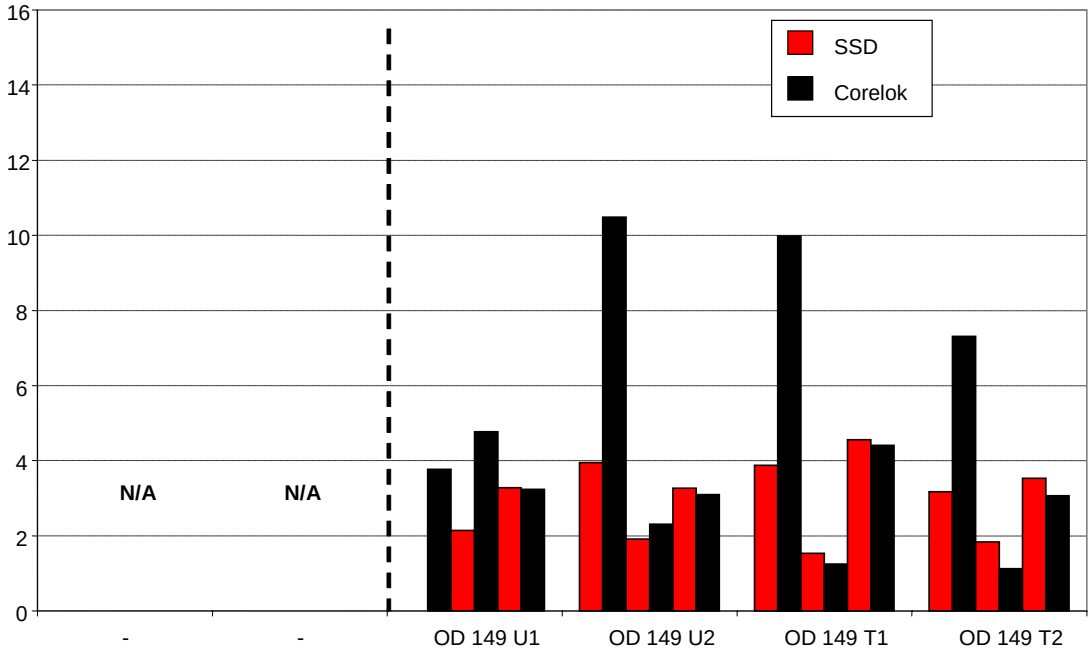

Figure G-25b. Total Air Void of Odessa SH 149, %.

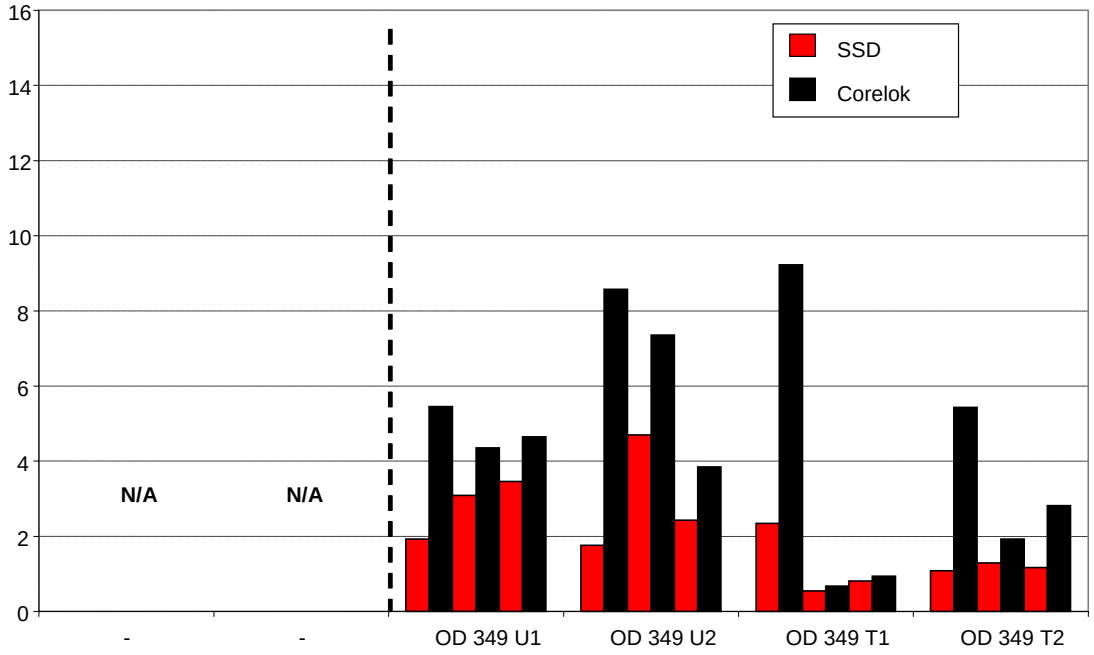

Figure G-26a. Accessible Air Void of Odessa SH 349, %.

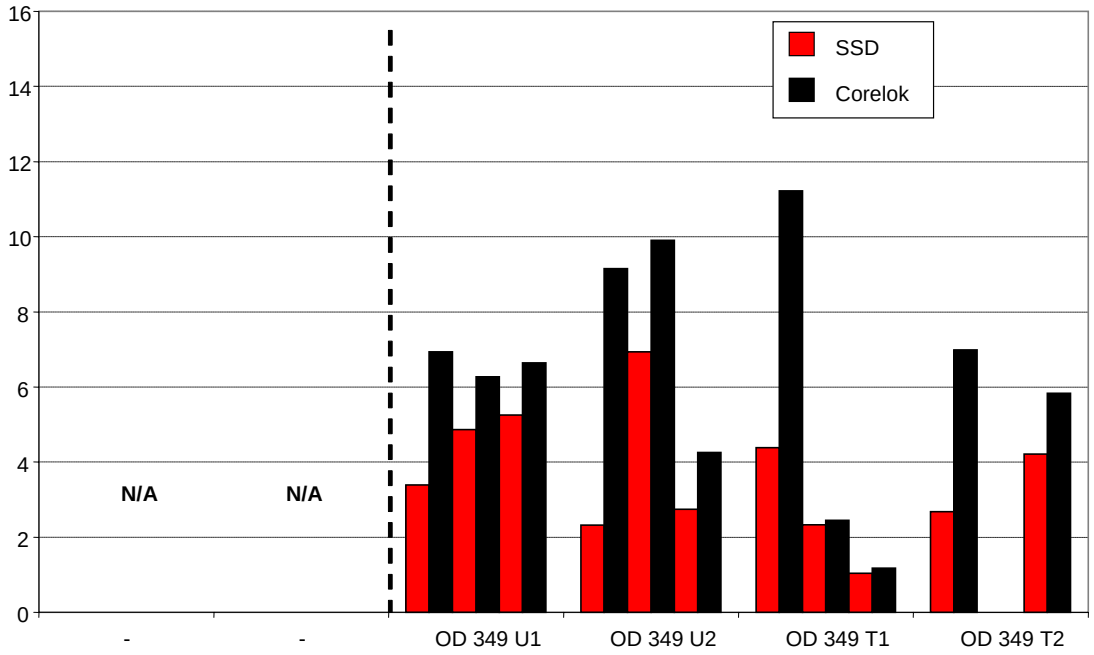

Figure G-26b. Total Air Void of Odessa SH 349, %.

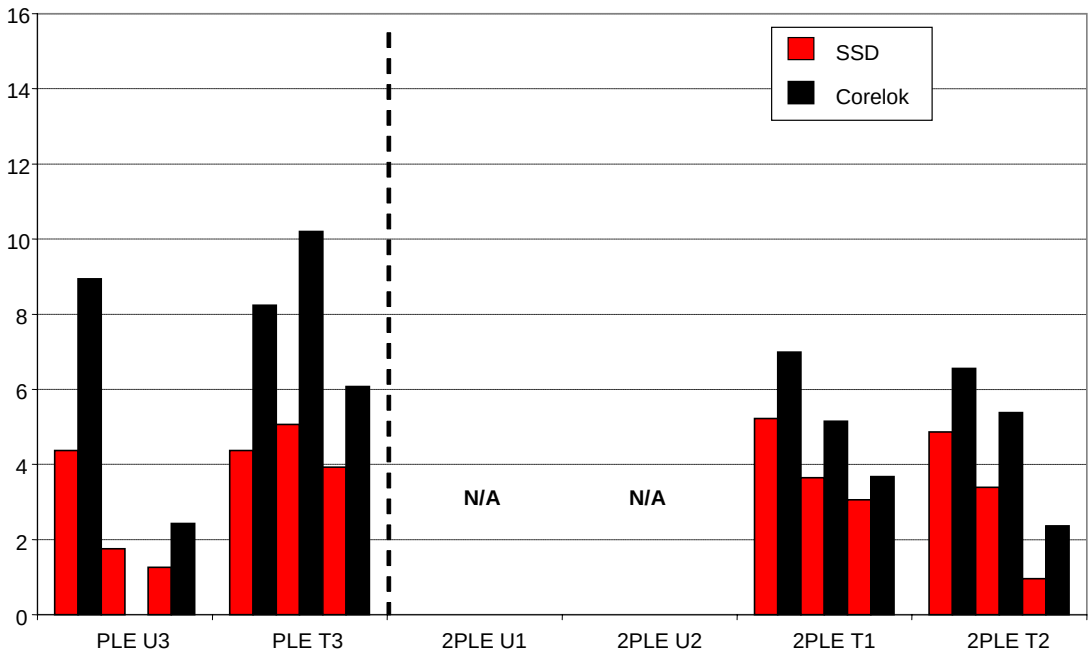

Figure G-27a. Accessible Air Void of 1st and 2nd Set Pleasanton Airport, %.

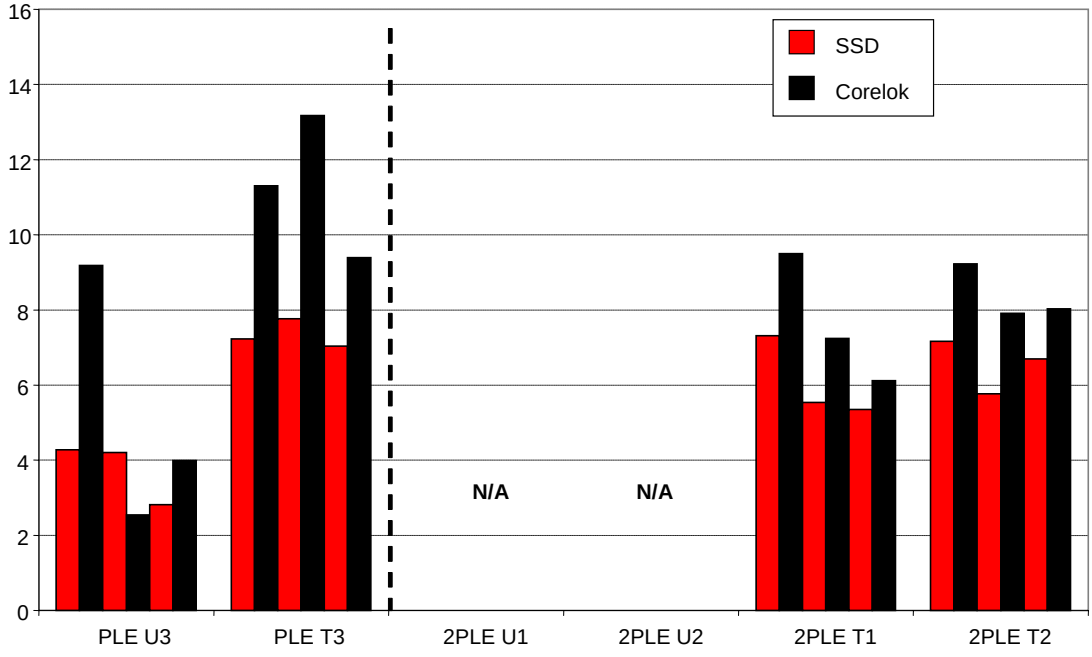

Figure G-27b. Total Air Void of 1st and 2nd Set Pleasanton Airport, %.

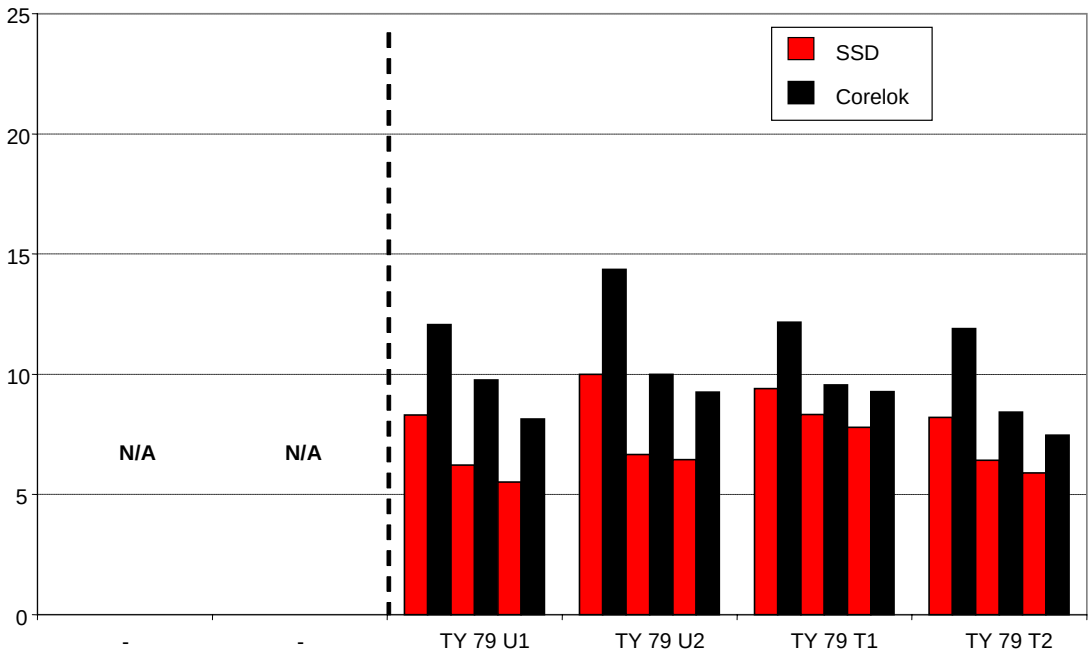

Figure G-28a. Accessible Air Void of Tyler US 79, %.

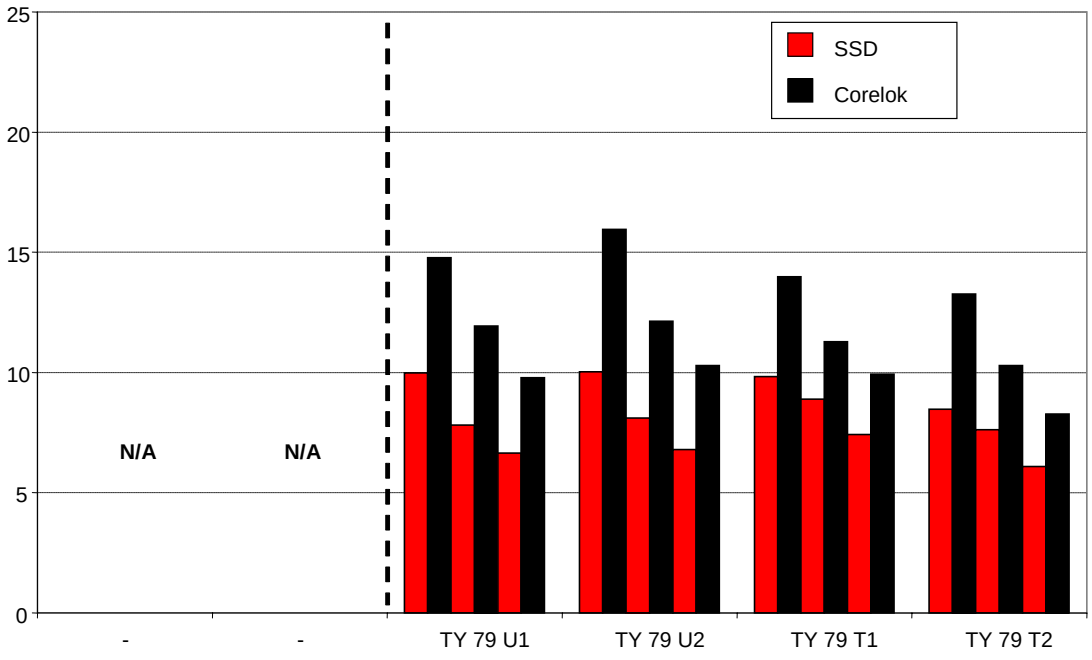

Figure G-28b. Total Air Void of Tyler US 79, %.

APPENDIX H

BINDER CONTENT OF CORE SAMPLES

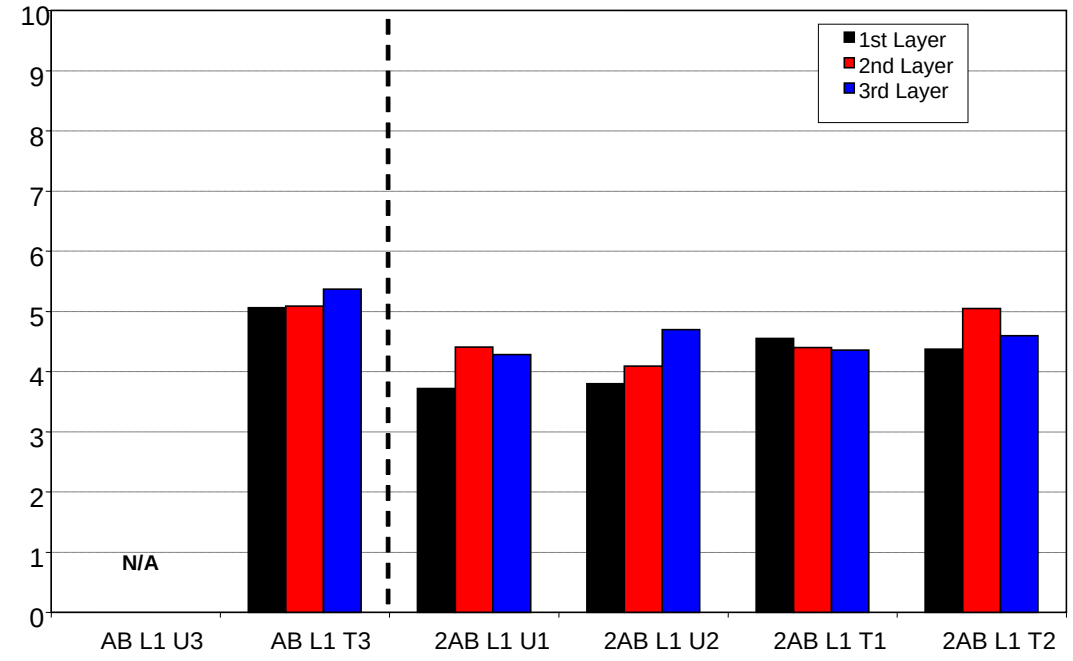

Figure H-1. Binder Content of 1st and 2nd Set Abilene SH 36 L1, %.

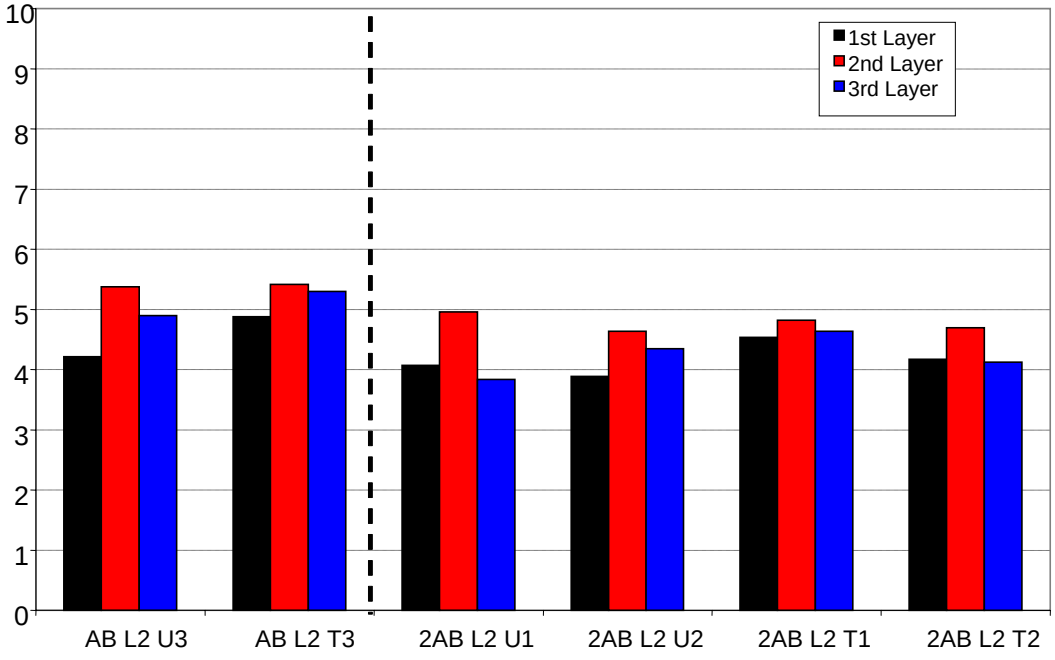

Figure H-2. Binder Content of 1st and 2nd Set Abilene SH 36 L2, %.

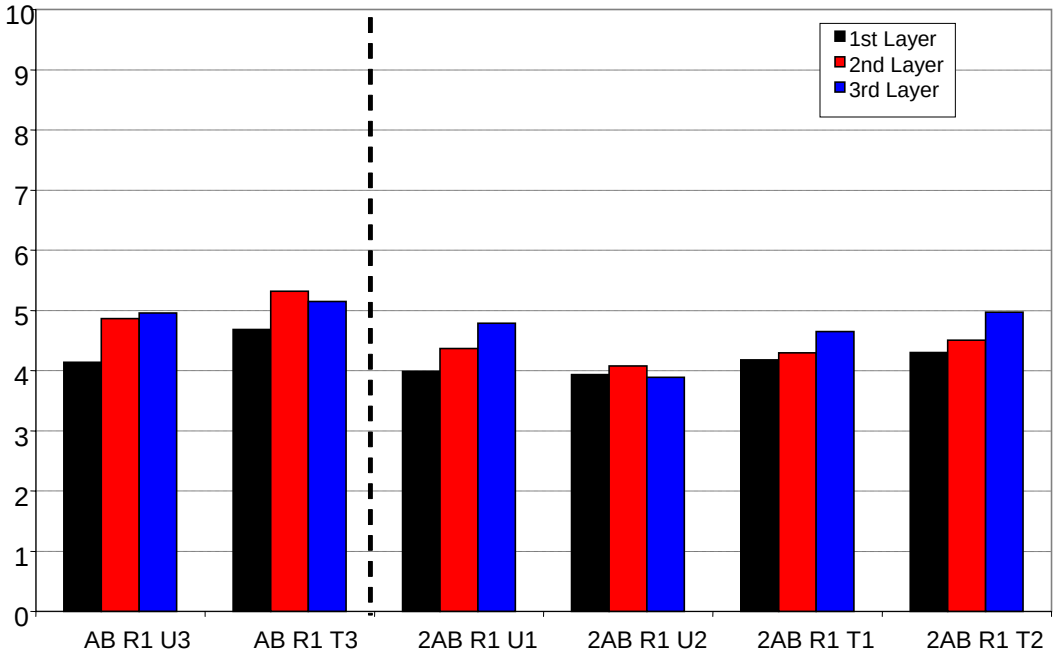

Figure H-3. Binder Content of 1st and 2nd Set Abilene SH 36 R1, %.

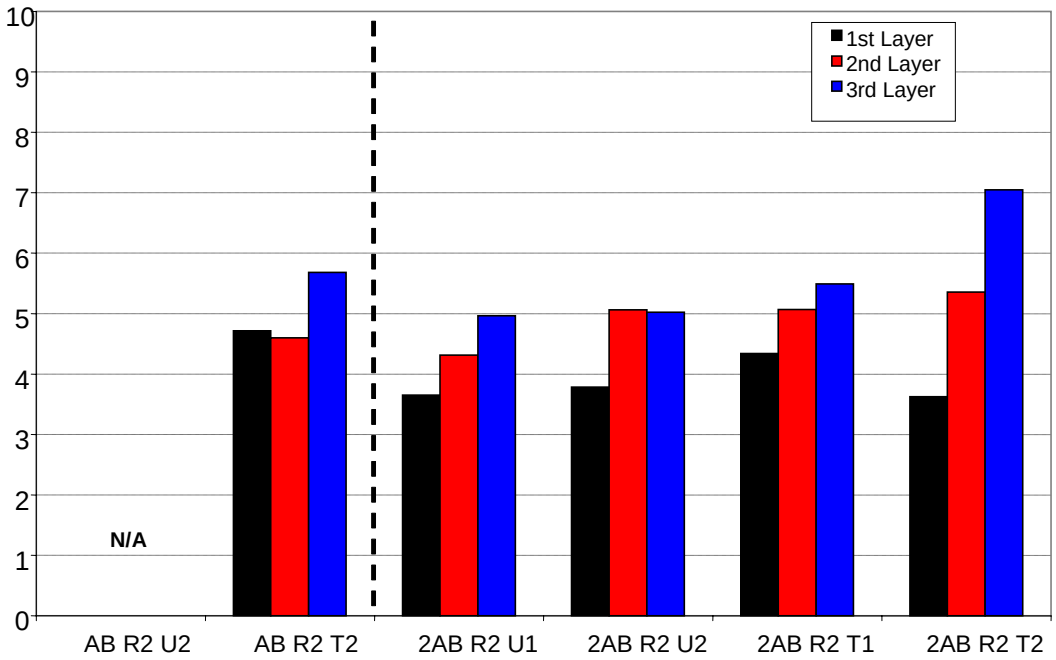

Figure H-4. Binder Content of 1st and 2nd Set Abilene SH 36 R2, %.

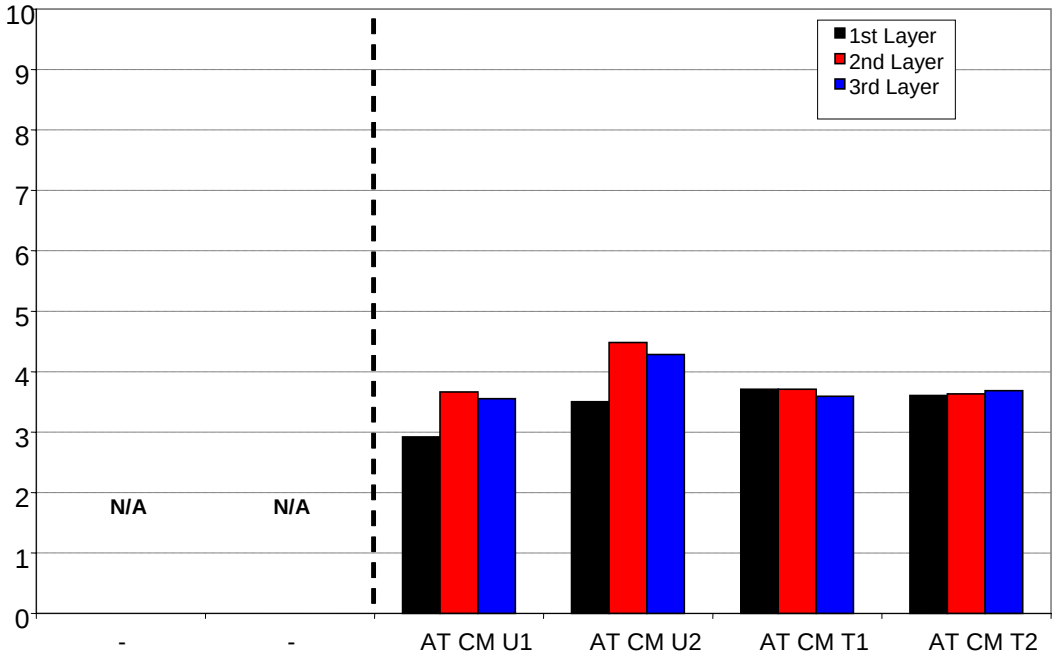

Figure H-5. Binder Content of Atlanta IH 20 CM, %.

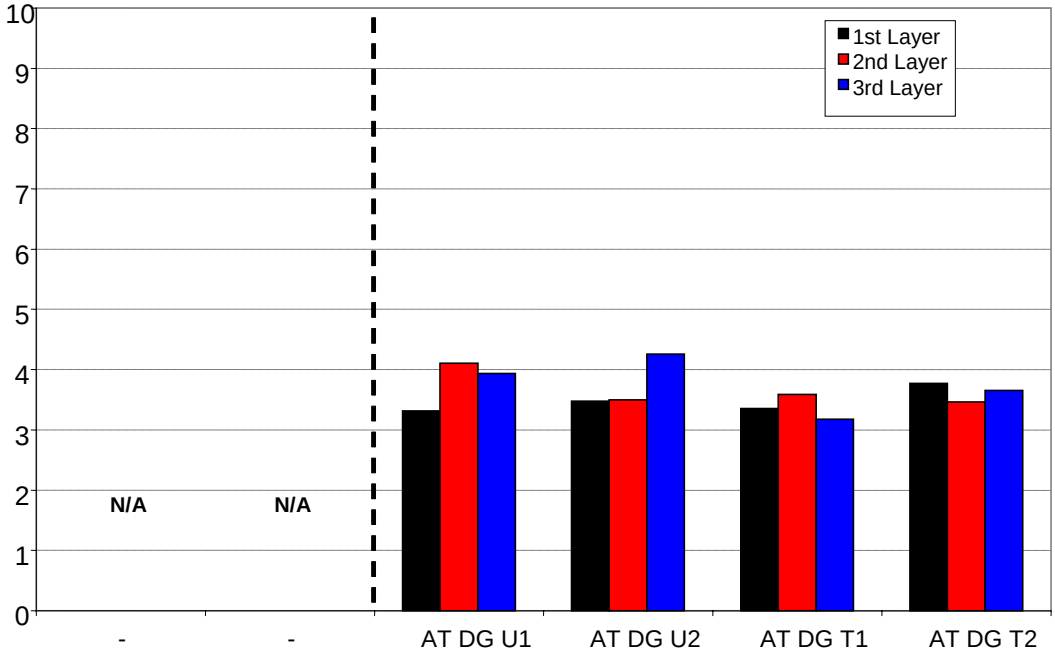

Figure H-6. Binder Content of Atlanta IH 20 DG, %

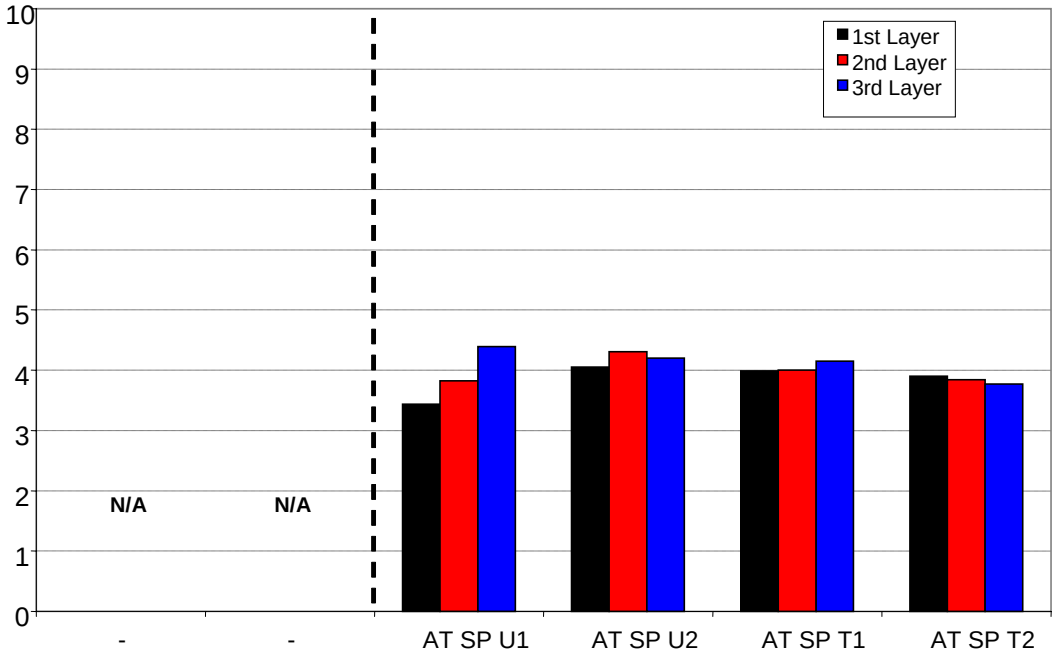

Figure H-7. Binder Content of Atlanta IH 20 SP, %.

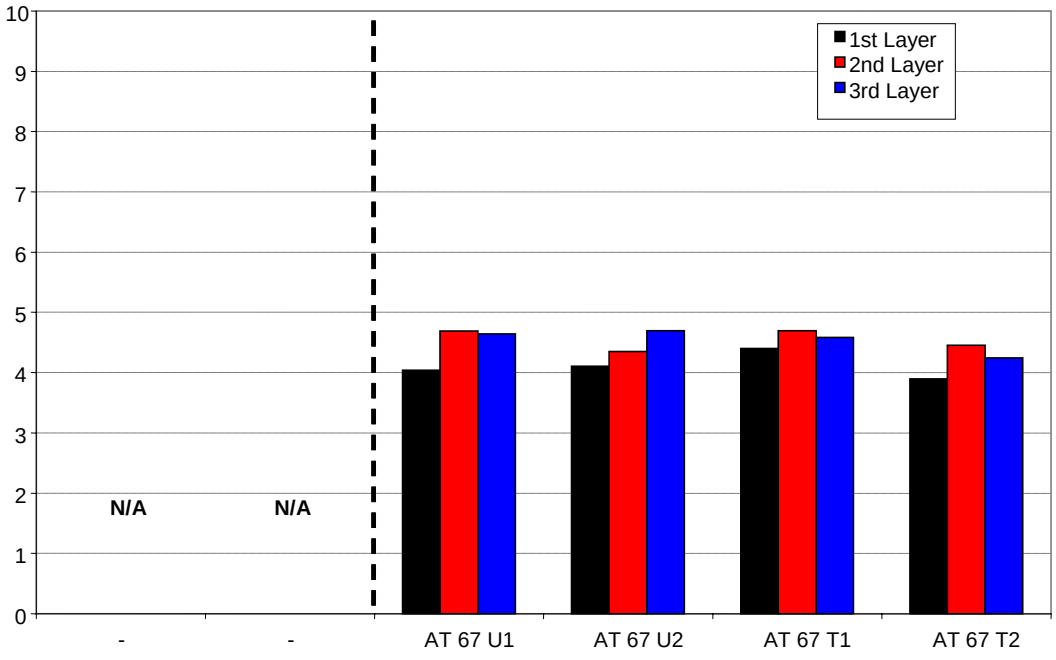

Figure H-8. Binder Content of Atlanta IH 20 67, %.

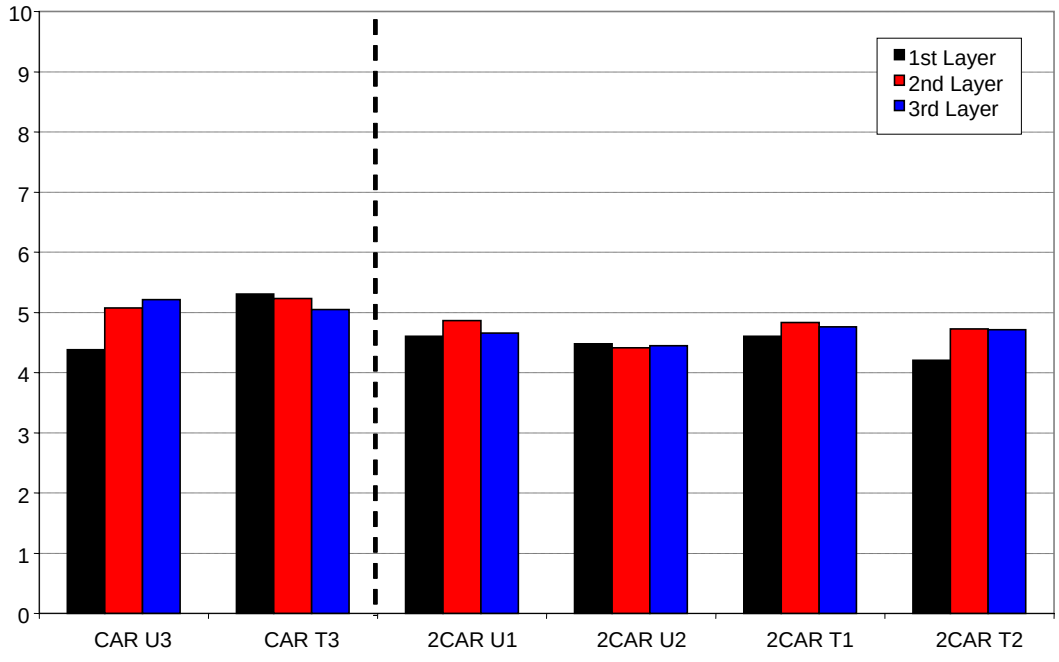

Figure H-9. Binder Content of 1st and 2nd Set Carrizo Springs Airport, %.

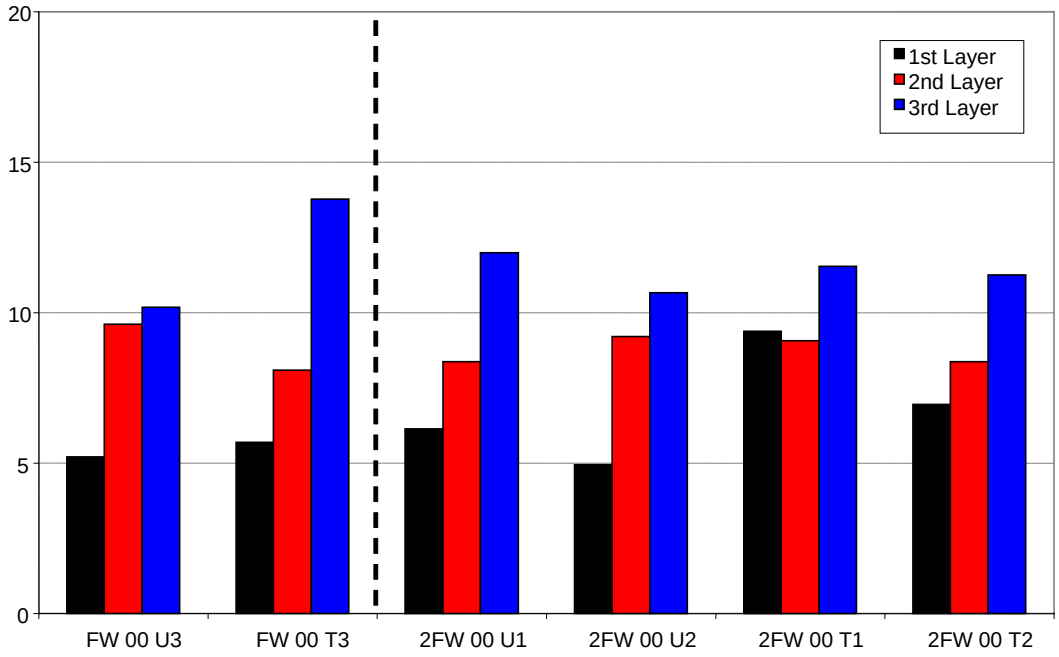

Figure H-10. Binder Content of 1st and 2nd Set Fort Worth FM 4 (2000), %.

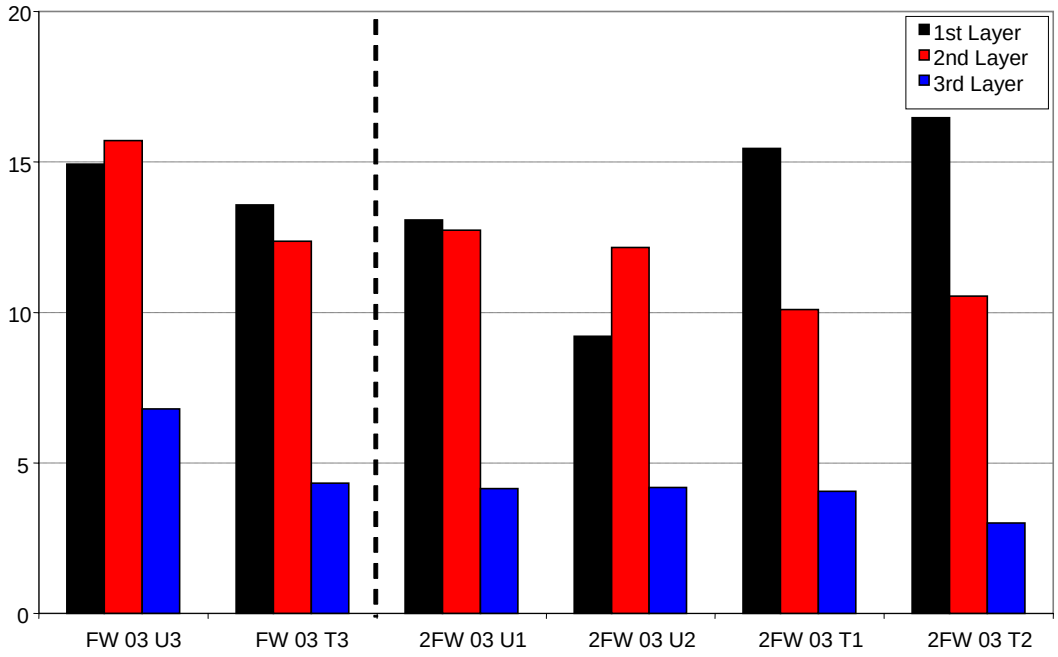

Figure H-11. Binder Content of 1st and 2nd Set Fort Worth FM 4 (2003), %.

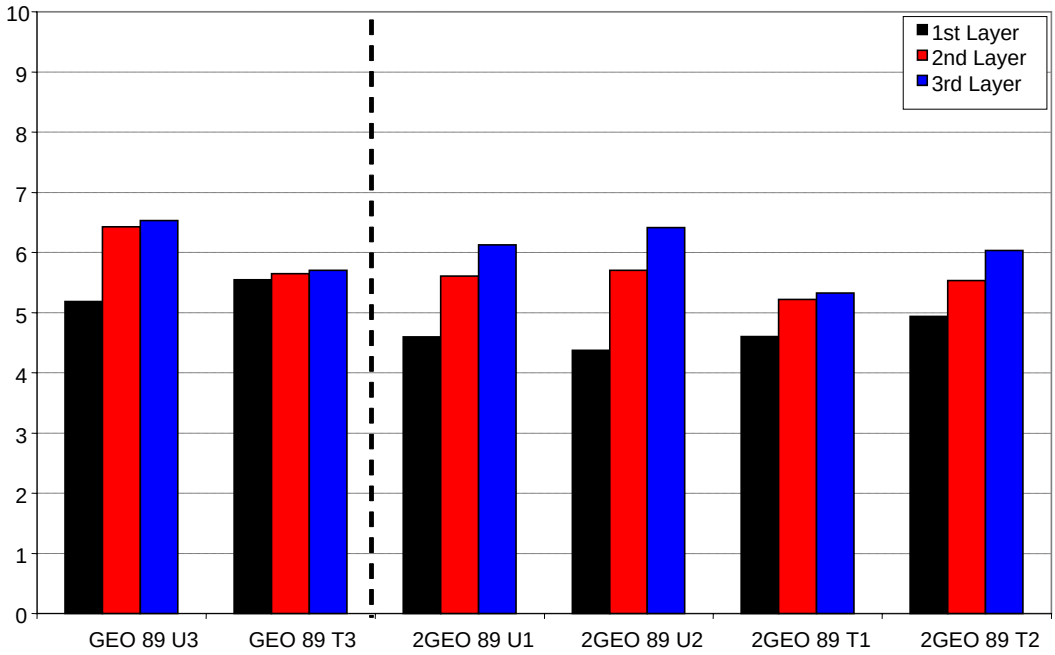

Figure H-12. Binder Content of 1st and 2nd Set Georgetown Airport (1989), %.

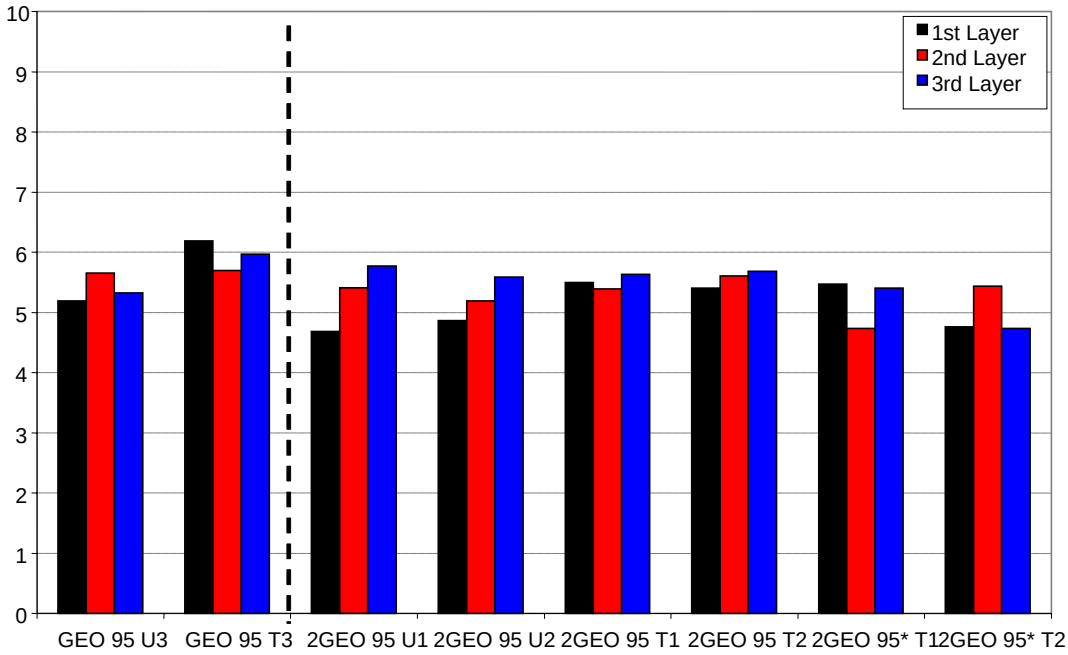

Figure H-13. Binder Content of 1st and 2nd Set Georgetown Airport (1995), %.

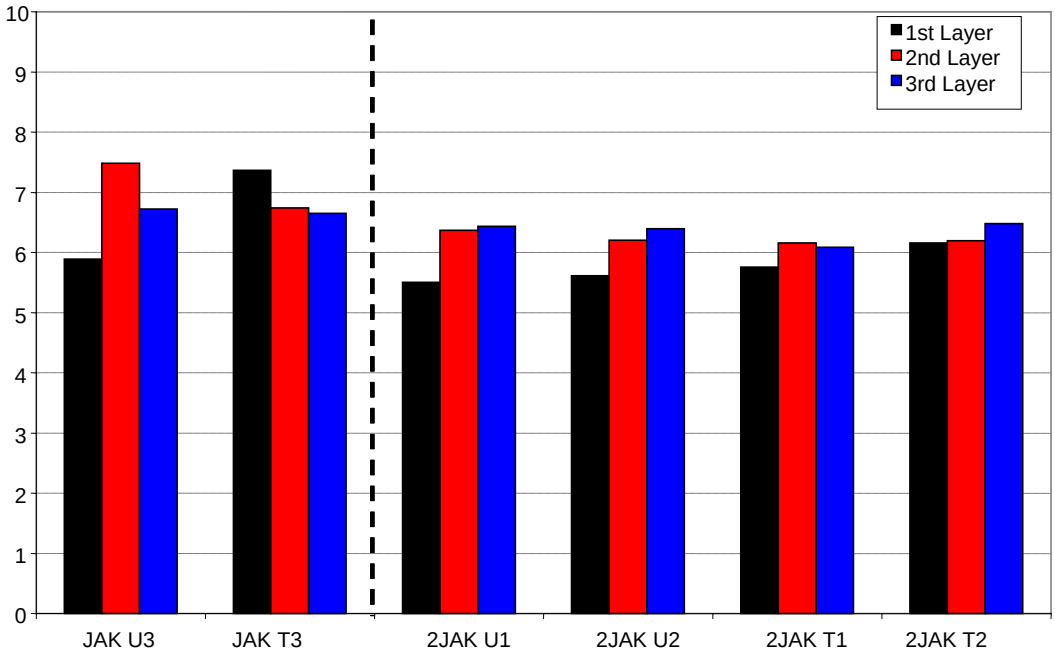

Figure H-14. Binder Content of 1st and 2nd Set Jacksonville Airport, %.

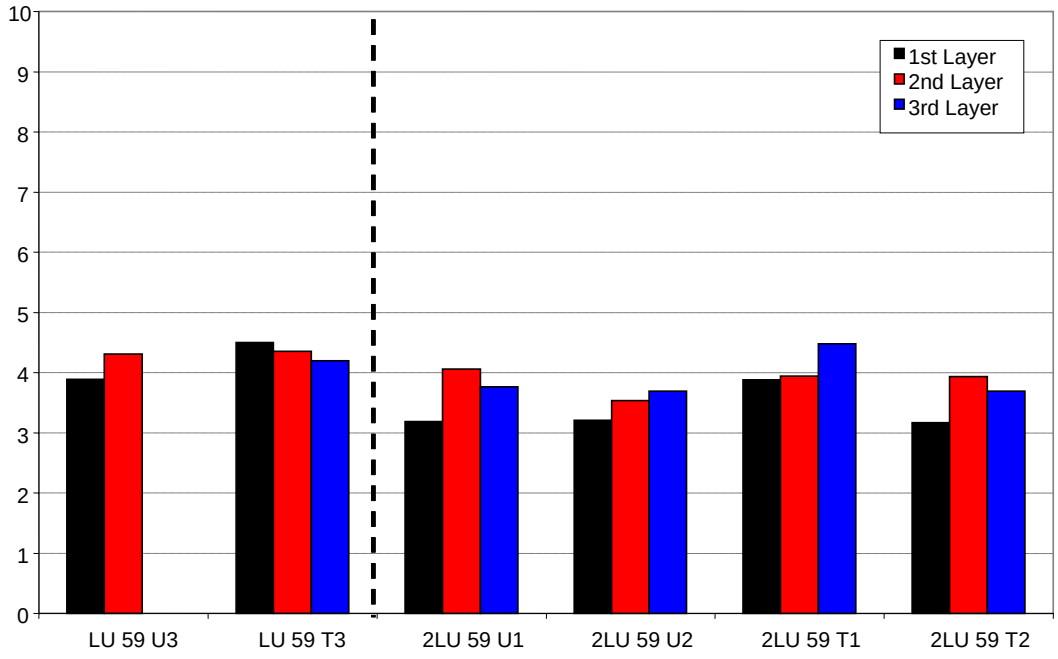

Figure H-15. Binder Content of 1st and 2nd Set Lufkin BUS 59, %.

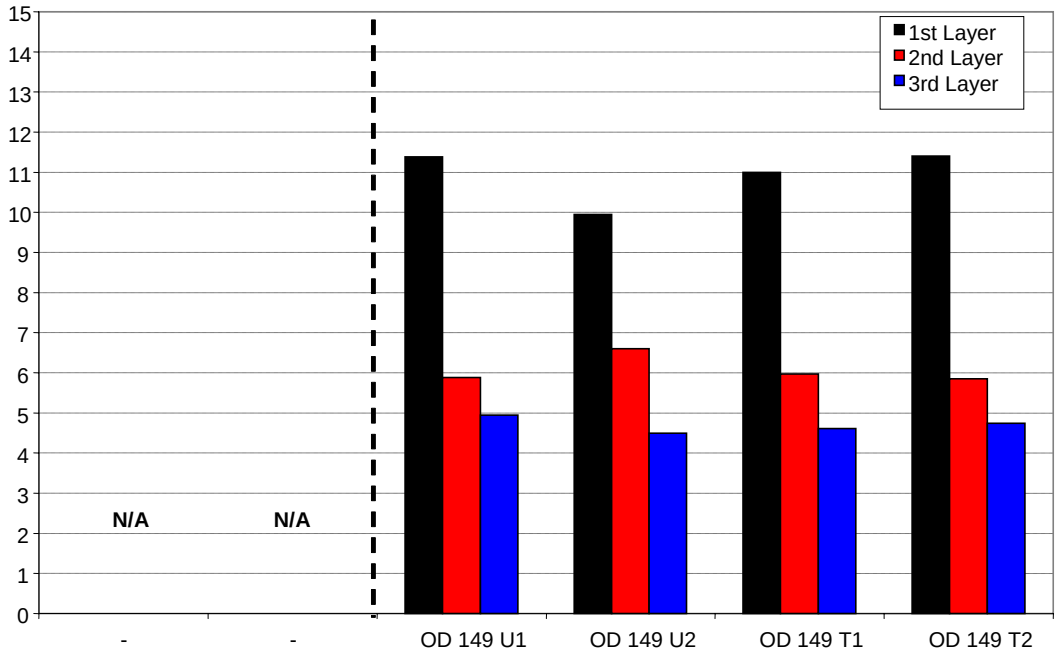

Figure H-16. Binder Content of Odessa SH 149, %.

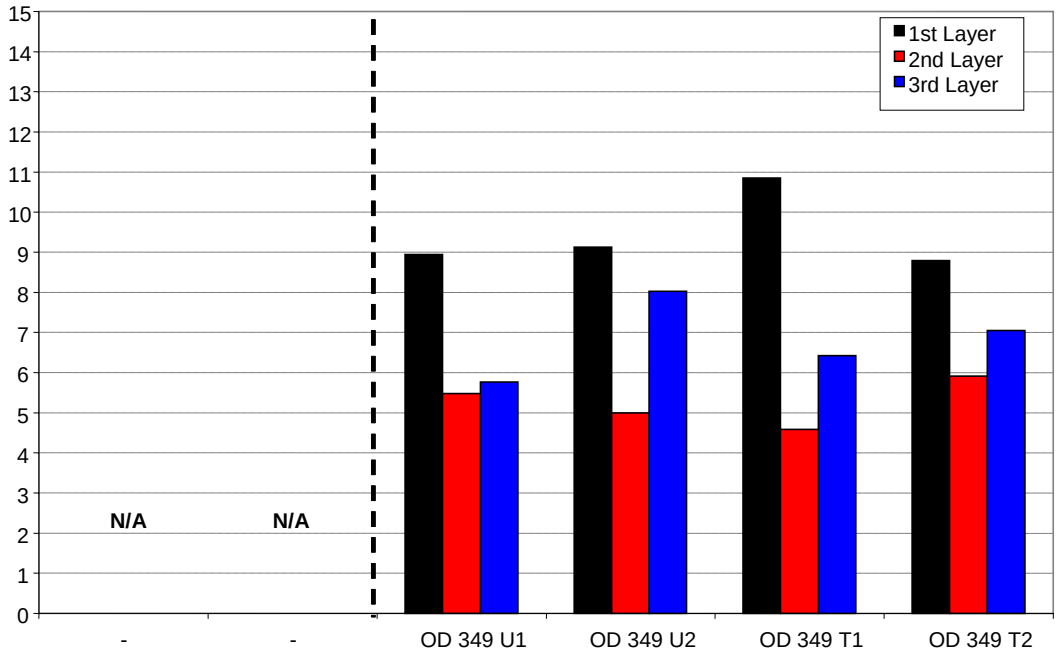

Figure H-17. Binder Content of Odessa SH 349, %.

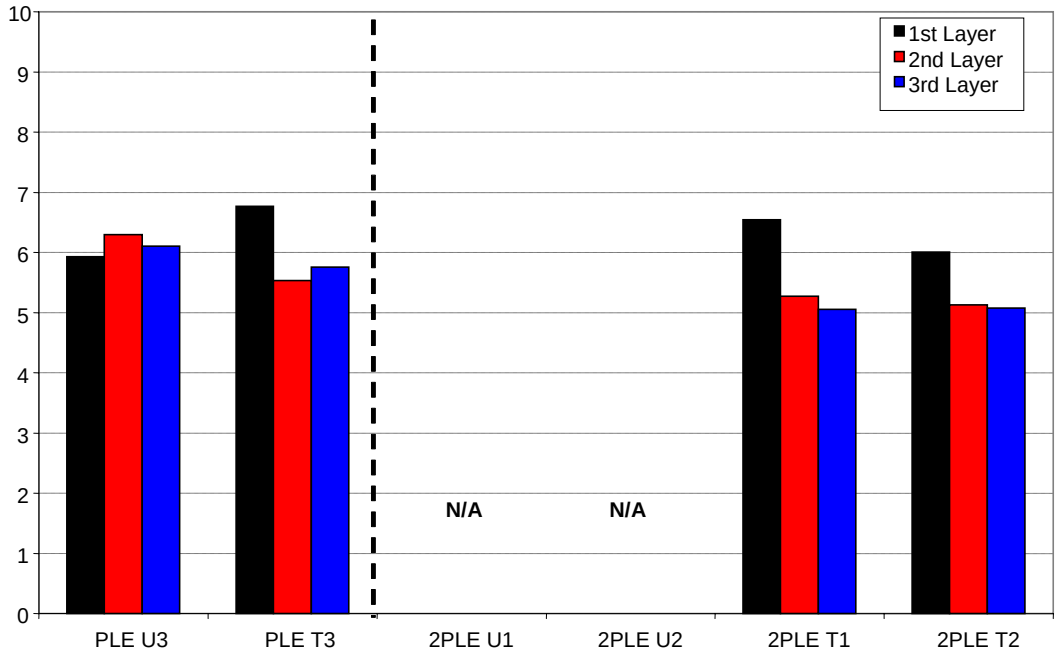

Figure H-18. Binder Content of 1st and 2nd Set Pleasanton Airport, %.

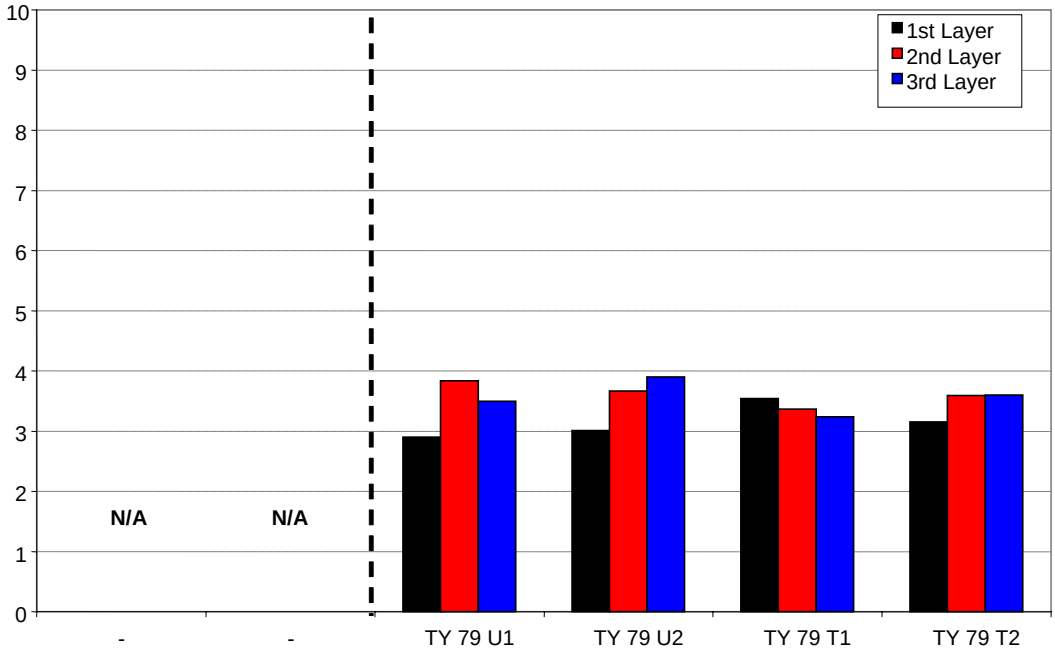

Figure H-19. Binder Content of Tyler US 79, %.

APPENDIX I

PROPERTIES OF THE FOG SEAL BINDERS

PROPERTIES OF THE FOG SEAL BINDERS

TEST METHOD FOR FOG SEAL EMULSIONS

Solvent Removal from Fog Seal Emulsion

The fog seal emulsions obtained from construction sites, most of the time, contain approximately 40 to 60 percent solvent (water, oil, etc.), used to reduce the viscosity of the fog seal material. In order to measure the physical properties of the fog seal base materials, the solvents must be removed from the emulsion. In this project, approximately 15 to 18 grams of fog seal emulsions in 3 oz containers were heated in the laboratory oven at 60 °C (used as an average pavement surface temperature) to effect solvent evaporation. Weight reduction of the samples was recorded every day for five days as shown in Figure I-1. According the this figure, after approximately 3 to 4 days, the weight change was less than 1 percent compared to the previous day, which assured that most of the solvent was evaporated. The solvent-free base materials were tested with DSR and SEC, respectively.

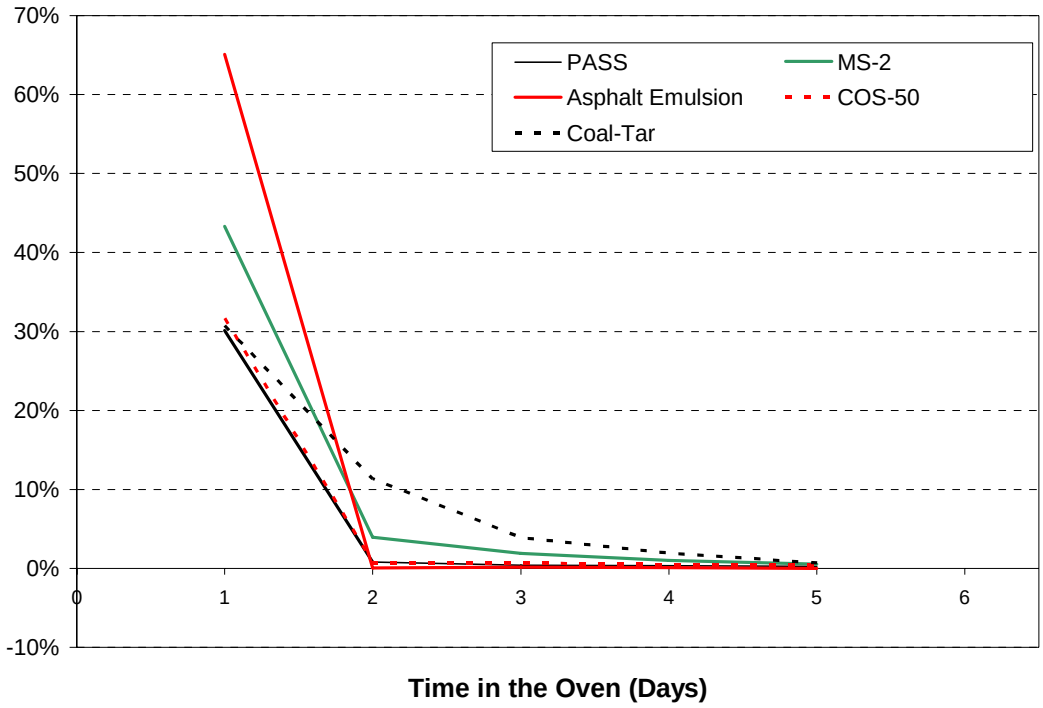

Figure I-1. Weight Reduction of Fog Seal Emulsions.

Dynamic Shear Rheometer Measurements

Two types of rheological property data were obtained from dynamic shear rheometry measurements: the viscosity master curve at 60 °C and an estimated ductility of the asphalt binder. A 2.5 cm diameter parallel-plate geometry with a 500 micrometer gap was used for the measurements. To acquire the viscosity master curve at the 60 °C reference temperature, complex viscosity measurements were obtained in a controlled-stress mode by performing two frequency sweeps at 60 °C and 80 °C over a frequency range of 100 to 0.1 rad/s. Then, time-temperature superposition was used to obtain a single viscosity master curve at 60 °C over a frequency range of 100-0.001 rad/s. At the lower end of the frequency range, the viscosity approaches a low shear rate limiting viscosity (also termed the "zero-shear" viscosity), a useful characteristic of the binder. An estimate of the binder's ductility at 15 °C and 1 cm/min extension rate can be calculated from DSR G' and G" at 44.7 °C and 10 rad/s (Ruan et al. 2003). The DSR function relationship is shown below:

$$\text{DSR Function} = \frac{G'}{\left(\eta'/G'\right)} = \frac{G'^{*}\omega}{\tan\delta} \qquad \text{(I-1)}$$

Where $\eta' = \frac{G''}{\omega}$ and $\frac{G''}{G'} = \tan\delta$

ω = Angular Frequency (rad/s)

δ = Phase Angle (degree)

From this DSR function, an estimate of the binder's ductility can be calculated according to the correlation of Ruan et al. (2003). This correlation is quite good for unmodified binders below ductility of about 10 cm but may underestimate the actual ductility significantly beyond 10 cm.

Size Exclusion Chromatography

Size exclusion chromatography, also called gel permeation chromatography, can be used to characterize the recovered fog seal base materials. The shape and relative size of the asphaltenes and maltenes peaks can be used as "fingerprinting," to compare the different base binders used in the different fog seal materials and to help identify them as asphalt materials versus light oils.

The molecular size distribution of asphalt materials was measured using a Waters GPC HPLC system with both refractive index and intrinsic viscosity detectors. Recovered fog seal asphalt binder material (0.2 g) was dissolved in 10 mL of Tetrahydrofuran, and this solution was passed through the GPC columns at a flow rate of 1.0 mL/min after filtering through a 0.4 µm PTFE syringe filter.

RECOVERED FOG SEAL BASE ASPHALT PROPERTIES

SEC Chromatograms

Figures I-2 through I-7 are SEC chromatograms of the emulsion materials. The materials were recovered from the emulsion by distilling off the water, following the procedure described above. The recovered materials were then tested in the SEC apparatus using the standard procedures described in Chapter 2.

The PASS, MS-2, COS-50, and asphalt emulsion materials, to a large degree, look very much like standard asphalt materials. The typical asphalt chromatogram exhibits an asphaltenes peak that elutes between about 22 and 26 minutes, and a maltenes peak that elutes after the asphaltenes peak. The PASS material, in addition to the asphalt, contains polymer, which is seen very clearly in the prominent peak that elutes at 20 minutes. The MS-2 (Figure I-3) and COS-50 (Figure I-4) materials show no polymer and the asphalt emulsion material (Figure I-5) shows only a very minimal amount of polymer. In all of these chromatograms, there are two traces. One is the refractive index detector trace and the other is an intrinsic viscosity detector trace that is especially suited for characterizing the presence of polymer materials. Of course, even though these four materials look basically like asphalt materials, they are, nevertheless, readily distinguishable from each other through their characteristic chromatographic patterns. In addition to the asphalt in these materials, each of the traces shows three negative peaks at about 37, 40, and 41.5 minutes. These are traces of water, nitrogen, and oxygen, respectively, and exist in virtually all of the chromatograms.

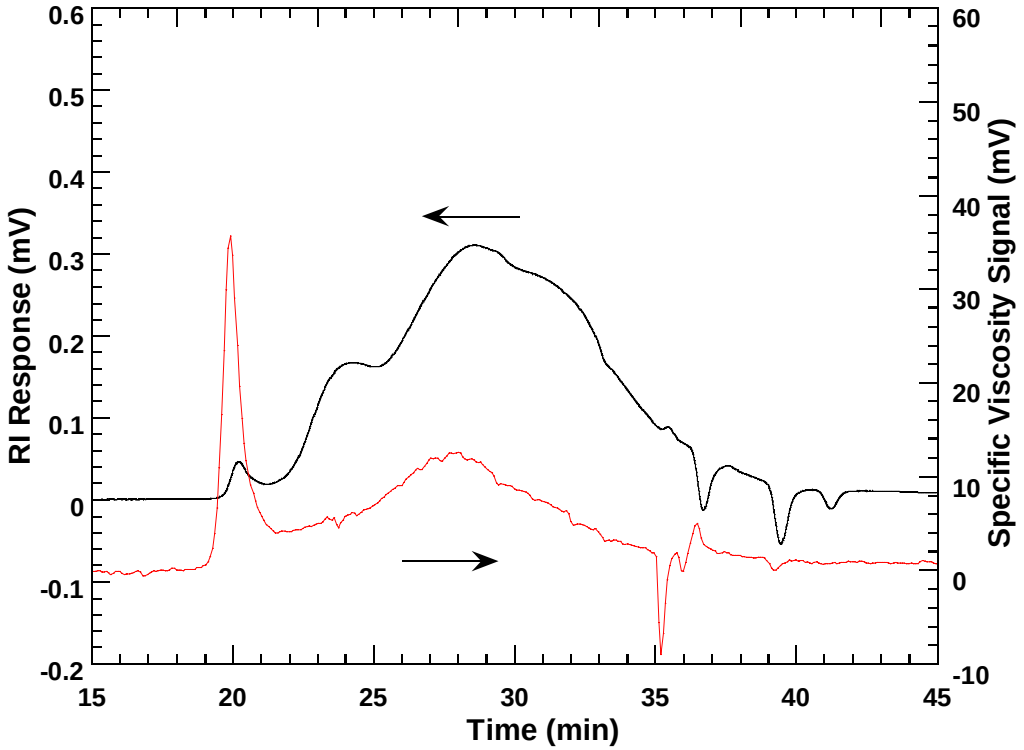

Figure I-2. SEC Chromatogram of the Recovered PASS Fog Seal Material.

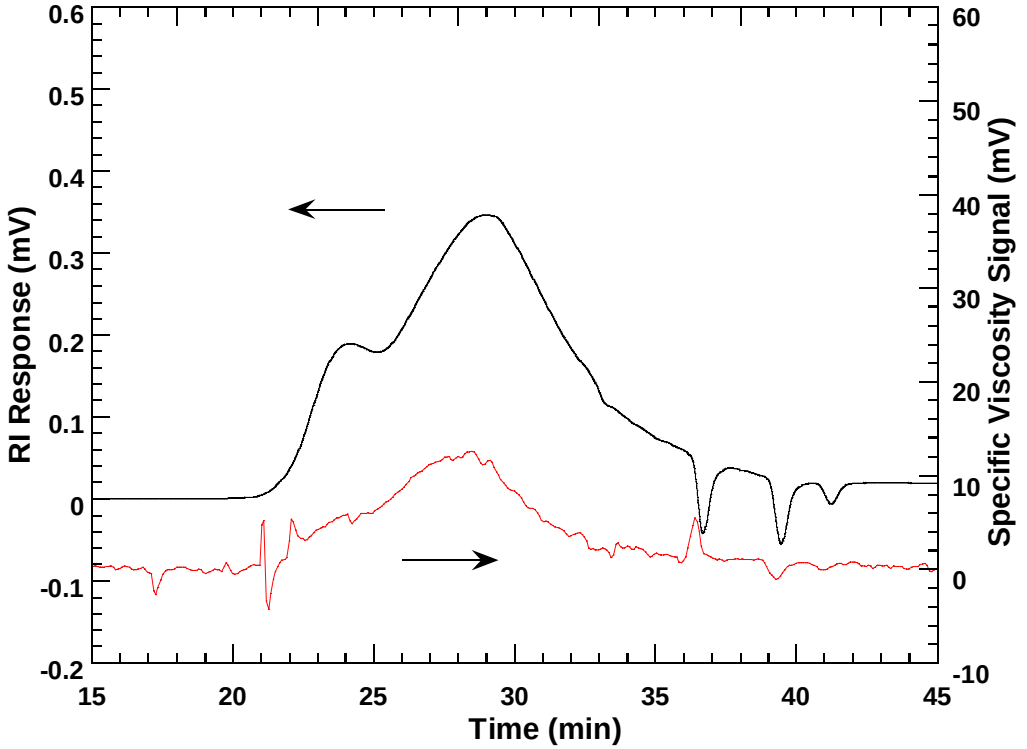

Figure I-3. SEC Chromatogram of the Recovered MS-2 Fog Seal Material.

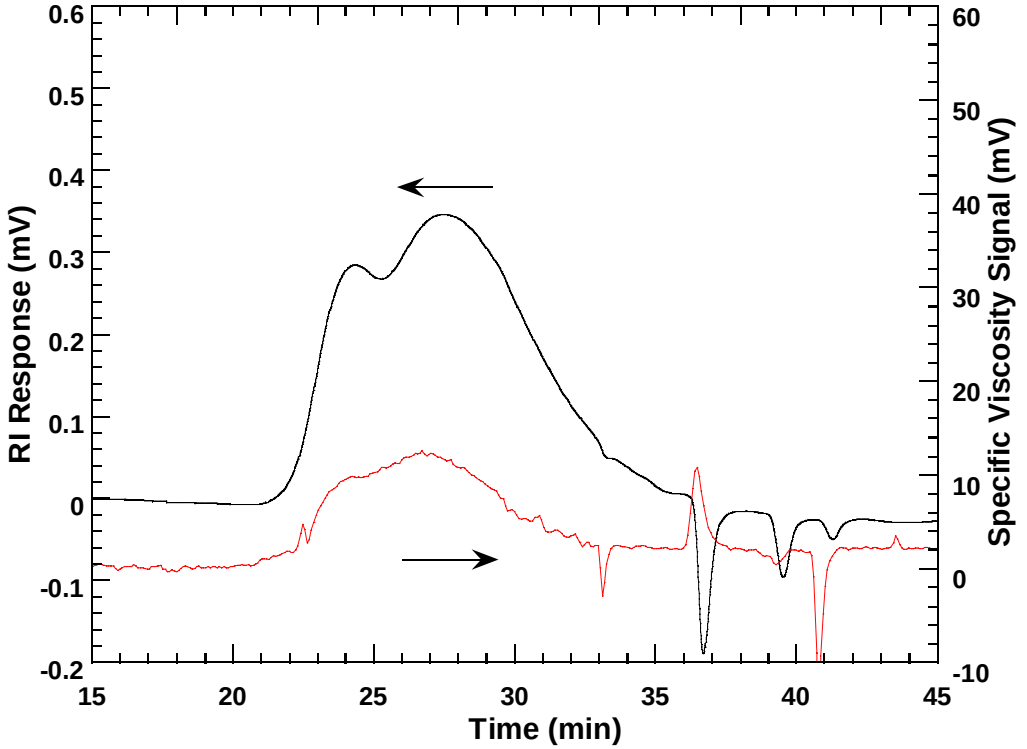

Figure I-4. SEC Chromatogram of the Recovered COS-50 Fog Seal Material.

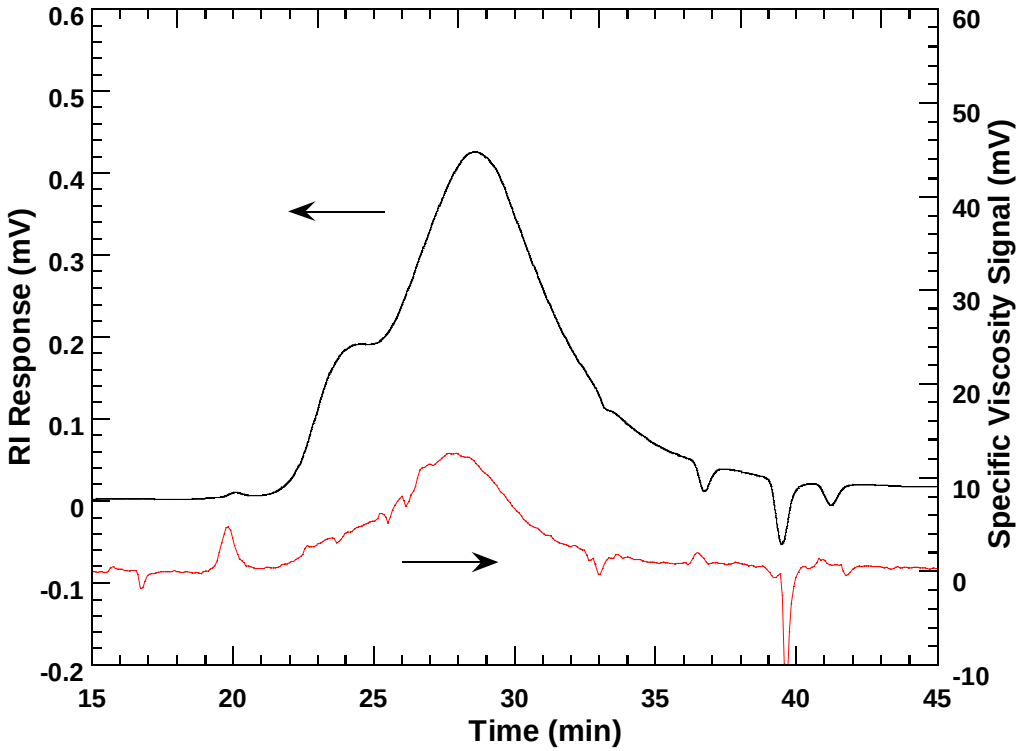

Figure I-5. SEC Chromatogram of the Recovered Asphalt Emulsion Fog Seal Material.

The coal tar and rejuvenator materials are decidedly different materials from the others (Figures I-6 and I-7). These are much lighter materials and elute beginning at about 35 minutes and ending at about 41 minutes. This establishes them as lighter components than almost any of the components in the asphalt emulsion materials, a fact that suggests that they would be much more volatile than the asphalt materials. However, because they appear at such a distinctive part of the chromatogram and have such a distinctive trace compared to the asphalt materials, they have the potential to serve as a good marker for the presence of the fog seal application and especially for its penetration below the surface into the pavement. The asphalt materials, because they look so much like asphalts, are much more difficult to distinguish from the original binder used in the pavements. Of course, if the PASS material were used over a pavement binder that did not have polymer, then the presence of the polymer in the recovered binder in the treated pavement would serve as a good indication of residual presence of the fog seal treatment. Detecting the MS-2, COS-50, and asphalt emulsion materials, however, is a much more problematic issue. One might also look for differences in the shape of the recovered binder at different layers, which may indicate the presence of the emulsion asphalt blended with the original binder.

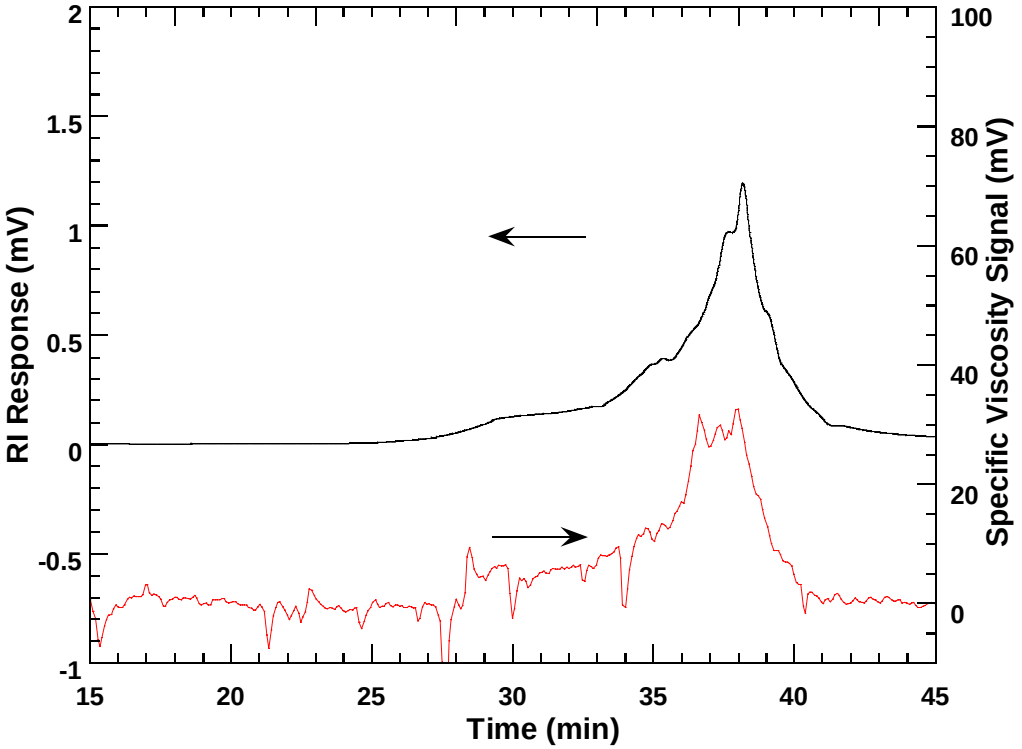

Figure I-6. SEC Chromatogram of the Recovered Coal Tar Rejuvenating Seal Material.

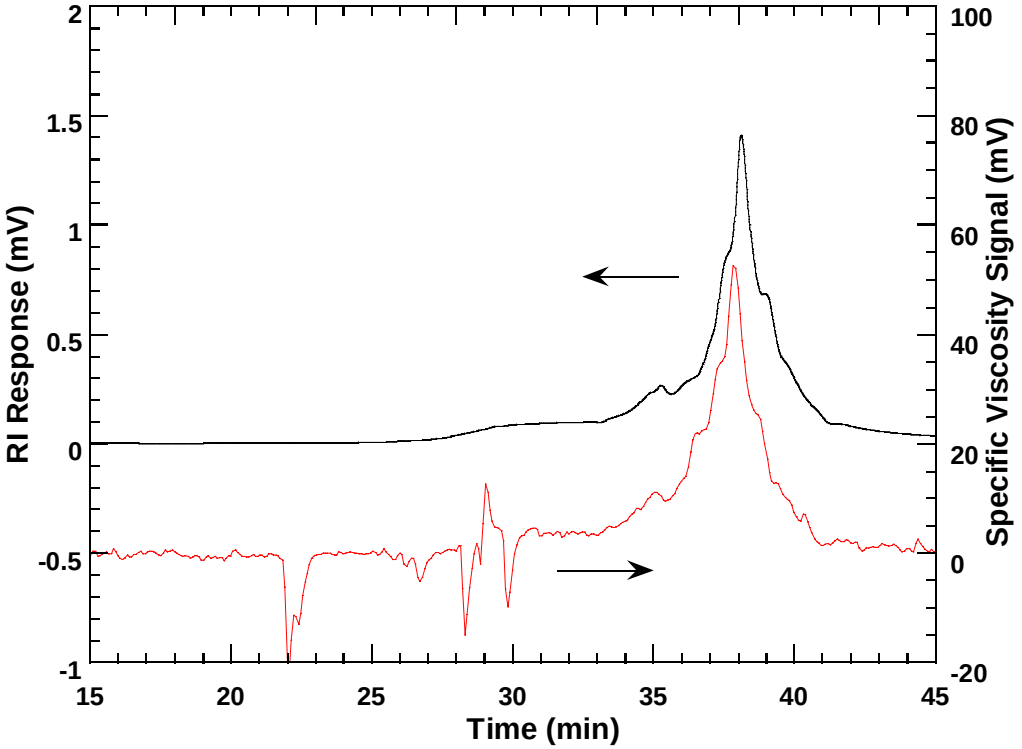

Figure I-7. SEC Chromatogram of the Recovered Rejuvenator Material.

Dynamic Complex Viscosity Master Curves of the Fog Seal Materials

The recovered fog seal asphalt materials were analyzed for their rheological properties. Dynamic complex viscosity master curves, at 60 °C for low frequencies, are shown in Figure I-8. The PASS, MS-2, and asphalt emulsion materials are much like conventional viscosity-graded AC-10 to AC-20 asphalts, having viscosities that range from 1000, to nearly 3000, poise. The COS-50 material is significantly harder, 30,000 poise.

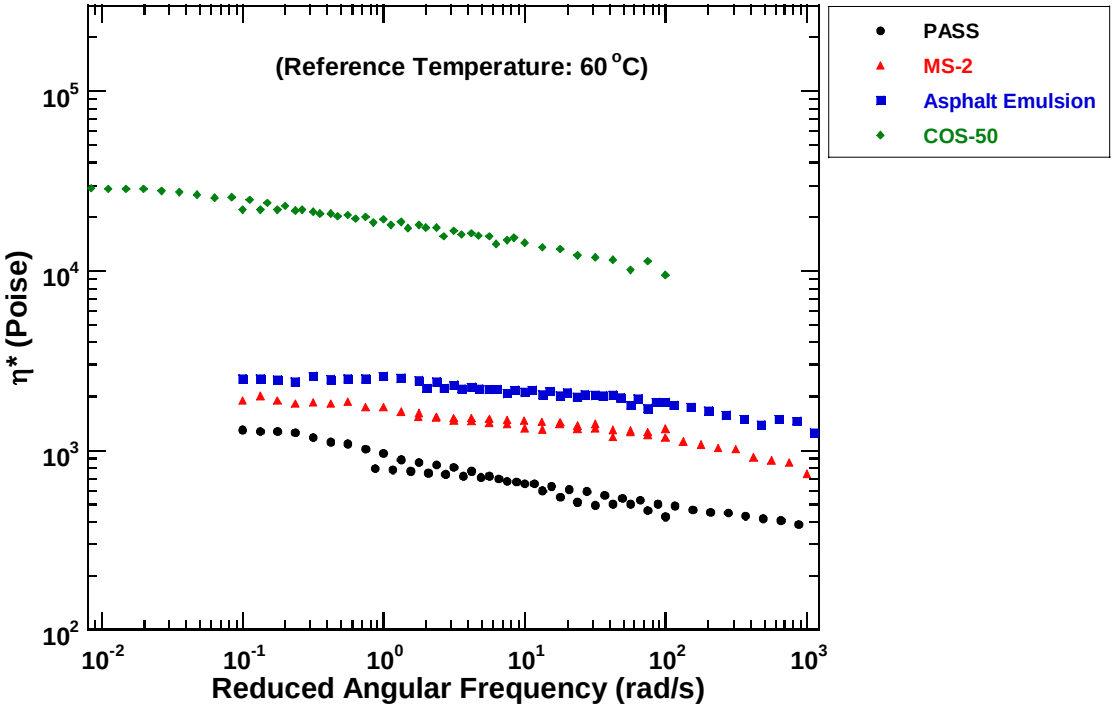

Figure I-8. Complex Viscosity Master Curves for Base Materials of Fog Seal Emulsions.

DSR Function and Calculated Ductility

Values of the DSR function for the recovered fog seal base materials were calculated using Equation I-1 and are shown in Table I-1. Also shown are the calculated ductility values, estimated using the correlation of Ruan et al. (2003). As noted above, this correlation is quite good for ductilities less than 10 cm but significantly underestimates the ductility above 10 cm.

Note that the COS-50 binder, at a calculated ductility of 12 cm, is much stiffer than the other asphalt materials. At this low a ductility, the COS-50 material would have no rejuvenation capability at all. The other materials are significantly softer.

Table I-1. DSR Function and Calculated Ductility Data for the Recovered Fog Seal Binders.[a]

Fog Seal Emulsion	DSR Function (G'/(η'/G'))	Calculated Ductility (cm)
PASS	6.25E-07	123
MS-2	1.91E-06	76
COS-50	1.26E-04	12
Asphalt Emulsion	2.32E-06	69

[a] η' and G' are measured at 44.7 °C, 10 rad/s and converted by TTSP to 15 °C, 0.005 rad/s

CONCLUSIONS

The fog seal materials evaluated in this project appear not to be well suited as rejuvenating materials. The asphalt materials, at best, are light asphalt materials (approximately unaged AC-10 viscosity grade) and at worst, correspond to a pavement binder aged at least to the level of a newly placed binder in Texas. In either case, they provide the pavement with more asphaltenes, of which it has no need. At the other extreme, the coal tar materials appear to be too light to be effectively absorbed by the *in situ* binder. The ideal rejuvenating material has been previously hypothesized to have no asphaltenes and to consist largely of aromatic components (Davison et al. 1994).